
The Electron

Riccardo Fantoni



June 3, 2025

To my Grandmother

nonna Jone

To my Parents

*my father and my mother a couple for
56 years, to their patience, never los-
ing hope, and extraordinary acumen*

Preface

The electron is the main actor of this assay, a mysterious character and at the same time omnipresent in our daily life that can be in multiple states at the same time. At the same time elementary and complex. We will initially follow a top-down causation [Ellis \[2011\]](#) to introduce it from symmetry principles and then a bottom-up causation to introduce various systems made of it.

It is an elementary particle and as such is described by a vector, a wave function, of a finite dimensional irreducible unitary representation of its group of symmetries (the Galileo group in the non-relativistic case and the Poincare' group in the relativistic case, extended to the parity transformation). The invariants of the group are the mass and the spin and the electron has spin 1/2. The spin-statistics theorem states that, as a consequence of Lorentz invariance and of locality, half integer spin particles must obey to Fermi statistics and integer spin particles must obey to Bose statistics. So many electrons must obey to the Pauli exclusion principle

Its role in a ionic crystal in the Feynman polaron problem, in atomic structure in the Mendeleev periodic system, and in the redox chemical bond is discussed as few electron systems examples.

The assay continues with the properties of a many electron system, the Jellium. Its ground state and finite temperature state are discussed from a (computational) theoretical point of view. Some phenomenology is also presented in the very end.

The assay then gives a description of the equation of state and structure of a white dwarf a stellar core remnant composed mostly of electron-degenerate matter which has a white hot color temperature and reddens as it cools down.

The assay is then concluded with a description of the renormalization group theory for phase transitions in statistical physics.

Of course the assay has no pretensions of completeness of any kind since the argument is so vast that one could devote to it a whole encyclopedia. Nonetheless the few arguments that are touched are rigorous and go somewhat in depth. It could certainly be an interesting reading for the graduate student but in some of its parts (especially Chapters 2,3, and 6) could become a valid instrument for researchers from the high- to the low-energy physics communities.

The project of the assay has been made possible by my rather fortunate encounters of many of the few 'maestri' in the field of relativistic quantum mechanics like prof. Adriano Di Giacomo from the physics department of the University of Pisa, Italy and prof. Robert Leigh from the department of physics of the University of Illinois at Urbana/Champaign among others, in the field of the electron gas like my first master advisor prof. Mario Pio Tosi from the Scuola Normale Superiore di Pisa, Italy, my second master advisor prof. David Matthew Ceperley from the National Center for Supercomputing Applications of the University of Illinois at Urbana/Champaign, and prof. Bernard Jancovici from the laboratory for theoretical physics of the University of Paris Sud at Orsay, France among others, and in the field of cosmology, gravitation, and compact objects in the Universe like my graduate courses prof. Stuart Shapiro from the University of Illinois at Urbana/Champaign among others.

I must mention the fact that the third chapter of the assay is the result of my first Ph.D. studies while working in the group of prof. David Matthew Ceperley on the Path Integral Monte Carlo (PIMC) method. The form that is presented here is the original version written on 1998 in preparation of my Ph.D. thesis which describes the results obtained with my own PIMC code. My advisor did not consider it sufficiently interesting to be worth a publication. As a matter of fact I would discover only in 2001 after I had to come back to Trieste in 2000 to give birth to my daughter that a certain Dr. Carlo Pierleoni from l' Aquila had just published exactly the same results in a three author Phys. Rev. Lett. collaboration.

The assay is organized in 9 chapters. In the first introductory chapter we describe the physical constants and properties of the *isolated electron* and give some historical background. In chapter two we show how the electron as an *elementary particle* can be described as a vector of a finite dimensional irreducible unitary representation of its group of symmetries and how relativistic quantum mechanics can explain the spin-statistics theorem. In the following chapters we start studying the *few electrons* and their interactions among themselves and with the environment. We will always see the electron as the protagonist of the interaction. So, in the third chapter we present the Feynman quantum polaron problem that sees one electron interacting with a crystal of ions. In chapter four we study the role of few electrons in the periodic system of the elements of Mendeleev. In the fifth chapter we see how few electrons determine the RedOx chemical bond between elements. In the following chapters we study *many electrons* in the thermodynamic limit. In chapter six we review some of our studies on the non-quantum electron gas, the plasma, on curved surfaces at that special value of the coupling constant that allows for an exact analytic solution of the many body statistical physics problem. In the seventh chapter we present some numerical work that has been done on the fully quantum electron gas, the Jellium, its ground state and finite temperature phase diagram properties. In chapter eight chapter we study a white dwarf, a compact object of the universe that has consumed all its nuclear fuel and support itself against gravity by the pressure of the residual cold electron gas. In the last ninth chapter we describe the properties of phase transition in statistical physics and the renormalization group and its universality properties explaining how in a neighborhood of a critical point it is often largely irrelevant the nature of the liquid studied being it Jellium or other.

References

- G. F. R. Ellis. Top-down causation and emergence: some comments on mechanisms. *Interface Focus*, 2011. doi: [10.1098/rsfs.2011.0062](https://doi.org/10.1098/rsfs.2011.0062).

Contents

Preface	i
References	ii
1 Introduction	1
References	16
Appendices	17
1.A Particle Data Group	17
References	25
2 The particle	27
2.1 Definition of Invariance	27
2.1.1 Conventions	28
2.2 Invariance in quantum mechanics	28
2.3 Invariance and time evolution	31
2.4 Galilean relativity	31
2.4.1 Spatial translations	31
2.4.2 Rotations	32
2.4.3 Galilean transformations	32
2.4.4 Galileo group	33
2.4.5 Parity invariance	34
2.4.6 Time reversal	35
2.5 Einstein Relativity	38
2.5.1 The irreducible unitary representation of the Poincaré group	42
2.5.2 Wave functions in coordinate space	53
2.6 The relativistic wave equations	54
2.6.1 Particles of spin 0	54
2.6.2 Particles of spin 1/2	57
2.6.3 Particles of spin 1	67
2.7 The second quantization	69
2.7.1 Fock space	70
2.7.2 Field operators	72
2.7.3 Transformation properties of the field operators	73
2.7.4 Locality and spin-statistics theorem	76

References	80
Appendices	81
2.A Commutators	81
2.B The Levi-Civita symbol	83
2.C Angular momentum	83
2.D SU(2)	85
2.E Velocity transformations	86
3 The Polaron	89
3.1 Introduction	89
3.2 The model	90
3.3 The observables	91
3.4 Discrete path integral expressions	92
3.5 Sampling the path	93
3.6 Choice of T_k and π_k	95
3.7 Correlated sampling	96
3.8 Numerical Results	98
3.9 Conclusions	102
References	107
Appendices	109
3.A Estimating errors	109
4 Mendeleev Periodic System	111
4.1 Electron states in the atom	111
4.2 Periodic Table	113
References	116
5 RedOx Chemical Reactions	117
5.1 Mathematical discovery in 1D	118
5.2 Mathematical discovery in 2D	119
References	122
6 Plasma living in a curved surface	123
6.1 Introduction	123
6.1.1 The surface	125
6.1.2 The Coulomb potential	126
6.1.3 The background	126
6.1.4 The total potential energy	126
6.1.5 The densities and distribution functions	127
6.2 The One-Component Plasma	127
6.2.1 The plane	128
6.2.2 The cylinder	130
6.2.3 The sphere	132
6.2.4 The pseudosphere	134
6.2.5 The Flamm paraboloid	144

6.3	The Two-Component Plasma	161
6.3.1	The plane	161
6.3.2	The sphere	164
6.3.3	The pseudosphere	166
6.3.4	The Flamm paraboloid	166
6.4	Conclusions	172
	References	173
	Appendices	175
6.A	Electrostatic potential of the background for the OCP in the pseudosphere	175
6.B	The flat limit for the OCP in the pseudosphere	176
6.C	Green's function of Laplace equation in Flamm's paraboloid	177
6.C.1	Laplace equation	177
6.C.2	Green's function of Laplace equation	178
6.D	The geodesic distance on the Flamm paraboloid	181
	References	182
7	The Electron Gas	183
7.1	The model	184
7.1.1	Lindhard theory of static screening in Jellium ground state	185
7.1.2	Ewald sums	187
7.2	Jellium in its ground state	188
7.2.1	Monte Carlo simulation (Diffusion)	188
7.2.2	Expectation values in DMC	189
7.2.3	Trial wave-function	191
7.2.4	The radial distribution function	195
7.2.5	Results for the radial distribution function and structure factor	197
7.2.6	Results for the internal energy	197
7.3	Jellium at finite temperature	197
7.3.1	Monte Carlo simulation (Path Integral)	197
7.3.2	Results for the radial distribution function and structure factor	207
7.3.3	Results for the internal energy	207
7.3.4	Phase diagram	211
7.4	Some physical realizations and phenomenology	212
7.4.1	Molten halides and some alloys of metallic elements	213
7.4.2	Structure of trivalent-metal halides	215
7.4.3	Chemical short-range order in liquid alloys	216
7.4.4	Liquid metals	217
	References	223
	Appendices	225
7.A	Ideal gas energy and exchange energy as a function of polarization	225
7.B	Jastrow, backflow, and three-body	226
7.C	The Random-Phase-Approximation	227
7.D	Analytic expressions for the non-interacting fermions ground state	228
7.D.1	Radial distribution function	228
7.D.2	Static structure factor	228

CONTENTS

7.D.3 Internal energy	229
7.E Radial distribution functions sum rules for the electron gas ground state	230
7.E.1 Cusp conditions	230
7.E.2 The Random-Phase-Approximation (RPA)	230
7.F The primitive action	231
7.G The pair-product action	233
7.H Linear-Response-Theory	234
7.H.1 Fluctuation-dissipation theorem	235
7.H.2 Kramers-Kronig relations	236
7.H.3 The dielectric function	237
7.I Long-range potentials with the Ewalds image technique	238
References	241
8 The White Dwarf	243
8.1 Introduction	243
8.2 The thermodynamics of the ideal quantum gas	244
8.2.1 Relativistic effects at high density in a gas of fermions	247
8.2.2 The onset of quantum statistics	248
8.2.3 The Chandrasekhar limit	250
8.3 The structure of the ideal quantum gas	252
8.4 Conclusions	254
References	256
Appendices	257
8.A The adiabatic equation of state	257
9 The Renormalization Group	259
9.1 Notation	259
9.2 The origin of RG	260
9.3 The decay of correlation functions	261
9.4 The challenges posed by critical phenomena	263
9.5 The critical exponents	266
9.5.1 The classical exponent values	267
9.5.2 The Ising exponent values	267
9.5.3 Exponent relations	268
9.6 The Gaussian model	268
9.7 The task of RG	268
9.8 The basis and formulation	270
References	280
List of Figures	281
Index	287

Chapter 1

Introduction

Composition:	Elementary particle Eichten et al. [1983]
Statistics:	Fermionic Navas et al. [2024]
Family:	Lepton Navas et al. [2024]
Generation:	First Navas et al. [2024]
Interactions:	Weak, electromagnetic, gravity Navas et al. [2024]
Symbol:	e^- , β^- Navas et al. [2024]
Antiparticle:	Positron Navas et al. [2024]
Theorized:	Richard Laming (1838-1851), Farrar [1969] G. Johnstone Stoney (1874) and others.
Discovered:	J. J. Thomson (1897) Thomson [1897]
Mass (m):	$9.1093837139(28) \times 10^{-31}$ kg Navas et al. [2024] $5.485799090441(97) \times 10^{-4}$ Da $[1822.888486209(53)]^{-1}$ Da
Mean lifetime:	$0.51099895069(16)$ MeV/ c^2 Navas et al. [2024]
Electric charge:	$> 6.6 \times 10^{28}$ years Agostini [2015] (stable)
Magnetic moment:	$-1 e$ Navas et al. [2024] $-1.602176634 \times 10^{-19}$ C Navas et al. [2024]
Spin:	$-9.2847646917(29) \times 10^{-24}$ J/T Navas et al. [2024]
Weak isospin:	$-1.00115965218128(18) \mu_B$ Navas et al. [2024]
Weak hypercharge:	$\frac{1}{2} \hbar$ Navas et al. [2024] LH: $-\frac{1}{2}$, RH: 0 Navas et al. [2024] LH: -1, RH: -2 Navas et al. [2024]

The **electron** e^- is a subatomic particle with a negative one elementary electric charge e . Electrons belong to the first generation of the lepton particle family, and are generally thought to be elementary particles because they have no known components or substructure Eichten et al. [1983]. The electron's mass, m , is approximately $\frac{1}{1836}$ that of the proton. Quantum mechanical properties of the electron include an intrinsic angular momentum (spin) of a half-integer value, expressed in units of the reduced Planck constant, \hbar . Being fermions, no two electrons can occupy the same quantum state, per the Pauli exclusion principle. Like all elementary particles, electrons

exhibit properties of both particles and waves: They can collide with other particles and can be diffracted like light. The wave properties of electrons are easier to observe with experiments than those of other particles like neutrons and protons because electrons have a lower mass and hence a longer de Broglie wavelength for a given energy. In Chapter 2 we will present the proof of the Pauli exclusion principle by first principles. We will introduce an elementary particle as a vector of a unitary irreducible representation of the group of the symmetries in our universe and prove the spin-statistics theorem which states that, as a consequence of Lorentz invariance and of locality, half integer spin particles must obey to Fermi statistics and integer spin particles must obey to Bose statistics.

Electrons play an essential role in numerous physical phenomena, such as electricity, magnetism, chemistry, and thermal conductivity; they also participate in gravitational, electromagnetic, and weak interactions. Since an electron has charge, it has a surrounding electric field; if that electron is moving relative to an observer, the observer will observe it to generate a magnetic field. Electromagnetic fields produced from other sources will affect the motion of an electron according to the Lorentz force law. Electrons radiate or absorb energy in the form of photons when they are accelerated [Pauli \[1973\]](#).

Laboratory instruments are capable of trapping individual electrons as well as electron plasma by the use of electromagnetic fields. Special telescopes can detect electron plasma in outer space. Electrons are involved in many applications, such as tribology or frictional charging, electrolysis, electrochemistry, battery technologies, electronics, welding, cathode-ray tubes, photoelectricity, photovoltaic solar panels, electron microscopes, radiation therapy, lasers, gaseous ionization detectors, and particle accelerators.

Interactions involving electrons with other subatomic particles are of interest in fields such as chemistry and nuclear physics. The Coulomb force interaction between the positive protons within atomic nuclei and the negative electrons without allows the composition of the two known as atoms. Ionization or differences in the proportions of negative electrons versus positive nuclei changes the binding energy of an atomic system. The exchange or sharing of the electrons between two or more atoms is the main cause of chemical bonding [Pauling \[1960\]](#). This will be briefly presented in Chapter 5.

Electrons participate in nuclear reactions, such as nucleosynthesis in stars, where they are known as β^- particles. Electrons can be created through beta decay of radioactive isotopes and in high-energy collisions, for instance, when cosmic rays enter the atmosphere. The antiparticle of the electron is called the positron; it is identical to the electron, except that it carries electrical charge of the opposite sign (See for example Section 2.6). When an electron collides with a positron, both particles can be annihilated, producing gamma ray photons.

The ancient Greeks noticed that amber attracted small objects when rubbed with fur. Along with lightning, this phenomenon is one of humanity's earliest recorded experiences with electricity. In his 1600 treatise *De Magnete*, the English scientist William Gilbert coined the Neo-Latin term *electrica*, to refer to those substances with property similar to that of amber which attract small objects after being rubbed. Both electric and electricity are derived from the Latin *electrum* (also the root of the alloy of the same name), which came from the Greek word for amber, *ηλεκτρον* (*élektron*).

In 1838, British natural philosopher Richard Laming first hypothesized the concept of an indivisible quantity of electric charge to explain the chemical properties of atoms [Farrar \[1969\]](#). Irish physicist George Johnstone Stoney named this charge “electron” in 1891, and J. J. Thomson and his team of British physicists (John S. Townsend and H. A. Wilson) identified it as a particle in 1897 during the cathode-ray tube experiment [Thomson \[1897\]](#). J. J. Thomson would subsequently in 1899 give estimates for the electron charge and mass as well: $e \sim 6.8 \times 10^{-10}$ esu and $m \sim 3 \times 10^{-26}$ g.

1. INTRODUCTION

The electron’s charge was more carefully measured by the American physicists Robert Millikan [\[1910\]](#) and Harvey Fletcher in their oil-drop experiment of 1909, the results of which were published in 1911. This experiment used an electric field to prevent a charged droplet of oil from falling as a result of gravity. This device could measure the electric charge from as few as 1-150 ions with an error margin of less than 0.3%. Comparable experiments had been done earlier by Abram Ioffe, who independently obtained the same result as Millikan using charged microparticles of metals, then published his results in 1913. However, oil drops were more stable than water drops because of their slower evaporation rate, and thus more suited to precise experimentation over longer periods of time. The experiment of Millikan took place in the Ryerson Physical Laboratory at the University of Chicago. Millikan received the Nobel Prize in Physics in 1923.

In particle physics, the electroweak interaction or electroweak force is the unified description of two of the fundamental interactions of nature: electromagnetism (electromagnetic interaction) and the weak interaction. Although these two forces appear very different at everyday low energies, the theory models them as two different aspects of the same force. Above the unification energy, on the order of 246 GeV,¹ they would merge into a single force. Thus, if the temperature is high enough — approximately 1015 K — then the electromagnetic force and weak force merge into a combined electroweak force [Glashow \[1959\]](#); [Salam and Ward \[1959\]](#); [Weinberg \[1967\]](#). In this standard model of electroweak interaction one initially supposes massless leptons. In 1964 Peter Higgs proposed the *Higgs mechanism* [Higgs \[1964\]](#). The Higgs field is a scalar field with two neutral and two electrically charged components that form a complex doublet of the weak isospin SU(2) symmetry. Its “Sombrero potential” leads it to take a nonzero value everywhere (including otherwise empty space), which breaks the weak isospin symmetry of the electroweak interaction and, via the Higgs mechanism, gives a rest mass to leptons, among which figures the electron, and the W^\pm , Z^0 gauge bosons through a rotation by the Winberg angle. After a 40-year search, a subatomic particle with the expected properties was discovered in 2012 by the ATLAS and CMS experiments at the Large Hadron Collider (LHC) at CERN near Geneva, Switzerland. Even if these scalar particles are plagued by triviality issues from a rigorous mathematical point of view [Fantoni and Klauder \[2021a\]](#); [Fantoni \[2021\]](#); [Fantoni and Klauder \[2021b,c, 2022a,b,c,d\]](#); [Klauder and Fantoni \[2023\]](#); [Fantoni \[2023, 2024\]](#).

Fermions with negative chirality² (also called “left-handed” fermions) have a weak isospin $T = \frac{1}{2}$ and can be grouped into doublets with $T_3 = \pm\frac{1}{2}$ that behave the same way under the weak interaction. By convention, electrically charged fermions are assigned T_3 with the same sign as their electric charge. In all cases, the corresponding anti-fermion has reversed chirality (“right-handed” antifermion) and reversed sign T_3 . Fermions with $T = T_3 = 0$ form singlets that do not undergo charged weak interactions. Particles with $T_3 = 0$ do not interact with W^\pm gauge bosons; however, they do all interact with the Z^0 gauge boson. The weak isospin conservation law relates to the conservation of T_3 ; weak interactions conserve T_3 . It is also conserved by the electromagnetic and strong interactions. However, interaction with the Higgs field does not conserve T_3 , as directly seen in propagating fermions, which mix their helicities by the mass terms that result from their Higgs couplings. Since the Higgs field vacuum expectation value is nonzero, particles interact with this field all the time, even in vacuum. Interaction with the Higgs field changes particles’ weak isospin. Only a specific combination of electric charge is conserved. The electric charge, $Q = T_3 + \frac{1}{2}Y_W$, where Y_W is the weak hypercharge. In 1961 Sheldon Glashow proposed this relation by analogy to the Gell-Mann-Nishijima formula for charge to isospin

¹The particular number 246 GeV is taken to be the vacuum expectation value $v = (G_F \sqrt{2})^{-1/2}$ of the Higgs field (where G_F is the Fermi coupling constant).

²The chirality and intrinsic helicity are two characteristic properties of massive and massless particles respectively. This will be used in Section 2.5.1.

Glashow [1961].

Have you ever asked yourselves how can we be certain that the Sun is a giant nuclear candle? If Galileo Galilei was here he would ask: “where are the proofs?” The proofs can be found in the Gran Sasso Laboratory where we measure the flux of solar neutrinos. Every second, on every centimeter square of the Earth, arrive something like sixty billions neutrinos. Night and Day. In fact, Earth is transparent to these mysterious particles that goes through anything without ever stopping. If our eyes could see the neutrinos, the night would not exist! And what do these neutrinos tell us? Performing the exact calculations, we discover that their flux corresponds exactly to that predicted for a perfectly regulated nuclear candle. But who controls this “fire”? The answer lies in the extraordinary discovery of Fermi first and Salam, Weinberg, and Glashow later: The weak charge, that Enrico Fermi identified as a new force of Nature. This is the “security valve” which allows the production of the Sun “fuel”: the neutrinos. Even if the Sun is made almost exclusively by protons and electrons, the Fermi force allows the necessary transformation for fusion to happen. Without this perfect regulation, the Sun would not be our “neverending” source of light and life.

We live in an electrically neutral environment; everything around us is electrically neutral; but our lives are moved by electrical unbalances, like the synapses in the neurons in our brain, or the nervous terminations moving our muscles. Already Luigi Galvani (Bologna, 9 September 1737 - Bologna, 4 December 1798) discovered biological electricity (with his theory on the electrical fluid in frogs) and some of its applications like the electrochemical cell, the galvanometer, or the galvanization. Alessandro Volta (Como, 18 February 1745 - Como, 5 March 1827) in the same period invented the first electrical generator, the “pila” in 1799. Our heart, our respiration, the chlorophyll photosynthesis³ of our sisters the plants, the biological rhythms are ruled by electrical unbalances. These are local unbalances since a global unbalance would result in a thermodynamic instability. After all the simplest mathematical model of an electron gas requires a uniform neutralizing background of positive charge which confines harmonically the electrons which would otherwise run away to infinity. This is commonly called a **One Component Plasma** in the non-quantum limit and will be studied in Chapter 6 or **Jellium** in the fully quantum regime and will be discussed in Chapter 7.

If we introduce a charge in an electron gas if the charge is negative it will create a hole around itself and it will soon be screened by the other charges far around it and neutrality is restored. If we introduce two like negative charges in an electron gas when they are close together the other charges will be unable to screen simultaneously both external charges so that in the two holes created around them there will be a region between them with a net positive charge (the one of the background) with a net resulting attraction between the two like negative charges.

If the external charge is positive it will also be screened far away but it may undergo *clustering* with the other charges. We will then have atom or molecule formation.

The **atom** of Democrito (Abdera, between 470 and 457 b.C. - between 360 and 350 b.C.) is itself neutral. It is the main actor in chemistry. It hasn't been easy to reach its modern mathematical model. First John Dalton (Eaglesfield, 5 or 6 September 1766 - Manchester, 27 July 1844) in 1803 described an atom as a heavy central particle surrounded by an atmosphere of caloric, the supposed substance of heat at the time. The size of the atom was determined by the diameter of the caloric atmosphere. He provided a method of calculating relative atomic weights for the chemical elements, which provides the means for the assignment of molecular formulas for all chemical substances. Later Sir Joseph John Thomson (Manchester, 18 December 1856 - Cambridge, 30 August 1940) believed that the corpuscles, the “electrons”, emerged from the atoms of the trace gas inside his cathode-ray tubes. He thus concluded that atoms were

³Certainly related to the photoelectric effect discovered by Albert Einstein (Ulma, 14 March 1879 – Princeton, 18 April 1955).

1. INTRODUCTION

divisible, and that the corpuscles were their building blocks. In 1904, he suggested a model of the atom, hypothesizing that it was a sphere of positive matter within which electrostatic forces determined the positioning of the corpuscles. To explain the overall neutral charge of the atom, he proposed that the corpuscles were distributed in a uniform sea of positive charge. In this “plum pudding model”, the electrons were seen as embedded in the positive charge like raisins in a plum pudding (although in Thomson’s model they were not stationary, but orbiting rapidly). Later Ernest Rutherford, 1st Baron Rutherford of Nelson (Brightwater, 30 August 1871 - Cambridge, 19 October 1937) in 1911 performed the Geiger–Marsden experiment, which demonstrated the nuclear nature of atoms by measuring the deflection of alpha particles passing through a thin gold foil. He was inspired to ask Geiger and Marsden in this experiment to look for alpha particles with very high deflection angles, which was not expected according to any theory of matter at that time. Such deflection angles, although rare, were found. Reflecting on these results in one of his last lectures, Rutherford was quoted as saying: “It was quite the most incredible event that has ever happened to me in my life. It was almost as incredible as if you fired a 15-inch shell at a piece of tissue paper and it came back and hit you.” It was Rutherford’s interpretation of this data that led him to propose the “nucleus”, a very small, charged region containing much of the atom’s mass. In 1912, Rutherford was joined by Niels Henrik David Bohr (Copenhagen, 7 October 1885 - Copenhagen, 18 November 1962) who postulated that electrons moved in specific orbits about the compact nucleus. Bohr adapted Rutherford’s nuclear structure to be consistent with Max Planck’s quantum hypothesis. The resulting Rutherford–Bohr model was the basis for quantum mechanical atomic physics of Heisenberg which remains valid today. In Chapter 4 we present the properties of the periodic system of the elements as can be predicted by quantum physics. And in Chapter 5 we present the relevance of the electron in a **chemical bond** between elements.

Stripping one or more electrons from an atom one gets an “**ion**” which is therefore positively charged. If we introduce an electron in a crystal of positive ions we call it a **polaron** which will be presented in Chapter 3. Condensed matter can be seen as composed of three subsystems: i. The lattice (elastic) made of nuclear coordinates and phonons; ii. the electrons with their Fermi surface or superconducting condensate; iii. the electromagnetic field with their photons or polaritons. When there is no (bulk) Fermi surface the electrons subsystem is incompressible with no autonomous low-energy degrees of freedom. The electrons are completely owned by the lattice and the density of the electrons is completely fixed by the local volume of the Brillouin zone and can only fluctuate in the presence of longitudinal phonons, so one has a band insulator. This is opposed to what happens for a polaron that is free to wander through the lattice or, for example, to the quantum Hall state [v. Klitzing et al. \[1980\]](#) where some of the electrons on the lattice plane are “captured” (by Landau quantization) by the magnetic flux (see also Chapter 6) and can flow with the electromagnetic drift velocity.

Charles-Augustin de Coulomb (Angoulême, 14 June 1736 - Paris, 23 August 1806) discovered the mathematical law of interaction between two charges of electrical charge q_1 and q_2 separated by a distance r . **Coulomb force** (in Gauss units)

$$\vec{F}_{12} = r \frac{q_1 q_2}{r^3}, \quad (1.0.1)$$

gives rise to an **electric field** around charge one $\vec{E}(r) = \vec{F}_{12}/q_2$. The electric field is generated by an electric potential $\vec{E}(r) = -\vec{\nabla}\varphi(r)$ with $\varphi(r) = q/r$, the Coulomb potential. The Coulomb potential satisfies to the equation of Baron Simón Denis Poisson (Pithiviers, 21 June 1781 - Paris,

25 April 1840) ⁴

$$\vec{\nabla}^2 \varphi(r) = -4\pi q \delta^3(r), \quad (1.0.4)$$

where δ^3 is a Dirac delta function in 3 dimensions. Poisson equation is the equation of Pierre-Simon, Marquis de Laplace (Beaumont-en-Auge, 23 March 1749 - Paris, 5 March 1827) with a source term due to the charge q . Later Johann Carl Friedrich Gauss (Braunschweig, 30 April 1777 - Gottinga, 23 February 1855) discovered that

$$4\pi q = - \int_{\Omega} \vec{\nabla}^2 \varphi(r) dr = - \int_{\partial\Omega} \mathbf{n} \cdot \vec{\nabla} \varphi(r) dS = \int_{\partial\Omega} \mathbf{n} \cdot \vec{E}(r) dS = \Phi_E, \quad (1.0.5)$$

which states the important mathematical result that the flux Φ_E of the electric field through any closed surface containing charge q is fixed. In Eq. (1.0.5) dr is the infinitesimal volume integral, dS is the infinitesimal surface element with \mathbf{n} its outward normal versor, Ω is the volume region considered in the volume integral, and $\partial\Omega$ is its bounding surface.

The representation of the electron as a pointwise particle poses the problem of an infinite self-energy diverging as $1/r$. On the other side the electrostatic energy for assembling a system on N point charges of charge q_i is that required to bring them close together from infinity

$$E = \frac{1}{2} \sum_{i \neq j=1}^N \frac{q_i q_j}{|\mathbf{r}_i - \mathbf{r}_j|}, \quad (1.0.6)$$

But again a divergence problem arises as soon as one introduces a charge density $\rho(\mathbf{r})$ to rewrite this energy with a continuous expression

$$E = \frac{1}{2} \int d\mathbf{r} \int d\mathbf{r}' \frac{\rho(\mathbf{r})\rho(\mathbf{r}')}{|\mathbf{r} - \mathbf{r}'|}, \quad (1.0.7)$$

where one readily recognize a divergence for a linear, planar, or spatial charge density. Also in these cases is necessary to deal with infinities.

An electron moving in an electric field $\vec{E} = -\vec{\nabla}\varphi$ and a magnetic field $\vec{B} = \vec{\nabla} \times \vec{A}$, where \vec{A} is the vector potential, is subject to the Lorentz force which in Gaussian units reads $\vec{F} = q(\vec{E} + \frac{\vec{v}}{c} \times \vec{B})$ where $q = -e$ is the electron charge, \vec{v} is the speed of the electron, and c is the speed of light. In order to reach to this result from the Hamilton equations of motion it is necessary to start with a classical Hamiltonian $H = \frac{1}{2m} (\vec{p} - \frac{q}{c} \vec{A})^2 + q\varphi$. This amounts to the following transformation recipe $\vec{p} \rightarrow \vec{p} - \frac{q}{c} \vec{A}$. If we start from a quantum Hamiltonian $\hat{H} = \frac{1}{2m} \hat{p}^2 = \frac{1}{2m} (\hat{\sigma} \cdot \hat{p})(\hat{\sigma} \cdot \hat{p})$, where $\hat{\sigma} = (\sigma_1, \sigma_2, \sigma_3)$ and σ_i are the Pauli matrices described in

⁴For charges living in n -dimensions we have

$$\varphi(r) = q \begin{cases} 1/r & n = 3 \\ -\ln(r/\ell) & n = 2 \\ -r & n = 1 \end{cases}, \quad (1.0.2)$$

where ℓ is a length. And the Poisson equation becomes

$$\vec{\nabla}^2 \varphi(r) = -q \delta^n(r) \begin{cases} 4\pi & n = 3 \\ 2\pi & n = 2 \\ 2 & n = 1 \end{cases}, \quad (1.0.3)$$

where δ^n is a Dirac delta function in n dimensions.

1. INTRODUCTION

Appendix 2.D such that $(\hat{\sigma} \cdot \hat{A})(\hat{\sigma} \cdot \hat{B}) = \hat{A} \cdot \hat{B} + i\hat{\sigma} \cdot (\hat{A} \times \hat{B})$ for any two operators \hat{A} and \hat{B} . After applying the transformation recipe required by classical electrodynamics we find

$$\hat{H} = \frac{1}{2m} \left(\hat{p} - \frac{q}{c} \vec{A} \right)^2 - \frac{q\hbar}{2mc} \hat{\sigma} \cdot \vec{B} + q\varphi, \quad (1.0.8)$$

where we have used $\hat{p} \times \vec{A} = -i\hbar(\vec{\nabla} \times \vec{A}) - \vec{A} \times \hat{p}$. The spin magnetic moment turns out to have a g-factor $g = 2$. This derivation from the nonrelativistic Schrödinger-Pauli theory is due to R. P. Feynman and is alternative to the one obtained by P. A. M. Dirac from the nonrelativistic limit of his equation. More generally a particle of spin s has an “intrinsic” magnetic moment μ . The corresponding quantum mechanical operator is proportional to the spin operator \hat{s} (for example $\hat{s} = \hat{\sigma}\hbar/2$ for particles of spin $s = 1/2$) and can therefore be written as $\hat{\mu} = \mu\hat{s}/s$. This contributes a term $-\hat{\mu} \cdot \vec{B}$ to the Hamiltonian. The intrinsic magnetic moment of the electron is consequently $-\mu_B$ where $\mu_B = e\hbar/2mc \approx 0.927 \times 10^{-20}$ erg/gauss. This quantity is called the *Bohr magneton*. A charged, spin $s = 1/2$, particle that does not possess any internal structure has a spin magnetic moment $\hat{\mu} = gq\hat{s}/2mc$. The full relativistic quantum electrodynamics (QED) theory predicts a correction to the spin magnetic moment that is called *anomalous magnetic moment* and denoted with $a = (g - 2)/2$. For the electron, the correction of first order in the fine-structure constant $\alpha = e^2/\hbar c$ is $a_e = \alpha/2\pi \approx 0.001\,161\,4$. This result was first found by Julian Schwinger in 1948 [Schwinger \[1948\]](#) and is engraved on his tombstone. As of 2016, the coefficients of the QED formula for the anomalous magnetic moment of the electron are known analytically up to α^3 and have been calculated up to order α^5 $a_e = 0.001\,159\,652\,181\,643(764)$. The QED prediction agrees with the experimentally measured value to more than 10 significant figures, making the magnetic moment of the electron one of the most accurately verified predictions in the history of physics. The current experimental value and uncertainty is: $a_e = 0.001\,159\,652\,180\,59(13)$. This required measuring g to an accuracy of around 1 part in 10 trillion.

Particularly interesting is an electron gas *living in* a surface. For this electrons the electric field lines cannot exit the “world” they live in, so for example on a flat surface they will interact with the logarithmic Coulomb pair potential of Eq. (1.0.2). This is different from electrons *moving on* a surface which will still interact with the $1/r$ Coulomb potential since for them the electric field lines can exit the two dimensional world [Abbott \[1884\]](#). Recently it became interesting to study an electron gas on a *curved* surface since the discovery of *graphene* which was isolated and characterized in 2004 by Andre Geim and Konstantin Novoselov at the University of Manchester [Novoselov et al. \[2004\]](#) using a piece of graphite and adhesive tape. In 2010, Geim and Novoselov were awarded the Nobel Prize in Physics for their “groundbreaking experiments regarding the two-dimensional material graphene”. Actually the two dimensional electron gas has an ancient history since it turned out to be one of the few non-one-dimensional non-quantum many body systems that admit an exact analytic solution for the statistical mechanics partition function at least at one special value of the coupling constant [Jancovici \[1981\]](#). This will be discussed in detail in Chapter 6. This early solution turned out to be an essential ingredient to determine a very efficient trial wave function for the ground state of the Landau problem of the fully quantum electron gas on a plane immersed in a strong magnetic field orthogonal to the plane [Laughlin \[1983\]](#). It becomes important in guessing a good functional form for the Jastrow factor of the trial wave function in a variational calculation. Moreover the two dimensional space has many nice features related to *conformal* geometry and more generally the theory of *holomorphic* functions and their conformal transformation, i.e. a holomorphic transformation of the complex plane that conserves the *harmonicity* properties of the real and imaginary parts of a holomorphic function (remember that the real and imaginary parts of any holomorphic function are independently solutions of the Laplace equation, i.e. they are harmonic functions). Last but not least the phase transition properties of the two dimensional electron gas is characterized by the unique

feature of the Kosterlitz-Thouless phenomenon [Kosterlitz and Thouless \[1973\]](#) of collapse of oppositely charged particles in a two component two dimensional plasma which is responsible for the transition between a high temperature conductive phase and a low temperature dielectric phase. The Kosterlitz-Thouless transition is not against the theorem that long-range order cannot exist in two dimensions at finite temperatures. Instead, it provides an explanation for how a system can exhibit a phase transition in two dimensions without establishing long-range order. The Kosterlitz-Thouless transition, which occurs in certain two-dimensional systems, is a phase transition that leads to a quasi-long-range ordered state. This means that the correlation between particles decays with a power-law rather than exponentially, as would be expected in a long-range ordered state [Martin \[1988\]](#), i.e. a state without exponential clustering among the particles.⁵ The theorem that states that long-range order cannot exist in two dimensions at finite temperatures is related to the concepts of spontaneous symmetry breaking and the Mermin-Wagner theorem. These theorems generally hold true for systems with short-range interactions and continuous symmetries. However, the Kosterlitz-Thouless transition demonstrates that a phase transition can occur even in the absence of long-range order, as the system transitions into a state with power-law correlations, a form of quasi-long-range order. So, in summary, the Kosterlitz-Thouless transition is not a contradiction to the theorem about long-range order in two dimensions but rather a specific example of a phase transition that occurs even when long-range order is not established. It highlights the importance of considering the nature of correlations, as the system transitions into a quasi-long-range ordered state with power-law decay.

From the first discoveries of electrostatics soon enough James Clerk Maxwell (Edinburgh, 13 June 1831 – Cambridge, 5 November 1879) wrote his equations for electrodynamics. The most synthetic way to write these important equations describing electromagnetism is through the geometric language of the differential forms (here we use Gauss units and set additionally the speed of light $c = 1$)

$$d \mathbf{F} = 0, \quad (1.0.9)$$

$$d \star \mathbf{F} = 4\pi \star \mathbf{J}. \quad (1.0.10)$$

Here d stands for an exterior derivative [Misner et al. \[1970\]](#), \star is the Hodge star that stands for the dual, $\mathbf{F} = dA$ is the **Faraday** two form that subtend the electromagnetic asymmetric tensor $F_{\mu\nu}$ containing the electric and magnetic fields, $A = (\varphi, \vec{A})$ is the electromagnetic 4-potential one form where φ is the electric scalar potential for the electric field $\vec{E} = -\vec{\nabla}\varphi - \partial\vec{A}/\partial t$ and \vec{A} the magnetic vector potential for the magnetic field $\vec{B} = \vec{\nabla} \times \vec{A}$, $\star F$ is **Maxwell** two form dual to Faraday, and $\star J$ is the **charge** three form with $J = (\rho, \vec{J})$ the 4-current density one form with ρ the electric charge density and \vec{J} the electric current density. So that the total charge Q inside a three dimensional hypersurface region S is $Q = \int_S \star J$. Also from $dd \star F = 0$ follows $d \star J = 0$ which is the law of conservation of charge. Eq. (1.0.9) summarizes Faraday's law and the non-existence of magnetic monopoles and it is a consequence of the general result that $dd = 0$. Eq. (1.0.10) summarizes Ampere's law with Maxwell's correction to take into account of the displacement current and Gauss's law.

The Maxwell equations are invariant under the gauge transformation $\vec{A} \rightarrow \vec{A} + \vec{\nabla}\psi$ and $\varphi \rightarrow \varphi - \partial\psi/\partial t$ with the gauge function $\psi(t, r)$ any scalar. Which means that electromagnetism has $U(1)$ gauge freedom.

Now, start with the scalar φ . Its gradient $d\varphi$ is a one form. Take its dual to get the three form $\star d\varphi$. Take its exterior derivative to get the four form $d \star d\varphi$. Take its dual, to get the

⁵It should be mentioned that among all possible long range potentials, it is only in the Coulomb case (of Eq. (1.0.2)) that a decay law of correlations faster than any inverse power is compatible with the structure of equilibrium equations of statistical mechanics, like the Born-Green-Yvon hierarchy [Alastuey and Martin \[1985\]](#); [Lighthill \[1959\]](#).

1. INTRODUCTION

scalar $\star d \star d\varphi = \square \varphi = -(\partial^2 \varphi / \partial t^2) + \vec{\nabla}^2 \varphi$. This is the Jean-Baptiste le Rond d'Alembert (16 November 1717 - 29 October 1783) wave operator.

Start with the one form A . Get the two form dA . Take its dual to get the two form $\star dA$. Take its exterior derivative to get the three form $d \star dA$. Take its dual, to get the one form $4\pi J = \star d \star dA$. This is the wave equation for the electromagnetic 4-potential. And from here follow the electromagnetic waves. For example for the zero component in vacuum in absence of charges one finds $\square \varphi = 0$ whose solution with forward and backward propagation along the direction k is of the form $\varphi(t, r) = f(k \cdot r - \omega t) + g(k \cdot r + \omega t)$, where $\omega = 2\pi/T$ is the angular frequency of the wave of period T , $k = 2\pi/\lambda$ is the wave vector for a wavelength λ , the speed of the wave is $\omega/k = \lambda/T = 1$, and f, g are arbitrary functions. Alternatively one may think of a spherical wave solution of the following kind, $\varphi_{s.w.}(t, r) \propto \exp[i(\pm kr - \omega t)]/r$.

In flat spacetime, express the coordinates of one electron as a function of his proper time as $a^\mu(\tau)$. The density-current 4-vector for this electron is then

$$J^\mu(x) = e \int \delta^4[x - a(\tau)] \dot{a}^\mu d\tau, \quad (1.0.11)$$

where $x \equiv (t, \mathbf{r})$ and as usual we denote with the dot a partial time derivative. This density-current drives the electromagnetic field, \mathbf{F} . Then Maxwell equation (1.0.10) becomes $F_{\mu,\nu}^\nu = 4\pi J_\mu$ where as usual the comma stands for a partial derivative. Or $A_{\nu,\nu\mu}^\nu - \eta^{\nu\alpha} A_{\mu,\alpha\nu} = 4\pi J_\mu$ where $\eta_{\mu\nu}$ is the metric of the Lorentz coordinate system of the flat spacetime. Make use of the gauge freedom to set Lorentz gauge, $A_{\nu,\nu} = 0$, to get

$$\square A_\mu = -4\pi J_\mu. \quad (1.0.12)$$

This can be solved through the Green's function method rewriting $A^\mu(x) = e \int G[x - a(\tau)] \dot{a}^\mu d\tau$ with the Green's function satisfying the following wave equation

$$\square G = -4\pi \delta^4(x). \quad (1.0.13)$$

The causal solution of this equation is given in terms of the retarded potential

$$A_\mu(t, \mathbf{r}) = \int \frac{J_\mu(t_{\text{retarded}}, \mathbf{r}')}{|\mathbf{r} - \mathbf{r}'|} d\mathbf{r}', \quad (1.0.14)$$

$$t_{\text{retarded}} = t - |\mathbf{r} - \mathbf{r}'|, \quad (1.0.15)$$

where remember that we chose the speed of light $c = 1$.

With reference to Fig. 1.1 we briefly discuss the radiation electromagnetic field of a current system Pauli [1973] consisting of a single pointwise electron $\vec{J} = \rho \vec{v}$ with $\vec{I} = \int \vec{J} d\mathbf{r} = e \vec{v}$, where \vec{v} is the electron velocity. The radiation zone is characterized by the points P shown in the figure such that $R \gg d$ and $R \gg \lambda$ with λ the wavelength of the radiation. Nothing at all is presupposed about the ratio d/λ . If a point O within the current system is chosen as the origin of coordinates as is shown in the figure, then $r_{PQ} \approx R - \mathbf{n} \cdot \mathbf{r}_Q$ where $\overline{OP} = R$, \mathbf{r}_Q is the position vector of a source point Q , and \mathbf{n} is a versor in the P direction. Considering the spherical wave solution to Eq. (1.0.12) we can replace r_{PQ} with R in the denominator but not in the exponent, so that

$$(A_\mu)_P = \frac{e^{i(kR - \omega t)}}{R} \int d\mathbf{r}_Q (J_\mu)_Q e^{-ik(\mathbf{n} \cdot \mathbf{r}_Q)}. \quad (1.0.16)$$

In the transition to the fields intensities $\mathbf{F} = dA$ we note that $\partial R / \partial \mathbf{r}_P = \mathbf{n}$. Moreover we note that

$$\frac{\partial}{\partial \mathbf{r}_P} \frac{e^{i k R}}{R} = e^{i k R} \frac{\partial}{\partial \mathbf{r}_P} \frac{1}{R} + \frac{1}{R} \frac{\partial}{\partial \mathbf{r}_P} e^{i k R}, \quad (1.0.17)$$

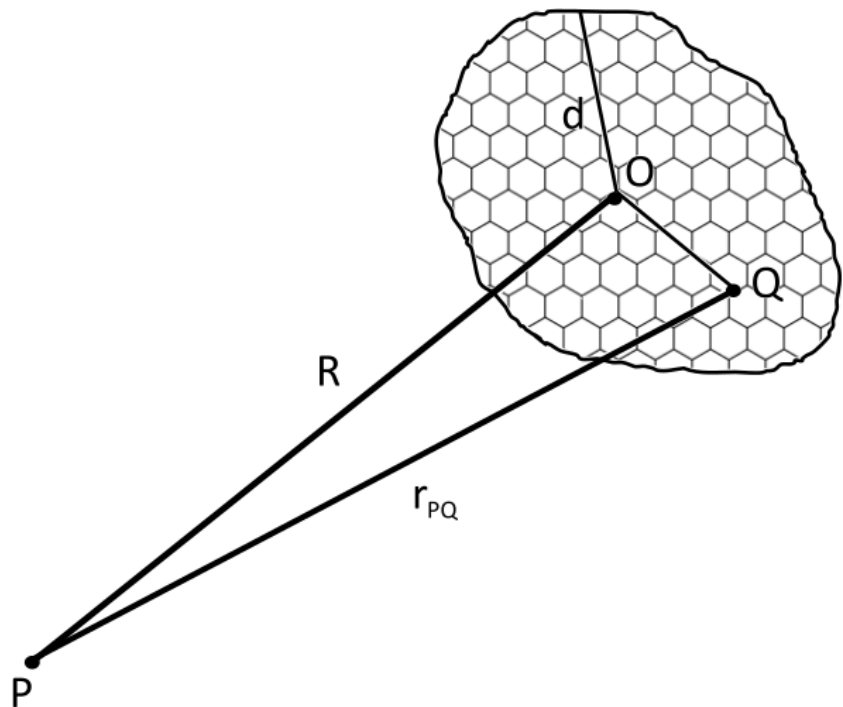


Figure 1.1: Radiation zone of a current system. The shaded area is where are the currents. The origin of the coordinate system O is chosen inside this region. Q is any point of the currents. P is where we measure the electromagnetic field radiated out. d is the linear extension of the current system.

1. INTRODUCTION

but since the gradient in the first term gives rise to an additional factor $1/R$ and the one in the second term gives rise to a multiplication by k we can neglect the first term altogether in the radiation zone where $kR \gg 1$. So $\vec{B} = \vec{\nabla}_P \times \vec{A} \approx ik\mathbf{n} \times \vec{A}$, $\vec{\nabla}_P \cdot \vec{A} \approx ik\mathbf{n} \cdot \vec{A}$, and thanks to the Lorentz gauge condition $\varphi \approx \mathbf{n} \cdot \vec{A}$. So $\vec{E} \approx ik[\vec{A} - \mathbf{n}(\mathbf{n} \cdot \vec{A})] = ik\vec{A}_{\perp}$.

If we now also require that $\lambda \gg d$ (or $kd \ll 1$), a condition frequently satisfied for antennas, the exponential function $e^{-ik(\mathbf{n} \cdot \mathbf{r}_Q)}$ can be expanded in a power series. This correspond to a decomposition of the radiation into multipoles. In the first approximation one sets $e^{-ik(\mathbf{n} \cdot \mathbf{r}_Q)} \approx 1$ so that we do not have to worry about retardation due to the position of the emitter within the current system. The Poynting vector in this dipole radiation approximation is then given by

$$\vec{S} = \frac{\vec{E} \times \vec{B}}{4\pi} = \frac{E^2}{4\pi} \mathbf{n}, \quad (1.0.18)$$

$$\vec{E} = ik \frac{e^{i(kR-\omega t)}}{R} \vec{I}_{\perp}, \quad (1.0.19)$$

where for the case of a linear oscillation parallel to the z axis $I_{\perp} = I \sin \theta$. The energy radiated per second is obtained by integrating the Poynting vector over the surface of a sphere containing the oscillating electron

$$\int \vec{S} \cdot \mathbf{n} dS = \frac{2}{3} \left(\frac{d\vec{I}}{dt} \right)_{\text{retarded}}^2, \quad (1.0.20)$$

where $dS = R^2 d\Omega$ and Ω the solid angle and we used the fact that $\omega/k = 1$ to reconstruct the time derivative.

Nikola Tesla (Smiljan, 10 July 1856 - New York, 7 January 1943) invented machines to transmit electricity without wires through alternating currents, electromagnetic induction generated by a varying in time magnetic field according to Eq. (1.0.9), and Maxwell displacement current generated by a varying in time electric field according to Eq. (1.0.10).

Very similar to the wave equation of d'Alembert is the Erwin Rudolf Josef Alexander Schrödinger (Vienna, 12 August 1887 - Vienna, 4 January 1961) equation for the wavefunction φ of a free particle of mass $m = 1/2$. This reads $i\hbar(\partial\varphi/\partial t) + \hbar^2 \vec{\nabla}^2 \varphi = 0$. The only difference with the d'Alembert equation is that it is of order one in time. And from here follows the wave-particle duality of quantum mechanics. For example for an eigenstate of eigenenergy E one may find a plane wave propagating along the direction of versor \mathbf{n} given by $\varphi_{p.w.}(t, \mathbf{r}) \propto \exp[(\pm i\sqrt{E}\mathbf{n} \cdot \mathbf{r} - iEt)/\hbar]$ or otherwise a spherical wave [Landau and Lifshitz \[1977\]](#) $\varphi_{s.w.}(t, \mathbf{r}) \propto \exp[(\pm i\sqrt{E}\mathbf{r} - iEt)/\hbar]/r$. The speed of this wave is \sqrt{E} .

One of the pillar thought experiments of quantum physics is the double slit experiment where a beam of electrons that impinges on a double slit may either produce an interference pattern on a screen posed behind the two slits as if the electron were waves or just a two bands pattern in correspondence of the two slits as if they were particles.

Clearly energy eigenstate of Schrödinger equation will have a well defined energy E and zero energy standard deviation ΔE . The eigenstate probability distribution, $|\varphi(t, \mathbf{r})|^2$, will be steady state carrying no information on the dynamics of the electrons. In other words if $\Delta E = 0$ then Heisenberg uncertainty principle, $\Delta E \Delta t \geq \hbar/2$ tells us that the time standard deviation must diverge. In this case the electrons will behave like waves and produce an interference patter in the two slit experiment.

Otherwise it is possible to create an electron “time wave-packet” by summing together several different energies eigenstates in a Fourier series in E so to have a finite non-zero standard deviation in energy. And as a consequence a finite standard deviation on time. This will allow to gather some dynamical information on the electrons beam.

But we can at the same time sum together several different momenta eigenstates in a Fourier series in p to create a “spacetime wave-packet” which according to the Heisenberg uncertainty principle $\Delta q \cdot \Delta p \geq 3\hbar/2$ will also have a finite position standard deviation. Here we denote with $q \equiv r$. This will allow the observer to predict the “classical” trajectory of the electron spacetime wave-packet. In this case, playing with the slit width and Δq we can observe the particle behavior of the electrons with the disappearance of the interference pattern in the two slit experiment.

Something similar can be done with the Coherent State (CS) of John Rider Klauder (Reading, January 24, 1932 – New York, October 24, 2024) [Klauder \[1963a,b, 1964\]](#); [McKenna and Klauder \[1964\]](#); [Klauder and McKenna \[1965\]](#)⁶

$$\varphi(q; Q, P) = \langle q | e^{-iQ\hat{p}/\hbar} e^{iP\hat{q}/\hbar} | 0 \rangle, \quad (1.0.21)$$

where \hat{q}, \hat{p} are the position and momentum operators in position representation respectively and $\varphi_0(q) = \langle q | 0 \rangle$ is a fiducial wavefunction such that $\langle 0 | \hat{q} | 0 \rangle = \langle 0 | \hat{p} | 0 \rangle = 0$. The time evolution of this wavefunction according to the quantum Hamiltonian $\hat{H}(\hat{q}, \hat{p})$ is then given by $\varphi(t, q; Q, P) = e^{-i\hat{H}t/\hbar} \varphi(q; Q, P) \approx \varphi(q; Q(t), P(t))$ where $Q(t)$ and $P(t)$ follow Hamilton’s equations of motion according to the corresponding classical Hamiltonian $H(Q, P)$, i.e. the one that has the functional form of the quantum mechanical Hamiltonian with explicit c-number substitution. Unfortunately this extremely useful time evolution property that holds exactly for the Harmonic Oscillator (HO) case,⁷ is lost for a more general potential energy $V(\hat{q})$ (see section 2B of Ref. [Klauder \[1963b\]](#)), for which it is in any case still possible to expand on a local minimum and approximate it there with a quadratic potential. If Klauder dynamical property would remain exact and valid for a generic potential it could be possible to perform a “quantum molecular dynamics” simulation on an electron liquid. We are thinking at a computer experiment that could be used to study the statistical properties of a many electrons system in thermodynamic equilibrium at a given temperature T . Unfortunately for the time being this has never been done and the only quantum simulation method available is the path integral Monte Carlo [Ceperley \[1995\]](#). Molecular dynamics being only available in the non-quantum regime.

The computer experiment with some of its most recent realization to study the Jellium will be presented in Chapter 7. Variational and diffusion Monte Carlo methods are able to study the ground state properties of Jellium. Path integral Monte Carlo methods are able to determine the finite non-zero temperature properties. The properties of interest are the structure, the pressure, the internal energy, and various other thermodynamic quantities, the superconducting fraction. Unfortunately the Monte Carlo method is exact only for boson (and boltzmann) fluids. For fermion fluids, the yet unsolved “sign problem” requires the formulation of some approximation in the numerical calculation. So that even computationally we are still unable to extract exact statistical mechanical properties for fermions. Another limitation of the path integral Monte Carlo is that, whereas it is able to describe the molecules formation from the constituent atomic species, it is unable to describe the atom formation from the constituent electrons and nuclei, unless for an highly diluted system. This is due to the fact that since the mass of an electron is three orders of magnitude smaller than the one of the nucleous the degeneracy temperature of the electons is three orders of magnitude bigger than the one of the nuclei, at a given density. Therefore it is very unlikely that an electron, with a world-line with many particle exchanges, will bind to a nucleous, which has a world-line with many less particle exchanges.

The computer experiment allows also to study the cumbersome problem of the fluid phases coexistence. Of interest here are the phase transitions of the electron gas. From a mathematical

⁶They were called ‘continuous representation’ by the inventor J. R. Klauder and later renamed CS by J. P. Gazeau who first used them.

⁷It holds exactly also for a general linear or quadratic Hamiltonian.

point of view a phase transition appears as a non analyticity of the thermodynamic quantities of a many body system in the thermodynamic limit. The most complete theory for phase transitions in statistical physics is the **Renormalization Group** which predicts universal behaviors for the liquid in a neighborhood of a phase transition being it Jellium or something else. This will be presented briefly in Chapter 9.

Of particular interest for our everyday life is the *solid state* Ashcroft and Mermin [1976]; Grosso and Parravicini [2013]; Martin et al. [2016]. We live in a world made of surfaces between different phases but the solid is all around us, the soil, the walls of our houses, our same selves. Electrons play a fundamental role in solids, in crystals, in glasses. First of all it is possible to make a distinction between solids that conduct electrons, the *metals*, and solids that do not, the *insulators*. This way to classify a solid on the base of its ability to conduct electrons has been refined and needed revision over the years as technological advances allowed the observation and later reproduction of some important emerging physical phenomena related to electrons conduction. Such as the discovery of *semiconductors* and *superconductors*. Probably the first physical theories of electron conduction are the the Drude Theory of Metals⁸ and the Sommerfeld Theory of Metals. Later theories dealt with the failure of the free electron model. Another way to classify a solid is through their crystal lattices characteristics in real and reciprocal space. As be determined by X-ray diffraction.

Electrons in a solid may be either tightly bound to the atoms forming the crystal or stripped from these atoms to form a gas around them. There are specific theories describing the electron energy levels in a periodic potential, the ones for the electrons in the gas, that form *bands*, and the ones for the bound electrons, that form *orbitals*, and their deformations. Usually the electrons in a solid should be described by a quantum theory, but the semiclassical limit may grasp already some general characteristic properties of their dynamics. Of course surface effect may play a role both as *finite size corrections* to the thermodynamic limit of the electron gas and for the chemical physics nature of the surface. Another important issue to take into account is the fact that since the mass of an electron is three orders of magnitude smaller than the one of the nucleus the degeneracy temperature of the electrons is three orders of magnitude bigger than the one of the nuclei, at a given density. Therefore it may be possible, to a first level of accuracy, to give a non-quantum description of the nuclei. In this respect a classical theory of a harmonic crystal may become a first meaningful approximation. Of course for a more faithful and complete description we should worry of a quantum theory of a harmonic crystal able to measure the *phonons* dispersion relations and other properties. Another important correction to this description would be to take care of anharmonic effects in crystals. Each of the four characteristic solids: insulators, semiconductors, metals, and superconductors, will have its own peculiarities in their theoretical descriptions.

In Chapter 8 we study the thermodynamic properties of a **white dwarf**, Shapiro and Teukolsky [1983] a star that has consumed all her nuclear energy ending in a plasma made of a core with iron nuclei and an halo made of an electron liquid that is cooling down, supporting itself against gravity by the pressure of the cold electrons. These are found in the lower-left corner of the Hertzsprung–Russell diagram below the main sequence that contains our sun.

References

E. A. Abbott. *Flatland: A Romance of Many Dimensions*. Seeley & Co., London, 1884.

⁸At room temperature the mean square velocities of the electrons in Drude theory are of the order of 10^5 m/s . The electrical current in a wire is instead quasi instantaneous because it is the result of a disturbance that propagates from one electron to another and is much faster than the drift velocity of electrons in the metal.

- M. Agostini. Test of electric charge conservation with Borexino. *Phys. Rev. Lett.*, 115:231802, 2015. doi: [10.1103/PhysRevLett.115.231802](https://doi.org/10.1103/PhysRevLett.115.231802).
- A. Alastuey and P. A. Martin. Decay of correlations in classical fluids with long-range forces. *J. Stat. Phys.*, 39:405, 1985. doi: [10.1007/BF01018670](https://doi.org/10.1007/BF01018670).
- N. W. Ashcroft and N. D. Mermin. *Solid State Physics*. Thomson Learning Inc, Australia, 1976.
- D. M. Ceperley. Path integrals in the theory of condensed helium. *Rev. Mod. Phys.*, 67:279, 1995. doi: [10.1103/RevModPhys.67.279](https://doi.org/10.1103/RevModPhys.67.279).
- E. J. Eichten, M. E. Peskin, and M. Peskin. New Tests for Quark and Lepton Substructure. *Phys. Rev. Lett.*, 50:811, 1983. doi: [10.1103/PhysRevLett.50.811](https://doi.org/10.1103/PhysRevLett.50.811).
- R. Fantoni. Monte Carlo evaluation of the continuum limit of $(\phi^4)_3$. *J. Stat. Mech.*, page 083102, 2021. doi: [10.1088/1742-5468/ac0f69](https://doi.org/10.1088/1742-5468/ac0f69).
- R. Fantoni. Scaled Affine Quantization of φ_3^{12} is Nontrivial. *Mod. Phys. Lett. A*, 38:2350167, 2023. doi: [10.1142/S0217732323501675](https://doi.org/10.1142/S0217732323501675).
- R. Fantoni. Continuum limit of the Green function in scaled affine φ_4^4 quantum Euclidean covariant relativistic field theory. *Quantum Rep.*, 6:134, 2024. doi: [10.3390/quantum6020010](https://doi.org/10.3390/quantum6020010).
- R. Fantoni and J. R. Klauder. Affine quantization of $(\varphi^4)_4$ succeeds while canonical quantization fails. *Phys. Rev. D*, 103:076013, 2021a. doi: [10.1103/PhysRevD.103.076013](https://doi.org/10.1103/PhysRevD.103.076013).
- R. Fantoni and J. R. Klauder. Monte Carlo evaluation of the continuum limit of the two-point function of the Euclidean free real scalar field subject to affine quantization. *J. Stat. Phys.*, 184:28, 2021b. doi: [10.1007/s10955-021-02818-x](https://doi.org/10.1007/s10955-021-02818-x).
- R. Fantoni and J. R. Klauder. Monte Carlo evaluation of the continuum limit of the two-point function of two Euclidean Higgs real scalar fields subject to affine quantization. *Phys. Rev. D*, 104:054514, 2021c. doi: [10.1103/PhysRevD.104.054514](https://doi.org/10.1103/PhysRevD.104.054514).
- R. Fantoni and J. R. Klauder. Eliminating Nonrenormalizability Helps Prove Scaled Affine Quantization of φ_4^4 is Nontrivial. *Int. J. Mod. Phys. A*, 37:2250029, 2022a. doi: [10.1142/S0217751X22500294](https://doi.org/10.1142/S0217751X22500294).
- R. Fantoni and J. R. Klauder. Kinetic Factors in Affine Quantization and Their Role in Field Theory Monte Carlo. *Int. J. Mod. Phys. A*, 37(14):2250094, 2022b. doi: [10.1142/S0217751X22500944](https://doi.org/10.1142/S0217751X22500944).
- R. Fantoni and J. R. Klauder. Scaled Affine Quantization of φ_4^4 in the Low Temperature Limit. *Eur. Phys. J. C*, 82:843, 2022c. doi: [10.1140/epjc/s10052-022-10807-x](https://doi.org/10.1140/epjc/s10052-022-10807-x).
- R. Fantoni and J. R. Klauder. Scaled Affine Quantization of Ultralocal φ_2^4 a comparative Path Integral Monte Carlo study with scaled Canonical Quantization. *Phys. Rev. D*, 106:114508, 2022d. doi: [10.1103/PhysRevD.106.114508](https://doi.org/10.1103/PhysRevD.106.114508).
- W. V. Farrar. Richard Laming and the Coal-Gas Industry, with His Views on the Structure of Matter. *Annals of Science*, 25:243, 1969. doi: [10.1080/00033796900200141](https://doi.org/10.1080/00033796900200141).
- S. Glashow. The renormalizability of vector meson interactions. *Nucl. Phys.*, 10:107, 1959.
- S. L. Glashow. Partial-symmetries of weak interactions. *Nucl. Phys.*, 22:579, 1961. doi: [10.1016/0029-5582\(61\)90469-2](https://doi.org/10.1016/0029-5582(61)90469-2).

- G. Grosso and G. P. Parravicini. *Solid State Physics*. Academic Pr., 2013.
- P. W. Higgs. Broken Symmetries and the Masses of Gauge Bosons. *Phys. Rev. Lett.*, 12:132, 1964. doi: [10.1103/PhysRevLett.13.508](https://doi.org/10.1103/PhysRevLett.13.508).
- B. Jancovici. Exact Results for the Two-Dimensional One-Component Plasma. *Phys. Rev. Lett.*, 46:386, 1981. doi: [10.1103/PhysRevLett.46.386](https://doi.org/10.1103/PhysRevLett.46.386).
- J. R. Klauder. Continuous-Representation Theory. I. Postulates of Continuous-Representation Theory. *J. Math. Phys.*, 4:1055, 1963a. doi: [10.1063/1.1704034](https://doi.org/10.1063/1.1704034).
- J. R. Klauder. Continuous-Representation Theory. II. Generalized Relation between Quantum and Classical Dynamics. *J. Math. Phys.*, 4:1058, 1963b. doi: [10.1063/1.1704035](https://doi.org/10.1063/1.1704035).
- J. R. Klauder. Continuous-Representation Theory. III. On Functional Quantization of Classical Systems. *J. Math. Phys.*, 5:177, 1964. doi: [10.1063/1.1704107](https://doi.org/10.1063/1.1704107).
- J. R. Klauder and R. Fantoni. The Magnificent Realm of Affine Quantization: valid results for particles, fields, and gravity. *Axioms*, 12:911, 2023. doi: [10.3390/axioms12100911](https://doi.org/10.3390/axioms12100911).
- J. R. Klauder and J. McKenna. Continuous-Representation Theory. V. Construction of a Class of Scalar Boson Field Continuous Representations. *J. Math. Phys.*, 6:68, 1965. doi: [10.1063/1.1704265](https://doi.org/10.1063/1.1704265).
- J. M. Kosterlitz and D. J. Thouless. Ordering, metastability and phase transitions in two-dimensional systems. *J. Phys. C*, 6:1181, 1973. doi: [10.1088/0022-3719/6/7/010](https://doi.org/10.1088/0022-3719/6/7/010).
- L. D. Landau and E. M. Lifshitz. *Quantum Mechanics. Non-relativistic Theory*, volume 3. Pergamon Press Ltd, Oxford, 1977. Course of Theoretical Physics.
- R. B. Laughlin. Anomalous Quantum Hall Effect: An Incompressible Quantum Fluid with Fractionally Charged Excitations. *Phys. Rev. Lett.*, 50:1395, 1983. doi: [10.1103/PhysRevLett.50.1395](https://doi.org/10.1103/PhysRevLett.50.1395).
- M. J. Lighthill. *Introduction to Fourier analysis and generalized functions*. Cambridge University Press, 1959.
- P. A. Martin. Sum rules in charged fluids. *Rev. Mod. Phys.*, 60:1075, 1988. doi: [10.1103/RevModPhys.60.1075](https://doi.org/10.1103/RevModPhys.60.1075).
- R. M. Martin, L. Reining, and D. M. Ceperley. *Interacting Electrons, Theory and Computational Approaches*. Cambridge, 2016.
- J. McKenna and J. R. Klauder. Continuous-Representation Theory. IV. Structure of a Class of Function Spaces Arising from Quantum Mechanics. *J. Math. Phys.*, 5:878, 1964. doi: [10.1063/1.1704190](https://doi.org/10.1063/1.1704190).
- R. A. Millikan. The isolation of an ion, a precision measurement of its charge, and the correction of Stokes's law. *Science*, 32:436, 1910. doi: [10.1126/science.32.822.436](https://doi.org/10.1126/science.32.822.436).
- C. W. Misner, K. S. Thorne, and J. A. Wheeler. *Gravitation*. C. W. Misner and K. S. Thorne and J. A. Wheeler, New York, 1970.
- S. Navas et al. Review of particle physics. *Phys. Rev. D*, 110(3):030001, 2024. doi: [10.1103/PhysRevD.110.030001](https://doi.org/10.1103/PhysRevD.110.030001).

- K. S. Novoselov, A. K. Geim, S. V. Morozov, D. Jiang, Y. Zhang, S. V. Dubonos, I. V. Grigorieva, and A. A. Firsov. Electric Field Effect in Atomically Thin Carbon Films. *Science*, 306:666, 2004. doi: [10.1126/science.1102896](https://doi.org/10.1126/science.1102896).
- W. Pauli. *Electrodynamics*, volume 1 of *Pauli Lectures on Physics*. MIT Press, Cambridge, Massachusetts, first edition, 1973.
- L. C. Pauling. *The Nature of the Chemical Bond and the Structure of Molecules and Crystals: an introduction to modern structural chemistry*. Cornell University Press, 1960. pp. 88–107.
- A. Salam and J. C. Ward. Weak and electromagnetic interactions. *Nuovo Cimento*, 11:568, 1959. doi: [10.1007/BF02726525](https://doi.org/10.1007/BF02726525).
- J. Schwinger. On Quantum-Electrodynamics and the Magnetic Moment of the Electron. *Phys. Rev.*, 73:416, 1948. doi: [10.1103/PhysRev.73.416](https://doi.org/10.1103/PhysRev.73.416).
- S. L. Shapiro and S. A. Teukolsky. *Black Holes, White Dwarfs, and Neutron Stars. The Physics of Compact Objects*. John Wiley & Sons Inc, New York, 1983.
- J. J. Thomson. Cathode Rays. *Philosophical Magazine*, 44:293, 1897. doi: [10.1080/14786449708621070](https://doi.org/10.1080/14786449708621070).
- K. v. Klitzing, G. Dorda, and M. Pepper. New method for high-accuracy determination of the fine-structure constant based on quantized Hall resistance. *Phys. Rev. Lett.*, 45:494, 1980. doi: [10.1103/PhysRevLett.45.494](https://doi.org/10.1103/PhysRevLett.45.494).
- S. Weinberg. A Model of Leptons. *Phys. Rev. Lett.*, 19:1264, 1967. doi: [10.1103/PhysRevLett.19.1264](https://doi.org/10.1103/PhysRevLett.19.1264).

Appendices

1.A Particle Data Group

We include here the particle listing for the electron from the Particle Data Group [Navas et al. \[2024\]](#) followed by an illustrative key.

e

$$J = \frac{1}{2}$$

e MASS (atomic mass units u)

The primary determination of an electron's mass comes from measuring the ratio of the mass to that of a nucleus, so that the result is obtained in u (atomic mass units). The conversion factor to MeV is more uncertain than the mass of the electron in u; indeed, the recent improvements in the mass determination are not evident when the result is given in MeV. In this datablock we give the result in u, and in the following datablock in MeV.

VALUE (10^{-6} u)	DOCUMENT ID	TECN	COMMENT
548.579909065±0.000000016	TIESINGA	21	RVUE 2018 CODATA value
• • • We do not use the following data for averages, fits, limits, etc. • • •			
548.579909070±0.000000016	MOHR	16	RVUE 2014 CODATA value
548.57990946 ± 0.00000022	MOHR	12	RVUE 2010 CODATA value
548.57990943 ± 0.00000023	MOHR	08	RVUE 2006 CODATA value
548.57990945 ± 0.00000024	MOHR	05	RVUE 2002 CODATA value
548.5799092 ± 0.0000004	¹ BEIER	02	CNTR Penning trap
548.5799110 ± 0.0000012	MOHR	99	RVUE 1998 CODATA value
548.5799111 ± 0.0000012	² FARNHAM	95	CNTR Penning trap
548.579903 ± 0.000013	COHEN	87	RVUE 1986 CODATA value

¹ BEIER 02 compares Larmor frequency of the electron bound in a $^{12}\text{C}^{5+}$ ion with the cyclotron frequency of a single trapped $^{12}\text{C}^{5+}$ ion.

² FARNHAM 95 compares cyclotron frequency of trapped electrons with that of a single trapped $^{12}\text{C}^{6+}$ ion.

e MASS

The mass is known more precisely in u (atomic mass units) than in MeV.

The conversion is: $1 \text{ u} = 931.494\ 102\ 42(28) \text{ MeV}/c^2$ (2018 CODATA value, TIESINGA 21). The conversion error dominates the uncertainty of the masses given below.

VALUE (MeV)	DOCUMENT ID	TECN	COMMENT
0.51099895000±0.00000000015	TIESINGA	21	RVUE 2018 CODATA value
• • • We do not use the following data for averages, fits, limits, etc. • • •			
0.5109989461 ± 0.0000000031	MOHR	16	RVUE 2014 CODATA value
0.510998928 ± 0.000000011	MOHR	12	RVUE 2010 CODATA value
0.510998910 ± 0.000000013	MOHR	08	RVUE 2006 CODATA value
0.510998918 ± 0.000000044	MOHR	05	RVUE 2002 CODATA value
0.510998901 ± 0.000000020	^{1,2} BEIER	02	CNTR Penning trap
0.510998902 ± 0.000000021	MOHR	99	RVUE 1998 CODATA value
0.510998903 ± 0.000000020	^{1,3} FARNHAM	95	CNTR Penning trap
0.510998895 ± 0.000000024	¹ COHEN	87	RVUE 1986 CODATA value
0.5110034 ± 0.0000014	COHEN	73	RVUE 1973 CODATA value

¹ Converted to MeV using the 1998 CODATA value of the conversion constant, 931.494013 ± 0.000037 MeV/u.

² BEIER 02 compares Larmor frequency of the electron bound in a $^{12}\text{C}^{5+}$ ion with the cyclotron frequency of a single trapped $^{12}\text{C}^{5+}$ ion.

³ FARNHAM 95 compares cyclotron frequency of trapped electrons with that of a single trapped $^{12}\text{C}^{6+}$ ion.

$(m_{e^+} - m_{e^-}) / m_{\text{average}}$

A test of *CPT* invariance.

VALUE	CL%	DOCUMENT ID	TECN	COMMENT
$<8 \times 10^{-9}$	90	¹ FEE	93	CNTR Positronium spectroscopy
• • • We do not use the following data for averages, fits, limits, etc. • • •				
$<4 \times 10^{-23}$	90	² DOLGOV	14	From photon mass limit
$<4 \times 10^{-8}$	90	CHU	84	CNTR Positronium spectroscopy

¹ FEE 93 value is obtained under the assumption that the positronium Rydberg constant is exactly half the hydrogen one.

² DOLGOV 14 result is obtained under the assumption that any mass difference between electron and positron would lead to a non-zero photon mass. The PDG 12 limit of 1×10^{-18} eV on the photon mass is in turn used to derive the value quoted here.

$|q_{e^+} + q_{e^-}|/e$

A test of *CPT* invariance. See also similar tests involving the proton.

VALUE	DOCUMENT ID	TECN	COMMENT
$<4 \times 10^{-8}$	¹ HUGHES	92	RVUE
• • • We do not use the following data for averages, fits, limits, etc. • • •			
$<2 \times 10^{-18}$	² SCHAEFER	95	THEO Vacuum polarization
$<1 \times 10^{-18}$	³ MUELLER	92	THEO Vacuum polarization

¹ HUGHES 92 uses recent measurements of Rydberg-energy and cyclotron-frequency ratios.

² SCHAEFER 95 removes model dependency of MUELLER 92.

³ MUELLER 92 argues that an inequality of the charge magnitudes would, through higher-order vacuum polarization, contribute to the net charge of atoms.

e MAGNETIC MOMENT ANOMALY

$\mu_e/\mu_B - 1 = (g-2)/2$

VALUE (units 10^{-6})	DOCUMENT ID	TECN	CHG	COMMENT
1159.65218062 ± 0.00000012 OUR AVERAGE				
1159.65218059 ± 0.00000013	¹ FAN	23	MRS	Single electron
1159.65218073 ± 0.00000028	HANNEKE	08	MRS	Single electron
1159.6521884 ± 0.0000043	VANDYCK	87	MRS	— Single electron
• • • We do not use the following data for averages, fits, limits, etc. • • •				
1159.65218128 ± 0.00000018	TIESINGA	21	RVUE	2018 CODATA value
1159.65218091 ± 0.00000026	MOHR	16	RVUE	2014 CODATA value
1159.65218076 ± 0.00000027	MOHR	12	RVUE	2010 CODATA value
1159.65218111 ± 0.00000074	² MOHR	08	RVUE	2006 CODATA value

1159.65218085 ± 0.00000076	³ ODOM	06	MRS	–	Single electron
1159.6521859 ± 0.0000038	MOHR	05	RVUE		2002 CODATA value
1159.6521869 ± 0.0000041	MOHR	99	RVUE		1998 CODATA value
1159.652193 ± 0.000010	COHEN	87	RVUE		1986 CODATA value
1159.6521879 ± 0.0000043	⁴ VANDYCK	87	MRS	+	Single positron

¹ FAN 23 report the most accurate measurement of the electron magnetic moment. A one-electron quantum cyclotron is used. We do not propagate at the moment this measurement to the fine structure and other physical constants. When discrepancies in the independent determinations of alpha are resolved, the new measurement uncertainty of 0.13 ppt is available for precise tests for BSM physics.

² MOHR 08 average is dominated by ODOM 06.

³ Superseded by HANNEKE 08 per private communication with Gerald Gabrielse.

⁴ This VANDYCK 87 result is for a positron. We do not take it into account for the average to avoid the assumption of CPT invariance.

($g_{e^+} - g_{e^-}$) / g_{average}

A test of *CPT* invariance.

VALUE (units 10^{-12})	CL%	DOCUMENT ID	TECN	COMMENT
– 0.5 ± 2.1		¹ VANDYCK 87	MRS	Penning trap
• • • We do not use the following data for averages, fits, limits, etc. • • •				
< 12	95	² VASSERMAN 87	CNTR	Assumes $m_{e^+} = m_{e^-}$
22 ± 64		SCHWINBERG 81	MRS	Penning trap

¹ VANDYCK 87 measured $(g_-/g_+) - 1$ and we converted it.

² VASSERMAN 87 measured $(g_+ - g_-)/(g-2)$. We multiplied by $(g-2)/g = 1.2 \times 10^{-3}$.

e ELECTRIC DIPOLE MOMENT (d)

A nonzero value is forbidden by both *T* invariance and *P* invariance.

VALUE (10^{-28} ecm)	CL%	DOCUMENT ID	TECN	COMMENT
< 0.041	90	¹ ROUSSY	23	ESR electrons in intramolecular electric field
• • • We do not use the following data for averages, fits, limits, etc. • • •				
< 0.11	90	² ANDREEV	18	CNTR ThO molecules
< 1.3	90	³ CAIRNCROSS	17	ESR $^{180}\text{Hf}^{19}\text{F}$ molecules
– 5570 ± 7980 ± 120		KIM	15	CNTR $\text{Gd}_3\text{Ga}_5\text{O}_{12}$ molecules
< 0.87	90	⁴ BARON	14	CNTR ThO molecules
< 6050	90	⁵ ECKEL	12	CNTR $\text{Eu}_{0.5}\text{Ba}_{0.5}\text{TiO}_3$ molecules
< 10.5	90	⁶ HUDSON	11	NMR YbF molecules
6.9 ± 7.4		REGAN	02	MRS ^{205}Tl beams
18 ± 12 ± 10		⁷ COMMINS	94	MRS ^{205}Tl beams
– 27 ± 83		⁷ ABDULLAH	90	MRS ^{205}Tl beams
– 1400 ± 2400		CHO	89	NMR TIF molecules
– 150 ± 550 ± 150		MURTHY	89	Cs, no <i>B</i> field

– 5000	± 11000	LAMOREAUX	87	NMR	^{199}Hg
19000	± 34000	SANDARS	75	MRS	Thallium
7000	± 22000	PLAYER	70	MRS	Xenon
< 30000	90	WEISSKOPF	68	MRS	Cesium

¹ ROUSSY 23 gives a measurement corresponding to this limit as $(-1.3 \pm 2.0 \pm 0.6) \times 10^{-30} \text{ ecm}$.

² ANDREEV 18 gives a measurement corresponding to this limit as $(4.3 \pm 3.1 \pm 2.6) \times 10^{-30} \text{ ecm}$.

³ CAIRNCROSS 17 gives a measurement corresponding to this limit as $(0.09 \pm 0.77 \pm 0.17) \times 10^{-28} \text{ ecm}$.

⁴ BARON 14 gives a measurement corresponding to this limit as $(-0.21 \pm 0.37 \pm 0.25) \times 10^{-28} \text{ ecm}$.

⁵ ECKEL 12 gives a measurement corresponding to this limit as $(-1.07 \pm 3.06 \pm 1.74) \times 10^{-25} \text{ ecm}$.

⁶ HUDSON 11 gives a measurement corresponding to this limit as $(-2.4 \pm 5.7 \pm 1.5) \times 10^{-28} \text{ ecm}$.

⁷ ABDULLAH 90, COMMINS 94, and REGAN 02 use the relativistic enhancement of a valence electron's electric dipole moment in a high-Z atom.

e^- MEAN LIFE / BRANCHING FRACTION

A test of charge conservation. See the “Note on Testing Charge Conservation and the Pauli Exclusion Principle” following this section in our 1992 edition (Physical Review **D45** S1 (1992), p. VI.10).

Most of these experiments are one of three kinds: Attempts to observe (a) the 255.5 keV gamma ray produced in $e^- \rightarrow \nu_e \gamma$, (b) the (K) shell x ray produced when an electron decays without additional energy deposit, e.g., $e^- \rightarrow \nu_e \bar{\nu}_e \nu_e$ (“disappearance” experiments), and (c) nuclear de-excitation gamma rays after the electron disappears from an atomic shell and the nucleus is left in an excited state. The last can include both weak boson and photon mediating processes. We use the best $e^- \rightarrow \nu_e \gamma$ limit for the Summary Tables.

Note that we use the mean life rather than the half life, which is often reported.

$e \rightarrow \nu_e \gamma$ and astrophysical limits

VALUE (yr)	CL%	DOCUMENT ID	TECN	COMMENT
$>6.6 \times 10^{28}$	90	AGOSTINI	15B	$e^- \rightarrow \nu \gamma$
• • • We do not use the following data for averages, fits, limits, etc. • • •				
$>1.22 \times 10^{26}$	68	¹ Klapdor-Kleingrothaus et al. 07	CNTR	$e^- \rightarrow \nu \gamma$
$>4.6 \times 10^{26}$	90	BACK	02	BORX $e^- \rightarrow \nu \gamma$
$>3.4 \times 10^{26}$	68	BELLI	00B	DAMA $e^- \rightarrow \nu \gamma$, liquid Xe
$>3.7 \times 10^{25}$	68	AHARONOV	95B	CNTR $e^- \rightarrow \nu \gamma$
$>2.35 \times 10^{25}$	68	BALYSH	93	CNTR $e^- \rightarrow \nu \gamma$, ^{76}Ge detector
$>1.5 \times 10^{25}$	68	AVIGNONE	86	CNTR $e^- \rightarrow \nu \gamma$
$>1 \times 10^{39}$	2	ORITO	85	ASTR Astrophysical argument
$>3 \times 10^{23}$	68	BELLOTTI	83B	CNTR $e^- \rightarrow \nu \gamma$

¹ The authors of A. Derbin et al, arXiv:0704.2047v1 argue that this limit is overestimated by at least a factor of 5.

² ORITO 85 assumes that electromagnetic forces extend out to large enough distances and that the age of our galaxy is 10^{10} years.

Disappearance and nuclear-de-excitation experiments

VALUE (yr)	CL%	DOCUMENT ID	TECN	COMMENT
$>6.4 \times 10^{24}$	68	¹ BELLI	99B	DAMA De-excitation of ^{129}Xe
• • • We do not use the following data for averages, fits, limits, etc. • • •				
$>1.2 \times 10^{24}$	90	ABGRALL	17	HPGE Ge K-shell disappearance
$>4.2 \times 10^{24}$	68	BELLI	99	DAMA Iodine L-shell disappearance
$>2.4 \times 10^{23}$	90	² BELLI	99D	DAMA De-excitation of ^{127}I (in NaI)
$>4.3 \times 10^{23}$	68	AHARONOV	95B	CNTR Ge K-shell disappearance
$>2.7 \times 10^{23}$	68	REUSSER	91	CNTR Ge K-shell disappearance
$>2 \times 10^{22}$	68	BELLOTTI	83B	CNTR Ge K-shell disappearance

¹ BELLI 99B limit on charge nonconserving e^- capture involving excitation of the 236.1 keV nuclear state of ^{129}Xe ; the 90% CL limit is 3.7×10^{24} yr. Less stringent limits for other states are also given.

² BELLI 99D limit on charge nonconserving e^- capture involving excitation of the 57.6 keV nuclear state of ^{127}I . Less stringent limits for the other states and for the state of ^{23}Na are also given.

LIMITS ON LEPTON-FLAVOR VIOLATION IN PRODUCTION

Forbidden by lepton family number conservation.

This section was added for the 2008 edition of this *Review* and is not complete. For a list of further measurements see references in the papers listed below.

$\sigma(e^+ e^- \rightarrow e^\pm \tau^\mp) / \sigma(e^+ e^- \rightarrow \mu^+ \mu^-)$

VALUE	CL%	DOCUMENT ID	TECN	COMMENT
$<8.9 \times 10^{-6}$	95	AUBERT	07P	BABR $e^+ e^-$ at $E_{\text{cm}} = 10.58$ GeV
• • • We do not use the following data for averages, fits, limits, etc. • • •				
$<1.8 \times 10^{-3}$	95	GOMEZ-CAD...	91	MRK2 $e^+ e^-$ at $E_{\text{cm}} = 29$ GeV

$\sigma(e^+ e^- \rightarrow \mu^\pm \tau^\mp) / \sigma(e^+ e^- \rightarrow \mu^+ \mu^-)$

VALUE	CL%	DOCUMENT ID	TECN	COMMENT
$<4.0 \times 10^{-6}$	95	AUBERT	07P	BABR $e^+ e^-$ at $E_{\text{cm}} = 10.58$ GeV
• • • We do not use the following data for averages, fits, limits, etc. • • •				
$<6.1 \times 10^{-3}$	95	GOMEZ-CAD...	91	MRK2 $e^+ e^-$ at $E_{\text{cm}} = 29$ GeV

e REFERENCES

FAN	23	PRL 130 071801	X. Fan <i>et al.</i>	(HARV, NWES)
ROUSSY	23	SCI 381 46	T.S. Roussy <i>et al.</i>	(COLO)
TIESINGA	21	RMP 93 025010	E. Tiesinga <i>et al.</i>	(NIST)
ANDREEV	18	NAT 562 355	V. Andreev <i>et al.</i>	(ACME Collab.)
ABGRALL	17	PRL 118 161801	N. Abgrall <i>et al.</i>	(MAJORANA Collab.)
CAIRNCROSS	17	PRL 119 153001	W.B. Cairncross <i>et al.</i>	(NIST, COLO)
MOHR	16	RMP 88 035009	P.J. Mohr, D.B. Newell, B.N. Taylor	(NIST)
AGOSTINI	15B	PRL 115 231802	M. Agostini <i>et al.</i>	(Borexino Collab.)
KIM	15	PR D91 102004	Y.J. Kim <i>et al.</i>	(IND, YALE, LANL)
BARON	14	SCI 343 269	J. Baron <i>et al.</i>	(ACME Collab.)
DOLGOV	14	PL B732 244	A.D. Dolgov, V.A. Novikov	
ECKEL	12	PRL 109 193003	S. Eckel, A.O. Sushkov, S.K. Lamoreaux	(YALE)
MOHR	12	RMP 84 1527	P.J. Mohr, B.N. Taylor, D.B. Newell	(NIST)
PDG	12	PR D86 010001	J. Beringer <i>et al.</i>	(PDG Collab.)
HUDSON	11	NAT 473 493	J.J. Hudson <i>et al.</i>	(LOIC)

HANNEKE	08	PRL 100 120801	D. Hanneke, S. Fogwell, G. Gabrielse	(HARV)
MOHR	08	RMP 80 633	P.J. Mohr, B.N. Taylor, D.B. Newell	(NIST)
AUBERT	07P	PR D75 031103	B. Aubert <i>et al.</i>	(BABAR Collab.)
KLAPDOR-K...	07	PL B644 109	H.V. Klapdor-Kleingrothaus, I.V. Krivosheina, I.V. Titkova	(HARV)
ODOM	06	PRL 97 030801	B. Odom <i>et al.</i>	(HARV)
MOHR	05	RMP 77 1	P.J. Mohr, B.N. Taylor	(NIST)
BACK	02	PL B525 29	H.O. Back <i>et al.</i>	(Borexino/SASSO Collab.)
BEIER	02	PRL 88 011603	T. Beier <i>et al.</i>	
REGAN	02	PRL 88 071805	B.C. Regan <i>et al.</i>	
BELLI	00B	PR D61 117301	P. Belli <i>et al.</i>	(DAMA Collab.)
BELLI	99	PL B460 236	P. Belli <i>et al.</i>	(DAMA Collab.)
BELLI	99B	PL B465 315	P. Belli <i>et al.</i>	(DAMA Collab.)
BELLI	99D	PR C60 065501	P. Belli <i>et al.</i>	(DAMA Collab.)
MOHR	99	JPCRD 28 1713	P.J. Mohr, B.N. Taylor	(NIST)
Also		RMP 72 351	P.J. Mohr, B.N. Taylor	(NIST)
AHARONOV	95B	PR D52 3785	Y. Aharonov <i>et al.</i>	(SCUC, PNL, ZARA+)
Also		PL B353 168	Y. Aharonov <i>et al.</i>	(SCUC, PNL, ZARA+)
FARNHAM	95	PRL 75 3598	D.L. Farnham, R.S. van Dyck, P.B. Schwinberg	(WASH)
SCHAEFER	95	PR A51 838	A. Schaefer, J. Reinhardt	(FRAN)
COMMINS	94	PR A50 2960	E.D. Commins <i>et al.</i>	
BALYSH	93	PL B298 278	A. Balysh <i>et al.</i>	(KIAE, MPIK, SASSO)
FEE	93	PR A48 192	M.S. Fee <i>et al.</i>	
HUGHES	92	PRL 69 578	R.J. Hughes, B.I. Deutch	(LANL, AARH)
MUELLER	92	PRL 69 3432	B. Muller, M.H. Thoma	(DUKE)
PDG	92	PR D45 S1	K. Hikasa <i>et al.</i>	(KEK, LBL, BOST+)
GOMEZ-CAD...	91	PRL 66 1007	J.J. Gomez-Cadenas <i>et al.</i>	(SLAC MARK-2 Collab.)
REUSSER	91	PL B255 143	D. Reusser <i>et al.</i>	(NEUC, CIT, PSI)
ABDULLAH	90	PRL 65 2347	K. Abdullah <i>et al.</i>	(LBL, UCB)
CHO	89	PRL 63 2559	D. Cho, K. Sangster, E.A. Hinds	(YALE)
MURTHY	89	PL 63 965	S.A. Murthy <i>et al.</i>	(AMHT)
COHEN	87	RMP 59 1121	E.R. Cohen, B.N. Taylor	(RISC, NBS)
LAMOREAUX	87	PRL 59 2275	S.K. Lamoreaux <i>et al.</i>	(WASH)
VANDYCK	87	PRL 59 26	R.S. van Dyck, P.B. Schwinberg, H.G. Dehmelt	(WASH)
VASSERMAN	87	PL B198 302	I.B. Vasserman <i>et al.</i>	(NOVO)
Also		PL B187 172	I.B. Vasserman <i>et al.</i>	(NOVO)
AVIGNONE	86	PR D34 97	F.T. Avignone <i>et al.</i>	(PNL, SCUC)
ORITO	85	PRL 54 2457	S. Orito, M. Yoshimura	(TOKY, KEK)
CHU	84	PRL 52 1689	S. Chu, A.P. Mills, J.L. Hall	(BELL, NBS, COLO)
BELLOTTI	83B	PL 124B 435	E. Bellotti <i>et al.</i>	(MILA)
SCHWINBERG	81	PRL 47 1679	P.B. Schwinberg, R.S. van Dyck, H.G. Dehmelt	(WASH)
SANDARS	75	PR A11 473	P.G.H. Sandars, D.M. Sternheimer	(OXF, BNL)
COHEN	73	JPCRD 2 664	E.R. Cohen, B.N. Taylor	(RISC, NBS)
PLAYER	70	JP B3 1620	M.A. Player, P.G.H. Sandars	(OXF)
WEISSKOPF	68	PRL 21 1645	M.C. Weisskopf <i>et al.</i>	(BRAN)

Illustrative Key to the Particle Listings

Name of particle. "Old" name used before 1986 renaming scheme also given if different. See the section "Naming Scheme for Hadrons" for details.

 $a_0(1200)$
 $I^G(J^{PC}) = 1^-(0^{++})$

Particle quantum numbers (where known).

OMITTED FROM SUMMARY TABLE

Evidence not compelling, may be a kinematic effect.

Indicates particle omitted from Particle Physics Summary Table, implying particle's existence is not confirmed.

Quantity tabulated below.

Top line gives our best value (and error) of quantity tabulated here, based on weighted average of measurements used. Could also be from fit, best limit, estimate, or other evaluation. See next page for details.

Footnote number linking measurement to text of footnote.

 $a_0(1200)$ MASS

VALUE (MeV)	EVTS	DOCUMENT ID	TECN	CHG	COMMENT
1206 ± 7 OUR AVERAGE					
1210 ± 8 ± 9	3000	FENNER 87	MMS	—	3.5 $\pi^- p$
1198 ± 10		PIERCE 83	ASPK	+	2.1 $K^- p$
1216 ± 11 ± 9	1500	MERRILL 81	HBC	0	3.2 $K^- p$
• • • We do not use the following data for averages, fits, limits, etc. • • •					
1192 ± 16	200	LYNCH 81	HBC	±	2.7 $\pi^- p$

General comments on particle.

Number of events above background.

Measured value used in averages, fits, limits, etc.

Error in measured value (often statistical only; followed by systematic if separately known; the two are combined in quadrature for averaging and fitting.)

Measured value not used in averages, fits, limits, etc. See the Introductory Text for explanations.

Arrow points to weighted average.

 Shaded pattern extends $\pm 1\sigma$ (scaled by "scale factor" S) from weighted average.

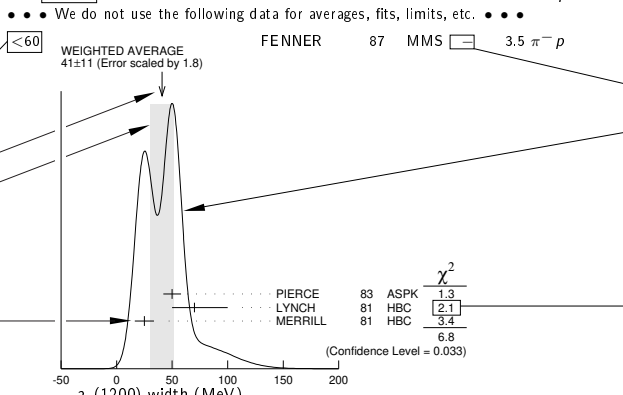
Value and error for each experiment.

 $a_0(1200)$ WIDTH

VALUE (MeV)	EVTS	DOCUMENT ID	TECN	CHG	COMMENT
41 ± 11 OUR AVERAGE					
50 ± 8		PIERCE 83	ASPK	+	2.1 $K^- p$
70 ± 30	200	LYNCH 81	HBC	±	2.7 $\pi^- p$
25 ± 5 ± 7		MERRILL 81	HBC	0	3.2 $K^- p$
• • • We do not use the following data for averages, fits, limits, etc. • • •					
<60		FENNER 87	MMS	—	3.5 $\pi^- p$

Scale factor > 1 indicates possibly inconsistent data.

Reaction producing particle, or general comments.



"Change bar" indicates result added or changed since previous edition.

Charge(s) of particle(s) detected.

Ideogram to display possibly inconsistent data. Curve is sum of Gaussians, one for each experiment (area of Gaussian = 1/error; width of Gaussian = ±error). See Introductory Text for discussion.

 Contribution of experiment to χ^2 (if no entry present, experiment not used in calculating χ^2 or scale factor because of very large error).

 Partial decay mode (labeled by Γ_i).

Mode	Fraction (Γ_i/Γ)	Scale factor/ Confidence level
$\Gamma_1 3\pi$	(65.2 ± 1.3) %	S=1.7
$\Gamma_2 K\bar{K}$	(34.8 ± 1.3) %	S=1.7
$\Gamma_3 \eta\pi^\pm$	< 5 $\times 10^{-4}$	CL=95%

Our best value for branching fraction as determined from data averaging, fitting, evaluating, limit selection, etc. This list is basically a compact summary of results in the Branching Ratio section below.

Branching ratio.

VALUE	DOCUMENT ID	TECN	CHG	COMMENT
0.652 ± 0.013 OUR FIT Error includes scale factor of 1.7.				
0.643 ± 0.010 OUR AVERAGE				
0.64 ± 0.01	PIERCE 83	ASPK	+	2.1 $K^- p$
0.74 ± 0.06	MERRILL 81	HBC	0	3.2 $K^- p$
• • • We do not use the following data for averages, fits, limits, etc. • • •				
0.48 ± 0.15	2 LYNCH 81	HBC	±	2.7 $\pi^- p$

2 Data has questionable background subtraction.

Weighted average of measurements of this ratio only.

Footnote (referring to LYNCH 81).

Confidence level for measured upper limit.

VALUE	DOCUMENT ID	TECN	CHG	COMMENT
0.348 ± 0.013 OUR FIT Error includes scale factor of 1.7.				
0.35 ± 0.05				
PIERCE 83	ASPK	+	2.1 $K^- p$	

 Branching ratio in terms of partial decay mode(s) Γ_i above.

References, ordered inversely by year, then author.

"Document id" used on data entries above.

Journal, report, preprint, etc. (See abbreviations on next page.)

VALUE	DOCUMENT ID	TECN	CHG	COMMENT
0.535 ± 0.030 OUR FIT Error includes scale factor of 1.7.				
0.50 ± 0.03				
MERRILL 81	HBC	0	3.2 $K^- p$	

 $0.71\Gamma_3/\Gamma$

VALUE (units 10^{-4})	CL%	DOCUMENT ID	TECN	CHG	COMMENT
<3.5	95	PIERCE 83	ASPK	+	2.1 $K^- p$

Partial list of author(s) in addition to first author.

Quantum number determinations in this reference.

Institution(s) of author(s). (See abbreviations on next page.)

 $a_0(1200)$ REFERENCES

FENNER 87	PRL 55 14
PIERCE 83	PL 123B 230
LYNCH 81	PR D24 610
MERRILL 81	PRL 47 143

H. Fenner et al.
J.H. Pierce
G.R. Lynch et al.
D.W. Merrill et al.

(SLAC) (FNAL) (JPF)
(CLEO Collab.) (SACL, CERN)

References

S. Navas et al. Review of particle physics. *Phys. Rev. D*, 110(3):030001, 2024. doi: [10.1103/PhysRevD.110.030001](https://doi.org/10.1103/PhysRevD.110.030001).

Chapter 2

The particle

In Relativistic Quantum Theory Berestetskii et al. [1971] we describe a pointwise, structureless, elementary, free particle through a finite dimensional irreducible unitary representation of its group of symmetries (the Galileo group in the non-relativistic case and the Poincaré group in the relativistic case, extended to the parity transformation). The invariants of the group are the mass and the spin. The wave functions of the particles are in bijective correspondence with the vectors of such representations, and the scalar product for such vectors is expressible in terms of wave functions. We determine the wave equation satisfied by the particles. In the relativistic case, the locality requirement, forces the introduction of “negative energy” solutions. It is an experimental fact that the number of particles may change in physical processes. Then, there exist transitions between states with different number of particles. We will present a formalism that allows to describe systems of many free particles, used in any many-body theory, relativistic or not, and known as Fock method. It allows to describe many particles states with the correct statistics and to introduce operators that change the number of particles (creation and annihilation operators). We will introduce the free field operators, and we will interpret in terms of field operators the negative energy solutions of the equations of free motion. We will denote as “antiparticles” the negative energy particles with a non-hermitian field operator. We construct the representation of the group on the many free particles states. And we prove the spin-statistics theorem which states that, as a consequence of Lorentz invariance and of locality, half integer spin particles must obey to *Fermi statistics* and integer spin particles must obey to *Bose statistics*.

This chapter is extracted from the “Theoretical Physics” course given by Prof. Adriano di Giacomo at the physics department of the University of Pisa in 1993.

2.1 Definition of Invariance

A reference frame is defined by a set of operative rules to measure physical quantities.

The same physical phenomenon can be observed from two different reference frames. In order for the two reference frames to be defined, the transformation between the quantities measured in the two frames must be known.

In a given reference frame a phenomenon obeys certain physical laws. A physical law is a relationship which poses conditions on the quantities measured at a given instant.

The frames are said to be equivalent respect to a class of phenomena if:

- a) Any physical situation realizable in one can also be realizable in the other.
- b) The time evolution laws are the same in the two frames.

The equivalence between frames produced by the invariance is an equivalence relationship in the mathematical sense: Given R, R', R'' three frames; R is equivalent to R , if R is equivalent to R' then R' is equivalent to R ; if R is equivalent to R' and R' is equivalent to R'' then R is equivalent to R'' .

The transformation laws between quantities in equivalent frames form a group:

- a) The identity transformation exists: The one between any frame and itself.
- b) Given any transformation, an inverse transformation exists which is itself an equivalence relationship respect to the class of phenomena in exam.
- c) The product of two equivalence relationships, defined as the application in succession and ordered of two transformations, is still an equivalence relationship.

The equivalence of a class of frames relative to a set of phenomena is called *invariance* of such phenomena relative to the group of transformations between the frames.

2.1.1 Conventions

Through the note we will conform to the following conventions:

Units

We will always use relativistic units with $\hbar = 1, c = 1$. In these units, we have for the elementary charge $e^2/4\pi = 1/137$.

Fourier transform

The tridimensional Fourier transform is

$$f(\mathbf{p}) = \int f(\mathbf{q}) e^{-i\mathbf{q} \cdot \mathbf{p}} d\mathbf{q}, \quad (2.1.1)$$

$$f(\mathbf{q}) = \int f(\mathbf{p}) e^{i\mathbf{q} \cdot \mathbf{p}} \frac{d\mathbf{p}}{(2\pi)^3}, \quad (2.1.2)$$

and analogously for the four-dimensional case.

Operators

We will not introduce a different symbol for the operators on the Hilbert space and their eigenvalues. The reader should understand the difference from the context of the various equations introduced.

2.2 Invariance in quantum mechanics

In quantum mechanics the invariance respect to a change of reference frame is defined as follows:

- a) The possible states in the two frames are the vectors of a same Hilbert space. The observables are the same. The transformation law is a mapping of the Hilbert space onto itself.
 - b) Starting from the same initial state the time evolution is the same in the two frames.
-

The invariance transformations are a group. So an invariance transformation is a realization of the group on an Hilbert space.

Let $|a\rangle$ be a state, in a certain frame, defined by the simultaneous measure of a complete set of commuting observables. Any vector of the form $x_a|a\rangle$ where x_a is an arbitrary phase factor, is an eigenstate of the same observables with the same eigenvalues. So it represents the same physical state. The phase is not observable. A measurement on $|a\rangle$ means to observe the probability that $|a\rangle$ contains a state $|b\rangle$ defined by the measure instruments. What one measures is

$$P_{ab} = |\langle b|a\rangle|^2, \quad (2.2.1)$$

where the phases x_a and x_b cancel. A vector of the Hilbert space modulo a phase is called a “ray” of the Hilbert space and will be denoted $|\{a\}\rangle$.

Wigner theorem: Given a bijective transformation between rays in a Hilbert space $|\{s\}\rangle \rightarrow |\{s'\}\rangle$ such that

$$|\langle \{s'_2\} | \{s'_1\} \rangle|^2 = |\langle \{s_2\} | \{s_1\} \rangle|^2 \quad \forall |\{s_1\}\rangle, |\{s_2\}\rangle \quad (2.2.2)$$

it is always possible to choose the phases in such a way that the transformation is realized on the Hilbert space vectors as a unitary or antiunitary transformation.

Proof:

1. Let $|e_n\rangle$ be an orthonormal complete base of the Hilbert space and let $|\{e_n\}\rangle$ be the correspondent rays. The transformed rays are orthonormal

$$\langle e_i | e_j \rangle = \delta_{ij} \implies |\langle \{e'_i\} | \{e'_j\} \rangle|^2 = \delta_{ij} \quad (2.2.3)$$

Let us choose in an arbitrary way a set of phases on the rays $|\{e'_i\}\rangle$, i.e. a set of vectors $|e'_i\rangle$ that represent the states. Then

$$\langle e'_i | e'_j \rangle = \delta_{ij}, \quad (2.2.4)$$

The set of vectors so obtained is also a complete base of the Hilbert space. In fact, if there exists a vector $|v'\rangle$ such that $\langle v'|v'\rangle \neq 0$ and $\langle v'|e'_n\rangle = 0 \quad \forall n$, then, by hypothesis, there would exist a vector $|v\rangle$ such that $\langle v|v\rangle \neq 0$ and $\langle v|e_n\rangle = 0 \quad \forall n$, against the hypothesis of completeness of the base $|e_n\rangle$.

2. Let $|F_k\rangle = |e_1\rangle + |e_k\rangle$. The generic representative of the transformed ray $|\{F'_k\}\rangle$ will be

$$|F'_k\rangle = x_k(|e'_1\rangle + y_k|e'_k\rangle), \quad (2.2.5)$$

with x_k and y_k phases factors. In fact

$$|\langle F_k | e_n \rangle| = \delta_{n1} + \delta_{nk} \implies |\langle F'_k | e'_n \rangle| = \delta_{n1} + \delta_{nk}. \quad (2.2.6)$$

Next I can define the following S transformation

$$|Se_1\rangle = |e'_1\rangle \quad |Se_k\rangle = y_k|e'_k\rangle \quad (2.2.7)$$

$$|SF_k\rangle = \frac{1}{x_k}|F'_k\rangle = |e'_1\rangle + y_k|e'_k\rangle. \quad (2.2.8)$$

With this choice

$$|SF_k\rangle = |Se_1\rangle + |Se_k\rangle. \quad (2.2.9)$$

In other words we realized the transformation S as a linear transformation on vectors of kind $|F_k\rangle$. Let us next extend this construction to all vectors of the Hilbert space.

3. Consider a generic vector

$$|v\rangle = \sum_n a_n |e_n\rangle. \quad (2.2.10)$$

Let us assume, without loss of generality, a_1 real. The correspondent ray $|\{v\}\rangle$ will be transformed into a ray $|\{v'\}\rangle$ with the following generic representative

$$|v'\rangle = \sum_n a'_n |e'_n\rangle, \quad (2.2.11)$$

and since by hypothesis

$$|\langle v|e_n\rangle|^2 = |\langle v'|e'_n\rangle|^2, \quad (2.2.12)$$

we have

$$|a'_n| = |a_n|. \quad (2.2.13)$$

We define

$$|Se_1\rangle = |e'_1\rangle, \quad (2.2.14)$$

$$|Se_n\rangle = y_n |e'_n\rangle \quad \forall n \neq 1, \quad (2.2.15)$$

with y_n some phase factors, so that for any vector belonging to the transformed ray $|\{v'\}\rangle$

$$|v'\rangle = x \left\{ a_1 |Se_1\rangle + \sum_{n=2}^{\infty} \frac{a'_n}{y_n} |Se_n\rangle \right\}, \quad (2.2.16)$$

with x a phase factor. We then define

$$|Sv\rangle = \frac{1}{x} |v'\rangle. \quad (2.2.17)$$

By hypothesis it must be

$$|\langle F_k|v\rangle|^2 = |a_1 + a_k|^2 = |\langle SF_k|Sv\rangle|^2 = \left| a_1 + \frac{a'_k}{y_k} \right|^2. \quad (2.2.18)$$

Since we also have $|a_k| = |a'_k|$ we require

$$\mathbf{Re}(a_1 a_k) = \mathbf{Re} \left(a_1 \frac{a'_k}{y_k} \right). \quad (2.2.19)$$

Then there are only two possibilities:

- i. $a_k = a'_k/y_k$
- ii. $a_k = (a'_k/y_k)^*$

or

- i. $|Sv\rangle = S(\sum_n a_n |e_n\rangle) = \sum_n a_n |Se_n\rangle$
- ii. $|Sv\rangle = S(\sum_n a_n |e_n\rangle) = \sum_n a_n^* |Se_n\rangle$

In the first case the operator S is linear, in the second is antilinear. We also have

- i. $\langle Sv_1|Sv_2\rangle = \langle v_1|v_2\rangle \quad \forall |v_1\rangle, |v_2\rangle$
- ii. $\langle Sv_1|Sv_2\rangle = \langle v_2|v_1\rangle \quad \forall |v_1\rangle, |v_2\rangle$

In the first case S is unitary, in the second it is antiunitary.

2.3 Invariance and time evolution

The requirement b) for invariance tells us that the evolution of the transformed must coincide with the transformation of the evolved

$$U(t, t')S(t')|\psi\rangle = S(t)U(t, t')|\psi\rangle, \quad (2.3.1)$$

where $U(t, t')$ is the time evolution operator. Since $|\psi\rangle$ is arbitrary we must have

$$S^\dagger(t)U(t, t')S(t') = U(t, t'). \quad (2.3.2)$$

If the Hamiltonian H is independent of time

$$U(t, t') = e^{-iH(t-t')}, \quad (2.3.3)$$

and we require

$$S(t) = e^{-iH(t-t')}S(t')e^{iH(t-t')}. \quad (2.3.4)$$

2.4 Galilean relativity

We require invariance under translations, rotations, and velocity transformations for pointwise non relativistic particles.

2.4.1 Spatial translations

Let us consider a reference frame R' translated by \mathbf{a} relative to the frame R . If the spatial translations are a symmetry of the system it must exist a unitary transformation $U(\mathbf{a})$ which relates the dynamical variables \mathbf{q}' and \mathbf{p}' in R' to the variables \mathbf{q} and \mathbf{p} in R . The transformation law must be

$$\mathbf{q}' = \mathbf{q} - \mathbf{a}, \quad (2.4.1)$$

$$\mathbf{p}' = \mathbf{p}. \quad (2.4.2)$$

It is easy to see that the unitary operator exists and is

$$U(\mathbf{a}) = e^{i\mathbf{a} \cdot \mathbf{p}}. \quad (2.4.3)$$

Since the transformation is unitary the commutation relations do not change

$$[q'_i, p'_j] = [q_i, p_j] = i\delta_{ij}, \quad (2.4.4)$$

$$[q'_i, q'_j] = [q_i, q_j] = 0, \quad (2.4.5)$$

$$[p'_i, p'_j] = [p_i, p_j] = 0, \quad (2.4.6)$$

where $\mathbf{q} = U(\mathbf{a})^\dagger \mathbf{q} U(\mathbf{a})$ and $\mathbf{p} = U(\mathbf{a})^\dagger \mathbf{p} U(\mathbf{a})$. Moreover from Hadamard lemma (2.A.11) follows immediately that Eqs. (2.4.1)-(2.4.2) are satisfied.

The invariance of the time evolution between two frames R and R' imposes

$$U^\dagger(\mathbf{a}, t)e^{-iH(t-t')}U(\mathbf{a}, t') = e^{-iH(t-t')}, \quad (2.4.7)$$

which means

$$[\mathbf{p}, H] = 0. \quad (2.4.8)$$

In other words, the momentum is a constant of motion. We can also write

$$\frac{\partial H}{\partial \mathbf{q}} = 0. \quad (2.4.9)$$

2.4.2 Rotations

A rotation is defined by a versor \hat{n} which indicates the axis of rotation and an angle θ . We define $\boldsymbol{\theta} = \theta \hat{n}$. The angles are taken as positive for anti-clockwise rotations. Let us consider a frame R' rotated by $\boldsymbol{\theta}$ relative to frame R . The component of a vector v will change according to

$$v'_i = R(\boldsymbol{\theta})_{ij} v_j, \quad (2.4.10)$$

where $R(\boldsymbol{\theta})$ is the rotation matrix. For infinitesimal transformations

$$\delta v = v' - v \approx -\boldsymbol{\theta} \wedge v. \quad (2.4.11)$$

If the quantum system is invariant under rotations it must be possible to construct a unitary transformation on the Hilbert space which realizes the transformation and commutes with the time evolution. Let us then consider the angular momentum

$$\mathbf{J} = \mathbf{q} \wedge \mathbf{p}. \quad (2.4.12)$$

It is easy to verify that for $v = q$ or $v = p$ we have

$$[\boldsymbol{\theta} \cdot \mathbf{J}, v] = -i\boldsymbol{\theta} \wedge v. \quad (2.4.13)$$

Then the transformation we are looking for is

$$U(\boldsymbol{\theta}) = e^{i\boldsymbol{\theta} \cdot \mathbf{J}}, \quad (2.4.14)$$

as can be readily verified for infinitesimal transformations

$$v' = U^\dagger(\boldsymbol{\theta})vU(\boldsymbol{\theta}) \approx v - i[\boldsymbol{\theta} \cdot \mathbf{J}, v] = v - \boldsymbol{\theta} \wedge v. \quad (2.4.15)$$

The transformation commutes with the time evolution if

$$[\mathbf{J}, H] = 0 \quad (2.4.16)$$

which means that H must be a scalar and the angular momentum a constant of motion. Since the transformation is unitary it preserves the commutation relations.

If the particle has a spin the generator of the rotations is the total angular momentum

$$\mathbf{J} = \mathbf{q} \wedge \mathbf{p} + \mathbf{s}. \quad (2.4.17)$$

2.4.3 Galilean transformations

If we go from a frame R to a frame R' moving relative to R with a constant speed v we must have

$$q' = q - tv, \quad (2.4.18)$$

$$p' = p - mv. \quad (2.4.19)$$

It is easy to verify that these laws of transformation are induced by the unitary operator

$$U(t, v) = e^{i(p t - q m) \cdot v}, \quad (2.4.20)$$

so that

$$U^\dagger(t, v)qU(t, v) = q - tv, \quad (2.4.21)$$

$$U^\dagger(t, v)pU(t, v) = p - mv. \quad (2.4.22)$$

If the Galilean transformation has to be an invariance we must also require

$$U(t, \mathbf{v}) = e^{-iH(t-t')} U(t', \mathbf{v}) e^{iH(t-t')}, \quad (2.4.23)$$

or

$$t\mathbf{p} - m\mathbf{q} = e^{-iH(t-t')} (t'\mathbf{p} - m\mathbf{q}) e^{iH(t-t')}. \quad (2.4.24)$$

If the system is invariant under translations $[\mathbf{p}, H] = 0$, so

$$(t - t')\mathbf{p} = m\mathbf{q} - m e^{-iH(t-t')} \mathbf{q} e^{iH(t-t')}. \quad (2.4.25)$$

For infinitesimal time differences we get

$$\frac{\mathbf{p}}{m} = i[H, \mathbf{q}] = \frac{\partial H}{\partial \mathbf{p}}. \quad (2.4.26)$$

So

$$H = \frac{\mathbf{p}^2}{2m}. \quad (2.4.27)$$

2.4.4 Galileo group

We analyzed the symmetries under translations, rotations, and Galileo transformations for a non relativistic system. The corresponding unitary transformations are

$$U(\mathbf{a}) = e^{i\mathbf{a} \cdot \mathbf{p}}, \quad (2.4.28)$$

$$U(\boldsymbol{\theta}) = e^{i\boldsymbol{\theta} \cdot \mathbf{J}}, \quad (2.4.29)$$

$$U(\mathbf{v}) = e^{-i\mathbf{v} \cdot \mathbf{K}} \quad \mathbf{K} = m\mathbf{q} - t\mathbf{p} \quad (2.4.30)$$

The group corresponding to the set of these transformations is called “Galileo group” and the corresponding invariance “galilean invariance”.

From the canonical commutation relationships, the following algebra for the group generators, follows

$$[p_\mu, p_\nu] = 0 \quad P_0 = H \quad (2.4.31)$$

$$[\mathbf{J}, H] = 0 \quad [J_i, p_j] = i\epsilon_{ijk}p_k \quad (2.4.32)$$

$$[J_i, J_j] = i\epsilon_{ijk}J_k \quad [J_i, K_j] = i\epsilon_{ijk}K_k \quad (2.4.33)$$

$$[K_i, K_j] = 0 \quad [K_i, p_j] = im\delta_{ij} \quad [K_i, H] = ip_i \quad (2.4.34)$$

In the Hilbert space of the physical system is then defined an unitary representation of the group that transforms the spec into itself.

If this representation is reducible it is possible to write the Hilbert space as a direct sum of one or more orthogonal Hilbert spaces each one transforming in itself. The generators are written as sum of the generators acting in each subspace and generators acting on different irreducible subspaces commute. The states in each subspace evolve with their Hamiltonian each in states belonging to the same subspace.

A physical system can then be written as a sum of irreducible representations of the Galileo group.

The simplest case is a particle without internal structure. In this case the only internal variable is the spin which commutes with the orbital variables. A complete set of state is

$$|\mathbf{p}\rangle|s, s_z\rangle. \quad (2.4.35)$$

Assuming the usual metric

$$\langle \mathbf{p}' | \mathbf{p} \rangle = (2\pi)^3 \delta^3(\mathbf{p} - \mathbf{p}'), \quad (2.4.36)$$

$$\langle s'_z | s_z \rangle = \delta_{s'_z s_z} \quad (2.4.37)$$

these states constitute an irreducible representation of the Galileo group if the states $|s_z\rangle$ are an irreducible representation of internal rotations. Let us show this explicitly:

$$p|\mathbf{p}\rangle = p|\mathbf{p}\rangle, \quad (2.4.38)$$

$$\begin{aligned} p e^{i\theta \cdot \mathbf{J}} |\mathbf{p}\rangle &= e^{i\theta \cdot \mathbf{J}} e^{-i\theta \cdot \mathbf{J}} p e^{i\theta \cdot \mathbf{J}} |\mathbf{p}\rangle \\ &= R(\theta) p e^{i\theta \cdot \mathbf{J}} |\mathbf{p}\rangle, \end{aligned} \quad (2.4.39)$$

where p on the right hand side denotes the momentum operator acting on the eigenstate $|\mathbf{p}\rangle$ and on the left denotes the eigenvalue. The eigenvalues of the rotated state is the rotated momentum. In the same way:

$$\begin{aligned} p e^{-iv \cdot \mathbf{K}} |\mathbf{p}\rangle &= e^{-iv \cdot \mathbf{K}} e^{iv \cdot \mathbf{K}} p e^{-iv \cdot \mathbf{K}} |\mathbf{p}\rangle \\ &= (\mathbf{p} - m\mathbf{v}) e^{-iv \cdot \mathbf{K}} |\mathbf{p}\rangle, \end{aligned} \quad (2.4.40)$$

so

$$e^{i\theta \cdot \mathbf{J}} |\mathbf{p}\rangle = |R(\theta)\mathbf{p}\rangle, \quad (2.4.41)$$

$$e^{-iv \cdot \mathbf{K}} |\mathbf{p}\rangle = |\mathbf{p} - m\mathbf{v}\rangle, \quad (2.4.42)$$

and we see that starting from any vector $|\mathbf{p}\rangle$ it is possible to reach any other vector $|\mathbf{p}'\rangle$ through successive applications of rotations or of Galileo transformations. The internal degrees of freedom only transform by rotations independently.

So a pointwise free particle is described by an irreducible unitary representation of the Galileo group.

2.4.5 Parity invariance

The parity transformation is defined by

$$\mathbf{p} \rightarrow -\mathbf{p} \quad \mathbf{q} \rightarrow -\mathbf{q} \quad \mathbf{s} \rightarrow \mathbf{s} \quad (2.4.43)$$

This is a canonical transformation since it does not change the commutation relations. The transformation operator is

$$U_P = e^{i\frac{\pi}{2}(\mathbf{p}+i\mathbf{q}) \cdot (\mathbf{p}-i\mathbf{q})}. \quad (2.4.44)$$

The parity transformation has square 1

$$U_P = U_P^{-1} = U_P^\dagger. \quad (2.4.45)$$

If the parity transformation is an invariance we must have

$$U_P^{-1} H U_P = H \quad (2.4.46)$$

or

$$[U_P, H] = 0. \quad (2.4.47)$$

Let us now prove Eq. (2.4.44) in the one-dimensional case

$$U_P = e^{i\frac{\pi}{2}(p^2 + q^2 - 1)}. \quad (2.4.48)$$

Apart from a phase this operator coincides with the time evolution operator of a harmonic oscillator of mass 1 and $\omega = 1$ from time $t = 0$ to time $t = \pi$. The Heisenberg equations for

$$q(t) = e^{iHt}q(0)e^{-iHt}, \quad (2.4.49)$$

$$p(t) = e^{iHt}p(0)e^{-iHt}, \quad (2.4.50)$$

are

$$\dot{q} = i[H, q], \quad (2.4.51)$$

$$\dot{p} = i[H, p], \quad (2.4.52)$$

with $H = (p^2 + q^2)/2$. They have solution

$$q(t) = q \cos t + p \sin t, \quad (2.4.53)$$

$$p(t) = p \cos t - q \sin t. \quad (2.4.54)$$

It follows for $t = \pi$

$$q(\pi) = U_P^\dagger q U_P = -q, \quad (2.4.55)$$

$$p(\pi) = U_P^\dagger p U_P = -p, \quad (2.4.56)$$

which is what we wanted.

2.4.6 Time reversal

The time reversal acts as follows

$$q \rightarrow q \quad p \rightarrow -p \quad s \rightarrow -s \quad t \rightarrow -t \quad (2.4.57)$$

This transformation cannot be realized by a unitary operator because in such case the commutation relations would be preserved. Instead we want, in one dimension,

$$[q, p] = i \rightarrow [q, -p] = -i \quad (2.4.58)$$

If the transformation is antiunitary this is possible:

$$[q', p'] = U_T^\dagger [q, p] U_T = U_T^\dagger i U_T = -i. \quad (2.4.59)$$

An antilinear operator is defined by

$$T|s_1\rangle = |Ts_1\rangle \quad T|s_2\rangle = |Ts_2\rangle \quad (2.4.60)$$

$$T(a|s_1\rangle + b|s_2\rangle) = a^*T|s_1\rangle + b^*T|s_2\rangle. \quad (2.4.61)$$

For a linear operator O

$$\langle a|Ob\rangle = \langle O^\dagger a|b\rangle = \langle b|O^\dagger a\rangle^*, \quad (2.4.62)$$

and the operator is Hermitian if

$$\langle a|Ob\rangle = \langle Oa|b\rangle. \quad (2.4.63)$$

For an antilinear operator T

$$\langle a|Tb\rangle = \langle b|T^\dagger a\rangle, \quad (2.4.64)$$

which is antilinear in $|a\rangle$ and in $|b\rangle$. An antilinear operator is antiunitary if

$$TT^\dagger = T^\dagger T = 1, \quad (2.4.65)$$

or

$$\langle a|T^\dagger Tb\rangle = \langle Tb|Ta\rangle = \langle a|b\rangle. \quad (2.4.66)$$

The transformed of O under T

$$O' = T^\dagger OT, \quad (2.4.67)$$

is still linear and

$$\langle b|T^\dagger OTa\rangle = \langle OTa|Tb\rangle = \langle Ta|O^\dagger Tb\rangle. \quad (2.4.68)$$

In particular for $O = i$ we find

$$T^\dagger iT = TiT^\dagger = -i. \quad (2.4.69)$$

The time reversal is realizable with an antiunitary operator:

$$T^\dagger qT = q \quad T^\dagger pT = -p \quad T^\dagger sT = -s \quad (2.4.70)$$

Moreover, in order to have invariance, we must require

$$T^\dagger HT = H. \quad (2.4.71)$$

If O is an observable

$$\langle b|OTa\rangle = \langle b|TT^\dagger OTa\rangle = \langle T^\dagger OTa|T^\dagger b\rangle. \quad (2.4.72)$$

So if $T^\dagger OT = \pm O$ we have

$$\langle b|OTa\rangle = \pm \langle Oa|T^\dagger b\rangle. \quad (2.4.73)$$

For eigenstates of O , $O|a\rangle = O_a|a\rangle$, we have

$$\langle b|OTa\rangle = \pm O_a \langle a|T^\dagger b\rangle = \pm O_a \langle b|Ta\rangle, \quad (2.4.74)$$

which means that $|Ta\rangle$ is an eigenstate of O with the transformed eigenvalue.

So for a state $|a\rangle = |p, s_z\rangle$ we have

$$|Ta\rangle = | -p, -s_z\rangle, \quad (2.4.75)$$

modulo a phase.

For a spinless particle with canonical variables \mathbf{q} and \mathbf{p} the time reversal is realized through

$$\langle \mathbf{q}|Ta\rangle = \psi_{Ta}(\mathbf{q}) = \psi_a^*(\mathbf{q}) = \langle \mathbf{q}|a\rangle^*, \quad (2.4.76)$$

on wave functions in coordinate representation. In fact we have

$$\langle a|T^\dagger pTb\rangle = \langle pTb|Ta\rangle = \int \psi_b(\mathbf{q})(-i\nabla)\psi_a^*(\mathbf{q}) d\mathbf{q} = - \int \psi_a^*(\mathbf{q})(-i\nabla)\psi_b(\mathbf{q}) d\mathbf{q} = -\langle a|pb\rangle \quad (2.4.77)$$

where we used an integration by parts. Analogously we verify

$$\langle a|T^\dagger qTb\rangle = \langle qTb|Ta\rangle = \langle a|qb\rangle. \quad (2.4.78)$$

The Hamiltonian is an Hermitian function of \mathbf{q} and \mathbf{p} . In the coordinate representation, \mathbf{q} is a real variable and $\mathbf{p} = -i\nabla$. The transformation $\mathbf{p} \rightarrow -\mathbf{p}$ is equivalent to a complex conjugation. We will have invariance under T if $H(\mathbf{q}, \mathbf{p}) = H(\mathbf{q}, -\mathbf{p})$ or if H is real. A Hamiltonian of the form

$$H = \frac{\mathbf{p}^2}{2m} + V(\mathbf{q}), \quad (2.4.79)$$

is invariant under T .

If the particle has spin, it is described by $2s+1$ functions of \mathbf{q}

$$\psi(\mathbf{q}) = \begin{pmatrix} \psi_1(\mathbf{q}) \\ \vdots \\ \psi_{2s+1}(\mathbf{q}) \end{pmatrix}. \quad (2.4.80)$$

The spin is represented by three matrices $\boldsymbol{\Sigma} = (\Sigma_1, \Sigma_2, \Sigma_3)$ independent from \mathbf{q} . We now take

$$\psi_{Ta}(\mathbf{q}) = U\psi_a^*(\mathbf{q}), \quad (2.4.81)$$

with U an unitary matrix independent from \mathbf{q} and acting on spin space. To have the correct spin transformations we must have

$$\langle a|T^\dagger sTb\rangle = \langle sTb|Ta\rangle = -\langle a|sb\rangle, \quad (2.4.82)$$

or

$$-\int \psi_a^\dagger \boldsymbol{\Sigma} \psi_b = \int \psi_b^{\text{Tr}} U^\dagger \boldsymbol{\Sigma} U \psi_a^*, \quad (2.4.83)$$

which means

$$U^{\text{Tr}} \boldsymbol{\Sigma}^{\text{Tr}} U^{\dagger \text{Tr}} = -\boldsymbol{\Sigma}, \quad (2.4.84)$$

and taking the complex conjugate, since $\boldsymbol{\Sigma}^\dagger = \boldsymbol{\Sigma}$, we find

$$U^\dagger \boldsymbol{\Sigma} U = -\boldsymbol{\Sigma}^*. \quad (2.4.85)$$

With the usual choice of phases in the angular momentum representation Σ_1 and Σ_3 are real matrices and Σ_2 is pure imaginary.

For example for spin 1/2 particles

$$\Sigma_3 = \frac{1}{2} \begin{pmatrix} 1 & 0 \\ 0 & -1 \end{pmatrix} \quad \Sigma_1 = \frac{1}{2} \begin{pmatrix} 0 & 1 \\ 1 & 0 \end{pmatrix} \quad \Sigma_2 = \frac{1}{2} \begin{pmatrix} 0 & i \\ -i & 0 \end{pmatrix} \quad (2.4.86)$$

Then apart from an unessential phase we find

$$U = e^{i\pi\Sigma_2}, \quad (2.4.87)$$

a rotation of π around the 2 axis, which changes sign to Σ_1 and Σ_3 . In conclusions we have

$$\psi_{Ta} = e^{i\pi\Sigma_2} \psi_a^*. \quad (2.4.88)$$

2.5 Einstein Relativity

The invariance under the Galileo group is valid in the limit of small velocities. But, actually, physics is invariant under Lorentz transformations in addition to spatial translations. This invariance is known as Einstein relativity.

The Lorentz group is defined as the group of linear transformations which leaves invariant the quadratic form

$$ds^2 = dt^2 - dx^2. \quad (2.5.1)$$

Let $dx = (dx^0, dx^1, dx^2, dx^3) = (dt, dx)$ we can write

$$ds^2 = g_{\mu\nu} dx^\mu dx^\nu, \quad (2.5.2)$$

where Einstein summation convention is used with

$$g_{\mu\nu} = g^{\mu\nu} = \begin{pmatrix} 1 & 0 & 0 & 0 \\ 0 & -1 & 0 & 0 \\ 0 & 0 & -1 & 0 \\ 0 & 0 & 0 & -1 \end{pmatrix} \quad g^{\mu\nu} g_{\nu\alpha} = \delta_\alpha^\mu \quad (2.5.3)$$

The Lorentz transformations are defined as the linear transformations

$$dx'^\mu = \Lambda_\nu^\mu dx^\nu, \quad (2.5.4)$$

such that

$$g_{\mu\nu} dx'^\mu dx'^\nu = g_{\mu\nu} \Lambda_\alpha^\mu \Lambda_\beta^\nu dx^\alpha dx^\beta. \quad (2.5.5)$$

Due to the arbitrariness of dx^μ we have

$$g_{\mu\nu} = g_{\alpha\beta} \Lambda_\mu^\alpha \Lambda_\nu^\beta, \quad (2.5.6)$$

or

$$g = \mathbf{\Lambda}^{\text{Tr}} g \mathbf{\Lambda}, \quad (2.5.7)$$

which defines the Lorentz group. Taking the 00 component in Eq. (2.5.6)

$$1 = g_{\alpha\beta} \Lambda_0^\alpha \Lambda_0^\beta = (\Lambda_0^0)^2 - \sum_i (\Lambda_0^i)^2, \quad (2.5.8)$$

or

$$(\Lambda_0^0)^2 \geq 1, \quad (2.5.9)$$

or

$$\Lambda_0^0 \geq 1 \quad \text{or} \quad \Lambda_0^0 \leq -1. \quad (2.5.10)$$

Taking the determinant in Eq. (2.5.6) follows

$$(\det \mathbf{\Lambda})^2 = 1, \quad (2.5.11)$$

or

$$\det \Lambda = \pm 1. \quad (2.5.12)$$

The transformations obtained continuously from the identity have $\Lambda^0_0 \geq 1$ and $\det \Lambda = 1$ and constitute the *proper* Lorentz group. The transformations with $\Lambda^0_0 \geq 1$ and $\det \Lambda = -1$ can be written as the product of the parity $P : x \rightarrow -x$ times a proper transformation. The ones with $\Lambda^0_0 \leq -1$ and $\det \Lambda = 1$ as a product of the time reversal $T : x^0 \rightarrow -x^0$ times the proper transformations. The ones with $\Lambda^0_0 \leq 1$ and $\det \Lambda = -1$ as PT times a proper transformation.

An infinitesimal proper transformation

$$\Lambda^\mu_{\mu'} = \delta^\mu_{\mu'} + \Omega^\mu_{\mu'}, \quad (2.5.13)$$

must satisfy Eq. (2.5.6). So

$$g_{\mu'\nu'} = g_{\mu'\nu'} + \Omega^\mu_{\mu'} g_{\mu\nu'} + \Omega^\nu_{\nu'} g_{\nu\mu'} + \mathcal{O}(\Omega^2). \quad (2.5.14)$$

Let

$$\Omega_{\mu\nu} = g_{\mu\alpha} \Omega^\alpha_\nu, \quad (2.5.15)$$

then we must have

$$\Omega_{\mu\nu} = -\Omega_{\nu\mu}. \quad (2.5.16)$$

The group has 6 parameters as the number of components of an antisymmetric 4×4 matrix. The most general 4×4 antisymmetric matrix can be written as

$$\Omega_{\mu\nu} = \frac{1}{2} \sum_{\rho\sigma} \omega_{(\rho\sigma)} M_{\mu\nu}^{(\rho\sigma)}, \quad (2.5.17)$$

$$M_{\mu\nu}^{(\rho\sigma)} = \delta^\rho_\mu \delta^\sigma_\nu - \delta^\rho_\nu \delta^\sigma_\mu = -M_{\mu\nu}^{(\sigma\rho)}. \quad (2.5.18)$$

We write

$$\left(M^{(\rho\sigma)} \right)^\mu_\nu = g^{\mu\alpha} M_{\alpha\nu}^{(\rho\sigma)}, \quad (2.5.19)$$

so

$$\Omega^\mu_\nu = g^{\mu\alpha} \Omega_{\alpha\nu} = g^{\mu\alpha} \frac{1}{2} \omega_{(\rho\sigma)} M_{\mu\nu}^{(\rho\sigma)} = \frac{1}{2} \omega_{(\rho\sigma)} \left(M^{(\rho\sigma)} \right)^\mu_\nu. \quad (2.5.20)$$

The matrices $M^{(\mu\nu)}$ satisfy the following algebra

$$[M^{(\alpha\beta)}, M^{(\mu\nu)}] = - \left(g^{\alpha\mu} M^{(\beta\nu)} + g^{\beta\nu} M^{(\alpha\mu)} - g^{\beta\mu} M^{(\alpha\nu)} - g^{\alpha\nu} M^{(\beta\mu)} \right). \quad (2.5.21)$$

We can then introduce

$$J^{(\mu\nu)} \equiv -i M^{(\mu\nu)}, \quad (2.5.22)$$

and

$$J^i = -\frac{1}{2} \epsilon_{0ijk} J^{(jk)}, \quad (2.5.23)$$

$$K^i = J^{(0i)}, \quad (2.5.24)$$

where $\epsilon_{\mu_0\mu_1\mu_2\mu_3}$ is the Levi-Civita symbol with $\epsilon_{0123} = 1$ ¹. Then Eq. (2.5.21) is rewritten as

$$[J^i, J^j] = i\epsilon_{ijk}J^k, \quad (2.5.28)$$

$$[J^i, K^j] = i\epsilon_{ijk}K^k, \quad (2.5.29)$$

$$[K^i, K^j] = -i\epsilon_{ijk}J^k. \quad (2.5.30)$$

The generators J^i are the rotations generators, which constitute a subgroup of the Lorentz transformations. The K^i are the generators of the velocity (v) transformations and are vectors, as follows from their commutation relations with the J^i . The infinitesimal transformations are then

$$\Lambda = 1 + i(\boldsymbol{\theta} \cdot \mathbf{J} - \boldsymbol{\alpha} \cdot \mathbf{K}). \quad (2.5.31)$$

The finite ones are

$$\Lambda = e^{\frac{i}{2} \sum_{\alpha\beta} J^{(\alpha\beta)} \omega_{(\alpha\beta)}} = e^{i(\boldsymbol{\theta} \cdot \mathbf{J} - \boldsymbol{\alpha} \cdot \mathbf{K})} \quad \mathbf{v} = (\tanh \alpha_1, \tanh \alpha_2, \tanh \alpha_3), \quad (2.5.32)$$

where $\boldsymbol{\theta}$ is the rotation angle vector and $\boldsymbol{\alpha}$ is the rapidity vector.

Under the Lorentz group the generators of the translations p_μ must transform as four-vectors

$$[J^{(\mu\nu)}, p^\alpha] = i(g^{\mu\alpha}p^\nu - g^{\alpha\nu}p^\mu), \quad (2.5.33)$$

or

$$[J, p^0] = -\delta p^0 = -J p^0 = 0, \quad (2.5.34)$$

which expresses the conservation of angular momentum, and

$$[J^i, p^j] = -\delta p^j = -J^i p^j = i\epsilon_{ijk}p^k, \quad (2.5.35)$$

which tells us that p is a vector. On the momenta the generators of the velocity transformations act as follows

$$[K^i, p^0] = -\delta p^0 = -K^i p^0 = ig^{00}p^i, \quad (2.5.36)$$

$$[K^i, p^j] = -\delta p^j = -K^i p^j = -ig^{ij}p^0. \quad (2.5.37)$$

The invariance under translations is written as

$$[p^\mu, p^\nu] = 0. \quad (2.5.38)$$

The commutation relations between the generators are then

$$[p^\mu, p^\nu] = 0, \quad (2.5.39)$$

$$[J^{(\mu\nu)}, p^\alpha] = i(g^{\mu\alpha}p^\nu - g^{\alpha\nu}p^\mu), \quad (2.5.40)$$

$$[J^{(\alpha\beta)}, J^{(\mu\nu)}] = i(g^{\alpha\mu}J^{(\beta\nu)} + g^{\beta\nu}J^{(\alpha\mu)} - g^{\beta\mu}J^{(\alpha\nu)} - g^{\alpha\nu}J^{(\beta\mu)}). \quad (2.5.41)$$

¹For any antisymmetric tensor $F^{\mu\nu}$ it is possible to use a decomposition of the following kind: $F^{\mu\nu} = (\mathbf{P}, \mathbf{A})$ with

$$A^1 = -F^{23} \quad A^2 = -F^{31} \quad A^3 = -F^{12} \quad (2.5.25)$$

$$P^1 = F^{01} \quad P^2 = F^{02} \quad P^3 = F^{03} \quad (2.5.26)$$

For the product of two tensors of this kind we have

$$\frac{1}{2} F_{\mu\nu}^{(1)} F^{(2)\mu\nu} = \mathbf{A}^{(1)} \cdot \mathbf{A}^{(2)} - \mathbf{P}^{(1)} \cdot \mathbf{P}^{(2)}. \quad (2.5.27)$$

They define the Lie algebra of a 10 parameters group known as the Poincaré group.

The Poincaré group is defined by the transformation laws

$$(\Lambda, a) : x \rightarrow x' = \Lambda x - a, \quad (2.5.42)$$

where a is a translation and Λ is a Lorentz transformation. We immediately find the multiplication properties of the group as

$$(\Lambda_1, a)(\Lambda_2, b) = (\Lambda_1 \Lambda_2, -\Lambda_1 b - a), \quad (2.5.43)$$

from which immediately follows that the translations are an abelian invariant subgroup. In fact applying repetitively Eq. (2.5.43) we find that the transformed by similitude of a translation $(1, a)$,

$$(\Lambda, c)(1, a)(\Lambda^{-1}, -c) = (1, \Lambda(c - a) - c), \quad (2.5.44)$$

is still a translation.

By Wigner theorem the states of a physical system are the basis of a unitary representation of the Poincaré group. An elementary system will be described by an irreducible representation of the Poincaré group.

We note that

$$J_{\pm} = \frac{J \pm iK}{2}, \quad (2.5.45)$$

obey the following commutation relations

$$[J_+^i, J_+^j] = i\epsilon_{ijk}J_+^k, \quad (2.5.46)$$

$$[J_-^i, J_-^j] = i\epsilon_{ijk}J_-^k, \quad (2.5.47)$$

$$[J_+^i, J_-^j] = 0. \quad (2.5.48)$$

So the generators of J_+ and J_- obey to the algebra $SU(2) \otimes SU(2)$. Let us show now that an irreducible representation of the Poincaré group, i.e. an elementary particle, is determined by the mass and the spin.

An irreducible representation is characterized by the value of the *invariants*, i.e. of the operators built with the generators of the group that commute with all the group generators. We then define

$$\Gamma_{\mu} = \frac{1}{2}\epsilon_{\mu\alpha\beta\sigma}J^{(\alpha\beta)}p^{\sigma}, \quad (2.5.49)$$

$$\Gamma_{\mu}p^{\mu} = 0, \quad (2.5.50)$$

$$g^{\mu} = J^{(\mu\nu)}p_{\nu}, \quad (2.5.51)$$

$$g^{\mu}p_{\mu} = 0. \quad (2.5.52)$$

One can prove Shirokov [1958a,b,c,d, 1959]² that

$$p^2 J^{(\mu\nu)} = g^{\mu}p^{\nu} - g^{\nu}p^{\mu} - \epsilon^{\sigma\mu\nu\lambda}\Gamma_{\sigma}p_{\lambda}. \quad (2.5.54)$$

²One can use the identity

$$\epsilon^{\sigma\mu\nu\lambda}\epsilon_{\sigma\alpha\beta\rho} = \det \begin{pmatrix} \delta_{\alpha}^{\mu} & \delta_{\beta}^{\mu} & \delta_{\rho}^{\mu} \\ \delta_{\alpha}^{\nu} & \delta_{\beta}^{\nu} & \delta_{\rho}^{\nu} \\ \delta_{\alpha}^{\lambda} & \delta_{\beta}^{\lambda} & \delta_{\rho}^{\lambda} \end{pmatrix}, \quad (2.5.53)$$

and the definition of Γ_{σ} to calculate the product $\epsilon^{\sigma\mu\nu\lambda}\Gamma_{\sigma}p_{\lambda}$.

This tells us that $J^{(\mu\nu)}$ can be expressed in terms of p_μ, Γ_μ , and g_μ if $p^2 = p_\mu p^\mu \neq 0$.

Moreover we have

$$[\Gamma_\mu, \Gamma_\nu] = i\epsilon_{\rho\mu\nu\lambda}\Gamma^\rho p^\lambda, \quad (2.5.55)$$

$$[g_\mu, \Gamma_\sigma] = -i\Gamma_\mu p_\sigma, \quad (2.5.56)$$

$$[g_\mu, p_\nu] = i(g_{\mu\nu}p^2 - p_\mu p_\nu), \quad (2.5.57)$$

$$[g_\mu, g_\nu] = -i(g^\mu p^\nu - g^\nu p^\mu - \epsilon^{\sigma\mu\nu\lambda}\Gamma_\sigma p_\lambda) \quad (2.5.58)$$

$$[p_\mu, \Gamma_\sigma] = 0. \quad (2.5.59)$$

An invariant should be constructed with the vectors p_μ, Γ_μ , and g_μ . Recalling that $g_\mu p^\mu = 0$ and $\Gamma_\mu p^\mu = 0$ the only independent invariants under the Lorentz group are

$$p^2, \Gamma^2, g^2, \Gamma_\mu g^\mu. \quad (2.5.60)$$

But g^2 and $\Gamma_\mu g^\mu$ do not commute with translations. Then the representation is determined by p^2, Γ^2 , and by the sign of p^0 , which is also invariant under the proper Lorentz group and commutes with translations, if $p^2 \geq 0$.

The physical interpretation of the two invariants is obvious:

- i. For the invariant p^2 we have 4 cases

$$p^2 > 0, \quad (2.5.61)$$

$$p^2 = 0 \quad p \neq 0, \quad (2.5.62)$$

$$p^2 = 0 \quad p = 0, \quad (2.5.63)$$

$$p^2 < 0. \quad (2.5.64)$$

Since $p^2 = m^2$ we will be interested only in the first two cases. In these two cases, for the representations of the proper group ($\Lambda_0^0 \geq 0$ and $\det \Lambda = 1$) we will have another invariant, namely the sign of p^0 .

- ii. The invariant Γ^2 can be calculated in the reference frame where $p = 0$. In such a frame

$$\Gamma = (\Gamma^0, \Gamma^1, \Gamma^2, \Gamma^3) = (\Gamma^0, \mathbf{\Gamma}) = (0, m\mathbf{J}) \quad \Gamma^2 = -m^2 J(J+1). \quad (2.5.65)$$

The modulus of \mathbf{J} in the rest frame is by definition the particle spin, so $\Gamma^2 = -m^2 s(s+1)$

Then the representation is determined by the mass m and by the spin s , exactly as in the nonrelativistic happens for the Galileo group.

2.5.1 The irreducible unitary representation of the Poincaré group

We want now to explicitly construct the irreducible unitary representations of the Poincaré group.

Massive particles

We can build a base of the Hilbert space which diagonalizes simultaneously the components p_μ of the four-momentum, which commute among themselves, and other observables which we will denote by now with σ . The vector of the base will have the form $|\mathbf{p}, \sigma\rangle$ with

$$p_i |\mathbf{p}, \sigma\rangle = p_i |\mathbf{p}, \sigma\rangle \quad p_0 |\mathbf{p}, \sigma\rangle = \text{sgn}(p_0) p_0 |\mathbf{p}, \sigma\rangle, \quad (2.5.66)$$

with $p_0 = p^0 = \sqrt{\mathbf{p}^2 + m^2}$ and $\mathbf{p} = (p^1, p^2, p^3) = (-p_1, -p_2, -p_3)$. We will call $U(\Lambda)$ the unitary operators which represents the generic Lorentz transformation Λ . We will have

$$U(\Lambda)|\mathbf{p}, \sigma\rangle = \sum_{\sigma'} \mathcal{R}(\Lambda, \mathbf{p})_{\sigma\sigma'} |\Lambda\mathbf{p}, \sigma'\rangle. \quad (2.5.67)$$

In fact, using the group algebra we have

$$U^\dagger(\Lambda)p_\mu U(\Lambda) = \Lambda^\nu_\mu p_\nu, \quad (2.5.68)$$

then

$$\begin{aligned} p_\mu U(\Lambda)|\mathbf{p}, \sigma\rangle &= U(\Lambda)U^\dagger(\Lambda)p_\mu U(\Lambda)|\mathbf{p}, \sigma\rangle \\ &= \Lambda^\nu_\mu p_\nu U(\Lambda)|\mathbf{p}, \sigma\rangle. \end{aligned} \quad (2.5.69)$$

So $U(\Lambda)|\mathbf{p}, \sigma\rangle$ belongs to the eigenvalue $(\Lambda\mathbf{p})_\mu$ of the four-momentum. And this proves Eq. (2.5.67). The Lorentz invariant measure, for momentum $\mathbf{p} = (p^0, p^1, p^2, p^3) = (p^0, \mathbf{p})$, is

$$d\Omega_{\mathbf{p}} = \frac{d^4 p}{(2\pi)^3} \delta(\sqrt{\mathbf{p}^2} - m)\theta(p_0) = \frac{d^3 \mathbf{p}}{(2\pi)^3 2p_0}. \quad (2.5.70)$$

One can easily verify that with the invariant normalization

$$\langle \mathbf{p}', \sigma' | \mathbf{p}, \sigma \rangle = (2\pi)^3 2p_0 \delta(\mathbf{p} - \mathbf{p}') \delta_{\sigma\sigma'}, \quad (2.5.71)$$

the matrix $\mathcal{R}(\Lambda, \mathbf{p})_{\sigma\sigma'}$ in Eq. (2.5.67) is unitary due to the unitarity of $U(\Lambda)$.

The operator Γ_μ commutes with all the components of p_μ . Then when applied to the state $|\mathbf{p}, \sigma\rangle$ it can only mix it with states of the same \mathbf{p} .

Let us start by considering the case $\mathbf{p}^2 = m^2 > 0$ with $\mathbf{p} = \mathbf{0}$, $|\mathbf{0}, \sigma\rangle$, for which

$$\mathbf{p}|\mathbf{0}, \sigma\rangle = \mathbf{0} \quad p_0|\mathbf{0}, \sigma\rangle = \text{sgn}(p_0)m|\mathbf{0}, \sigma\rangle. \quad (2.5.72)$$

On this subspace $\Gamma_\mu = \frac{1}{2}\epsilon_{\mu\alpha\beta\gamma}J^{(\alpha\beta)}p^\gamma$ can be easily calculated

$$\Gamma_0 = 0 \quad \mathbf{\Gamma} = m\mathbf{J} = ms. \quad (2.5.73)$$

The angular momentum of the rest frame is called spin by definition. The dimension of the subspace is $2s + 1$.

For the variable σ we can take the eigenvalue of one of the spin component, i.e. s_3 .

If $U(\Lambda_p)$ is a Lorentz transformation which brings the momentum from $\mathbf{0}$ to a certain value \mathbf{p} , since Γ^μ is a four-vector, we will have

$$U^\dagger(\Lambda_p)\Gamma^\mu U(\Lambda_p) = (\Lambda_p)^\mu_\nu \Gamma^\nu. \quad (2.5.74)$$

If we call $\bar{\Gamma}_{\sigma'\sigma}^\mu$ the representative of the Γ^μ on the subspace $|\mathbf{0}, \sigma\rangle$ we will have

$$\begin{aligned} \Gamma^\mu U(\Lambda_p)|\mathbf{0}, \sigma\rangle &= U(\Lambda_p)U^\dagger(\Lambda_p)\Gamma^\mu U(\Lambda_p)|\mathbf{0}, \sigma\rangle \\ &= U(\Lambda_p)(\Lambda_p)^\mu_\nu \Gamma^\nu |\mathbf{0}, \sigma\rangle \\ &= (\Lambda_p)^\mu_\nu \bar{\Gamma}_{\sigma'\sigma}^\nu U(\Lambda_p)|\mathbf{0}, \sigma\rangle. \end{aligned} \quad (2.5.75)$$

Then $(\Lambda_p)^\mu_\nu \bar{\Gamma}_{\sigma'\sigma}^\nu$ is the representative of Γ^μ on the subspace $|\mathbf{p}, \sigma\rangle$, in the representation in which the base vectors are $|\mathbf{p}, \sigma\rangle = U(\Lambda_p)|\mathbf{0}, \sigma\rangle$.

The Lorentz transformation $U(\Lambda_p)$ which brings the momentum from $\mathbf{0}$ to p is not univocally defined: it is indetermined on the right by a transformation of the small group³ of the initial momentum $\mathbf{0}$ and on the left by a transformation of the small group of the final momentum p .

For each choice of these transformations we will have a choice of the base vectors $U(\Lambda_p)|\mathbf{0}, \sigma\rangle$ and of the representative of Γ^μ . We will adopt, in the following, a standard choice for $U(\Lambda_p)$. Namely a simple velocity transformation $e^{-i\alpha \cdot K}$ in the p direction, which sends the momentum from $\mathbf{0}$ to p . The base vectors are then

$$|p, \sigma\rangle = U(\Lambda_p)|\mathbf{0}, \sigma\rangle = e^{-i\alpha \cdot K}|\mathbf{0}, \sigma\rangle, \quad (2.5.76)$$

and

$$\Gamma^\mu(p) = (\Lambda_p)^\mu_\nu \Gamma^\nu(\mathbf{0}) = \left(p \cdot s, ms + \frac{(p \cdot s)p}{p^0 + m} \right). \quad (2.5.77)$$

This can be proved as follows. We can write for a general velocity transformation

$$\Lambda_p = \begin{pmatrix} \gamma & -\gamma \beta^{\text{Tr}} \\ -\gamma \beta & \mathbf{1} + (\gamma - 1)\beta \beta^{\text{Tr}}/\beta^2 \end{pmatrix} \quad \gamma = \frac{1}{\sqrt{1 - \beta^2}}, \quad (2.5.78)$$

with

$$-\gamma \beta = \frac{p}{m} \implies \gamma = \frac{p_0}{m} \quad \text{and} \quad (\gamma - 1)/\beta^2 = \frac{p_0^2}{m(p_0 + m)} \quad (2.5.79)$$

The transformation we are looking for is then

$$(\Lambda_p)^\mu_\nu = \delta^\mu_\nu - \frac{1}{p_0 + m} \left[m \delta^\mu_0 \delta^0_\nu + \delta^\mu_0 p_\nu + \frac{p^\mu p_\nu}{m} - \delta^0_\nu p^\mu \left(1 + 2 \frac{p_0}{m} \right) \right], \quad (2.5.80)$$

from which we immediately find Eq. (2.5.77).

To complete the construction of the representation we could now look for the representative of g_μ defined in (2.5.51), using the commutation relations (2.5.55)-(2.5.59), and construct the representative of the generic $J^{(\mu\nu)}$ using Eq. (2.5.54). Alternatively we may proceed as follows:

- a) Let us first consider the rotations. If Λ is a rotation R_θ

$$U(R_\theta)|p, \sigma\rangle = U(R_\theta)U(\Lambda_p)U^\dagger(R_\theta)U(R_\theta)|\mathbf{0}, \sigma\rangle. \quad (2.5.81)$$

We know that

$$U(\Lambda_p) = e^{-i\alpha \cdot K}, \quad (2.5.82)$$

and since

$$U^\dagger(R_\theta)KU(R_\theta) = R_\theta K, \quad (2.5.83)$$

we have

$$U(R_\theta)U(\Lambda_p)U^\dagger(R_\theta) = e^{-i(R_\theta \alpha) \cdot K}, \quad (2.5.84)$$

and

$$U(R_\theta)|p, \sigma\rangle = \left(e^{i\theta \cdot s} \right)_{\sigma' \sigma} |R_\theta p, \sigma'\rangle. \quad (2.5.85)$$

³The small group of p is the subgroup of the transformations which leaves p unchanged.

b) For a Lorentz transformation sending \mathbf{p} into \mathbf{p}'

$$U(\Lambda)|\mathbf{p}, \sigma\rangle = U(\Lambda_{\mathbf{p}'})U^\dagger(\Lambda_{\mathbf{p}'})U(\Lambda)U(\Lambda_{\mathbf{p}})|\mathbf{0}, \sigma\rangle. \quad (2.5.86)$$

The matrix $U^\dagger(\Lambda_{\mathbf{p}'})U(\Lambda)U(\Lambda_{\mathbf{p}})$ belongs to the small group of $\mathbf{p} = \mathbf{0}$, i.e. it is a rotation $R(\Lambda, \mathbf{p})$ in the subspace $|\mathbf{0}, \sigma\rangle$. To determine it we just need to calculate

$$\Lambda_{\mathbf{p}'}^{-1}\Lambda\Lambda_{\mathbf{p}}, \quad (2.5.87)$$

using the formula (2.5.80) and the explicit one (2.5.78). If we call $\mathcal{R}(\Lambda, \mathbf{p})_{\sigma'\sigma}$ the representative of such a rotation in the space $|\mathbf{0}, \sigma\rangle$ we will have

$$U(\Lambda)|\mathbf{p}, \sigma\rangle = \mathcal{R}(\Lambda, \mathbf{p})_{\sigma'\sigma}|\Lambda\mathbf{p}, \sigma\rangle. \quad (2.5.88)$$

Explicitly, if Λ is a velocity transformation with velocity β in the direction $\hat{\mathbf{n}}$, we find

$$\begin{aligned} (\Lambda_{\mathbf{p}'}^{-1}\Lambda\Lambda_{\mathbf{p}},)^{\mu}_{\nu} &= \begin{pmatrix} \bar{\mathcal{R}}_0^0 & \bar{\mathcal{R}}_0^j \\ \bar{\mathcal{R}}_i^0 & \bar{\mathcal{R}}_i^j \end{pmatrix} = \begin{pmatrix} \frac{p'_0}{m} & -\frac{p'_j}{m} \\ -\frac{p'_i}{m} & \delta_{ik} + \frac{p'_i p'_k}{m(p'_0 + m)} \end{pmatrix} \times \\ &\quad \begin{pmatrix} \gamma & -\gamma\beta n_l \\ -\gamma\beta n_k & \delta_{kl} + (\gamma - 1)n_k n_l \end{pmatrix} \begin{pmatrix} \frac{p_0}{m} & \frac{p_j}{m} \\ \frac{p_l}{m} & \delta_{lj} + \frac{m p_l p_j}{m(p_0 + m)} \end{pmatrix}. \end{aligned} \quad (2.5.89)$$

To first order in β

$$p'_0 = \gamma p_0 - \gamma\beta\hat{\mathbf{n}} \cdot \mathbf{p} = p_0 - \boldsymbol{\beta} \cdot \mathbf{p} + \mathcal{O}(\beta^2), \quad (2.5.90)$$

$$\mathbf{p}' = -\gamma\beta\hat{\mathbf{n}}p_0 + \mathbf{p} + (\gamma - 1)\hat{\mathbf{n}}(\hat{\mathbf{n}} \cdot \mathbf{p}) = \mathbf{p} - \boldsymbol{\beta}p_0 + \mathcal{O}(\beta^2), \quad (2.5.91)$$

and

$$\bar{\mathcal{R}}_i^j = \delta_i^j + \frac{\beta}{p_0 + m}(n^i p_j - p^i n_j) + \mathcal{O}(\beta^2). \quad (2.5.92)$$

Recalling that in the vector representation $(J^i)_{jk} = i\epsilon_{jik}$ and using $\epsilon_{ijk}\epsilon_{ilm} = \delta_{jl}\delta_{km} - \delta_{jm}\delta_{kl}$ we finally find

$$\mathcal{R} \approx 1 - i\frac{\boldsymbol{\beta} \wedge \mathbf{p}}{p_0 + m} \cdot \mathbf{J}. \quad (2.5.93)$$

The finite transformation $\mathcal{R}(\Lambda, \mathbf{p})$ is then of the following form

$$\mathcal{R}(\Lambda, \mathbf{p}) = e^{-i\frac{\boldsymbol{\beta} \wedge \mathbf{p}}{p_0 + m} \cdot \mathbf{J}}. \quad (2.5.94)$$

This rotation is called the Wigner rotation.

The transformations on the wave functions can be determined from the one on the states. The generic $|\phi\rangle$ is written as

$$|\phi\rangle = \int d\Omega_{\mathbf{p}} \varphi_{\sigma}(\mathbf{p}) |\mathbf{p}, \sigma\rangle, \quad (2.5.95)$$

and the scalar product

$$\langle \phi' | \phi \rangle = \int d\Omega_{\mathbf{p}} \varphi'^*(\mathbf{p}) \varphi(\mathbf{p}). \quad (2.5.96)$$

Under a transformation $U(\Lambda, a)$

$$|\Lambda\phi\rangle = U(\Lambda, a)|\phi\rangle = \int d\Omega_{\mathbf{p}} e^{-ipa} \varphi_\sigma(\mathbf{p}) \mathcal{R}(\Lambda, \mathbf{p})_{\sigma'\sigma} |\Lambda\mathbf{p}, \sigma'\rangle. \quad (2.5.97)$$

Changing variables from \mathbf{p} to $\Lambda^{-1}\mathbf{p}$ and using the fact that the measure is invariant we find

$$|\Lambda\phi\rangle = \int d\Omega_{\mathbf{p}} e^{-i(\Lambda^{-1}\mathbf{p})a} \mathcal{R}_{\sigma'\sigma} \varphi_\sigma(\Lambda^{-1}\mathbf{p}) |\mathbf{p}, \sigma'\rangle, \quad (2.5.98)$$

or

$$(\Lambda\varphi)_\sigma(\mathbf{p}) = \mathcal{R}_{\sigma\sigma'} \varphi_{\sigma'}(\Lambda^{-1}\mathbf{p}). \quad (2.5.99)$$

The matrix \mathcal{R} is given by Eq. (2.5.85) for the rotations and by Eq. (2.5.89) for the velocity transformations and is unitary respect to the metric $\langle \phi' | \phi \rangle$.

For an infinitesimal transformation Eq. (2.5.99) gives the form of the generators:

- a) For an infinitesimal rotation of an angle $\boldsymbol{\theta}$

$$\Lambda^{-1}\mathbf{p} \approx \mathbf{p} + \boldsymbol{\theta} \wedge \mathbf{p} \quad \mathcal{R} \approx 1 + i\boldsymbol{\theta} \cdot \mathbf{s}, \quad (2.5.100)$$

so

$$\delta\varphi_\sigma \equiv (\Lambda\varphi_\sigma) - \varphi_\sigma \approx i\boldsymbol{\theta} \cdot \mathbf{s}_{\sigma\sigma'} \varphi_{\sigma'} + (\boldsymbol{\theta} \wedge \mathbf{p}) \frac{\partial}{\partial \mathbf{p}} \varphi_\sigma. \quad (2.5.101)$$

The generator is defined by $\delta\varphi = i(\boldsymbol{\theta} \cdot \mathbf{J})\varphi$ so

$$\mathbf{J} = \mathbf{s} - ip \wedge \frac{\partial}{\partial \mathbf{p}}. \quad (2.5.102)$$

- b) For a velocity transformation

$$\Lambda^{-1}\mathbf{p} \approx \mathbf{p} + \beta p_0 \quad \mathcal{R} \approx 1 - i \frac{\boldsymbol{\beta} \wedge \mathbf{p}}{p_0 + m} \cdot \mathbf{s}, \quad (2.5.103)$$

so

$$\delta\varphi_\sigma \approx -i(\boldsymbol{\beta} \cdot \mathbf{K})\varphi_\sigma = -i \frac{\boldsymbol{\beta} \wedge \mathbf{p}}{p_0 + m} \cdot \mathbf{s}_{\sigma\sigma'} \varphi_{\sigma'} + \boldsymbol{\beta} \cdot p_0 \frac{\partial}{\partial \mathbf{p}} \varphi_\sigma, \quad (2.5.104)$$

or

$$\mathbf{K} = \frac{\mathbf{p} \wedge \mathbf{s}}{p_0 + m} + ip_0 \frac{\partial}{\partial \mathbf{p}}. \quad (2.5.105)$$

One can verify that the generators \mathbf{J} and \mathbf{K} satisfy the algebra of the group. This completes the construction of the representation of the group on the Hilbert space of the multiplets of functions $\varphi(\mathbf{p})$ with the metric of Eq. (2.5.96).

The Helicity

We just saw that states can be taken as simultaneous eigenstates of p^2 and Γ^2 and accordingly labeled as $|m, s, \dots\rangle$, with

$$p^2|m, s, \dots\rangle = m^2|m, s, \dots\rangle, \quad (2.5.106)$$

$$\Gamma^2|m, s, \dots\rangle = -ms(s+1)|m, s, \dots\rangle. \quad (2.5.107)$$

What are the additional quantum numbers we can use to label the states? They must be eigenvalues of operators which commute with each other. So we are free to consider states of definite four-momentum p_μ . Since the mass is already fixed, it is only necessary to specify in addition the three-momentum p , the energy being determined by $p^0 = \sqrt{m^2 + p^2}$. We cannot simultaneously give definite value for the third component of the angular momentum operator J^3 because J and p do not commute. However there is an angular momentum operator which commutes with p , namely the *helicity*. This operator is the component of the spin along the direction of the momentum, $J \cdot p / |p|$, and its eigenvalues are labeled a . Thus the complete specification of the momentum eigenstates of a massive particle is $|m, s; p, a\rangle$ with

$$p_\mu|m, s; p, a\rangle = p_\mu|m, s; p, a\rangle, \quad (2.5.108)$$

$$\frac{\mathbf{J} \cdot \mathbf{p}}{|p|}|m, s; p, a\rangle = a|m, s; p, a\rangle. \quad (2.5.109)$$

Massless particles

Let us consider the base $|p, \sigma\rangle$. For $p^2 = 0$ it does not exist a rest frame. We will take as the standard state the state with

$$p^\mu = (\bar{p}, 0, 0, \bar{p}), \quad (2.5.110)$$

with \bar{p} chosen arbitrarily. We will call $|\bar{p}, \sigma\rangle$ the corresponding subspace. We will assume $\text{sgn}(p^0) = 1$. The discussion for $\text{sgn}(p^0) = -1$ is analogous.

On the states $|\bar{p}, \sigma\rangle$, Γ^μ acts mixing them, since it commutes with p^μ . The condition $\Gamma^\mu p_\mu = 0$ gives

$$\bar{p}(\Gamma^0 - \Gamma^3) = 0. \quad (2.5.111)$$

We will define

$$\Gamma^0 = \bar{p}\tilde{\Gamma} \quad \Gamma^\pm = \Gamma^1 \pm \Gamma^2. \quad (2.5.112)$$

The the commutation rule

$$[\Gamma_\mu, \Gamma_\nu] = i\epsilon_{\mu\nu\rho\lambda}\Gamma^\rho p^\lambda, \quad (2.5.113)$$

gives

$$[\Gamma^\pm, \tilde{\Gamma}] = \mp\Gamma^\pm, \quad (2.5.114)$$

$$[\Gamma^+, \Gamma^-] = 0, \quad (2.5.115)$$

$$[\Gamma^2, \tilde{\Gamma}] = 0, \quad (2.5.116)$$

$$[\Gamma^2, \Gamma^\pm] = 0. \quad (2.5.117)$$

Moreover

$$\Gamma^2 = \Gamma^+ \Gamma^-, \quad (2.5.118)$$

since $\Gamma_0^2 - \Gamma_3^2 = 0$.

In a unitary representation $\Gamma^+ = (\Gamma^-)^\dagger$. If we diagonalize $\tilde{\Gamma}$,

$$\tilde{\Gamma}|\bar{p}, a\rangle = a|\bar{p}, a\rangle, \quad (2.5.119)$$

from Eq. (2.5.114) the operators Γ^+ and Γ^- are the operators of higher and lowering of a respectively. Their representative is then

$$(\Gamma^+)_m n = b_n \delta_{m,n+1}, \quad (2.5.120)$$

$$(\Gamma^-)_m n = b_m^* \delta_{n,m+1}. \quad (2.5.121)$$

$$(2.5.122)$$

Then Eq. (2.5.118) imposes $\Gamma^2 = |b_n|^2 = \alpha^2$, independent from n . If $\alpha \neq 0$ the Γ^μ representation is infinite dimensional. In order to have a finite number of states of fixed spin and momentum it must be $\alpha = 0$. This implies $\Gamma^+ = \Gamma^- = 0$ and, by Eq. (2.5.118), $\Gamma^2 = 0$. So we can say that

$$\Gamma^\mu = \tilde{\Gamma} p^\mu. \quad (2.5.123)$$

The physical significance of $\tilde{\Gamma}$ can be obtained from the definition (2.5.49) of Γ^μ

$$\tilde{\Gamma} = \frac{\mathbf{J} \cdot \mathbf{p}}{|\mathbf{p}|}. \quad (2.5.124)$$

$\tilde{\Gamma}$ is the projection of the spin on the direction of motion, i.e. the helicity.

From Eq. (2.5.123) follows that $\tilde{\Gamma}$ is an invariant. For a massless particle the helicity is a Poincaré invariant. The representation is one dimensional. The helicity is a pseudoscalar: A representation with a fixed helicity defines a system which is not invariant under parity because the transformed state has opposite helicity and is not a possible state. The invariance under parity requires the direct sum of the representations with opposite helicity. The photon exists in the two states of helicity ± 1 .

We will define the generic state $|p\rangle$ with $|p| = |\bar{p}|$ through a rotation starting from the state $|\bar{p}\rangle$. The rotation sending \bar{p} into p is undetermined on the right for a rotation around the direction of \bar{p} and on the left for a rotation around the direction of p . We will choose $|p\rangle$ adopting a standard convention for the Euler angles that define it, i.e.

$$R_p = R_z(\varphi) R_y(\theta) R_z(-\varphi), \quad (2.5.125)$$

where θ and φ are the polar angles of p . This convention is equivalent to define R_p as a rotation of θ around $\mathbf{n}_3 \wedge \hat{\mathbf{p}}$, with \mathbf{n}_3 the versor along the 3 axis and $\hat{\mathbf{p}} = \mathbf{p}/|\mathbf{p}|$.

With this convention

$$|p\rangle = U(R_p)|\bar{p}\rangle. \quad (2.5.126)$$

It is easy to verify that $|p\rangle$ has the same helicity, a , of $|\bar{p}\rangle$. In fact

$$\frac{\mathbf{J} \cdot \mathbf{p}}{|\mathbf{p}|}|p\rangle = U(R_p)U^{-1}(R_p)\frac{\mathbf{J} \cdot \mathbf{p}}{|\mathbf{p}|}U(R_p)|\bar{p}\rangle = U(R_p)\frac{\mathbf{J} \cdot \mathbf{p}}{|\mathbf{p}|}|\bar{p}\rangle = a|\bar{p}\rangle = a|p\rangle. \quad (2.5.127)$$

We will define the state $|\bar{p}'\rangle$ with \bar{p}'_μ of the form (2.5.110) and $\bar{p}' \neq \bar{p}$ through the transformation

$$|\bar{p}'\rangle = U(\Lambda_{\bar{p}'})|\bar{p}\rangle, \quad (2.5.128)$$

where $U(\Lambda_{\bar{p}'})$ is a pure velocity transformation along the 3 axis which sends \bar{p} into \bar{p}' without rotations around \bar{p} or \bar{p}' . The rotated states of $|\bar{p}'\rangle$ will be defined with the convention (2.5.126).

Once fixed the base in this way let us now construct the representation. If $U(\Lambda)$ is the representative of the generic Lorentz transformation sending \mathbf{p} into \mathbf{p}'

$$U(\Lambda)|\mathbf{p}\rangle = U(\Lambda)U(R_p)|\bar{p}\rangle = U(R_{\mathbf{p}'})U^\dagger(R_{\mathbf{p}'})U(\Lambda)U(R_p)U^\dagger(\Lambda_{\bar{p}'})U(\Lambda_{\bar{p}'})|\bar{p}'\rangle. \quad (2.5.129)$$

It is easy to see that

$$\mathcal{U} = R_{\mathbf{p}'}^{-1}\Lambda R_p\Lambda_{\bar{p}'}^{-1}, \quad (2.5.130)$$

is a transformation that leaves \bar{p}'_μ unchanged, i.e. an element of the small group of \bar{p}'_μ . The algebra of such a group is formed by the generators $\epsilon_{\mu\nu\rho\sigma}J^{(\nu\rho)}\bar{p}'^\sigma$, i.e. $\mathbf{J} \cdot \bar{p}'/|\bar{p}'|, \Gamma^+, \Gamma^-$. Now Γ^+ and Γ^- are identically zero in the representation under exam, thus \mathcal{U} is a rotation around the 3 axis of a well defined angle $\bar{\varphi}$.

A rotation of an angle $\bar{\varphi}$ around the 3 axis is represented by

$$R_3(\bar{\varphi})|\bar{p}'\rangle = e^{ia\bar{\varphi}}|\bar{p}'\rangle, \quad (2.5.131)$$

where a is the helicity. Then Eq. (2.5.129) becomes

$$U(\Lambda)|\mathbf{p}\rangle = e^{ia\bar{\varphi}}|\Lambda\mathbf{p}\rangle. \quad (2.5.132)$$

If Λ is an infinitesimal rotation of parameter $\delta\boldsymbol{\theta}$ we find

$$\begin{aligned} 1 + i\bar{\varphi}J_3 &\approx e^{i\theta\mathbf{J}\cdot(\mathbf{n}_3 \wedge \hat{\mathbf{p}})}(1 + i\delta\boldsymbol{\theta}\cdot\mathbf{J})e^{-i\theta\mathbf{J}\cdot(\mathbf{n}_3 \wedge \hat{\mathbf{p}}')} \\ &\approx 1 + i\delta\boldsymbol{\theta}\cdot\mathbf{J} - \theta[\mathbf{J}\cdot(\mathbf{n}_3 \wedge \hat{\mathbf{p}}), \delta\boldsymbol{\theta}\cdot\mathbf{J}] \\ &\approx 1 + i\delta\boldsymbol{\theta}\cdot\mathbf{J} - i\theta[(\mathbf{J}\cdot\hat{\mathbf{p}})\delta\theta_3 - J_3(\hat{\mathbf{p}}\cdot\delta\boldsymbol{\theta})], \end{aligned} \quad (2.5.133)$$

where in the first equality we used the fact that $\Lambda_{\bar{p}'} = 1$, in the second the fact that for infinitesimal rotations we may choose $\mathbf{p}' \approx \mathbf{p}$ in the second exponential, and in the third the use of the infinitesimal rotations. We then find

$$\bar{\varphi} = \delta\theta_3(1 - \hat{p}_3\theta) + \delta\boldsymbol{\theta}\cdot\hat{\mathbf{p}}\theta, \quad (2.5.134)$$

and choosing $\theta = |\mathbf{p}|/(|\mathbf{p}| + p_3)$

$$\bar{\varphi} = \delta\boldsymbol{\theta}\cdot\frac{\mathbf{p} + |\mathbf{p}|\mathbf{n}_3}{|\mathbf{p}| + p_3}. \quad (2.5.135)$$

Analogously if Λ is an infinitesimal Lorentz transformation of parameter $\delta\boldsymbol{\beta}$ we find

$$\bar{\varphi} = \frac{\delta\beta_1 p_2 - \delta\beta_2 p_1}{|\mathbf{p}| + p_3}. \quad (2.5.136)$$

The generic state of the particle is written as

$$|\Phi\rangle = \int d\Omega_{\mathbf{p}} \Phi(\mathbf{p})|\mathbf{p}\rangle, \quad (2.5.137)$$

with the scalar product

$$\langle \Phi' | \Phi \rangle = \int d\Omega_p \Phi'^*(p) \Phi(p). \quad (2.5.138)$$

For a generic Lorentz transformation

$$U(\Lambda) |\Phi\rangle = \int d\Omega_p \Phi(p) e^{ia\bar{\varphi}(\Lambda, p)} |\Lambda p\rangle = \int d\Omega_p \Phi(\Lambda^{-1}p) e^{ia\bar{\varphi}(\Lambda, \Lambda^{-1}p)} |p\rangle. \quad (2.5.139)$$

The generators on the space of the $\Phi(p)$ functions are

$$J = -ip \wedge \frac{\partial}{\partial p} + s, \quad (2.5.140)$$

$$K = ip^0 \frac{\partial}{\partial p} + \chi, \quad (2.5.141)$$

with

$$s_1 = a \frac{p_1}{|p| + p_3} \quad s_2 = a \frac{p_2}{|p| + p_3} \quad s_3 = a, \quad (2.5.142)$$

$$\chi_1 = a \frac{p_2}{|p| + p_3} \quad \chi_2 = -a \frac{p_1}{|p| + p_3} \quad \chi_3 = 0. \quad (2.5.143)$$

This generators obey the commutation relations of the algebra (2.5.28)-(2.5.30) and are hermitian with the metric (2.5.138).

This completes the construction of the group representation on the Hilbert space of functions $\Phi(p)$ for a zero mass particle.

The Wigner rotation

We here want to calculate explicitly the Wigner rotation for a finite Lorentz transformation, for a massive particle. The velocity transformation is written as

$$U(\Lambda) = e^{-iK \cdot y}, \quad (2.5.144)$$

with

$$K = ip_0 \frac{\partial}{\partial p} + \frac{p \wedge s}{p_0 + m}. \quad (2.5.145)$$

For zero spin

$$e^{y \cdot p_0 \frac{\partial}{\partial p}} \varphi(p) = \varphi(\Lambda^{-1}p). \quad (2.5.146)$$

For non-zero spin

$$U(\Lambda) \varphi(p) = e^{y \cdot p_0 \frac{\partial}{\partial p} - iy \cdot \frac{p \wedge s}{p_0 + m}} \varphi(p), \quad (2.5.147)$$

where φ has $2s + 1$ components. The operator $U(\Lambda)$ is the exponential of two operators which do not commute.

In general given two operators A and B one has

$$e^{A+B} = e^A \sum_{n=0}^{\infty} \int_0^1 dx_1 \cdots dx_n T(B(x_1) \cdots B(x_n)), \quad (2.5.148)$$

where $B(x) = e^{-x^A} B e^{x^A}$ and T is the usual time ordered product

$$T(B(x_1) \cdots B(x_n)) = \frac{1}{n!} \sum_{\substack{\text{permutations} \\ \text{of } \{i_k\}}} \theta(x_{i_1} - x_{i_2}) \cdots \theta(x_{i_{n-1}} - x_n) B(x_1) \cdots B(x_n). \quad (2.5.149)$$

If A and B commute $B(x) = B$ and Eq. (2.5.148) gives $e^{A+B} = e^A e^B$. Eq. (2.5.148) can be proved observing that $U(\lambda) = e^{\lambda(A+B)}$ obeys the equation

$$\frac{d}{d\lambda} U(\lambda) = (A + B)U(\lambda) \quad U(0) = 1. \quad (2.5.150)$$

Let

$$W(\lambda) = e^{\lambda A} \sum_{n=0}^{\infty} \int_0^{\lambda} dx_1 \cdots dx_n T(B(x_1) \cdots B(x_n)). \quad (2.5.151)$$

One easily verifies that

$$\frac{d}{d\lambda} W(\lambda) = (A + B)W(\lambda) \quad (2.5.152)$$

with $W(0) = 1$. Then we must have $U(\lambda) = W(\lambda)$ and for $\lambda = 1$ Eq. (2.5.148) is recovered.

Let now

$$A = \mathbf{y} \cdot \mathbf{p}_0 \frac{\partial}{\partial \mathbf{p}} \quad B = -i\mathbf{y} \cdot \frac{\mathbf{p} \wedge \mathbf{s}}{\mathbf{p}_0 + m}. \quad (2.5.153)$$

We will have

$$B(x) = e^{-xy \cdot \mathbf{p}_0 \frac{\partial}{\partial \mathbf{p}}} B(\mathbf{p}) e^{xy \cdot \mathbf{p}_0 \frac{\partial}{\partial \mathbf{p}}} = B(\Lambda_{-x}^{-1} \mathbf{p}), \quad (2.5.154)$$

where Λ_x is the Lorentz transformation with parameter xy . In the numerator of B , due to the vector products, only enters the component of \mathbf{p} orthogonal to \mathbf{y} and this is invariant under the transformation. So

$$B(x) = -i\mathbf{y} \cdot \frac{\mathbf{p} \wedge \mathbf{s}}{\Lambda_{-x}^{-1} \mathbf{p}_0 + m}. \quad (2.5.155)$$

The $B(x)$ all commute with themselves and

$$\int_0^1 dx_1 \cdots dx_n T(B(x_1) \cdots B(x_n)) = \frac{1}{n!} \left[\int_0^1 B(x) dx \right]^n, \quad (2.5.156)$$

and

$$U(\Lambda) = e^{\mathbf{y} \cdot \mathbf{p}_0 \frac{\partial}{\partial \mathbf{p}}} e^{\int_0^1 b(x) dx}, \quad (2.5.157)$$

Moreover

$$U(\Lambda)\varphi(\mathbf{p}) = e^{-i\mathbf{y} \cdot \int_0^1 dx \frac{\mathbf{p} \wedge \mathbf{s}}{\Lambda_{-x}^{-1} \mathbf{p}_0 + m}} \varphi(\Lambda^{-1} \mathbf{p}), \quad (2.5.158)$$

Then the Wigner rotation is

$$e^{i\mathbf{s} \cdot (\mathbf{p} \wedge \mathbf{y}) \int_0^1 \frac{dx}{\Lambda_{-x}^{-1} \mathbf{p}_0 + m}}. \quad (2.5.159)$$

The integral can easily be evaluated if we parametrize p_μ in the form \mathbf{p}_\perp , $p_0 = m_t \cosh y_0$, $p_\parallel = m_t \sinh y_0$, and $m_t = \sqrt{m^2 + \mathbf{p}_\perp^2}$. Using this parametrization we find

$$\begin{aligned} \int_0^1 \frac{dx}{\Lambda_{1-x}^{-1} p_0 + m} &= \int_0^1 \frac{dx}{m_t \cosh[y_0 + y(1-x)] + m} \\ &= \frac{1}{y} \int_0^y \frac{dz}{m_t \cosh(y_0 + z) + m} \\ &= \frac{1}{y p_\perp} \varphi, \\ \varphi &= \arcsin \left[\frac{m_t + m \cosh(y_0 + z)}{m + m_t \cosh(y_0 + z)} \right]_{z=0}^{z=y}, \end{aligned} \quad (2.5.160)$$

is the angle of the Wigner rotation.

Discrete transformations

We want now to discuss the discrete transformations, specifically the spatial inversion and the time reversal.

The spatial inversion Π sends

$$\mathbf{p} \rightarrow -\mathbf{p} \quad \mathbf{J} \rightarrow \mathbf{J} \quad \mathbf{K} \rightarrow -\mathbf{K}. \quad (2.5.161)$$

We immediately find a representation

$$\Pi|\mathbf{p}\rangle = \eta|-\mathbf{p}\rangle, \quad (2.5.162)$$

and on the wave functions

$$\varphi_a(\mathbf{p}) \rightarrow -\eta \varphi_a(-\mathbf{p}), \quad (2.5.163)$$

where η is a phase factor which must be ± 1 since $\Pi^2 = 1$. It is easy to show that the transformation (2.5.163) is unitary

$$\begin{aligned} \langle \Pi a' | \Pi a \rangle &= \int d\Omega_{\mathbf{p}} \varphi_a'^{\dagger}(-\mathbf{p}) \varphi_a(-\mathbf{p}) \\ &= \int d\Omega_{\mathbf{p}} \varphi_a'^{\dagger}(\mathbf{p}) \varphi_a(\mathbf{p}) = \langle a' | a \rangle, \end{aligned} \quad (2.5.164)$$

Moreover $\langle \Pi a' | p \Pi a \rangle = -\langle a' | p a \rangle$ or

$$\Pi^\dagger p \Pi = -p, \quad (2.5.165)$$

and

$$\Pi^\dagger J \Pi = J, \quad (2.5.166)$$

$$\Pi^\dagger K \Pi = -K, \quad (2.5.167)$$

since we assumed η independent of \mathbf{p} .

A representation of the time reversal T is in terms of the antiunitary operator

$$\varphi(\mathbf{p}) \rightarrow \eta_T C \varphi^*(-\mathbf{p}), \quad (2.5.168)$$

where the unitary matrix C is defined in Section 2.4.6 and η_T is a phase independent of p . So that

$$\begin{aligned}\langle a' | T^\dagger p T a \rangle &= \langle T a | p T a' \rangle = \int d\Omega_p \varphi_a^{\text{Tr}}(-p) p \varphi_{a'}^*(-p) \\ &= - \int d\Omega_p \varphi_{a'}^\dagger(p) p \varphi_a(p) = -\langle a' | p a \rangle\end{aligned}\quad (2.5.169)$$

or

$$T^\dagger p T = -p, \quad (2.5.170)$$

Similarly

$$\begin{aligned}\langle a' | T^\dagger J T a \rangle &= \langle T a | J T a' \rangle = \int d\Omega_p \varphi_a^{\text{Tr}}(-p) C^* \left(-ip \wedge \frac{\partial}{\partial p} + s \right) C^{\text{Tr}} \varphi_{a'}^*(-p) \\ &= \int d\Omega_p \varphi_{a'}^\dagger(-p) \left(ip \wedge \frac{\partial}{\partial p} - s \right) \varphi_a(-p),\end{aligned}\quad (2.5.171)$$

where we integrated by parts and used $C s^{\text{Tr}} C^\dagger = C s^* C^\dagger = -s$ (see Eq. (2.4.85)). So $\langle T a | J T a' \rangle = -\langle a' | J a \rangle$ or

$$T^\dagger J T = -J. \quad (2.5.172)$$

Similarly

$$T^\dagger K T = K. \quad (2.5.173)$$

2.5.2 Wave functions in coordinate space

In relativistic mechanics the coordinates, $x = (x^0, x^1, x^2, x^3) = (t, \mathbf{x})$, play a privileged role. The constant speed of light principle, together with the relativity principle, implies that a signal cannot propagate at a speed greater than c . This implies, for example, that the regions with $x^2 < 0$ are causally disconnected from the events at $x = (0, \mathbf{0})$. This statement is simple in coordinate space but it does not have an equally explicit expression in other representations.

It is then convenient to associate to a state a wave function $\psi(x)$ which describes the state point by point in space-time. For the description to be effectively linked to the point event it is necessary that $\psi(x)$ transforms *locally*.

For a Lorentz transformations Λ this means

$$\psi(x) \xrightarrow{\Lambda} \psi'(x) = S(\Lambda)\psi(\Lambda^{-1}x), \quad (2.5.174)$$

or

$$\psi'(\Lambda x) = S(\Lambda)\psi(x), \quad (2.5.175)$$

where $S(\Lambda)$ does not depend on the point and it is a representation of the Lorentz group.

For a translation, a , we require

$$\psi(x) \xrightarrow{a} \psi'(x) = \psi(x + a). \quad (2.5.176)$$

Introducing

$$p_\mu \psi(x) = i \frac{\partial}{\partial x^\mu} \psi(x), \quad (2.5.177)$$

the momentum eigenstate $\psi_p(x)$ can be written as follows

$$\psi_p(x) = e^{-ipx}\psi_p(0), \quad (2.5.178)$$

where in the exponent we use the simplified notation $px \equiv p_\mu x^\mu$.

If the time evolution is local we will need that $\psi(x)$ obeys to a partial differential equation with derivatives of *finite order*. In what follows we will try to build local wave functions for spin 0, 1/2, 1 particles. Of course the states of these particles are defined by the unitary irreducible representations of the Poincaré group. Our wave functions will have to be in bijective correspondence with the vectors of such representations, and the scalar product for such vectors will have to be expressible in terms of wave functions. Relative to this metric of the Hilbert space the symmetry transformations on the $\psi(x)$ will have to be unitary. We will verify that the representations of the Lorentz group $S(\Lambda)$ will necessarily be finite dimensional.

We conclude observing that

$$\psi'(0) = S(\Lambda)\psi(0), \quad (2.5.179)$$

in fact Λ is the small group of point $x = 0$. If we call $U(\Lambda)$ the unitary operator which represents the Lorentz transformation Λ we will have

$$U(\Lambda)\psi(x) = U(\Lambda)e^{-ipx}\psi(0) = U(\Lambda)e^{-ipx}U^{-1}(\Lambda)U(\Lambda)\psi(0), \quad (2.5.180)$$

but

$$U(\Lambda)e^{-ipx}U^{-1}(\Lambda) = e^{-i(\Lambda p)x} = e^{-ip(\Lambda^{-1}x)}, \quad (2.5.181)$$

and, since $U(\Lambda)\psi(0) = S(\Lambda)\psi(0)$,

$$U(\Lambda)\psi(x) = e^{-ip(\Lambda^{-1}x)}S(\Lambda)\psi(0) = S(\Lambda)\psi(\Lambda^{-1}x). \quad (2.5.182)$$

2.6 The relativistic wave equations

In Section 2.5 we introduced the Poincaré group and showed that a structureless particle is described by a unitary irreducible representation of this group identified by the mass and by the spin. We will now find the relativistic wave equations of free motion for these particles.

2.6.1 Particles of spin 0

For a spin 0 particle any given state $|s\rangle$ can be represented as

$$|s\rangle = \int d\Omega_p \varphi_s(p)|p\rangle, \quad (2.6.1)$$

$\varphi_s(p) = \langle p|s\rangle$ is the wave function in the representation were the momenta are diagonal. The wave function associated to the state $|p\rangle$, $\psi_p(x)$, must have the form (2.5.178). By the superposition principle

$$\langle x|s\rangle = \psi_s(x) = \int d\Omega_p \varphi_s(p)e^{-ipx}\psi_p(0). \quad (2.6.2)$$

To determine $\psi_p(0)$ let us consider the effect of a Lorentz transformation

$$|s\rangle \xrightarrow{\Lambda} \int d\Omega_p \varphi_s(p)|\Lambda p\rangle = \int d\Omega_p \varphi_s(\Lambda^{-1}p)|p\rangle, \quad (2.6.3)$$

and on the wave function

$$\psi_s(x) \xrightarrow{\Lambda} \int d\Omega_p \varphi_s(\Lambda^{-1}p) e^{-ipx} \psi_p(0) = \int d\Omega_p \varphi_s(p) e^{-ip(\Lambda^{-1}x)} \psi_{\Lambda p}(0). \quad (2.6.4)$$

This transformation is certainly local if $\psi_{\Lambda p}(0) = \psi_p(0)$. This means that $\psi_p(0)$ must be an invariant constructed with p_μ . Since $p^2 = m^2$, such an invariant must be a constant, that can be chosen equal to 1.

So

$$\psi_s(x) = \int d\Omega_p \varphi_s(p) e^{-ipx}. \quad (2.6.5)$$

Under translation

$$\psi_s(x) \xrightarrow{a} \psi'(x) = \psi_s(x + a). \quad (2.6.6)$$

Under Lorentz transformation

$$\psi_s(x) \xrightarrow{\Lambda} \psi'(x) = \psi_s(\Lambda^{-1}x). \quad (2.6.7)$$

The function $\psi_s(x)$ in Eq. (2.6.5) transforms locally and the requirement $p^2 = m^2$ implies that it obeys the Klein-Gordon equation

$$(\square + m^2)\psi_s(x) = 0, \quad (2.6.8)$$

where

$$\square = \frac{\partial^2}{\partial t^2} - \sum_{i=1}^3 \frac{\partial^2}{\partial x_i^2}, \quad (2.6.9)$$

is the d' Alambert operator. Eq. (2.6.8) is invariant under transformations of the Poincaré group.

Not all solutions of Eq. (2.6.8) are of kind (2.6.5). Eq. (2.6.8) admits also solutions with negative energy. As a matter of fact the wave function of Eq. (2.6.5) obeys to the following equation

$$\left(i \frac{\partial}{\partial x^0} - \sqrt{m^2 - \nabla^2} \right) \psi_s(x) = 0, \quad (2.6.10)$$

which is non-local. The requirement for a local equation imposes to have negative energy solutions as well.

The general solution of Eq. (2.6.8) can be easily obtained working in Fourier space

$$\psi_s(x) = \int \frac{d^4 p}{(2\pi)^4} e^{-ipx} \tilde{\psi}_s(p). \quad (2.6.11)$$

Then Eq. (2.6.8) becomes

$$(p^2 - m^2) \tilde{\psi}_s(p) = 0, \quad (2.6.12)$$

or

$$\tilde{\psi}_s(p) = \varphi_s(p) 2\pi \delta(p^2 - m^2). \quad (2.6.13)$$

Integrating over p_0 in Eq. (2.6.11)

$$\psi_s(x) = \int \frac{d^3 p}{(2\pi)^3 2p_0} [\varphi_s(\mathbf{p}, p_0) e^{-ipx} + \varphi_s(\mathbf{p}, -p_0) e^{ip_0 x^0 + ip \cdot r}]. \quad (2.6.14)$$

We then define

$$\varphi_s(\mathbf{p}, p_0) = \varphi_s^+(\mathbf{p}), \quad (2.6.15)$$

$$\varphi_s(\mathbf{p}, -p_0) = \varphi_s^-(\mathbf{p}), \quad (2.6.16)$$

so that

$$\psi_s(x) = \int d\Omega_{\mathbf{p}} [\varphi_s^+(\mathbf{p}) e^{-ipx} + \varphi_s^-(\mathbf{p}) e^{ipx}]. \quad (2.6.17)$$

A natural scalar product can be introduced as follows. Given two solutions of the Klein-Gordon equation (2.6.8), $\psi_a(x)$ and $\psi_b(x)$, the quantity

$$J_\mu^{(a,b)}(x) = i\psi_a^* \overleftrightarrow{\partial}_\mu \psi_b = i[\psi_a^* \partial_\mu \psi_b - (\partial_\mu \psi_a^*) \psi_b], \quad (2.6.18)$$

where $\partial_\mu \equiv \partial/\partial x^\mu$, is conserved, i.e.

$$\partial^\mu J_\mu^{(a,b)}(x) = 0. \quad (2.6.19)$$

Then, due to Gauss theorem, if the ψ go to zero sufficiently rapidly at spatial infinity, the integral extended to an hypersurface of spatial kind extended to infinity,

$$\int d\sigma^\mu J_\mu^{(a,b)}(x), \quad (2.6.20)$$

is independent from the surface ($d\sigma^\mu$ is the oriented normal). It can be calculated on a surface $x^0 = \text{constant}$

$$\int d\sigma^\mu J_\mu^{(a,b)}(x) = \int dx J_0^{(a,b)}(t, x). \quad (2.6.21)$$

We will define the scalar product $\langle a|b \rangle$ through

$$\begin{aligned} \langle a|b \rangle &= \int d\sigma^\mu J_\mu^{(a,b)}(x) \\ &= \int d\Omega_{\mathbf{p}} [\varphi_a^{+*}(\mathbf{p}) \varphi_b^+(\mathbf{p}) - \varphi_a^{-*}(\mathbf{p}) \varphi_b^-(\mathbf{p})]. \end{aligned} \quad (2.6.22)$$

The generators of the group in this representation are

$$\begin{aligned} p_\mu &= i \frac{\partial}{\partial x^\mu}, \\ J^{(\mu\nu)} &= -i \left(x^\mu \frac{\partial}{\partial x^\nu} - x^\nu \frac{\partial}{\partial x^\mu} \right), \end{aligned} \quad (2.6.23)$$

which are hermitians under the metric of Eq. (2.6.22).

The Eq. (2.6.10) satisfied by these wave functions is non-local. In order to have a local equation, like (2.6.8), it is necessary to put together positive and negative energy solutions. Actually, the Klein-Gordon Eq. (2.6.8) is second order in the temporal derivative, while, once the Hamiltonian is known, the evolution equation should be of the first order.

2.6.2 Particles of spin 1/2

The irreducible representations of the Poincaré group corresponding to particles of mass m and spin 1/2 are in correspondence with vectors $|r, \mathbf{p}\rangle$, where r is the eigenvalue of one component of the spin in the rest frame.

Any state $|a\rangle$ of the Hilbert space generated like so is of the following form

$$|a\rangle = \int d\Omega_{\mathbf{p}} \sum_{r=1}^2 \varphi_a(r, \mathbf{p}) |r, \mathbf{p}\rangle. \quad (2.6.24)$$

The infinitesimal transformations of the Lorentz group are $\varphi_a(r, \mathbf{p}) \rightarrow \varphi_{\Lambda a}(r, \mathbf{p})$, with

$$\varphi_{\Lambda a}(r, \mathbf{p}) = \left[1 + i\boldsymbol{\theta} \cdot \left(\frac{1}{i} \mathbf{p} \wedge \frac{\partial}{\partial \mathbf{p}} + s \right) - i\boldsymbol{\alpha} \cdot \left(ip_0 \frac{\partial}{\partial \mathbf{p}} + \frac{\mathbf{p} \wedge s}{p_0 + m} \right) \right]_{rr'} \varphi_a(r', \mathbf{p}). \quad (2.6.25)$$

We will now construct local wave functions for these states. The locality under translations fixes the form of the wave functions corresponding to eigenstates of momentum

$$\psi_{r, \mathbf{p}}(x) = \psi_{r, \mathbf{p}}(0) e^{-ipx}. \quad (2.6.26)$$

We will call $\psi_{r, \mathbf{p}}(0) \equiv u(r, \mathbf{p})$. Due to the superposition principle we will have

$$\psi_a(x) = \int d\Omega_{\mathbf{p}} \sum_{r=1}^2 \varphi_a(r, \mathbf{p}) u(r, \mathbf{p}) e^{-ipx}. \quad (2.6.27)$$

To find an explicit form for the local wave functions we will adopt the following strategy. We will assume specific properties of local transformations for $\psi_a(x)$. We will write an equation explicitly covariant under the Poincaré group transformations and will later prove that the solutions of this equation give a unitary representation of the Poincaré group. And will express the scalar product between states in terms of these wave functions.

Locality under group transformations requires

$$\psi_a(x) \xrightarrow{\Lambda} \psi_{\Lambda a}(x) = S(\Lambda) \psi_a(\Lambda^{-1}x), \quad (2.6.28)$$

where $S(\Lambda)$ is a finite dimensional representation of the Lorentz group. The Lorentz group is locally isomorphic to $SU(2) \otimes SU(2)$. Hence the finite dimensional representations are fixed by two numbers (n_+, n_-) which determine the representations of the two groups $SU(2)$ with generators

$$\mathbf{J}_+ = \frac{\mathbf{J} + i\mathbf{K}}{2}, \quad (2.6.29)$$

$$\mathbf{J}_- = \frac{\mathbf{J} - i\mathbf{K}}{2}. \quad (2.6.30)$$

We will heuristically construct the ψ with representations of dimension 2.

There exist two inequivalent representations of dimension 2. The $(\frac{1}{2}, 0)$ and the $(0, \frac{1}{2})$. In the two representations the group generators, defined by the infinitesimal transformations

$$\boldsymbol{\Lambda} \approx 1 + i\boldsymbol{\theta} \cdot \mathbf{J} - i\boldsymbol{\alpha} \cdot \mathbf{K}, \quad (2.6.31)$$

are given by

$$\left(\frac{1}{2}, 0 \right) : \quad \begin{cases} \mathbf{J} = \frac{\boldsymbol{\sigma}}{2} \\ \mathbf{K} = -i\frac{\boldsymbol{\sigma}}{2} \end{cases}, \quad (2.6.32)$$

$$\left(0, \frac{1}{2} \right) : \quad \begin{cases} \mathbf{J} = \frac{\boldsymbol{\sigma}}{2} \\ \mathbf{K} = i\frac{\boldsymbol{\sigma}}{2} \end{cases}. \quad (2.6.33)$$

The corresponding finite transformations are

$$S_{(\frac{1}{2},0)}(\Lambda) = e^{i\theta \cdot \frac{\sigma}{2} - \alpha \cdot \frac{\sigma}{2}}, \quad (2.6.34)$$

$$S_{(0,\frac{1}{2})}(\Lambda) = e^{i\theta \cdot \frac{\sigma}{2} + \alpha \cdot \frac{\sigma}{2}}, \quad (2.6.35)$$

with

$$S_{(0,\frac{1}{2})}(\Lambda) = S_{(\frac{1}{2},0)}^{\dagger}(\Lambda)^{-1}. \quad (2.6.36)$$

We will call ξ the spinors which transform according to $(\frac{1}{2}, 0)$ and η the ones transforming according to $(0, \frac{1}{2})$.

Since J is an axial vector, whereas K is a polar vector, we have under parity

$$(\frac{1}{2}, 0) \xleftrightarrow{P} (0, \frac{1}{2}). \quad (2.6.37)$$

Then in order to construct a representation invariant under parity we need to consider a reducible representation of the Lorentz group for $S(\Lambda)$, namely

$$(\frac{1}{2}, 0) \oplus (0, \frac{1}{2}). \quad (2.6.38)$$

The vectorial space for this representation is composed by spinors of 4 components of the form

$$\begin{pmatrix} \xi \\ \eta \end{pmatrix}. \quad (2.6.39)$$

In such representation, the generators of the Lorentz group are

$$J = \begin{pmatrix} \frac{\sigma}{2} & 0 \\ 0 & \frac{\sigma}{2} \end{pmatrix}, \quad (2.6.40)$$

$$K = \begin{pmatrix} -i\frac{\sigma}{2} & 0 \\ 0 & i\frac{\sigma}{2} \end{pmatrix}. \quad (2.6.41)$$

Using the following identities for the Pauli matrices

$$[\theta \cdot \sigma, \sigma] = -2i\theta \wedge \sigma, \quad (2.6.42)$$

$$\{\alpha \cdot \sigma, \sigma\} = 2\alpha, \quad (2.6.43)$$

where $[\dots]$ stands for the commutator and $\{\dots\}$ for the anticommutator, we easily find that

$$\begin{aligned} S_{(\frac{1}{2},0)}(\Lambda)(p_0 + p \cdot \sigma)S_{(\frac{1}{2},0)}^{\dagger}(\Lambda) &= p_0 + p \cdot \sigma + i[\theta \cdot \frac{\sigma}{2}, p_0 + p \cdot \sigma] - \{\alpha \cdot \frac{\sigma}{2}, p_0 + p \cdot \sigma\} + \dots \\ &= p_0 + p \cdot \sigma + \frac{i}{2}[\theta \cdot \sigma, p \cdot \sigma] - \alpha \cdot \sigma p_0 - \frac{1}{2}\{\alpha \cdot \sigma, p \cdot \sigma\} + \dots \\ &= (p_0 - \alpha \cdot p + \dots) + \sigma \cdot (p - \theta \wedge p - \alpha p_0 + \dots) \\ &= p'_0 + \sigma \cdot p', \end{aligned} \quad (2.6.44)$$

where in the vector representation we used

$$(iJ_i)_{jk} = \epsilon_{ijk}, \quad (2.6.45)$$

$$(iK_i)_{j0} = (iK_i)_{0j} = \delta_{ij}, \quad (2.6.46)$$

and p' is the Lorentz transformed of p

$$p'_\mu = \Lambda^\nu_\mu p_\nu. \quad (2.6.47)$$

Then an equation of the form

$$(p^0 + \mathbf{p} \cdot \boldsymbol{\sigma})\eta = c\xi, \quad (2.6.48)$$

where c is a scalar, is covariant under Lorentz transformations. In fact, calling $S = S_{(\frac{1}{2}, 0)}(\Lambda)$, we have

$$S(p^0 + \mathbf{p} \cdot \boldsymbol{\sigma})\eta = cS\xi, \quad (2.6.49)$$

or

$$S(p^0 + \mathbf{p} \cdot \boldsymbol{\sigma})S^\dagger S^\dagger{}^{-1}\eta = cS\xi'. \quad (2.6.50)$$

Due to Eq. (2.6.36) $S^\dagger{}^{-1}\eta = \eta'$ and using Eq. (2.6.44)

$$(p^{0'} + \mathbf{p}' \cdot \boldsymbol{\sigma})\eta' = \xi', \quad (2.6.51)$$

so the equation has the same form in all reference frames. Analogously we show that $(p^0 - \mathbf{p} \cdot \boldsymbol{\sigma})\xi$ transforms as $(0, \frac{1}{2})$. The most general system of first order covariant equations has then the following form

$$(p^0 + \mathbf{p} \cdot \boldsymbol{\sigma})\eta = c\xi, \quad (2.6.52)$$

$$(p^0 - \mathbf{p} \cdot \boldsymbol{\sigma})\xi = c'\eta, \quad (2.6.53)$$

and invariance under parity imposes $c = c'$. Multiplying the first equation by $(p^0 - \mathbf{p} \cdot \boldsymbol{\sigma})$ and using the second equation we find

$$p^{0^2} - \mathbf{p}^2 = c^2. \quad (2.6.54)$$

Then if we want to describe a particle we must identify c with the mass m . In terms of bispinors we have

$$\begin{pmatrix} 0 & p^0 + \mathbf{p} \cdot \boldsymbol{\sigma} \\ p^0 - \mathbf{p} \cdot \boldsymbol{\sigma} & 0 \end{pmatrix} \begin{pmatrix} \xi \\ \eta \end{pmatrix} = m \begin{pmatrix} \xi \\ \eta \end{pmatrix}. \quad (2.6.55)$$

We give a more symmetric form to this equation by introducing the 4×4 matrices

$$\gamma^0 = \begin{pmatrix} 0 & 1 \\ 1 & 0 \end{pmatrix}, \quad \boldsymbol{\gamma} = \begin{pmatrix} 0 & -\boldsymbol{\sigma} \\ \boldsymbol{\sigma} & 0 \end{pmatrix}, \quad (2.6.56)$$

and the bispinor $\psi = \begin{pmatrix} \xi \\ \eta \end{pmatrix}$. We will also introduce

$$\gamma^5 = \begin{pmatrix} 1 & 0 \\ 0 & -1 \end{pmatrix} = i\gamma^0\gamma^1\gamma^2\gamma^3 = -\frac{i}{4!}\epsilon_{\mu\nu\sigma\tau}\gamma^\mu\gamma^\nu\gamma^\sigma\gamma^\tau. \quad (2.6.57)$$

We then find

$$(\gamma^0 p^0 - \boldsymbol{\gamma} \cdot \mathbf{p})\psi = m\psi, \quad (2.6.58)$$

or

$$\gamma^\mu p_\mu \psi = m\psi. \quad (2.6.59)$$

Introducing the notation $\not{p} = \gamma^\mu p_\mu$ we have

$$(\not{p} - m)\psi = 0. \quad (2.6.60)$$

This equation is known as the Dirac equation.

Applying the Lorentz transformation $S(\Lambda)$ in the representation $(\frac{1}{2}, 0) \oplus (0, \frac{1}{2})$ to the Dirac equation

$$S(\Lambda)\gamma^\mu p_\mu S^{-1}(\Lambda)S(\Lambda)\psi = mS(\Lambda)\psi. \quad (2.6.61)$$

Since the bispinor transforms under $S(\Lambda)$ the covariance imposes

$$S(\Lambda)\gamma^\mu S^{-1}(\Lambda) = \Lambda^\mu_\nu \gamma^\nu, \quad (2.6.62)$$

which means that γ^μ transform as a four-vector.

In coordinate representation

$$(i\not{\partial} - m)\psi = 0, \quad (2.6.63)$$

and by construction the solutions of this equation transform locally under Lorentz transformations. Of course in order to know whether they represent the states of a spin 1/2 particle of mass m we must verify that they are in bijective correspondence with the states defined in terms of the representations of the Poincaré group, and that a transformation on the states corresponds to a transformation on the wave functions.

We have

$$\{\gamma^\mu, \gamma^\nu\} = 2g^{\mu\nu}, \quad (2.6.64)$$

we can define the covariant component of the gamma matrices

$$\gamma_\mu = g_{\mu\nu}\gamma^\nu, \quad (2.6.65)$$

and we find

$$\{\gamma_\mu, \gamma_\nu\} = 2g_{\mu\nu}. \quad (2.6.66)$$

Also

$$\{\gamma^\mu, \gamma^5\} = 0, \quad (2.6.67)$$

and

$$\gamma^{0\dagger} = \gamma^0 \quad \gamma^{i\dagger} = -\gamma^i, \quad (2.6.68)$$

or

$$\gamma^{\mu\dagger} = \gamma^0 \gamma^\mu \gamma^0. \quad (2.6.69)$$

Using the matrices γ^μ it is possible to write in a compact form the Lorentz transformations in the representation $(\frac{1}{2}, 0) \oplus (0, \frac{1}{2})$. Consider the matrices

$$\sigma_{\mu\nu} = \frac{1}{2i}[\gamma_\mu, \gamma_\nu]. \quad (2.6.70)$$

Under the transformation $S(\Lambda)\sigma_{\mu\nu}S^{-1}(\Lambda)$ they transform as an antisymmetric tensor of rank 2. One can verify that

$$K^i = \frac{1}{2}\sigma^{oi} \quad J^i = \frac{1}{2}\epsilon^{oijk}\sigma_{jk} \quad i, j, k = 1, 2, 3. \quad (2.6.71)$$

The tensor $\sigma_{\mu\nu}$ represents the generators of the Lorentz group and we can write

$$S(\Lambda) = e^{\frac{i}{4}\omega^{\mu\nu}\sigma_{\mu\nu}}. \quad (2.6.72)$$

Moreover $\sigma_{\mu\nu}/2$ satisfies the algebra (2.5.41).

The matrix γ^0 has the role of exchanging the representations $(\frac{1}{2}, 0)$ and $(0, \frac{1}{2})$, so it coincides with the parity operator up to a phase,

$$\psi_a(x) \xrightarrow{P} \psi_{Pa}(x) = \eta_P \gamma^0 \psi_a(x^0, -x). \quad (2.6.73)$$

From the anticommutation rules (2.6.64) follows

$$\gamma^0 \gamma^i \gamma^0 = -\gamma^i \quad i = 1, 2, 3 \quad \gamma^0 \gamma^0 \gamma^0 = \gamma^0. \quad (2.6.74)$$

It is interesting to consider the set of the 16 matrices

$$1, \gamma^5, \gamma^\mu, \gamma^5 \gamma^\mu, \sigma^{\mu\nu}. \quad (2.6.75)$$

From the definition follow that the properties of Lorentz transformation of the matrices (2.6.75) are

1	scalar
γ^5	pseudoscalar
γ^μ	vector
$\gamma^5 \gamma^\mu$	pseudovector
$\sigma^{\mu\nu}$	antisymmetric tensor

(2.6.76)

These 16 matrices are linearly independent (in fact they transform differently under Lorentz transformations) so they constitute a complete basis for the 4×4 matrices, i.e. any 4×4 matrix can be written in the form

$$\sum_{a=1}^{16} c_a \Gamma^a, \quad (2.6.77)$$

where $\{\Gamma^a\}$ is the set of 16 matrices (2.6.75).

Note that if ψ and ψ' are two bispinors, $\psi'^\dagger \psi$ is not a scalar density. In fact

$$\psi'^\dagger(x) \psi(x) \xrightarrow{(a, \Lambda)} \psi'^\dagger(\Lambda^{-1}x + a) S^\dagger(\Lambda) S(\Lambda) \psi(\Lambda^{-1}x + a), \quad (2.6.78)$$

and $S^\dagger S \neq 1$. The representation $S(\Lambda)$ is not unitary as follows from its definition (2.6.32)-(2.6.33) and as should be expected since the Lorentz group is not compact. But we have

$$S^\dagger(\Lambda) \gamma^0 = \gamma^0 S^{-1}(\Lambda). \quad (2.6.79)$$

Then, upon defining $\bar{\psi}' = \psi^\dagger \gamma^0$, $\bar{\psi}' \psi$ is a scalar density

$$\begin{aligned} \bar{\psi}'(x) \psi(x) &\xrightarrow{(a, \Lambda)} \bar{\psi}'^\dagger(\Lambda^{-1}x + a) S^\dagger(\Lambda) \gamma^0 S(\Lambda) \psi(\Lambda^{-1}x + a) \\ &= \bar{\psi}'(\Lambda^{-1}x + a) \psi(\Lambda^{-1}x + a). \end{aligned} \quad (2.6.80)$$

Let us finally mention the following formulas,

$$\text{Tr}\{\gamma^{\mu_1}\gamma^{\mu_2} \cdot \gamma^{\mu_{2n+1}}\} = 0, \quad (2.6.81)$$

$$\text{Tr}\{\gamma^\mu\gamma^\nu\} = 4g^{\mu\nu}, \quad (2.6.82)$$

$$\text{Tr}\{\gamma^\mu\gamma^\nu\gamma^\rho\gamma^\sigma\} = 4\{g^{\mu\nu}g^{\rho\sigma} - g^{\mu\rho}g^{\nu\sigma} + g^{\mu\sigma}g^{\nu\rho}\}, \quad (2.6.83)$$

$$\text{Tr}\{\gamma^5\gamma^\mu\gamma^\nu\gamma^\rho\gamma^\sigma\} = -4i\epsilon^{\mu\nu\rho\sigma}, \quad (2.6.84)$$

$$\gamma_\mu A\gamma^\mu = -2A, \quad (2.6.85)$$

$$\gamma_\mu A\bar{B}\gamma^\mu = 4AB, \quad (2.6.86)$$

$$\gamma_\mu A\bar{B}\bar{C}\gamma^\mu = -2\bar{C}BA. \quad (2.6.87)$$

Dirac equation solutions: momentum eigenstates

Multiplying Eq. (2.6.60) by γ^0 we find

$$p^0\psi = (\boldsymbol{\alpha} \cdot \mathbf{p} + \gamma^0 m)\psi, \quad (2.6.88)$$

where $\boldsymbol{\alpha} = \gamma^0\boldsymbol{\gamma}$. Now we do a change of representation where we diagonalize γ^0

$$\psi \rightarrow U\psi \quad \gamma^\mu \rightarrow U\gamma^\mu U^{-1} \quad U = \frac{1}{\sqrt{2}} \begin{pmatrix} 1 & 1 \\ 1 & -1 \end{pmatrix} = U^{-1}, \quad (2.6.89)$$

explicitly

$$U \begin{pmatrix} \xi \\ \eta \end{pmatrix} = \begin{pmatrix} \frac{\xi + \eta}{\sqrt{2}} \\ \frac{\xi - \eta}{\sqrt{2}} \end{pmatrix} \equiv \begin{pmatrix} \varphi \\ \chi \end{pmatrix}. \quad (2.6.90)$$

After this transformation the algebra of the γ matrices remains the same. The γ matrices are rewritten as follows

$$\gamma^0 = \begin{pmatrix} 1 & 0 \\ 0 & -1 \end{pmatrix} \quad \boldsymbol{\gamma} = \begin{pmatrix} 0 & \boldsymbol{\sigma} \\ -\boldsymbol{\sigma} & 0 \end{pmatrix} \quad \gamma^5 = \begin{pmatrix} 0 & 1 \\ 1 & 0 \end{pmatrix}. \quad (2.6.91)$$

Since γ^0 is diagonal in the non-relativistic limit the states in this representation have definite parity. This is known as *Pauli representation*. The one of Eq. (2.6.56) as *spinorial or Kramers representation*.

Let us now find the solution with definite momentum and positive energy in the form

$$\psi_p(x) = e^{-ipx}u(r, \mathbf{p}), \quad (2.6.92)$$

suggested by translational invariance.

In the Pauli representation we find then

$$p^0 u_1 - \boldsymbol{\sigma} \cdot \mathbf{p} u_2 = mu_1, \quad (2.6.93)$$

$$-p^0 u_2 + \boldsymbol{\sigma} \cdot \mathbf{p} u_1 = mu_2, \quad (2.6.94)$$

where $p^0 = \sqrt{\mathbf{p}^2 + m^2}$ and $u = \begin{pmatrix} u_1 \\ u_2 \end{pmatrix}$.

These equations admit two independent solutions labeled by two Pauli spinors (bidimensional) w_1 and w_2 orthonormal

$$u(r, p) = c \begin{pmatrix} w_r \\ \frac{\boldsymbol{\sigma} \cdot \mathbf{p}}{p^0 + m} w_r \end{pmatrix} \quad w_r^\dagger w_s = \delta_{rs}. \quad (2.6.95)$$

Since we know that $\bar{u}u$ must be invariant, we find

$$\begin{aligned} \bar{u}u &= u^\dagger \gamma^0 u = w_r^\dagger w_r c^2 \left(1 - \frac{\boldsymbol{\sigma}^\dagger \cdot \mathbf{p} \boldsymbol{\sigma} \cdot \mathbf{p}}{(p^0 + m)^2} \right) \\ &= c^2 \left(1 - \frac{\mathbf{p}^2}{(p^0 + m)^2} \right) \\ &= c^2 \frac{2m}{p^0 + m} = \text{invariant.} \end{aligned} \quad (2.6.96)$$

We then choose conveniently $c = \sqrt{p^0 + m}$ so that

$$u(r, p) = \begin{pmatrix} \sqrt{p^0 + m} w_r \\ \frac{\boldsymbol{\sigma} \cdot \mathbf{p}}{\sqrt{p^0 + m}} w_r \end{pmatrix}, \quad (2.6.97)$$

$$\bar{u}(r, p)u(s, p) = 2m\delta_{rs}. \quad (2.6.98)$$

As a standard base for the spinors w_r we can take the eigenstates of σ_z

$$w_1 = \begin{pmatrix} 1 \\ 0 \end{pmatrix} \quad w_2 = \begin{pmatrix} 0 \\ 1 \end{pmatrix}. \quad (2.6.99)$$

As in the scalar case the Dirac equation admits also negative energy solutions. These will be of the following kind

$$\tilde{\psi}(x) = e^{ip^0 t + i\mathbf{p} \cdot \mathbf{x}} \tilde{u}(r, p), \quad (2.6.100)$$

Proceeding as in the previous case we find

$$\tilde{u}(r, p) = \begin{pmatrix} -\frac{\boldsymbol{\sigma} \cdot \mathbf{p}}{\sqrt{p^0 + m}} \tilde{w}_r \\ \frac{\sqrt{p^0 + m}}{\sqrt{p^0 + m}} \tilde{w}_r \end{pmatrix}. \quad (2.6.101)$$

Calling $v(r, p) = \tilde{u}(r, -p)$ we find

$$v(r, p) = \begin{pmatrix} \frac{\boldsymbol{\sigma} \cdot \mathbf{p}}{\sqrt{p^0 + m}} \tilde{w}_r \\ \frac{\sqrt{p^0 + m}}{\sqrt{p^0 + m}} \tilde{w}_r \end{pmatrix}, \quad (2.6.102)$$

$$\bar{v}(r, p)v(s, p) = -2m\delta_{rs}. \quad (2.6.103)$$

The spinors u and v satisfy the following algebraic equations

$$(\not{p} - m)u(r, p) = 0, \quad (2.6.104)$$

$$(\not{p} + m)v(r, p) = 0, \quad (2.6.105)$$

and constitute a complete set of spinors for the description of the momentum eigenstates. The four solutions found form a set of independent vectors, orthogonal respect to the γ^0 metric

$$\bar{u}(r, \mathbf{p})u(s, \mathbf{p}) = 2m\delta_{rs}, \quad (2.6.106)$$

$$\bar{v}(r, \mathbf{p})v(s, \mathbf{p}) = -2m\delta_{rs}, \quad (2.6.107)$$

$$\bar{u}(r, \mathbf{p})v(s, \mathbf{p}) = \bar{v}(r, \mathbf{p})u(s, \mathbf{p}) = 0. \quad (2.6.108)$$

Due to the completeness of the set we also have

$$\sum_{r=1}^2 u(r, \mathbf{p})\bar{u}(r, \mathbf{p}) = \not{p} + m, \quad (2.6.109)$$

$$\sum_{r=1}^2 v(r, \mathbf{p})\bar{v}(r, \mathbf{p}) = \not{p} - m. \quad (2.6.110)$$

Transformation properties and connection with the Poincaré group representations

We will now explicitly study the effect of the Lorentz transformation $S(\Lambda)$ on the solutions we just found. We will find that they realize a representation of the Poincaré group for a spin 1/2 particle.

A Lorentz transformation sends solutions with momentum p to solutions with momentum $p' = \Lambda p$. In fact, using the covariance property of the γ matrices we find

$$S(\Lambda)(\not{p} - m)u(r, \mathbf{p}) = (\not{p}' - m)S(\Lambda)u(r, \mathbf{p}) = 0. \quad (2.6.111)$$

In the Pauli representation we find for a rotation $R(\boldsymbol{\theta})$

$$J = \begin{pmatrix} \boldsymbol{\sigma} & 0 \\ \frac{1}{2} & \boldsymbol{\sigma} \\ 0 & \frac{1}{2} \end{pmatrix} \quad S(R(\boldsymbol{\theta})) = \begin{pmatrix} e^{i\boldsymbol{\theta} \cdot \frac{\boldsymbol{\sigma}}{2}} & 0 \\ 0 & e^{i\boldsymbol{\theta} \cdot \frac{\boldsymbol{\sigma}}{2}} \end{pmatrix}, \quad (2.6.112)$$

so

$$S(R(\boldsymbol{\theta}))u(r, \mathbf{p}) = \begin{pmatrix} \sqrt{p^0 + m}e^{i\boldsymbol{\theta} \cdot \frac{\boldsymbol{\sigma}}{2}}w_r \\ (R^{-1}(\boldsymbol{\theta})\boldsymbol{\sigma}) \cdot \mathbf{p}e^{i\boldsymbol{\theta} \cdot \frac{\boldsymbol{\sigma}}{2}}w_r \\ \sqrt{p^0 + m} \end{pmatrix} = \begin{pmatrix} \sqrt{p^0 + m}e^{i\boldsymbol{\theta} \cdot \frac{\boldsymbol{\sigma}}{2}}w_r \\ \boldsymbol{\sigma} \cdot (R(\boldsymbol{\theta})\mathbf{p})e^{i\boldsymbol{\theta} \cdot \frac{\boldsymbol{\sigma}}{2}}w_r \\ \sqrt{p^0 + m} \end{pmatrix}, \quad (2.6.113)$$

and

$$e^{i\boldsymbol{\theta} \cdot \frac{\boldsymbol{\sigma}}{2}}w_r = \sum_{r'} \mathcal{R}(\boldsymbol{\theta})_{r'r} w_{r'} \quad (2.6.114)$$

$$\mathcal{R}(\boldsymbol{\theta})_{r'r} = \left(e^{i\boldsymbol{\theta} \cdot \frac{\boldsymbol{\sigma}}{2}} \right)_{r'r} \quad (2.6.115)$$

$$S(R(\boldsymbol{\theta}))u(r, \mathbf{p}) = \sum_{r'} \mathcal{R}(\boldsymbol{\theta})_{r'r} u(r', R\mathbf{p}). \quad (2.6.116)$$

A transformation of rapidity $\boldsymbol{\alpha}$ is given by

$$S(\Lambda_{\boldsymbol{\alpha}}) = \begin{pmatrix} e^{-\boldsymbol{\alpha} \cdot \frac{\boldsymbol{\sigma}}{2}} & 0 \\ 0 & e^{\boldsymbol{\alpha} \cdot \frac{\boldsymbol{\sigma}}{2}} \end{pmatrix} = \begin{pmatrix} \cosh \frac{\alpha}{2} - \hat{\boldsymbol{\alpha}} \cdot \boldsymbol{\sigma} \sinh \frac{\alpha}{2} & 0 \\ 0 & \cosh \frac{\alpha}{2} + \hat{\boldsymbol{\alpha}} \cdot \boldsymbol{\sigma} \sinh \frac{\alpha}{2} \end{pmatrix}, \quad (2.6.117)$$

and in the Pauli representation

$$US(\Lambda_{\alpha})U^{-1} = \begin{pmatrix} \cosh \frac{\alpha}{2} & -\hat{\alpha} \cdot \sigma \sinh \frac{\alpha}{2} \\ -\hat{\alpha} \cdot \sigma \sinh \frac{\alpha}{2} & \cosh \frac{\alpha}{2} \end{pmatrix}. \quad (2.6.118)$$

We then find explicitly

$$\begin{pmatrix} \cosh \frac{\alpha}{2} & -\hat{\alpha} \cdot \sigma \sinh \frac{\alpha}{2} \\ -\hat{\alpha} \cdot \sigma \sinh \frac{\alpha}{2} & \cosh \frac{\alpha}{2} \end{pmatrix} \begin{pmatrix} \sqrt{p^0 + m} w_r \\ \frac{\sigma \cdot p}{\sqrt{p^0 + m}} w_r \end{pmatrix} = \begin{pmatrix} \sqrt{p'^0 + m} e^{-i\varphi \sigma \cdot \hat{\alpha} \wedge \hat{p}} w_r \\ \frac{\sigma \cdot p'}{\sqrt{p'^0 + m}} e^{-i\varphi \sigma \cdot \hat{\alpha} \wedge \hat{p}} w_r \end{pmatrix},$$

where

$$\tan \varphi = \frac{|\mathbf{p}| \sinh \frac{\alpha}{2}}{(p^0 + m) \cosh \frac{\alpha}{2} - p_{\parallel} \sinh \frac{\alpha}{2}}. \quad (2.6.119)$$

Here we used Eqs. (2.D.23) and (2.D.24) and $p_{\parallel} = \hat{\alpha} \cdot \mathbf{p}$. The matrix $\mathcal{R} = e^{-i\varphi \sigma \cdot \hat{\alpha} \wedge \hat{p}}$ is a rotation of an angle $-2\varphi \hat{\alpha} \wedge \hat{p}$ which acts on the components of the spinor w . Explicitly

$$S(\Lambda_{\alpha})u(r, \mathbf{p}) = \sum_{r'} \mathcal{R}(\Lambda_{\alpha}, \mathbf{p})_{r' r} u(r', \Lambda_{\alpha} \mathbf{p}). \quad (2.6.120)$$

For an infinitesimal transformation ($\alpha \ll 1$)

$$\varphi \approx \frac{\alpha}{2} \frac{|\mathbf{p}|}{p^0 + m}, \quad (2.6.121)$$

$$\mathcal{R} \approx 1 - i \frac{\sigma}{2} \cdot \frac{\alpha \wedge \mathbf{p}}{p^0 + m} = 1 + i s \cdot \frac{\mathbf{p} \wedge \alpha}{p^0 + m}. \quad (2.6.122)$$

So in general we find

$$S(\Lambda)u(r, \mathbf{p}) = \sum_{r'} \mathcal{R}(\Lambda, \mathbf{p})_{r' r} u(r', \Lambda \mathbf{p}), \quad (2.6.123)$$

where \mathcal{R} is the Wigner rotation associated to the transformation Λ . And an identical formula holds for $v(r, \mathbf{p})$.

Let us now consider any solution of the Dirac equation

$$\psi(x) = \sum_{r=1}^2 \int d\Omega_{\mathbf{p}} [\varphi_r^+(p)u(r, \mathbf{p})e^{-ipx} + \varphi_r^-(p)v(r, \mathbf{p})e^{ipx}]. \quad (2.6.124)$$

By construction the Poincaré group is realized in a local way on the space of these solutions

$$T_a : \psi(x) \xrightarrow{a} \psi'(x) = \psi(x + a), \quad (2.6.125)$$

$$\Lambda : \psi(x) \xrightarrow{\Lambda} \psi'(x) = \psi(\Lambda^{-1}x). \quad (2.6.126)$$

For infinitesimal transformations, recalling that $(\Lambda^{-1}x)^{\mu} \approx x^{\mu} - \omega_{\nu}^{\mu} x^{\nu}$, we have

$$\psi(x) \xrightarrow{a} (1 + a^{\mu} \partial_{\mu})\psi(x), \quad (2.6.127)$$

$$\psi(x) \xrightarrow{\Lambda} (1 + \frac{i}{2} \omega^{\mu\nu} \sigma_{\mu\nu} - \omega^{\mu\nu} x_{\nu} \partial_{\mu})\psi(x). \quad (2.6.128)$$

And the generators are

$$p_\mu = i\partial_\mu, \quad (2.6.129)$$

$$J_{(\mu\nu)} = \sigma_{\mu\nu} + \frac{1}{i}(x_\mu\partial_\nu - x_\nu\partial_\mu). \quad (2.6.130)$$

For the translations we find

$$\varphi_r^+(\mathbf{p}) \xrightarrow{a} e^{-ipa}\varphi_r^+(\mathbf{p}), \quad (2.6.131)$$

$$\varphi_r^-(\mathbf{p}) \xrightarrow{a} e^{ipa}\varphi_r^-(\mathbf{p}), \quad (2.6.132)$$

which are the usual transformations laws, in the momentum representation, for the eigenstates of the momenta \mathbf{p} and $-\mathbf{p}$ respectively.

For Lorentz transformations we find

$$\begin{aligned} \psi(x) &\xrightarrow{\Lambda} \sum_{r,r'=1}^2 \int d\Omega_{\mathbf{p}} \left[\varphi_r^+(\mathbf{p}) \mathcal{R}(\Lambda, \mathbf{p})_{r'r} u(r', \Lambda\mathbf{p}) e^{-ip(\Lambda^{-1}x)} + \right. \\ &\quad \left. \varphi_r^-(\mathbf{p}) \mathcal{R}(\Lambda, \mathbf{p})_{r'r} v(r', \Lambda\mathbf{p}) e^{ip(\Lambda^{-1}x)} \right] \\ &= \sum_{r,r'=1}^2 \int d\Omega_{\mathbf{p}} \left[\varphi_r^+(\Lambda^{-1}\mathbf{p}) \mathcal{R}(\Lambda, \Lambda^{-1}\mathbf{p})_{r'r} u(r', \mathbf{p}) e^{-ipx} + \right. \\ &\quad \left. \varphi_r^-(\Lambda^{-1}\mathbf{p}) \mathcal{R}(\Lambda, \Lambda^{-1}\mathbf{p})_{r'r} v(r', \mathbf{p}) e^{ipx} \right]. \end{aligned} \quad (2.6.133)$$

So the law of transformation on the functions φ^\pm is

$$\varphi_r^+(\mathbf{p}) \xrightarrow{\Lambda} \sum_{r'} \mathcal{R}(\Lambda, \Lambda^{-1}\mathbf{p})_{rr'} \varphi_r^+(\Lambda^{-1}\mathbf{p}), \quad (2.6.134)$$

$$\varphi_r^-(\mathbf{p}) \xrightarrow{\Lambda} \sum_{r'} \mathcal{R}(\Lambda, \Lambda^{-1}\mathbf{p})_{rr'} \varphi_r^-(\Lambda^{-1}\mathbf{p}). \quad (2.6.135)$$

This law of transformation is identical with the one constructed in Section 2.5.1. The generators can be found recalling that for rotations and velocity infinitesimal transformations we have

$$\mathcal{R}(\boldsymbol{\theta}) \approx 1 + i\frac{\boldsymbol{\sigma}}{2} \cdot \boldsymbol{\theta}, \quad (2.6.136)$$

$$\mathcal{R}(\boldsymbol{\alpha}) \approx 1 - i\frac{\boldsymbol{\sigma}}{2} \cdot \frac{\boldsymbol{\alpha} \wedge \mathbf{p}}{p^0 + m}. \quad (2.6.137)$$

The result is

$$\mathbf{J} = \frac{\boldsymbol{\sigma}}{2} - ip \wedge \frac{\partial}{\partial \mathbf{p}}, \quad (2.6.138)$$

$$\mathbf{K} = \frac{1}{2} \frac{\mathbf{p} \wedge \boldsymbol{\sigma}}{p^0 + m} + ip^0 \frac{\partial}{\partial \mathbf{p}}, \quad (2.6.139)$$

which coincides with the expressions (2.5.102) and (2.5.105).

Let us now write the scalar product in terms of the $\psi(x)$. Let ψ_a and ψ_b be two solutions of the Dirac equation. Then the quantity

$$J_{(a,b)}^\mu(x) = \bar{\psi}_b(x) \gamma^\mu \psi_a(x), \quad (2.6.140)$$

is conserved

$$\partial_\mu J_{(a,b)}^\mu(x) = 0, \quad (2.6.141)$$

as can easily be proved from the Dirac equation and recalling that $\gamma^0\gamma^0 = 1$ and $\gamma^0\gamma^\mu\gamma^0 = \gamma^\mu$. $J_{(a,b)}^\mu$ transforms as a four-vector under Lorentz transformations

$$\begin{aligned} J_{(a,b)}^\mu(x) &\xrightarrow{\Lambda} \bar{\psi}_b(\Lambda^{-1}x)S^{-1}(\Lambda)\gamma^\mu S(\Lambda)\psi_a(\Lambda^{-1}x) \\ &= (\Lambda^{-1})^\mu{}_\nu \bar{\psi}_b(\Lambda^{-1}x)\gamma^\nu \psi_a(\Lambda^{-1}x), \end{aligned} \quad (2.6.142)$$

where we used Eq. (2.6.62) and (2.6.79). The conservation law is thus covariant. Applying Gauss theorem as in the scalar case, the integral extended to any space-like surface with normal $d\sigma^\mu$,

$$\int d\sigma_\mu J_{(a,b)}^\mu(x), \quad (2.6.143)$$

is independent from the chosen surface. Choosing a surface $x^0 = \text{constant}$, it is independent from x^0 . We thus define

$$\langle a|b\rangle = \int dx \bar{\psi}_b(x, t)\gamma^0\psi_a(x, t) = \int dx \bar{\psi}_b(x, 0)\gamma^0\psi_a(x, 0). \quad (2.6.144)$$

Respect to this scalar product, since it is Lorentz invariant and clearly translational invariant, the transformations of Eqs. (2.6.127)-(2.6.128) are realized as unitary operators. It can be easily shown that their generators (2.6.129)-(2.6.130) are hermitian respect to this scalar product.

Using the equations

$$u^\dagger(r, p)u(s, p) = v^\dagger(r, p)v(s, p) = 2p^0\delta_{rs}, \quad (2.6.145)$$

$$u^\dagger(r, p)v(s, -p) = 0, \quad (2.6.146)$$

we obtain

$$\langle a|b\rangle = \int d\Omega_p \left[\varphi_b^{+*}(p)\varphi_a^+(p) + \varphi_b^{-*}(p)\varphi_a^-(p) \right]. \quad (2.6.147)$$

So the scalar product coincides, in the two subspaces relative to positive and negative energies, with the scalar product originally introduced for the representation of the Poincaré group.

We have then realized, in a local way, a unitary irreducible representation of the Poincaré group, extended to the parity transformations, for particles of mass m and spin 1/2.

2.6.3 Particles of spin 1

The most simple Lorentz transformation which contains spin 1 is the $(\frac{1}{2}, \frac{1}{2})$ representation, i.e the one of four-vectors. For this representation $|s_z|$ can assume the values 0 and 1.

A local wave function $W^\mu(x)$ transforms according to the law

$$W^\mu(x) \xrightarrow{\Lambda} \Lambda^\mu{}_\nu W^\nu(\Lambda^{-1}x). \quad (2.6.148)$$

For the state with definite momentum

$$W_p^\mu(x) = e^{-ipx}\varepsilon^\mu(r, p), \quad (2.6.149)$$

For the spin to be 1, in the rest frame the four-vector $\varepsilon^\mu(p)$ must have only spatial components. This means

$$\varepsilon^\mu(r, p)p_\mu = 0. \quad (2.6.150)$$

Then in addition to the Klein-Gordon equation

$$(\square + m^2)W^\mu(x) = 0, \quad (2.6.151)$$

$W^\mu(x)$ must satisfy the constraint (2.6.150) which in coordinate representation translates into

$$\partial_\mu W^\mu(x) = 0. \quad (2.6.152)$$

The Eqs. (2.6.151) and (2.6.152) are equivalent to the system

$$G_{\mu\nu}(x) = \partial_\mu W_\nu(x) - \partial_\nu W_\mu(x), \quad (2.6.153)$$

$$\partial_\mu G^{\mu\nu}(x) - m^2 W^\nu(x) = 0. \quad (2.6.154)$$

In fact applying ∂_ν to the second equation and using the antisymmetry of $G_{\mu\nu}$ we find

$$m^2 \partial_\mu W^\mu(x) = 0, \quad (2.6.155)$$

which coincides with Eq. (2.6.152) when $m \neq 0$. On the other hand if $\partial_\mu W^\mu(x) = 0$ the Eq. (2.6.154) coincides with (2.6.151).

The Eqs. (2.6.153) and (2.6.154) has both positive and negative energy solutions. The general solution is of the form

$$W^\mu(x) = \sum_{r=1}^3 \int d\Omega_p [W(r, p)\varepsilon^\mu(r, p)e^{-ipx} + \tilde{W}(r, p)\varepsilon^{\mu*}(r, p)e^{ipx}], \quad (2.6.156)$$

where $\varepsilon_\mu(r, p)$ are independent vectors that obey to Eq. (2.6.150).

By construction such solution is an irreducible representation of the Poincaré group.

We can define a scalar product, exactly in the same way we did for the spin 0 case,

$$\langle a|b\rangle = -i \int d\sigma^\nu W_{a\mu}^*(x) \overset{\leftrightarrow}{\partial}_\nu W_b^\mu(x) \quad (2.6.157)$$

$$= - \int d\Omega_p W_{a\mu}^*(p) W_b^\mu(p), \quad (2.6.158)$$

where

$$W_{a\mu}(p) = \sum_{r=1}^3 W_a(r, p)\varepsilon_\mu(r, p). \quad (2.6.159)$$

Note that

$$\sum_{r=1}^3 \varepsilon_\mu(r, p)\varepsilon_\nu^*(r, p) = -g_{\mu\nu} + \frac{p_\mu p_\nu}{m^2}, \quad (2.6.160)$$

represents the density matrix for unpolarized states. The proof is straightforward in the rest frame. The covariance fixes the form in other frames.

Let us give, for completeness, an explicit representation of the base $\varepsilon^\mu(r, \mathbf{p})$. In the rest frame we can choose any three spatial orthonormal vectors. Let them be $\boldsymbol{\varepsilon}(r, \mathbf{0})$. For particles with momentum \mathbf{p} we can define, according to Eq. (2.5.174),

$$\varepsilon^\mu(r, \mathbf{p}) = S(\Lambda_{\mathbf{p}})\varepsilon(r, \mathbf{0}) = (\Lambda_{\mathbf{p}})^\mu_\nu \varepsilon^\nu(r, \mathbf{0}), \quad (2.6.161)$$

where we used the fact that ε^μ transform as a four-vector. Using then the explicit expression (2.5.80) we have

$$\varepsilon^0(r, \mathbf{p}) = \frac{\mathbf{p} \cdot \boldsymbol{\varepsilon}(r, \mathbf{0})}{m}, \quad (2.6.162)$$

$$\boldsymbol{\varepsilon}(r, \mathbf{p}) = \boldsymbol{\varepsilon}(r, \mathbf{0}) + \mathbf{p} \frac{\mathbf{p} \cdot \boldsymbol{\varepsilon}(r, \mathbf{0})}{m(p^0 + m)}. \quad (2.6.163)$$

The canonical base is the one where $\varepsilon^i(r, \mathbf{0}) = \delta_{ir}$. Choosing instead as a base the eigenstates of s_z we have

$$\boldsymbol{\varepsilon}(+1, \mathbf{0}) = -\frac{i}{\sqrt{2}}(e_x + ie_y), \quad (2.6.164)$$

$$\boldsymbol{\varepsilon}(0, \mathbf{0}) = ie_z, \quad (2.6.165)$$

$$\boldsymbol{\varepsilon}(-1, \mathbf{0}) = \frac{i}{\sqrt{2}}(e_x - ie_y), \quad (2.6.166)$$

where e_x, e_y, e_z are the versors of the axes.

In the vectorial case the Wigner matrix \mathcal{R} is defined by

$$\mathcal{R}(\Lambda)_{r'r}\varepsilon^\mu(r', \mathbf{p}) = \Lambda^\mu_\nu \varepsilon^\nu(r, \Lambda^{-1}\mathbf{p}). \quad (2.6.167)$$

2.7 The second quantization

It is an experimental fact that the number of particles may change in physical processes: An hydrogen atom in the state $2P$ is composed by an electron and a proton and decays into an atom in its fundamental state plus a photon, an electron which pass through the Coulomb field of nucleus is accelerated and emit photons (Bremsstrahlung), when a positron annihilates with an electron their mass is converted in energy in the form of two photons, in the scattering between two high energy protons many pions are produced, Then, exist transitions between states with different number of particles. In Section 2.7.1 we will present a formalism that allows to describe systems of many free particles, used in any many-body theory, relativistic or not, and known as Fock method. It allows to describe many particles states with the correct statistics and to introduce operators that change the number of particles (creation and annihilation operators).

In Section 2.7.2 we will introduce the free field operators, and we will interpret in terms of field operators the negative energy solutions of the equations of free motion.

The relativistic equations of motion can be rederived in the Lagrangian formalism and it can be shown that the Fock second quantization is equivalent to the canonical quantization of a system of an infinite number of degrees of freedom.

The Lagrangian formalism is indispensable to write theories of non-free particles: In interaction.

2.7.1 Fock space

Let us consider an orthonormal complete base $|i\rangle$ for the single particle states. For example the base $|r, p\rangle$ of the positive energy states for relativistic particles introduced in Section 2.6.

If the particles are bosons, in the state $|i\rangle$ can coexist an arbitrary number n_i of free particles.

If the particles are fermions, in the state $|i\rangle$ can exist at most one particle.

In both cases, assigning the occupation numbers $\{n_i\}$ in the various states $|i\rangle$ determines completely the state of the system, since the state must be symmetric for the bosons and completely antisymmetric for the fermions.

Bosons

For any state $|i\rangle$ the observable number of particles in such state, n_i , has integer eigenvalues: $1, 2, 3, \dots$

His spectrum is the one of an harmonic oscillator. As for the harmonic oscillator is possible to define a rising (creation) operator b_i^\dagger and a lowering (annihilation) operator b_i of the eigenvalue of n_i . The commutation properties are

$$[b_i, b_i^\dagger] = 1 \quad [b_i, b_j] = [b_i^\dagger, b_j^\dagger] = 0, \quad (2.7.1)$$

We then define $n_i = b_i^\dagger b_i$ with

$$[n_i, b_i] = -b_i \quad [n_i, b_i^\dagger] = b_i^\dagger. \quad (2.7.2)$$

The lower state $|0_i\rangle$ corresponds to zero particles in the state $|i\rangle$ and $b_i|0_i\rangle = 0$ with $\langle 0_i | 0_i \rangle = 1$. The normalized state with n_i particles is then

$$\frac{(b_i^\dagger)^{n_i}}{\sqrt{n_i!}} |0_i\rangle = |n_i\rangle. \quad (2.7.3)$$

A state identified by the set of occupation numbers $\{n_i\}$ in the different states $|i\rangle$ can be written as

$$|n_{i_1}, \dots, n_{i_k}, \dots\rangle = \prod_{i_1} \frac{(b_{i_1}^\dagger)^{n_{i_1}}}{\sqrt{n_{i_1}!}} |0\rangle \quad (2.7.4)$$

where $|0\rangle = \prod_i |0_i\rangle$ is the vacuum. It is automatically symmetric under particle exchange if

$$[b_i, b_k] = [b_i^\dagger, b_k^\dagger] = 0. \quad (2.7.5)$$

The “harmonic oscillators” correspondent to different modes are independent and we must also have

$$[b_i, b_k^\dagger] = \delta_{ik}. \quad (2.7.6)$$

The total number of particles is

$$N = \sum_i n_i = \sum_i b_i^\dagger b_i, \quad (2.7.7)$$

Moreover $\langle 0 | 0 \rangle = 1$.

Fermions

For the fermions the occupation number can be 0 or 1 and the state must be completely antisymmetric under particle exchange. This can be realized by associating to each single particle state an harmonic anti-oscillator, requiring anticommutation between operators relative to different modes

$$[b_i, b_k]_+ = [b_i^\dagger, b_k^\dagger]_+ = 0 \quad [b_i, b_k^\dagger]_+ = \delta_{ik}, \quad (2.7.8)$$

$$n_i = b_i^\dagger b_i \quad N = \sum_i n_i \quad b_i |0_i\rangle = 0, \quad (2.7.9)$$

$$[n_i, b_k] = -b_i \delta_{ik} \quad [n_i, b_k^\dagger] = b_i^\dagger \delta_{ik}. \quad (2.7.10)$$

The subscript + indicates the anticommutator. The possible states in the mode $|i\rangle$ are $|0_i\rangle$ and $b_i^\dagger |0_i\rangle = |1_i\rangle$. $b_i^{\dagger 2} |0_i\rangle = 0$ because the operator b_i^\dagger anticommutes with itself. Moreover

$$b_i b_i^\dagger |0_i\rangle = (-b_i b_i^\dagger + 1) |0_i\rangle = |0_i\rangle. \quad (2.7.11)$$

Observations

Given an operator O written in terms of creation and annihilation operators we will denote with $:O:$ the normal ordered operator for bosons or the antinormal ordered operator for fermions. For bosons it is obtained from O displacing all creation operators to the left and all annihilation operators to the right and for fermions is obtained from O displacing all creation operators to the left and all annihilation operators to the right times $(-1)^n$, with n the number of needed exchanges of a creation and an annihilation operator. For example for bosons $:bb^\dagger: = b^\dagger b = bb^\dagger - 1$. Normal ordering is not linear. For example $:bb^\dagger: = :1 + b^\dagger b: = :1: + :b^\dagger b: = 1 + b^\dagger b \neq b^\dagger b$. For fermions $:bb^\dagger: = -b^\dagger b = bb^\dagger - 1$. In particular we will always have $\langle 0| :O: 0\rangle = 0$ on the vacuum. We usually refer to the normal order as the Wick order.

The (anti)commutation relations are invariant under unitary changes of base. Let V be a unitary transformation from the base $|1_i\rangle$ for the single particle states to the base $|1_\alpha\rangle$

$$|1_\alpha\rangle = \sum_i V_{\alpha i} |1_i\rangle \quad |1_i\rangle = \sum_i V_{i\alpha}^\dagger |1_\alpha\rangle, \quad (2.7.12)$$

with $VV^\dagger = V^\dagger V = 1$. If $|1_i\rangle = b_i^\dagger |0\rangle$ then $|1_\alpha\rangle = \sum_i V_{\alpha i} b_i^\dagger |0\rangle$. Defining

$$b_\alpha^\dagger = \sum_i V_{\alpha i} b_i^\dagger \quad b_\alpha = \sum_i V_{i\alpha}^\dagger b_i, \quad (2.7.13)$$

we have

$$[b_\alpha, b_\beta]_\pm = [b_\alpha^\dagger, b_\beta^\dagger]_\pm = 0, \quad (2.7.14)$$

$$[b_\alpha, b_\beta^\dagger]_\pm = \sum_{ij} V_{\alpha i}^* V_{\beta j} [b_i, b_j^\dagger]_\pm = \sum_i V_{\alpha i}^* V_{\beta i} = (VV^\dagger)_{\beta\alpha} = \delta_{\alpha\beta}. \quad (2.7.15)$$

The vacuum remains unchanged.

If the index i that label the states is continuous, as for the momentum p in the base $|r, p\rangle$ for free particles, the (anti)commutation rules must be modified replacing the δ_{ik} in the Eqs. (2.7.6) and (2.7.8) the diagonal element of the identity matrix in the chosen representation. For the states $|r, p\rangle$

$$[b(r, p), b(r', p')]_\pm = [b^\dagger(r, p), b^\dagger(r', p')]_\pm = 0, \quad (2.7.16)$$

$$[b(r, p), b^\dagger(r', p')]_\pm = \delta_{rr'} (2\pi)^3 2p^0 \delta(p - p'), \quad (2.7.17)$$

where \pm denotes the commutator or anticommutator. This choice give the correct states normalization. In fact

$$\langle r, p | r', p' \rangle = \langle 0 | b(r, p) b^\dagger(r', p') | 0 \rangle = \langle 0 | [b(r, p), b^\dagger(r', p')]_\pm | 0 \rangle = \delta_{rr'} (2\pi)^3 2p^0 \delta(p - p'). \quad (2.7.18)$$

The density of occupation number is $b^\dagger(r, p)b(r, p)$ and the total number of particles is

$$N = \int d\Omega_p \sum_r b^\dagger(r, p) b(r, p). \quad (2.7.19)$$

The commutation rules for N are

$$[N, b(r, p)] = -b(r, p) \quad [N, b^\dagger(r, p)] = b^\dagger(r, p). \quad (2.7.20)$$

2.7.2 Field operators

Let

$$|s\rangle = \int d\Omega_p \sum_r \varphi_s(r, p) |r, p\rangle, \quad (2.7.21)$$

be any single particle state. It can be written as

$$|s\rangle = \int d\Omega_p \sum_r \varphi_s(r, p) b^\dagger(r, p) |0\rangle, \quad (2.7.22)$$

with

$$\langle r', p' | s \rangle = \langle 0 | b(r', p') s \rangle = \int d\Omega_p \sum_r \varphi_s(r, p) \langle 0 | b(r', p') b^\dagger(r, p) | 0 \rangle, \quad (2.7.23)$$

but

$$\langle 0 | b(r', p') b^\dagger(r, p) | 0 \rangle = \delta_{rr'} (2\pi)^3 2p^0 \delta(p - p'), \quad (2.7.24)$$

and so

$$\langle 0 | b(r', p') s \rangle = \varphi_s(r', p'). \quad (2.7.25)$$

The operator $b(r, p)$ extracts from a state the component with momentum p . We can construct an operator which acts in the same way on the x space. For a particle of any spin let us consider the positive energy solutions and build the following operator

$$\varphi_+(x) = \int d\Omega_p \sum_r b(r, p) u(r, p) e^{-ipx}. \quad (2.7.26)$$

The operator $\varphi_+(x)$ has the same number of components of the function $u(r, p)$: 1 for spin 0, 4 for spin 1/2 and 1. In any case from Eq. (2.7.26) follows

$$\langle 0 | \varphi_+(x) s \rangle = \int d\Omega_p \sum_r \varphi_s(r, p) u(r, p) e^{-ipx} = \varphi_s(x), \quad (2.7.27)$$

where $\varphi_s(x)$ is the wave function of the state $|s\rangle$.

The operator $\varphi_+(x)$ defined in Eq. (2.7.26) is called field operator or better the positive energy component of the field operator. The subscript + indicates that it contains only positive energies.

The operator $\varphi_+(x)$ is a linear superposition of solutions $u(r, p)e^{-ipx}$ with positive energy of the wave equation, so it is a solution with positive energy of the wave equation.

Let us give the explicit formulas for the field operator

$$\text{spin 0} \quad \varphi_+(x) = \int d\Omega_p b(p) e^{-ipx}, \quad (2.7.28)$$

$$\text{spin } \frac{1}{2} \quad \psi_+(x) = \int d\Omega_p \sum_{r=1}^2 u(r, p) b(r, p) e^{-ipx}, \quad (2.7.29)$$

$$\text{spin 1} \quad W_+^\mu(x) = \int d\Omega_p \sum_{r=1}^3 \varepsilon_\mu^r(r, p) b(r, p) e^{-ipx}. \quad (2.7.30)$$

It is possible to invert these formulas using the expressions for the scalar products defined in the various cases (2.6.22), (2.6.144), and (2.6.157)

$$\text{spin 0} \quad b(p) = i \int d\sigma^\mu e^{ipx} \overleftrightarrow{\partial}_\mu \varphi_+(x) = i \int dx e^{ipx} \overleftrightarrow{\partial}_0 \varphi_+(x), \quad (2.7.31)$$

$$\text{spin } \frac{1}{2} \quad b(r, p) = \int dx u^\dagger(r, p) e^{ipx} \psi_+(x), \quad (2.7.32)$$

$$\text{spin 1} \quad b(r, p) = -i \int dx \varepsilon_\mu^*(r, p) e^{ipx} \overleftrightarrow{\partial}_0 W_+^\mu(x). \quad (2.7.33)$$

All observables can be expressed in terms of $b^\dagger(r, p)$ and $b(r, p)$. Then they can be expressed in terms of the fields and of their first derivatives for spin 0 and 1 particles, and in terms of the fields for spin 1/2 particles.

2.7.3 Transformation properties of the field operators

The invariance under a symmetry group implies the existence of a unitary representation of the group which send the Hilbert space into itself.

For a free particle the symmetry group is the Poincaré group and the representation is irreducible. We want now construct the representation of the group on the many free particles states.

Let $U(\Lambda, a) = T_a U(\Lambda)$ be a transformation of the group with Lorentz matrix Λ and translation parameter a^μ . On the single particle states we know that

$$U(\Lambda, a)|r, p\rangle = e^{-i(\Lambda p)a} \mathcal{R}(\Lambda, p)_{r'r}|r', \Lambda p\rangle, \quad (2.7.34)$$

where \mathcal{R} is a unitary matrix which represents the Wigner rotation. To construct the representation of the group in the Fock space we assume that the vacuum is invariant

$$U(\Lambda, a)|0\rangle = |0\rangle, \quad (2.7.35)$$

and we set

$$U(\Lambda, a)b^\dagger(r, p)U^\dagger(\Lambda, a) = e^{-i(\Lambda p)a} \mathcal{R}(\Lambda, p)_{r'r}b^\dagger(r', \Lambda p). \quad (2.7.36)$$

This representation realizes the (2.7.34) and transforms independently the many particles states. For the annihilation operator we will then have

$$U(\Lambda, a)b(r, p)U^\dagger(\Lambda, a) = e^{i(\Lambda p)a} \mathcal{R}(\Lambda, p)_{rr'}^* b(r', \Lambda p). \quad (2.7.37)$$

We define the transformed of $b(r, p)$ as follows ⁴

$$b(r, p) \rightarrow U^\dagger(\Lambda, a)b(r, p)U(\Lambda, a). \quad (2.7.39)$$

From Eq. (2.7.37), recalling that

$$U^{-1}(\Lambda, a) = U(\Lambda^{-1}, -\Lambda^{-1}a), \quad (2.7.40)$$

we find

$$U^\dagger(\Lambda, a)b(r, p)U(\Lambda, a) = e^{-ipa} \mathcal{R}(\Lambda, \Lambda^{-1}p)_{rr'} b(r', \Lambda^{-1}p), \quad (2.7.41)$$

$$U^\dagger(\Lambda, a)b^\dagger(r, p)U(\Lambda, a) = e^{ipa} \mathcal{R}(\Lambda, \Lambda^{-1}p)_{rr'}^* b(r', \Lambda^{-1}p). \quad (2.7.42)$$

$$(2.7.43)$$

To derive Eq. (2.7.41) we used

$$\mathcal{R}(\Lambda^{-1}, p)_{rr'}^* = \mathcal{R}(\Lambda^{-1}, p)_{rr'}^\dagger, \quad (2.7.44)$$

and

$$\mathcal{R}(\Lambda^{-1}, p)_{rr'}^\dagger = \mathcal{R}(\Lambda, \Lambda^{-1}p)_{rr'}. \quad (2.7.45)$$

Eq. (2.7.45) can be derived observing that \mathcal{R} is unitary, that

$$|r, p\rangle = U(\Lambda)U^\dagger(\Lambda)|r, p\rangle = U(\Lambda)\mathcal{R}(\Lambda^{-1}, p)_{rr'}|r', \Lambda^{-1}p\rangle \quad (2.7.46)$$

$$= \mathcal{R}(\Lambda, \Lambda^{-1}p)_{rr'}\mathcal{R}(\Lambda^{-1}, p)_{rr'}|r'', p\rangle, \quad (2.7.47)$$

and that $|r, p\rangle$ is a complete base at fixed p . Since the transformation (2.7.41) is unitary in Fock space it leaves unchanged the commutation relations.

The generators of the unitary transformation $U(\Lambda, a)$ can be explicitly constructed as hermitian operators on Fock space. For infinitesimal transformations

$$U(\Lambda, a) \approx 1 - ip_\mu a^\mu + i\boldsymbol{\theta} \cdot \mathbf{J} - i\boldsymbol{\alpha} \cdot \mathbf{K}. \quad (2.7.48)$$

We recall that for infinitesimal rotations

$$\mathcal{R}(\Lambda)_{rr'} \approx \delta_{rr'} + i\boldsymbol{\theta} \cdot \mathbf{s}_{rr'}, \quad (2.7.49)$$

$$b(r, \Lambda^{-1}p) \approx b(r, p + \boldsymbol{\theta} \wedge p) \approx b(r, p) + \boldsymbol{\theta} \cdot \left(p \wedge \frac{\partial}{\partial p} \right) b(r, p), \quad (2.7.50)$$

and for infinitesimal velocity transformations

$$\mathcal{R}(\Lambda)_{rr'} \approx \delta_{rr'} - i \frac{\boldsymbol{\alpha} \wedge p}{p^0 + m} \cdot \mathbf{s}_{rr'}, \quad (2.7.51)$$

$$b(r, \Lambda^{-1}p) \approx b(r, p + \boldsymbol{\alpha} p^0) \approx b(r, p) + \boldsymbol{\alpha} \cdot p^0 \frac{\partial}{\partial p} b(r, p). \quad (2.7.52)$$

⁴Note that here we must define the transformed operator using the inverse transformation respect to the one that applies to regular observables for which the measure in the two reference frames must coincide. In fact

$$\varphi_s(r, p) = \langle 0 | bs \rangle \rightarrow \langle 0 | U^\dagger b U s \rangle \equiv \langle 0 | b' s \rangle, \quad (2.7.38)$$

where b' is the transformed operator and in the last equation we used the fact that $U|0\rangle = |0\rangle$ and $U|s\rangle = |s'\rangle$.

Using Eqs. (2.7.41) and (2.7.48) we derive the commutation relations for the generators

$$[p_\mu, b(r, \mathbf{p})] = -p_\mu b(r, \mathbf{p}), \quad (2.7.53)$$

$$[J, b(r, \mathbf{p})] = -\left(s - i\mathbf{p} \wedge \frac{\partial}{\partial \mathbf{p}}\right)_{rr'} b(r', \mathbf{p}), \quad (2.7.54)$$

$$[\mathbf{K}, b(r, \mathbf{p})] = -\left(\frac{\mathbf{p} \wedge s}{p^0 + m} + ip^0 \frac{\partial}{\partial \mathbf{p}}\right)_{rr'} b(r', \mathbf{p}). \quad (2.7.55)$$

Taking the hermitian conjugate and recalling that the s matrices are hermitian we find

$$[p_\mu, b^\dagger(r, \mathbf{p})] = p_\mu b^\dagger(r, \mathbf{p}), \quad (2.7.56)$$

$$[J, b^\dagger(r, \mathbf{p})] = \left(s + i\mathbf{p} \wedge \frac{\partial}{\partial \mathbf{p}}\right)_{r'r} b^\dagger(r', \mathbf{p}), \quad (2.7.57)$$

$$[\mathbf{K}, b^\dagger(r, \mathbf{p})] = \left(\frac{\mathbf{p} \wedge s}{p^0 + m} - ip^0 \frac{\partial}{\partial \mathbf{p}}\right)_{r'r} b^\dagger(r', \mathbf{p}). \quad (2.7.58)$$

It is possible to give an explicit representation for the operators p_μ , J , and \mathbf{K} in terms of the operators b and b^\dagger

$$p_\mu = \int d\Omega_p \sum_r b^\dagger(r, \mathbf{p}) p_\mu b(r, \mathbf{p}), \quad (2.7.59)$$

$$J = \int d\Omega_p \sum_r b^\dagger(r, \mathbf{p}) \left(s - i\mathbf{p} \wedge \frac{\partial}{\partial \mathbf{p}}\right)_{rr'} b(r, \mathbf{p}), \quad (2.7.60)$$

$$\mathbf{K} = \int d\Omega_p \sum_r b^\dagger(r, \mathbf{p}) \left(\frac{\mathbf{p} \wedge s}{p^0 + m} + ip^0 \frac{\partial}{\partial \mathbf{p}}\right)_{rr'} b(r, \mathbf{p}), \quad (2.7.61)$$

so that these operators satisfy the commutation rules (2.7.53)-(2.7.55).

Let us now treat the transformation properties of the field operator. The Eq. (2.7.41) induces the following transformation

$$U^\dagger(\Lambda, a)\varphi_+(x)U(\Lambda, a) = \int d\Omega_p e^{-ipx} \sum_r u(r, \mathbf{p}) e^{-ipa} \mathcal{R}(\Lambda, \Lambda^{-1}\mathbf{p})_{rr'} b(r', \Lambda^{-1}\mathbf{p}). \quad (2.7.62)$$

Changing variables $\mathbf{p} \rightarrow \Lambda\mathbf{p}$ and using Eq. (2.6.123) we find

$$\varphi'(x) \equiv U^\dagger(\Lambda, a)\varphi_+(x)U(\Lambda, a) = S(\Lambda)\varphi_+(\Lambda^{-1}x + \Lambda^{-1}a), \quad (2.7.63)$$

which is the correct transformation law for a local operator⁵. Indicating with x' the transformed event we can also write

$$\varphi'_+(x') = U^\dagger\varphi_+(x')U = S(\Lambda)\varphi_+(x). \quad (2.7.64)$$

This equation allows to write down immediately the action of the generators of the Poincaré group on the field operators. Denoting with $J_{(\mu\nu)}$ and p_μ the generators in the Fock space

$$U(T_a) = e^{-ia^\mu p_\mu} \quad U(\Lambda) = e^{\frac{i}{2}\omega^{\mu\nu} J_{(\mu\nu)}}, \quad (2.7.65)$$

and with $\sigma_{\mu\nu}$ the generator of the group in the representation under which φ transforms, i.e. the generator of the $S(\Lambda)$ matrix, from Eq. (2.7.63) follows

$$[p_\mu, \varphi_+(x)] = -i\partial_\mu \varphi_+(x), \quad (2.7.66)$$

$$[J_{(\mu\nu)}, \varphi_+(x)] = -[\sigma_{\mu\nu} - i(x_\mu \partial_\nu - x_\nu \partial_\mu)] \varphi_+(x), \quad (2.7.67)$$

as follows from Eqs. (2.6.129) and (2.6.130).

⁵We recall that $(\Lambda, a)^{-1}x = (T_a\Lambda)^{-1}x = \Lambda^{-1}T_{-a}x = \Lambda^{-1}x + \Lambda^{-1}a$.

2.7.4 Locality and spin-statistics theorem

In constructing the relativistic theory it is necessary to deal with local operators commuting at spacelike distances. In fact, since a signal can not propagate at speeds higher than that of light, measures occurred at spatial distances must not influence each other. As observed in Section 2.7.2 all observables can be written in terms of fields and their first derivatives. If the (anti)commutators between these quantities are zero for spacelike distances it will be possible to construct a theory that satisfies causality.

From the commutators between the operators $b(r, p)$ and $b^\dagger(r, p)$ we can easily calculate the commutators between the fields and their derivatives. Let us consider first the scalar field

$$[\varphi_+(x), \varphi_+(y)] = 0, \quad (2.7.68)$$

$$[\varphi_+(x), \varphi_+^\dagger(y)] = F_+(x - y), \quad (2.7.69)$$

$$[\varphi_+(x), \partial_0 \varphi_+^\dagger(y)] = \frac{\partial}{\partial y^0} F_+(x - y), \quad (2.7.70)$$

where Eq. (2.7.70) follows from Eq. (2.7.69).

The function F_+ is invariant under translations and under Lorentz transformations. It is in fact a c-number, i.e. as an operator in the Fock space it is proportional to the identity, because such is $[b(r, p), b^\dagger(r, p)]$. From Eq. (2.7.69) follows that

$$U^\dagger(\Lambda, a)[\varphi_+(x), \varphi_+^\dagger(x)]U(\Lambda, a) = F_+(x - y)U^\dagger(\Lambda, a)U(\Lambda, a) = F_+(x - y). \quad (2.7.71)$$

But the first member is also equal to

$$[\varphi_+(\Lambda^{-1}(x + a)), \varphi_+^\dagger(\Lambda^{-1}(x + a))] = F_+(\Lambda^{-1}(x - y)), \quad (2.7.72)$$

and this proves the invariance of F_+ under the Poincaré group.

Explicitly we have

$$F_+(x - y) = \int d\Omega_p e^{-ip(x-y)}. \quad (2.7.73)$$

If x and y are at spacelike distances it is always possible to bring them to be simultaneous ($x^0 = y^0$) through a Lorentz transformation. To study the behavior of F_+ at spacelike distances it is sufficient to study it at equal times ($x^0 = y^0$). We then have

$$F_+(0, x - y) = \int d\Omega_p e^{ip \cdot (x-y)}, \quad (2.7.74)$$

$$\left. \frac{\partial}{\partial y^0} F_+(x^0 - y^0, x - y) \right|_{y^0=x^0} = \frac{i}{2} \int \frac{dp}{(2\pi)^3} e^{ip \cdot (x-y)} = \frac{i}{2} \delta(x - y). \quad (2.7.75)$$

The integral in Eq. (2.7.74) can be easily calculated in terms of Bessel functions

$$F_+(0, x - y) = \frac{m}{(2\pi)^2 |x - y|} K_0(m|x - y|). \quad (2.7.76)$$

F_+ is different from zero at spacelike distances of the order of the Compton wavelength of the particle ($\ell = h/mc$). So a theory constructed in terms of just the φ_+ is non local.

But we remember that next to the positive energy solutions exist the “negative energy” solutions of the Klein-Gordon equation. In the Fock space context a dependence of the kind e^{ipx} is associated to a creation operator, rather than to a destruction operator as in the expansion

for φ_+ . While considering the negative energy solutions is then natural to introduce a “negative frequency” field

$$\varphi_-(x) = \int d\Omega_p e^{ipx} d^\dagger(p). \quad (2.7.77)$$

The operators $d^\dagger(p)$ and $d(p)$ are operator independent from $b^\dagger(p)$ and $b(p)$, i.e. they describe a different particle, and so they commute with them.

Let us now construct the field

$$\varphi(x) = \varphi_+(x) + \varphi_-(x), \quad (2.7.78)$$

or

$$\varphi(x) = \int d\Omega_p [d(p)e^{-ipx} + d^\dagger(p)e^{ipx}], \quad (2.7.79)$$

$$\varphi^\dagger(x) = \int d\Omega_p [d^\dagger(p)e^{ipx} + d(p)e^{-ipx}]. \quad (2.7.80)$$

$$(2.7.81)$$

The commutators now becomes

$$[\varphi(x), \varphi(y)] = [\varphi^\dagger(x), \varphi^\dagger(y)] = 0, \quad (2.7.82)$$

$$[\varphi(x), \varphi^\dagger(y)] = F_+(x - y) - F_+(y - x), \quad (2.7.83)$$

$$[\varphi(x), \partial_0 \varphi^\dagger(y)] = \frac{\partial}{\partial y^0} [F_+(x - y) - F_+(y - x)]. \quad (2.7.84)$$

At equal times, at spacelike distances, we have

$$[\varphi(x^0, x), \varphi^\dagger(x^0, y)] = 0, \quad (2.7.85)$$

$$[\varphi(x^0, x), \partial_0 \varphi^\dagger(x^0, y)] = i\delta(x - y). \quad (2.7.86)$$

The theory is now *local*.

We note that the minus sign in the Eqs. (2.7.83) and (2.7.84) depends by the choice of commutation relation: The locality in Eqs. (2.7.85) and (2.7.86) would have been destroyed if we would have chosen the Fermi statistics. This is a manifestation of the so called *spin-statistics theorem*.

We note that since $\varphi(x)$ is a superposition of solutions of the Klein-Gordon equation it itself satisfies to such equation

$$(\square + m^2)\varphi(x) = 0. \quad (2.7.87)$$

Note that since $b(p) \neq d(p)$ the scalar field is not hermitian. This is also called a *charged* scalar field. The hermitian field is called *neutral*. The particle described by the creation operator d^\dagger is called *antiparticle*.

Let us now treat the spin 1/2 case. For the Dirac field,

$$\psi_+(x) = \int d\Omega_p \sum_r u(r, p) b(r, p) e^{-ipx}, \quad (2.7.88)$$

we have

$$\begin{aligned} [\psi_+^\alpha(x), \psi_+^\beta(y)]_+ &= \int d\Omega_p \sum_r u^\alpha(r, p) u^\beta(r, p) e^{-ip(x-y)} \\ &= \int d\Omega_p [(\not{p} + m)\gamma^0]^{\alpha\beta} e^{-ip(x-y)}, \end{aligned} \quad (2.7.89)$$

where we used the anticommutation relations for the b, b^\dagger and we used the Eq. (2.6.109) for the projector on the positive energies states.

Omitting the indexes α, β and using the anticommutation rules of the γ matrices we can then write

$$[\psi_+(x), \psi_+^\dagger(y)]_+ = \left(i \frac{\partial}{\partial x^0} + m\gamma^0 + i\gamma^0 \boldsymbol{\gamma} \cdot \boldsymbol{\nabla} \right) F_+(x - y), \quad (2.7.90)$$

where F_+ is again given by Eq. (2.7.74). At equal times

$$[\psi_+(x^0, \mathbf{x}), \psi_+^\dagger(x^0, \mathbf{y})]_+ = \frac{i}{2} \delta(\mathbf{x} - \mathbf{y}) + (m\gamma^0 + i\gamma^0 \boldsymbol{\gamma} \cdot \boldsymbol{\nabla}) F_+(x - y), \quad (2.7.91)$$

which is non-local.

In analogy to what we did in the scalar case we introduce

$$\psi_-(x) = \int d\Omega_{\mathbf{p}} \sum_r v(r, \mathbf{p}) b^\dagger(r, \mathbf{p}) e^{ipx}, \quad (2.7.92)$$

where d^\dagger is the creation operator for a new particle

$$[d(r, \mathbf{p}), d^\dagger(r', \mathbf{p}')]_+ = \delta_{rr'} 2p^0 (2\pi)^3 \delta(\mathbf{p} - \mathbf{p}'), \quad (2.7.93)$$

$$[d, d]_+ = [d^\dagger, d^\dagger]_+ = [b, d]_+ = [b, d^\dagger]_+ = [b^\dagger, d]_+ = [b^\dagger, d^\dagger]_+ 0, \quad (2.7.94)$$

and $\psi(x) = \psi_+(x) + \psi_-(x)$, with

$$\psi(x) = \int d\Omega_{\mathbf{p}} \sum_r [u(r, \mathbf{p}) b(r, \mathbf{p}) e^{-ipx} + v(r, \mathbf{p}) d^\dagger(r, \mathbf{p}) e^{ipx}], \quad (2.7.95)$$

$$\psi^\dagger(x) = \int d\Omega_{\mathbf{p}} \sum_r [u^\dagger(r, \mathbf{p}) b^\dagger(r, \mathbf{p}) e^{ipx} + v^\dagger(r, \mathbf{p}) d(r, \mathbf{p}) e^{-ipx}]. \quad (2.7.96)$$

Then

$$[\psi(x), \psi(y)]_+ = [\psi^\dagger(x), \psi^\dagger(y)]_+ = 0, \quad (2.7.97)$$

$$\begin{aligned} [\psi(x), \psi^\dagger(y)]_+ &= \int d\Omega_{\mathbf{p}} \left[(\not{p} + m) \gamma^0 e^{-ip(x-y)} + (\not{p} - m) \gamma^0 e^{ip(x-y)} \right] \\ &= \int d\Omega_{\mathbf{p}} \left[\left(i\gamma^\mu \frac{\partial}{\partial x^\mu} + m \right) \gamma^0 e^{-ip(x-y)} + \left(i\gamma^\mu \frac{\partial}{\partial y^\mu} - m \right) \gamma^0 e^{ip(x-y)} \right] \\ &= \left(i\gamma^\mu \frac{\partial}{\partial x^\mu} + m \right) \gamma^0 [F_+(x - y) - F_+(y - x)]. \end{aligned} \quad (2.7.98)$$

At equal times, using $\gamma^0 \gamma^0 = 1$, we find

$$[\psi(x^0, \mathbf{x}), \psi^\dagger(x^0, \mathbf{y})]_+ = i\delta(\mathbf{x} - \mathbf{y}), \quad (2.7.99)$$

which is again local. Again we must notice that in order to have Eq. (2.7.99) in a local form it was essential to choose the anticommutators. The commutator would have brought a minus sign for the vv^\dagger term in Eq. (2.7.98) and to a non-local result. This is a manifestation of the spin-statistic theorem.

Since ψ is a linear superposition of Dirac equation solutions, it itself is a solution of the Dirac equation

$$(i\not{\partial} - m)\psi(x) = 0. \quad (2.7.100)$$

Let us conclude with the case of a massive vectorial field. The analysis is identical to the scalar case. For a vectorial field we define

$$W_\mu(x) = \int d\Omega_p \sum_{r=1}^3 [\varepsilon_\mu(r, p)b(r, p)e^{-ipx} + \varepsilon_\mu^*(r, p)d^\dagger(r, p)e^{ipx}], \quad (2.7.101)$$

$$W_\mu^\dagger(x) = \int d\Omega_p \sum_{r=1}^3 [\varepsilon_\mu^*(r, p)b^\dagger(r, p)e^{ipx} + \varepsilon_\mu(r, p)d(r, p)e^{-ipx}]. \quad (2.7.102)$$

The commutation rules can be easily derived recalling Eq. (2.6.160)

$$[W_\mu(x), W_\nu^\dagger(y)] = -\left(g_{\mu\nu} + \frac{1}{m^2} \frac{\partial}{\partial x^\mu} \frac{\partial}{\partial x^\nu}\right) \times [F_+(x-y) - F_+(y-x)], \quad (2.7.103)$$

$$[W_\mu(x^0, x), W_\nu^\dagger(x^0, y)] = -\frac{i}{2m^2} [g_{\mu 0}\partial_\nu + g_{0\nu}\partial_\mu]\delta(x-y), \quad (2.7.104)$$

$$[W_\mu(x^0, x), \partial_0 W_\nu^\dagger(x^0, y)] = -\left(g_{\mu\nu} + \frac{\partial_\mu\partial_\nu}{m^2}\right) i\delta(x-y). \quad (2.7.105)$$

Also in this case the use of the Bose statistics has been essential for the locality of (2.7.104). Again this is a manifestation of the spin-statistics theorem.

The vectorial field W_μ will satisfy to the following system of equations

$$(\square + m^2)W^\mu(x) = 0, \quad (2.7.106)$$

$$\partial_\mu W^\mu = 0 \quad (2.7.107)$$

The spin-statistics theorem states that, as a consequence of Lorentz invariance and of locality, half integer spin particles must obey to Fermi statistics and integer spin particles must obey to Bose statistics.

As we saw in the various cases, the introduction of the negative energy solutions does not interfere with the Lorentz structure of the fields. Since the commutation rules of the operators b and d are identical we can write the action of the group on the whole Fock space generated by b^\dagger and d^\dagger . In particular the generators are given by

$$p_\mu = \int d\Omega_p \sum_r [b^\dagger(r, p)p_\mu b(r, p) + d^\dagger(r, p)p_\mu d(r, p)], \quad (2.7.108)$$

$$\begin{aligned} \mathbf{J} = & \int d\Omega_p \sum_r \left[b^\dagger(r, p) \left(s - ip \wedge \frac{\partial}{\partial p} \right)_{rr'} b(r, p) + \right. \\ & \left. d^\dagger(r, p) \left(s - ip \wedge \frac{\partial}{\partial p} \right)_{rr'} d(r, p) \right], \end{aligned} \quad (2.7.109)$$

$$\begin{aligned} \mathbf{K} = & \int d\Omega_p \sum_r \left[b^\dagger(r, p) \left(\frac{\mathbf{p} \wedge \mathbf{s}}{p^0 + m} + ip^0 \frac{\partial}{\partial p} \right)_{rr'} b(r, p) + \right. \\ & \left. d^\dagger(r, p) \left(\frac{\mathbf{p} \wedge \mathbf{s}}{p^0 + m} + ip^0 \frac{\partial}{\partial p} \right)_{rr'} d(r, p) \right], \end{aligned} \quad (2.7.110)$$

as can be inferred by Eqs. (2.7.59)-(2.7.61).

On the field operators Eqs. (2.7.66) and (2.7.67) now give

$$[p_\mu, \varphi(x)] = -i\partial_\mu \varphi(x), \quad (2.7.111)$$

$$[J_{(\mu\nu)}, \varphi(x)] = -[\sigma_{\mu\nu} - i(x_\mu\partial_\nu - x_\nu\partial_\mu)]\varphi(x), \quad (2.7.112)$$

From the point of view of the Poincaré group it is evident from the construction and from the generators (2.7.108)-(2.7.110) that the antiparticle states are identical to the particle ones: they describe a system of free particles of mass m .

References

- V. B. Berestetskiĭ, E. M. Lifshitz, and L. P. Pitaevskiĭ. *Relativistic Quantum Theory*. Pergamon Press Ltd, Oxford, 1971.
- Y. M. Shirokov. A Group-Theoretical Consideration on the Basis of Relativistic Quantum Mechanics. I. The General Properties of the Inhomogeneous Lorentz Group. *JETP*, 6:664, 1958a.
- Y. M. Shirokov. A Group-Theoretical Consideration on the Basis of Relativistic Quantum Mechanics. II. Classification of the Irreducible Representations of the Inhomogeneous Lorentz Group. *JETP*, 6:919, 1958b.
- Y. M. Shirokov. A Group-Theoretical Consideration on the Basis of Relativistic Quantum Mechanics. III. Irreducible Representations of the Classes P_0 and O_0 , and the Non-Completely-Reducible Representations of the Inhomogeneous Lorentz Group. *JETP*, 6:929, 1958c.
- Y. M. Shirokov. A Group-Theoretical Consideration of the Basis of Relativistic Quantum Mechanics. IV. Space Reflections in Quantum Theory. *JETP*, 7:493, 1958d.
- Y. M. Shirokov. A Group-Theoretical Consideration of the Basis of Relativistic Quantum Mechanics. V. *JETP*, 9:620, 1959.

Appendices

2.A Commutators

The commutator of two operators A and B is defined as

$$[A, B] = AB - BA. \quad (2.A.1)$$

The commutator satisfies to the following Lie algebra relations

$$[A, A] = 0, \quad (2.A.2)$$

$$[A, B] = -[B, A], \quad (2.A.3)$$

$$[A, [B, C]] + [B, [C, A]] + [C, [A, B]] = 0, \quad (2.A.4)$$

where the third one is known as the Jacobi identity.

For three operators A, B , and C we also have

$$[A, B + C] = [A, B] + [A, C], \quad (2.A.5)$$

$$[A, BC] = B[A, C] + [A, B]C. \quad (2.A.6)$$

If $[A, B] = \alpha \in \mathbb{C}$ then

$$[A, B^2] = B[A, B] + [A, B]B = 2\alpha B, \quad (2.A.7)$$

$$[A, B^3] = B[A, B^2] + [A, B]B^2 = 3\alpha B^2, \quad (2.A.8)$$

$$\dots \\ [A, B^n] = n\alpha B^{n-1}. \quad (2.A.9)$$

Then, given a smooth function f , using its Taylor series expansion, we readily obtain

$$[A, f(B)] = \alpha \frac{df(B)}{dB}. \quad (2.A.10)$$

In general we can prove the following lemma:

Hadamard lemma: Given any two operators A and B we have

$$e^A B e^{-A} = B + [A, B] + \frac{1}{2!} [A, [A, B]] + \frac{1}{3!} [A, [A, [A, B]]] + \dots \quad (2.A.11)$$

Proof: Consider the function $f(s) = e^{sA} B e^{-sA}$. We want $f(1)$. Taylor expand $f(s)$ around $s = 0$

$$f(s) = f(0) + s f'(0) + \frac{1}{2!} s^2 f''(0) + \frac{1}{3!} s^3 f'''(0) + \dots, \quad (2.A.12)$$

but it is easy to see that

$$f'(s) = e^{sA} ABe^{-sA} - e^{sA} BAe^{-sA} = e^{sA}[A, B]e^{-sA}, \quad (2.A.13)$$

$$f''(s) = e^{sA}[A, [A, B]]e^{-sA}, \quad (2.A.14)$$

$$f'''(s) = e^{sA}[A, [A, [A, B]]]e^{-sA}, \quad (2.A.15)$$

and so on.

Another important result is the Baker–Campbell–Hausdorff formula:

Baker–Campbell–Hausdorff formula: Given any two operators A and B we have

$$\ln(e^A e^B) = A + B + \frac{1}{2}[A, B] + \frac{1}{12}([A, [A, B]] + [B, [B, A]]) - \frac{1}{24}[B, [A, [A, B]]] + \dots \quad (2.A.16)$$

Proof: Consider

$$\frac{1}{1-x} = 1 + x + x^2 + x^3 + \dots \quad (2.A.17)$$

or

$$\frac{1}{1+x} = 1 - x + x^2 - x^3 + \dots \quad (2.A.18)$$

integrate respect to x

$$\ln(1+x) = x - \frac{1}{2}x^2 + \frac{1}{3}x^3 - \frac{1}{4}x^4 + \dots \quad (2.A.19)$$

or

$$\ln(x) = (x-1) - \frac{1}{2}(x-1)^2 + \frac{1}{3}(x-1)^3 - \frac{1}{4}(x-1)^4 + \dots \quad (2.A.20)$$

Now

$$\begin{aligned} \ln(e^A e^B) &= \sum_{k=1} \frac{(-1)^{k-1}}{k} \left(\sum_{m,n=0} \frac{A^m B^n}{m!n!} - 1 \right)^k \\ &= \left(A + B + AB + \frac{A^2 + B^2}{2} \dots \right) - \frac{1}{2} (A^2 + B^2 + AB + BA \dots) + \dots \\ &= A + B + \frac{1}{2}[A, B] + \dots \end{aligned} \quad (2.A.21)$$

Commutators are of fundamental importance in a *Lie algebra*: a vector space \mathfrak{g} together with an operation called the Lie bracket, an alternating bilinear map $\mathfrak{g} \times \mathfrak{g} \rightarrow \mathfrak{g}$, that satisfies the Jacobi identity. In other words, a Lie algebra is an algebra over a field for which the multiplication operation (called the Lie bracket) is alternating and satisfies the Jacobi identity. The Lie bracket of two vectors x and y is denoted $[x, y]$. A Lie algebra is typically a non-associative algebra. However, every associative algebra gives rise to a Lie algebra, consisting of the same vector space with the commutator Lie bracket, $[x, y] = xy - yx$.

Lie groups are smooth differentiable manifolds and as such can be studied using differential calculus, in contrast with the case of more general topological groups. One of the key ideas in the theory of Lie groups is to replace the global object, the group, with its local or linearized version, which Lie himself called its “infinitesimal group” and which has since become known as its Lie algebra or the tangent space to the manifold at the identity.

The following theorem is also of great importance:

Theorem: Given two hermitian operators A and B which commutes, $[A, B] = 0$, they can be diagonalized simultaneously on the same orthonormal base of vectors of the Hilbert space.

2.B The Levi-Civita symbol

The Levi-Civita symbol $\epsilon_{i_1 i_2 \dots i_n}$ is defined as a total antisymmetric n rank tensor with $\epsilon_{012\dots n} = 1$.

In two dimensions

$$\epsilon_{ij}\epsilon_{ik} = \delta_{jk}, \quad (2.B.1)$$

$$\epsilon_{ij}\epsilon_{ij} = 2, \quad (2.B.2)$$

where in the first equation we contracted one index and in the second equation we contracted both indexes.

In three dimensions

$$\epsilon_{ijk}\epsilon_{ilm} = \delta_{jl}\delta_{km} - \delta_{jm}\delta_{kl}, \quad (2.B.3)$$

$$\epsilon_{ijk}\epsilon_{ijl} = 3\delta_{kl} - \delta_{kl} = 2\delta_{kl}, \quad (2.B.4)$$

$$\epsilon_{ijk}\epsilon_{ijk} = 6. \quad (2.B.5)$$

In general

$$\epsilon_{i_1 i_2 \dots i_n} \epsilon_{j_1 j_2 \dots j_n} = \det \begin{pmatrix} \delta_{i_1 j_1} & \cdots & \delta_{i_1 j_n} \\ \vdots & \ddots & \\ \delta_{i_n j_1} & & \delta_{i_n j_n} \end{pmatrix}. \quad (2.B.6)$$

Also for an $n \times n$ matrix \mathbf{A} with $(\mathbf{A})_{ij} = a_{ij}$ we have

$$\det(\mathbf{A}) = \epsilon_{i_1 i_2 \dots i_n} a_{1i_1} a_{2i_2} \cdots a_{ni_n}, \quad (2.B.7)$$

$$\det(\mathbf{A}) \epsilon_{j_1 j_2 \dots j_n} = \epsilon_{i_1 i_2 \dots i_n} a_{i_1 j_1} a_{i_2 j_2} \cdots a_{i_n j_n}. \quad (2.B.8)$$

2.C Angular momentum

Consider the angular momentum hermitian operator $\hat{\mathbf{L}}$, where the hat denotes the operator. Then the following commutation relations hold

$$[\hat{L}_i, \hat{L}_j] = i\epsilon_{ijk}\hat{L}_k. \quad (2.C.1)$$

Then define

$$\hat{L}^2 = \sum_{i=1}^3 \hat{L}_i^2, \quad (2.C.2)$$

$$\hat{L}_\pm = \hat{L}_1 \pm i\hat{L}_2. \quad (2.C.3)$$

We can then prove the following relations

$$[\hat{L}^2, \hat{L}_i] = 0, \quad (2.C.4)$$

$$[\hat{L}_+, \hat{L}_-] = 2\hat{L}_3, \quad (2.C.5)$$

$$[\hat{L}_3, \hat{L}_\pm] = \pm \hat{L}_\pm, \quad (2.C.6)$$

and

$$\hat{L}^2 = \hat{L}_+ \hat{L}_- + \hat{L}_3^2 - \hat{L}_3 = \hat{L}_- \hat{L}_+ + \hat{L}_3^2 + \hat{L}_3 \quad (2.C.7)$$

Since \widehat{L}^2 commutes with \widehat{L}_3 we can diagonalize them simultaneously so that

$$\widehat{L}^2|\psi_{L,M}\rangle = \mathcal{L}^2|\psi_{L,M}\rangle, \quad (2.C.8)$$

$$\widehat{L}_3|\psi_{L,M}\rangle = M|\psi_{L,M}\rangle, \quad (2.C.9)$$

where, since $\widehat{L}^2 - \widehat{L}_3^2 = \widehat{L}_1^2 + \widehat{L}_2^2$, we called L the maximum value of $|M|$ for a given value \mathcal{L} . Then

$$\widehat{L}_3\widehat{L}_\pm|\psi_{L,M}\rangle = (M \pm 1)\widehat{L}_\pm|\psi_{L,M}\rangle, \quad (2.C.10)$$

$$\widehat{L}_+|\psi_{L,L}\rangle = 0. \quad (2.C.11)$$

From Eq. (2.C.7) follows

$$0 = \widehat{L}_-\widehat{L}_+|\psi_{L,L}\rangle = (\widehat{L}^2 - \widehat{L}_3^2 - \widehat{L}_3)|\psi_{L,L}\rangle, \quad (2.C.12)$$

or $\mathcal{L}^2 = L(L+1)$. Also M can assume $2L+1$ values, namely $M = L, L-1, \dots, -L$. And $2L = 0, 1, 2, 3, \dots$

For the orbital angular momentum $\widehat{\mathbf{L}} = \widehat{\mathbf{r}} \wedge \widehat{\mathbf{p}}$. In the coordinate representation $\widehat{\mathbf{r}} = \mathbf{r}$ and $\widehat{\mathbf{p}} = -i\nabla_r$. From the commutation relations for position and momentum

$$[\widehat{r}_i, \widehat{r}_j] = 0, \quad (2.C.13)$$

$$[\widehat{p}_i, \widehat{p}_j] = 0, \quad (2.C.14)$$

$$[\widehat{r}_i, \widehat{p}_j] = i\delta_{ij}, \quad (2.C.15)$$

follows

$$[\widehat{L}_i, \widehat{r}_j] = i\epsilon_{ijk}\widehat{r}_k, \quad (2.C.16)$$

$$[\widehat{L}_i, \widehat{p}_j] = i\epsilon_{ijk}\widehat{p}_k, \quad (2.C.17)$$

and again Eq. (2.C.1). Using spherical coordinates

$$r_1 = r \sin \theta \cos \phi, \quad r_2 = r \sin \theta \sin \phi, \quad r_3 = r \cos \theta, \quad (2.C.18)$$

we find in particular

$$\widehat{L}_3 = -i\frac{\partial}{\partial \phi}. \quad (2.C.19)$$

So we see that the eigenvalue equation

$$\widehat{L}_3\psi_{L,M}(\mathbf{r}) = M\psi_{L,M}(\mathbf{r}), \quad (2.C.20)$$

has solution

$$\psi_{L,M} = f(r, \theta)e^{iM\phi}, \quad (2.C.21)$$

where f is an arbitrary function. If the function $\psi_{L,M}$ has to be single valued, it must be periodic in ϕ with period 2π . Hence we find that additionally for the orbital case we must have $M = 0, \pm 1, \pm 2, \dots$, i.e. L must be an integer.

If we have to add the angular momentum of two different systems, $\widehat{\mathbf{L}} = \widehat{\mathbf{L}}^{(1)} + \widehat{\mathbf{L}}^{(2)}$, we can either choose the set of commuting operators $\{(\widehat{L}^{(1)})^2, (\widehat{L}^{(2)})^2, \widehat{L}_3^{(1)}, \widehat{L}_3^{(2)}\}$ or the other one $\{(\widehat{L}^{(1)})^2, (\widehat{L}^{(2)})^2, \widehat{L}^2, \widehat{L}_3\}$, since $[\widehat{L}^{(1)}, \widehat{L}^{(2)}] = 0$.

2.D SU(2)

The special unitary group of degree n , $SU(n)$, is the group of $n \times n$ unitary matrices with determinant 1. Its dimension as a real manifold is $n^2 - 1 = 3$. Topologically it is compact and simply connected. Algebraically it is a simple Lie group.

Consider the 2×2 complex matrices A which are unitary $A^\dagger A = 1$ and with determinant equal to 1. The most general 2×2 complex matrix can be written as

$$A = \begin{pmatrix} z_1 & z_2 \\ z_3 & z_4 \end{pmatrix} \quad z_i = \rho_i e^{i\varphi_i}. \quad (2.D.1)$$

Imposing unitarity is the same as imposing the three following conditions

$$z_1^* z_1 + z_3^* z_3 = 1, \quad (2.D.2)$$

$$z_2^* z_2 + z_4^* z_4 = 1, \quad (2.D.3)$$

$$z_1^* z_2 + z_3^* z_4 = 0. \quad (2.D.4)$$

Imposing that the determinant is 1 amounts to setting

$$z_1 z_4 - z_2 z_3 = 1. \quad (2.D.5)$$

This four conditions can be rewritten as follows

$$\rho_1^2 + \rho_3^2 = 1, \quad (2.D.6)$$

$$\rho_2^2 + \rho_4^2 = 1, \quad (2.D.7)$$

$$\rho_1 \rho_2 e^{i(\varphi_2 - \varphi_1)} + \rho_3 \rho_4 e^{i(\varphi_4 - \varphi_3)} = 0, \quad (2.D.8)$$

$$\rho_1 \rho_4 e^{i(\varphi_1 + \varphi_4)} - \rho_2 \rho_3 e^{i(\varphi_2 - \varphi_3)} = 1. \quad (2.D.9)$$

Taking the modulus of Eq. (2.D.8) gives $\rho_1 \rho_2 = \rho_3 \rho_4$. When we use this relation in Eqs. (2.D.6) and (2.D.7) we find $\rho_1 = \rho_4$ and $\rho_2 = \rho_3$. Then Eq. (2.D.8) gives $\varphi_2 - \varphi_1 + \varphi_3 - \varphi_4 = \pi$ which when used in Eq. (2.D.9) gives

$$\rho_1^2 + \rho_2^2 = e^{-i(\varphi_1 + \varphi_4)}, \quad (2.D.10)$$

which in turn is satisfied by $\rho_1^2 + \rho_2^2 = 1$ and $\varphi_1 + \varphi_4 = 0$. Then we end up with matrices of the form

$$A = \begin{pmatrix} \rho_1 e^{i\varphi_1} & \pm \sqrt{1 - \rho_1^2} e^{i\varphi_2} \\ \mp \sqrt{1 - \rho_1^2} e^{-i\varphi_2} & \rho_1 e^{-i\varphi_1} \end{pmatrix}. \quad (2.D.11)$$

In other words we can say that

$$SU(2) = \left\{ \begin{pmatrix} \alpha & -\beta^* \\ \beta & \alpha^* \end{pmatrix} \mid \alpha, \beta \in \mathbb{C}, \quad |\alpha|^2 + |\beta|^2 = 1 \right\}. \quad (2.D.12)$$

The Lie algebra $SU(2)$ of the group is obtained through the exponential map as the 2×2 complex matrices ia such that $A = e^{ia}$. Then the unitarity of A implies that a be hermitian and the condition for A to have determinant 1 implies that a be traceless. It is easy to prove that $SU(n)$ has dimension $2n(n-1)/2 + n - 1 = n^2 - 1$ and

$$SU(2) = \{i\boldsymbol{\theta} \cdot \boldsymbol{\sigma} \mid \boldsymbol{\theta} \in \mathbb{R}^3\}, \quad (2.D.13)$$

with σ_i the Pauli matrices

$$\sigma_1 = \sigma_x = \begin{pmatrix} 0 & 1 \\ 1 & 0 \end{pmatrix}, \quad (2.D.14)$$

$$\sigma_2 = \sigma_y = \begin{pmatrix} 0 & -i \\ i & 0 \end{pmatrix}, \quad (2.D.15)$$

$$\sigma_3 = \sigma_z = \begin{pmatrix} 1 & 0 \\ 0 & -1 \end{pmatrix}. \quad (2.D.16)$$

If we add to the Pauli matrices the identity matrix

$$1 = \begin{pmatrix} 1 & 0 \\ 0 & 1 \end{pmatrix} = \sigma_1^2 = \sigma_2^2 = \sigma_3^2 = -i\sigma_1\sigma_2\sigma_3, \quad (2.D.17)$$

we obtain a base for the vector space of hermitian 2×2 complex matrices.

The Pauli matrices are unitary and some of their properties are as follows

$$\det(\sigma_i) = -1, \quad (2.D.18)$$

$$\text{Tr}(\sigma_i) = 0, \quad (2.D.19)$$

$$\det(\mathbf{a} \cdot \boldsymbol{\sigma}) = -|\mathbf{a}|^2, \quad (2.D.20)$$

$$[\sigma_i, \sigma_j] = 2i\epsilon_{ijk}\sigma_k, \quad (2.D.21)$$

$$\{\sigma_i, \sigma_j\} = 2\delta_{ij}1, \quad (2.D.22)$$

$$(\mathbf{a} \cdot \boldsymbol{\sigma})(\mathbf{b} \cdot \boldsymbol{\sigma}) = (\mathbf{a} \cdot \mathbf{b})1 + i(\mathbf{a} \wedge \mathbf{b}) \cdot \boldsymbol{\sigma}, \quad (2.D.23)$$

$$e^{ia(\hat{\mathbf{n}} \cdot \boldsymbol{\sigma})} = 1 \cos a + i(\hat{\mathbf{n}} \cdot \boldsymbol{\sigma}) \sin a. \quad (2.D.24)$$

The Pauli matrices offer a representation for the spin 1/2 operator s as follows

$$s = \frac{\boldsymbol{\sigma}}{2}. \quad (2.D.25)$$

There exists a 2 : 1 group homomorphism between $SU(2)$ and $SO(3)$.

2.E Velocity transformations

A velocity transformation with $\beta = (0, 0, \beta)$ is $x' = \Lambda x$ with

$$\begin{pmatrix} x'^0 \\ x'^1 \\ x'^2 \\ x'^3 \end{pmatrix} = \begin{pmatrix} \gamma & 0 & 0 & -\gamma\beta \\ 0 & 1 & 0 & 0 \\ 0 & 0 & 1 & 0 \\ -\gamma\beta & 0 & 0 & \gamma \end{pmatrix} \begin{pmatrix} x^0 \\ x^1 \\ x^2 \\ x^3 \end{pmatrix}, \quad (2.E.1)$$

where $\gamma = 1/\sqrt{1-\beta^2}$. The velocity transformation can be cast into another useful form by defining a parameter α called the *rapidity* (or hyperbolic angle) such that

$$e^\alpha = \gamma(1+\beta) = \sqrt{\frac{1+\beta}{1-\beta}}, \quad (2.E.2)$$

and thus

$$e^{-\alpha} = \gamma(1-\beta) = \sqrt{\frac{1-\beta}{1+\beta}}. \quad (2.E.3)$$

So

$$\gamma = \cosh \alpha = \frac{e^\alpha + e^{-\alpha}}{2}, \quad (2.E.4)$$

$$\beta\gamma = \sinh \alpha = \frac{e^\alpha - e^{-\alpha}}{2}, \quad (2.E.5)$$

$$(2.E.6)$$

and therefore

$$\beta = \tanh \alpha. \quad (2.E.7)$$

We then have

$$\begin{pmatrix} x'^0 \\ x'^1 \\ x'^2 \\ x'^3 \end{pmatrix} = \begin{pmatrix} \cosh \alpha & 0 & 0 & -\sinh \alpha \\ 0 & 1 & 0 & 0 \\ 0 & 0 & 1 & 0 \\ -\sinh \alpha & 0 & 0 & \cosh \alpha \end{pmatrix} \begin{pmatrix} x^0 \\ x^1 \\ x^2 \\ x^3 \end{pmatrix}, \quad (2.E.8)$$

with

$$\begin{pmatrix} \cosh \alpha & 0 & 0 & -\sinh \alpha \\ 0 & 1 & 0 & 0 \\ 0 & 0 & 1 & 0 \\ -\sinh \alpha & 0 & 0 & \cosh \alpha \end{pmatrix} = \exp \left[-i\alpha \begin{pmatrix} 0 & 0 & 0 & -i \\ 0 & 0 & 0 & 0 \\ 0 & 0 & 0 & 0 \\ -i & 0 & 0 & 0 \end{pmatrix} \right] = \exp(-i\alpha K^3), \quad (2.E.9)$$

where the simpler Lie-algebraic hyperbolic rotation generator iK^3 is called a *boost* generator.

Chapter 3

The Polaron

3.1 Introduction

An electron in a ionic crystal polarizes the lattice in its neighborhood. An electron moving with its accompanying distortion of the lattice has sometimes been called a “polaron” [??](#). Since 1933 Landau addresses the possibility whether an electron can be self-trapped (ST) in a deformable lattice [???](#). This fundamental problem in solid state physics has been intensively studied for an optical polaron in an ionic crystal [??????](#). Bogoliubov approached the polaron strong coupling limit with one of his canonical transformations. Feynman used his path integral formalism and a variational principle to develop an all coupling approximation for the polaron ground state [?](#). Its extension to finite temperatures appeared first by Osaka [??](#), and more recently by Castrigiano *et al.* [???](#). Recently the polaron problem has gained new interest as it could play a role in explaining the properties of the high T_c superconductors [?](#). The polaron problem has also been studied to describe an impurity in a Bose-Einstein ultracold quantum gas condensate of atoms [?](#). In this context evidence for a transition between free and self-trapped optical polarons is found. For the solid state optical polaron no ST state has been found yet [???](#).

The acoustic modes of lattice vibration are known to be responsible for the appearance of the ST state [???](#). Contrary to the optical mode which interacts with the electron through Coulombic force and is dispersionless, the acoustic phonons have a linear dispersion coupled to the electron through a short range potential which is believed to play a crucial role in forming the ST state [?](#). Acoustic modes have also been widely studied [?](#). Sumi and Toyozawa generalized the optical polaron model by including a coupling to the acoustic modes [?](#). Using Feynman’s variational approach, they found that the electron is ST with a very large effective mass as the acoustic coupling exceeds a critical value. Emin and Holstein also reached a similar conclusion within a scaling theory [?](#) in which the Gaussian trial wave function is essentially identical to the harmonic trial action used in the Feynman’s variational approach in the adiabatic limit [?](#).

The ST state distinguishes itself from an extended state (ES) where the polaron has lower mass and a bigger radius. A polaronic phase transition separates the two states with a breaking of translational symmetry in the ST one [?](#). The variational approach is unable to clearly assess the existence of the phase transition [?](#). In particular Gerlach and Löwen [?](#) concluded that no phase transition exists in a large class of polarons. The three dimensional acoustic polaron is not included in the class but Fisher *et al.* [?](#) argued that its ground state is delocalized.

In a recent work [Fantoni \[2012a\]](#) we employed for the first time a specialized path integral Monte Carlo (PIMC) method [Ceperley \[1995\]](#); [?](#) to the continuous, highly non-local, acoustic polaron problem at low temperature which is valid at all values of the coupling strength and solves

the problem exactly (in a Monte Carlo sense). The method differs from previously employed methods [???????](#) and hinges on the Lévy construction and the multilevel Metropolis method with correlated sampling. In such work the potential energy was calculated and it was shown that like the effective mass it usefully signals the transition between the ES and the ST state. Properties of ES and ST states were explicitly shown through the numerical simulation.

Aim of the chapter is to give a detailed description of the PIMC method used in that calculation and some additional numerical results in order to complement the brief paper of Ref. [Fantoni \[2012a\]](#). In particular it is presented a calculation of the properties of an acoustic polaron in three dimensions in thermal equilibrium at a given low temperature using the path integral Monte Carlo method. The specialized numerical method used is described in full details, thus complementing Ref. [Fantoni \[2012a\]](#), and it appears to be the first time it has been used in this context. These results are in favor of the presence of a phase transition from a localized state to an extended state for the electron as the phonon-electron coupling constant decreases. The phase transition manifests itself with a jump discontinuity in the potential energy as a function of the coupling constant and it affects the properties of the path of the electron in imaginary time: In the weak coupling regime the electron is in an extended state whereas in the strong coupling regime it is found in a self-trapped state.

The chapter is organized as follows: in section [3.2](#) we describe the acoustic polaron model and Hamiltonian, in section [3.3](#) we describe the observables we are going to compute in the simulation, in section [3.4](#) we describe the PIMC numerical scheme employed, in section [3.5](#) we describe the multilevel Metropolis method for sampling the path, in section [3.6](#) we describe the choice of the transition probability and the level action, in section [3.7](#) we describe the correlated sampling. Section [3.8](#) is for the results, and section [3.9](#) is for final remarks.

3.2 The model

The acoustic polaron can be described by the following quasi-continuous model [??](#),

$$\hat{H} = \frac{\hat{p}^2}{2m} + \sum_k \hbar\omega_k \hat{a}_k^\dagger \hat{a}_k + \sum_k (i\Gamma_k \hat{a}_k e^{ik\hat{x}} + \text{H.c.}) . \quad (3.2.1)$$

Here \hat{x} and \hat{p} are the electron coordinate and momentum operators respectively and \hat{a}_k is the annihilation operator of the acoustic phonon with wave vector k . The first term in the Hamiltonian is the kinetic energy of the electron, the second term the energy of the phonons and the third term the coupling energy between the electron and the phonons. The electron coordinate x is a continuous variable, while the phonons wave vector k is restricted by the Debye cut-off k_o . The acoustic phonons have a dispersion relation $\omega_k = uk$ (u being the sound velocity) and they interact with the electron of mass m through the interaction vertex $\Gamma_k = \hbar u k_o (S/N)^{1/2} (k/k_o)^{1/2}$ according to the deformation potential analysis of Ref. [?.](#) S is the coupling constant between the electron and the phonons and N the number of unit cells in the crystal with $N/V = (4\pi/3)(k_o/2\pi)^3$ by Debye approximation and V the crystal volume.

Using the path integral representation (see Ref. [? section 8.3](#)), the phonon part in the Hamiltonian can be exactly integrated owing to its quadratic form in phonon coordinates, and one can write the partition function for a polaron in thermal equilibrium at an absolute temperature T ($\beta = 1/k_B T$, with k_B Boltzmann constant) as follows,

$$Z = \int dx \iint_{x=x(0)}^{x=x(\hbar\beta)} e^{-\frac{1}{\hbar}\mathcal{S}[x(t), \dot{x}(t), t]} \mathcal{D}x(t) , \quad (3.2.2)$$

where the action \mathcal{S} is given by ?¹

$$\begin{aligned}\mathcal{S} &= \frac{m}{2} \int_0^{\hbar\beta} \dot{x}^2(t) dt - \frac{1}{2\hbar} \int_0^{\hbar\beta} dt \int_0^{\hbar\beta} ds \int \frac{dk}{(2\pi)^3} \Gamma_k^2 e^{ik \cdot (x(t) - x(s)) - \omega_k |t-s|} \\ &= \mathcal{S}_f + \mathcal{U} .\end{aligned}\quad (3.2.3)$$

Here \mathcal{S}_f is the *free particle action*, and \mathcal{U} the *inter-action* and we denoted with a dot a time derivative as usual. Using dimensionless units $\hbar = m = uk_o = k_B = V = 1$ the action becomes,

$$\mathcal{S} = \int_0^\beta \frac{\dot{x}^2(t)}{2} dt + \int_0^\beta dt \int_0^\beta ds V_{eff}(|x(t) - x(s)|, |t-s|) , \quad (3.2.4)$$

with the electron moving subject to an effective retarded potential,

$$V_{eff} = -\frac{S}{2I_D} \int_{q \leq 1} dq q e^{i\sqrt{\frac{2}{\gamma}}q \cdot (x(t) - x(s)) - q|t-s|} \quad (3.2.5)$$

$$= -\frac{3S}{2} \sqrt{\frac{\gamma}{2}} \frac{1}{|x(t) - x(s)|} \int_0^1 dq q^2 \sin\left(\sqrt{\frac{2}{\gamma}}q|x(t) - x(s)|\right) e^{-q|t-s|} , \quad (3.2.6)$$

where $q = k/k_o$, $I_D = \int_{q \leq 1} dq = 4\pi/3$, and we have introduced a non-adiabatic parameter γ defined as the ratio of the average phonon energy, $\hbar u k_o$ to the electron band-width, $(\hbar k_o)^2/2m$. This parameter is of order of 10^{-2} in typical ionic crystals with broad band so that the ST state is well-defined ?. In our simulation we took $\gamma = 0.02$. Note that the integral in (3.2.6) can be solved analytically and the resulting function tabulated.

3.3 The observables

In particular the internal energy E of the polaron is given by,

$$E = -\frac{1}{Z} \frac{\partial Z}{\partial \beta} = \frac{1}{Z} \int dx \iint e^{-\mathcal{S}} \frac{\partial \mathcal{S}}{\partial \beta} \mathcal{D}x = \left\langle \frac{\partial \mathcal{S}}{\partial \beta} \right\rangle , \quad (3.3.1)$$

where the internal energy tends to the ground state energy in the large $\beta \rightarrow \infty$ limit.

Scaling the Euclidean time $t = \beta t'$ and $s = \beta s'$ in Eq. (3.2.4), deriving \mathcal{S} with respect to β , and undoing the scaling, we get,

$$\begin{aligned}\frac{\partial \mathcal{S}}{\partial \beta} &= -\frac{1}{\beta} \int_0^\beta \frac{\dot{x}^2}{2} dt - \frac{S}{2I_D} \int_0^\beta dt \int_0^\beta ds \times \\ &\int_{q \leq 1} dq q e^{i\sqrt{\frac{2}{\gamma}}q \cdot (x(t) - x(s)) - q|t-s|} \frac{1}{\beta} (2 - q|t-s|) ,\end{aligned}\quad (3.3.2)$$

where the first term is the kinetic energy contribution to the internal energy, \mathcal{K} , and the last term is the potential energy contribution, \mathcal{P} ,

$$\begin{aligned}\mathcal{P} &= -\frac{3S}{2\beta} \int_0^\beta dt \int_0^\beta ds \int_0^1 dq q^3 \frac{\sin\left(\sqrt{\frac{2}{\gamma}}q|x(t) - x(s)|\right)}{\sqrt{\frac{2}{\gamma}}q|x(t) - x(s)|} e^{-q|t-s|} \times \\ &\quad (2 - q|t-s|) .\end{aligned}\quad (3.3.3)$$

¹This is an approximation as $e^{-\beta\omega_k}$ is neglected. The complete form is obtained by replacing $e^{-\omega_k|t-s|}$ by $e^{-\omega_k|t-s|}/(1 - e^{-\beta\omega_k}) + e^{\omega_k|t-s|}e^{-\beta\omega_k}/(1 - e^{-\beta\omega_k})$. But remember that β is large.

So that,

$$E = \langle \mathcal{K} + \mathcal{P} \rangle . \quad (3.3.4)$$

An expression for \mathcal{K} not involving the polaron speed, can be obtained by taking the derivative with respect to β after having scaled both the time, as before, and the coordinate $x = \sqrt{\beta}x'$. Undoing the scaling in the end one gets,

$$\begin{aligned} \mathcal{K} &= -\frac{S}{4\beta I_D} \int_0^\beta dt \int_0^\beta ds \int_{q \leq 1} dq q e^{i\sqrt{\frac{2}{\gamma}}\mathbf{q} \cdot (\mathbf{x}(t) - \mathbf{x}(s)) - q|t-s|} \times \\ &\quad \left[i\sqrt{\frac{2}{\gamma}}\mathbf{q} \cdot (\mathbf{x}(t) - \mathbf{x}(s)) \right] \end{aligned} \quad (3.3.5)$$

$$\begin{aligned} &= -\frac{3S}{4\beta} \int_0^\beta dt \int_0^\beta ds \int_0^1 dq q^3 \left[\cos\left(\sqrt{\frac{2}{\gamma}}q|\mathbf{x}(t) - \mathbf{x}(s)|\right) - \right. \\ &\quad \left. \frac{\sin\left(\sqrt{\frac{2}{\gamma}}q|\mathbf{x}(t) - \mathbf{x}(s)|\right)}{\sqrt{\frac{2}{\gamma}}q|\mathbf{x}(t) - \mathbf{x}(s)|} \right] e^{-q|t-s|} . \end{aligned} \quad (3.3.6)$$

In the following we will explain how we calculated the potential energy $P = \langle \mathcal{P} \rangle$.

3.4 Discrete path integral expressions

Generally we are interested in calculating the density matrix $\hat{\rho} = \exp(-\beta\hat{H})$ in the electron coordinate basis, namely,

$$\rho(\mathbf{x}_a, \mathbf{x}_b; \beta) = \iint_{\mathbf{x}=\mathbf{x}_a}^{\mathbf{x}=\mathbf{x}_b} e^{-\mathcal{S}} \mathcal{D}\mathbf{x}(t) . \quad (3.4.1)$$

To calculate the path integral, we first choose a subset of all paths. To do this ,we divide the independent variable, Euclidean time, into *steps* of width

$$\tau = \beta/M . \quad (3.4.2)$$

This gives us a set of *times*, $t_k = k\tau$ spaced a distance τ apart between 0 and β with $k = 0, 1, 2, \dots, M$.

At each time t_k we select the special point $x_k = \mathbf{x}(t_k)$, the k^{th} *time slice*. We construct a path by connecting all points so selected by straight lines. It is possible to define a sum over all paths constructed in this manner by taking a multiple integral over all values of x_k for $k = 1, 2, \dots, M-1$ where $x_0 = \mathbf{x}_a$ and $x_M = \mathbf{x}_b$ are the two fixed ends. The resulting equation is,

$$\rho(\mathbf{x}_a, \mathbf{x}_b; \beta) = \lim_{\tau \rightarrow 0} \frac{1}{A} \int_{-\infty}^{\infty} \int_{-\infty}^{\infty} \cdots \int_{-\infty}^{\infty} e^{-\mathcal{S}} \frac{dx_1}{A} \cdots \frac{dx_{M-1}}{A} , \quad (3.4.3)$$

where the normalizing factor $A = (2\pi\tau)^{3/2}$.

The simplest discretized expression for the action can then be written as follows,

$$\mathcal{S} = \sum_{k=1}^M \frac{(\mathbf{x}_{k-1} - \mathbf{x}_k)^2}{2\tau} + \tau^2 \sum_{i=1}^M \sum_{j=1}^M V(t_i, t_j) , \quad (3.4.4)$$

where $V(t_i, t_j) = V_{eff}(|x_i - x_j|, |i - j|)$ is a symmetric two variables function, $V(s, t) = V(t, s)$. In our simulation we tabulated this function taking $|x_i - x_j| = 0, 0.1, 0.2, \dots, 10$ and $|i - j| = 0, 1, \dots, M$.

In writing Eq. (3.4.4) we used the following approximate expressions,

$$\dot{x}_k = \frac{x_k - x_{k-1}}{\tau} + O(\tau) , \quad (3.4.5)$$

$$\int_{t_{k-1}}^{t_k} \dot{x}^2(t) dt = \dot{x}_k^2 \tau + O(\tau^2) , \quad (3.4.6)$$

$$\int_{t_{i-1}}^{t_i} \int_{t_{j-1}}^{t_j} V(s, t) ds dt = V(t_i, t_j) \tau^2 + O(\tau^3) . \quad (3.4.7)$$

If we take $V = 0$ in Eq. (3.4.4) the $M - 1$ Gaussian integrals in (3.4.3) can be done analytically. The result is the exact free particle density matrix,

$$\rho_f(x_a, x_b; \beta) = (2\pi\beta)^{-3/2} e^{\frac{1}{2\beta}(x_a - x_b)^2} . \quad (3.4.8)$$

Thus approximations (3.4.5) and (3.4.6) allow us to rewrite the polaron density matrix as follows,

$$\rho(x_a, x_b; \beta) = \int \cdots \int dx_1 \cdots dx_{M-1} \rho_f(x_a, x_1; \tau) \cdots \rho_f(x_{M-1}, x_M; \tau) \times e^{\tau^2 \sum_i \sum_j V(t_i, t_j)} . \quad (3.4.9)$$

In the next section we will see that this expression offers a useful starting point for the construction of an algorithm for the sampling of the path: the Lévy construction and the analogy with classical polymer systems or the classical isomorphism described in Ceperley [1995]).

The partition function is the trace of the density matrix,

$$Z = \int dx \rho(x, x; \beta) . \quad (3.4.10)$$

This restrict the path integral to an integral over closed paths only. In other words the paths we need to consider in calculating Z (and hence F) are closed by the *periodic boundary condition*, $x_M = x_0 = x$.

To calculate the internal energy we need then to perform the following M dimensional integral,

$$E = \frac{1}{Z} \int_{-\infty}^{\infty} \int_{-\infty}^{\infty} \cdots \int_{-\infty}^{\infty} dx_0 dx_1 \cdots dx_{M-1} e^{-S} (\mathcal{P} + \mathcal{K}) \Big|_{x_M = x_0} . \quad (3.4.11)$$

To do this integral we use the Monte Carlo simulation technique described next.

3.5 Sampling the path

The total configuration space to be integrated over is made of elements $s = [x_0, x_1, \dots, x_M]$ where x_k are the path time slices subject to the periodic boundary condition $x_M = x_0$. In the simulation we wish to sample these elements from the probability distribution,

$$\pi(s) = \frac{e^{-S}}{Z} , \quad (3.5.1)$$

where the partition function Z normalizes the function π in this space.

The idea is to find an efficient way to move the path in a random walk sampled by π , through configuration space.

In order to be able to make the random walk diffuse fast through configuration space, as τ decreases, is necessary to use multislices moves [Ceperley \[1995\]](#).

In our simulation we chose to use the bisection method (a particular multilevel Monte Carlo sampling method [Ceperley \[1995\]](#)). That's how an l levels move is constructed. Clip out of the path $m = 2^l$ subsequent time slices $x_i, x_{i+1}, \dots, x_{i+m}$ (choosing i randomly). In the first level we keep x_i and x_{i+m} fixed and, following Lévy construction for a Brownian bridge ?, we move the bisecting point at $i + m/2$ to,

$$x_{i+m/2} = \frac{x_i + x_{i+m}}{2} + \boldsymbol{\eta} \quad (3.5.2)$$

where $\boldsymbol{\eta}$ is a normally distributed random vector with mean zero and standard deviation $\sqrt{\tau m/4}$. As shown in next section this kind of transition rule samples the path using a transition probability distribution $T \propto \exp(-\mathcal{S}_f)$. Thus we will refer to it as *free particle sampling*.

Having sampled $x_{i+m/2}$, we proceed to the second level bisecting the two new intervals $(0, i + m/2)$ and $(i + m/2, i + m)$ generating points $x_{i+m/4}$ and $x_{i+3m/4}$ with the same algorithm. We continue recursively, doubling the number of sampled points at each level, stopping only when the time difference of the intervals is τ .

In this way we are able to partition the full configuration s into l levels, $s = (s_0, s_1, \dots, s_l)$ where: $s_0 = [x_0, \dots, x_i, x_{i+m}, \dots, x_{M-1}]$, unchanged; $s_1 = [x_{i+m/2}]$, changed in level 1; $s_2 = [x_{i+m/4}, x_{i+3m/4}]$, changed in level 2; ...; $s_l = [x_{i+1}, x_{i+2}, \dots, x_{i+m-1}]$ changed in level l .

To construct the random walk we use the multilevel Metropolis method ?? [Ceperley \[1995\]](#). Call (s'_1, \dots, s'_l) the new trial positions in the sense of a Metropolis rejection method, the unprimed ones are the corresponding old positions with $s_0 = s'_0$.

In order to decide if the sampling of the path should continue beyond level k , we need to construct the probability distribution π_k for level k . This, usually called the *level action*, is a function of s_0, s_1, \dots, s_k proportional to the reduced distribution function of s_k conditional on s_0, s_1, \dots, s_{k-1} . The optimal choice for the level action would thus be,

$$\pi_k^*(s_0, s_1, \dots, s_k) = \int ds_{k+1} \dots ds_l \pi(s) . \quad (3.5.3)$$

This is only a guideline. Non optimal choices will lead to slower movement through configuration space. One needs to require only that feasible paths (closed ones) have non zero level action, and that the action at the last level be exact,

$$\pi_l(s_0, s_1, \dots, s_l) = \pi(s) . \quad (3.5.4)$$

Given the level action $\pi_k(s)$ the optimal choice for the transition probability $T_k(s_k)$, for s_k contingent on the levels already sampled, is given by,

$$T_k^*(s_k) = \frac{\pi_k(s)}{\pi_{k-1}(s)} . \quad (3.5.5)$$

One can show that T_k^* will be a normalized probability if and only if π_k is chosen as in (3.5.3). In general one need to require only that T_k be a probability distribution non zero for feasible paths. In our simulation we used the free particle transition probability of the Lévy construction as a starting point for a more efficient correlated sampling that will be described in a later section.

Once the partitioning and the sampling rule are chosen, the sampling proceeds past level k with probability,

$$A_k(s') = \min \left[1, \frac{T_k(s_k)\pi_k(s')\pi_{k-1}(s)}{T_k(s'_k)\pi_k(s)\pi_{k-1}(s')} \right] . \quad (3.5.6)$$

That is we compare A_k with a uniformly distributed random number in $(0, 1)$, and if A_k is larger, we go on to sample the next level. If A_k is smaller, we make a new partitioning of the initial path, and start again from level 1. Here π_0 needed in the first level can be set equal to 1, since it will cancel out of the ratio.

This acceptance probability has been constructed so that it satisfies a form of “detailed balance” for each level k ,

$$\frac{\pi_k(s)}{\pi_{k-1}(s)} T_k(s'_k) A_k(s') = \frac{\pi_k(s')}{\pi_{k-1}(s')} T_k(s_k) A_k(s) . \quad (3.5.7)$$

The moves will always be accepted if the transition probabilities and level actions are set to their optimal values.

The total transition probability for a trial move making it through all l levels is,

$$P(s \rightarrow s') = \prod_{k=1}^l T_k(s') A_k(s') . \quad (3.5.8)$$

By multiplying Eq. (3.5.7) from $k = 1$ to $k = l$ and using Eq. (3.5.4), one can verify that the total move satisfy the detailed balance condition,

$$\pi(s) P(s \rightarrow s') = \pi(s') P(s' \rightarrow s) . \quad (3.5.9)$$

Thus if there are no barriers or conserved quantities that restrict the walk to a subset of the full configuration space (i.e. assuming the random walk to be ergodic) the algorithm will asymptotically converge to π , independent of the particular form chosen for the transition probabilities, T_k , and the level actions, π_k . We will call *equilibration time* the number of moves needed in the simulation to reach convergence.

Whenever the last level is reached, one calculates the properties (\mathcal{K} and \mathcal{P}) on the new path s' , resets the initial path to the new path, and start a new move. We will call Monte Carlo step (MCS) any attempted move.

3.6 Choice of T_k and π_k

In our simulation we started moving the path with the Lévy construction described in the preceding section. We will now show that this means that we are sampling an approximate T^* with free particle sampling.

For the free particle case ($\mathcal{U} = 0$) one can find analytic expressions for the optimal level action π_k^* and the optimal transition rule T_k^* . For examples for the first level, Eq. (3.5.3) gives,

$$\pi_1^*(x_{i+m/2}) \propto \rho_f(x_i, x_{i+m/2}; \tau m/2) \rho_f(x_{i+m/2}, x_{i+m}; \tau m/2) \quad (3.6.1)$$

$$\propto e^{\frac{1}{m\tau}(x_i - x_{i+m/2})^2} e^{\frac{1}{m\tau}(x_{i+m/2} - x_{i+m})^2} \quad (3.6.2)$$

$$\propto e^{\frac{2}{m\tau} [x_{i+m/2} - (\frac{x_i + x_{i+m}}{2})]^2} . \quad (3.6.3)$$

This justify the Lévy construction and shows that it exactly samples the free particle action (i.e. $A_k = 1$ for all k 's). This also imply that for the interacting system we can introduce a *level inter action*, $\tilde{\pi}_k$ such that,

$$\tilde{\pi}_k = \int ds_{k+1} \dots ds_l \tilde{\pi}(s) , \quad (3.6.4)$$

with

$$\tilde{\pi}(s) = \frac{e^{-\mathcal{U}}}{Z} . \quad (3.6.5)$$

So that the acceptance probability will have the simplified expression,

$$A_k(s') = \min \left[1, \frac{\tilde{\pi}_k(s') \tilde{\pi}_{k-1}(s)}{\tilde{\pi}_k(s) \tilde{\pi}_{k-1}(s')} \right] . \quad (3.6.6)$$

For the k^{th} level inter action we chose the following expression,

$$\tilde{\pi}_k \propto \exp \left[-(\tau \ell_k)^2 \sum_{i=1}^{[M/\ell_k]} \sum_{j=1}^{[M/\ell_k]} V(i\ell_k \tau, j\ell_k \tau) \right] , \quad (3.6.7)$$

where $\ell_k = m/2^k$. In the last level $\ell_l = 1$ and the level inter action $\tilde{\pi}_l$ reduces to the exact inter action $\tilde{\pi}$ thus satisfying Eq. (3.5.4).

It's important to notice that during the simulation we never need to calculate the complete level inter action since in the acceptance probabilities enter only ratios of level inter actions calculated on the old and on the new path. For example if for the move we clipped out the interval t_i, \dots, t_{i+m} with $i+m < M$ ², we have,

$$\ln \frac{\tilde{\pi}_k(s')}{\tilde{\pi}_k(s)} = -(\tau \ell_k)^2 \left\{ \sum_{m=0}^{2^k} \sum_{n=0}^{2^k} V(t_i + m\ell_k \tau, t_i + n\ell_k \tau) + \sum_{m=1}^{i-1} \sum_{n=0}^{2^k} V(m\ell_k \tau, t_i + n\ell_k \tau) + \sum_{m=i+m+1}^M \sum_{n=0}^{2^k} V(m\ell_k \tau, t_i + n\ell_k \tau) \right\} , \quad (3.6.8)$$

which is computationally much cheaper than (3.6.7).

3.7 Correlated sampling

When the path reaches equilibrium (i.e. $P(s \rightarrow s') \approx \pi(s')$) if we calculate,

$$\sigma(t_0/\tau) = \sqrt{\left\langle \left[x(t) - \left(\frac{x(t+t_0) + x(t-t_0)}{2} \right) \right]^2 \right\rangle} , \quad (3.7.1)$$

we see that these deviations are generally smaller than the free particle standard deviations used in the Lévy construction (see Fig. 3.7.1),

²When $i+m \geq M$ there is a minor problem with the periodic boundary conditions and Eq. (3.6.8) will change.

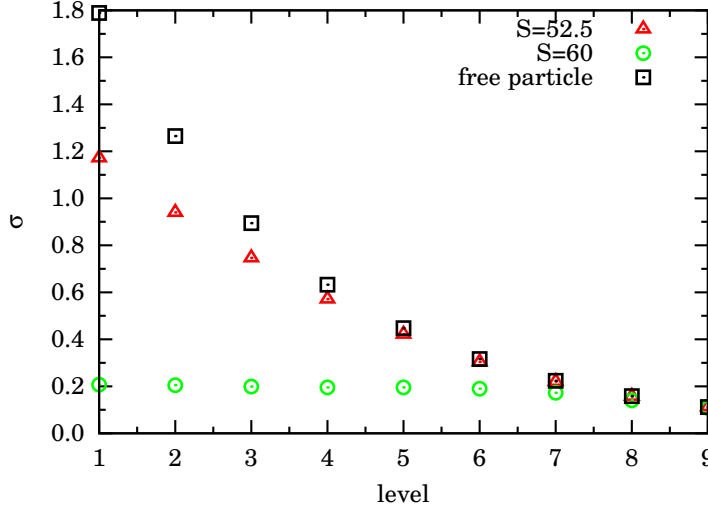


Figure 3.7.1: Shows the deviations (3.7.1) for a simulation with $S = 60$ and $S = 52.5$, $\tau = 0.025$, $l = 9$. The free particle standard deviations (3.7.2) are plotted for comparison. For $S = 60$ the path is localized while for $S = 52.5$ is unlocalized i.e. closer to the free particle path.

$$\sigma_f(\ell_k) = \sqrt{\ell_k \tau / 2} . \quad (3.7.2)$$

As Fig. 3.7.1 shows, the discrepancy gets bigger as ℓ_k increases.

We thus corrected the sampling rule for the correct deviations. For example for the first level we used,

$$T_1(x_{i+m/2}) \propto e^{-\frac{(x_{i+m/2} - \bar{x})^2}{2\sigma_f^2(m/2)}}, \quad (3.7.3)$$

where $\bar{x} = (x_i + x_{i+m})/2$. Since the level action is given by,

$$\pi_1(x_{i+m/2}) \propto e^{-\frac{(x_{i+m/2} - \bar{x})^2}{2\sigma_f^2(m/2)}} \tilde{\pi}_1(x_{i+m/2}), \quad (3.7.4)$$

we can define a function,

$$P_1 \propto e^{-\frac{(x_{i+m/2} - \bar{x})^2}{2\sigma_f^2(m/2)} \left[\frac{1}{\sigma_f^2(m/2)} - \frac{1}{\sigma_f^2(m/2)} \right]}, \quad (3.7.5)$$

and write the acceptance probability,

$$A_1(s') = \min \left[1, \frac{P_1(s)}{P_1(s')} \frac{\tilde{\pi}_1(s') \tilde{\pi}_0(s)}{\tilde{\pi}_1(s) \tilde{\pi}_0(s')} \right] . \quad (3.7.6)$$

Which is a generalization of Eq. (3.6.6).

We maintain the acceptance ratios in $[0.15, 0.65]$ by decreasing (or increasing) the number of levels in the multilevel algorithm as the acceptance ratios becomes too low (or too high).

In the Appendix we report some remarks on the error analysis in our MC simulations.

3.8 Numerical Results

We simulated the acoustic polaron fixing the adiabatic coupling constant $\gamma = 0.02$ and the inverse temperature $\beta = 15$. Such temperature is found to be well suited to extract close to ground state properties of the polaron. The path was M time slices long and the time step was $\tau = \beta/M$. For a given coupling constant S we computed the potential energy P extrapolating (with a linear χ square fit) to the continuum time limit, $\tau \rightarrow 0$, three points corresponding to time-steps chosen in the interval $\tau \in [1/100, 1/30]$. An example of extrapolation is shown in Fig. 3.8.1 for the particular case $\beta = 15$, $\gamma = 0.02$, and $S = 60$.

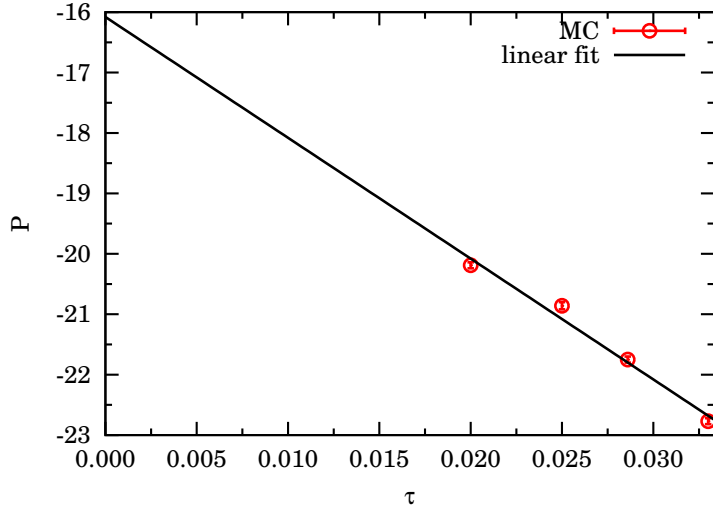


Figure 3.8.1: Shows the time step, τ , extrapolation for the potential energy, $P = \langle \mathcal{P} \rangle$. We run at $\beta = 15$, $\gamma = 0.02$, and $S = 60$. The extrapolated value to the continuum limit is in this case $P = -16.1(5)$ which is in good agreement with the result of Ref. ?.

In Fig. 3.8.4 and Tab. 3.8.1 we show the results for the potential energy as a function of the coupling strength. With the coupling constant $S = 52.5$ we generated the equilibrium path which turns out to be unlocalized (see Fig. 3.8.3). Changing the coupling constant to $S = 60$ and taking the unlocalized path as the initial path we saw the phase transition described in Fig. 3.8.2. the path after the phase transition is localized (see Fig. 3.8.3).

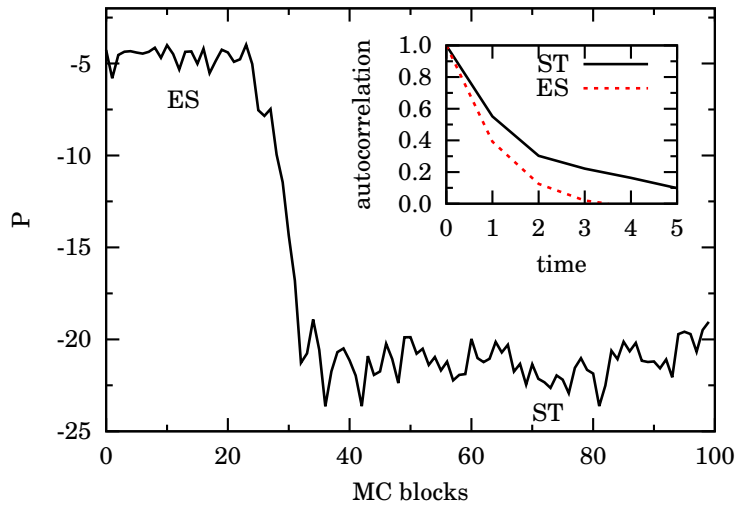


Figure 3.8.2: At $S = 60$ the results for the potential energy \mathcal{P} at each MC block (5×10^3 MCS) starting from an initial unlocalized path obtained by a previous simulation at $S = 52.5$. We can see that after about 30 blocks there is a transition from the ES state to the ST state. In the inset is shown the autocorrelation function, defined in Eq. (3.A.8), for the potential energy, for the two states. The correlation time, in MC blocks, is shorter in the unlocalized phase than in the localized one. The computer time necessary to carry on a given number of Monte Carlo steps is longer for the unlocalized phase.

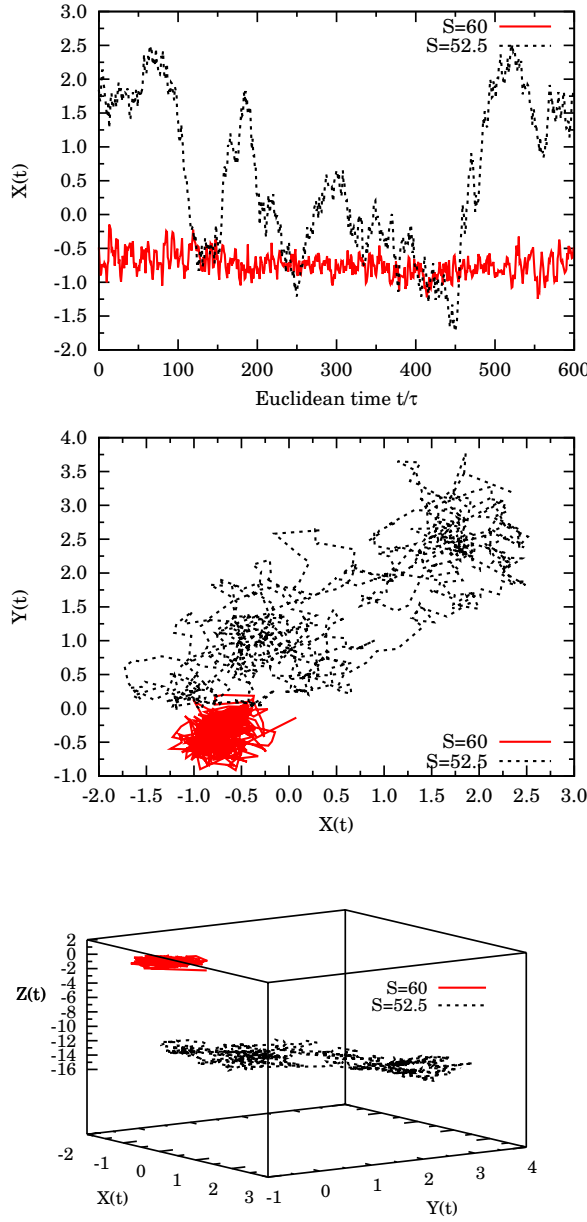


Figure 3.8.3: The top panel shows the polaron (closed) path $x(t)$ as a function of Euclidean time t in units of τ at equilibrium during the simulation. The middle panel shows the projection on the $x - y$ plane of the path. The bottom panel shows the three-dimensional path. We see clearly how both path has moved from the initial path located on the origin but the path at $S = 52.5$ is much less localized than the one at $S = 60$.

Note that since S and τ appear in the combination $S\tau^2$ in \mathcal{U} (and $S\tau$ in \mathcal{F}) the same phase

transition from an ES to a ST state will be observed increasing the temperature. With the same Hamiltonian we are able to describe two very different behaviors of the acoustic polaron as the temperature changes.

In Fig. 3.8.4 we show the behavior of the potential energy as a function of the coupling strength. The numerical results suggests the existence of a phase transition between two different regimes which corresponds to the so called ES and ST states for the weak and strong coupling region respectively. We found that paths related to ES and ST are characteristically distinguishable. Two typical paths for the ES and ST regimes involved in Fig. 3.8.4 is illustrated in Fig. 3.8.3. The path in ES state changes smoothly in a large time scale, whereas the path in ST state do so abruptly in a small time scale with a much smaller amplitude which is an indication that the polaron hardly moves. The local fluctuations in the results for the potential energy has an autocorrelation function (defined in Eq. (3.A.8)) which decay much more slowly in the ES state than in the ST state as shown in the inset of Fig. 3.8.2. Concerning the critical property of the transition between the ES and ST states our numerical results are in favor of the presence of a discontinuity in the potential energy. In the large β limit at $\beta = 15$ and fixing the adiabatic coupling constant to $\gamma = 0.02$, the ST state appear at a value of the coupling constant between $S = 52.5$ and $S = 55$. With the increase of β , the values for the potential energy $P = \langle \mathcal{P} \rangle$ increase in the weak coupling regime but decrease in the strong coupling region.

From second order perturbation theory (see Ref. ? section 8.2) follows that the energy shift $E(\gamma, S)$ is given by $-3S\gamma[1/2 - \gamma + \gamma^2 \ln(1 + 1/\gamma)]$ from which one extracts the potential energy shift by taking $P(\gamma, S) = \gamma dE(\gamma, S)/d\gamma$. From the Feynman variational approach of Ref. ? follows that in the weak regime the energy shift is $-3S\gamma[1/2 - \gamma + \gamma \ln(1 + 1/\gamma)]$ and in the strong coupling regime $-S + 3\sqrt{S/5\gamma}$.

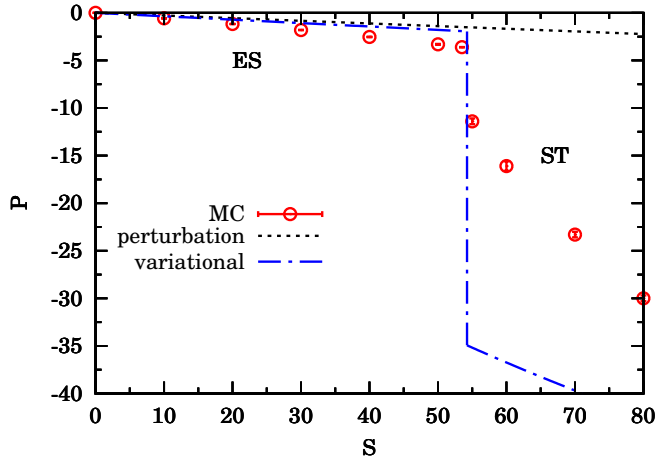


Figure 3.8.4: Shows the behavior of the potential energy P as a function of the coupling constant S . The points are the MC results (see Tab. 3.8.1), the dashed line is the second order perturbation theory result (perturbation) valid in the weak coupling regime and the dot-dashed line is the variational approach from Ref. ? (variational) in the weak and strong coupling regimes.

Table 3.8.1: MC results for P as a function of S at $\beta = 15$ and $\gamma = 0.02$ displayed in Fig. 3.8.4. The runs were made of 5×10^5 MCS (with 5×10^4 MCS for the equilibration) for the ES states and 5×10^6 MCS (with 5×10^5 MCS for the equilibration) for the ST states.

S	P
10	-0.573(8)
20	-1.17(2)
30	-1.804(3)
40	-2.53(3)
50	-3.31(4)
53.5	-3.61(1)
55	-11.4(3)
60	-16.1(5)
70	-23.3(3)
80	-30.0(3)

3.9 Conclusions

In this chapter we presented a specialized path integral Monte Carlo method to study the low temperature behavior of an acoustic polaron. At an inverse temperature $\beta = 15$ (close to the ground state of the polaron) and at a non-adiabatic parameter $\gamma = 0.02$ typical of ionic crystals we found numerical evidence for a phase transition between an extended state in the weak coupling regime and a self-trapped one in the strong coupling regime at a value of the phonons-electron coupling constant $S = 54.3(7)$. The transition also appears looking at the potential energy as a function of the coupling constant where a jump discontinuity is observed. Comparison with the perturbation theory and the variational calculation of Ref. ? is also presented.

The specialized path integral Monte Carlo simulation method used as an unbiased way to study the properties of the acoustic polaron has been presented in full detail. It is based on the Lévy construction and the multilevel Metropolis method with correlated sampling. Some remarks on the estimation of the errors in the Monte Carlo calculation are also given in the Appendix. This complement our previous paper [Fantoni \[2012a\]](#) where fewer details on the Monte Carlo method had been given.

This method differs from previously adopted methods ????????. Unlike the method of Ref. ? this path integral is in real space rather than in Fourier space, Refs. ?? put the polaron on a lattice and not on the continuum as is done here, while Refs. ? use PIMC single slice move whereas the multilevel PIMC used here instead is a general sampling method which can efficiently make multislice moves. The efficiency ξ (see the Appendix) for the potential energy increases respect to the single slice sampling because the coarsest movements are sampled and rejected before the finer movements are even constructed. In Ref. ? the Lévy construction was used as is done here but the Metropolis test was performed after the entire path had been reconstructed, using an effective action, and not at each intermediate level of the reconstruction. In Ref. ? the simpler Lévy reconstruction scheme was also found to be satisfactory for the efficient sampling of the polaron configuration space even at strong coupling. Even if here it is not implemented the method of Ref. ? we expect the method presented in this chapter to be of comparable efficiency to the one of these authors. In fact it is true that the Lévy construction is computationally cheap but guiding the path as it is been reconstructed starting already from the first levels as done here should have the advantage of refining the sampling since the path is guided through configuration space starting from the small displacements.

Although these results are of a numerical nature and one only probed the acoustic polaron for one value of the non-adiabatic parameter γ the analysis support the existence of a local-

ization phase transition as the phonons-electron coupling constant S is increased at constant temperature or as the temperature is decreased at constant S . More so, considering the fact that the introduction of a cut-off parameter have shown to work successfully in renormalization treatments.

References

- E. A. Abbott. *Flatland: A Romance of Many Dimensions*. Seeley & Co., London, 1884.
- A. C. Aitken. *Determinants and Matrices*. Interscience, New York, 1956.
- A. Alastuey and B. Jancovici. On the classical two-dimensional one-component Coulomb plasma. *J. Phys. (France)*, 42:1, 1981. doi: [10.1051/jphys:019810042010100](https://doi.org/10.1051/jphys:019810042010100).
- D. V. Anosov. Geodesic flows on closed riemannian manifolds of negative curvature. *Proc. Steklov Inst. Math.*, 90, 1967.
- V. I. Arnold and A. Avez. *Ergodic problems of Classical Mechanics*. W. A. Benjamin, Inc., New York, Amsterdam, 1968.
- V. I. Arnold, V. V. Kozlov, and A. I. Neishtadt. *Mathematical aspects of Classical and Celestial Mechanics*. Springer, 1993. 2nd printing 1997 of the 2nd edition 1993 which was originally published as “Dynamical Systems III”, volume 3 of the “Encyclopedia of Mathematical Sciences”. Translated by A. Iacob. Edited by: R. V. Gamkrelidze and V. I. Arnold. (see remark to theorem 20 of chapter 6).
- E. Artin. Ein mechanisches system mit quai-ergodischen bahnen. *Abh. Math. Sem. d.*, 3:170–175, 1924. Hamburgischen Universität.
- C. W. J. Beenakker and H. van Houten. Quantum transport in semiconductor nanostructures. *Solid State Physics*, 44, 1991.
- E. W. Brown, B. K. Clark, J. L. DuBois, and D. M. Ceperley. Path-Integral Monte Carlo Simulation of the Warm Dense Homogeneous Electron Gas. *Phys. Rev. Lett.*, 110:146405, 2013a. doi: [10.1103/PhysRevLett.110.146405](https://doi.org/10.1103/PhysRevLett.110.146405).
- E. W. Brown, J. L. DuBois, M. Holzmann, and D. M. Ceperley. Exchange-correlation energy for the three-dimensional homogeneous electron gas at arbitrary temperature. *Phys. Rev. B*, 88 (R):081102, 2013b. doi: [10.1103/PhysRevB.88.081102](https://doi.org/10.1103/PhysRevB.88.081102).
- J. M. Caillol. Exact results for a two-dimensional one-component plasma on a sphere. *J. Phys. (France) - Lett.*, 42:L–245, 1981. doi: [10.1051/jphyslet:019810042012024500](https://doi.org/10.1051/jphyslet:019810042012024500).
- J. M. Caillol, D. Levesque, J. J. Weis, and J. P. Hansen. A monte carlo study of the classical two-dimensional one-component plasma. *J. Stat. Phys.*, 28:325, 1982. doi: [10.1007/BF01012609](https://doi.org/10.1007/BF01012609).
- D. M. Ceperley. Introduction to quantum monte carlo methods applied to the electron gas. In G. F. Giuliani and G. Vignale, editors, *Proceedings of the International School of Physics Enrico Fermi*, pages 3–42, Amsterdam, 2004. IOS Press. Course CLVII.
- P. Choquard. The two-dimensional one-component plasma on a periodic strip. *Helv. Phys. Acta*, 54:332, 1981.

- P. Choquard, P. J. Forrester, and E. R. Smith. The two-dimensional one-component plasma at $\Gamma = 2$: The semiperiodic strip. *J. Stat. Phys.*, **33**:13, 1983. doi: [10.1007/BF01009744](https://doi.org/10.1007/BF01009744).
- F. Cornu and B. Jancovici. On the two-dimensional Coulomb gas. *J. Stat. Phys.*, **49**:33, 1987. doi: [10.1007/BF01009953](https://doi.org/10.1007/BF01009953).
- F. Cornu and B. Jancovici. The electrical double layer: A solvable model. *J. Chem. Phys.*, **90**: 2444, 1989. doi: [10.1063/1.455986](https://doi.org/10.1063/1.455986).
- P. Debye and E. Hückel. Zur theorie der elektrolyte. *Phys. Z.*, **9**:185, 1923.
- S. F. Edwards and A. Lenard. Exact Statistical Mechanics of a One Dimensional System with Coulomb Forces. II. The Method of Functional Integration. *J. Math. Phys.*, **3**:778, 1961. doi: [10.1063/1.1724281](https://doi.org/10.1063/1.1724281).
- R. Fantoni. Localization of acoustic polarons at low temperatures: A path-integral Monte Carlo approach. *Phys. Rev. B*, **86**:144304, 2012a. doi: [10.1103/PhysRevB.86.144304](https://doi.org/10.1103/PhysRevB.86.144304).
- R. Fantoni. The density of a fluid on a curved surface. *J. Stat. Mech.*, page P10024, 2012b. doi: [10.1088/1742-5468/2012/10/P10024](https://doi.org/10.1088/1742-5468/2012/10/P10024).
- R. Fantoni. Exact results for one dimensional fluids through functional integration. *J. Stat. Phys.*, **163**:1247, 2016. doi: [10.1007/s10955-016-1510-3](https://doi.org/10.1007/s10955-016-1510-3).
- R. Fantoni and G. Téllez. Two dimensional one-component plasma on a Flamm's paraboloid. *J. Stat. Phys.*, **133**:449, 2008. doi: [10.1007/s10955-008-9616-x](https://doi.org/10.1007/s10955-008-9616-x).
- R. Fantoni, B. Jancovici, and G. Téllez. Pressures for a One-Component Plasma on a Pseudo-sphere. *J. Stat. Phys.*, **112**:27, 2003. doi: [10.1023/A:1023671419021](https://doi.org/10.1023/A:1023671419021).
- R. Fantoni, J. W. O. Salari, and B. Klumperman. The structure of colloidosomes with tunable particle density: Simulation vs experiment. *Phys. Rev. E*, **85**:061404, 2012. doi: [10.1103/PhysRevE.85.061404](https://doi.org/10.1103/PhysRevE.85.061404).
- P. J. Forrester. The two-dimensional one-component plasma at $\Gamma = 2$: metallic boundary. *J. Phys. A: Math. Gen.*, **18**:1419, 1985. doi: [10.1088/0305-4470/18/9/023](https://doi.org/10.1088/0305-4470/18/9/023).
- P. J. Forrester. Density and correlation functions for the two-component plasma at $\Gamma = 2$ near a metal wall. *J. Chem. Phys.*, **95**:4545, 1991. doi: [10.1063/1.461745](https://doi.org/10.1063/1.461745).
- P. J. Forrester and B. Jancovici. The two-dimensional two-component plasma plus background on a sphere: Exact results. *J. Stat. Phys.*, **84**:337, 1996. doi: [10.1007/BF02179646](https://doi.org/10.1007/BF02179646).
- P. J. Forrester, B. Jancovici, and J. Madore. The two-dimensional Coulomb gas on a sphere: Exact results. *J. Stat. Phys.*, **69**:179, 1992. doi: [10.1007/BF01053789](https://doi.org/10.1007/BF01053789).
- M. Gaudin. L'isotherme critique d'un plasma sur réseau ($\beta = 2, d = 2, n = 2$). *J. Phys. (France)*, **46**:1027, 1985. doi: [10.1051/jphys:019850046070102700](https://doi.org/10.1051/jphys:019850046070102700).
- J. Ginibre. Statistical Ensembles of Complex, Quaternion, and Real Matrices. *J. Math. Phys.*, **6**:440, 1965. doi: [10.1063/1.1704292](https://doi.org/10.1063/1.1704292).
- J. Hadamard. Les surfaces à courbures opposées et leurs lignes géodésiques. *J. Math. Pures et Appl.*, **4**:27–73, 1898.
- E. H. Hauge and P. C. Hemmer. *Phys. Norvegica*, **5**:209, 1971.

- D. Henderson, M. Holovko, and A. Trokhymchuk, editors. *Ionic Soft Matter: Modern Trends in Theory and Applications*. NATO Science Series. Springer, Dordrecht, 2005.
- J. D. Jackson. *Classical Electrodynamics*. John Wiley & Sons, Inc., United States of America, third edition, 1999. Sections 3.9 & 3.11.
- B. Jancovici. Exact Results for the Two-Dimensional One-Component Plasma. *Phys. Rev. Lett.*, **46**:386, 1981a. doi: [10.1103/PhysRevLett.46.386](https://doi.org/10.1103/PhysRevLett.46.386).
- B. Jancovici. Exact Results for the Two-Dimensional One-Component Plasma. *Phys. Rev. Lett.*, **46**:386, 1981b. doi: [10.1103/PhysRevLett.46.386](https://doi.org/10.1103/PhysRevLett.46.386).
- B. Jancovici. Pressure and Maxwell Tensor in a Coulomb Fluid. *J. Stat. Phys.*, **99**:1281, 2000. doi: [10.1023/A:1018640806624](https://doi.org/10.1023/A:1018640806624).
- B. Jancovici and G. Téllez. Coulomb systems seen as critical systems: Ideal conductor boundaries. *J. Stat. Phys.*, **82**:609, 1996. doi: [10.1007/BF02179788](https://doi.org/10.1007/BF02179788).
- B. Jancovici and G. Téllez. Two-Dimensional Coulomb Systems on a Surface of Constant Negative Curvature. *J. Stat. Phys.*, **91**:953, 1998. doi: [10.1023/A:1023079916489](https://doi.org/10.1023/A:1023079916489).
- B. Jancovici and G. Téllez. Charge Fluctuations for a Coulomb Fluid in a Disk on a Pseudosphere. *J. Stat. Phys.*, **116**:205, 2004. doi: [10.1023/B:JOSS.0000037207.05672.5b](https://doi.org/10.1023/B:JOSS.0000037207.05672.5b).
- B. Jancovici, G. Manificat, and C. Pisani. Coulomb systems seen as critical systems: Finite-size effects in two dimensions. *J. Stat. Phys.*, **76**:307, 1994. doi: [10.1007/BF02188664](https://doi.org/10.1007/BF02188664).
- C. Jayewardena. *Helv. Phys. Acta*, **61**:636, 1988.
- J. M. Kosterlitz and D. J. Thouless. Ordering, metastability and phase transitions in two-dimensional systems. *J. Phys. C*, **6**:1181, 1973. doi: [10.1088/0022-3719/6/7/010](https://doi.org/10.1088/0022-3719/6/7/010).
- Y. Kwon, D. M. Ceperley, and R. M. Martin. Transient-estimate Monte Carlo in the two-dimensional electron gas. *Phys. Rev. B*, **53**:7376, 1996. doi: [10.1103/PhysRevB.53.7376](https://doi.org/10.1103/PhysRevB.53.7376).
- L. Šamaj. Is the Two-Dimensional One-Component Plasma Exactly Solvable? *J. Stat. Phys.*, **117**:131, 2004. doi: [10.1023/B:JOSS.0000044056.19438.2c](https://doi.org/10.1023/B:JOSS.0000044056.19438.2c).
- L. D. Landau and E. M. Lifshitz. *Quantum Mechanics. Non-relativistic Theory*, volume 3. Pergamon Press Ltd, Oxford, 1977. Course of Theoretical Physics.
- R. B. Laughlin. Anomalous Quantum Hall Effect: An Incompressible Quantum Fluid with Fractionally Charged Excitations. *Phys. Rev. Lett.*, **50**:1395, 1983. doi: [10.1103/PhysRevLett.50.1395](https://doi.org/10.1103/PhysRevLett.50.1395).
- A. Lenard. Exact Statistical Mechanics of a One Dimensional System with Coulomb Forces. *J. Math. Phys.*, **2**:682, 1961. doi: [10.1063/1.1703757](https://doi.org/10.1063/1.1703757).
- N. H. March and M. P. Tosi. *Coulomb liquids*. Academic Press, 1984.
- P. A. Martin. Sum rules in charged fluids. *Rev. Mod. Phys.*, **60**:1075, 1988. doi: [10.1103/RevModPhys.60.1075](https://doi.org/10.1103/RevModPhys.60.1075).
- M. L. Mehta. *Random Matrices*. Academic Press, 1991.

- L. Merchán and G. Téllez. Confined Coulomb Systems with Adsorbing Boundaries: The Two-Dimensional Two-Component Plasma. *J. Stat. Phys.*, **114**:735, 2004. doi: [10.1023/B:JOSS.0000012507.14488.a3](https://doi.org/10.1023/B:JOSS.0000012507.14488.a3).
- M. L. Metha. *Random Matrices*. Academic, New York, 1967.
- B. Militzer, E. L. Pollock, and D. M. Ceperley. Path integral Monte Carlo calculation of the momentum distribution of the homogeneous electron gas at finite temperature. *High Energy Density Physics*, **30**:13, 2003. doi: [10.1016/j.hedp.2018.12.004](https://doi.org/10.1016/j.hedp.2018.12.004).
- M. L. Rosinberg and L. Blum. The ideally polarizable interface: A solvable model and general sum rules. *J. Chem. Phys.*, **81**:3700, 1984. doi: [10.1063/1.448121](https://doi.org/10.1063/1.448121).
- C. Rovelli. *Quantum Gravity*. Cambridge University, Cambridge, 2004.
- C. Rovelli. General relativistic statistical mechanics. *Phys. Rev. D*, **87**:084055, 2013. doi: [10.1103/PhysRevD.87.084055](https://doi.org/10.1103/PhysRevD.87.084055).
- R. P. Salazar and G. Téllez. Exact Energy Computation of the One Component Plasma on a Sphere for Even Values of the Coupling Parameter. *J. Stat. Phys.*, **164**:969, 2016. doi: [10.1007/s10955-016-1562-4](https://doi.org/10.1007/s10955-016-1562-4).
- A. Salzberg and S. Prager. Equation of State for a Two-Dimensional Electrolyte. *J. Chem. Phys.*, **38**:2587, 1963. doi: [10.1063/1.1733553](https://doi.org/10.1063/1.1733553).
- S. Samuel. Grand partition function in field theory with applications to sine-Gordon field theory. *Phys. Rev. D*, **18**:1916, 1978. doi: [10.1103/PhysRevD.18.1916](https://doi.org/10.1103/PhysRevD.18.1916).
- R. R. Sari and D. Merlini. On the ν -dimensional one-component classical plasma: The thermodynamic limit problem revisited. *J. Stat. Phys.*, **14**:91, 1976. doi: [10.1007/BF01011761](https://doi.org/10.1007/BF01011761).
- Y. G. Sinai. On the foundations of the ergodic hypothesis for a dynamical system. *Dokl. Akad. Nauk.*, **153**(6), 1963. [Sov. Math. Dokl. **4**, 1818-1822 (1963)].
- F. Steiner. Quantum chaos and hyperbolic geometry. Technical report, Université de Hambourg, Semestre d' été 1995. Troisième cycle de la physique en suisse romande, cours du Professeur Frank Steiner.
- B. Tanatar and D. M. Ceperley. Ground state of the two-dimensional electron gas. *Phys. Rev. B*, **39**:5005, 1989. doi: [10.1103/PhysRevB.39.5005](https://doi.org/10.1103/PhysRevB.39.5005).
- G. Tarjus, F. Saussset, and P. Viot. *Advances in Chem. Phys.*, **148**:251, 2010.
- G. Téllez. Two-component plasma in a gravitational field. *J. Chem. Phys.*, **106**:8572, 1997. doi: [10.1063/1.473912](https://doi.org/10.1063/1.473912).
- G. Téllez. Two-component plasma in a gravitational field: thermodynamics. *J. Phys. A: Mathematical and General*, **31**:5277, 1998. doi: [10.1088/0305-4470/31/23/010](https://doi.org/10.1088/0305-4470/31/23/010).
- G. Téllez and P. Forrester. Expanded Vandermonde Powers and Sum Rules for the Two-Dimensional One-Component Plasma. *J. Stat. Phys.*, **148**:824, 2012. doi: [10.1007/s10955-012-0551-5](https://doi.org/10.1007/s10955-012-0551-5).
- G. Téllez and P. J. Forrester. Exact Finite-Size Study of the 2D OCP at $\Gamma = 4$ and $\Gamma = 6$. *J. Stat. Phys.*, **97**:489, 1999. doi: [10.1023/A:1004654923170](https://doi.org/10.1023/A:1004654923170).

- G. Téllez and L. Merchán. Solvable Model for Electrolytic Soap Films: The Two-Dimensional Two-Component Plasma. *J. Stat. Phys.*, 108:495, 2002. doi: [10.1023/A:1015725807258](https://doi.org/10.1023/A:1015725807258).
- L. Šamaj. The Statistical mechanics of the classical two-dimensional Coulomb gas is exactly solved. *J. Phys. A*, 36:5913, 2003. doi: [10.1088/0305-4470/36/22/312](https://doi.org/10.1088/0305-4470/36/22/312).
- J. Zinn-Justin. *Quantum Field Theory and Critical Phenomena*. Clarendon Press, Oxford, second edition, 1993.

Appendices

3.A Estimating errors

Since asymptotic convergence is guaranteed, the main issue is whether configuration space is explored thoroughly in a reasonable amount of computer time. Let us define a measure of the convergence rate and of the efficiency of a given random walk. This is needed to compare the efficiency of different transition rules, to estimate how long the runs should be, and to calculate statistical errors.

The rate of convergence is a function of the property being calculated. Let $\mathcal{O}(s)$ be a given property, and let its value at step k of the random walk be \mathcal{O}_k . Let the estimator for the mean and variance of a random walk with N MCS be,

$$O = \langle \mathcal{O}_k \rangle = \frac{1}{N} \sum_{k=0}^{N-1} \mathcal{O}_k , \quad (3.A.1)$$

$$\sigma^2(\mathcal{O}) = \langle (\mathcal{O}_k - O)^2 \rangle . \quad (3.A.2)$$

Then the estimator for the variance of the mean will be,

$$\sigma^2(O) = \langle \left(\frac{1}{N} \sum_k \mathcal{O}_k - \frac{1}{N} \sum_k O \right)^2 \rangle \quad (3.A.3)$$

$$= \frac{1}{N^2} \langle \left[\sum_k (\mathcal{O}_k - O) \right]^2 \rangle \quad (3.A.4)$$

$$= \frac{1}{N^2} \left\{ \sum_k \langle (\mathcal{O}_k - O)^2 \rangle + 2 \sum_{i < j} \langle (\mathcal{O}_i - O)(\mathcal{O}_j - O) \rangle \right\} \quad (3.A.5)$$

$$= \frac{\sigma^2(\mathcal{O})}{N} \left\{ 1 + \frac{2}{N\sigma^2(\mathcal{O})} \sum_{i < j} \langle (\mathcal{O}_i - O)(\mathcal{O}_j - O) \rangle \right\} \quad (3.A.6)$$

$$= \frac{\sigma^2(\mathcal{O}) k_{\mathcal{O}}}{N} . \quad (3.A.7)$$

The quantity $k_{\mathcal{O}}$ is called the *correlation time* and can be calculated given the autocorrelation function for $A_k = \mathcal{O}_k - O$. The estimator for the *autocorrelation function*, c_k , can be constructed observing that in the infinite random walk, $\langle A_i A_j \rangle$ has to be a function of $|i - j|$ only. Thus the estimator can be written,

$$c_k = \frac{\langle A_0 A_k \rangle}{\sigma^2(\mathcal{O})} = \frac{1}{(N - k)\sigma^2(\mathcal{O})} \sum_{n=1}^{N-k} A_n A_{n+k} . \quad (3.A.8)$$

So that the estimator for the correlation time will be,

$$k_{\mathcal{O}} = 1 + \frac{2}{N} \sum_{k=1}^N (N - k) c_k . \quad (3.A.9)$$

To determine the true statistical error in a random walk, one needs to estimate this correlation time. To do this, is very important that the total length of the random walk be much greater than $k_{\mathcal{O}}$. Otherwise the result and the error will be unreliable. Runs in which the number of steps $N \gg k_{\mathcal{O}}$ are called *well converged*.

The correlation time gives the average number of steps needed to decorrelate the property \mathcal{O} . It will depend crucially on the transition rule and has a minimum value of 1 for the optimal rule (while $\sigma(\mathcal{O})$ is independent of the sampling algorithm).

Normally the equilibration time will be at least as long as the equilibrium correlation time, but can be longer. Generally the equilibration time depends on the choice for the initial path. To lower this time is important to choose a physical initial path. Since the polaron system is isotropic, we chose the initial path with all time slices set to $\vec{0}$.

The efficiency of a random walk procedure (for the property \mathcal{O}) is defined as how quickly the error bars decrease as a function of the computer time, $\xi_{\mathcal{O}} = 1/\sigma^2(\mathcal{O})N\mathcal{T} = 1/\sigma^2(\mathcal{O})k_{\mathcal{O}}\mathcal{T}$ where \mathcal{T} is the computer time per step. The efficiency depends not only on the algorithm but also on the computer and the implementation.

Chapter 4

Mendeleev Periodic System

In this chapter we revisit Sections §67 and §73 of Landau and Lifshitz [1977].

4.1 Electron states in the atom

In the non-relativistic approximation,¹ the stationary states of the atom are determined by Schrödinger's equation for the system of electrons, which move in the Coulomb field of the nucleus and interact electrically with one another; the spin operators of the electrons do not appear in this equation. As we know, for a system of particles in a centrally symmetric external field the total orbital angular momentum L and the parity of the state are conserved. Hence each stationary state of the atom will be characterized by a definite value of the orbital angular momentum L and by its parity. Moreover, the coordinate wave functions of the stationary states of a system of identical particles have a certain permutational symmetry determined by the total spin S of the electrons. Hence every stationary state of the atom is characterized also by the total spin S of the electrons.

The energy level having given values of S and L is degenerate to a degree equal to the number of different possible directions in space of the vectors S and L . The degree of the degeneracy from the directions of L and S is respectively $2L + 1$ and $2S + 1$. Consequently, the total degree of the degeneracy of a level with given L and S is equal to the product $(2L + 1)(2S + 1)$.

There is a generally accepted notation to denote the atomic energy levels (or, as they are called, the spectral terms of the atoms). States with different values of the total orbital angular

¹The electromagnetic interaction of the electrons contains relativistic effects, which depend on their spins. These effects have the result that the energy of the atom depends not only on the absolute magnitudes of the vectors \mathbf{L} and \mathbf{S} but also on their relative positions. Strictly speaking, when the relativistic interactions are taken into account the orbital angular momentum \mathbf{L} and the spin \mathbf{S} of the atom are not separately conserved. Only the total angular momentum $\mathbf{J} = \mathbf{L} + \mathbf{S}$ is conserved; this is a universal and exact law which follows from the isotropy of space relative to a closed system. For this reason, the exact energy levels must be characterized by the values J of the total angular momentum. However, if the relativistic effects are comparatively small (as often happens), they can be allowed for as a perturbation. Thus, as a result of the relativistic effects, a level with given values of L and S is split into a number of levels with different values of J . This splitting is called the *fine structure* (or the *multiplet splitting*) of the level. Here we will neglect relativistic effects so that we can consider L and S as separately conserved quantities.

momentum L are denoted by capital Latin letters, as follows:

$$\begin{array}{ccccccccccccc} L, l & = & 0 & 1 & 2 & 3 & 4 & 5 & 6 & 7 & 8 & 9 & 10 & \dots \\ l & \rightarrow & s & p & d & f & g & h & i & k & l & m & n & \dots \\ L & \rightarrow & S & P & D & F & G & H & I & K & L & M & N & \dots \end{array}$$

where the lower case letters denote quantum numbers of single electron states and the upper case ones denotes quantum numbers of the many electron states. Above and to the left of this letter is placed the number $2S + 1$, called the multiplicity of the term. Below and to the right of the letter is placed the value of the total angular momentum J (here $\mathbf{J} = \mathbf{L} + \mathbf{S}$ is the total angular momentum of the system of electrons in the atom). Thus the symbol $^2P_{1/2}$ denotes the level with $L = 1, S = 1/2, J = 1/2$.

An atom with more than one electron is a complex system of mutually interacting electrons moving in the field of the nucleus. For such a system we can, strictly speaking, consider only states of the system as a whole. Nevertheless, it is found that we can, with fair accuracy, introduce the idea of the states of each individual electron in the atom, as being the stationary states of the motion of each electron in some effective centrally symmetric field due to the nucleus and to all the other electrons. These fields are in general different for different electrons in the atom, and they must all be defined simultaneously, since each of them depends on the states of all the other electrons. Such a field is said to be *self-consistent*.

Since the self-consistent field is centrally symmetric, each state of the electron is characterized by a definite value of its orbital angular momentum l . The states of an individual electron with a given l are numbered (in order of increasing energy) by the *principal quantum number* n , which takes the values $n = l + 1, l + 2, \dots$; this choice of the order of numbering is made in accordance with what is usual for the hydrogen atom. However, the sequence of levels of increasing energy for various l in complex atoms is in general different from that found in the hydrogen atom. In the latter, the energy is independent of l , so that the states with larger values of n always have higher energies. In complex atoms, on the other hand, the level with $n = 5, l = 0$, for example, is found to lie below that with $n = 4, l = 2$.

The states of individual electrons with different values of n and l are customarily denoted by a figure which gives the value of the principal quantum number, followed by a letter which gives the value of l : thus $4d$ denotes the state with $n = 4, l = 2$. A complete description of the atom demands that, besides the values of the total L, S , and J , the states of all the electrons should also be enumerated. Thus the symbol $1s\ 2p\ ^3P_0$ denotes a state of the helium atom in which $L = 1, S = 1, J = 0$ and the two electrons are in the $1s$ and $2p$ states. If several electrons are in states with the same l and n , this is usually shown for brevity by means of an index: thus $3p^2$ denotes two electrons in the $3p$ state. The distribution of the electrons in the atom among states with different l and n is called the *electron configuration*.

For given values of n and l , the electron can have different values of the projections of the orbital angular momentum (m) and of the spin (σ) on the z -axis. For a given l , the number m takes $2l + 1$ values; the number σ is restricted to only two values, $\pm \frac{1}{2}$. Hence there are altogether $2(2l + 1)$ different states with the same n and l ; these states are said to be *equivalent*. According to Pauli's principle there can be only one electron in each such state. Thus at most $2(2l + 1)$ electrons in an atom can simultaneously have the same n and l . An assembly of electrons occupying all the states with the given n and l is called a *closed shell* of the type concerned.

The difference in energy between atomic levels having different L and S but the same electron configuration is due to the electrostatic interaction of the electrons. These energy differences are usually small, and several times less than the distances between the levels of different configurations. The following empirical principle (Hund's rule; F. Hund 1925) is known concerning the

relative position of levels with the same configuration but different L and S : The term with the greatest possible value of S (for the given electron configuration) and the greatest possible value of L (for this S) has the lowest energy.² We shall show how the possible atomic terms can be found for a given electron configuration. If the electrons are not equivalent, the possible value of L and S are determined immediately from the rule for the addition of angular momenta. Thus, for instance, with the configurations np , $n'p$ (n, n' being different) the total angular momentum L can take the values 2, 1, 0, and the total spin $S = 0, 1$; combining these, we obtain the terms $^{1,3}S$, $^{1,3}P$, $^{1,3}D$. If we are concerned with equivalent electrons, however, restrictions imposed by Pauli's principle make their appearance.

When Hund's rule is applied to determine the ground term of an atom from a known electron configuration, only the unfilled shell need be considered, since the moments of electrons in closed shells cancel out. For example, let there be four d electrons outside the closed shells in an atom. The magnetic quantum number of the d electron can take five values: $0, \pm 1, \pm 2$. Hence all four electrons can have the same spin component $\sigma = \frac{1}{2}$, and the maximum possible total spin is $S = 2$. We must then assign to the electrons different values of m so as to give the maximum value of $M_L = \sum m = 2$. This means that the maximum value of L for $S = 2$ is also 2, and the term is 5D .

4.2 Periodic Table

The elucidation of the nature of the periodic variation of properties, observed in the series of elements when they are placed in order of increasing atomic number (D. I. Mendeleev 1869)³, requires an examination of the peculiarities in the successive completion of the electron shells of atoms. The theory of the periodic system is due to N. Bohr (1922).

When we pass from one atom to the next, the charge is increased by unity and one electron is added to the envelope. At first sight we might expect the binding energy of each of the successively added electrons to vary monotonically as the atomic number increases. The actual variation, however, is entirely different.

In the normal state of the hydrogen atom there is only one electron, in the $1s$ state. In the atom of the next element, helium, another $1s$ electron is added; the binding energy of the $1s$ electrons in the helium atom is, however, considerably greater than in the hydrogen atom. This is a natural consequence of the difference between the field in which the electron moves in the hydrogen atom and the field encountered by an electron added to the He^+ ion. At large distances these fields are approximately the same, but near the nucleus with charge $Z = 2$ the field of the He^+ ion is stronger than that of the hydrogen nucleus with $Z = 1$. In the lithium atom ($Z = 3$), the third electron enters the $2s$ state, since no more than two electrons can be in $1s$ states at the same time. For a given Z the $2s$ energy level³ lies above the $1s$ level; as the nuclear charge increases, both levels become lower. In the transition from $Z = 2$ to $Z = 3$, however, the former

²The requirement that S should be as large as possible can be explained as follows. Let us consider, for example, a system of two electrons. Here we can have $S = 0$ or $S = 1$; the spin 1 corresponds to an antisymmetrical coordinate wave function $\psi(r_1, r_2)$. For $r_1 = r_2$, this function vanishes; in other words, in the state with $S = 1$ the probability of finding the two electrons close together is small. This means that their electrostatic repulsion is comparatively small, and hence the energy is less. Similarly, for a system of several electrons, the "most antisymmetrical" coordinate wave function corresponds to the greatest spin.

³In an hydrogen-like atom Bohr's formula for the energy levels is as follows:

$$E = -\frac{mZ^2e^4}{2\hbar^2(1 + m/M)} \frac{1}{n^2}, \quad (4.2.1)$$

where Ze is the charge of the nucleus, M its mass, m the mass of the electron, and n is the principal quantum number. We notice that the dependence on the mass of the nucleus is only very slight.

effect is predominant, and so the binding energy of the third electron in the lithium atom is considerably less than those of the electrons in the helium atom. Next, in the atoms from Be ($Z = 4$) to Ne ($Z = 10$), first one more $2s$ electron and then six $2p$ electrons are successively added. The binding energies of these electrons increase on the average, owing to the increasing nuclear charge. The next electron added, on going to the sodium atom ($Z = 11$), enters the $3s$ state, and the binding energy again diminishes markedly, since the effect of going to a higher shell predominates over that of the increase of the nuclear charge. This picture of the filling up of the electron envelope is characteristic of the whole sequence of elements. All the electron states can be divided into successively occupied groups such that, as the states of each group are occupied in a series of elements, the binding energy increases on the average, but when the states of the next group begin to be occupied the binding energy decreases noticeably. Figure 4.2.1 shows those ionization potentials of elements that are known from spectroscopic data; they give the binding energies of the electrons added as we pass from each element to the next.

The different states are distributed as follows into successively occupied groups:

$1s$	2 electrons
$2s\ 2p$	8 electrons
$3s\ 3p$	8 electrons
$4s\ 3d\ 4p$	18 electrons
$5s\ 4d\ 5p$	18 electrons
$6s\ 4f\ 5d\ 6p$	32 electrons
$7s\ 6d\ 5f \dots$	

The first group is occupied in H and He; the occupation of the second and third groups corresponds to the first two (short) periods of the periodic system, containing 8 elements each. Next follow two long periods of 18 elements each, and a long period containing the rare-earth elements and 32 elements in all. The final group of states is not completely occupied in the natural (and artificial transuranic) elements.

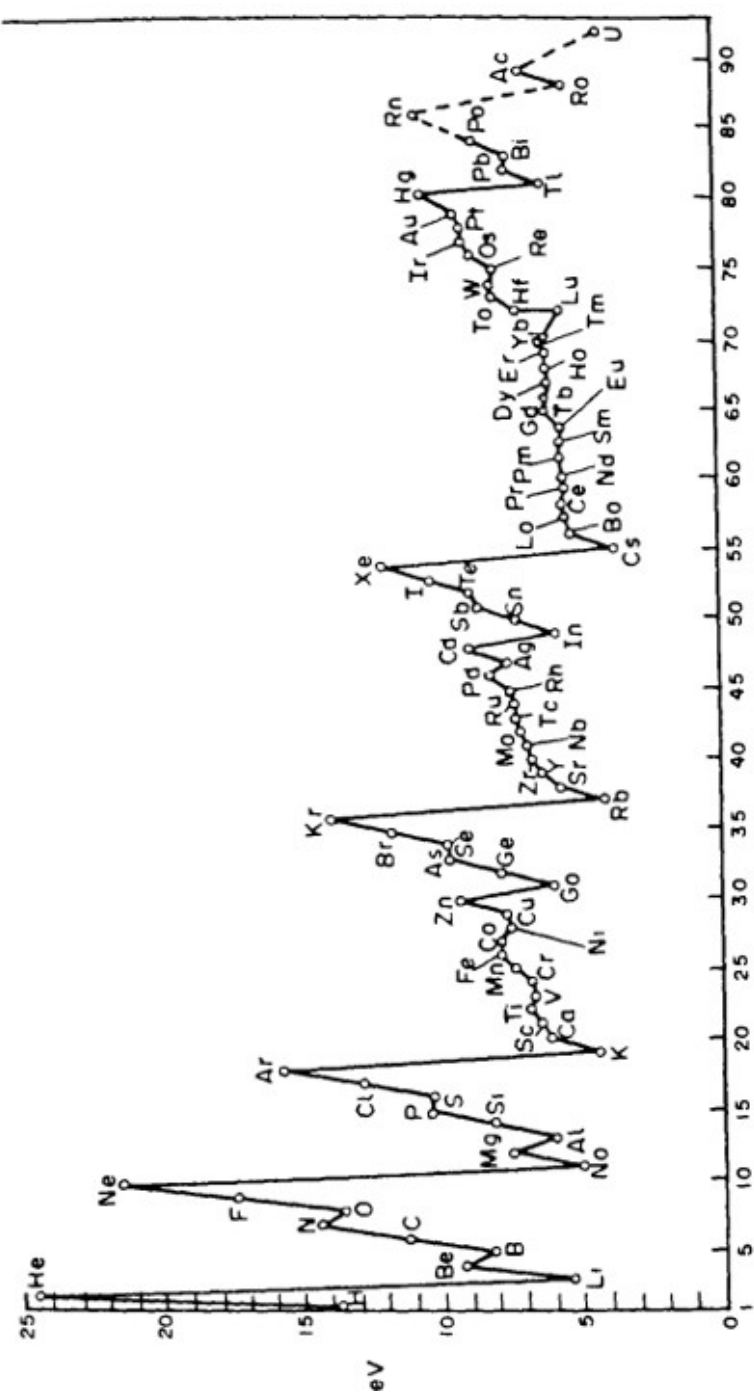
To understand the variation of the properties of the elements as the states of each group are occupied, the following property of d and f states, which distinguishes them from s and p states, is important. The curves of the effective potential energy of the centrally symmetric field (composed of the electrostatic field and the centrifugal field) for an electron in a heavy atom have a rapid and almost vertical drop to a deep minimum near the origin; they then begin to rise, and approach zero asymptotically.⁴ For s and p states, the rising parts of these curves are very close together. This means that the electron is at approximately the same distance from the nucleus in these states. The curves for the d states, and particularly for the f states, on the other hand, pass considerably further to the left; the classically accessible region which they delimit ends considerably closer in than that for the s and p states with the same total electron energy. In other words, an electron in the d and f states is mainly much closer to the nucleus than in the s and p states.

Many properties of atoms (including the chemical properties of elements) depend principally on the outer regions of the electron envelopes. The above characteristic of the d and f states

⁴The Schrödinger's equation in a centrally symmetric field being:

$$\frac{\hbar^2}{2\mu} \left[-\frac{1}{r^2} \frac{\partial}{\partial r} \left(r^2 \frac{\partial \psi}{\partial r} \right) + \frac{l^2}{r^2} \psi \right] + U(r)\psi = E\psi, \quad (4.2.2)$$

with μ is the reduced mass of the two-body problem, $\psi = R(r)Y_{l,m}(\theta, \phi)\chi_\sigma$, the spherical harmonics satisfy $l^2 Y_{l,m} = l(l+1)Y_{l,m}$, here l is the orbital angular momentum operator, and χ_σ is a spin $\frac{1}{2}$ spinor. In a Coulomb field $U(r) = -\alpha/r$ where $\alpha = Ze^2$ and $\mu = mM/(m+M)$ with m the electron mass and M the nucleus mass.



is very important in this connection. Thus, for instance, when the $4f$ states are being filled (in the rare-earth elements; see below), the added electrons are located considerably closer to the nucleus than those in the states previously occupied. As a result, these electrons have practically no effect on the chemical properties, and all the rare-earth elements are chemically very similar.

The elements containing complete d and f shells (or not containing these shells at all) are called elements of the *principal groups*; those in which the filling up of these states is actually in progress are called elements of the *intermediate groups*. These groups of elements are conveniently considered separately.

References

- R. Fantoni, B. Jancovici, and G. Téllez. Pressures for a One-Component Plasma on a Pseudosphere. *J. Stat. Phys.*, 112:27, 2003. doi: [10.1023/A:1023671419021](https://doi.org/10.1023/A:1023671419021).
- B. Jancovici. Exact Results for the Two-Dimensional One-Component Plasma. *Phys. Rev. Lett.*, 46:386, 1981a. doi: [10.1103/PhysRevLett.46.386](https://doi.org/10.1103/PhysRevLett.46.386).
- B. Jancovici. Exact Results for the Two-Dimensional One-Component Plasma. *Phys. Rev. Lett.*, 46:386, 1981b. doi: [10.1103/PhysRevLett.46.386](https://doi.org/10.1103/PhysRevLett.46.386).
- B. Jancovici. Sum rules for inhomogeneous Coulomb fluids, and ideal conductor boundary conditions. *J. Phys. (France)*, 47:389, 1986. doi: [10.1051/jphys:01986004703038900](https://doi.org/10.1051/jphys:01986004703038900).
- B. Jancovici. Charge fluctuations in finite coulomb systems. *J. Stat. Phys.*, 110:879, 2003. doi: [10.1023/A:1022172105290](https://doi.org/10.1023/A:1022172105290).

Chapter 5

RedOx Chemical Reactions

RedOx (reduction-oxidation or oxidation-reduction) is a type of chemical reaction in which the oxidation states of the reactants change. Oxidation is the loss of electrons or an increase in the oxidation state, while reduction is the gain of electrons or a decrease in the oxidation state. The oxidation and reduction processes occur simultaneously in the chemical reaction.

Oxidation is a process in which a substance loses electrons. Reduction is a process in which a substance gains electrons. The processes of oxidation and reduction occur simultaneously and cannot occur independently. In redox processes, the reductant transfers electrons to the oxidant. Thus, in the reaction, the reductant or reducing agent loses electrons and is oxidized, and the oxidant or oxidizing agent gains electrons and is reduced. The pair of an oxidizing and reducing agent that is involved in a particular reaction is called a redox pair. A redox couple is a reducing species and its corresponding oxidizing form. The oxidation alone and the reduction alone are each called a half-reaction because two half-reactions always occur together to form a whole reaction. In electrochemical reactions the oxidation and reduction processes do occur simultaneously but are separated in space.

Electronegativity, symbolized as χ , is the tendency for an atom of a given chemical element to attract shared electrons (or electron density) when forming a chemical bond. An atom's electronegativity is affected by both its atomic number and the distance at which its valence electrons reside from the charged nucleus. The higher the associated electronegativity, the more an atom or a substituent group attracts electrons. Electronegativity serves as a simple way to quantitatively estimate the bond energy, and the sign and magnitude of a bond's chemical polarity, which characterizes a bond along the continuous scale from covalent to ionic bonding. The loosely defined term electropositivity is the opposite of electronegativity: it characterizes an element's tendency to donate valence electrons.

On the most basic level, electronegativity is determined by factors like the nuclear charge (the more protons an atom has, the more "pull" it will have on electrons) and the number and location of other electrons in the atomic shells (the more electrons an atom has, the farther from the nucleus the valence electrons will be, and as a result, the less positive charge they will experience — both because of their increased distance from the nucleus and because the other electrons in the lower energy core orbitals will act to shield the valence electrons from the positively charged nucleus).

The term "electronegativity" was introduced by Jöns Jacob Berzelius in 1811, though the concept was known before that and was studied by many chemists including Avogadro. In spite of its long history, an accurate scale of electronegativity was not developed until 1932, when Linus Pauling proposed an electronegativity scale which depends on bond energies, as a development

of valence bond theory. ? It has been shown to correlate with a number of other chemical properties. Electronegativity cannot be directly measured and must be calculated from other atomic or molecular properties. Several methods of calculation have been proposed, and although there may be small differences in the numerical values of the electronegativity, all methods show the same periodic trends between elements.

The most commonly used method of calculation is that originally proposed by Linus Pauling. This gives a dimensionless quantity, commonly referred to as the *Pauling scale*, on a relative scale running from 0.79 to 3.98 (hydrogen = 2.20). When other methods of calculation are used, it is conventional (although not obligatory) to quote the results on a scale that covers the same range of numerical values: this is known as an electronegativity in Pauling units.

As it is usually calculated, electronegativity is not a property of an atom alone, but rather a property of an atom in a molecule. Pauling [1960] Even so, the electronegativity of an atom is strongly correlated with the first ionization energy. The electronegativity is slightly negatively correlated (for smaller electronegativity values) and rather strongly positively correlated (for most and larger electronegativity values) with the electron affinity. It is to be expected that the electronegativity of an element will vary with its chemical environment, ? but it is usually considered to be a transferable property, that is to say that similar values will be valid in a variety of situations.

Caesium is the least electronegative element (0.79); fluorine is the most (3.98).

5.1 Mathematical discovery in 1D

In two Journals of Mathematical Physics, Edwards and Lenard Lenard [1961]; ? have been able to study a mathematical model of a particularly simplified electron gas, one living in one dimension in the non-quantum limit and made of two oppositely charged species, and to solve its statistical physics exactly analytically. Notwithstanding the simplicity of their model, that could not undergo phase transitions ¹, it turned out to be rich enough to account for and predict chemical bonding. This rather amusing discovery puts them in the position of probably the first chemical physicists to describe a RedOx chemical bond. It was extraordinary how they could carry out this discovery from a purely rigorous mathematically analytic and exact point of view.

The abstract to the first paper of Lenard Lenard [1961] reads:

¹This is a rather general property shared by one dimensional many impenetrable bodies models in the non-quantum limit ?.

A system consisting of an equal number of positively and negatively charged “sheets” is considered in thermal equilibrium, with motion restricted to one dimension. The configurational part of the partition function can be represented as a sum of terms, each a simple algebraic expression. The summation is performed with the technique of generating functions. The asymptotic form in the limit of an infinite system is obtained from the pole of the generating function closest to the origin. This pole is the solution of a certain transcendental equation for which an explicit analytic representation in terms of an infinite continued fraction is available. It is shown that this equation is identical with the characteristic equation associated with the even Mathieu functions of even order.

In the limit, when the ratio of interparticle force to pressure is small, the system behaves as an ideal gas, the deviations from this state being expandable in powers of the square root of this ratio. In the opposite limit of large ratio, the particles associate in pairs of opposite charge, thus behaving like an ideal gas of neutral “molecules” which have an internal vibrational degree of freedom.

The analysis may be generalized to include the effect of a constant external electric field. For a given pressure there is a critical field which can never be surpassed without disrupting equilibrium.

The abstract to the second paper of Lenard ? reads:

The statistical mechanics of a one-dimensional system of charged sheets is studied in the formalism of the grand canonical ensemble. It is shown that the grand partition function may be expressed as a Wiener integral, i.e., as an average of a certain functional of Brownian motion paths. This functional integral is then expressed in terms of the fundamental solution of a partial differential equation of diffusion type. This depends on a theorem of Kac whose proof is also given. The generality of this method is discussed. When all charges are integral multiples of a common unit the problem is reduced to the determination of the largest characteristic value of an ordinary differential operator with periodic coefficients. An invariance property of the thermodynamic potential is shown to imply charge neutrality in the infinite system limit: A theorem is proven which, in certain cases, excludes the possibility of a thermodynamic phase transition. The method is generalized to yield exact expressions for the n -particle reduced density functions. Some properties of the two-particle functions are discussed.

5.2 Mathematical discovery in 2D

Two years after Lenard discovery of clustering in a classical two component plasma living in one dimension, Salzberg and Prager ? observed the same clustering phenomenon in the same classical two component plasma, that they call an electrolyte, but now living in two dimensions. Once again they do this in a completely analytic and exact way. They will write:

[Our equation of state] also seems to predict negative pressures below a critical temperature [equal to half the ionic strength]. Before this temperature is reached, however, the [partition function] becomes infinite, specifically when $2k_B T$ [(here k_B is Boltzmann constant and T the absolute temperature)] equals the absolute product of the largest positive and the largest negative charge in the system. Possibly what happens at this point may be interpreted as ion pair formation; in any case, it seems unwise to trust [our classical equation of state] at lower temperatures without further investigation.

References

- Proceedings of the International Conference on Materials & Mechanism of Superconductivity, High Temperature Superconductors V. In Y-Sheng He, Pei-Heng Wu, Li-Fang Xu, and Zong-Xian Zhao, editor, *Physica*, volume 282C-287C, Amsterdam, 1997.
- C. Alexandrou and R. Rosenfelder. Stochastic solution to highly nonlocal actions: the polaron problem. *Phys. Rep.*, 215:1, 1992. doi: [10.1016/0370-1573\(92\)90150-X](https://doi.org/10.1016/0370-1573(92)90150-X).
- C. Alexandrou, W. Fleischer, and R. Rosenfelder. Fourier path integrals, partial averaging, and the polaron problem. *Phys. Rev. Lett.*, 65:2615, 1990. doi: [10.1103/PhysRevLett.65.2615](https://doi.org/10.1103/PhysRevLett.65.2615).
- J. Bardeen and W. Shockley. Deformation Potentials and Mobilities in Non-Polar Crystals. *Phys. Rev.*, 80:72, 1950. doi: [10.1103/PhysRev.80.72](https://doi.org/10.1103/PhysRev.80.72).
- D. P. L. Castrigiano and N. Kokiantonis. Classical paths for a quadratic action with memory and exact evaluation of the path integral. *Phys. Lett. A*, 96:55, 1983. doi: [10.1016/0375-9601\(83\)90588-1](https://doi.org/10.1016/0375-9601(83)90588-1).
- D. P. L. Castrigiano, N. Kokiantonis, and H. Stierstorfer. Free energy and effective mass of the polaron at finite temperatures. *Phys. Lett. A*, 104:364, 1984. doi: [10.1016/0375-9601\(84\)90818-1](https://doi.org/10.1016/0375-9601(84)90818-1).
- D. M. Ceperley. Path integrals in the theory of condensed helium. *Rev. Mod. Phys.*, 67:279, 1995. doi: [10.1103/RevModPhys.67.279](https://doi.org/10.1103/RevModPhys.67.279).
- D. M. Ceperley and E. L. Pollock. Path-integral computation of the low-temperature properties of liquid ^4He . *Phys. Rev. Lett.*, 56:351, 1986. doi: [10.1103/PhysRevLett.56.351](https://doi.org/10.1103/PhysRevLett.56.351).
- D. M. Ceperley and E. L. Pollock. Path-integral simulation of the superfluid transition in two-dimensional ^4He . *Phys. Rev. B*, 39:2084, 1989. doi: [10.1103/PhysRevB.39.2084](https://doi.org/10.1103/PhysRevB.39.2084).
- M. Creutz and B. Freedman. A statistical approach to quantum mechanics. *Ann. Phys.*, 132:427, 1981. doi: [10.1016/0003-4916\(81\)90074-9](https://doi.org/10.1016/0003-4916(81)90074-9).
- J. T. Devreese and A. S. Alexandrov. Fröhlich polaron and bipolaron: recent developments. *Rep. Prog. Phys.*, 72:066501, 2009. doi: [10.1088/0034-4885/72/6/066501](https://doi.org/10.1088/0034-4885/72/6/066501).
- D. Emin and T. Holstein. Adiabatic Theory of an Electron in a Deformable Continuum. *Phys. Rev. Lett.*, 36:323, 1976. doi: [10.1103/PhysRevLett.36.323](https://doi.org/10.1103/PhysRevLett.36.323).
- R. Fantoni. Localization of acoustic polarons at low temperatures: A path-integral Monte Carlo approach. *Phys. Rev. B*, 86:144304, 2012. doi: [10.1103/PhysRevB.86.144304](https://doi.org/10.1103/PhysRevB.86.144304).

- R. P. Feynman. Slow Electrons in a Polar Crystal. *Phys. Rev.*, 97:660, 1955. doi: [10.1103/PhysRev.97.660](https://doi.org/10.1103/PhysRev.97.660).
- R. P. Feynman. *Statistical Mechanics: A Set of Lectures*. Addison-Wesley Publishing Company Inc, Reading, 1972. Section 9.6; Chapter 8.
- R. P. Feynman and A. R. Hibbs. *Quantum Mechanics and Path Integrals*. McGraw-Hill Inc, New York, 1965. pp. 292-293.
- M. P. A. Fisher and W. Zwerger. Ground-state symmetry of a generalized polaron. *Phys. Rev. B*, 34:5912, 1986. doi: [10.1103/PhysRevB.34.5912](https://doi.org/10.1103/PhysRevB.34.5912).
- H. Fröhlich. Electrons in lattice fields. *Adv. Phys.*, 3:325, 1954. doi: [10.1080/00018735400101213](https://doi.org/10.1080/00018735400101213).
- H. Fröhlich, H. Pelzer, and S. Zienau. Properties of slow electrons in polar materials. *Phil. Mag.*, 41:221, 1950. doi: [10.1080/14786445008521794](https://doi.org/10.1080/14786445008521794).
- B. Gerlach and H. Löwen. Analytical properties of polaron systems or: Do polaronic phase transitions exist or not? *Rev. Mod. Phys.*, 63:63, 1991. doi: [10.1103/RevModPhys.63.63](https://doi.org/10.1103/RevModPhys.63.63).
- J. M. Hammersley and C. D. Handscomb. *Monte Carlo Methods*. Chapman and Hall, London, 1964.
- D. C. Khandekar and S. V. Lawande. Feynman path integrals: Some exact results and applications. *Phys. Rep.*, 137:115, 1986. doi: [10.1016/0370-1573\(86\)90029-3](https://doi.org/10.1016/0370-1573(86)90029-3).
- P. E. Kornilovitch. Trotter-number scaling in Monte Carlo studies of the small polaron. *J. Phys.: Condens. Matter*, 9:10675, 1997. doi: [10.1088/0953-8984/9/48/011](https://doi.org/10.1088/0953-8984/9/48/011).
- P. E. Kornilovitch. Path-integral approach to lattice polarons. *J. Phys.: Condens. Matter*, 19: 255213, 2007. doi: [10.1088/0953-8984/19/25/255213](https://doi.org/10.1088/0953-8984/19/25/255213).
- C. G. Kuper and G. D. Whitfield, editors. *Polarons and Excitons*. Oliver and Boyd, Edinburgh, 1963. page 211.
- L. D. Landau and S. I. Pekar. Effective Mass of a Polaron. *Zh. Eksp. Teor. Fiz.*, 18:419, 1948.
- L. D. Landau. The Movement of Electrons in the Crystal Lattice. *Phys. Z. Sowjetunion*, 3:644, 1933. doi: [10.1016/b978-0-08-010586-4.50015-8](https://doi.org/10.1016/b978-0-08-010586-4.50015-8).
- P. Lévy. Sur certains processus stochastiques homogènes. *Compositio Math.*, 7:283, 1939.
- B. A. Mason and S. D. Sarma. Path-integral study of localization in the generalized polaron problem. *Phys. Rev. B*, 33:1412, 1986. doi: [10.1103/PhysRevB.33.1412](https://doi.org/10.1103/PhysRevB.33.1412).
- T. K. Mitra, A. Chatterjee, and S. Mukhopadhyay. Polarons. *Phys. Rep.*, 91:153, 1987. doi: [10.1016/0370-1573\(87\)90087-1](https://doi.org/10.1016/0370-1573(87)90087-1).
- Y. Ōsaka. Polaron State at a Finite Temperature. *Prog. Theor. Phys.*, 22:437, 1959. doi: [10.1143/PTP.22.437](https://doi.org/10.1143/PTP.22.437).
- Y. Osaka. Polaron Mobility at Finite Temperature (Weak Coupling Limit). *J. Phys. Soc. Jpn.*, 21:423, 1965. doi: [10.1143/JPSJ.21.423](https://doi.org/10.1143/JPSJ.21.423).
- F. M. Peeters and J. T. Devreese. On the Existence of a Phase Transition for the Fröhlich Polaron. *Phys. Stat. Sol.*, 112:219, 1982. doi: [10.1002/pssb.2221120125](https://doi.org/10.1002/pssb.2221120125).

- F. M. Peeters and J. T. Devreese. Acoustical polaron in three dimensions: The ground-state energy and the self-trapping transition. *Phys. Rev. B*, 32:3515, 1985. doi: [10.1103/PhysRevB.32.3515](https://doi.org/10.1103/PhysRevB.32.3515).
- S. Pekar. Local Quantum States of Electrons in an Ideal Ion Crystal. *Zh. eksper. teor. Fiz.*, 16: 341, 1946.
- A. Sumi and Y. Toyozawa. Discontinuity in the Polaron Ground State. *J. Phys. Soc. Jpn.*, 35: 137, 1973. doi: [10.1143/JPSJ.35.137](https://doi.org/10.1143/JPSJ.35.137).
- M. Takahashi and M. Imada. Monte Carlo Calculation of Quantum Systems. *J. Phys. Soc. Jpn.*, 53:963, 1983. doi: [10.1143/JPSJ.53.963](https://doi.org/10.1143/JPSJ.53.963).
- J. Tempere, W. Casteels, M. K. Oberthaler, S. Knoop, E. Timmermans, and J. T. Devreese. Feynman path-integral treatment of the BEC-impurity polaron. *Phys. Rev. B*, 80:184504, 2009. doi: [10.1103/PhysRevB.80.184504](https://doi.org/10.1103/PhysRevB.80.184504).
- J. T. Titantah, C. Pierleoni, and S. Ciuchi. Free Energy of the Fröhlich Polaron in Two and Three Dimensions. *Phys. Rev. Lett.*, 87:206406, 2001. doi: [10.1103/PhysRevLett.87.206406](https://doi.org/10.1103/PhysRevLett.87.206406).
- Y. Toyozawa. Self-Trapping of an Electron by the Acoustical Mode of Lattice Vibration. I. *Prog. Theor. Phys.*, 26:29, 1961. doi: [10.1143/PTP.26.29](https://doi.org/10.1143/PTP.26.29).
- X. Wang. *Mod. Phys. Lett. B*, 12:775, 1998.

Chapter 6

Plasma living in a curved surface at some special temperature

The simplest statistical mechanics model of a Coulomb plasma in two spatial dimensions admits an exact analytic solution at some special temperature in several (curved) surfaces. We present in a unifying perspective these solutions for the (non-quantum) plasma, made of point particles carrying an absolute charge e , in thermal equilibrium at a temperature $T = e^2/2k_B$, with k_B Boltzmann's constant, discussing the importance of having an exact solution, the role of the curvature of the surface, and the density correlation functions of the plasma.

6.1 Introduction

The physics of fluids of particles living in (curved) surfaces is a well known chapter of surface physics. It arises in situations in which particles are adsorbed or confined on a substrate with nonzero curvature, be it the wall of a porous material, or a membrane, a vesicle, a micelle for example made of amphiphilic surfactant molecules such as lipids, or a biological membrane, or the surface of a large solid particle, or an interface in an oil-water emulsion [Fantoni et al. \[2012\]](#). On the other hand it often occurs that by lowering the number of spatial dimensions, the statistical mechanics problem of a given fluid in the whole space, greatly simplifies, to the point of becoming, in certain cases, exactly solvable analytically in the continuum. A relevant feature of such low dimensional exactly solvable fluids is that they often play an important role as exact standards and guides to test approximate solutions and numerical experiments for (higher dimensional) fluid's models. In a more general context, the few exact analytical results have helped form new qualitative insights given by sum rules and in clarifying the nature of the long distance asymptotic decay of the truncated two (or more) particle distribution functions [Martin \[1988\]](#); [Tarjus et al. \[2010\]](#).

In the statistical physics of continuous fluids, those where the particles are allowed to move in a continuous space, one finds examples of exactly solvable ones especially among the non-quantum in lower dimensions (one and two).

Coulomb systems [March and Tosi \[1984\]](#); [Henderson et al. \[2005\]](#) such as plasmas, electrolytes, or generally ionic materials are made of charged particles interacting through the long-range Coulomb law. They are an important chapter of ionic condensed matter (in systems like molten salts, transition metal ions in solution, molten alkali halides, ...) or ionic soft matter (in systems like natural or synthetic saline environments like aqueous and non aqueous electrolyte solutions,

polyelectrolytes, colloidal suspensions, ...). The simplest model of a Coulomb system is the one-component plasma (OCP), also called *jellium*: an assembly of identical point charges of charge e , embedded in a neutralizing uniform background of the opposite sign. Here we consider the classical (i.e. non-quantum) equilibrium statistical mechanics of the OCP. According to the proof of Sari and Merlini [Sari and Merlini \[1976\]](#) which goes through “H-stability” and the “cheese theorem”, the OCP must have a well behaved thermodynamic limit. Though this model might seem, at first sight, oversimplified as to bear little resemblance to molten salts or liquid metals, it is nevertheless of great value in clarifying general effects which emerge as a direct consequence of long-range Coulomb’s interaction. This model constitutes the basic link between the microscopic description and the phenomenology of ionic condensed and soft matter.

The two-dimensional version (2D OCP) of the OCP has been much studied. Provided that the Coulomb potential due to a point-charge is defined as the solution of the Poisson equation “in” a two-dimensional world, i.e., is a logarithmic function $-\ln r$ of the distance r to that point-charge, the 2D OCP mimics many generic properties of the three-dimensional Coulomb systems. In this case the electric field lines are not allowed to leave the surface as it happens in the satirical novella of Edwin Abbott Abbott [Abbott \[1884\]](#). Of course, this toy logarithmic model does not describe real charged particles, such as electrons confined on a quasi two dimensional surface, which nevertheless interact through the three dimensional Coulomb potential $1/r$. One motivation for studying the 2D OCP is that its equilibrium statistical mechanics is analytically exactly solvable at one special temperature: both the analytic form of the thermodynamical quantities and of the correlation functions can be found exactly.

The OCP is exactly solvable at any temperatures in one dimension [Edwards and Lenard \[1961\]](#); [Fantoni \[2016\]](#). In two dimensions, Jancovici and Alastuey [Ginibre \[1965\]](#); [Metha \[1967\]](#); [Jancovici \[1981b\]](#); [Alastuey and Jancovici \[1981\]](#) proved that the OCP is exactly solvable analytically at a special value of the coupling constant, $\Gamma = \beta e^2 = 2$ where $\beta = 1/k_B T$ with k_B Boltzmann’s constant and T the absolute temperature, on a plane. Since then, a growing interest in two-dimensional plasmas has lead to study this system on various flat geometries [Rosinberg and Blum \[1984\]](#); [Jancovici et al. \[1994\]](#); [Jancovici and Téllez \[1996\]](#) and two-dimensional curved surfaces like the cylinder [Choquard \[1981\]](#); [Choquard et al. \[1983\]](#), the sphere [Caillol \[1981\]](#); [Téllez and Forrester \[1999\]](#); [Jancovici \[2000\]](#); [Salazar and Téllez \[2016\]](#), the pseudosphere [Jancovici and Téllez \[1998\]](#); [Fantoni et al. \[2003\]](#); [Jancovici and Téllez \[2004\]](#), and Flamm paraboloid [Fantoni and Téllez \[2008\]](#). Among these surfaces only the last one, due to Flamm, is of non-constant curvature. The sphere is the surface of constant positive curvature and the pseudosphere is the surface of constant negative curvature.

How the properties of a system are affected by the curvature of the space in which the system lives is a question which arises in general relativity. This is an incentive for studying simple toy models.

The two-component plasma (TCP) is a neutral mixture of point-wise particles of charge $\pm e$. The equation of state of the TCP living in a plane is known since the work of Salzberg and Prager [Salzberg and Prager \[1963\]](#). In the plasma the attraction between oppositely charged particles competes with the thermal motion and makes the partition function of the finite system diverge when $\Gamma = \beta e^2 \geq 2$, where $\beta = 1/k_B T$ with k_B Boltzmann constant. The system becomes unstable against the collapse of pairs of oppositely charged particles, and as a consequence all thermodynamic quantities diverge, so that the point particle model is well behaved only for $\Gamma < 2$ [Hauge and Hemmer \[1971\]](#) when the Boltzmann factor for unlike particles is integrable at small separations of the charges. In this case rescaling the particles coordinates so as to stay in the unit disk one easily proves that the grand canonical partition function is a function of $\sqrt{\zeta_- \zeta_+} V^{(1-\Gamma/4)}$, where V is the volume occupied by the plasma and ζ_{\pm} the fugacities of the two charge species, and as a consequence the equation of state is $\beta p = n(1 - \Gamma/4)$ where $n = \rho_+ + \rho_-$ is the total particle

number density. However, if the collapse is avoided by some short range repulsion (hard cores for instance), the model remains well defined for lower temperatures. Then, for $\Gamma > 4$ the long range Coulomb attraction binds positive and negative particles in pairs of finite polarizability. Thus, at some critical value $\Gamma_c \sim 4$ the system undergoes the Kosterlitz-Thouless transition Kosterlitz and Thouless [1973] between a high temperature ($\Gamma < 4$) conductive phase and a low temperature ($\Gamma > 4$) dielectric phase. For $\Gamma \geq 2$ it is necessary to regularize the system of point charges allowing for a short-range strong repulsion between unlike charge which may be modeled as hard (impenetrable) disks, i.e. giving a physical dimension to the particles to prevent the collapse. The same behavior also occurs in the TCP living in one dimension Lenard [1961]; Fantoni [2016].

The structure of the TCP living in a plane at the special value $\Gamma = 2$ of the coupling constant is also exactly solvable analytically Gaudin [1985]; Cornu and Jancovici [1987]. Through the use of an external potential it has also been studied in various confined geometries Cornu and Jancovici [1989]; Forrester [1991]; Téllez and Merchán [2002]; Merchán and Téllez [2004] and in a gravitational field Téllez [1997, 1998]. It has been studied in surfaces of constant curvature as the sphere Forrester et al. [1992]; Forrester and Jancovici [1996], the pseudosphere Jancovici and Téllez [1998], and on the Flamm paraboloid of non-constant curvature Fantoni [2012]. Unlike the OCP where the properties of the van der Monde determinant allowed the analytical solution a Cauchy identity is used for the solution of the TCP. Unlike in the one-component case where the solution was possible for the plasma confined in a region of the surface now this is not possible, anymore, without the use of an external potential. In these cases the external potential is rather given by $-(\Gamma/e^2) \ln \sqrt{g}$ where g is the determinant of the metric tensor of the Riemannian surface Fantoni [2012b]. On a curved surface, even though the finite system partition function will still be finite for $\Gamma < 2$ since the surface is locally flat, the structure will change respect to the flat case.

Purpose of this chapter is to describe the state of the art for the studies on the exactly solvable statistical physics models of a plasma on a (curved) surface. In section 6.2 we will treat the OCP in the various surfaces and in section 6.3 the TCP in the various surfaces. Except for the OCP on the plane we will stop at the solution for the partition function and the densities of the finite OCP. If the reader wishes he can refer to the original papers for the resulting expressions in the thermodynamic limit. The solutions for the TCP do not give the results for the finite system but only its thermodynamic limit. For the OCP we use the canonical ensemble for the plane, the cylinder and the sphere, and the grand canonical ensemble for the pseudosphere and the Flamm paraboloid on half surface with grounded horizon. For the TCP we only use the grand canonical ensemble. When appropriate we point out the ensemble inequivalence which arise for the finite system.

6.1.1 The surface

We will generally consider Riemannian surfaces S with a coordinate frame $q = (x^1, x^2)$ and with a metric

$$ds^2 = g_{\mu\nu}(q) dx^\mu dx^\nu, \quad (6.1.1)$$

with $g_{\mu\nu}$ the metric tensor. We will denote with $g(q)$ the Jacobian of the transformation to an orthonormal coordinate reference frame, i.e. the determinant of the metric tensor $g_{\mu\nu}$. The surface may be embeddable in the three dimensional space or not. It is important to introduce a disk Ω_R of radius R and its boundary $\partial\Omega_R$. The connection coefficients, the Christoffel symbols, in a coordinate frame are

$$\Gamma_{\mu\beta\gamma} = \frac{1}{2}(g_{\mu\beta,\gamma} + g_{\mu\gamma,\beta} - g_{\beta\gamma,\mu}), \quad (6.1.2)$$

where the comma denotes a partial derivative as usual. The Riemann tensor in a coordinate frame reads

$$R^\alpha_{\beta\gamma\delta} = \Gamma^\alpha_{\beta\delta,\gamma} - \Gamma^\alpha_{\beta\gamma,\delta} + \Gamma^\alpha_{\mu\gamma}\Gamma^\mu_{\beta\delta} - \Gamma^\alpha_{\mu\delta}\Gamma^\mu_{\beta\gamma}, \quad (6.1.3)$$

in a two-dimensional space has only $2^2(2^2 - 1/12) = 1$ independent component. The scalar curvature is then given by the following indexes contractions (the trace of the Ricci curvature tensor),

$$\mathcal{R} = R^\mu_{\mu} = R^{\mu\nu}_{\mu\nu}, \quad (6.1.4)$$

and the (intrinsic) Gaussian curvature is $K = \mathcal{R}/2$. In an embeddable surface we may define also a (extrinsic) mean curvature $H = (k_1 + k_2)/2$, where the principal curvatures k_i , $i = 1, 2$ are the eigenvalues of the shape operator or equivalently the second fundamental form of the surface and $1/k_i$ are the principal radii of curvature. The Euler characteristic of the disk Ω_R is given by

$$\chi = \frac{1}{2\pi} \left(\int_{\Omega_R} K dS + \int_{\partial\Omega_R} k dl \right), \quad (6.1.5)$$

where k is the geodesic curvature of the boundary $\partial\Omega_R$.

6.1.2 The Coulomb potential

The *Coulomb potential* $G(\mathbf{q}, \mathbf{q}_0)$ created at \mathbf{q} by a unit charge at \mathbf{q}_0 is given by the Green function of the Laplacian

$$\Delta G(\mathbf{q}, \mathbf{q}_0) = -2\pi\delta^{(2)}(\mathbf{q}; \mathbf{q}_0), \quad (6.1.6)$$

with appropriate boundary conditions. Here Δ is the Laplace-Beltrami operator. This equation can often be solved by using the decomposition of G as a Fourier series.

6.1.3 The background

The Coulomb potential generated by the *background*, with a constant surface charge density $\rho_b = -en_b$ satisfies the Poisson equation

$$\Delta v_b = -2\pi\rho_b. \quad (6.1.7)$$

The Coulomb potential of the background can be obtained by solving Poisson equation with the appropriate boundary conditions. Also, it can be obtained from the Green function computed in the previous section

$$v_b(\mathbf{q}) = \int G(\mathbf{q}, \mathbf{q}') \rho_b(\mathbf{q}') dS'. \quad (6.1.8)$$

This integral can be performed easily by using the Fourier series decomposition of Green's function G .

6.1.4 The total potential energy

The *total potential energy* of the plasma is then

$$\begin{aligned} V_N &= V_N^{pp} + V_N^{pb} + V_N^0 = \frac{e^2}{2} \sum_{i \neq j} G(|\mathbf{q}_i - \mathbf{q}_j|) + e \sum_i \int_{\Omega_R} v_b(|\mathbf{q} - \mathbf{q}_i|) d\mathbf{q} + \\ &\quad \frac{1}{2} \iint_{\Omega_R} \rho_b v_b(|\mathbf{q} - \mathbf{q}'|) d\mathbf{q} d\mathbf{q}', \end{aligned} \quad (6.1.9)$$

where the last term V_N^0 is the self energy of the background and the first two terms V_N^{pp} and V_N^{pb} are the interaction potential energy between the charges at \mathbf{q}_i , $i = 1, \dots, N$ and between the charges and the background, respectively.

6.1.5 The densities and distribution functions

Given either the canonical partition function in a fixed region $\Omega \in \mathcal{S}$ of a Riemannian surface \mathcal{S} , $Z_N(\Gamma)$ with $\Gamma = \beta e^2$ the coupling constant, or the grand canonical one $\Xi[\{\lambda_p(\mathbf{q})\}, \Gamma]$, with λ_p some position dependent fugacities, we can define the *n-body density functions*. Denoting with $p = (p, \mathbf{q})$ the species p and the position \mathbf{q} of a particle of this species, we have,

$$\begin{aligned} \rho^{(n)}(\mathbf{p}_1, \dots, \mathbf{p}_n; N, \Gamma) &= \rho(\mathbf{p}_1; N, \Gamma) \cdots \rho(\mathbf{p}_n; N, \Gamma) g_{p_1 \dots p_n}(\mathbf{q}_1, \dots, \mathbf{q}_n; N, \Gamma) \\ &= \left\langle \sum_{i_1, \dots, i_n}^{DP} \delta^{(2)}(\mathbf{q}_1; \mathbf{q}_{i_1}) \delta_{p_1, p_{i_1}} \cdots \delta^{(2)}(\mathbf{q}_n; \mathbf{q}_{i_n}) \delta_{p_n, p_{i_n}} \right\rangle_{N, \Gamma} \end{aligned} \quad (6.1.10)$$

where $\delta_{p,q}$ is the Kronecker delta, $\delta^{(2)}$ is the Dirac delta function on the curved surface such that $\int \delta^{(2)}(\mathbf{q}; \mathbf{q}') dS = 1$ with $dS = \sqrt{g(\mathbf{q})} d\mathbf{q}$ the elementary surface area on \mathcal{S} , $\langle \dots \rangle_{N, \Gamma} = \sum_{p_1, \dots, p_N} \int_{\Omega} \dots e^{-\beta V_N} dS_1 \cdots dS_N / Z_N$ is the thermal average in the canonical ensemble, \sum^{DP} denotes the inclusion in the sum only of addends containing the product of delta functions relative to different particles, and we omitted the superscript ⁽¹⁾ in the one-body densities. The g_{p_1, \dots, p_n} are known as the *n-body distribution functions*. It is convenient to introduce another set of correlation functions which decay to zero as two groups of particles are largely separated [Martin \[1988\]](#), namely the *truncated* (Ursell) correlation functions,

$$\rho^{(n)T}(\mathbf{p}_1, \dots, \mathbf{p}_n; N, \Gamma) = \rho^{(n)}(\mathbf{p}_1, \dots, \mathbf{p}_n; N, \Gamma) - \sum \prod_{m < n} \rho^{(m)T}(\mathbf{p}_{i_1}, \dots, \mathbf{p}_{i_m}; N, \Gamma), \quad (6.1.11)$$

where the sum of products is carried out over all possible partitions of the set $(1, \dots, n)$ into subsets of cardinal number $m < n$.

In terms of the grand canonical partition function we will have,

$$\rho^{(n)}(\mathbf{p}_1, \dots, \mathbf{p}_n; \{\lambda_p\}, \Gamma) = \prod_{i=1}^n \lambda_{p_i}(\mathbf{q}_i) \frac{1}{\Xi[\{\lambda_p\}, \Gamma]} \frac{\delta^{(n)} \Xi[\{\lambda_p\}, \Gamma]}{\delta \lambda_{p_1}(\mathbf{q}_1) \cdots \delta \lambda_{p_n}(\mathbf{q}_n)}, \quad (6.1.12)$$

and

$$\rho^{(n)T}(\mathbf{p}_1, \dots, \mathbf{p}_n; \{\lambda_p\}, \Gamma) = \prod_{i=1}^n \lambda_{p_i}(\mathbf{q}_i) \frac{\delta^{(n)} \ln \Xi[\{\lambda_p\}, \Gamma]}{\delta \lambda_{p_1}(\mathbf{q}_1) \cdots \delta \lambda_{p_n}(\mathbf{q}_n)}. \quad (6.1.13)$$

We may also use the notation $\rho^{(n)}(\mathbf{p}_1, \dots, \mathbf{p}_n; \{\lambda_p\}, \Gamma) = \rho_{p_1 \dots p_n}^{(n)}(\mathbf{q}_1, \dots, \mathbf{q}_n; \{\lambda_p\}, \Gamma)$ where for example in the two-component mixture each $p = \pm$ denotes either a positive or a negative charge. And sometimes we may omit the dependence from the number of particles, the fugacities, and the coupling constant. From the structure it is possible to derive the thermodynamic properties of the plasma (but not the contrary).

6.2 The One-Component Plasma

An *one-component plasma* is a system of N identical particles of charge e embedded in a uniform neutralizing background of opposite charge.

6.2.1 The plane

The metric tensor in the Cartesian coordinates $\mathbf{q} = (x, y)$ of the *plane* is,

$$\mathbf{g} = \begin{pmatrix} 1 & 0 \\ 0 & 1 \end{pmatrix}, \quad (6.2.1)$$

and the curvature is clearly zero. We will use polar coordinates $\mathbf{q} = (r, \varphi)$ with $r = \sqrt{x^2 + y^2}$ and $\varphi = \arctan(y/x)$.

The Coulomb potential

The Coulomb interaction potential between a particle at \mathbf{q} and a particle at \mathbf{q}_0 a distance $r = |\mathbf{q} - \mathbf{q}_0|$ from one another is

$$G(\mathbf{q}, \mathbf{q}_0) = -\ln(|\mathbf{q} - \mathbf{q}_0|/L), \quad (6.2.2)$$

where L is a length scale.

The background

If one assumes the particles to be confined in a disk $\Omega_R = \{\mathbf{q} \in \mathcal{S} | 0 \leq \varphi \leq 2\pi, 0 \leq r \leq R\}$ of area $\mathcal{A}_R = \pi R^2$ the background potential is

$$v_b(r) = en_b \frac{\pi}{2} \left(r^2 - R^2 + 2R^2 \ln \frac{R}{L} \right), \quad (6.2.3)$$

where $r = |\mathbf{q}|$.

The total potential energy

The total potential energy of the system is then given by Eq. (6.1.9). Developing all the terms and using $n_b = n = N/\mathcal{A}_R$ (this is not a necessary condition since we can imagine a situation where $n_b \neq n$. In this case the system would not be electrically neutral) we then find

$$V_N/e^2 = - \sum_{i < j} \ln \left(\frac{r_{ij}}{L} \right) + \frac{n_b \pi}{2} \sum_i r_i^2 + n_b^2 \pi^2 R^4 \left(-\frac{3}{8} + \frac{1}{2} \ln \frac{R}{L} \right), \quad (6.2.4)$$

where $r_{ij} = |\mathbf{q}_i - \mathbf{q}_j|$ and $r_i = |\mathbf{q}_i|$. This can be rewritten as follows

$$\begin{aligned} V_N/e^2 &= - \sum_{i < j} \ln \left(\frac{r_{ij}}{R} \right) + \frac{N}{2} \sum_i \left(\frac{r_i}{R} \right)^2 + \\ &\quad N^2 \left(-\frac{3}{8} + \frac{1}{2} \ln \frac{R}{L} \right) - \frac{N(N-1)}{2} \ln \left(\frac{R}{L} \right). \end{aligned} \quad (6.2.5)$$

We can then introduce the new variables Jancovici [1981b] $z_i = \sqrt{N} \mathbf{q}_i / R$ to find

$$V_N/e^2 = f(\{z_i\}) + f_c \quad (6.2.6)$$

$$f = - \sum_{i < j} \ln z_{ij} + \frac{1}{2} \sum_i z_i^2, \quad (6.2.7)$$

$$f_c = \frac{N(N-1)}{4} \ln(n\pi L^2) + N^2 \left(-\frac{3}{8} + \frac{1}{2} \ln \frac{R}{L} \right). \quad (6.2.8)$$

We can always choose $L = R$ so that in the thermodynamic limit $\lim_{N \rightarrow \infty} f_c/N = -\ln(n\pi L^2)/4$ and the excess Helmholtz free energy per particle

$$a_{\text{exc}} = F_{\text{exc}}/N \rightarrow -\frac{e^2}{4} \ln(\pi n L^2) + a_0(T), \quad (6.2.9)$$

with a_0 some function of the temperature T alone. Therefore, the equation of state has the simple form

$$p = (1/\beta - e^2/4)n, \quad (6.2.10)$$

where $\beta = 1/k_B T$ with k_B Boltzmann's constant.

Partition function and densities at a special temperature

At the special temperature $T_0 = e^2/2k_B$ the partition function can be found exactly analytically using the properties of the van der Monde determinant [Jancovici \[1981b\]](#); [Alastuey and Jancovici \[1981\]](#). Using polar coordinates $z_i = (z_i, \theta_i)$, one obtains at T_0 a Boltzmann factor

$$e^{-\beta V_N} = A_N e^{-\sum_i z_i^2} \left| \prod_{i < j} (Z_i - Z_j) \right|^2, \quad (6.2.11)$$

where A_N is a constant and $Z_i = z_i \exp(i\theta_i)$. This expression can be integrated upon variables z_i ($0 \leq z_i \leq \sqrt{N}$) by expanding the van der Monde determinant $\prod(Z_i - Z_j)$. One obtains the partition function

$$Z_N(2) = \int e^{-\beta V_N} dz_1 \cdots dz_N = A_N \pi^N N! \prod_{j=1}^N \gamma(j, N), \quad (6.2.12)$$

where

$$\gamma(j, N) = \int_0^{\sqrt{N}} e^{-z^2} z^{2(j-1)} 2z dz = \int_0^N e^{-t} t^{j-1} dt, \quad (6.2.13)$$

is the incomplete gamma function. Taking the thermodynamic limit of $-[\ln(Z_N(2)/A_R^N)]/N \rightarrow \beta a_{\text{exc}}(2)$ we obtain the Helmholtz free energy per particle

$$a_{\text{exc}}(2) = -\frac{e^2}{4} \ln(\pi n L^2) + \frac{e^2}{2} \left[1 - \frac{1}{2} \ln(2\pi) \right]. \quad (6.2.14)$$

One can also obtain the n -body distribution functions from the truncated densities [Martin \[1988\]](#) as follows

$$g(1, \dots, n; N) = e^{-\sum_{i=1}^n z_i^2} \det [K_N(Z_i \bar{Z}_j)]_{i,j=1,\dots,n}, \quad (6.2.15)$$

where \bar{Z} is the complex conjugate of Z and

$$K_N(x) = \sum_{i=1}^N \frac{x^{i-1}}{\gamma(i, N)}. \quad (6.2.16)$$

In the thermodynamic limit $N \rightarrow \infty$, $\gamma(i, N) \rightarrow (i - 1)!$, and $K_N(x) \rightarrow e^x$. In this limit, one obtains from Eq. (6.2.15) the following explicit distribution functions Jancovici [1981b]

$$g(1) = 1, \quad (6.2.17)$$

$$g(1, 2) = 1 - e^{-\pi n r_{12}^2}, \quad (6.2.18)$$

$$g(1, 2, 3) = \dots \quad (6.2.19)$$

This Gaussian falloff is in agreement with the general result according to which, among all possible long-range pair potentials, it is only in the Coulomb case that a decay of correlations faster than any inverse power is compatible with the structure of equilibrium equations like the Born-Green-Yvon hierachic set (see Ref. Martin [1988] section II.B.3). A somewhat surprising result is that the correlations does not have the typical exponential falloff typical of the high-temperature Debye-Hückel approximation Debye and Hückel [1923]. One easily checks that the distribution functions obey the perfect screening and other sum rules.

Expansions around $\Gamma = 2$ suggests that the pair correlation function changes from the exponential form to an oscillating one for a region with $\Gamma > 2$. This behavior of the pair correlation function as the coupling is stronger has been observed in Monte Carlo simulations Caillol et al. [1982]. For sufficient high values of Γ (low temperatures) the 2D OCP begins to crystallize and there are several works where the freezing transition is found. For the case of the sphere Caillol et al. Caillol et al. [1982] localized the coupling parameter for melting at $\Gamma \approx 140$. In the limit $\Gamma \rightarrow \infty$ the 2D OCP becomes a Wigner crystal. In particular, the spatial configuration of the charges which minimizes the energy at zero temperature for the 2D OCP on a plane is the usual hexagonal lattice. Nowadays, the corresponding Wigner crystal of the 2D OCP on sphere or Thomson problem may be solved numerically Fantoni et al. [2012].

6.2.2 The cylinder

The cylinder may be useful to compare an exactly soluble fluid with the results from its Monte Carlo simulation for example, where one needs to use periodic boundary conditions. The two dimensional system studied in the simulation would actually live on a torus but the cylinder is already a relevant step forward in this direction.

The metric tensor in the cartesian coordinates $q = (x, y)$ is,

$$g = \begin{pmatrix} 1 & 0 \\ 0 & 1 \end{pmatrix}, \quad (6.2.20)$$

and again the curvature is zero.

The Coulomb potential

We now consider Choquard [1981]; Choquard et al. [1983] a rectangular disk $\Omega_{L,W} = \{q \in \mathcal{S} | -L/2 \leq x \leq L/2, -W/2 \leq y \leq W/2\}$. We then solve Eq. (6.1.6) imposing periodicity in y with period W expanding G in a Fourier series in y where the coefficients are functions of x and written as inverse Fourier transforms. The solution is

$$\begin{aligned} G(q_1, q_2) = & -\frac{\pi}{W}|x_1 - x_2| + \\ & \frac{\text{sgn}(x_1 - x_2)}{2} \ln \left\{ 1 - 2e^{-\frac{2\pi}{W}|x_1 - x_2|} \cos \frac{2\pi}{W}(y_1 - y_2) + e^{-\frac{4\pi}{W}|x_1 - x_2|} \right\} \end{aligned} \quad (6.2.21)$$

where $\text{sgn}(x) = |x|/x$ is the sign of x . The term proportional to $|x_1 - x_2|$ comes from the constant term in the Fourier series solution, while the other terms sum to give the logarithmic part.

The background

The potential of the background (6.1.7) is then

$$v_b(x) = en_b \frac{\pi}{4} (L^2 + 4x^2), \quad (6.2.22)$$

since the second term on the right hand side of Eq. (6.2.21) is an odd function of $x_1 - x_2$.

The total potential energy

The total potential energy (6.1.9) for $n_b = n = N/WL$ can then be written as

$$V_N/e^2 = \sum_{i < j} G(\mathbf{q}_i, \mathbf{q}_j) + \pi n \sum_i x_i^2 + B_N, \quad (6.2.23)$$

where B_N is a constant irrelevant to the distribution function.

Partition function and densities at a special temperature

The energy of Eq. (6.2.23) can be inserted into the formula for the canonical partition function $Z_N(\Gamma)$ at $\Gamma = \beta e^2 = 2$ to obtain

$$\begin{aligned} Z_N(2) = & A_N \int_{-L/2}^{L/2} dx_N \int_{-L/2}^{x_N} dx_{N-1} \cdots \int_{-L/2}^{x_2} dx_1 e^{-2\pi n \sum_i x_i^2} \times \\ & \int_{-W/2}^{W/2} dy_1 \cdots \int_{-W/2}^{W/2} dy_N \prod_{i < j} \left(e^{\frac{2\pi}{W}(x_i+x_j)} \left| e^{-\frac{2\pi}{W}(x_i-iy_i)} - e^{-\frac{2\pi}{W}(x_j-iy_j)} \right|^2 \right) \end{aligned} \quad (6.2.24)$$

Where A_N is a constant. Now we notice that the y -dependent part of the integrand is contained in the square modulus of a van der Monde determinant. We use the permutation notation to write the expansion of the determinant and its conjugate as follows

$$\begin{aligned} & \int_{-W/2}^{W/2} dy_1 \cdots \int_{-W/2}^{W/2} dy_N \prod_{i < j} \left| e^{-\frac{2\pi}{W}(x_i-iy_i)} - e^{-\frac{2\pi}{W}(x_j-iy_j)} \right|^2 = \\ & \sum_{P,Q} \epsilon(P) \epsilon(Q) \prod_{i=1}^N \left(e^{-\frac{2\pi x_i}{W}[P(i)+Q(i)-2]} \int_{-W/2}^{W/2} dy_i e^{-\frac{2\pi i y_i}{W}[P(i)-Q(i)]} \right), \end{aligned} \quad (6.2.25)$$

where the sums are over the $N!$ permutations, $\epsilon(P)$ denotes the sign of permutation P . Only permutations for which $P(i) = Q(i)$, $1 \leq i \leq N$ contribute. Recalling that $n = N/WL$ we obtain

$$\begin{aligned} Z_N(2) = & A_N W^N \sum_P \int_{-L/2}^{L/2} dx_N \int_{-L/2}^{x_N} dx_{N-1} \cdots \int_{-L/2}^{x_2} dx_1 \times \\ & \prod_{i=1}^N e^{-2\pi n \left\{ x_i^2 - 2x_i \frac{L}{2} \left[1 - 2 \frac{P(i)-1}{N} \right] \right\}}. \end{aligned} \quad (6.2.26)$$

For permutation P , make the substitution $x_i = z_{P(i)}$, $1 \leq i \leq N$. We then have a sum over ordered integrals over the z_i . The integrand is the same for each permutation and each possible ordering of the z_i occurs exactly once. Hence, the sum over ordered integrals may be written as

an unrestricted multiple integral over $[-L/2, L/2]^N$. Renaming $z_i = x_i$ for $1 \leq i \leq N$ and using the appropriately defined B_N , we obtain

$$Z_N(2) = B_N W^N \prod_{i=1}^N \int_{-L/2}^{L/2} dx_i e^{-2\pi n [x_i - \frac{L}{2}(1 - 2\frac{i-1}{N})]^2} \quad (6.2.27)$$

This equation describes the canonical partition function for an assembly of N independent harmonic oscillators with mean position evenly spaced on $[-L/2, L/2]$. Using the correct form of B_N we may now take the thermodynamic limit of $-\ln(Z_N(2)/\mathcal{A}_R^N)/N$ to obtain for the excess free energy per particle $\beta a_{\text{exc}}(2) = \beta a_{\text{exc,plane}}(2) + M$ where $a_{\text{exc,plane}}(2)$ is expression (6.2.14) with the choice $L = W/2\pi$ and $M = \pi/6nW^2$ is a Madelung constant for the potential in the semiperiodic boundary conditions used.

To calculate the one-particle distribution function in the finite system we simply leave out the integrations over x_1 and y_1 . Define $x_0 = -L/2, x_{N+1} = L/2$, and the ordering of the x variables with $x_0 \leq x_2 \leq x_3 \leq \dots \leq x_p \leq x_1 < x_{p+1} \leq \dots \leq x_N \leq x_{N+1}$. There are $(N-1)!$ orderings, each giving the same contribution to $g(1; N)$. We use the van der Monde determinant representation of the integrand and carry out the integrations over y_2, \dots, y_N giving $P(i) = Q(i)$, $2 \leq i \leq N$, and so $P(1) = Q(1)$ by default. Collect all the integrals with $P(1) = q$ and change variables with $x_i = z_{P(i)}$, $2 \leq i \leq N$; $P(i) \neq q$ and $x_1 = z_q$. This generates ordered integrals with respect to $(N-l)$ of the z_i , all possible orderings occurring exactly once. An unrestricted integral over

$$\{z_1, \dots, z_{q-1}, z_{q+1}, \dots, z_N\} \in [-L/2, L/2]^{N-1}, \quad (6.2.28)$$

results. The final form for the one-particle distribution function is then

$$g(1; N) = \frac{1}{Wn} \sum_{q=1}^N e^{-2\pi n [x_1 - \frac{L}{2}(1 - 2\frac{q-1}{N})]^2} / I(q, L, N), \quad (6.2.29)$$

$$I(i, L, N) = \int_{-L/2}^{L/2} dx e^{-2\pi n [x_1 - \frac{L}{2}(1 - 2\frac{i-1}{N})]^2}. \quad (6.2.30)$$

The higher orders distribution functions are determined in Ref. Choquard et al. [1983].

6.2.3 The sphere

The metric tensor in the polar coordinates $\mathbf{q} = (\theta, \varphi)$ is now,

$$g = \begin{pmatrix} a^2 & 0 \\ 0 & a^2 \sin^2 \theta \end{pmatrix}, \quad (6.2.31)$$

where a is the radius of the sphere. The sphere is embeddable in the three dimensional Euclidean space. The intrinsic Gaussian curvature of the sphere is a constant $K = 1/a^2$ and the surface area of the sphere is $\mathcal{A}_S = 4\pi a^2$. So the sphere is the surface of constant positive curvature by Liemann's theorem. Also by Minding's theorem we know that surfaces with the same constant curvature are locally isometric.

The Coulomb potential

The Coulomb interaction between a particle at \mathbf{r}_i and a particle at \mathbf{r}_j is

$$G(\mathbf{r}_i, \mathbf{r}_j) = -\ln(r_{ij}/L), \quad (6.2.32)$$

$$r_{ij} = 2a \sin(\theta_{ij}/2), \quad (6.2.33)$$

$$\varphi_{ij} = \arccos(\mathbf{r}_i \cdot \mathbf{r}_j / a^2), \quad (6.2.34)$$

where \mathbf{r}_k is the three-dimensional vector from the center of the sphere to particle k on the sphere surface and r_{ij} is the length of the chord joining \mathbf{r}_i and \mathbf{r}_j .

The background

The background potential is then a constant

$$v_b = en_b 2\pi a^2 \left(-1 + \ln \frac{4a^2}{L^2} \right). \quad (6.2.35)$$

The total potential energy

The total potential energy of the system (6.1.9) is then

$$V_N/e^2 = -\frac{1}{2} \sum_{i < j} \ln \left[\frac{2a^2}{L^2} (1 - \cos \theta_{ij}) \right] - \frac{N^2}{4} \left(1 - \ln \frac{4a^2}{L^2} \right). \quad (6.2.36)$$

Partition function and densities at a special temperature

At $\Gamma = \beta e^2 = 2$ the excess canonical partition function is

$$Z_N(2) = e^{N^2/2} \left(\frac{L}{2a} \right)^N \int \prod_{i=1}^N dq_i \prod_{j < k} \left(\frac{1 - \cos \theta_{jk}}{2} \right), \quad (6.2.37)$$

where denoting with $g = \det[g_{\mu\nu}]$ we have $dq = dS = \sqrt{g} dq^1 dq^2 = a^2 \sin \theta d\theta d\varphi$. Introducing the Cayley-Klein parameters defined by

$$\alpha_i = \cos \frac{\theta_i}{2} e^{i\varphi_i/2}, \quad (6.2.38)$$

$$\beta_i = -i \sin \frac{\theta_i}{2} e^{-i\varphi_i/2}, \quad (6.2.39)$$

we can write

$$1 - \cos \theta_{ij} = 2|\alpha_i \beta_j - \alpha_j \beta_i|^2. \quad (6.2.40)$$

The integrand of Eq. (6.2.37) takes the form

$$\prod_{i < j} \left(\frac{1 - \cos \theta_{jk}}{2} \right) = \left| \prod_{k=1}^N \beta_k^{N-1} \prod_{i < j} \left(\frac{\alpha_i}{\beta_i} - \frac{\alpha_j}{\beta_j} \right) \right|^2. \quad (6.2.41)$$

The second product in the right hand side of this equation is a van der Monde determinant. Expanding it and inserting in Eq. (6.2.37) we find

$$Z_N(2) = e^{N^2/2} (2\pi L)^N a^N N! \prod_{k=1}^N \frac{(k-1)!(N-k)!}{N!}. \quad (6.2.42)$$

This result is similar to the result (6.2.12) on the plane apart from the fact that now only complete gamma functions are involved. The excess free energy per particle is identical to the result (6.2.14) for the plane.

For the distribution functions we find [Caillol \[1981\]](#)

$$g(1, 2, \dots, n; N) = \det[(\alpha_i \bar{\alpha}_j + \beta_i \bar{\beta}_j)^{N-1}], \quad (6.2.43)$$

where $\bar{\alpha}$ is the complex conjugate of α . In particular

$$g(1; N) = 1, \quad (6.2.44)$$

$$g(1, 2; N) = 1 - \left(\frac{1 + \cos \theta_{12}}{2} \right)^{N-1}. \quad (6.2.45)$$

The system appears to be homogeneous for all N and the distribution functions are invariant under a rotation of the sphere.

The thermodynamic limit is obtained defining $\rho_i = R\theta_i$ and taking the limit $N \rightarrow \infty$ and $R \rightarrow \infty$ at n constant, keeping ρ_i and φ_i constant for each particle i . For an infinitely large sphere the particles will be situated in the tangent plane at the North pole and there positions will be characterized by the polar coordinates (ρ_i, φ_i) . The solution for the planar geometry of section [6.2.1](#) is thereby recovered.

6.2.4 The pseudosphere

The pseudosphere is non-embeddable in the three dimensional Euclidean space and it is a non-compact Riemannian surface of constant negative curvature. Unlike the sphere it has an infinite area and this fact makes it interesting from the point of view of statistical physics because one can take the thermodynamic limit on it.

Riemannian surfaces of negative curvature play a special role in the theory of dynamical systems [Steiner \[Semestre d' été 1995\]](#). Hadamard study of the geodesic flow of a point particle on a such surface [Hadamard \[1898\]](#) has been of great importance for the future development of ergodic theory and of modern chaos theory. In 1924 the mathematician Emil Artin [\[1924\]](#) studied the dynamics of a free point particle of mass m on a pseudosphere closed at infinity by a reflective boundary (a billiard). Artin's billiard belongs to the class of the so called Anosov systems. All Anosov systems are ergodic and posses the mixing property [Arnold and Avez \[1968\]](#). Sinai [\[1963\]](#) translated the problem of the Boltzmann-Gibbs gas into a study of the by now famous "Sinai's billiard", which in turn could relate to Hadamard's model of 1898. Recently, smooth experimental versions of Sinai's billiard have been fabricated at semiconductor interfaces as arrays of nanometer potential wells and have opened the new field of mesoscopic physics [Beenakker and van Houten \[1991\]](#).

The following important theorem holds for Anosov systems [Arnold et al. \[1993\]](#), [Anosov \[1967\]](#):

Theorem 6.2.1 *Let M be a connected, compact, orientable analytic surface which serves as the configurational manifold of a dynamical system whose Hamiltonian is $H = K + U$. Let the dynamical system be closed and its total energy be h . Consider the manifold \mathcal{M} defined by the Maupertuis Riemannian metric $ds^2 = 2(h - U)K dt^2$ on M , where t is time. If the curvature of \mathcal{M} is negative everywhere then the dynamical system is an Anosov system and in particular is ergodic on $M_h = \{h = H\}$.*

If the dynamical system is composed of N particles, the same conclusions hold, we need only require that the curvature be negative when we keep the coordinates of all the particles but anyone constant.

The metric tensor of the pseudosphere in the coordinates $q = (\theta, \varphi)$ with $\theta \in [0, \infty[$ is,

$$g = \begin{pmatrix} a^2 & 0 \\ 0 & a^2 \sinh^2 \theta \end{pmatrix}, \quad (6.2.46)$$

where a is the “radius” of the pseudosphere.

Introducing the alternative coordinates $q = (r, \varphi)$ with $r/2a = \tanh(\theta/2)$ we find

$$\mathbf{g} = \begin{pmatrix} [1 - (r/2a)^2]^{-2} & 0 \\ 0 & r^2[1 - (r/2a)^2]^{-2} \end{pmatrix}. \quad (6.2.47)$$

These are the polar coordinates $\omega = (r/2a, \varphi)$ of a disk of the unitary disk, $\mathcal{D} = \{\omega \in \mathbb{C} \mid |\omega| < 1\}$, which with such a metric is called the *Poincaré disk*.

A third set of coordinates used is $q = (x, y)$ obtained from $(r/2a, \varphi)$ through the Cayley transformation,

$$z = x + iy = \frac{\omega + i}{1 + i\omega}. \quad (6.2.48)$$

which establishes a bijective transformation between the unitary disk and the complex half plane,

$$\mathcal{H} = \{z = x + iy \mid x \in \mathbb{R}, y > 0\}. \quad (6.2.49)$$

The center of the unitary disk corresponds to the point $z_o = i$, “the center of the plane”. The metric becomes,

$$\mathbf{g} = \begin{pmatrix} a^2/y^2 & 0 \\ 0 & a^2/y^2 \end{pmatrix}. \quad (6.2.50)$$

The complex half plane with such a metric is called the *hyperbolic plane*, and the metric the *Poincaré's metric*.

Cayley transformation is a particular Möbius transformation. Poincaré metric is invariant under Möbius transformations. And any transformation that preserves Poincaré metric is a Möbius transformation.

The geodesic distance d_{01} between any two points $q_0 = (\tau_0, \varphi_0)$ and $q_1 = (\tau_1, \varphi_1)$ on the pseudosphere \mathcal{S} is given by,

$$\cosh(d_{01}/a) = \cosh \tau_1 \cosh \tau_0 - \sinh \tau_1 \sinh \tau_0 \cos(\varphi_1 - \varphi_0). \quad (6.2.51)$$

Given the set of points Ω_d at a geodesic distance from the origin less or equal to d ,

$$\Omega_d = \{(\tau, \varphi) \in \mathcal{S} \mid \tau a \leq d, \varphi \in [0, 2\pi)\}, \quad (6.2.52)$$

that we shall call a disk of radius d , we can determine its circumference,

$$\begin{aligned} \mathcal{C} &= \mathcal{L}(\partial\Omega_d) = a \int_{\tau=d/a}^{\infty} \sqrt{\dot{\tau}^2 + \sinh^2 \tau \dot{\varphi}^2} dt \\ &= 2\pi a \sinh\left(\frac{d}{a}\right) \underset{d \rightarrow \infty}{\sim} \pi a e^{d/a}, \end{aligned} \quad (6.2.53)$$

and its area,

$$\begin{aligned} \mathcal{A} &= \mathcal{V}(\Omega_d) = \int_0^{2\pi} d\varphi \int_0^{d/a} d\tau a^2 \sinh \tau \\ &= 4\pi a^2 \sinh^2\left(\frac{d}{2a}\right) \underset{d \rightarrow \infty}{\sim} \pi a^2 e^{d/a}. \end{aligned} \quad (6.2.54)$$

The Laplace-Beltrami operator on \mathcal{S} is,

$$\begin{aligned}\Delta &= \frac{1}{\sqrt{g}} \frac{\partial}{\partial q^\mu} \left(\sqrt{g} g^{\mu\nu} \frac{\partial}{\partial q^\nu} \right) \\ &= \frac{1}{a^2} \left(\frac{1}{\sinh \tau} \frac{\partial}{\partial \tau} \sinh \tau \frac{\partial}{\partial \tau} + \frac{1}{\sinh^2 \tau} \frac{\partial^2}{\partial \varphi^2} \right),\end{aligned}\quad (6.2.55)$$

where g is the determinant of the metric tensor $g = \det[g_{\mu\nu}]$.

The characteristic component of the Riemann tensor is,

$$R^\tau_{\varphi\tau\varphi} = -\sinh^2 \tau. \quad (6.2.56)$$

The Gaussian curvature is given by

$$R^{\tau\varphi}_{\tau\varphi} = g^{\varphi\varphi} R^\tau_{\varphi\tau\varphi} = -\frac{1}{a^2}, \quad (6.2.57)$$

except at its singular cusp, in agreement with Hilbert's theorem. Contraction gives the components of the Ricci tensor,

$$R^\tau_\tau = R^\varphi_\varphi = -\frac{1}{a^2}, \quad R^\tau_\varphi = 0, \quad (6.2.58)$$

and further contraction gives the scalar curvature,

$$R = -\frac{2}{a^2}. \quad (6.2.59)$$

The ensemble of N identical point-wise particles of charge e are constrained to move in a connected and compact domain $\Omega \subset \mathcal{S}$ by an infinite potential barrier on the boundary of the domain $\partial\Omega$ with a number density $n = N/\mathcal{V}(\Omega)$.

The Coulomb potential

The pair Coulomb potential between two unit charges a geodesic distance d apart, satisfies Poisson equation on \mathcal{S} ,

$$\Delta G(d) = -2\pi\delta^{(2)}(d), \quad (6.2.60)$$

where $\delta^{(2)}(d_{01}) = \delta(q_0 - q_1)/\sqrt{g}$ is the Dirac delta function on the curved manifold. Poisson equation admits a solution vanishing at infinity,

$$G(d_{ij}) = -\ln \left[\tanh \left(\frac{d_{ij}}{2a} \right) \right]. \quad (6.2.61)$$

The background

If we choose $\Omega = \Omega_{a\tau_0}$, the electrostatic potential of the background inside Ω can be chosen (see appendix 6.A) to be just a function of τ ,

$$v_b(\tau) = en_b 2\pi a^2 \left\{ \ln \left[\frac{1 - \tanh^2(\tau_0/2)}{1 - \tanh^2(\tau/2)} \right] + \sinh^2(\tau_0/2) \ln[\tanh^2(\tau_0/2)] \right\}. \quad (6.2.62)$$

Ergodicity

Consider a closed one component Coulomb plasma of N charges and total energy h , confined in the domain $\Omega_{a\tau_0} \subset \mathcal{S}$. Let the coordinates of particle i be $\mathbf{q}_i = q_{(i)}^\alpha \vec{e}_\alpha = (q_{(i)}^1, q_{(i)}^2) \in \Omega_{a\tau_0}$, where $\vec{e}_\alpha = \partial/\partial q^\alpha$ ($\alpha = 1, 2$) is a coordinate basis for \mathcal{S} . The trajectory of the dynamical system,

$$\mathcal{T}_{t_0} = \{q^N(t) \equiv (\mathbf{q}_1, \dots, \mathbf{q}_N) \mid t \in [0, t_0]\}, \quad (6.2.63)$$

is a geodesic on the $2N$ dimensional manifold \mathcal{M} defined by the metric,

$$\mathcal{G}_{\alpha\beta} = (h - V_N) g_{\mu\nu}(\mathbf{q}_i) \otimes \cdots \otimes g_{\mu\nu}(\mathbf{q}_N), \quad (6.2.64)$$

on \mathcal{S}^N . We now assume $n_b = n$ and rewrite $V_N^{pb} = v_1 + v_{pb}$ where

$$v_1 = N 2\pi a^2 e^2 n \{\ln[1 - \tanh^2(\tau_0/2)] + \sinh^2(\tau_0/2) \ln[\tanh^2(\tau_0/2)]\}, \quad (6.2.65)$$

is a constant. Since the interaction between the particles is repulsive we conclude that, up to an additive constant ($V_N^0 + v_1$), the potential V_N is a positive function of the coordinates of the particles. Since v_{pb} and V_N^{pp} are positive on $\Omega_{a\tau_0}$ we have,

$$\mathcal{G}_{\alpha\beta} < \mathcal{G}'_{\alpha\beta} = (h - V_N^0 - v_1) g_{\mu\nu}(\mathbf{q}_i) \otimes \cdots \otimes g_{\mu\nu}(\mathbf{q}_N), \quad (6.2.66)$$

where \mathcal{G}' has a negative curvature along the coordinates of any given particle. In the next subsection we will calculate the curvature of \mathcal{G} along the coordinates of one particle. According to the theorem stated in the introduction we will require the curvature to be negative everywhere on \mathcal{S}^N . This will determine a condition on the kinetic and potential energy of the system, sufficient for its ergodicity to hold on M_h .

Let $\tilde{\mathbf{p}}_i = p_{(i)\alpha} \tilde{\omega}^\alpha$ be the momentum of charge i , where $\tilde{\omega}^\alpha = \tilde{d}q^\alpha$ are the 1-forms of the dual coordinate basis, and define $p^N(t) \equiv (\tilde{\mathbf{p}}_1, \dots, \tilde{\mathbf{p}}_N)$, $q^N(t) \equiv (\mathbf{q}_1, \dots, \mathbf{q}_N)$. The ergodicity of the system tells us that given any dynamical quantity $A(q^N, p^N)$, its time average,

$$\langle A \rangle_t = \lim_{T \rightarrow \infty} \frac{1}{T} \int_0^T A(q^N, p^N) dt, \quad (6.2.67)$$

coincides with its microcanonical phase space average,

$$\langle A \rangle_h = \frac{\int_{M_{ps}} A(q^N, p^N) \delta(h - H) d^{4N} \mu_{ps}}{\int_{M_{ps}} \delta(h - H) d^{4N} \mu_{ps}}, \quad (6.2.68)$$

where the phase space of the system is,

$$\begin{aligned} M_{ps} = \{&(q^N, p^N) \mid \mathbf{q}_i \in \mathcal{S} \quad i = 1, \dots, N; \\ &p_{(i)\alpha} \in [-\infty, \infty] \quad i = 1, \dots, N, \alpha = 1, 2\}, \end{aligned} \quad (6.2.69)$$

the phase space measure is,

$$d^{4N} \mu_{ps} = \prod_{\alpha=1}^2 dq_{(1)}^\alpha \cdots dq_{(N)}^\alpha dp_{(1)\alpha} \cdots dp_{(N)\alpha}, \quad (6.2.70)$$

and δ is the Dirac delta function.

Calculation of the curvature of \mathcal{M}

We calculate the curvature of \mathcal{M} along particle 1 using Cartan structure equations. Let $K = h - U(\tau, \varphi)$ be the kinetic energy of the N particle system of total energy h , as a function of the coordinates of particle 1 (all the other particles having fixed coordinates). We choose an orthonormal basis,

$$\begin{cases} \tilde{\omega}^{\hat{\tau}} = a\sqrt{K}\tilde{d}\tau \\ \tilde{\omega}^{\hat{\varphi}} = a \sinh(\tau)\sqrt{K}\tilde{d}\varphi \end{cases} \quad (6.2.71)$$

By Cartan second theorem we know that the connection 1-form satisfies $\tilde{\omega}_{\hat{\alpha}\hat{\beta}} + \tilde{\omega}_{\hat{\beta}\hat{\alpha}} = 0$. Then we must have,

$$\begin{cases} \tilde{\omega}^{\hat{\tau}}_{\hat{\tau}} = \tilde{\omega}^{\hat{\varphi}}_{\hat{\varphi}} = 0 \\ \tilde{\omega}^{\hat{\tau}}_{\hat{\varphi}} = -\tilde{\omega}^{\hat{\varphi}}_{\hat{\tau}} = -\tilde{\omega}^{\hat{\varphi}}_{\hat{\tau}} \end{cases} \quad (6.2.72)$$

We use Cartan first theorem to calculate $\tilde{\omega}^{\hat{\tau}}_{\hat{\varphi}}$,

$$\begin{aligned} \tilde{d}\tilde{\omega}^{\hat{\tau}} &= -\tilde{\omega}^{\hat{\tau}}_{\hat{\varphi}} \wedge \tilde{\omega}^{\hat{\varphi}} \\ &= \tilde{d}(a\sqrt{K}\tilde{d}\tau) \\ &= a K^{\frac{1}{2}},_{\varphi} \tilde{d}\varphi \wedge \tilde{d}\tau = 0, \end{aligned} \quad (6.2.73)$$

where in the last equality we used the fact that the pair interaction is a function of $\varphi_i - \varphi_j$ and that the interaction with the background is a function of τ only (being the system confined in a domain which is symmetric under translations of φ). We must then conclude that $\tilde{\omega}^{\hat{\tau}}_{\hat{\varphi}}$ is either zero or proportional to $\tilde{\omega}^{\hat{\varphi}}$. We proceed then calculating,

$$\begin{aligned} \tilde{d}\tilde{\omega}^{\hat{\varphi}} &= -\tilde{\omega}^{\hat{\varphi}}_{\hat{\tau}} \wedge \tilde{\omega}^{\hat{\tau}} \\ &= \tilde{d}(a \sinh(\tau)\sqrt{T}\tilde{d}\varphi) \\ &= a(\sinh(\tau)K^{\frac{1}{2}}),_{\tau} \tilde{d}\tau \wedge \tilde{d}\varphi, \end{aligned} \quad (6.2.74)$$

which tells us that indeed,

$$\tilde{\omega}^{\hat{\varphi}}_{\hat{\tau}} = \frac{(\sinh(\tau)K^{\frac{1}{2}}),_{\tau}}{a \sinh(\tau)K} \tilde{\omega}^{\hat{\varphi}}. \quad (6.2.75)$$

Next we calculate the characteristic component of the curvature 2-form $\mathcal{R}^{\hat{\alpha}}_{\hat{\beta}} = \tilde{d}\tilde{\omega}^{\hat{\alpha}}_{\hat{\beta}} + \tilde{\omega}^{\hat{\alpha}}_{\hat{\gamma}} \wedge \tilde{\omega}^{\hat{\gamma}}_{\hat{\beta}}$,

$$\begin{aligned} \mathcal{R}^{\hat{\tau}}_{\hat{\varphi}} &= \tilde{d}\tilde{\omega}^{\hat{\tau}}_{\hat{\varphi}} \\ &= \tilde{d}[-(\sinh(\tau)K^{\frac{1}{2}}),_{\tau} K^{-\frac{1}{2}} \tilde{d}\varphi] \\ &= -\frac{[(\sinh(\tau)K^{\frac{1}{2}}),_{\tau} K^{-\frac{1}{2}}],_{\tau}}{a^2 \sinh(\tau)K} \tilde{\omega}^{\hat{\tau}} \wedge \tilde{\omega}^{\hat{\varphi}}. \end{aligned} \quad (6.2.76)$$

and use Cartan third theorem to read off the characteristic component of the Riemann tensor,

$$R^{\hat{\tau}}_{\hat{\varphi}\hat{\tau}\hat{\varphi}} = -\frac{[(\sinh(\tau)K^{\frac{1}{2}}),_{\tau} K^{-\frac{1}{2}}],_{\tau}}{a^2 \sinh(\tau)K}. \quad (6.2.77)$$

We find then for the scalar curvature,

$$\begin{aligned} R = R^{\hat{\alpha}\hat{\beta}}_{\hat{\alpha}\hat{\beta}} &= 2R^{\hat{\tau}\hat{\phi}}_{\hat{\tau}\hat{\phi}} \\ &= -\frac{2}{a^2} \left\{ \frac{[(\sinh(\tau) K^{\frac{1}{2}})_{,\tau} K^{-\frac{1}{2}}]_{,\tau}}{\sinh(\tau) K} \right\}, \end{aligned} \quad (6.2.78)$$

which can be rewritten in terms of the Laplacian as follows,

$$R = -\frac{2}{a^2 K} \left\{ 1 + \frac{1}{2K} \left[-a^2 \Delta U + \frac{U_{,\varphi\varphi}}{\sinh^2 \tau} - \frac{(U_{,\tau})^2}{K} \right] \right\}. \quad (6.2.79)$$

For finite values of h , the condition for R to be negative on all the accessible region of \mathcal{S}^N is then,

$$2\pi a^2 q^2 n - \frac{U_{,\varphi\varphi}}{\sinh^2 \tau} + \frac{(U_{,\tau})^2}{K} < 2K. \quad (6.2.80)$$

Ergodicity of the semi-ideal Coulomb plasma

Consider a one component Coulomb plasma where we switch off the mutual interactions between the particles, leaving unchanged the interaction between the particles and the neutralizing background ($U = V_N^0 + V_N^{pb}$). We will call it the “semi-ideal” system. Define,

$$\Omega(h, \tau_0) = \{q^N | q_i \in \Omega_{a\tau_0} \quad \forall i, h - U(q^N) \geq 0\}, \quad (6.2.81)$$

and call $h' = h - V_N^0 - v_1$ and

$$\begin{aligned} f(N) &= -N \ln[1 - \tanh^2(\tau_0/2)] = N \ln[1 + \sinh^2(\tau_0/2)] \\ &= N \ln \left(1 + \frac{N}{4\pi a^2 n} \right). \end{aligned} \quad (6.2.82)$$

We will have ($\alpha = 2\pi a^2 n e^2$)

$$r = \inf_{q^N \in \Omega(h, \tau_0)} 2K^2 = \begin{cases} 2[h' - \alpha f(N)]^2 & h' > \alpha f(N) \\ 0 & h' \leq \alpha f(N) \end{cases}, \quad (6.2.83)$$

Notice that for large N , at constant n , we have (see appendix 6.A),

$$-V_N^0/\alpha = \frac{\alpha}{e^2} \left[-2 \frac{N}{4\pi a^2 n} + \ln \left(1 + \frac{N}{4\pi a^2 n} \right) + \frac{1}{2} \right] + O(1/N), \quad (6.2.84)$$

$$-v_1/\alpha = f(N) + N - \frac{\alpha}{e^2} + O(1/N). \quad (6.2.85)$$

Using the extensive property of the energy we may assume that $h = Nh_0$, where h_0 is the total energy per particle. Then for large N we will have

$$h' = Nh_0 + \alpha f(N) + \left(\frac{\alpha}{e} \right)^2 \left[\ln \left(1 + \frac{N}{4\pi a^2 n} \right) - \frac{1}{2} \right] + O(1/N) > \alpha f(N), \quad (6.2.86)$$

if $h_0 \geq 0$.

On the other hand for $h' > \alpha f(N)$ we have

$$\begin{aligned} l &= \sup_{q^N \in \Omega(h, \tau_0)} [\alpha K + (U, \tau)^2] \leqslant \sup_{q^N \in \Omega(h, \tau_0)} [\alpha K] + \sup_{q^N \in \Omega(h, \tau_0)} [(U, \tau)^2] \\ &= l_+ = \alpha h' + \alpha^2 \tanh^2(\tau_0/2), \end{aligned} \quad (6.2.87)$$

Condition (6.2.80) is always satisfied if $l < r$. Then the semi-ideal system is ergodic if,

$$h' > h'_+ = \alpha f(N) + \frac{\alpha}{4} \left[1 + \sqrt{1 + 8f(N) + 8 \tanh^2(\tau_0/2)} \right], \quad (6.2.88)$$

where h'_+ is the largest root of the equation $l_+ = r$. Recalling that $\tanh^2(\tau_0/2) \rightarrow 1$ at large N , one can verify that, given Eq. (6.2.86), Eq. (6.2.88) must be satisfied at large N if $h_0 > 0$.

We conclude that the semi ideal system is certainly ergodic if the total enery is extensive and the total energy per particle is positive.

Partition function and densities at a special temperature

Working with the set of coordinates (r, φ) on the pseudosphere (the Poincaré disk representation), the particle i -particle j interaction term in the Hamiltonian can be written as Jancovici and Téllez [1998]

$$G(d_{ij}) = -\ln \tanh(d_{ij}/2a) = -\ln \left| \frac{(z_i - z_j)/2a}{1 - (z_i \bar{z}_j/4a^2)} \right|, \quad (6.2.89)$$

where $z_j = r_j e^{i\varphi_j}$ and \bar{z}_j is the complex conjugate of z_j . This interaction (6.2.89) happens to be the Coulomb interaction in a flat disc of radius $2a$ with ideal conductor walls. Therefore, it is possible to use the techniques which have been developed Forrester [1991]; Jancovici and Téllez [1996] for dealing with ideal conductor walls, in the grand canonical ensemble.

The grand canonical partition function of the OCP at fugacity ζ with a fixed background density n_b , when $\Gamma = \beta e^2 = 2$, is

$$\Xi(2) = C_0 \left[1 + \sum_{N=1}^{\infty} \frac{1}{N!} \int \prod_{i=1}^N \frac{r_i dr_i d\varphi_i}{[1 - (r_i^2/4a^2)]} \prod_{i < j} \left| \frac{(z_i - z_j)/2a}{1 - (z_i \bar{z}_j/4a^2)} \right|^2 \prod_{i=1}^N \zeta(r_i) \right] \quad (6.2.90)$$

where for $N = 1$ the product $\prod_{i < j}$ must be replaced by 1. We have defined a position-dependent fugacity $\zeta(r) = \zeta[1 - r^2/4a^2]^{4\pi n_b a^2 - 1} e^C$ which includes the particle-background interaction (6.2.62) and only one factor $[1 - r^2/4a^2]^{-1}$ from the integration measure $dS = [1 - r^2/4a^2]^{-2} dr$. This should prove to be convenient later. The e^C factor is

$$e^C = \exp \left[4\pi n_b a^2 \left(\ln \cosh^2 \frac{\tau_0}{2} - \sinh^2 \frac{\tau_0}{2} \ln \tanh^2 \frac{\tau_0}{2} \right) \right] \quad (6.2.91)$$

which is a constant term coming from the particle-background interaction term (6.2.62) and

$$\ln C_0 = \frac{(4\pi n_b a^2)^2}{2} \left[\ln \cosh^2 \frac{\tau_0}{2} + \sinh^2 \frac{\tau_0}{2} \left(\sinh^2 \frac{\tau_0}{2} \ln \tanh^2 \frac{\tau_0}{2} - 1 \right) \right] \quad (6.2.92)$$

which comes from the background-background interaction. Notice that for large domains, when $\tau_0 \rightarrow \infty$, we have

$$e^C \sim \left[\frac{e^{\tau_0+1}}{4} \right]^{4\pi n_b a^2} \quad (6.2.93)$$

and

$$\ln C_0 \sim -\frac{(4\pi n_b a^2)^2 e^{\tau_0}}{4} \quad (6.2.94)$$

Let us define a set of reduced complex coordinates $u_i = (z_i/2a)$ inside the Poincaré disk and its corresponding images $u_i^* = (2a/\bar{z}_i)$ outside the disk. By using the following Cauchy identity Aitken [1956]

$$\det \left(\frac{1}{u_i - u_j^*} \right)_{(i,j) \in \{1, \dots, N\}^2} = (-1)^{N(N-1)/2} \frac{\prod_{i < j} (u_i - u_j)(u_i^* - u_j^*)}{\prod_{i,j} (u_i - u_j^*)} \quad (6.2.95)$$

the particle-particle interaction term together with the $[1 - (r_i^2/4a^2)]^{-1}$ other term from the integration measure can be cast into the form

$$\prod_{i < j} \left| \frac{(z_i - z_j)/2a}{1 - (z_i \bar{z}_j/4a^2)} \right|^2 \prod_{i=1}^N [1 - (r_i^2/4a^2)]^{-1} = \det \left(\frac{1}{1 - u_i \bar{u}_j} \right)_{(i,j) \in \{1, \dots, N\}^2} \quad (6.2.96)$$

The grand canonical partition function then is

$$\Xi(2) = \left[1 + \sum_{N=1}^{\infty} \frac{1}{N!} \int \prod_{i=1}^N d^2 r_i \prod_{i=1}^N \zeta(r_i) \det \left(\frac{1}{1 - u_i \bar{u}_j} \right) \right] C_0 \quad (6.2.97)$$

We shall now show that this expression can be reduced to an infinite continuous determinant, by using a functional integral representation similar to the one which has been developed for the two-component Coulomb gas Zinn-Justin [1993]. Let us consider the Gaussian partition function

$$Z_0 = \int \mathcal{D}\psi \mathcal{D}\bar{\psi} \exp \left[\int \bar{\psi}(r) M^{-1}(z, \bar{z}') \psi(r') d^2 r d^2 r' \right] \quad (6.2.98)$$

The fields ψ and $\bar{\psi}$ are anticommuting Grassmann variables. The Gaussian measure in (6.2.98) is chosen such that its covariance is equal to¹

$$\langle \bar{\psi}(r_i) \psi(r_j) \rangle = M(z_i, \bar{z}_j) = \frac{1}{1 - u_i \bar{u}_j} \quad (6.2.99)$$

where $\langle \dots \rangle$ denotes an average taken with the Gaussian weight of (6.2.98). By construction we have

$$Z_0 = \det(M^{-1}) \quad (6.2.100)$$

Let us now consider the following partition function

$$Z = \int \mathcal{D}\psi \mathcal{D}\bar{\psi} \exp \left[\int \bar{\psi}(r) M^{-1}(z, \bar{z}') \psi(r') d^2 r d^2 r' + \int \zeta(r) \bar{\psi}(r) \psi(r) d^2 r \right] \quad (6.2.101)$$

which is equal to

$$Z = \det(M^{-1} + \zeta) \quad (6.2.102)$$

and then

$$\frac{Z}{Z_0} = \det[M(M^{-1} + \zeta)] = \det[1 + K] \quad (6.2.103)$$

¹Actually the operator M should be restricted to act only on analytical functions for its inverse M^{-1} to exist.

where

$$K(\mathbf{r}, \mathbf{r}') = M(z, \bar{z}') \zeta(r') = \frac{\zeta(r')}{1 - u\bar{u}'} \quad (6.2.104)$$

The results which follow can also be obtained by exchanging the order of the factors M and $M^{-1} + \zeta$ in (6.2.103), i.e. by replacing $\zeta(r')$ by $\zeta(r)$ in (6.2.104), however using the definition (6.2.104) of K is more convenient. Expanding the ratio Z/Z_0 in powers of ζ we have

$$\frac{Z}{Z_0} = 1 + \sum_{N=1}^{\infty} \frac{1}{N!} \int \prod_{i=1}^N d^2 r_i \prod_{i=1}^N \zeta(r_i) \langle \bar{\psi}(\mathbf{r}_1)\psi(\mathbf{r}_1) \cdots \bar{\psi}(\mathbf{r}_N)\psi(\mathbf{r}_N) \rangle \quad (6.2.105)$$

Now, using Wick theorem for anticommuting variables Zinn-Justin [1993], we find that

$$\langle \bar{\psi}(\mathbf{r}_1)\psi(\mathbf{r}_1) \cdots \bar{\psi}(\mathbf{r}_N)\psi(\mathbf{r}_N) \rangle = \det M(z_i, \bar{z}_j) = \det \left(\frac{1}{1 - u_i \bar{u}_j} \right) \quad (6.2.106)$$

Comparing equations (6.2.105) and (6.2.97) with the help of equation (6.2.106) we conclude that

$$\Xi(2) = C_0 \frac{Z}{Z_0} = C_0 \det(1 + K) \quad (6.2.107)$$

The problem of computing the grand canonical partition function has been reduced to finding the eigenvalues of the operator K . The eigenvalue problem for K reads

$$\int \zeta e^C \frac{\left(1 - \frac{r'^2}{4a^2}\right)^{4\pi n_b a^2 - 1}}{1 - \frac{z\bar{z}'}{4a^2}} \Phi(\mathbf{r}') r' dr' d\varphi' = \lambda \Phi(\mathbf{r}) \quad (6.2.108)$$

For $\lambda \neq 0$ we notice from equation (6.2.108) that $\Phi(\mathbf{r}) = \Phi(z)$ is an analytical function of z . Because of the circular symmetry it is natural to try $\Phi(z) = \Phi_\ell(z) = z^\ell = r^\ell e^{i\ell\varphi}$ with ℓ a positive integer. Expanding

$$\frac{1}{1 - \frac{z\bar{z}'}{4a^2}} = \sum_{n=0}^{\infty} \left(\frac{z\bar{z}'}{4a^2} \right)^n \quad (6.2.109)$$

and replacing $\Phi_\ell(z) = z^\ell$ in equation (6.2.108) one can show that Φ_ℓ is actually an eigenfunction of K with eigenvalue

$$\lambda_\ell = 4\pi a^2 \zeta e^C B_{t_0}(\ell + 1, 4\pi n_b a^2) \quad (6.2.110)$$

with $t_0 = r_0^2/4a^2 = \tanh^2(\tau_0/2)$ and

$$B_{t_0}(\ell + 1, 4\pi n_b a^2) = \int_0^{t_0} (1 - t)^{4\pi n_b a^2 - 1} t^\ell dt \quad (6.2.111)$$

the incomplete beta function. So we finally arrive to the result for the grand potential

$$\beta\Omega = -\ln \Xi(2) = -\ln C_0 - \sum_{\ell=0}^{\infty} \ln (1 + 4\pi a^2 \zeta e^C B_{t_0}(\ell + 1, 4\pi n_b a^2)) \quad (6.2.112)$$

with e^C and $\ln C_0$ given by equations (6.2.91) and (6.2.92). This result is valid for any disk domain of radius $a\tau_0$. A more explicit expression of the grand potential for large domains $\tau_0 \rightarrow \infty$ can also be obtained Fantoni et al. [2003].

As usual one can compute the density by doing a functional derivative of the grand potential with respect to the position-dependent fugacity:

$$n^{(1)}(\mathbf{r}) = \left(1 - \frac{r^2}{4a^2}\right)^2 \zeta(r) \frac{\delta \ln \Xi(2)}{\delta \zeta(r)} \quad (6.2.113)$$

The factor $[1 - (r^2/4a^2)]^2$ is due to the curvature Jancovici and Téllez [1998], so that $n^{(1)}(\mathbf{r}) dS$ is the average number of particles in the surface element $dS = [1 - (r^2/4a^2)]^{-2} dr$. Using a Dirac-like notation, one can formally write

$$\ln \Xi(2) = \text{Tr} \ln(1 + K) + \ln C_0 = \int \langle \mathbf{r} | \ln(1 + \zeta(r)M) | \mathbf{r} \rangle dr + \ln C_0 \quad (6.2.114)$$

Then, doing the functional derivative (6.2.113), one obtains

$$n^{(1)}(\mathbf{r}) = \left(1 - \frac{r^2}{4a^2}\right)^2 \zeta(r) \langle \mathbf{r} | (1 + K)^{-1} M | \mathbf{r} \rangle = 4\pi a \left(1 - \frac{r^2}{4a^2}\right)^2 \zeta(r) \tilde{G}(\mathbf{r}, \mathbf{r}) \quad (6.2.115)$$

where we have defined $\tilde{G}(\mathbf{r}, \mathbf{r}')$ by² $\tilde{G} = (1 + K)^{-1} M / 4\pi a$. More explicitly, \tilde{G} is the solution of $(1 + K)\tilde{G} = M / 4\pi a$, that is

$$\tilde{G}(\mathbf{r}, \mathbf{r}') + \zeta e^C \int \tilde{G}(\mathbf{r}'', \mathbf{r}') \frac{\left(1 - \frac{r''^2}{4a^2}\right)^{4\pi n_b a^2 - 1}}{1 - \frac{z\bar{z}''}{4a^2}} d\mathbf{r}'' = \frac{1}{4\pi a \left[1 - \frac{z\bar{z}'}{4a^2}\right]} \quad (6.2.116)$$

and the density is given by

$$n^{(1)}(\mathbf{r}) = 4\pi a \zeta e^C \left(1 - \frac{r^2}{4a^2}\right)^{4\pi n_b a^2 + 1} \tilde{G}(\mathbf{r}, \mathbf{r}) \quad (6.2.117)$$

From the integral equation (6.2.116) one can see that $\tilde{G}(\mathbf{r}, \mathbf{r}')$ is an analytical function of z . Trying a solution of the form

$$\tilde{G}(\mathbf{r}, \mathbf{r}') = \sum_{\ell=0}^{\infty} a_{\ell}(\mathbf{r}') z^{\ell} \quad (6.2.118)$$

into equation (6.2.116) yields

$$\tilde{G}(\mathbf{r}, \mathbf{r}') = \frac{1}{4\pi a} \sum_{\ell=0}^{\infty} \left(\frac{z\bar{z}'}{4a^2}\right)^{\ell} \frac{1}{1 + 4\pi a^2 \zeta e^C B_{t_0}(\ell + 1, 4\pi n_b a^2)} \quad (6.2.119)$$

Then the density is given by

$$n^{(1)}(\mathbf{r}) = \zeta e^C \left(1 - \frac{r^2}{4a^2}\right)^{4\pi n_b a^2 + 1} \sum_{\ell=0}^{\infty} \left(\frac{r^2}{4a^2}\right)^{\ell} \frac{1}{1 + 4\pi a^2 \zeta e^C B_{t_0}(\ell + 1, 4\pi n_b a^2)} \quad (6.2.120)$$

After some calculation (see appendix 6.B), it can be shown that, in the limit $a \rightarrow \infty$, the result for the flat disk in the canonical ensemble Jancovici [1981a]

$$\frac{n^{(1)}(\mathbf{r})}{n_b} = \exp(-\pi n_b r^2) \sum_{\ell=0}^{N_b-1} \frac{(\pi n_b r^2)^{\ell}}{\gamma(\ell + 1, N_b)} \quad (6.2.121)$$

²The factor $4\pi a$ is there just to keep the same notations as in Ref. Jancovici and Téllez [1998].

is recovered. up to a correction due to the non-equivalence of ensembles in finite systems. In (6.2.121), γ is the incomplete gamma function

$$\gamma(\ell + 1, x) = \int_0^x t^\ell e^{-t} dt \quad (6.2.122)$$

In that flat-disk case, in the thermodynamic limit (half-space), $n^{(1)}(r_0) = n_{\text{contact}} \rightarrow n_b \ln 2$.

In a flat space, the neighborhood of the boundary of a large domain has a volume which is a negligible fraction of the whole volume. This is why, for the statistical mechanics of ordinary fluids, usually there is a thermodynamic limit: when the volume becomes infinite, quantities such as the free energy per unit volume or the pressure have a unique limit, independent of the domain shape and of the boundary conditions. However, even in a flat space, the one-component plasma is special. For the OCP, it is possible to define several non-equivalent pressures, some of which, for instance the kinetic pressure [Fantoni et al. \[2003\]](#), obviously are surface-dependent even in the infinite-system limit.

Even for ordinary fluids, statistical mechanics on a pseudosphere is expected to have special features, which are essentially related to the property that, for a large domain, the area of the neighborhood of the boundary is of the same order of magnitude as the whole area. Although some bulk properties, such as correlation functions far away from the boundary, will exist, extensive quantities such as the free energy or the grand potential are strongly dependent on the boundary neighborhood and surface effects. For instance, in the large-domain limit, no unique limit is expected for the free energy per unit area F/\mathcal{A} or the pressure $-(\partial F/\partial \mathcal{A})_{\beta, N}$.

In the present section, we have studied the 2D OCP on a pseudosphere, for which surface effects are expected to be important for both reasons: because we are dealing with a one-component plasma and because the space is a pseudosphere. Therefore, although the correlation functions far away from the boundary have unique thermodynamic limits [Jancovici and Téllez \[1998\]](#), many other properties are expected to depend on the domain shape and on the boundary conditions. This is why we have considered a special well-defined geometry: the domain is a disk bounded by a plain hard wall, and we have studied the corresponding large-disk limit. Our results have been derived only for that geometry.

6.2.5 The Flamm paraboloid

The metric tensor of *Flamm's paraboloid* in the coordinates $q = (r, \varphi)$ is now,

$$g = \begin{pmatrix} (1 - 2M/r)^{-1} & 0 \\ 0 & r^2 \end{pmatrix}, \quad (6.2.123)$$

where M is a constant. This is an embeddable surface in the three-dimensional Euclidean space with cylindrical coordinates (r, φ, Z) with $ds^2 = dZ^2 + dr^2 + r^2 d\varphi^2$, whose equation is

$$Z(r) = \pm 2\sqrt{2M(r - 2M)}. \quad (6.2.124)$$

This surface is illustrated in Fig. 6.2.1. It has a hole of radius $2M$. As the hole shrinks to a point (limit $M \rightarrow 0$) the surface becomes flat. We will from now on call the $r = 2M$ region of the surface its “horizon”. The Schwarzschild geometry in general relativity is a vacuum solution to the Einstein field equation which is spherically symmetric and in a two dimensional world its spatial part is a Flamm paraboloid \mathcal{S} . In general relativity, M (in appropriate units) is the mass of the source of the gravitational field.

The “Schwarzschild wormhole” provides a path from the upper “universe” \mathcal{S}_+ ($Z > 0$) to the lower one \mathcal{S}_- ($Z < 0$). These are both multiply connected surfaces. We will study the OCP on

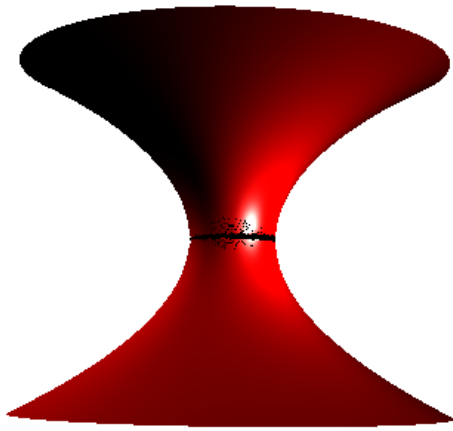


Figure 6.2.1: The Riemannian surface \mathcal{S} of Eq. (6.2.124).

a single universe, on the whole surface, and on a single universe with the “horizon” (the region $r = 2M$) grounded.

Since the curvature of the surface is not a constant but varies from point to point, the plasma will not be uniform even in the thermodynamic limit.

The system of coordinates (r, φ) with the metric (6.2.123) has the disadvantage that it requires two charts to cover the whole surface \mathcal{S} . It can be more convenient to use the variable

$$u = \frac{Z}{4M} = \pm \sqrt{\frac{r}{2M} - 1} \quad (6.2.125)$$

instead of r . Replacing r as a function of Z using equation (6.2.124) gives the following metric when using the system of coordinates $q = (u, \varphi)$,

$$\mathbf{g} = \begin{pmatrix} (4M)^2(1+u^2) & 0 \\ 0 & 4M^2(1+u^2)^2 \end{pmatrix}, \quad (6.2.126)$$

The region $u > 0$ corresponds to \mathcal{S}_+ and the region $u < 0$ to \mathcal{S}_- .

Let us consider that the OCP is confined in a disk defined as

$$\Omega_R^+ = \{q = (r, \varphi) \in \mathcal{S}_+ | 0 \leq \varphi \leq 2\pi, 2M \leq r \leq R\}. \quad (6.2.127)$$

The area of this disk is given by

$$\mathcal{A}_R = \int_{\Omega_R} dS = \pi \left[\sqrt{R(R-2M)(3M+R)} + 6M^2 \ln \left(\frac{\sqrt{R} + \sqrt{R-2M}}{\sqrt{2M}} \right) \right], \quad (6.2.128)$$

where $dS = \sqrt{g} dr d\varphi$ and $g = \det[g_{\mu\nu}]$. The perimeter is $C_R = 2\pi R$.

The Riemann tensor characteristic component is

$$R^r_{\varphi r \varphi} = -\frac{M}{r}. \quad (6.2.129)$$

The scalar curvature is then given by the following indexes contractions

$$\mathcal{R} = R^\mu_\mu = R^{\mu\nu}_{\mu\nu} = 2R^{r\varphi}_{r\varphi} = 2g^{\varphi\varphi}R^r_{\varphi r\varphi} = -\frac{2M}{r^3}, \quad (6.2.130)$$

and the (intrinsic) Gaussian curvature is $K = \mathcal{R}/2 = -M/r^3$. The (extrinsic) mean curvature of the manifold turns out to be $H = -\sqrt{M/8r^3}$.

The Euler characteristic (6.1.5) of the disk Ω_R^+ turns out to be $\chi = 0$, in agreement with the Gauss-Bonnet theorem $\chi = 2 - 2h - b$ where $h = 0$ is the number of handles and $b = 2$ the number of boundaries.

We can also consider the case where the system is confined in a “double” disk

$$\Omega_R = \Omega_R^+ \cup \Omega_R^-, \quad (6.2.131)$$

with $\Omega_R^- = \{q = (r, \varphi) \in \mathcal{S}_- | 0 \leq \varphi \leq 2\pi, 2M \leq r \leq R\}$, the disk image of Ω_R^+ on the lower universe \mathcal{S}_- portion of \mathcal{S} . The Euler characteristic of Ω_R is also $\chi = 0$.

The fact that the Euler characteristic is zero implies that the asymptotic expansion in the thermodynamic limit of the free energy does not exhibit the logarithmic corrections predicted by Ref. Jancovici et al. [1994].

The Laplacian for a function f is

$$\begin{aligned} \Delta f &= \frac{1}{\sqrt{g}} \frac{\partial}{\partial q^\mu} \left(\sqrt{g} g^{\mu\nu} \frac{\partial}{\partial q^\nu} \right) f \\ &= \left[\left(1 - \frac{2M}{r} \right) \frac{\partial^2}{\partial r^2} + \frac{1}{r^2} \frac{\partial^2}{\partial \varphi^2} + \left(\frac{1}{r} - \frac{M}{r^2} \right) \frac{\partial}{\partial r} \right] f, \end{aligned} \quad (6.2.132)$$

where $q \equiv (r, \varphi)$. In appendix 6.C, we show how, finding the Green function of the Laplacian, naturally leads to consider the system of coordinates (x, φ) , with

$$x = (\sqrt{u^2 + 1} + u)^2. \quad (6.2.133)$$

The range for the variable x is $]0, +\infty[$. The lower paraboloid \mathcal{S}_- corresponds to the region $0 < x < 1$ and the upper one \mathcal{S}_+ to the region $x > 1$. A point in the upper paraboloid with coordinate (x, φ) has a mirror image by reflection ($u \rightarrow -u$) in the lower paraboloid, with coordinates $(1/x, \varphi)$, since if

$$x = (\sqrt{u^2 + 1} + u)^2 \quad (6.2.134)$$

then

$$\frac{1}{x} = (\sqrt{u^2 + 1} - u)^2. \quad (6.2.135)$$

In the upper paraboloid \mathcal{S}_+ , the new coordinate x can be expressed in terms of the original one, r , as

$$x = \frac{(\sqrt{r} + \sqrt{r - 2M})^2}{2M}. \quad (6.2.136)$$

Using this system of coordinates, the metric takes the form of a flat metric multiplied by a conformal factor

$$g = \begin{pmatrix} (M/2)^2(1 + 1/x)^4 & 0 \\ 0 & (M/2)^2(1 + 1/x)^4 x^2 \end{pmatrix}, \quad (6.2.137)$$

The Laplacian also takes a simple form

$$\Delta f = \frac{4}{M^2 (1 + \frac{1}{x})^4} \Delta_{\text{flat}} f \quad (6.2.138)$$

where

$$\Delta_{\text{flat}} f = \frac{\partial^2 f}{\partial x^2} + \frac{1}{x} \frac{\partial f}{\partial x} + \frac{1}{x^2} \frac{\partial^2 f}{\partial \varphi^2} \quad (6.2.139)$$

is the Laplacian of the flat Euclidean space \mathbb{R}^2 . The determinant of the metric is now given by $g = [M^2 x(1+x^{-1})^4/4]^2$.

With this system of coordinates (x, φ) , the area of a disk Ω_R^+ of radius R , in the original system (r, φ) , is given by

$$\mathcal{A}_R = \frac{\pi M^2}{4} p(x_m) \quad (6.2.140)$$

with

$$p(x) = x^2 + 8x - \frac{8}{x} - \frac{1}{x^2} + 12 \ln x \quad (6.2.141)$$

and $x_m = (\sqrt{R} + \sqrt{R-2M})^2/(2M)$.

The Coulomb potential $G(x, \varphi; x_0, \varphi_0)$ created at (x, φ) by a unit charge at (x_0, φ_0) is given by the Green function of the Laplacian

$$\Delta G(x, \varphi; x_0, \varphi_0) = -2\pi \delta^{(2)}(x, \varphi; x_0, \varphi_0) \quad (6.2.142)$$

with appropriate boundary conditions. The Dirac distribution on \mathcal{S} is given by

$$\delta^{(2)}(x, \varphi; x_0, \varphi_0) = \frac{4}{M^2 x(1+x^{-1})^4} \delta(x-x_0) \delta(\varphi-\varphi_0) \quad (6.2.143)$$

Notice that using the system of coordinates (x, φ) the Laplacian Green function equation takes the simple form

$$\Delta_{\text{flat}} G(x, \varphi; x_0, \varphi_0) = -2\pi \frac{1}{x} \delta(x-x_0) \delta(\varphi-\varphi_0) \quad (6.2.144)$$

which is formally the same Laplacian Green function equation for flat space.

We shall consider three different situations: when the particles can be in the whole surface \mathcal{S} , or when the particles are confined to the upper paraboloid universe \mathcal{S}_+ , confined by a hard wall or by a grounded perfect conductor.

The geodesic distance on the Flamm paraboloid is determined in appendix 6.D.

Coulomb potential in the whole surface (ws)

To complement the Laplacian Green function equation (6.2.142), we impose the usual boundary condition that the electric field $-\nabla G$ vanishes at infinity ($x \rightarrow \infty$ or $x \rightarrow 0$). Also, we require the usual interchange symmetry $G(x, \varphi; x_0, \varphi_0) = G(x_0, \varphi_0; x, \varphi)$ to be satisfied. Additionally, due to the symmetry between each universe \mathcal{S}_+ and \mathcal{S}_- , we require that the Green function satisfies the symmetry relation

$$G^{\text{ws}}(x, \varphi; x_0, \varphi_0) = G^{\text{ws}}(1/x, \varphi; 1/x_0, \varphi_0) \quad (6.2.145)$$

The Laplacian Green function equation (6.2.142) can be solved, as usual, by using the decomposition as a Fourier series, as shown in appendix 6.C. Since equation (6.2.142) reduces to the flat Laplacian Green function equation (6.2.144), the solution is the standard one

$$G(x, \varphi; x_0, \varphi_0) = \sum_{n=1}^{\infty} \frac{1}{n} \left(\frac{x_-}{x_+} \right)^n \cos[n(\varphi - \varphi_0)] + g_0(x, x_0) \quad (6.2.146)$$

where $x_> = \max(x, x_0)$ and $x_< = \min(x, x_0)$. The Fourier coefficient for $n = 0$, has the form

$$g_0(x, x_0) = \begin{cases} a_0^+ \ln x + b_0^+, & x > x_0 \\ a_0^- \ln x + b_0^-, & x < x_0. \end{cases} \quad (6.2.147)$$

The coefficients a_0^\pm, b_0^\pm are determined by the boundary conditions that g_0 should be continuous at $x = x_0$, its derivative discontinuous $\partial_x g_0|_{x=x_0^+} - \partial_x g_0|_{x=x_0^-} = -1/x_0$, and the boundary condition at infinity $\nabla g_0|_{x \rightarrow \infty} = 0$ and $\nabla g_0|_{x \rightarrow 0} = 0$. Unfortunately, the boundary condition at infinity is trivially satisfied for g_0 , therefore g_0 cannot be determined only with this condition. In flat space, this is the reason why the Coulomb potential can have an arbitrary additive constant added to it. However, in our present case, we have the additional symmetry relation (6.2.145) which should be satisfied. This fixes the Coulomb potential up to an additive constant b_0 . We find

$$g_0(x, x_0) = -\frac{1}{2} \ln \frac{x_>}{x_<} + b_0, \quad (6.2.148)$$

and summing explicitly the Fourier series (6.2.146), we obtain

$$G^{\text{ws}}(x, \varphi; x_0, \varphi_0) = -\ln \frac{|z - z_0|}{\sqrt{|zz_0|}} + b_0, \quad (6.2.149)$$

where we defined $z = xe^{i\varphi}$ and $z_0 = x_0 e^{i\varphi_0}$. Notice that this potential does not reduce exactly to the flat one when $M = 0$. This is due to the fact that the whole surface \mathcal{S} in the limit $M \rightarrow 0$ is not exactly a flat plane \mathbb{R}^2 , but rather it is two flat planes connected by a hole at the origin, this hole modifies the Coulomb potential.

Coulomb potential in the half surface (hs) confined by hard walls

We consider now the case when the particles are restricted to live in the half surface \mathcal{S}_+ , $x > 1$, and they are confined by a hard wall located at the “horizon” $x = 1$. The region $x < 1$ (\mathcal{S}_-) is empty and has the same dielectric constant as the upper region occupied by the particles. Since there are no image charges, the Coulomb potential is the same G^{ws} as above. However, we would like to consider here a new model with a slightly different interaction potential between the particles. Since we are dealing only with half surface, we can relax the symmetry condition (6.2.145). Instead, we would like to consider a model where the interaction potential reduces to the flat Coulomb potential in the limit $M \rightarrow 0$. The solution of the Laplacian Green function equation is given in Fourier series by equation (6.2.146). The zeroth order Fourier component g_0 can be determined by the requirement that, in the limit $M \rightarrow 0$, the solution reduces to the flat Coulomb potential

$$G^{\text{flat}}(\mathbf{r}, \mathbf{r}') = -\ln \frac{|\mathbf{r} - \mathbf{r}'|}{L} \quad (6.2.150)$$

where L is an arbitrary constant length. Recalling that $x \sim 2r/M$, when $M \rightarrow 0$, we find

$$g_0(x, x_0) = -\ln x_> - \ln \frac{M}{2L} \quad (6.2.151)$$

and

$$G^{\text{hs}}(x, \varphi; x_0, \varphi_0) = -\ln |z - z_0| - \ln \frac{M}{2L}. \quad (6.2.152)$$

Coulomb potential on half surface with a grounded horizon (gh)

Let us consider now that the particles are confined to \mathcal{S}_+ by a grounded perfect conductor at $x = 1$ which imposes Dirichlet boundary condition to the electric potential. The Coulomb potential can easily (see appendix 6.C) be found from the Coulomb potential G^{ws} (6.2.149) using the method of images

$$G^{\text{gh}}(x, \varphi; x_0, \varphi_0) = -\ln \frac{|z - z_0|}{\sqrt{|zz_0|}} + \ln \frac{|z - \bar{z}_0^{-1}|}{\sqrt{|z\bar{z}_0^{-1}|}} = -\ln \left| \frac{z - z_0}{1 - z\bar{z}_0^{-1}} \right| \quad (6.2.153)$$

where the bar over a complex number indicates its complex conjugate. We will call this the grounded horizon Green function. Notice how its shape is the same of the Coulomb potential on the pseudosphere [Fantoni et al. \[2003\]](#) or in a flat disk confined by perfect conductor boundaries [Jancovici and Téllez \[1996\]](#).

This potential can also be found using the Fourier decomposition. Since it will be useful in the following, we note that the zeroth order Fourier component of G^{gh} is

$$g_0(x, x_0) = \ln x_- . \quad (6.2.154)$$

The background

The Coulomb potential generated by the background, with a constant surface charge density ρ_b satisfies the Poisson equation, for $r > 2M$,

$$\Delta v_b = -2\pi\rho_b , \quad (6.2.155)$$

Assuming that the system occupies an area \mathcal{A}_R , the background density can be written as $\rho_b = -qN_b/\mathcal{A}_R = -qn_b$, where we have defined here $n_b = N_b/\mathcal{A}_R$ the number density associated to the background. For a neutral system $N_b = N$. The Coulomb potential of the background can be obtained by solving Poisson equation with the appropriate boundary conditions for each case. Also, it can be obtained from the Green function computed in the previous section

$$v_b(x, \varphi) = \int G(x, \varphi; x', \varphi') \rho_b dS' \quad (6.2.156)$$

This integral can be performed easily by using the Fourier series decomposition (6.2.146) of the Green function G . Recalling that $dS = \frac{1}{4}M^2x(1+x^{-1})^4 dx d\varphi$, after the angular integration is done, only the zeroth order term in the Fourier series survives

$$v_b(x, \varphi) = \frac{\pi\rho_b M^2}{2} \int_1^{x_m} g_0(x, x') x' \left(1 + \frac{1}{x'}\right)^4 dx' . \quad (6.2.157)$$

The previous expression is for the half surface case and the grounded horizon case. For the whole surface case, the lower limit of integration should be replaced by $1/x_m$, or, equivalently, the integral multiplied by a factor two.

Using the explicit expressions for g_0 , (6.2.148), (6.2.151), and (6.2.154) for each case, we find, for the whole surface,

$$v_b^{\text{ws}}(x, \varphi) = -\frac{\pi\rho_b M^2}{8} [h(x) - h(x_m) + 2p(x_m) \ln x_m - 4b_0 p(x_m)] \quad (6.2.158)$$

where $p(x)$ was defined in equation (6.2.141), and

$$h(x) = x^2 + 16x + \frac{16}{x} + \frac{1}{x^2} + 12(\ln x)^2 - 34 . \quad (6.2.159)$$

Notice the following properties satisfied by the functions p and h

$$p(x) = -p(1/x), \quad h(x) = h(1/x) \quad (6.2.160)$$

and

$$p(x) = xh'(x)/2, \quad p'(x) = 2x \left(1 + \frac{1}{x}\right)^4 \quad (6.2.161)$$

where the prime stands for the derivative.

The background potential for the half surface case, with the pair potential $-\ln(|z-z'|M/2L)$ is

$$v_b^{\text{hs}}(x, \varphi) = -\frac{\pi\rho_b M^2}{8} \left[h(x) - h(x_m) + 2p(x_m) \ln \frac{x_m M}{2L} \right]. \quad (6.2.162)$$

Also, the background potential in the half surface case, but with the pair potential $-\ln(|z-z'|/\sqrt{|zz'|}) + b_0$ is

$$v_b^{\text{hs}}(x, \varphi) = -\frac{\pi\rho_b M^2}{8} \left[h(x) - \frac{h(x_m)}{2} + p(x_m) \left(\ln \frac{x_m}{x} - 2b_0 \right) \right]. \quad (6.2.163)$$

Finally, for the grounded horizon case,

$$v_b^{\text{gh}}(x, \varphi) = -\frac{\pi\rho_b M^2}{8} [h(x) - 2p(x_m) \ln x]. \quad (6.2.164)$$

Partition function and densities at a special temperature

We will now show how at the special value of the coupling constant $\Gamma = \beta e^2 = 2$ the partition function and n -body correlation functions can be calculated exactly.

The 2D OCP on half surface with potential $-\ln|z-z'| - \ln M/(2L)$

For this case, we work in the canonical ensemble with N particles and the background neutralizes the charges: $N_b = N$, and $n = N/\mathcal{A}_R = n_b$. The potential energy of the system takes the explicit form

$$\begin{aligned} V^{\text{hs}} &= -e^2 \sum_{1 \leq i < j \leq N} \ln |z_i - z_j| + \frac{e^2}{2} \alpha \sum_{i=1}^N h(x_i) + \frac{e^2}{2} N \ln \frac{M}{2L} - \frac{e^2}{4} N \alpha h(x_m) \\ &\quad + \frac{e^2}{2} N^2 \ln x_m - \frac{e^2}{4} \alpha^2 \int_1^{x_m} h(x) p'(x) dx \end{aligned} \quad (6.2.165)$$

where we have used the fact that $dS = \pi M^2 x (1 + x^{-1})^4 dx / 2 = \pi M^2 p'(x) dx / 4$, and we have defined

$$\alpha = \frac{\pi n_b M^2}{4}. \quad (6.2.166)$$

Integrating by parts the last term of (6.2.165) and using (6.2.161), we find

$$\begin{aligned} V^{\text{hs}} &= -e^2 \sum_{1 \leq i < j \leq N} \ln |z_i - z_j| + \frac{e^2}{2} \alpha \sum_{i=1}^N h(x_i) + \frac{e^2}{2} N \ln \frac{M}{2L} + \frac{e^2}{2} N^2 \ln x_m \\ &\quad + \frac{e^2}{2} \alpha^2 \int_1^{x_m} \frac{[p(x)]^2}{x} dx - \frac{e^2}{2} N \alpha h(x_m). \end{aligned} \quad (6.2.167)$$

When $\beta e^2 = 2$, the canonical partition function can be written as

$$Z^{\text{hs}} = \frac{1}{\Lambda^{2N}} Z_0^{\text{hs}} \exp(-\beta F_0^{\text{hs}}) \quad (6.2.168)$$

with

$$-\beta F_0^{\text{hs}} = -N \ln \frac{M}{2L} - N^2 \ln x_m - \alpha^2 \int_1^{x_m} \frac{[p(x)]^2}{x} dx + N\alpha h(x_m) \quad (6.2.169)$$

and

$$Z_0^{\text{hs}}(2) = \frac{1}{N!} \int \prod_{i=1}^N dS_i e^{-\alpha h(x_i)} \prod_{1 \leq i < j \leq N} |z_i - z_j|^2. \quad (6.2.170)$$

where $\Lambda = \sqrt{2\pi\beta\hbar^2/m}$ is the de Broglie thermal wavelength. $Z_0(2)$ can be computed using the original method for the OCP in flat space Jancovici [1981b]; Alastuey and Jancovici [1981], which was originally introduced in the context of random matrices Mehta [1991]; Ginibre [1965], and which was presented in section 6.2.1. By expanding the van der Monde determinant $\prod_{i < j} (z_i - z_j)$ and performing the integration over the angles, the partition function can be written as

$$Z_0^{\text{hs}}(2) = \prod_{k=0}^{N-1} \mathcal{B}_N(k), \quad (6.2.171)$$

where

$$\mathcal{B}_N(k) = \int x^{2k} e^{-\alpha h(x)} dS \quad (6.2.172)$$

$$= \frac{\alpha}{n_b} \int_1^{x_m} x^{2k} e^{-\alpha h(x)} p'(x) dx. \quad (6.2.173)$$

In the flat limit $M \rightarrow 0$, we have $x \sim 2r/M$, with r the radial coordinate of flat space \mathbb{R}^2 , and $h(x) \sim p(x) \sim x^2$. Then, \mathcal{B}_N reduces to

$$\mathcal{B}_N(k) \sim \frac{1}{n_b \alpha^k} \gamma(k+1, N) \quad (6.2.174)$$

where $\gamma(k+1, N) = \int_0^N t^k e^{-t} dt$ is the incomplete Gamma function. Replacing into (6.2.171), we recover the partition function (6.2.14) for the OCP in a flat disk of radius R Alastuey and Jancovici [1981]

$$\ln Z^{\text{hs}}(2) = \frac{N}{2} \ln \frac{\pi L^2}{n_b \Lambda^4} + \frac{3N^2}{4} - \frac{N^2}{2} \ln N + \sum_{k=1}^N \ln \gamma(k, N). \quad (6.2.175)$$

Following Jancovici [1981b], we can also find the k -body distribution functions

$$\mathcal{K}_N^{(k)\text{hs}}(\mathbf{q}_1, \dots, \mathbf{q}_k) = \det[\mathcal{K}_N^{\text{hs}}(\mathbf{q}_i, \mathbf{q}_j)]_{(i,j) \in \{1, \dots, k\}^2}, \quad (6.2.176)$$

where $\mathbf{q}_i = (x_i, \varphi_i)$ is the position of the particle i , and

$$\mathcal{K}_N^{\text{hs}}(\mathbf{q}_i, \mathbf{q}_j) = \sum_{k=0}^{N-1} \frac{z_i^k \bar{z}_j^k e^{-\alpha[h(|z_i|) + h(|z_j|)]/2}}{\mathcal{B}_N(k)}. \quad (6.2.177)$$

where $z_k = x_k e^{i\varphi_k}$. In particular, the one-body density is given by

$$n^{\text{hs}}(x) = \mathcal{K}_N(\mathbf{q}, \mathbf{q}) = \sum_{k=0}^{N-1} \frac{x^{2k} e^{-\alpha h(x)}}{\mathcal{B}_N(k)}. \quad (6.2.178)$$

The density shows a peak in the neighborhoods of each boundary, tends to a finite value at the boundary and to the background density far from it, in the bulk. This is shown in Fig. 6.2.2

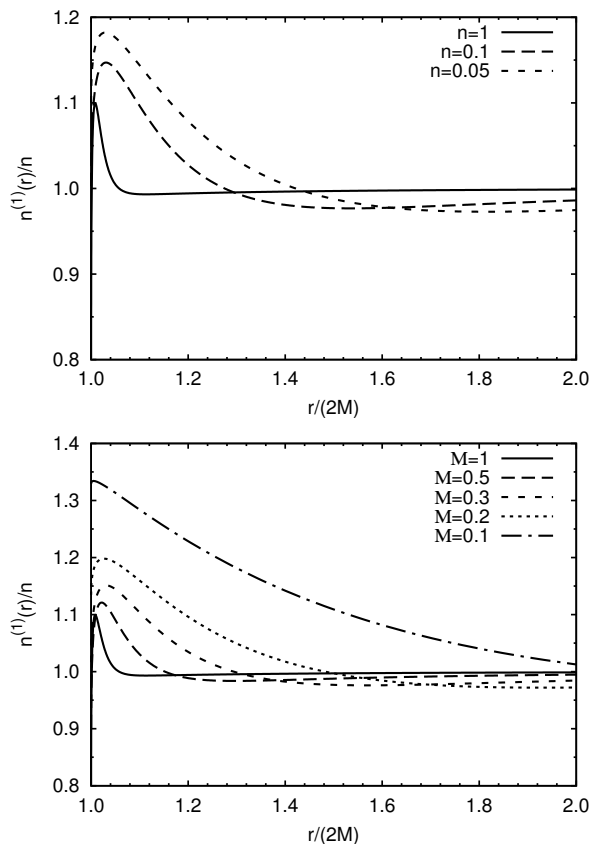


Figure 6.2.2: The one body density $n^{\text{hs}}(r)/n$ of Eq. (6.2.178), for the 2D OCP on just one universe of the surface \mathcal{S} , obtained with $N = 300$. On the left at fixed $M = 1$ and on the right at fixed $n = 1$.

Internal screening

Internal screening means that at equilibrium, a particle of the system is surrounded by a polarization cloud of opposite charge. It is usually expressed in terms of the simplest of the multipolar sum rules [Martin \[1988\]](#): the charge or electroneutrality sum rule, which for the OCP reduces to the relation

$$\int n^{(2)\text{hs}}(\mathbf{q}_1, \mathbf{q}_2) dS_2 = (N - 1)n^{(1)\text{hs}}(\mathbf{q}_1), \quad (6.2.179)$$

This relation is trivially satisfied because of the particular structure (6.2.176) of the correlation function expressed as a determinant of the kernel $\mathcal{K}_N^{\text{hs}}$, and the fact that $\mathcal{K}_N^{\text{hs}}$ is a projector

$$\int dS_3 \mathcal{K}_N^{\text{hs}}(\mathbf{q}_1, \mathbf{q}_3) \mathcal{K}_N^{\text{hs}}(\mathbf{q}_3, \mathbf{q}_2) = \mathcal{K}_N^{\text{hs}}(\mathbf{q}_1, \mathbf{q}_2). \quad (6.2.180)$$

Indeed,

$$\begin{aligned} \int n^{(2)\text{hs}}(\mathbf{q}_1, \mathbf{q}_2) dS_2 &= \int [\mathcal{K}_N^{\text{hs}}(\mathbf{q}_1, \mathbf{q}_1) \mathcal{K}_N^{\text{hs}}(\mathbf{q}_2, \mathbf{q}_2) - \mathcal{K}_N^{\text{hs}}(\mathbf{q}_1, \mathbf{q}_2) \mathcal{K}_N^{\text{hs}}(\mathbf{q}_2, \mathbf{q}_1)] dS_2 \\ &= \int n^{(1)\text{hs}}(\mathbf{q}_1) n^{(1)\text{hs}}(\mathbf{q}_2) dS_2 - \mathcal{K}_N^{\text{hs}}(\mathbf{q}_1, \mathbf{q}_1) \\ &= (N - 1)n^{(1)\text{hs}}(\mathbf{q}_1). \end{aligned} \quad (6.2.181)$$

External screening

External screening means that, at equilibrium, an external charge introduced into the system is surrounded by a polarization cloud of opposite charge. When an external infinitesimal point charge Q is added to the system, it induces a charge density $\rho_Q(\mathbf{q})$. External screening means that

$$\int \rho_Q(\mathbf{q}) dS = -Q. \quad (6.2.182)$$

Using linear response theory we can calculate ρ_Q to first order in Q as follows. Imagine that the charge Q is at \mathbf{q} . Its interaction energy with the system is $\hat{H}_{\text{int}} = Q\hat{\phi}(\mathbf{q})$ where $\hat{\phi}(\mathbf{q})$ is the microscopic electric potential created at \mathbf{q} by the system. Then, the induced charge density at \mathbf{q}' is

$$\rho_Q(\mathbf{q}') = -\beta \langle \hat{\rho}(\mathbf{q}') \hat{H}_{\text{int}} \rangle_T = -\beta Q \langle \hat{\rho}(\mathbf{q}') \hat{\phi}(\mathbf{q}) \rangle_T, \quad (6.2.183)$$

where $\hat{\rho}(\mathbf{q}')$ is the microscopic charge density at \mathbf{q}' , $\langle AB \rangle_T = \langle AB \rangle - \langle A \rangle \langle B \rangle$, and $\langle \dots \rangle$ is the thermal average. Assuming external screening (6.2.182) is satisfied, one obtains the Carnie-Chan sum rule [Martin \[1988\]](#)

$$\beta \int \langle \hat{\rho}(\mathbf{q}') \hat{\phi}(\mathbf{q}) \rangle_T dS' = 1. \quad (6.2.184)$$

Now in a uniform system starting from this sum rule one can derive the second moment Stillinger-Lovett sum rule [Martin \[1988\]](#). This is not possible here because our system is not homogeneous since the curvature is not constant throughout the surface but varies from point to point. If we apply the Laplacian respect to \mathbf{q} to this expression and use Poisson equation

$$\Delta_{\mathbf{q}} \langle \hat{\rho}(\mathbf{q}') \hat{\phi}(\mathbf{q}) \rangle_T = -2\pi \langle \hat{\rho}(\mathbf{q}') \hat{\rho}(\mathbf{q}) \rangle_T, \quad (6.2.185)$$

we find

$$\int \rho_e^{(2)}(\mathbf{q}', \mathbf{q}) dS' = 0 , \quad (6.2.186)$$

where $\rho_e^{(2)}(\mathbf{q}', \mathbf{q}) = \langle \hat{\rho}(\mathbf{q}') \hat{\rho}(\mathbf{q}) \rangle_T$ is the excess pair charge density function. Eq. (6.2.186) is another way of writing the charge sum rule Eq. (6.2.179) in the thermodynamic limit.

The 2D OCP on the whole surface with potential $-\ln(|z - z'|/\sqrt{|zz'|})$

Until now we studied the 2D OCP on just one universe. Let us find the thermodynamic properties of the 2D OCP on the whole surface \mathcal{S} . In this case, we also work in the canonical ensemble with a global neutral system. The position $z_k = x_k e^{i\varphi_k}$ of each particle can be in the range $1/x_m < x_k < x_m$. The total number particles N is now expressed in terms of the function p as $N = 2\alpha p(x_m)$. Similar calculations to the ones of the previous section lead to the following expression for the partition function, when $\beta e^2 = 2$,

$$Z^{\text{ws}} = \frac{1}{\Lambda_{2N}} Z_0^{\text{ws}} \exp(-\beta F_0^{\text{ws}}) \quad (6.2.187)$$

now, with

$$-\beta F_0^{\text{ws}} = Nb_0 + N\alpha h(x_m) - \frac{N^2}{2} \ln x_m - \alpha^2 \int_{1/x_m}^{x_m} \frac{[p(x)]^2}{x} dx \quad (6.2.188)$$

and

$$Z_0^{\text{ws}}(2) = \frac{1}{N!} \prod_{i=1}^N \int dS_i e^{-\alpha h(x_i)} x_i^{-N+1} \prod_{1 \leq i < j \leq N} |z_i - z_j|^2 . \quad (6.2.189)$$

Expanding the van der Monde determinant and performing the angular integrals we find

$$Z_0^{\text{ws}}(2) = \prod_{k=0}^{N-1} \tilde{\mathcal{B}}_N(k) \quad (6.2.190)$$

with

$$\tilde{\mathcal{B}}_N(k) = \int x^{2k-N+1} e^{-\alpha h(x)} dS \quad (6.2.191)$$

$$= \frac{\alpha}{n} \int_{1/x_m}^{x_m} x^{2k-N+1} e^{-\alpha h(x)} p'(x) dx . \quad (6.2.192)$$

The function $\tilde{\mathcal{B}}_N(k)$ is very similar to \mathcal{B}_N , and its asymptotic behavior for large values of N can be obtained by Laplace method as explained in Ref. [Fantoni and Téllez \[2008\]](#).

The one body density for the 2D OCP on the whole manifold is drawn in Fig. 6.2.3. From the figure we can see how the peaks in the neighborhood of the horizon are now disappeared. The density approaches the horizon with zero slope.

The 2D OCP on the half surface with potential $-\ln(|z - z'|/\sqrt{|zz'|})$

In this case, we have $N = \alpha p(x_m)$. In this case the partition function at $\beta e^2 = 2$ is

$$Z^{\text{hs}} = Z_0^{\text{hs}} e^{-\beta F_0^{\text{hs}}} \quad (6.2.193)$$

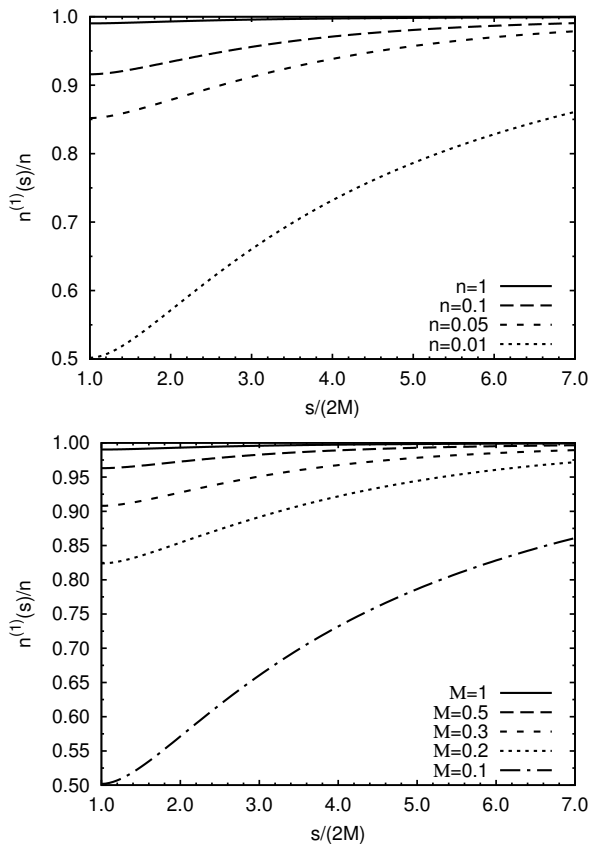


Figure 6.2.3: The one body density $n^{(1)}(s)/n$, where $s = 2Mx$, for the 2D OCP on the whole manifold, obtained using Eq. (6.2.192) with $N = 300$. On the left at fixed $M = 1$ and on the right at fixed $n = 1$.

with

$$-\beta F_0^{\text{hs}} = \alpha^2 p(x_m) h(x_m) - p(x_m)^2 \ln x_m + \int_1^{x_m} \frac{[p(x)]^2}{x} dx - Nb_0 \quad (6.2.194)$$

and

$$Z_0^{\text{hs}}(2) = \prod_{k=0}^{N-1} \hat{\mathcal{B}}_N(k) \quad (6.2.195)$$

with

$$\hat{\mathcal{B}}_N(k) = \frac{\alpha}{n_b} \int_1^{x_m} x^{2k+1} e^{-\alpha h(x)} dx \quad (6.2.196)$$

In Fig. 6.2.4 we compare the one body density obtained in this case with the one of the previous section.

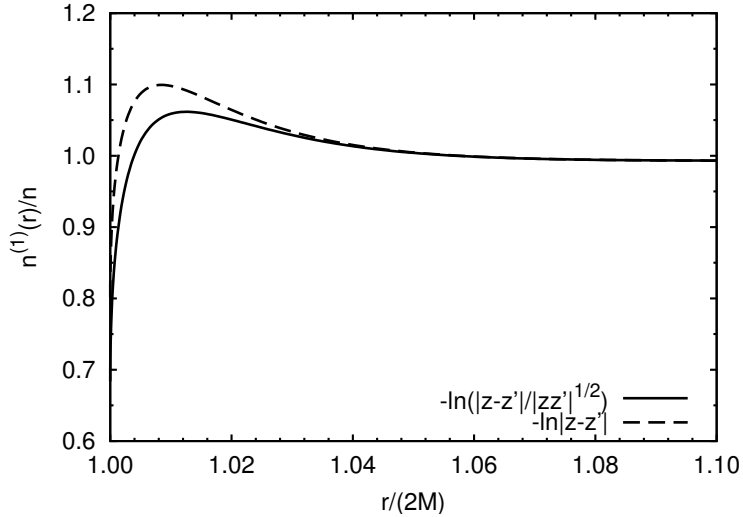


Figure 6.2.4: The one body density $n^{(1)}(r)/n$, for the 2D OCP on just one universe of the surface \mathcal{S} , obtained using both the pair potential $-\ln|z-z'|$ and $-\ln(|z-z'|/\sqrt{|zz'|})$ at fixed $M = n = 1$.

The grounded horizon case

In order to find the partition function for the system in the half space, with a metallic grounded boundary at $x = 1$, when the charges interact through the pair potential of Eq. (6.2.153) it is convenient to work in the grand canonical ensemble instead, and use the techniques developed in Refs. [Forrester \[1985\]](#); [Jancovici and Téllez \[1996\]](#). We consider a system with a fixed background density ρ_b . The fugacity $\zeta = e^{\beta\mu}/\Lambda^2$, where μ is the chemical potential, controls the average number of particles $\langle N \rangle$, and in general the system is non-neutral $\langle N \rangle \neq N_b$, where $N_b = \alpha p(x_m)$. The excess charge is expected to be found near the boundaries at $x = 1$ and $x = x_m$, while in the bulk the system is expected to be locally neutral. In order to avoid the collapse of a particle into the metallic boundary, due to its attraction to the image charges, we confine the particles to be in a disk domain $\tilde{\Omega}_R$, where $x \in [1 + w, x_m]$. We introduced a small gap w between the metallic boundary and the domain containing the particles, the geodesic width of this gap is

$W = \sqrt{\alpha p'(1)/(2\pi n_b)} w$. On the other hand, for simplicity, we consider that the fixed background extends up to the metallic boundary.

In the potential energy of the system (6.1.9) we should add the self energy of each particle, that is due to the fact that each particle polarizes the metallic boundary, creating an induced surface charge density. This self energy is $\frac{e^2}{2} \ln[|x^2 - 1|M/2L]$, where the constant $\ln(M/2L)$ has been added to recover, in the limit $M \rightarrow 0$, the self energy of a charged particle near a plane grounded wall in flat space.

The grand partition function, when $\beta e^2 = 2$, is

$$\Xi(2) = e^{-\beta F_0^{\text{gh}}} \left[1 + \sum_{N=1}^{\infty} \frac{\zeta^N}{N!} \int \prod_{i=1}^N dS_i \prod_{i < j} \left| \frac{z_i - z_j}{1 - z_i \bar{z}_j} \right|^2 \prod_{i=1}^N (|z_i|^2 - 1)^{-1} \prod_{i=1}^N e^{-\alpha[h(x_i) - 2N_b \ln x_i]} \right] \quad (6.2.197)$$

where for $N = 1$ the product $\prod_{i < j}$ must be replaced by 1. The domain of integration for each particle is $\tilde{\Omega}_R$. We have defined a rescaled fugacity $\zeta = 2L\zeta/M$ and

$$-\beta F_0^{\text{gh}} = \alpha N_b h(x_m) - N_b^2 \ln x_m - \alpha^2 \int_1^{x_m} \frac{[p(x)]^2}{x} dx \quad (6.2.198)$$

which is very similar to F_0^{hs} , except that here $N_b = \alpha p(x_m)$ is not equal to N the number of particles.

Let us define a set of reduced complex coordinates $u_i = z_i$ and its corresponding images $u_i^* = 1/\bar{z}_i$. By using Cauchy identity (6.2.95),

$$\det \left(\frac{1}{u_i - u_j^*} \right)_{(i,j) \in \{1, \dots, N\}^2} = (-1)^{N(N-1)/2} \frac{\prod_{i < j} (u_i - u_j)(u_i^* - u_j^*)}{\prod_{i,j} (u_i - u_j^*)}, \quad (6.2.199)$$

the particle-particle interaction and self energy terms can be cast into the form

$$\prod_{i < j} \left| \frac{z_i - z_j}{1 - z_i \bar{z}_j} \right|^2 \prod_{i=1}^N (|z_i|^2 - 1)^{-1} = (-1)^N \det \left(\frac{1}{1 - z_i \bar{z}_j} \right)_{(i,j) \in \{1, \dots, N\}^2}. \quad (6.2.200)$$

The grand canonical partition function is then

$$\Xi(2) = e^{-\beta F_0^{\text{gh}}} \left[1 + \sum_{N=1}^{\infty} \frac{1}{N!} \int \prod_{i=1}^N dS_i \prod_{i=1}^N [-\zeta(x_i)] \det \left(\frac{1}{1 - z_i \bar{z}_j} \right) \right], \quad (6.2.201)$$

with $\zeta(x) = \zeta e^{-\alpha[h(x) - 2N_b \ln x]}$. We now notice that we already found an analogous expression (6.2.97) when studying the pseudosphere. We therefore proceed as we did for that case. For ease of reading we repeat here the relevant steps reducing this expression to a Fredholm determinant Forrester [1985]. Then let us consider the Gaussian partition function

$$Z_0 = \int \mathcal{D}\psi \mathcal{D}\bar{\psi} \exp \left[\int \bar{\psi}(q) A^{-1}(z, \bar{z}') \psi(q') dS dS' \right] \quad (6.2.202)$$

The fields ψ and $\bar{\psi}$ are anticommuting Grassmann variables. The Gaussian measure in (6.2.202) is chosen such that its covariance is equal to

$$\langle \bar{\psi}(q_i) \psi(q_j) \rangle = A(z_i, \bar{z}_j) = \frac{1}{1 - z_i \bar{z}_j} \quad (6.2.203)$$

where $\langle \dots \rangle$ denotes an average taken with the Gaussian weight of (6.2.202). By construction we have

$$Z_0 = \det(A^{-1}) \quad (6.2.204)$$

Let us now consider the following partition function

$$Z = \int \mathcal{D}\psi \mathcal{D}\bar{\psi} \exp \left[\int \bar{\psi}(q) A^{-1}(z, \bar{z}') \psi(q') dS dS' - \int \zeta(x) \bar{\psi}(q) \psi(q) dS \right] \quad (6.2.205)$$

which is equal to

$$Z = \det(A^{-1} - \zeta) \quad (6.2.206)$$

and then

$$\frac{Z}{Z_0} = \det[A(A^{-1} - \zeta)] = \det(1 + K) \quad (6.2.207)$$

where K is an integral operator (with integration measure dS) with kernel

$$K(q, q') = -\zeta(x') A(z, \bar{z}') = -\frac{\zeta(x')}{1 - z\bar{z}'} \quad (6.2.208)$$

Expanding the ratio Z/Z_0 in powers of ζ we have

$$\frac{Z}{Z_0} = 1 + \sum_{N=1}^{\infty} \frac{1}{N!} \int \prod_{i=1}^N dS_i (-1)^N \prod_{i=1}^N \zeta(x_i) \langle \bar{\psi}(q_1) \psi(q_1) \cdots \bar{\psi}(q_N) \psi(q_N) \rangle \quad (6.2.209)$$

Now, using Wick theorem for anticommuting variables Zinn-Justin [1993], we find that

$$\langle \bar{\psi}(q_1) \psi(q_1) \cdots \bar{\psi}(q_N) \psi(q_N) \rangle = \det A(z_i, \bar{z}_j) = \det \left(\frac{1}{1 - z_i \bar{z}_j} \right) \quad (6.2.210)$$

Comparing equations (6.2.209) and (6.2.201) with the help of equation (6.2.210) we conclude that

$$\Xi(2) = e^{-\beta F_0^{\text{gh}}} \frac{Z(2)}{Z_0(2)} = e^{-\beta F_0^{\text{gh}}} \det(1 + K) \quad (6.2.211)$$

The problem of computing the grand canonical partition function has been reduced to finding the eigenvalues λ of the operator K . The eigenvalue problem for K reads

$$-\int_{\tilde{\Omega}_R} \frac{\zeta(x')}{1 - z\bar{z}'} \Phi(x', \varphi') dS' = \lambda \Phi(x, \varphi) \quad (6.2.212)$$

For $\lambda \neq 0$ we notice from equation (6.2.212) that $\Phi(x, \varphi) = \Phi(z)$ is an analytical function of $z = xe^{i\varphi}$ in the region $|z| > 1$. Because of the circular symmetry, it is natural to try $\Phi(z) = \Phi_\ell(z) = z^{-\ell}$ with $\ell \geq 1$ a positive integer. Expanding

$$\frac{1}{1 - z\bar{z}'} = -\sum_{n=1}^{\infty} (z\bar{z}')^{-n} \quad (6.2.213)$$

and replacing $\Phi_\ell(z) = z^{-\ell}$ in equation (6.2.212) we show that Φ_ℓ is indeed an eigenfunction of K with eigenvalue

$$\lambda_\ell = \zeta \mathcal{B}_{N_b}^{\text{gh}}(N_b - \ell) \quad (6.2.214)$$

where

$$\mathcal{B}_{N_b}^{\text{gh}}(k) = \frac{\alpha}{n_b} \int_{1+w}^{x_m} x^{2k} e^{-\alpha h(x)} p'(x) dx \quad (6.2.215)$$

which is very similar to \mathcal{B}_N defined in Eq. (6.2.173), except for the small gap w in the lower limit of integration. So, we arrive to the result for the grand potential

$$\beta\Omega = -\ln \Xi(2) = \beta F_0 - \sum_{\ell=1}^{\infty} \ln \left[1 + \zeta \mathcal{B}_{N_b}^{\text{gh}}(N_b - \ell) \right]. \quad (6.2.216)$$

As usual one can compute the density by doing a functional derivative of the grand potential with respect to a position-dependent fugacity $\zeta(\mathbf{q})$

$$n^{\text{gh}}(\mathbf{q}) = \zeta(\mathbf{q}) \frac{\delta \ln \Xi(2)}{\delta \zeta(\mathbf{q})}. \quad (6.2.217)$$

For the present case of a curved space, we shall understand the functional derivative with the rule $\delta\zeta(\mathbf{q}')/\delta\zeta(\mathbf{q}) = \delta^{(2)}(\mathbf{q}; \mathbf{q}')$ where $\delta^{(2)}(\mathbf{q}; \mathbf{q}') = \delta(x - x')\delta(\varphi - \varphi')/\sqrt{g}$ is the Dirac distribution on the curved surface.

Using a Dirac-like notation, one can formally write

$$\ln \Xi(2) = \text{Tr} \ln(1 + K) - \beta F_0^{\text{gh}} = \int \langle \mathbf{q} | \ln(1 - \zeta(\mathbf{q})A) | \mathbf{q} \rangle dS - \beta F_0^{\text{gh}} \quad (6.2.218)$$

Then, doing the functional derivative (6.2.217), one obtains

$$n^{\text{gh}}(\mathbf{q}) = \zeta \langle \mathbf{q} | (1 + K)^{-1}(-A) | \mathbf{q} \rangle = \zeta \tilde{G}(\mathbf{q}, \mathbf{q}) \quad (6.2.219)$$

where we have defined $\tilde{G}(\mathbf{q}, \mathbf{q}')$ by $\tilde{G} = (1 + K)^{-1}(-A)$. More explicitly, G is the solution of $(1 + K)\tilde{G} = -A$, that is

$$\tilde{G}(\mathbf{q}, \mathbf{q}') - \int_{\tilde{\Omega}_R} \zeta(x'') \frac{\tilde{G}(x'', \mathbf{q}')}{1 - z\bar{z}''} dS'' = -\frac{1}{1 - z\bar{z}'}. \quad (6.2.220)$$

From this integral equation, one can see that $\tilde{G}(\mathbf{q}, \mathbf{q}')$ is an analytical function of z in the region $|z| > 1$. Then, we look for a solution in the form of a Laurent series

$$\tilde{G}(\mathbf{q}, \mathbf{q}') = \sum_{\ell=1}^{\infty} a_{\ell}(\mathbf{r}') z^{-\ell} \quad (6.2.221)$$

into equation (6.2.220) yields

$$\tilde{G}(\mathbf{q}, \mathbf{q}') = \sum_{\ell=1}^{\infty} \frac{(z\bar{z}')^{-\ell}}{1 + \lambda_{\ell}}. \quad (6.2.222)$$

Recalling that $\lambda_{\ell} = \zeta \mathcal{B}_N^{\text{gh}}(N_b - \ell)$, the density is given by

$$n^{\text{gh}}(x) = \zeta \sum_{k=-\infty}^{N_b-1} \frac{x^{2k} e^{-\alpha h(x)}}{1 + \zeta \mathcal{B}_N^{\text{gh}}(k)} \quad (6.2.223)$$

The density reaches the background density far from the boundaries. In this case, the fugacity and the background density control the density profile close to the metallic boundary (horizon). In the bulk and close to the outer hard wall boundary, the density profile is independent of the fugacity. In Fig. 6.2.5 we show the density for various choices of the parameters M, n , and ζ . The figure shows how the density tends to the background density far from the horizon. The value of the density at the horizon depends on n and ζ .

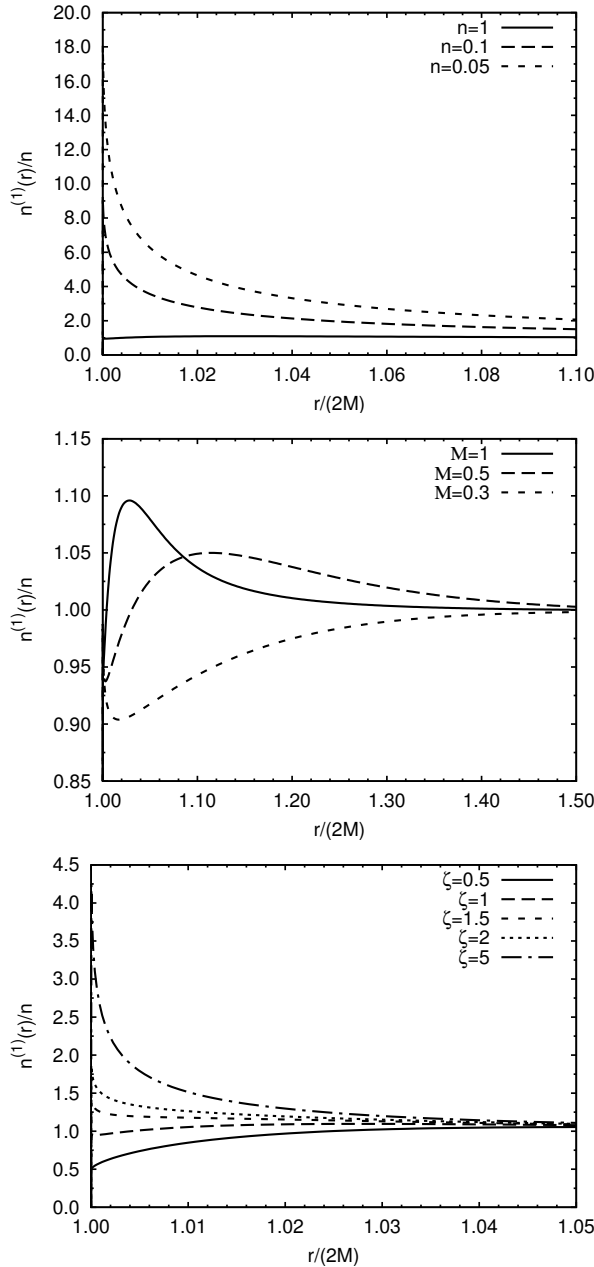


Figure 6.2.5: The one body density $n^{\text{gh}}(r)/n$ obtained truncating the sum of Eq. (6.2.223) after the first 300 terms and choosing $(\sqrt{R} + \sqrt{R - 2M})^2/2M = 10$. On top on the left at fixed $M = \zeta = 1$ and on the right at fixed $n = \zeta = 1$. On the bottom at fixed $M = n = 1$.

6.3 The Two-Component Plasma

A two-component plasma is a neutral mixture of two species of $2N$ point charges of opposite charge $\pm e$.

6.3.1 The plane

We represent the Cartesian components of the position $q = (x, y)$ of a particle by the complex number $z = x + iy$. For a system of N positive charges with complex coordinates u_i and N negative charges with complex coordinates v_i the Boltzmann factor at $\Gamma = \beta e^2 = 2$ is,

$$\begin{aligned} e^{2\sum_{i < j} \left[\ln \frac{|u_i - u_j|}{L} + \ln \frac{|v_i - v_j|}{L} \right] - 2\sum_{i,j} \ln \frac{|u_i - v_j|}{L}} &= L^{2N} \left| \frac{\prod_{i < j} (u_i - u_j)(v_i - v_j)}{\prod_{i,j} (u_i - v_j)} \right|^2 \\ &= L^{2N} \left| \det \left(\frac{1}{u_i - v_j} \right)_{(i,j) \in \{1, \dots, N\}^2} \right|^2, \end{aligned} \quad (6.3.1)$$

where the last equality stems from the Cauchy identity (6.2.95). Following Ref. Cornu and Jancovici [1987], it is convenient to start with a discretized model for which there are no divergencies. Two interwoven sublattices U and V are introduced. The positive (negative) particles sit on the sublattice $U(V)$. Each lattice site is occupied no or one particle. A possible external potential is described by position dependent fugacities $\zeta_+(u_i)$ and $\zeta_-(v_i)$. The the grand partition function reorganized as a sum including only neutral systems is

$$\Xi(2) = 1 + \sum_{N=1}^{\infty} L^{2N} \prod_{i=1}^N \zeta_+(u_i) \zeta_-(v_i) \sum_{\substack{u_1, \dots, u_N \in U \\ v_1, \dots, v_N \in V}} \left| \det \left(\frac{1}{u_i - v_j} \right)_{(i,j) \in \{1, \dots, N\}^2} \right|^2, \quad (6.3.2)$$

where the sums are defined with the prescription that configurations which differ only by a permutation of identical particles are counted only once. This grand partition function is the determinant of an anti-Hermitian matrix \mathbf{M} explicitly shown in Ref. Cornu and Jancovici [1989].

When passing to the continuum limit in the element \mathbf{M}_{ij} one should replace u_i or v_i by z and u_j or v_j by z' , i.e. $i \rightarrow z$ and $j \rightarrow z'$. Each lattice site is characterized by its complex coordinate z and an isospinor which is $(\begin{smallmatrix} 1 \\ 0 \end{smallmatrix})$ if the site belongs to the positive sublattice U and $(\begin{smallmatrix} 0 \\ 1 \end{smallmatrix})$ if it belongs to the negative sublattice V . We then define a matrix \mathbf{M} by

$$\langle z | \mathbf{M} | z' \rangle = \frac{\sigma_x + i\sigma_y}{2} \frac{L}{z - z'} + \frac{\sigma_x - i\sigma_y}{2} \frac{L}{\bar{z} - \bar{z}'}, \quad (6.3.3)$$

where the σ are the 2×2 Pauli matrices operating in the isospinor space.

The matrix \mathbf{M} can be expressed in terms of a simple Dirac operator $\not{d} = \sigma_x \partial_x + \sigma_y \partial_y$ as follows,

$$\langle z | \mathbf{M} | z' \rangle = L(\sigma_x \partial_x + \sigma_y \partial_y) \ln |z - z'|, \quad (6.3.4)$$

and the grand partition function can be rewritten as

$$\begin{aligned} \Xi(2) &= \det \left\{ \mathbf{1} \delta^{(2)}(z; z') + \left[\zeta_+(z) \frac{\mathbf{1} + \sigma_z}{2} + \zeta_-(z) \frac{\mathbf{1} - \sigma_z}{2} \right] \langle z | \mathbf{M} | z' \rangle \right\} \\ &= \det[\mathbf{1} + \mathcal{K}^{-1}], \end{aligned} \quad (6.3.5)$$

where $\mathbf{1}$ is the 2×2 identity matrix and

$$\boldsymbol{\lambda} = \zeta_+ \frac{\mathbf{1} + \boldsymbol{\sigma}_z}{2} + \zeta_- \frac{\mathbf{1} - \boldsymbol{\sigma}_z}{2}, \quad (6.3.6)$$

$$\boldsymbol{\kappa}^{-1} = \boldsymbol{\lambda} \boldsymbol{\mathcal{M}}. \quad (6.3.7)$$

Then, since $\Delta \ln |z| = 2\pi\delta(r)\delta(\varphi)/r = 2\pi\delta(z)$, where ($r = |z|$, $\varphi = \arg z$) are the polar coordinates in the plane, the inverse operator is $\boldsymbol{\kappa} = \boldsymbol{\mathcal{O}}\mathbf{m}^{-1}$, where

$$\mathbf{m}(z) = m_+(z) \frac{\mathbf{1} + \boldsymbol{\sigma}_z}{2} + m_-(z) \frac{\mathbf{1} - \boldsymbol{\sigma}_z}{2}, \quad (6.3.8)$$

$$\boldsymbol{\mathcal{O}} = \boldsymbol{\sigma}_x \partial_x + \boldsymbol{\sigma}_y \partial_y = \hat{\emptyset}. \quad (6.3.9)$$

Here $m_{\pm}(z) = 2\pi L\zeta_{\pm}(z)/S$ are rescaled position dependent fugacities and S is the area per lattice site which appears when the discrete sums are replaced by integrals.

We then find

$$\ln \Xi(2) = \text{Tr} \{ \ln [\mathbf{1} + \boldsymbol{\kappa}^{-1}] \},$$

which expresses the well known equivalence between the 2D OCP at $\Gamma = 2$ and a free Fermi field [Samuel \[1978\]](#).

The one-body densities and n -body truncated densities [Martin \[1988\]](#) can be obtained in the usual way by taking functional derivatives of the logarithm of the grand partition function with respect to the fugacities ζ_{\pm} . Marking the sign of the particle charge at z_i by an index $p_i = \pm$, and defining the matrix

$$R_{p_1 p_2}(z_1, z_2) = \langle z_1 p_1 | \boldsymbol{\kappa}^{-1} (1 + \boldsymbol{\kappa}^{-1})^{-1} | z_2 p_2 \rangle, \quad (6.3.10)$$

it can then be shown [Cornu and Jancovici \[1987, 1989\]](#) that they are given by

$$\rho_{p_1}^{(1)}(z_1) = R_{p_1 p_1}(z_1, z_1), \quad (6.3.11)$$

$$\rho_{p_1 p_2}^{(2)T}(z_1, z_2) = -R_{p_1 p_2}(z_1, z_2) R_{p_2 p_1}(z_2, z_1), \quad (6.3.12)$$

$$\rho_{p_1 p_2, \dots, p_n}^{(n)T}(z_1, z_2, \dots, z_n) = (-)^{n+1} \sum_{(i_1, i_2, \dots, i_n)} R_{p_{i_1} p_{i_2}}(z_{i_1}, z_{i_2}) \cdots R_{p_{i_n} p_{i_1}}(z_{i_n}, z_{i_1}) \quad (6.3.13)$$

where the summation runs over all cycles (i_1, i_2, \dots, i_n) built with $\{1, 2, \dots, n\}$.

Symmetries of Green's function R

Since $\mathbf{m}^\dagger = \mathbf{m}$ and $\boldsymbol{\mathcal{O}}^\dagger = -\boldsymbol{\mathcal{O}}$ we find

$$\overline{R_{p_1 p_2}(z_1, z_2)} = \langle z_2 p_2 | \mathbf{m}(z) (\mathbf{m}(z) - \boldsymbol{\mathcal{O}})^{-1} | z_1 p_1 \rangle. \quad (6.3.14)$$

Expanding in $\boldsymbol{\mathcal{O}}$ and comparing with the definition $R_{p_1 p_2}(z_1, z_2) = \langle z_1 p_1 | \mathbf{m}(z) (\mathbf{m}(z) + \boldsymbol{\mathcal{O}})^{-1} | z_2 p_2 \rangle$ we find

$$\overline{R_{pp}(z_1, z_2)} = R_{pp}(z_2, z_1), \quad (6.3.15)$$

$$\overline{R_{p-p}(z_1, z_2)} = -R_{-pp}(z_2, z_1). \quad (6.3.16)$$

From which also follows that $R_{pp}(z_1, z_1)$ has to be real. If $\zeta_+ = \zeta_-$ then we additionally must have

$$R_{pp}(z_1, z_2) = R_{-p-p}(z_1, z_2). \quad (6.3.17)$$

Two-body truncated correlation functions and perfect screening sum rule

For the two-body truncated correlation functions of Eq. (6.3.12) we then find

$$\rho_{++}^{(2)T}(z_1, z_2) = -|R_{++}(z_1, z_2)|^2, \quad (6.3.18)$$

$$\rho_{+-}^{(2)T}(z_1, z_2) = |R_{+-}(z_1, z_2)|^2. \quad (6.3.19)$$

Notice that the total correlation function for the like particles $h_{++}(z_1, z_2) = \rho_{++}^{(2)T}(z_1, z_2) / \rho_{+}^{(1)}(z_1) \rho_{+}^{(1)}(z_2)$ goes to -1 when the particles coincide $z_1 \rightarrow z_2$ as follows from the structure of Eqs. (6.3.11) and (6.3.12). Moreover the truncated densities of any order has to decay to zero as two groups of particles are infinitely separated. In particular $|R_{++}(z_1, z_2)| = |R_{++}(r_1, r_2, \varphi_2 - \varphi_1)|$ has to decay to zero as $|q_1 - q_2| \rightarrow \infty$.

The perfect screening sum rule has to be satisfied for the symmetric mixture

$$\int [\rho_{+-}^{(2)T}(z_1, z_2) - \rho_{++}^{(2)T}(z_1, z_2)] \sqrt{g_1} dr_1 d\varphi_1 = \rho_{\pm}(z_2), \quad (6.3.20)$$

where g_1 is g calculated on particle 1.

Determination of Green's function R

The Green function matrix \mathbf{R} is the solution of a system of four coupled partial differential equations, namely

$$(\mathbf{1} + \mathcal{K}^{-1}) \mathcal{K} \mathbf{R}(z_1, z_2) = (\mathbf{1} + \mathcal{K}) \mathbf{R}(z_1, z_2) = \mathbf{1} \delta^{(2)}(z_1; z_2) \quad (6.3.21)$$

where $\delta^{(2)}(z_1; z_2) = (\sqrt{g})^{-1} \delta(r - r_0) \delta(\varphi - \varphi_0)$, with $\sqrt{g} = r$ is the Dirac delta function on the plane which we will call $\delta(z_1 - z_2)$ the flat Dirac delta and $\mathbf{1}$ is the 2×2 identity matrix. These coupled equations can be rewritten as follows

$$[\mathcal{O} + \mathbf{m}(z_1)] \mathbf{R}(z_1, z_2) = \mathbf{m}(z_1) \delta^{(2)}(z_1; z_2).$$

If instead of \mathbf{R} one uses $\mathbf{R} = \mathbf{Gm}$, \mathbf{G} satisfies the equation

$$[\mathcal{O} + \mathbf{m}(z_1)] \mathbf{G}(z_1, z_2) = \mathbf{1} \delta^{(2)}(z_1; z_2). \quad (6.3.22)$$

By combining the components of this equation one obtains decoupled equations for G_{++} and G_{--} as follows

$$\{m_+(z_1) + A^\dagger [m_-(z_1)]^{-1} A\} G_{++}(z_1, z_2) = \delta^{(2)}(r_1, \varphi_1; r_2, \varphi_2), \quad (6.3.23)$$

$$\{m_-(z_1) + A [m_+(z_1)]^{-1} A^\dagger\} G_{--}(z_1, z_2) = \delta^{(2)}(r_1, \varphi_1; r_2, \varphi_2), \quad (6.3.24)$$

where $A = \partial_x + i\partial_y$, while

$$G_{-+}(z_1, z_2) = -[m_-(z_1)]^{-1} A G_{++}(z_1, z_2), \quad (6.3.25)$$

$$G_{+-}(z_1, z_2) = +[m_+(z_1)]^{-1} A^\dagger G_{--}(z_1, z_2), \quad (6.3.26)$$

Then Eq. (6.3.54) can be rewritten in Cartesian coordinates as

$$\left[m_+ m_- - \frac{1}{r_1} \partial_{r_1} (r_1 \partial_{r_1}) - \frac{1}{r_1^2} \partial_{\varphi_1}^2 \right] G_{++}(z_1, z_2) = \frac{m_-}{r_1} \delta(r_1 - r_2) \delta(\varphi_1 - \varphi_2). \quad (6.3.27)$$

which, when $m_+(z) = m_-(z) = m$, has the following solution Cornu and Jancovici [1989, 1987]

$$G_{++}(z_1, z_2) = \frac{m}{2\pi} K_0(m|q_1 - q_2|), \quad (6.3.28)$$

$$G_{-+}(z_1, z_2) = \frac{m}{2\pi} \frac{(x_1 - x_2) + i(y_1 - y_2)}{|q_1 - q_2|} K_1(m|q_1 - q_2|), \quad (6.3.29)$$

where K_0 and K_1 are modified Bessel functions. These functions decay at large distances on a characteristic length scale m^{-1} . The n -body truncated densities (6.3.13) are well defined quantities for the point particle system. The two-body truncated densities, for example, have the simple forms

$$\rho_{++}^{(2)T}(r) = -\left(\frac{m^2}{2\pi}\right)^2 K_0^2(mr), \quad (6.3.30)$$

$$\rho_{+-}^{(2)T}(r) = -\left(\frac{m^2}{2\pi}\right)^2 K_1^2(mr). \quad (6.3.31)$$

The one-body densities, however, as given by Eq. (6.3.11), are infinite since $K_0(mr)$ diverges logarithmically as $r \rightarrow 0$. This divergence can be suppressed by a short distance cutoff R . We replace the point particles by small hard discs of diameter R and use a regularized form of Eq. (6.3.11),

$$\rho_{\pm} = \frac{m^2}{2\pi} K_0(mR) \sim \frac{m^2}{2\pi} \left[\ln \frac{2}{mR} - \gamma \right], \quad (6.3.32)$$

where $\gamma = 0.5772$ is Euler's constant. Keeping the point charge expression for the correlation functions for separations larger than R the perfect screening rule (6.3.20) is satisfied.

Integrating $\rho_+ + \rho_- = m\partial(\beta p)/\partial m$, from Eq. (6.3.32) one obtains for the pressure p ,

$$\beta p = \frac{1}{2}(\rho_+ + \rho_-) + \frac{m^2}{4\pi}. \quad (6.3.33)$$

The same result can be obtained by using the regularized form of Eq. (6.3.5). In the limit $mR \rightarrow 0$ one finds the expected result for an ideal gas of collapsed neutral pairs.

6.3.2 The sphere

We consider the stereographic projection Forrester et al. [1992] of the sphere of radius a on the plane tangent to its south pole. The coordinates of the point $p = (x, y)$ stereographic projection of a point $q = (\theta, \varphi)$ of the sphere from the north pole is given in terms of the complex coordinate $z = x + iy$ by $z = 2ae^{i\varphi}\cotan(\theta/2)$. This projection is a conformal transformation. The conformal metric in the new coordinates (x, y) is then

$$g = \begin{pmatrix} e^\omega & 0 \\ 0 & e^\omega \end{pmatrix}, \quad (6.3.34)$$

with the conformal factor given by

$$e^\omega = \sin^2 \frac{\theta}{2} = \frac{1}{1 + (|z|/2a)^2}. \quad (6.3.35)$$

The length r_{ij} (6.2.33) of the chord joining two particles i and j has a simple relation with its projection $|z_i - z_j|$,

$$r_{ij} = e^{\omega_i/2}|z_i - z_j|e^{\omega_j/2} = \sin \frac{\theta_i}{2}|z_i - z_j| \sin \frac{\theta_j}{2}. \quad (6.3.36)$$

We can then follow the same steps as in section 6.3.1 with $z - z'$ replaced by $e^{\omega/2}(z - z')e^{\omega'/2}$. In particular the matrix \mathbf{M} will now become,

$$\langle z | \mathbf{M} | z' \rangle = \frac{\sigma_x + i\sigma_y}{2} \frac{L}{e^{\omega/2}(z - z')e^{\omega'/2}} + \frac{\sigma_x - i\sigma_y}{2} \frac{L}{e^{\omega/2}(\bar{z} - \bar{z}')e^{\omega'/2}}, \quad (6.3.37)$$

In the inverse operator \mathcal{K} we now have

$$\mathcal{O} = e^{-3\omega/2}\mathcal{J}e^{\omega/2} = \mathcal{D}, \quad (6.3.38)$$

since the Dirac delta function on the sphere $\delta^{(2)}(z; z') = e^{-2\omega}\delta(z - z')$ where δ is the flat Dirac delta function.

Thus, the Dirac operator \mathcal{J} in the plane has to be replaced by \mathcal{D} defined by (6.3.38). It turns out that \mathcal{D} is the Dirac operator on the sphere. The Dirac operators in curved spaces have been investigated by many authors.

Thermodynamic properties

If we define $m = 2\pi L\zeta/S$ in terms of the fugacity ζ and the area per lattice site S (a local property of the surface), we have

$$\ln \Xi(2) = \text{Tr} \ln[1 + m\mathcal{D}^{-1}]. \quad (6.3.39)$$

The eigenvalues of \mathcal{D} are Jayewardena [1988] $\pm in/a$ where n is any positive integer, with multiplicity $2n$. Thus the pressure is given by

$$\beta p = \frac{\ln \Xi(2)}{4\pi a^2} = \frac{1}{8\pi a^2} \text{Tr} \ln[1 - m^2 \mathcal{D}^{-2}] = \frac{1}{2\pi a^2} \sum_{n=1}^{\infty} n \ln \left[1 + \frac{m^2 a^2}{n^2} \right], \quad (6.3.40)$$

and the densities are

$$\rho_+ + \rho_- = m \frac{\partial}{\partial m} (\beta p) = \frac{m^2}{4\pi a^2} \text{Tr} \frac{1}{m^2 - \mathcal{D}^2} = \frac{m^2}{\pi} \sum_{n=1}^{\infty} \frac{n}{m^2 a^2 + n^2}. \quad (6.3.41)$$

These pressure and densities are divergent quantities, unless they are regularized by a short distance cutoff, as in the planar case. In the limit $a \rightarrow \infty$, setting $k = n/a$, one retrieves the non-regularized planar results.

Determination of Green's function G

Eq. (6.3.22) now becomes

$$(\mathcal{D} + \mathbf{m})\mathbf{G}(\mathbf{p}, \mathbf{p}') = e^{-2\omega} \mathbf{1} \delta(\mathbf{p} - \mathbf{p}'), \quad (6.3.42)$$

which in terms of

$$\mathbf{G}(\mathbf{p}, \mathbf{p}') = e^{\omega/2} \mathbf{G}(\mathbf{p}, \mathbf{p}') e^{\omega'/2}, \quad (6.3.43)$$

can be rewritten as

$$(\partial + \mathbf{m}e^\omega) \mathbf{G}(p, p') = \mathbf{1}\delta(p - p'). \quad (6.3.44)$$

This equation has a remarkably simple interpretation. $\mathbf{G}(p, p')$ is the Green function of the planar problem with a position dependent fugacity $me^\omega = m/[1 + (r/2a)^2]$. This equation correctly reduces to the flat analogue (6.3.22) in the $a \rightarrow \infty$ limit. Moreover, it admits solutions in term of some hypergeometric functions [Forrester et al. \[1992\]](#).

6.3.3 The pseudosphere

The pseudosphere has already been discussed in section 6.2.4.

We then observe that the curved system can be mapped onto a flat system in the Poincaré disk. The Boltzmann factor gain a multiplicative contribution $[1 - (r_i/2a)^2]$ for each particle and in the computation of the partition function the area element $dS_i = [1 - (r_i/2a)^2]^{-2} dr_i$. Thus, the original system with a constant fugacity ζ maps onto a flat system with a position dependent fugacity $\zeta[1 - (r_i/2a)^2]^{-1}$.

The Dirac operator on the pseudosphere is then,

$$\mathcal{D} = \left(1 - \frac{r^2}{4a^2}\right)^{3/2} \partial \left(1 - \frac{r^2}{4a^2}\right)^{-1/2}. \quad (6.3.45)$$

Determination of Green's function G

Eq. (6.3.43) now becomes,

$$\mathbf{G}(z_1, z_2) = \left(1 - \frac{r_1^2}{4a^2}\right)^{-1/2} \mathbf{G}(z_1, z_2) \left(1 - \frac{r_2^2}{4a^2}\right)^{-1/2}, \quad (6.3.46)$$

and Eq. (6.3.44) becomes,

$$\left[\partial + \frac{\mathbf{m}}{1 - (r/2a)^2}\right] \mathbf{G}(z, z') = \mathbf{1}\delta(z - z'). \quad (6.3.47)$$

where δ is the flat Dirac delta.

Thus \mathbf{G} is the Green function of $\mathcal{D} + \mathbf{m}$ on the pseudosphere. The solution of these coupled partial differential equations can be found in terms of hypergeometric functions [Téllez \[1998\]](#). Again the flat limit results by taking $a \rightarrow \infty$ at a fixed value of m .

Thermodynamic properties

If we define $m = 4\pi a \zeta / S$ in terms of the fugacity ζ and the area per lattice site S (a local property of the surface), we have,

$$\Xi(2) = \det[1 + m\mathcal{D}^{-1}]. \quad (6.3.48)$$

Then the equation of state can be obtained integrating $n = m\partial(\beta p)/\partial m$ where $n = 2\rho_+$. The one-body density ρ_+ can be obtained from Eq. (6.3.11) where $\mathbf{R} = \mathbf{G}\mathbf{m}$. However, the integration cannot be performed in terms of known functions for arbitrary m .

6.3.4 The Flamm paraboloid

Flamm's paraboloid has already been discussed in section 6.2.5.

Half surface with an insulating horizon

When the TCP lives in the half surface with an insulating horizon the Coulomb potential is given by Eq. (6.2.152). We will use $u_i = s_i e^{i\varphi_i}$ and $v_j = s_j e^{i\varphi_j}$ to denote the complex coordinates of the positively and negatively charged particles respectively, where, according to (6.2.136), we set $s = (\sqrt{r} + \sqrt{r - 2M})^2/2M > 1$. Note that the following small M behaviors holds: $s = 2r/M - 2 - M/2r + O(M^2)$ and $\sqrt{g} = rM/2 + O(M^2)$.

The Boltzmann factor at $\Gamma = \beta e^2 = 2$ now becomes

$$\left(\frac{2L}{M}\right)^{2N} \left| \det \left(\frac{1}{u_i - v_j} \right)_{(i,j) \in \{1, \dots, N\}^2} \right|^2, \quad (6.3.49)$$

where L is a length scale.

We can then repeat the analysis of Eqs. (6.3.1)-(6.3.20) noticing that now $\delta^{(2)}(z_1; z_2) = (\sqrt{g})^{-1} \delta(s - s_0) \delta(\varphi - \varphi_0)$ is the Dirac delta function on the curved surface and $\delta(s - s_0) \delta(\varphi - \varphi_0)/s = \delta(z - z_0)$ is the flat Dirac delta. Which gives the following,

$$m_{\pm}(z) = (2\pi L \zeta_{\pm} \sqrt{g}/sS)(2/M)^2, \quad (6.3.50)$$

rescaled position dependent fugacities which tends to $\tilde{m}_{\pm} = 2\pi L \zeta_{\pm}/S$, the ones of the flat system, in the $M \rightarrow 0$ limit. Here S is a local property of the surface independent of its curvature. Moreover Eqs. (6.3.4) and (6.3.9) read

$$\langle z | \mathbf{M}_{hs} | z' \rangle = \frac{2L}{M} (\boldsymbol{\sigma}_x \partial_x + \boldsymbol{\sigma}_y \partial_y) \ln |z - z'|, \quad (6.3.51)$$

$$\mathbf{O}_{hs} = \frac{2}{M} (\boldsymbol{\sigma}_x \partial_x + \boldsymbol{\sigma}_y \partial_y) = \frac{2}{M} \hat{\mathcal{O}}. \quad (6.3.52)$$

Determination of Green's function R

Upon defining $\mathbf{R} = \mathbf{Gm}$, \mathbf{G} satisfies the equation

$$[\mathbf{O} + \mathbf{m}(z_1)] \mathbf{G}(z_1, z_2) = \mathbf{1}(4/M^2) \delta(z_1; z_2). \quad (6.3.53)$$

which in the flat limit $M \rightarrow 0$ reduces to Eq. (6.3.22). Unfortunately this equation does not admit an analytical solution for \mathbf{G} . By combining the components of this equation one obtains decoupled equations for G_{++} and G_{--} as follows

$$\{m_+(z_1) + A^\dagger [m_-(z_1)]^{-1} A\} G_{++}(z_1, z_2) = \frac{4}{M^2} \delta(s_1, \varphi_1; s_2, \varphi_2), \quad (6.3.54)$$

$$\{m_-(z_1) + A [m_+(z_1)]^{-1} A^\dagger\} G_{--}(z_1, z_2) = \frac{4}{M^2} \delta(s_1, \varphi_1; s_2, \varphi_2), \quad (6.3.55)$$

while

$$G_{-+}(z_1, z_2) = -[m_-(z_1)]^{-1} A G_{++}(z_1, z_2), \quad (6.3.56)$$

$$G_{+-}(z_1, z_2) = +[m_+(z_1)]^{-1} A^\dagger G_{--}(z_1, z_2), \quad (6.3.57)$$

Then Eq. (6.3.54) can be rewritten in Cartesian coordinates as

$$\begin{aligned} & \left\{ m_+(z_1)m_-(z_1) - \left(\frac{2}{M}\right)^2 [(\partial_{x_1}^2 + \partial_{y_1}^2) - \right. \\ & \left. \frac{4(-x_1 + iy_1)}{s_1^2(1+s_1)}(\partial_{x_1} + i\partial_{y_1})] \right\} G_{++}(z_1, z_2) = \\ & \left(\frac{2}{M}\right)^4 \frac{\tilde{m}_-\sqrt{g_1}}{s_1^2} \delta(s_1 - s_2) \delta(\varphi_1 - \varphi_2) = \\ & \left(\frac{2}{M}\right)^4 \frac{\tilde{m}_-\sqrt{g_1}}{\sqrt{x_1^2 + y_1^2}} \delta(x_1 - x_2) \delta(y_1 - y_2), \end{aligned} \quad (6.3.58)$$

where $s = \sqrt{x^2 + y^2}$. From the expression of the gradient in polar coordinates follows

$$\begin{cases} \partial_x = \cos \varphi \partial_s - \frac{\sin \varphi}{s} \partial_\varphi, \\ \partial_y = \sin \varphi \partial_s + \frac{\cos \varphi}{s} \partial_\varphi. \end{cases} \quad (6.3.59)$$

Which allows us to rewrite Eq. (6.3.58) in polar coordinates as

$$\begin{aligned} & \left[\tilde{m}_+ \tilde{m}_- \left(1 + \frac{1}{s_1}\right)^8 - \left(\frac{2}{M}\right)^2 \left(\frac{1}{s_1} \partial_{s_1} (s_1 \partial_{s_1}) + \frac{1}{s_1^2} \partial_{\varphi_1}^2 + \right. \right. \\ & \left. \left. \frac{4}{s_1(1+s_1)} \partial_{s_1} + \frac{4i}{s_1^2(1+s_1)} \partial_{\varphi_1} \right) \right] G_{++}(z_1, z_2) = \\ & \left(\frac{2}{M}\right)^4 \frac{\tilde{m}_-\sqrt{g_1}}{s_1^2} \delta(s_1 - s_2) \delta(\varphi_1 - \varphi_2). \end{aligned} \quad (6.3.60)$$

From this equation we immediately see that $G_{++}(z_1, z_2)$ cannot be real. Notice that in the flat limit $M \rightarrow 0$ we have $s \sim 2r/M$ and Eq. (6.3.60) reduces to

$$\begin{aligned} & \left[\tilde{m}_+ \tilde{m}_- - \frac{1}{r_1} \partial_{r_1} (r_1 \partial_{r_1}) - \frac{1}{r_1^2} \partial_{\varphi_1}^2 \right] G_{++}(z_1, z_2) = \\ & \frac{\tilde{m}_-}{r_1} \delta(r_1 - r_2) \delta(\varphi_1 - \varphi_2). \end{aligned} \quad (6.3.61)$$

which, when $\tilde{m}_+ = \tilde{m}_- = \tilde{m}$, has the following well known solution [Cornu and Jancovici \[1989, 1987\]](#)

$$G_{++}(z_1, z_2) = \frac{\tilde{m}}{2\pi} K_0(\tilde{m}|r_1 - r_2|), \quad (6.3.62)$$

where K_0 is a modified Bessel function.

Let us from now on restrict to the case of equal fugacities of the two species. Then $\zeta_- = \zeta_+ = \zeta$ with

$$\tilde{m} = \frac{2\pi L}{S} \zeta = \frac{2\pi L e^{\beta\mu}}{\Lambda^2} = \left(2\pi L \frac{me^2}{4\pi\hbar^2}\right) e^{2\mu/e^2}, \quad (6.3.63)$$

where \hbar is Planck's constant, m is the mass of the particles, and μ the chemical potential. So \tilde{m} has the dimensions of an inverse length. From the symmetry of the problem we can say that

$G_{++} = G_{++}(s_1, s_2; \varphi_1 - \varphi_2)$. We can then express the Green function as the following Fourier series expansion

$$G_{++}(s_1, s_2; \varphi) = \frac{1}{2\pi} \sum_{k=-\infty}^{\infty} g_{++}(s_1, s_2; k) e^{ik\varphi}. \quad (6.3.64)$$

Then, using the expansion of the Dirac delta function, $\sum_k e^{ik\varphi} = 2\pi\delta(\varphi)$, we find that g_{++} , a continuous real function symmetric under exchange of s_1 and s_2 , has to satisfy the following equation

$$\begin{aligned} [Q_0(k, s_1) + Q_1(s_1) \partial_{s_1} + Q_2(s_1) \partial_{s_1}^2] g_{++}(s_1, s_2; k) = \\ \left(\frac{2}{M}\right)^2 \tilde{m} s_1^3 (1 + s_1)^5 \delta(s_1 - s_2), \end{aligned} \quad (6.3.65)$$

where

$$\begin{aligned} Q_0(k, s) &= \tilde{m}^2 (1 + s)^9 + \left(\frac{2}{M}\right)^2 k s^6 (4 + k(1 + s)), \\ Q_1(s) &= -\left(\frac{2}{M}\right)^2 s^7 (5 + s), \\ Q_2(s) &= -\left(\frac{2}{M}\right)^2 s^8 (1 + s). \end{aligned}$$

And the coefficients Q_i are polynomials of up to degree 9.

Method of solution

We start from the homogeneous form of Eq. (6.3.65). We note that, for a given k , the two linearly independent solutions $f_\alpha(s; k)$ and $f_\beta(s; k)$ of this linear homogeneous second order ordinary differential equation are not available in the mathematical literature to the best of our knowledge. Assuming we knew those solutions we would then find the Green function, $g_{++}(s_1, s_2; k)$, writing Jackson [1999]

$$f(t_1, t_2; k) = c_k f_\alpha(s_<; k) f_\beta(s_>; k), \quad (6.3.66)$$

where $s_< = \min(s_1, s_2)$, $s_> = \max(s_1, s_2)$, and f_β has the correct behavior at large s . Then we determine c_k by imposing the kink in f due to the Dirac delta function at $s_1 = s_2$ as follows

$$\partial_{s_1} f(s_1, s_2; k)|_{s_1=s_2+\epsilon} - \partial_{s_1} f(s_1, s_2; k)|_{s_1=s_2-\epsilon} = -\tilde{m} \frac{(1 + s_2)^4}{s_2^5}, \quad (6.3.67)$$

where ϵ is small and positive.

The Green function, symmetric under exchange of s_1 and s_2 , is reconstructed as follows

$$G_{++}(z_1, z_2) = G_{++}(s_1, s_2; \varphi) = \frac{1}{2\pi} \sum_{k=-\infty}^{\infty} c_k f_\alpha(s_<; k) f_\beta(s_>; k) e^{ik\varphi} \quad (6.3.68)$$

Whole surface

On the whole surface, using Eq. (6.2.149) with $b_0 = -\ln(L_0/L)$, we can now write the Boltzmann factor at a coupling constant $\Gamma = \beta e^2 = 2$ as follows,

$$\left| \det \left(\frac{L}{L_0} \frac{\sqrt{|u_j v_j|}}{u_i - v_j} \right)_{(i,j) \in \{1, \dots, N\}^2} \right|^2, \quad (6.3.69)$$

where L_0 is another length scale.

The grand partition function will then be,

$$\Xi(2) = \det [\mathbf{1} + \mathcal{K}_{ws}^{-1}] , \quad (6.3.70)$$

where now Eqs. (6.3.4) and the ones following read,

$$\langle z | \mathcal{M}_{ws} | z' \rangle = \frac{L}{L_0} (\boldsymbol{\sigma}_x \partial_x + \boldsymbol{\sigma}_y \partial_y) \ln |z - z'| , \quad (6.3.71)$$

$$\mathcal{K}_{ws}^{-1} = \boldsymbol{\lambda}_{ws} \mathcal{M}_{ws} , \quad (6.3.72)$$

$$\boldsymbol{\lambda}_{ws} = \zeta_+ |z| \frac{\mathbf{1} + \boldsymbol{\sigma}_z}{2} + \zeta_- |z| \frac{\mathbf{1} - \boldsymbol{\sigma}_z}{2} , \quad (6.3.73)$$

$$\mathbf{K}_{ws} = \mathcal{M}_{ws}^{-1} \boldsymbol{\lambda}_{ws}^{-1} , \quad (6.3.74)$$

$$\boldsymbol{\lambda}_{ws}^{-1} = \frac{1}{\zeta_+ |z|} \frac{\mathbf{1} + \boldsymbol{\sigma}_z}{2} + \frac{1}{\zeta_- |z|} \frac{\mathbf{1} - \boldsymbol{\sigma}_z}{2} . \quad (6.3.75)$$

Introducing position dependent fugacities

$$m_{\pm}(z) = \frac{2\pi(L/L_0)\zeta_{\pm}\sqrt{g}}{Ss} = \tilde{m}_{\pm} \frac{\sqrt{g}}{s} , \quad (6.3.76)$$

where now $\tilde{m}_{\pm}/L_0 \rightarrow \tilde{m}_{\pm}$, we can rewrite

$$\mathcal{K}_{ws} = \frac{\boldsymbol{\sigma}_x + i\boldsymbol{\sigma}_y}{2} a_- + \frac{\boldsymbol{\sigma}_x - i\boldsymbol{\sigma}_y}{2} a_+ , \quad (6.3.77)$$

with the operators

$$a_- = -\frac{\bar{z}}{m_-(z)|z|^3} + \frac{1}{m_-(z)|z|} (\partial_x - i\partial_y) , \quad (6.3.78)$$

$$a_+ = -\frac{z}{m_+(z)|z|^3} + \frac{1}{m_+(z)|z|} (\partial_x + i\partial_y) . \quad (6.3.79)$$

Then the equation for the Green functions are

$$(1 - a_- a_+) R_{++}(z_1, z_2) = \delta^{(2)}(z_1; z_2) , \quad (6.3.80)$$

$$(1 - a_+ a_-) R_{--}(z_1, z_2) = \delta^{(2)}(z_1; z_2) , \quad (6.3.81)$$

$$R_{+-} = -a_- R_{--} , \quad (6.3.82)$$

$$R_{-+} = -a_+ R_{++} . \quad (6.3.83)$$

The equation for R_{++} in the symmetric mixture case is

$$\begin{aligned} & \left[m^2(z_1) - \frac{2}{s_1^4} + \frac{2\partial_{s_1}}{s_1^3} - \frac{\partial_{s_1}^2}{s_1^2} - \frac{-i\partial_{\varphi_1} + \partial_{\varphi_1}^2}{s_1^4} \right] R_{++}(z_1, z_2) = \\ & \frac{m^2(z_1)}{\sqrt{g_1}} \delta(s_1 - s_2) \delta(\varphi_1 - \varphi_2) = \frac{\tilde{m}^2 \sqrt{g_1}}{s_1^2} \delta(s_1 - s_2) \delta(\varphi_1 - \varphi_2) , \end{aligned} \quad (6.3.84)$$

From this equation we see that $R_{++}(z_1, z_2)$ will now be real.

By expanding Eq. (6.3.84) in a Fourier series in the azimuthal angle we now find

$$\begin{aligned} [Q_0(k, s_1) + Q_1(s_1)\partial_{s_1} + Q_2(s_1)\partial_{s_1}^2]g_{++}(s_1, s_2; k) = \\ \left(\frac{M}{2}\right)^2 \tilde{m}s_1^3(1+s_1)^4\delta(s_1 - s_2), \end{aligned} \quad (6.3.85)$$

where

$$\begin{aligned} Q_0(k, s) &= \left(\frac{M}{2}\right)^4 \tilde{m}^2(1+s)^8 + s^4(k^2 - k - 2), \\ Q_1(s) &= 2s^5, \\ Q_2(s) &= -s^6. \end{aligned}$$

And the coefficients Q_i are now polynomials of up to degree 8.

In the flat limit we find, for $G_{++} = R_{++}/\tilde{m}$, the following equation

$$\begin{aligned} \left[\tilde{m}^2 - \frac{2}{r_1^4} + \frac{2\partial_{r_1}}{r_1^3} - \frac{\partial_{r_1}^2}{r_1^2} - \frac{-i\partial_{\varphi_1} + \partial_{\varphi_1}^2}{r_1^4}\right]G_{++}(z_1, z_2) = \\ \frac{\tilde{m}}{r_1}\delta(r_1 - r_2)\delta(\varphi_1 - \varphi_2). \end{aligned} \quad (6.3.86)$$

We then see that we now do not recover the TCP in the plane Cornu and Jancovici [1989, 1987]. This has to be expected because in the flat limit, Flamm's paraboloid reduces to two planes connected by the origin.

After the Fourier expansion of Eq. (6.3.64) we now get

$$[P_0(k, r_1) + P_1(r_1)\partial_{r_1} + P_2(r_1)\partial_{r_1}^2]g_{++}(r_1, r_2; k) = \tilde{m}\delta(r_1 - r_2), \quad (6.3.87)$$

where

$$\begin{aligned} P_0(k, r) &= \tilde{m}^2r + \frac{k^2 - k - 2}{r^3}, \\ P_1(r) &= \frac{2}{r^2}, \\ P_2(r) &= -\frac{1}{r}. \end{aligned}$$

The homogeneous form of this equation admits the following two linearly independent solutions

$$\begin{aligned} f_1(r; -1) &= [D_{-1/2}(i\sqrt{2\tilde{m}r}) + \overline{D_{-1/2}(i\sqrt{2\tilde{m}r})}]/2 \\ f_2(r; -1) &= D_{-1/2}(\sqrt{2\tilde{m}r}) \quad \left. \begin{array}{l} \\ \end{array} \right\} \quad k = -1, \\ f_1(r; 2) &= [D_{-1/2}((-2)^{1/4}\sqrt{\tilde{m}r}) + \overline{D_{-1/2}((-2)^{1/4}\sqrt{\tilde{m}r})}]/2 \\ f_2(r; 2) &= [D_{-1/2}(i(-2)^{1/4}\sqrt{\tilde{m}r}) + \overline{D_{-1/2}(i(-2)^{1/4}\sqrt{\tilde{m}r})}]/2 \quad \left. \begin{array}{l} \\ \end{array} \right\} \quad k = 2, \\ f_1(t; k) &= \sqrt{r}I_{-\sqrt{7-4k+4k^2/4}}(\tilde{m}r^2/2) \\ f_2(t; k) &= \sqrt{r}I_{\sqrt{7-4k+4k^2/4}}(\tilde{m}r^2/2) \quad \left. \begin{array}{l} \\ \end{array} \right\} \quad \text{else}, \end{aligned}$$

where $D_\nu(x)$ are parabolic cylinder functions and $I_\mu(x)$ are the modified Bessel functions of the first kind which diverge as $e^x/\sqrt{2\pi x}$ for large $x \gg |\mu^2 - 1/4|$.

Again we write $g_{++}(r_1, r_2; k) = c_k f_\alpha(r_<; k) f_\beta(r_>; k)$ and impose the kink condition,

$$\partial_{r_1} g_{++}(r_1, r_2; k)|_{r_1=r_2+\epsilon} - \partial_{r_1} g_{++}(r_1, r_2; k)|_{r_1=r_2-\epsilon} = -\tilde{m}r_2 , \quad (6.3.88)$$

to find the c_k . The Green function is then reconstructed using Eq. (6.3.68). But we immediately see that curiously $|G_{++}|$ diverges. Even the structure of the plasma is not well defined in this situation. The collapse of opposite charges at the horizon shrinking to the origin makes the structure of the plasma physically meaningless.

6.4 Conclusions

We presented a review of the analytical exact solutions of the one-component and two-component plasma at the special value of the coupling constant $\Gamma = 2$ in various Riemannian surfaces. Starting from the pioneering work Jancovici [1981b] of Bernard Jancovici in 1981 showing the analytic exact solution for the Jellium on the plane, many other curved surfaces with a conformal metric has been considered. Namely: the cylinder, the sphere, the pseudosphere, and the Flamm paraboloid. From a physical point of view we can see the curvature of the surface as an additional external field acting on the system of charges moving in the corresponding flat space Fantoni [2012b]. Even if this point of view does not take into account the fact that the Coulomb pair potential always reflect its harmonicity inside the given surface. For this reason we did not try a unifying treatment but rather a detailed presentation of each case individually as characteristic of the diverse scenarios which stem out of the various surfaces so far studied in the literature.

In our review we put light on the description of the surface, of the Coulomb potential (and the background potential for the OCP) in the surface, and of the exact solution for the partition function and for the correlation functions. The surfaces considered exhaust to the best of our knowledge all the cases considered in the literature until now. We hope that the review could be a valuable instrument for the reader who needs to have a broad overview on this fascinating exactly solvable fluid model giving the opportunity of finding in one place a self contained summary of various results appeared in the literature at different times and in different journals. We did our best to fill in all the conceptual gaps between the lines so that the reader can follow the various derivations without needing to refer to the original papers which would require an interruption of the reading. This choice required a certain degree of detail which we thought necessary in place of a more conversational presentation.

We decided to leave out the results of taking the thermodynamic limit of the various finite OCP expressions. If the reader desires he can always go back to the original references to find this lacking piece of information. It is well known that Coulomb systems have to exhibit critical finite-size effects Jancovici et al. [1994]. The last surface considered, Flamm's paraboloid, is the only surface of non-constant curvature considered. Nonetheless the one-body density of the plasma is a constant even in this surface in the thermodynamic limit Fantoni [2012b]. On the Flamm paraboloid two different thermodynamic limits can be considered Fantoni and Téllez [2008]: the one where the radius R of the disk confining the plasma is allowed to become very big while keeping the surface hole radius M constant, and the one where both $R \rightarrow \infty$ and $M \rightarrow \infty$ with the ratio R/M kept constant (fixed shape limit). When the horizon shrinks to a point the upper half surface reduces to a plane and one recovers the well known result valid for the one-component plasma on the plane. In the same limit the whole surface reduces to two flat planes connected by a hole at the origin. When only one-half of the surface is occupied by the plasma the density shows a peak in the neighborhoods of each boundary, tends to a finite value at the

boundary and to the background density far from it, in the bulk. In the thermodynamic limit at fixed shape, we find that the density profile is the same as in flat space near a hard wall. In the grounded horizon case the density reaches the background density far from the boundaries. In this case, the fugacity and the background density control the density profile close to the metallic boundary (horizon). In the bulk and close to the outer hard wall boundary, the density profile is independent of the fugacity. In the thermodynamic limit at fixed shape, the density profile is the same as for a flat space.

The importance of having an exactly soluble many-body systems at least at one special temperature relies in the fact that it can serve as a guide for numerical experiments or for approximate solutions of the same system at other temperatures or for different more realistic systems. For example the 2D OCP thermodynamics and structure can now be efficiently expanded in Jack polynomials for even values of the coupling constant Γ L. Šamaj [2004]; Téllez and Forrester [1999, 2012]. And the TCP can be solved in the whole stability range of temperatures Šamaj [2003].

The original 1981 work of Jancovici Jancovici [1981b] has been important for the understanding of the fractional quantum Hall effect in the Laughlin development Laughlin [1983] of a Jastrow correlation factor of the variational wave function of the Landau problem Landau and Lifshitz [1977] for an Hall system in its ground state. We expect the results on the curved surface to be relevant in the developments towards a general relativistic statistical mechanics Rovelli [2013] which is still missing. The main difficulty being the lack of a canonical Hamiltonian in a generally covariant theory where the dynamics is only given relationally rather than in terms of evolution in physical time. And without a Hamiltonian it is difficult to even start doing statistical physics Rovelli [2004].

The quantum 2D OCP does not admit an analytic exact solution but it has been studied through a computer experiment either in its ground state Tanatar and Ceperley [1989]; Kwon et al. [1996] or at finite temperature Militzer et al. [2003]; Ceperley [2004]; Brown et al. [2013a,b].

References

- L. D. Landau and E. M. Lifshitz. *Quantum Mechanics. Non-relativistic Theory*, volume 3. Pergamon Press Ltd, Oxford, 1977. Course of Theoretical Physics.
- D. Mendeleev. The natural system of elements and its application to the indication of the properties of undiscovered elements. *Journal of the Russian Chemical Society*, 3:25, 1871.

Appendices

6.A Electrostatic potential of the background for the OCP in the pseudosphere

In this appendix we give the expression for the electrostatic potential of the background,

$$v_b(q_1) = \int \rho_b G(d_{10}) dS_0 = -n_b e \int_{\Omega} G(d_{10}) dS_0. \quad (6.A.1)$$

The electric potential of the background satisfies equation (6.1.7). Using the coordinates (r, φ) we have,

$$v''_b(r) + \frac{1}{r} v'_b(r) = \alpha_b \frac{4a^2}{(1-r^2)^2}, \quad (6.A.2)$$

where $\alpha_b = -2\pi\rho_b$ and we denote with a prime a derivative with respect to r . This differential equation admits the following solution for v'_b ,

$$\begin{aligned} v'_b(r) &= e^{-\int_{r_0}^r \frac{1}{r'} dr'} \left[v'_b(r_0) + 4a^2 \int_{r_0}^r \frac{\alpha_b}{(1-r'^2)^2} e^{\int_{r_0}^{r'} \frac{1}{s} ds} dr' \right] \\ &= \frac{r_0 v'_b(r_0)}{r} + \frac{4a^2}{r} \int_{r_0}^r \alpha_b \frac{r'}{(1-r'^2)^2} dr'. \end{aligned} \quad (6.A.3)$$

Since the potential has to be chosen continuous at r_0 we set $v'_b(r_0) = 2a^2\alpha_b r_0/(1-r_0^2)$ to find,

$$v'_b(r) = 2a^2\alpha_b \begin{cases} \frac{r}{1-r^2} & r \leq r_0 \\ \frac{r_0^2}{1-r_0^2} \frac{1}{r} & r > r_0 \end{cases},$$

where $r_0 = \tanh(\tau_0/2)$. For the potential inside $\Omega_{a\tau_0}$ we then have,

$$v_b(r) = -\alpha_b a^2 \ln(1-r^2) + \text{constant}, \quad (6.A.4)$$

or using the coordinates (τ, φ) ,

$$v_b(\tau) = -\alpha_b a^2 \ln[1 - \tanh^2(\tau/2)] + \text{constant}. \quad (6.A.5)$$

We need to adjust the additive constant in such a way that this potential at $\tau = \tau_0$ has the

correct value corresponding to the total background charge. We then have,

$$\begin{aligned} \text{constant} &= v_b(0) = -en \int_{\Omega_{a\tau_0}} G(\tau a) dS \\ &= 2\pi a^2 qn \int_0^{\tau_0} \ln[\tanh(\tau/2)] \sinh \tau d\tau \\ &= \alpha_b a^2 [\ln[1 - \tanh^2(\tau_0/2)] + \sinh^2(\tau_0/2) \ln[\tanh^2(\tau_0/2)]]. \end{aligned} \quad (6.A.6)$$

We reach then the following expression for the potential inside $\Omega_{a\tau_0}$,

$$v_b(\tau) = \alpha_b a^2 \left\{ \ln \left[\frac{1 - \tanh^2(\tau_0/2)}{1 - \tanh^2(\tau/2)} \right] + \sinh^2(\tau_0/2) \ln[\tanh^2(\tau_0/2)] \right\}. \quad (6.A.7)$$

The self energy of the background is,

$$\begin{aligned} V_N^0 &= \frac{1}{2} \int_S \rho_b v_b dS \\ &= \frac{1}{2} \rho_b \alpha_b a^2 2\pi a^2 \left\{ \int_0^{\tau_0} \ln \left[\frac{1 - \tanh^2(\tau_0/2)}{1 - \tanh^2(\tau/2)} \right] \sinh \tau d\tau + \right. \\ &\quad \left. \sinh^2(\tau_0/2) \ln[\tanh^2(\tau_0/2)] \int_0^{\tau_0} \sinh \tau d\tau \right\} \\ &= -2a^4 (\pi \rho_b)^2 \{1 - \cosh \tau_0 + 4 \ln[\cosh(\tau_0/2)] + 2 \sinh^4(\tau_0/2) \ln[\tanh^2(\tau_0/2)]\}. \end{aligned} \quad (6.A.8)$$

Notice that if we drop the last term on the right hand side of this equation, i.e. if we adjust the additive constant so that the potential of the background vanishes on the boundary $\partial\Omega_{a\tau_0}$, then in the limit $a \rightarrow \infty$ we recover the self energy of the flat system $N^2 e^2/8$.

6.B The flat limit for the OCP in the pseudosphere

In this Appendix we study the flat limit $a \rightarrow \infty$ of the expressions found for the density in section 6.2.4. We shall study the limit $a \rightarrow \infty$ for a finite system and then take the thermodynamic limit. Since for a large system on the pseudosphere boundary effects are of the same order as bulk effects it is not clear a priori whether computing these two limits in different order would give the same results. In Ref. [Fantoni et al. \[2003\]](#) we show that it does.

For a finite disk of radius $d = a\tau_0$, we have in the flat limit $a \rightarrow \infty$, $d \sim r_0$. In equation (6.2.223), in the limit $a \rightarrow \infty$, the term e^C given by (6.2.91) becomes

$$e^C \sim \left(\frac{r_0^2}{4a^2} \right)^{-N_b} e^{N_b} \quad (6.B.1)$$

where $N_b = \pi n_b r_0^2$ is the number of particles in the background in the flat limit. Since for large a , $t_0 = r_0^2/4a^2$ is small, the incomplete beta function in equation (6.2.223) is

$$B_{t_0}(\ell+1, \alpha) = \int_0^{t_0} e^{(\alpha-1)\ln(1-t)} t^\ell dt \sim \int_0^{t_0} e^{-(\alpha-1)t} t^\ell dt \sim \frac{\gamma(\ell+1, N_b)}{\alpha^{\ell+1}} \quad (6.B.2)$$

Expanding $(1 - (r^2/4a^2))^{4\pi n_b a^2} \sim \exp(-\pi n_b r^2)$ in equation (6.2.223) we finally find the density as a function of the distance r from the center

$$n^{(1)}(r) = n_b e^{-\pi n_b r^2} \sum_{\ell=0}^{\infty} \frac{(\pi n_b r^2)^\ell}{\alpha^{\ell-N_b} N_b^{N_b} e^{-N_b} (n_b/\zeta) + \gamma(\ell+1, N_b)} \quad (6.B.3)$$

When $\alpha \rightarrow \infty$ the terms for $\ell > N_b$ in the sum vanish because $\alpha^{\ell-N_b} \rightarrow \infty$. Then

$$n^{(1)}(r) = n_b e^{-\pi n_b r^2} \sum_{\ell=0}^{E(N_b)-1} \frac{(\pi n_b r^2)^\ell}{\gamma(\ell+1, N_b)} + \Delta n^{(1)}(r) \quad (6.B.4)$$

The first term is the density for a flat OCP in the canonical ensemble with a background with $E(N_b)$ elementary charges ($E(N_b)$ is the integer part of N_b). The second term is a correction due to the inequivalence of the ensembles for finite systems and it depends on whether N_b is an integer or not. If N_b is not an integer

$$\Delta n^{(1)}(r) = n_b \frac{(\pi n_b r^2)^{E(N_b)} e^{-\pi n_b r^2}}{\gamma(E(N_b) + 1, N_b)} \quad (6.B.5)$$

and if N_b is an integer

$$\Delta n^{(1)}(r) = n_b \frac{(\pi n_b r^2)^{N_b} e^{-\pi n_b r^2}}{N_b^{N_b} e^{-N_b} (n_b/\zeta) + \gamma(N_b + 1, N_b)} \quad (6.B.6)$$

In any case in the thermodynamic limit $r_0 \rightarrow \infty$, $N_b \rightarrow \infty$, this term $\Delta n^{(1)}(r)$ vanishes giving the known results for the OCP in a flat space in the canonical ensemble [Jancovici \[1981b,a\]](#). Integrating the profile density (6.B.4) one finds the average number of particles. For a finite system it is interesting to notice that the average total number of particles N is

$$N = E(N_b) + 1 \quad (6.B.7)$$

for N_b not an integer and

$$N = N_b + \frac{1}{1 + \frac{N_b^{N_b} e^{-N_b} n_b}{\zeta \gamma(N_b + 1, N_b)}} \quad (6.B.8)$$

for N_b an integer. In both cases the departure from the neutral case $N = N_b$ is at most of one elementary charge as it was noticed before [Jancovici \[1986, 2003\]](#).

6.C Green's function of Laplace equation in Flamm's paraboloid

In this appendix, we illustrate the calculation of the Green function, for the various situations considered, using the original system of coordinates (r, φ) .

6.C.1 Laplace equation

We first find a solution $v(q)$, not circularly symmetric, to Laplace equation

$$\Delta v = 0, \quad (6.C.1)$$

through the separation of variables technique. We then write

$$v(r, \varphi) = R(r)\phi(\varphi), \quad (6.C.2)$$

so that Laplace equation splits into the two ordinary differential equations

$$\phi'' = -k^2\phi, \quad (6.C.3)$$

$$(r^2 - 2Mr)R'' + (r - M)R' = k^2R. \quad (6.C.4)$$

Taking care of the boundary condition $\phi(\varphi + 2\pi) = \phi(\varphi)$ we find that the first equation admits solution only when k is an integer. The solutions being

$$\phi_n = C_+ e^{in\varphi} + C_- e^{-in\varphi} \quad n = 0, 1, 2, 3, \dots \quad (6.C.5)$$

The solutions of the second equation are

$$R_n = \begin{cases} C_1 \cosh(na) + C_2 \sinh(na) & r > 2M \\ C_1 \cos(na) + C_2 \sin(na) & r < 2M \end{cases} \quad (6.C.6)$$

where

$$a = \begin{cases} 2 \arctan \sqrt{\frac{r}{2M-r}} & r < 2M \\ 2 \ln \frac{\sqrt{r} + \sqrt{r-2M}}{\sqrt{2M}} & r > 2M \end{cases} \quad (6.C.7)$$

Here C_- , C_+ , C_1 , and C_2 are the integration constants.

Then the general solution is real for $C_+ = C_- = C_0$

$$v(r, \varphi) = \sum_{n=0}^{\infty} R_n(r) \phi_n(\varphi) = \begin{cases} C_0 \left(C_1 + C_2 \frac{\sin a}{\cos \varphi - \cos a} \right) & r < 2M \\ C_0 \left(C_1 + C_2 \frac{\sinh a}{\cos \varphi - \cosh a} \right) & r > 2M \end{cases} \quad (6.C.8)$$

If we require the Coulomb potential to go to zero at $r = \infty$ we must choose $C_1 - C_2 = 0$ so that (for $C_0 = 1$)

$$v(r, \varphi) = \begin{cases} 1 + \frac{\sin a}{\cos \varphi - \cos a} & r < 2M \\ 1 + \frac{\sinh a}{\cos \varphi - \cosh a} & r > 2M \end{cases} \quad (6.C.9)$$

Moreover $v(2M, \varphi) = 1$.

6.C.2 Green's function of Laplace equation

We now want to find the Coulomb potential generated at $q = (r, \varphi)$ by a charge at $q_0 = (r_0, \varphi_0)$ with $r_0 > 2M$. We then have to solve the Poisson equation

$$\Delta G(r, \varphi; r_0, \varphi_0) = -2\pi\delta(r - r_0)\delta(\varphi - \varphi_0)/\sqrt{g}, \quad (6.C.10)$$

where $g = \det(g_{\mu\nu}) = r^2/(1 - 2M/r)$. To this end we expand the Green function G and the second delta function in a Fourier series as follows

$$G(r, \varphi; r_0, \varphi_0) = \sum_{n=-\infty}^{\infty} e^{in(\varphi - \varphi_0)} g_n(r, r_0), \quad (6.C.11)$$

$$\delta(\varphi - \varphi_0) = \frac{1}{2\pi} \sum_{n=-\infty}^{\infty} e^{in(\varphi - \varphi_0)}, \quad (6.C.12)$$

to get an ordinary differential equation for g_n

$$\left[\left(1 - \frac{2M}{r} \right) \frac{\partial^2}{\partial r^2} + \left(\frac{1}{r} - \frac{M}{r^2} \right) \frac{\partial}{\partial r} - \frac{n^2}{r^2} \right] g_n(r, r_0) = -\delta(r - r_0)/\sqrt{g}. \quad (6.C.13)$$

To solve this equation we first solve the homogeneous one for $r < r_0$: $g_{n,-}(r, r_0)$ and $r > r_0$: $g_{n,+}(r, r_0)$. This equation was already solved in (6.C.6) for $n \neq 0$

$$g_{n,\pm} = A_{n,\pm}(\sqrt{r} + \sqrt{r - 2M})^{2n} + B_{n,\pm}(\sqrt{r} + \sqrt{r - 2M})^{-2n} \quad (6.C.14)$$

and for $n = 0$ one finds

$$g_{0,\pm} = A_{0,\pm} + B_{0,\pm} \ln(\sqrt{r} + \sqrt{r - 2M}) . \quad (6.C.15)$$

The form of the solution immediately suggest that it is more convenient to work with the variable $x = (\sqrt{r} + \sqrt{r - 2M})^2/(2M)$. For this reason, we introduced this new system of coordinates (x, φ) which is used in the main text.

We then impose the following boundary conditions: (i) the solution at $r = r_0$ should be continuous, (ii) the first derivative at $r = r_0$ should have a jump due to the delta function, (iii) at $r = 2M$ the solution should tend to the solution of the flat system ($M \rightarrow 0$), and (iv) the solution should vanish at $r = \infty$, namely,

$$g_{n,-}(r_0, r_0) = g_{n,+}(r_0, r_0) , \quad (6.C.16)$$

$$g'_{n,-}(r_0, r_0) = g'_{n,+}(r_0, r_0) + \frac{1}{\sqrt{r_0(r_0 - 2M)}} , \quad (6.C.17)$$

$$B_{n,-} = 0 \quad \text{for } n > 0 , \quad A_{n,-} = 0 \quad \text{for } n < 0 , \quad (6.C.18)$$

$$A_{n,+} = 0 \quad \text{for } n > 0 , \quad B_{n,+} = 0 \quad \text{for } n < 0 . \quad (6.C.19)$$

Performing the Fourier series of Eq. (6.C.11) then leads to the following result,

$$G^{\text{hs}}(r, \varphi; r_0, \varphi_0) = -\ln|z - z_0| , \quad (6.C.20)$$

where the complex coordinates $z = (\sqrt{r} + \sqrt{r - 2M})^2 e^{i\varphi}$ and $z_0 = (\sqrt{r_0} + \sqrt{r_0 - 2M})^2 e^{i\varphi_0}$ have been introduced. This solution reduces to the correct Coulomb green function on a plane as $M \rightarrow 0$ and it is the Coulomb potential on one universe of the surface \mathcal{S} .

In order to find the Coulomb potential on the whole surface we can then start from the definition (6.2.125) and go back to the $s = (\sqrt{r} + \sqrt{r - 2M})^2$ variable. If we do this we find as solutions,

$$s_{\pm} = 2M(\sqrt{u^2 + 1} \pm u)^2 , \quad (6.C.21)$$

So that for the Coulomb potential one can choose one of the two definitions depending on which charge is in the upper or lower universe. Neglecting an additive constant we could then set

$$G^{\text{ws}}(u, \varphi; u_0, \varphi_0) = -\ln|z - z_0| , \quad (6.C.22)$$

where $z = (\sqrt{u^2 + 1} + u)^2 e^{i\varphi}$ and $z_0 = (\sqrt{u_0^2 + 1} + u_0)^2 e^{i\varphi_0}$. Actually this potential as it stands does not have the correct symmetry properties under the exchange of the charges from one universe to the other. It can easily be shown that if z is a point in the upper universe then $1/z$ is its symmetric in the lower universe. Then we should expect that if we take $z_0 = 1$ (in the horizon) the potential created at z should be the same as the one created at $1/z$, by symmetry. More generally, one should have $G^{\text{ws}}(z, z_0) = G^{\text{ws}}(1/z, 1/z_0)$.

We then need to revise the calculations of the Coulomb potential. We define the Coulomb potential as the solution of Poisson equation with the boundary condition that the electric field vanishes at infinity (this also happens for a flat space). However it turns out that with this

boundary condition one still have several different solutions, and contrary to the flat case, there are some that differ in more than a constant term. One can see this by solving Poisson equation using the Fourier transform, the constants of integration for the term which does not depend on the angular variable cannot be determined.

However one can impose some additional conditions. For instance we expect the Coulomb potential to be symmetric in the exchange of z and z_0 . The previous solution $-\ln|z - z_0|$ does satisfy this, but it is not the unique solution with this property. Additionally, we can impose the symmetry relation $G^{\text{ws}}(z, z_0) = G^{\text{ws}}(1/z, 1/z_0)$. Then one finds the solution

$$G^{\text{ws}}(z, z_0) = -\ln(|z - z_0|/\sqrt{|zz_0|}) . \quad (6.C.23)$$

We have not verified if this is the only solution (up to a constant) satisfying this symmetry, but we think so. For the whole surface we think that we should use this Coulomb potential instead of the original one, which does not treat on the same foot the upper and lower parts of the surface. However we have noticed that this potential does not reduce to the flat one when $M = 0$, but this is normal: if we work with the whole surface the limit $M = 0$ is not exactly the flat one, it is two flat planes connected by a hole at the origin, this hole modifies the Coulomb potential.

The grounded horizon case

Imagine now that the horizon at $r = 2M$ is a perfect conductor. We then start from

$$g_{n,\pm} = A_{n,\pm} \cosh \left[2n \ln(\sqrt{r} + \sqrt{r - 2M}) \right] + B_{n,\pm} \sinh \left[2n \ln(\sqrt{r} + \sqrt{r - 2M}) \right] . \quad (6.C.24)$$

We fix the four integration constants, for each n , requiring that: (i) the solution at $r = r_0$ should be continuous, (ii) the first derivative at $r = r_0$ should have a jump due to the delta function, (iii) at $r = 2M$ the solution should vanish, and (iv) the solution has the correct behavior at $r = \infty$, namely,

$$g_{n,-}(r_0, r_0) = g_{n,+}(r_0, r_0) , \quad (6.C.25)$$

$$g'_{n,-}(r_0, r_0) = g'_{n,+}(r_0, r_0) + \frac{1}{\sqrt{r_0(r_0 - 2M)}} , \quad (6.C.26)$$

$$g_{n,-}(2M, r_0) = 0 , \quad (6.C.27)$$

$$A_{n,+} = B_{n,+} \quad \text{for } n \geq 0 , \quad A_{n,+} = -B_{n,+} \quad \text{for } n < 0 . \quad (6.C.28)$$

Performing the Fourier series of Eq. (6.C.11) then leads to the following result for $r > r_0$

$$G(r, \varphi; r_0, \varphi_0) = -\ln \sqrt{\frac{1 + c^2 - 2c \cos(\varphi - \varphi_0)}{1 + b^2 - 2b \cos(\varphi - \varphi_0)}} + 2 \ln \frac{\sqrt{r_0} + \sqrt{r_0 - 2M}}{\sqrt{2M}} , \quad (6.C.29)$$

$$b = \left(\frac{\sqrt{r} + \sqrt{r - 2M}}{\sqrt{r_0} + \sqrt{r_0 - 2M}} \right)^2 , \quad (6.C.30)$$

$$c = \left(\frac{(\sqrt{r} + \sqrt{r - 2M})(\sqrt{r_0} + \sqrt{r_0 - 2M})}{2M} \right)^2 , \quad (6.C.31)$$

and the solution for $r < r_0$ is obtained by merely exchanging r with r_0 .

In terms of the complex numbers z and z_0 this can be rewritten as follows

$$G^{\text{gh}}(r, \varphi; r_0, \varphi_0) = -\ln \left| \frac{(z - z_0)/2M}{1 - z\bar{z}_0/4M^2} \right| \quad (6.C.32)$$

where the bar over a complex number indicates its complex conjugate. We will call this the grounded horizon green function. Notice how its shape is the same of the Coulomb potential on the pseudosphere [Fantoni et al. \[2003\]](#) M playing the role of the complex radius. This green function could have been found from the Coulomb one (6.C.20) by using the images method from electrostatics.

6.D The geodesic distance on the Flamm paraboloid

The geodesics are determined by the following equation

$$\ddot{r} + (\Gamma_{rrr}\dot{r}^2 + \Gamma_{r\varphi\varphi}\dot{\varphi}^2)/g_{rr} = 0, \quad (6.D.1)$$

$$\ddot{\varphi} + 2\Gamma_{\varphi\varphi r}\dot{\varphi}\dot{r}/g_{\varphi\varphi} = 0, \quad (6.D.2)$$

where the dot stands for a total differentiation with respect to time and the Christoffel symbols are as follows

$$\Gamma_{rrr} = g_{rr,r}/2, \quad (6.D.3)$$

$$\Gamma_{\varphi\varphi r} = -\Gamma_{r\varphi\varphi} = g_{\varphi\varphi,r}/2. \quad (6.D.4)$$

Here the comma means partial differentiation as usual.

The geodesics equation (6.D.1)-(6.D.2) is then

$$\ddot{r} - \left[\frac{M}{(r-2M)^2} \dot{r}^2 + r\dot{\varphi}^2 \right] \left(1 - \frac{2M}{r} \right) = 0, \quad (6.D.5)$$

$$\ddot{\varphi} + \frac{2}{r}\dot{\varphi}\dot{r} = 0, \quad (6.D.6)$$

The geodesic distance between two points on the surface is

$$d(q_1, q_2) = \int_{t_1}^{t_2} \frac{ds}{dt} dt = \int_{r_1}^{r_2} y dr = \int_{r_1}^{r_2} \sqrt{\frac{1}{1 - \frac{2M}{r}} + r^2 x^2} dr$$

where $x(r) = d\varphi/dr$ and $y(r) = ds/dr$.

Using $\dot{\varphi} = x\dot{r}$ in Eqs. (6.D.5) and (6.D.6) we find

$$x' = \left(\frac{2}{r} + \frac{M}{r^2 - 2Mr} \right) x + r \left(1 - \frac{2M}{r} \right) x^3, \quad (6.D.7)$$

where the prime stands for differentiation with respect to r .

The solution for $x(r)$ and $y(r)$ are as follows

$$x(r) = \pm \sqrt{\frac{15r^3(2M-r)}{r^4(30M^2 - 24Mr + 5r^2) - C}}, \quad (6.D.8)$$

$$y(r) = \sqrt{r^2 x^2 + \frac{r}{r-2M}}, \quad (6.D.9)$$

with C the integration constant, so that,

$$d(q, q_0) = \int_{r_0}^r y(r') dr', \quad (6.D.10)$$

$$\varphi - \varphi_0 = \int_{r_0}^r x(r') dr'. \quad (6.D.11)$$

References

- S. F. Edwards and A. Lenard. Exact Statistical Mechanics of a One Dimensional System with Coulomb Forces. II. The Method of Functional Integration. *J. Math. Phys.*, 3:778, 1961. doi: [10.1063/1.1724281](https://doi.org/10.1063/1.1724281).
- G. Gallavotti, S. Miracle-Sole, and D. Ruelle. Absence of phase transitions in one-dimensional systems with hard cores. *Physics Letters A*, 26:350, 1968. doi: [10.1016/0375-9601\(68\)90367-8](https://doi.org/10.1016/0375-9601(68)90367-8).
- N. N. Greenwood and A. Earnshaw. *Chemistry of the Elements*. Pergamon, 1960. p. 30.
- A. Lenard. Exact Statistical Mechanics of a One Dimensional System with Coulomb Forces. *J. Math. Phys.*, 2:682, 1961. doi: [10.1063/1.1703757](https://doi.org/10.1063/1.1703757).
- L. Pauling. The Nature of the Chemical Bond. IV. The Energy of Single Bonds and the Relative Electronegativity of Atoms. *Journal of the American Chemical Society*, 54:3570, 1932. doi: [10.1021/ja01348a011](https://doi.org/10.1021/ja01348a011).
- L. C. Pauling. *The Nature of the Chemical Bond and the Structure of Molecules and Crystals: an introduction to modern structural chemistry*. Cornell University Press, 1960. pp. 88–107.
- A. M. Salzberg and S. Prager. Equation of State for a Two-Dimensional Electrolyte. *J. Chem. Phys.*, 38:2587, 1963. doi: [10.1063/1.1733553](https://doi.org/10.1063/1.1733553).

Chapter 7

The Electron Gas

A gas of electrons would be thermodynamically unstable if not made electrically neutral by introducing a uniform background of opposite charge which gives rise to a harmonic confining potential to the gas which would otherwise explode to infinity. After all we all live in a neutral world. This simplest model of an electron gas is called the *Jellium* in the quantum regime where the Fermi statistics play a role through the Pauli exclusion principle and a One Component Plasma (OCP) in the opposite classical regime where the statistics reduces to the one of Boltzmann. More complicated albeit more realistic models of an electron gas are obtained by a more detailed description of the neutralizing background. This can for example be described by a system of positive charges (ions) which again make the whole system of charges globally neutral. Therefore one can think of a Two Component Plasma (TCP) or more generally of a multicomponent one. Another important complication consists in describing the charges as not ideally pointwise but with finite dimension. The simplest system of this kind is the *primitive model* which consists of uniformly charged hard spheres of n different species. The spheres belonging to specie $\mu = 1, 2, \dots, n$ have a diameter σ_μ and carry a total charge $z_\mu e$, where e is the elementary charge. The spheres are globally neutral, $\sum_\mu x_\mu z_\mu = 0$, where x_μ is the molar fraction of species μ , and move in a continuum medium of dielectric constant ϵ . One could for example study the restricted case $\sigma_\mu = \sigma$ and $|z_\mu| = z$ for all μ .

These have been historically the first models examined. And for these models there exist few exact analytic results, various approximate analytic or numerical results from integral equations theories (like the Percus-Yevick, the Mean-Spherical-Approximation, the Hyper-Netted-Chain, and many others), and various exact numerical results from Monte Carlo methods. [Pines and Nozières \[1966\]](#); [Feenberg \[1969\]](#); [March and Tosi \[1984\]](#); [Hansen and McDonald \[1986\]](#)

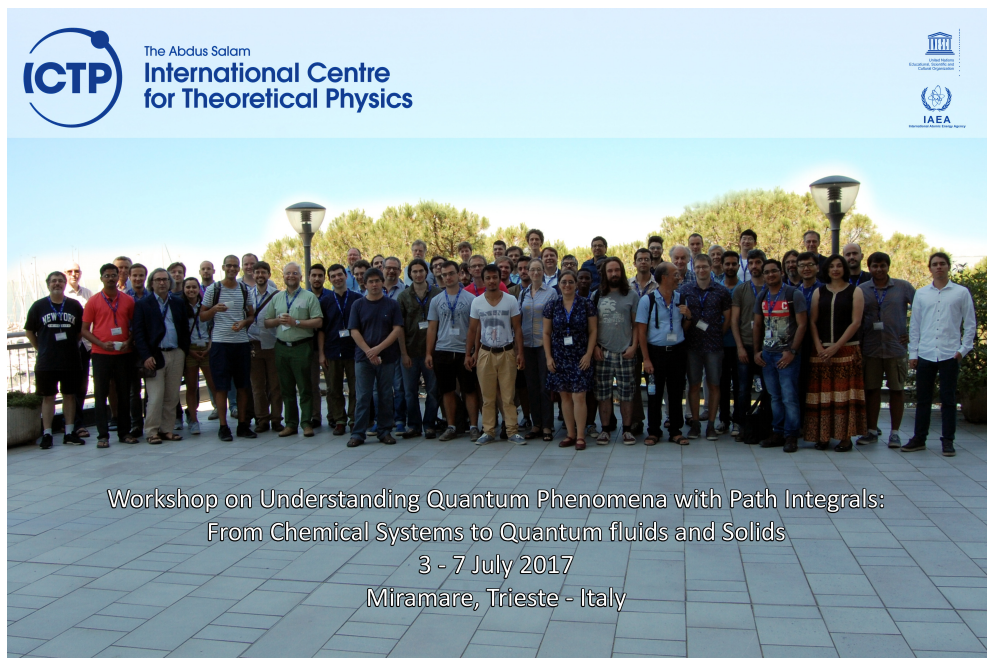
Here we will just mention some of the few exact analytic results. Beginning from the exact solution of the one dimensional OCP of Edwards and Lenard [Fantoni \[2016\]](#) and the TCP of Salzberg and Prager where the chemical bond is analytically seen through the clustering responsible for the molecule formation [Fantoni \[2012\]](#). An interesting exact analytic solution for the two dimensional OCP at a particular value of the coupling constant $\Gamma = \beta e^2 = 2$ with $\beta = 1/k_B T$, k_B Boltzmann constant and T absolute temperature, is available on various surface of constant curvature: The plane [Jancovici \[1981\]](#), the cylinder [Choquard \[1981\]](#), the sphere [Caillo \[1981\]](#), the pseudosphere [Fantoni et al. \[2003\]](#). And on non-constant curvature surfaces like the Flamm's paraboloid [Fantoni and Téllez \[2008\]](#) Is the two dimensional OCP Exactly Solvable? [L. Šamaj \[2004\]](#). These solutions make use of the properties of the Vandermonde determinant. At the same coupling constant a Cauchy identity allows the solution of the TCP.

In the quantum regime we do not know about any analytic exact solution. But the Jellium

has been studied with Monte Carlo methods both in its ground state, at zero temperature, or at finite temperature, through path integral. In this chapter we review some recent and less recent results in these directions on a flat space by David Ceperley and collaborators or on a curved space [Fantoni \[2018, 2023\]](#).

The primitive model in the quantum regime and in two dimensions opens the new exotic field of anyons and *fractional statistics* [Fantoni \[2021\]](#); [Lerda \[1992\]](#). ¹

7.1 The model



The *Jellium* model of [Wigner March and Tosi \[1984\]](#); [Singwi and Tosi \[1981\]](#); [Ichimaru \[1982\]](#); [Martin \[1988\]](#) is an assembly of N_+ spin up pointwise electrons and N_- spin down pointwise electrons of charge e moving in a positive inert background that ensures charge neutrality. The total number of electrons is $N = N_+ + N_-$ and the average particle number density is $n = N/\Omega$, where Ω is the volume of the electron fluid. In the volume Ω there is a uniform neutralizing background with a charge density $\rho_b = -en$. So that the total charge of the system is zero. The fluid polarization is then $\xi = |N_+ - N_-|/N$: $\xi = 0$ in the unpolarized (paramagnetic) case and $\xi = 1$ in the fully polarized (ferromagnetic) case.

Setting lengths in units of $a = (4\pi n/3)^{-1/3}$ and energies in Rydberg's units, $\text{Ry} = \hbar^2/2ma_0^2$,

¹Actually in order to allow for fractional statistics in two dimensions it is sufficient that the particles be impenetrable which may be already assured even by pointwise electrons since the Coulomb repulsion diverges at contact.

where m is the electron mass and $a_0 = \hbar^2/me^2$ is the Bohr radius, the Hamiltonian of Jellium is

$$\mathcal{H} = -\frac{1}{r_s^2} \sum_{i=1}^N \nabla_{r_i}^2 + V(R) , \quad (7.1.1)$$

$$V = \frac{1}{r_s} \left(2 \sum_{i < j} \frac{1}{|r_i - r_j|} + \sum_{i=1}^N r_i^2 + v_0 \right) , \quad (7.1.2)$$

where $R = (r_1, r_2, \dots, r_N)$ with r_i the coordinate of the i th electron, $r_s = a/a_0$, and v_0 a constant containing the self energy of the background.

The kinetic energy scales as $1/r_s^2$ and the potential energy (particle-particle, particle-background, and background-background interaction) scales as $1/r_s$, so for small r_s (high electronic densities), the kinetic energy dominates and the electrons behave like an ideal gas. In the limit of large r_s , the potential energy dominates and the electrons crystallize into a Wigner crystal [Wigner \[1934\]](#). No liquid phase is realizable within this model since the pair-potential has no attractive parts even though a superconducting state [Leggett \[1975\]](#) may still be possible (see chapter 8.9 of Ref. [Giuliani and Vignale \[2005\]](#) and Ref. [Pollock and Ceperley \[1987\]](#)).

The Jellium has been solved either by integral equation theories in its ground state [Singwi et al. \[1968\]](#) or by computer experiments in its ground state [Ceperley and Alder \[1980\]](#) and at finite temperature [Brown et al. \[2013\]](#).

Some details on the linear response theory for the Jellium can be found in appendixes 4 and 5 of Ref. [March and Tosi \[1984\]](#). Some details on the sum rules for the dielectric function can be found in appendix 6 of Ref. [March and Tosi \[1984\]](#). Some details on the moments of density fluctuation spectrum in the plasma can be found in appendix 7 of Ref. [March and Tosi \[1984\]](#). And some details on the Lindhard theory of dynamic screening can be found in appendix 8 of Ref. [March and Tosi \[1984\]](#).

7.1.1 Lindhard theory of static screening in Jellium ground state

Suppose we switch on an appropriately screened test charge potential δV , actually the so called Hartree potential, in a free electron gas.² The Hartree potential $\delta V(r)$ created at a distance r from a static point charge of magnitude e at the origin, should be evaluated self-consistently from the Poisson equation,

$$\nabla^2 \delta V(r) = -4\pi e^2 [\delta(r) + \delta n(r)] , \quad (7.1.3)$$

where $\delta n(r)$ is the change in electronic density induced by the foreign charge. The electron density $n(r)$ may be written as

$$n(r) = 2 \sum_k |\psi_k(r)|^2 , \quad (7.1.4)$$

where $\psi_k(r)$ are single-electron orbitals, the sum over k is restricted to occupied orbitals ($|k| \leq k_F$, where k_F is the Fermi wave vector) and the factor 2 comes from the sum over spin orientations. We must now calculate how the orbitals in the presence of the foreign charge, differ from plane waves $\exp(ik \cdot r)$. We use for this purpose the Schrödinger equation,

$$\nabla^2 \psi_k(r) + [k^2 - \frac{2m}{\hbar^2} \delta V(r)] \psi_k(r) = 0 , \quad (7.1.5)$$

²A brief review of the linear response theory to an external perturbation of the fluid is given in Appendix 7.H.

having imposed that the orbitals reduce to plane waves with energy $\hbar^2 k^2 / (2m)$ at large distance³.

With the aforementioned boundary condition the Schrödinger equation may be converted into an integral equation,

$$\psi_{\mathbf{k}}(\mathbf{r}) = \frac{1}{\sqrt{\Omega}} e^{i\mathbf{k} \cdot \mathbf{r}} + \frac{2m}{\hbar^2} \int G_{\mathbf{k}}(\mathbf{r} - \mathbf{r}') \delta V(\mathbf{r}') \psi_{\mathbf{k}}(\mathbf{r}') d\mathbf{r}' , \quad (7.1.6)$$

with $G_{\mathbf{k}}(\mathbf{r}) = -\exp(i\mathbf{k} \cdot \mathbf{r})/(4\pi r)$ and Ω the volume of the system.

Within linear response theory we can replace $\psi_{\mathbf{k}}(\mathbf{r})$ by $\Omega^{-1/2} \exp(i\mathbf{k} \cdot \mathbf{r})$ inside the integral. This yields

$$\delta n(\mathbf{r}) = -\frac{mk_F^2}{2\pi^3 \hbar^2} \int j_1(2k_F|\mathbf{r} - \mathbf{r}'|) \frac{\delta V(\mathbf{r}')}{|\mathbf{r} - \mathbf{r}'|^2} d\mathbf{r}' , \quad (7.1.7)$$

with $j_1(x)$ being the first-order spherical Bessel function $[\sin(x) - x \cos(x)]/x^2$. Using this result in the Poisson equation we get

$$\nabla^2 \delta V(\mathbf{r}) = -4\pi e^2 \delta(\mathbf{r}) + \frac{2mk_F^2 e^2}{\pi^2 \hbar^2} \int j_1(2k_F|\mathbf{r} - \mathbf{r}'|) \frac{\delta V(\mathbf{r}')}{|\mathbf{r} - \mathbf{r}'|^2} d\mathbf{r}' , \quad (7.1.8)$$

which is easily soluble in Fourier transform. Writing $\delta V(k) = 4\pi e^2/[k^2 \varepsilon(k)]$ we find,

$$\varepsilon(k) = 1 + \frac{2mk_F e^2}{\pi k^2 \hbar^2} \left[1 + \frac{k_F}{k} \left(\frac{k^2}{4k_F^2} - 1 \right) \ln \left| \frac{k - 2k_F}{k + 2k_F} \right| \right] , \quad (7.1.9)$$

which is the static dielectric function in RPA.

For $k \rightarrow 0$ this expression gives $\varepsilon(k) \rightarrow 1 + k_{TF}^2/k^2$ with $k_{TF} = 3\omega_p^2/v_F^2$ (ω_p being the plasma frequency and v_F the Fermi velocity) i.e. the result of the Thomas-Fermi theory. However $\varepsilon(k)$ has a singularity at $k = \pm 2k_F$, where its derivative diverges logarithmically⁴. This singularity in $\delta V(k)$ determines, after Fourier transform, the behavior of $\delta V(r)$ at large r . $\delta V(r)$ turns out to be an oscillating function⁵ rather than a monotonically decreasing function as in the Thomas-Fermi theory. Indeed,

$$\delta V(r) = \int \frac{dk}{(2\pi)^3} \frac{4\pi e^2}{k^2 \varepsilon(k)} e^{ik \cdot r} = \frac{e^2}{i\pi r} \int_{-\infty}^{\infty} dk \frac{e^{ikr}}{k \varepsilon(k)} , \quad (7.1.10)$$

and the integrand has non-analytic behavior at $q = \pm 2k_F$,

$$\left[\frac{1}{k \varepsilon(k)} \right]_{k \rightarrow \pm 2k_F} = -A(k - (\pm)2k_F) \ln |k - (\pm)2k_F| + \text{regular terms} , \quad (7.1.11)$$

with $A = (k_{TF}^2/4k_F^2)/(k_{TF}^2 + 8k_F^2)$. Hence,

$$\begin{aligned} \delta V(r)|_{r \rightarrow \infty} &= -\frac{Ae^2}{i\pi r} \int_{-\infty}^{\infty} dk e^{ikr} [(k - 2k_F) \ln |k - 2k_F| \\ &\quad + (k + 2k_F) \ln |k + 2k_F|] = -2Ae^2 \frac{\cos(2k_F r)}{r^3} . \end{aligned} \quad (7.1.12)$$

³This approach (which lead to the Random-Phase-Approximation, RPA) is approximate insofar as the potential entering the Schrödinger equation has been taken as the Hartree potential, thus neglecting exchange and correlation between an incoming electron and the electronic screening cloud.

⁴The discontinuity in the momentum distribution across the Fermi surface introduces a singularity in elastic scattering processes with momentum transfer equal to $2k_F$.

⁵J. Friedel, *N. Cimento Suppl.* **7**, 287 (1958).

This result is based on a theorem on Fourier transforms⁶, stating that the asymptotic behavior of $\delta V(r)$ is determined by the low- k behavior as well as the singularities of $\delta V(k)$. Obviously, in the present case the asymptotic contribution from the singularities is dominant over the exponential decay of Thomas-Fermi type. The result implies that the screened ion-ion interaction in a metal has oscillatory character and ranges over several shells of neighbors.

7.1.2 Ewald sums

Periodic boundary conditions are necessary for extrapolating results of the finite system to the thermodynamic limit. Suppose the bare pair-potential, in infinite space, is $v(r)$,

$$v(r) = \int \frac{dk}{(2\pi)^3} e^{-ik \cdot r} \tilde{v}(k), \quad \tilde{v}(k) = \int dr e^{ik \cdot r} v(r). \quad (7.1.13)$$

The best pair-potential of the finite system is given by

$$v_I(r) = \sum_{\mathbf{L}} v(|\mathbf{r} + \mathbf{L}|) - \tilde{v}(0)/\Omega. \quad (7.1.14)$$

where the \mathbf{L} sum is over the Bravais lattice of the simulation cell $\mathbf{L} = (m_x L, m_y L, m_z L)$ where m_x, m_y, m_z range over all positive and negative integers and $\Omega = L^3$. We have also added a uniform background of the same density but opposite charge. Converting this to k -space and using the Poisson sum formula we get

$$v_I(r) = \frac{1}{\Omega} \sum'_{\mathbf{k}} \tilde{v}(k) e^{-ik \cdot r}, \quad (7.1.15)$$

where the prime indicates that we omit the $\mathbf{k} = 0$ term; it cancels out with the background. The \mathbf{k} sum is over reciprocal lattice vectors of the simulation box $\mathbf{k}_n = (2\pi n_x/L, 2\pi n_y/L, 2\pi n_z/L)$ where n_x, n_y, n_z range over all positive and negative integers.

Because both sums, Eq. (7.1.14) and Eq. (7.1.15), are so poorly convergent [Allen and Tildesley \[1987\]](#) (see Appendix 7.I) we follow the scheme put forward by [Natoli et al. Natoli and Ceperley \[1995\]](#) for approximating the image potential by a sum in k -space and a sum in r -space,

$$v_a(\mathbf{r}) = \sum_{\mathbf{L}} v_s(|\mathbf{r} + \mathbf{L}|) + \sum_{|\mathbf{k}| \leq k_c} v_l(k) e^{ik \cdot r} - \tilde{v}(0)/\Omega, \quad (7.1.16)$$

where $v_s(r)$ is chosen to vanish smoothly as r approaches r_c , where r_c is less than half of the distance across the simulation box in any direction. If either r_c or k_c go to infinity then $v_a \rightarrow v_I$. [Natoli et al.](#) show that in order to minimize the error in the potential, it is appropriate to minimize $\chi^2 = \int_{\Omega} [v_I(r) - v_a(r)]^2 dr/\Omega$. And choose for $v_s(r)$ an expansion in a fixed number of radial functions. This same technique has also been applied to treat the pseudo-potential described in section 7.2.3.

Now let us work with N particles of charge e in a periodic box and let us compute the total potential energy of the unit cell. Particles i and j are assumed to interact with a potential $e^2 v(r_{ij}) = e^2 v(|\mathbf{r}_i - \mathbf{r}_j|)$. The potential energy for the N particle system is

$$V = \sum_{i < j} e^2 v_I(r_{ij}) + \sum_i e^2 v_M, \quad (7.1.17)$$

⁶M. Lighthill, “Introduction to Fourier Analysis and Generalized Functions” (University Press, Cambridge 1958)

where $v_M = \frac{1}{2} \lim_{r \rightarrow 0} [v_I(r) - v(r)]$ is the interaction of a particle with its own images; it is a Madelung constant [March and Tosi \[1984\]](#) for particle i interacting with the perfect lattice of the simulation cell. If this term were not present, particle i would only see $N - 1$ particles in the surrounding cells instead of N .

7.2 Jellium in its ground state

The ground state properties of Jellium has been for the first time found by Ceperley and Alder [Ceperley and Alder \[1980\]](#) through a diffusion Monte Carlo method [Kolarenc and Mitas \[2011\]](#). Since then better wave-functions and optimization methods have been developed, better schemes to minimize finite-size effect have been devised, and vastly improved computational facilities are available. Today, new modern techniques are available to optimize Slater-Jastrow wave-functions [Foulkes et al. \[2001\]](#) with backflow and three-body correlations [Kwon et al. \[1998\]](#) and Helmann and Feynman (HF) measures [Toulouse et al. \[2007\]](#) to calculate the RDF, particularly the on-top value, which suffers from poor statistical sampling in its conventional histogram implementation. Other useful tools are the twist-averaged boundary conditions [Lin et al. \[2001\]](#) and RPA-based corrections [Chiesa et al. \[2006\]](#) to minimize finite-size effects.

7.2.1 Monte Carlo simulation (Diffusion)

Consider the Schrödinger equation for the many-body wave-function, $\phi(R, t)$ (the wave-function can be assumed to be real, since both the real and imaginary parts of the wave-function separately satisfy the Schrödinger equation), in imaginary time, with a constant shift E_T in the zero of the energy. This is a diffusion equation in a $3N$ -dimensional space [Anderson \[1976\]](#). If E_T is adjusted to be the ground-state energy, E_0 , the asymptotic solution is a steady state solution, corresponding to the ground-state eigenfunction $\phi_0(R)$ (provided $\phi(R, 0)$ is not orthogonal to ϕ_0).

Solving this equation by a random-walk process with branching is inefficient, because the branching rate, which is proportional to the total potential $V(R)$, can diverge to $+\infty$. This leads to large fluctuations in the weights of the diffusers and to slow convergence when calculating averages. However, the fluctuations, and hence the statistical uncertainties, can be greatly reduced [Kalos et al. \[1974\]](#) by the technique of importance sampling [Hammersley and Handscomb \[1964\]](#).

One simply multiplies the Schrödinger equation by a known trial wave-function $\Psi(R)$ that approximate the unknown ground-state wave-function, and rewrites it in terms of a new probability distribution

$$f(R, t) = \phi(R, t)\Psi(R) , \quad (7.2.1)$$

whose normalization is given in Eq. (7.B.1). This leads to the following diffusion equation

$$-\frac{\partial f(R, t)}{\partial t} = -\lambda \nabla^2 f(R, t) + [E_L(R) - E_T]f(R, t) + \lambda \nabla \cdot [f(R, t)\mathbf{F}(R)] . \quad (7.2.2)$$

Here $\lambda = \hbar^2/(2m)$, t is the imaginary time measured in units of \hbar , $E_L(R) = [H\Psi(R)]/\Psi(R)$ is the local energy of the trial wave-function, and

$$\mathbf{F}(R) = \nabla \ln \Psi^2(R) . \quad (7.2.3)$$

The three terms on the right hand side of Eq. (7.2.2) correspond, from left to right, to diffusion, branching, and drifting, respectively.

At sufficiently long times the solution to Eq. (7.2.2) is

$$f(R, t) \approx N_0 \Psi(R) \phi_0(R) \exp[-(E_0 - E_T)t], \quad (7.2.4)$$

where $N_0 = \int \phi_0(R) \phi(R, 0) dR$. If E_T is adjusted to be E_0 , the asymptotic solution is a stationary solution and the average $\langle E_L(R) \rangle_f$ of the local energy over the stationary distribution gives the ground-state energy E_0 . If we set the branching to zero $E_L(R) = E_T$ then this average would be equal to the expectation value $\int \Psi(R) H \Psi(R) dR$, since the stationary solution to Eq. (7.2.2) would then be $f = f_{\text{vmc}} = \Psi^2$. In other words, without branching we would obtain the variational energy of Ψ , rather than E_0 , as in a Variational Monte Carlo (VMC) calculation.

The time evolution of $f(R, t)$ is given by

$$f(R', t + \tau) = \int dR G(R', R; \tau) f(R, t), \quad (7.2.5)$$

where the Green's function $G(R', R; \tau) = \Psi(R') \langle R' | \exp[-\tau(H - E_T)] | R \rangle \Psi^{-1}(R)$ is a transition probability for moving the set of coordinates from R to R' in a time τ . Thus G is a solution of the same differential equation, Eq. (7.2.2), but with the initial condition $G(R', R; 0) = \delta(R' - R)$. For short times τ an approximate solution for G is

$$G(R', R; \tau) = (4\pi\lambda\tau)^{-3N/2} e^{-|R' - R - \lambda\tau\mathbf{F}(R)|^2/4\lambda\tau} e^{-\tau\{(E_L(R) + E_L(R'))/2 - E_T\}} + O(\tau^2). \quad (7.2.6)$$

To compute the ground-state energy and other expectation values, the N -particle distribution function $f(R, t)$ is represented, in diffusion Monte Carlo, by an average over a time series of generations of walkers each of which consists of a fixed number of n_w walkers. A walker is a pair $(R_\alpha, \omega_\alpha)$, $\alpha = 1, 2, \dots, n_w$, with R_α a $3N$ -dimensional particle configuration with statistical weight ω_α . At time t , the walkers represent a random realization of the N -particle distribution, $f(R, t) = \sum_{\alpha=1}^{n_w} \omega_\alpha^t \delta(R - R_\alpha^t)$. The ensemble is initialized with a VMC sample from $f(R, 0) = \Psi^2(R)$, with $\omega_\alpha^0 = 1/n_w$ for all α . Note that if the trial wave-function were the exact ground-state then there would be no branching and it would be sufficient $n_w = 1$. A given walker (R^t, ω^t) is advanced in time (diffusion and drift) as $R^{t+\tau} = R^t + \chi + \lambda\tau\nabla \ln \Psi^2(R^t)$ where χ is a normally distributed random $3N$ -dimensional vector with variance $2\lambda\tau$ and zero mean [Kalos and Whitlock \[1986\]](#). In order to satisfy detailed balance we accept the move with a probability $A(R, R'; \tau) = \min[1, W(R, R')]$, where $W(R, R') = [G(R, R'; \tau)\Psi^2(R')]/[G(R', R; \tau)\Psi^2(R)]$. This step would be unnecessary if G were the exact Green's function, since W would be unity. Finally, the weight ω_α^t is replaced by $\omega_\alpha^{t+\tau} = \omega_\alpha^t \Delta\omega_\alpha^t$ (branching), with $\Delta\omega_\alpha^t = \exp\{-\tau[(E_L(R_\alpha^t) + E_L(R_\alpha^{t+\tau}))/2 - E_T]\}$.

However, for the diffusion interpretation to be valid, f must always be positive, since it is a probability distribution. But we know that the many-fermions wave-function $\phi(R, t)$, being antisymmetric under exchange of a pair of particles of the parallel spins, must have nodes, i.e. points R where it vanishes. In the fixed-nodes approximation one restricts the diffusion process to walkers that do not change the sign of the trial wave-function. One can easily demonstrate that the resulting energy, $\langle E_L(R) \rangle_f$, will be an upper bound to the exact ground-state energy; the best possible upper bound with the given boundary condition [Ceperley \[1991\]](#).

A detailed description of the algorithm used for the DMC calculation can be found in Ref. [Umrigar et al. \[1993\]](#).

7.2.2 Expectation values in DMC

In a DMC calculation there are various different possibilities to measure the expectation value of a physical observable, as for example the RDF. If $\langle \mathcal{O} \rangle_f$ is the measure and $\langle \dots \rangle_f$ the statistical

average over the probability distribution f we will, in the following, use the word *estimator* to indicate the function \mathcal{O} itself, unlike the more common use of the word to indicate the usual Monte Carlo estimator $\sum_{i=1}^N \mathcal{O}_i/N$ of the average, where $\{\mathcal{O}_i\}$ is the set obtained evaluating \mathcal{O} over a finite number N of points distributed according to f . Whereas the average from different estimators must give the same result, the variance, the square of the statistical error, can be different for different estimators.

The local estimator and the extrapolated measure

To obtain ground-state expectation values of quantities \mathcal{O} that do not commute with the Hamiltonian we introduce the local estimator $\mathcal{O}_L(R) = [\mathcal{O}\Psi(R)]/\Psi(R)$ and then compute the average over the DMC walk, the so called mixed measure, $\overline{\mathcal{O}}^{\text{mix}} = \langle \mathcal{O}_L(R) \rangle_f = \int \phi_0(R) \mathcal{O}\Psi(R) dR / \int \phi_0(R) \Psi(R) dR$. This is inevitably biased by the choice of the trial wave-function. A way to remedy to this bias is the use of the forward walking method Liu et al. [1974]; Barnett et al. [1991] or the reptation quantum Monte Carlo method Baroni and Moroni [1999] to reach pure estimates. Otherwise this bias can be made of leading order δ^2 , with $\delta = \phi_0 - \Psi$, introducing the extrapolated measure

$$\overline{\mathcal{O}}^{\text{ext}} = 2\overline{\mathcal{O}}^{\text{mix}} - \overline{\mathcal{O}}^{\text{var}}, \quad (7.2.7)$$

where $\overline{\mathcal{O}}^{\text{var}} = \langle \mathcal{O}_L \rangle_{f_{\text{vmc}}}$ is the variational measure. If the mixed measure equals the variational measure then the trial wave-function has maximum overlap with the ground-state.

The Hellmann and Feynman measure

Toulouse et al. Toulouse et al. [2007]; Assaraf and Caffarel [2003] observed that the zero-variance property of the energy Ceperley and Kalos [1979] can be extended to an arbitrary observable, \mathcal{O} , by expressing it as an energy derivative through the use of the Hellmann-Feynman theorem.

In a DMC calculation the Hellmann-Feynman theorem takes a form different from the one in a VMC calculation. Namely we start with the eigenvalue expression $(H^\lambda - E^\lambda)\Psi^\lambda = 0$ for the ground-state of the perturbed Hamiltonian $H^\lambda = H + \lambda\mathcal{O}$, take the derivative with respect to λ , multiply on the right by the ground-state at $\lambda = 0$, ϕ_0 , and integrate over the particle coordinates to get

$$\int dR \phi_0 (H^\lambda - E^\lambda) \frac{\partial \Psi^\lambda}{\partial \lambda} = \int dR \phi_0 \left(\frac{\partial E^\lambda}{\partial \lambda} - \frac{\partial H^\lambda}{\partial \lambda} \right) \Psi^\lambda. \quad (7.2.8)$$

Then we notice that due to the Hermiticity of the Hamiltonian, at $\lambda = 0$ the left hand side vanishes, so that we get Fantoni [2013]

$$\frac{\int dR \phi_0 \mathcal{O} \Psi^\lambda}{\int dR \phi_0 \Psi^\lambda} \Big|_{\lambda=0} = \frac{\partial E^\lambda}{\partial \lambda} \Big|_{\lambda=0}. \quad (7.2.9)$$

This relation holds only in the $\lambda \rightarrow 0$ limit unlike the more common form Landau and Lifshitz [1977] which holds for any λ . Also it resembles Eq. (3) of Ref. Gaudoin and Pitarke [2007].

Given $E^\lambda = \int dR \phi_0(R) H^\lambda \Psi^\lambda(R) / \int dR \phi_0(R) \Psi^\lambda(R)$ the “Hellmann and Feynman” (HF) measure in a DMC calculation is

$$\overline{\mathcal{O}}^{\text{HF}} = \frac{dE^\lambda}{d\lambda} \Big|_{\lambda=0} \approx \langle \mathcal{O}_L(R) \rangle_f + \langle \Delta \mathcal{O}_L^\alpha(R) \rangle_f + \langle \Delta \mathcal{O}_L^\beta(R) \rangle_f. \quad (7.2.10)$$

The α correction is [Fantoni \[2013\]](#)

$$\Delta\mathcal{O}_L^\alpha(R) = \left[\frac{H\Psi'}{\Psi'} - E_L(R) \right] \frac{\Psi'(R)}{\Psi(R)} . \quad (7.2.11)$$

This expression coincides with Eq. (18) of Ref. [Toulouse et al. \[2007\]](#). In a VMC calculation this term, usually, does not contribute to the average, with respect to $f_{\text{vmc}} = \Psi^2$, due to the Hermiticity of the Hamiltonian. This is of course not true in a DMC calculation. We will then define a Hellmann and Feynman variational (HFv) estimator as $\mathcal{O}^{\text{HFv}} = \mathcal{O}_L(R) + \Delta\mathcal{O}_L^\alpha(R)$. The β correction is [Fantoni \[2013\]](#)

$$\Delta\mathcal{O}_L^\beta(R) = [E_L(R) - E_0] \frac{\Psi'(R)}{\Psi(R)} , \quad (7.2.12)$$

where $E_0 = E^{\lambda=0}$. Which differs from Eq. (19) of Ref. [Toulouse et al. \[2007\]](#) by a factor of one half. This term is necessary in a DMC calculation not to bias the measure. The extrapolated Hellmann and Feynman measure will then be

$$\overline{\mathcal{O}}^{\text{HF-ext}} = 2\overline{\mathcal{O}}^{\text{HF}} - \langle \mathcal{O}^{\text{HFv}} \rangle_{f_{\text{vmc}}} . \quad (7.2.13)$$

Both corrections α and β to the local estimator depends on the auxiliary function, $\Psi' = \partial\Psi^\lambda/\partial\lambda|_{\lambda=0}$. Of course if we had chosen $\Psi^{\lambda=0}$, on the left hand side of Eq. (7.2.10), as the exact ground state wave-function, ϕ_0 , instead of the trial wave-function, then both corrections would have vanished. When the trial wave-function is sufficiently close to the exact ground state function a good approximation to the auxiliary function can be obtained from first order perturbation theory for $\lambda \ll 1$. So the Hellmann and Feynman measure is affected by the new source of bias due to the choice of the auxiliary function independent from the bias due to the choice of the trial wave-function.

It is convenient to rewrite Eqs. (7.2.11) and (7.2.12) in terms of the logarithmic derivative $Q(R) = \Psi'(R)/\Psi(R)$ as follows

$$\Delta\mathcal{O}_L^\alpha(R) = -\frac{1}{r_s^2} \sum_{k=1}^N [\nabla_{r_k}^2 Q(R) + 2v_k(R) \cdot \nabla_{r_k} Q(R)] , \quad (7.2.14)$$

$$\Delta\mathcal{O}_L^\beta(R) = [E_L(R) - E]Q(R) , \quad (7.2.15)$$

where $v_k(R) = \nabla_{r_k} \ln \Psi(R)$ is the drift velocity of the trial wave-function. For each observable a specific form of Q has to be chosen.

7.2.3 Trial wave-function

We chose the trial wave-function of the Bijl-Dingle-Jastrow [Bijl \[1940\]](#); [Dingle \[1949\]](#); [Jastrow \[1955\]](#) or product form

$$\Psi(R) \propto D(R) \exp \left(-\sum_{i < j} u(r_{ij}) \right) . \quad (7.2.16)$$

The function $D(R)$ is the exact wave-function of the non-interacting fermions (the Slater determinant) and serves to give the trial wave-function the desired antisymmetry

$$D(R) = \frac{1}{\sqrt{N_+!}} \det(\varphi_{n,m}^+) \frac{1}{\sqrt{N_-!}} \det(\varphi_{n,m}^-) , \quad (7.2.17)$$

where for the fluid phase $\varphi_{n,m}^\sigma = e^{ik_n \cdot r_m} \delta_{\sigma_m, \sigma} / \sqrt{\Omega}$ with k_n a reciprocal lattice vector of the simulation box such that $|k_n| \leq k_F^\sigma$, σ the z -component of the spin ($\pm 1/2$), r_m the coordinates of particle m , and σ_m its spin z -component. For the unpolarized fluid there are two separate determinants for the spin-up and the spin-down states because the Hamiltonian is spin independent. For the polarized fluid there is a single determinant. For the general case of N_+ spin-up particles the polarization will be $\xi = |N_+ - N_-|/N$ and the Fermi wave-vector for the spin-up (spin-down) particles will be $k_F^\pm = (1 \pm \xi)^{1/3} k_F$ with $k_F = (3\pi^2 n)^{1/3} = (9\pi/4)^{1/3}/(a_0 r_s)$ the Fermi wave-vector of the paramagnetic fluid. On the computer we fill closed shells so that N_σ is always odd. We only store k_n for each pair $(k_n, -k_n)$ and use sines and cosines instead of $\exp(ik_n \cdot r_i)$ and $\exp(-ik_n \cdot r_j)$.

The second factor (the Jastrow factor) includes in an approximate way the effects of particle correlations, through the “pseudo-potential”, $u(r)$, which is repulsive.

In the crystal phase, the orbitals are Gaussians centered around body-centered-cubic lattice sites with a width chosen variationally.

The pseudo-potential

Here we will consider a system where the particles interact with a bare potential

$$v_\mu(r) = \frac{\text{erf}(\mu r)}{r}, \quad (7.2.18)$$

whose Fourier transform is

$$\tilde{v}_\mu(k) = \frac{4\pi}{k^2} e^{-k^2/4\mu^2}, \quad (7.2.19)$$

so that for $\mu \rightarrow \infty$ we recover the Jellium and in the opposite limit $\mu \rightarrow 0$ we recover the non-interacting electron gas.

Neglecting the cross term between the Jastrow and the Slater determinant in Eq. (7.B.6) (third term) and the Madelung constant, the variational energy per particle can be approximated as follows,

$$\begin{aligned} e_V &= \frac{\langle E_L(R) \rangle_f}{N} = \frac{\int \Psi(R) H \Psi(R) dR}{N} \approx e_F + \frac{1}{2\Omega} \sum_k' [e^2 \tilde{v}_\mu(k) - 2\lambda k^2 \tilde{u}(k)] [S(k) - 1] + \\ &\quad \frac{1}{N\Omega^2} \sum_{k,k'}' \lambda \mathbf{k} \cdot \mathbf{k}' \tilde{u}(k) \tilde{u}(k') \langle \rho_{\mathbf{k}+\mathbf{k}'} \rho_{-\mathbf{k}-\mathbf{k}'} \rangle_f + \dots, \end{aligned} \quad (7.2.20)$$

where $e_F = (3/5)\lambda \sum_\sigma N_\sigma (k_F^\sigma)^2 / N$ is the non-interacting fermions energy per particle, $\tilde{u}(k)$ is the Fourier transform of the pseudo-potential $u(r)$, $\tilde{v}_\mu(k) = 4\pi \exp(-k^2/4\mu^2)/k^2$ is the Fourier transform of the bare pair-potential, $S(k)$ is the static structure factor for a given $u(r)$ (see Sec. 7.2.4), $\rho_k = \sum_{i=1}^N \exp(i\mathbf{k} \cdot \mathbf{r}_i)$ is the Fourier transform of the total number density $\rho(\mathbf{r}) = \sum_i \delta(\mathbf{r} - \mathbf{r}_i)$, and the trailing dots stand for the additional terms coming from the exclusion of the $j = k$ term in the last term of Eq. (7.B.6). Next we make the Random-Phase-Approximation Feynman [1972] and we keep only the terms with $\mathbf{k} + \mathbf{k}' = \mathbf{0}$ in the last term. This gives

$$e_V \approx e_F + \frac{1}{2\Omega} \sum_k' \left\{ [e^2 \tilde{v}_\mu(k) - 2\lambda k^2 \tilde{u}(k)] [S(k) - 1] - 2n\lambda [k \tilde{u}(k)]^2 S(k) \right\} + \dots. \quad (7.2.21)$$

In the limit $k \rightarrow 0$ we have to cancel the Coulomb singularity and we get $\tilde{u}^2(k) = me^2\tilde{v}_\mu(k)/(\hbar^2 nk^2) \simeq [(4\pi e^2/k^2)/(\hbar\omega_p)]^2$ (where $\omega_p = \sqrt{4\pi ne^2/m}$ is the plasmon frequency) or in adimensional units

$$\tilde{u}(k) = \sqrt{\frac{r_s}{3}} \frac{4\pi}{k^2}, \quad \text{small } k. \quad (7.2.22)$$

This determines the correct behavior of $\tilde{u}(k)$ as $k \rightarrow 0$ or the long range behavior of $u(r)$

$$u(r) = \sqrt{\frac{r_s}{3}} \frac{1}{r}, \quad \text{large } r. \quad (7.2.23)$$

Now to construct the approximate pseudo-potential, we start from the expression

$$\epsilon = e_F + \frac{1}{2\Omega} \sum_k' [e^2\tilde{v}_\mu(k) - \mathcal{A}\lambda k^2\tilde{u}(k)][S(k) - 1], \quad (7.2.24)$$

and use the following perturbation approximation, for how $S(k)$ depends on $\tilde{u}(k)$ Gaskell [1961, 1962],

$$\frac{1}{S(k)} = \frac{1}{S^x(k)} + \mathcal{B}n\tilde{u}(k), \quad (7.2.25)$$

where \mathcal{A} and \mathcal{B} are constant to be determined and $S^x(k)$ the structure factor for the non-interacting fermions (see Eq. (7.D.5)), which is $S^x = \sum_\sigma S_{\sigma,\sigma}^x$ with

$$S_{\sigma,\sigma}^x(k) = \begin{cases} \frac{n_\sigma}{n} \frac{y_\sigma}{2} (3 - y_\sigma^2) & y_\sigma < 1 \\ \frac{n_\sigma}{n} & \text{else} \end{cases} \quad (7.2.26)$$

where $n_\sigma = N_\sigma/\Omega$ and $y_\sigma = k/(2k_F^\sigma)$.

Minimizing ϵ with respect to $u(k)$, we obtain Ceperley [2004]

$$\mathcal{B}n\tilde{u}(k) = -\frac{1}{S^x(k)} + \left[\frac{1}{S^x(k)} + \frac{\mathcal{B}ne^2\tilde{v}_\mu(k)}{\lambda\mathcal{A}k^2} \right]^{1/2}, \quad (7.2.27)$$

This form is optimal at both long and short distances but not necessarily in between. In particular, for any value of ξ , the small k behavior of $\tilde{u}(k)$ is $\sqrt{2r_s/3\mathcal{A}\mathcal{B}(4\pi/k^2)}$ which means that

$$u(r) = \sqrt{\frac{2r_s}{3\mathcal{A}\mathcal{B}}} \frac{1}{r}, \quad \text{large } r. \quad (7.2.28)$$

The large k behavior of $\tilde{u}(k)$ is $(r_s/\mathcal{A})\tilde{v}_\mu(k)/k^2$, for any value of ξ , which in r space translates into

$$\frac{du(r)}{dr} \Big|_{r=0} = \begin{cases} -\frac{r_s}{2\mathcal{A}} & \mu \rightarrow \infty \\ 0 & \mu \text{ finite} \end{cases} \quad (7.2.29)$$

In order to satisfy the cusp condition for particles of antiparallel spins (any reasonable pseudo-potential has to obey to the cusp conditions (see Ref. Foulkes et al. [2001] Section IVF) which prevent the local energy from diverging whenever any two electrons ($\mu = \infty$) come together) we

need to choose $\mathcal{A} = 1$, then the correct behavior at large r (7.2.22) is obtained fixing $\mathcal{B} = 2$ ⁷. We will call this Jastrow \mathcal{J}_1 in the following.

It turns out that, at small μ , but not for the Coulomb case, a better choice is given by Ceperley [1978]

$$2n\tilde{u}(k) = -\frac{1}{S^x(k)} + \left[\left(\frac{1}{S^x(k)} \right)^2 + \frac{2ne^2\tilde{v}_\mu(k)}{\lambda k^2} \right]^{1/2}, \quad (7.2.30)$$

which still has the correct long (7.2.28) and short (7.2.29) range behaviors. We will call this Jastrow \mathcal{J}_2 in the following. This is expected since, differently from \mathcal{J}_1 , \mathcal{J}_2 satisfies the additional exact requirement $\lim_{\mu \rightarrow 0} u(r) = 0$, as immediately follows from the definition (7.2.30). Then at small μ (and any r_s), the trial wave-function is expected to be very close to the stationary solution of the diffusion problem.

The backflow and three-body correlations

As shown in Appendix 7.B, the trial wave-function of Eq. (7.2.16) can be further improved by adding three-body (3B) and backflow (BF) correlations Kwon et al. [1993, 1998] as follows

$$\Psi(R) = \tilde{D}(R) \exp \left[- \sum_{i < j} \tilde{u}(r_{ij}) - \sum_{l=1}^N \mathbf{G}(l) \cdot \mathbf{G}(l) \right]. \quad (7.2.31)$$

Here

$$\tilde{D}(R) = \frac{1}{\sqrt{N_+!}} \det(\tilde{\varphi}_{n,m}^+) \frac{1}{\sqrt{N_-!}} \det(\tilde{\varphi}_{n,m}^-), \quad (7.2.32)$$

with $\tilde{\varphi}_{n,m}^\sigma = e^{ik_n \cdot x_m} \delta_{\sigma_m, \sigma} / \sqrt{\Omega}$ and x_m quasi-particle coordinates defined as

$$x_i = r_i + \sum_{j \neq i}^N \eta(r_{ij})(r_i - r_j). \quad (7.2.33)$$

The displacement of the quasi-particle coordinates x_i from the real coordinate r_i incorporates effects of hydrodynamic backflow Feynman and Cohen [1956], and changes the nodes of the trial wave-function. The backflow correlation function $\eta(r)$, is parametrized as Kwon et al. [1998]

$$\eta(r) = \lambda_B \frac{1 + s_B r}{r_B + w_B r + r^4}, \quad (7.2.34)$$

which has the long-range behavior $\sim 1/r^3$.

Three-body correlations are included through the vector functions

$$\mathbf{G}(i) = \sum_{j \neq i}^N \xi(r_{ij})(r_i - r_j). \quad (7.2.35)$$

⁷Note that the probability distribution in a variational calculation is (from Eq. (7.2.16)) $\Psi^2(R) \propto D^2(R) \exp[-2U(R)]$ with $U(R) = \sum_{i < j} u(r_{ij})$. Then if one formally writes $D^2(R) = \exp[-2W(R)]$, Ψ^2 becomes the probability distribution for a classical fluid with potential $W + U$ at an inverse temperature $\beta = 2$. Then one sees that with the choice $\mathcal{B} = 2$, Eq (7.2.25) coincides with the well known Random-Phase-Approximation in the theory of classical fluids (see Ref. Hansen and McDonald [1986] Section 6.5) where W is the potential of the reference fluid and U the perturbation.

We call $\xi(r)$ the three-body correlation function which is parametrized as Panoff and Carlson [1989]

$$\xi(r) = a \exp \{ -[(r - b)c]^2 \} . \quad (7.2.36)$$

To cancel the two-body term arising from $\mathbf{G}(l) \cdot \mathbf{G}(l)$, we use $\tilde{u}(r) = u(r) - 2\xi^2(r)r^2$

The backflow and three-body correlation functions are then chosen to decay to zero with a zero first derivative at the edge of the simulation box.

7.2.4 The radial distribution function

The radial distribution function (RDF) is proportional to the probability of finding another particle of the fluid inside a spherical shell of radius r and thickness dr centered on any one particle on which you sit. This observable gives us informations about the structure of the fluid. We will see here how it can be measured in a DMC calculation. In appendix 7.D we give some details on the determination of the RDF for the ideal gas and in appendix 7.E we give some details on exact relationships that must be satisfied by the RDF of the interacting fluid, the *sum rules*.

Definition of the radial distribution function

The spin-resolved RDF is defined as Hill [1956]; Feenberg [1969]

$$g_{\sigma,\sigma'}(\mathbf{r}, \mathbf{r}') = \frac{\left\langle \sum_{i,j \neq i} \delta_{\sigma,\sigma_i} \delta_{\sigma',\sigma_j} \delta(\mathbf{r} - \mathbf{r}_i) \delta(\mathbf{r}' - \mathbf{r}_j) \right\rangle}{n_\sigma(\mathbf{r}) n_{\sigma'}(\mathbf{r}')} , \quad (7.2.37)$$

$$n_\sigma(\mathbf{r}) = \left\langle \sum_{i=1}^N \delta_{\sigma,\sigma_i} \delta(\mathbf{r} - \mathbf{r}_i) \right\rangle , \quad (7.2.38)$$

where here, and in the following, $\langle \dots \rangle$ will denote the expectation value respect to the ground-state. Two exact conditions follow immediately from the definition: i. the zero-moment sum rule

$$\sum_{\sigma,\sigma'} \int d\mathbf{r} d\mathbf{r}' n_\sigma(\mathbf{r}) n_{\sigma'}(\mathbf{r}') [g_{\sigma,\sigma'}(\mathbf{r}, \mathbf{r}') - 1] = -N , \quad (7.2.39)$$

also known as the charge (monopole) sum rule in the sequence of multipolar sum rules in the framework of charged fluids Martin [1988], ii. $g_{\sigma,\sigma}(\mathbf{r}, \mathbf{r}) = 0$ due to the Pauli exclusion principle.

For the homogeneous and isotropic fluid $n_\sigma(\mathbf{r}) = N_\sigma/\Omega$ where N_σ is the number of particles of spin σ and $g_{\sigma,\sigma'}$ depends only on the distance $r = |\mathbf{r} - \mathbf{r}'|$, so that

$$g_{\sigma,\sigma'}(r) = \frac{1}{4\pi r^2} \frac{\Omega}{N_\sigma N_{\sigma'}} \left\langle \sum_{i,j \neq i} \delta_{\sigma,\sigma_i} \delta_{\sigma',\sigma_j} \delta(r - r_{ij}) \right\rangle . \quad (7.2.40)$$

The total (spin-summed) radial distribution function will be

$$\begin{aligned} g(r) &= \frac{1}{n^2} \sum_{\sigma,\sigma'} n_\sigma n_{\sigma'} g_{\sigma,\sigma'}(r) \\ &= \left(\frac{1+\xi}{2} \right)^2 g_{+,+}(r) + \left(\frac{1-\xi}{2} \right)^2 g_{-,-}(r) + \frac{1-\xi^2}{2} g_{+,-}(r) . \end{aligned} \quad (7.2.41)$$

From the structure to the thermodynamics

As it is well known the knowledge of the RDF gives access to the thermodynamic properties of the system. The mean potential energy per particle can be directly obtained from $g(r)$ and the bare pair-potential $v_\mu(r)$ as follows

$$e_p = \sum_{\sigma, \sigma'} \frac{n_\sigma n_{\sigma'}}{2n} \int dr e^2 v_\mu(r) [g_{\sigma, \sigma'}(r) - 1] , \quad (7.2.42)$$

where we have explicitly taken into account of the background contribution. Suppose that $e_p(r_s)$ is known as a function of the coupling strength r_s . The virial theorem for a system with Coulomb interactions ($v_\infty(r) = 1/r$) gives $N(2e_k + e_p) = 3P\Omega$ with $P = -d(Ne_0)/d\Omega$ the pressure and $e_0 = e_k + e_p$ the mean total ground-state energy per particle. We then find

$$e_p(r_s) = 2e_0(r_s) + r_s \frac{de_0(r_s)}{dr_s} = \frac{1}{r_s} \frac{d}{dr_s} [r_s^2 e_0(r_s)] , \quad (7.2.43)$$

which integrates to

$$e_0(r_s) = e_F + \frac{1}{r_s^2} \int_0^{r_s} dr'_s r'_s e_p(r'_s) . \quad (7.2.44)$$

We can rewrite the ground-state energy per particle of the ideal Fermi gas, in reduced units, as

$$e_F = \left(\frac{9\pi}{4} \right)^{2/3} \frac{3}{10} \phi_5(\xi) \frac{1}{r_s^2} , \quad (7.2.45)$$

where $\phi_n(\xi) = (1 - \xi)^{n/3} + (1 + \xi)^{n/3}$. And for the exchange potential energy per particle in the Coulomb case

$$e_p^x = - \left(\frac{2}{3\pi^5} \right)^{1/3} \frac{9\pi}{8} \phi_4(\xi) \frac{1}{r_s} , \quad (7.2.46)$$

which follows from Eq. (7.2.42) and Eqs. (7.D.2)-(7.D.3). The expression for finite μ can be found in Ref. [Paziani et al. \[2006\]](#) (see their Eqs. (15)-(16)).

Definition of the static structure factor

If we introduce the microscopic spin dependent number density

$$\rho_\sigma(\mathbf{r}) = \sum_{i=1}^N \delta_{\sigma, \sigma_i} \delta(\mathbf{r} - \mathbf{r}_i) , \quad (7.2.47)$$

and its Fourier transform $\rho_{\mathbf{k}, \sigma}$, then the spin-resolved static structure factors are defined as $S_{\sigma, \sigma'}(\mathbf{k}) = \langle \rho_{\mathbf{k}, \sigma} \rho_{-\mathbf{k}, \sigma'} \rangle / N$, which, for the homogeneous and isotropic fluid, can be rewritten as

$$S_{\sigma, \sigma'}(\mathbf{k}) = \frac{n_\sigma}{n} \delta_{\sigma, \sigma'} + \frac{n_\sigma n_{\sigma'}}{n} \int [g_{\sigma, \sigma'}(r) - 1] e^{-i\mathbf{k} \cdot \mathbf{r}} dr + \frac{n_\sigma n_{\sigma'}}{n} (2\pi)^3 \delta(\mathbf{k}) , \quad (7.2.48)$$

From now on we will ignore the delta function at $\mathbf{k} = 0$. The total (spin-summed) static structure factor is $S = \sum_{\sigma, \sigma'} S_{\sigma, \sigma'}$. Due to the charge sum rule (7.2.39) we must have $\lim_{k \rightarrow 0} S(k) = 0$. In Sec. 7.E.2 we will show that the small k behavior of $S(k)$ has to start from the term of order k^2 .

7.2.5 Results for the radial distribution function and structure factor

The radial distribution function and structure factor have been calculated through DMC by Ortiz and Ballone [Ortiz and Ballone \[1994\]](#). In Fig. 7.2.1 we show their results for the radial distribution function and in Fig. 7.2.2 their results for the structure factor.

7.2.6 Results for the internal energy

The behavior of the internal energy of the Jellium in its ground state has been determined through DMC by Ceperley and Alder [Ceperley and Alder \[1980\]](#). Their result is shown in Fig. 7.2.3. Three phases of the fluid appeared, for $r_s < 75$ the stable phase is the one of the unpolarized Jellium, for $75 < r_s < 100$ the one of the polarized fluid, and for $r_s > 100$ the one of the Wigner crystal. The Wigner formula of Eq. (7.D.11) turns out to be a rather good approximation. They used systems from $N = 38$ to $N = 246$ electrons.

7.3 Jellium at finite temperature

For the Jellium at finite temperature it is convenient to introduce the *electron degeneracy parameter* $\Theta = T/T_F$, where T_F is the Fermi temperature

$$T_F = T_D \frac{(2\pi)^2}{2[(2 - \xi)\alpha_3]^{2/3}}, \quad (7.3.1)$$

here ξ is the polarization of the fluid that can be either $\xi = 0$, for the unpolarized case, and $\xi = 1$, for the fully polarized case, $\alpha_3 = 4\pi/3$, and

$$T_D = \frac{n^{2/3} \hbar^2}{m k_B}, \quad (7.3.2)$$

is the degeneracy temperature, for temperatures higher than T_D quantum effects are less relevant.

The state of the fluid will then depend also upon the *Coulomb coupling parameter*, $\Gamma = e^2/r_s a_0 k_B T$ [Brown et al. \[2013\]](#).

7.3.1 Monte Carlo simulation (Path Integral)

The *density matrix* of a many-fermion system at temperature $k_B T = \beta^{-1}$ can be written as an integral over all paths $\{R_t\}$

$$\rho_F(R_\beta, R_0; \beta) = \frac{1}{N!} \sum_{\mathcal{P}} (-1)^{\mathcal{P}} \oint_{\mathcal{P} R_0 \rightarrow R_\beta} dR_t \exp(-S[R_t]). \quad (7.3.3)$$

the path $R(t)$ begins at $\mathcal{P} R_0$ and ends at R_β and \mathcal{P} is a permutation of particles labels. For nonrelativistic particles interacting with a potential $V(R)$ the *action* of the path, $S[R_t]$, is given by (see appendix 7.F)

$$S[R_t] = \int_0^\beta dt \left[\frac{r_s^2}{4} \left| \frac{dR(t)}{dt} \right|^2 + V(R_t) \right]. \quad (7.3.4)$$

Thermodynamic properties, such as the energy, are related to the diagonal part of the density matrix, so that the path returns to its starting place or to a permutation \mathcal{P} after a time β .

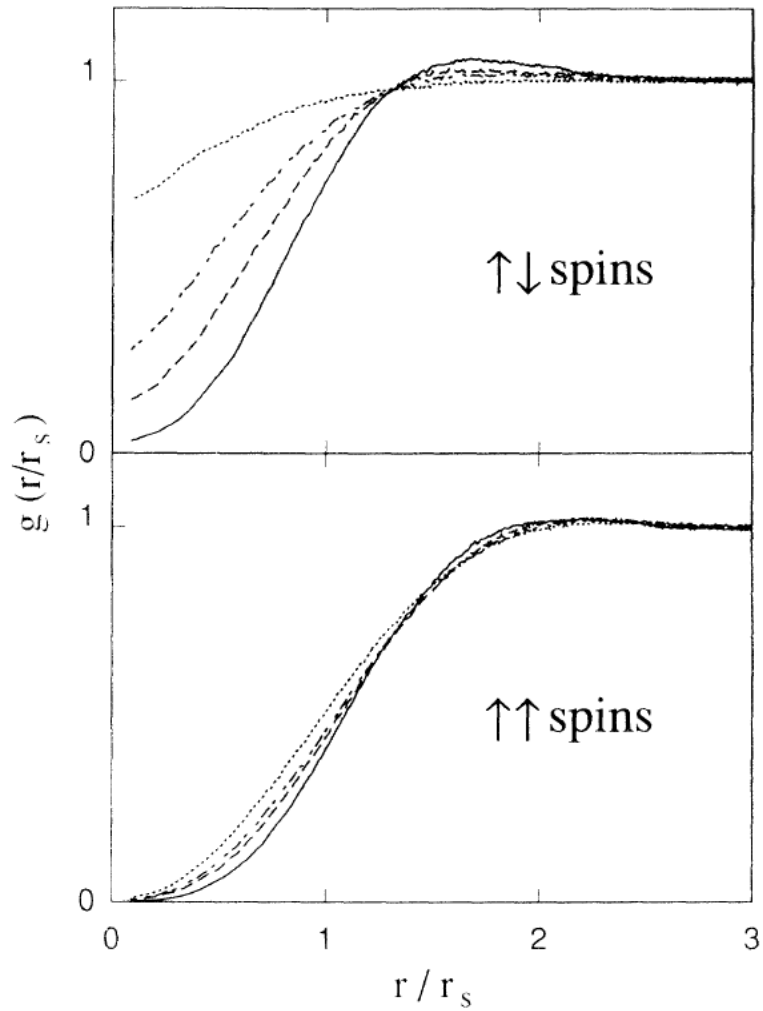


Figure 7.2.1: Radial distribution function $g(r)$ computed by DMC method (mixed estimator) for the unpolarized $\xi = 0$ case and the fully polarized $\xi = 1$ case. $r_s = 1$ (dotted line), $r_s = 3$ (dash-dotted line), $r_s = 5$ (dashed line), and $r_s = 10$ (full line). r is in units of a Bohr radius. (Figure reproduced here by courtesy of the authors of Ref. [Ortiz and Ballone \[1994\]](#))

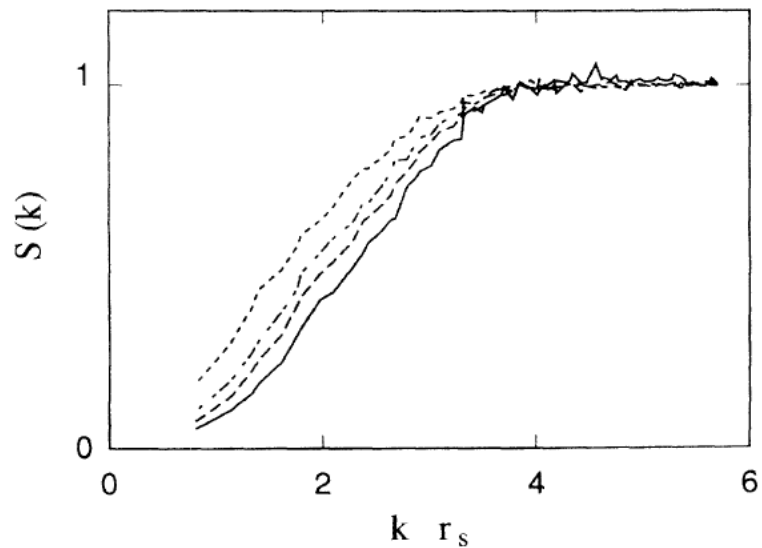


Figure 7.2.2: Structure factor $S(k)$ computed by the DMC method (mixed estimator). The r_s considered and the symbols are the same as those of Fig. 7.2.1. (Figure reproduced here by courtesy of the authors of Ref. [Ortiz and Ballone \[1994\]](#))

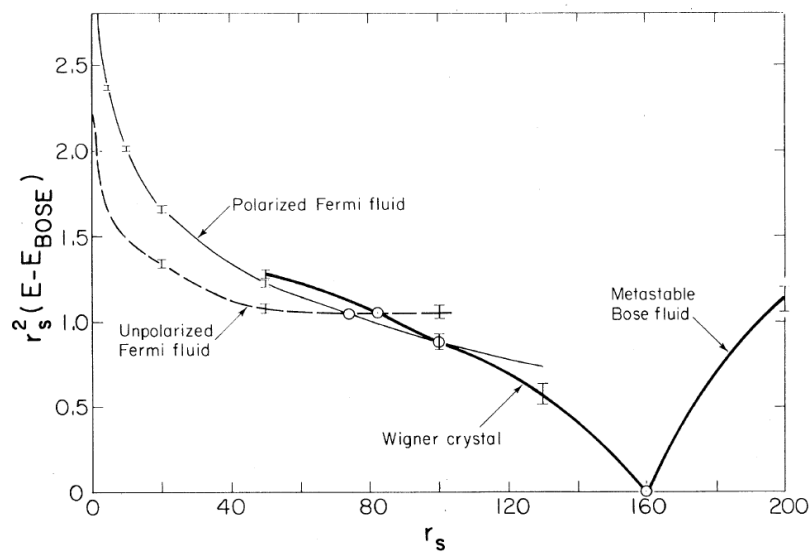


Figure 7.2.3: The energy of the four phases studied relative to that of the lowest boson state times r_s^2 in Rydbergs as a function of r_s in Bohr radii. The boson system undergoes Wigner crystallization at $r_s = 160 \pm 10$. The fermion system has two phase transitions, crystallization at $r_s = 100 \pm 20$ and depolarization at $r_s = 75 \pm 5$. (Figure reproduced here by courtesy of the authors of Ref. [Ceperley and Alder \[1980\]](#))

To perform Monte Carlo calculations of the integrand, one makes imaginary time discrete, so that one has a finite (and hopefully small) number of time slices and thus a classical system of N particles in M time slices; an equivalent NM particle classical system of “polymers” Ceperley [1995].

Note that in addition to sampling the path, the permutation is also sampled. This is equivalent to allowing the ring polymers to connect in different ways. This macroscopic “percolation” of the polymers is directly related to superfluidity as Feynman Feynman [1953a,b,c] first showed. Any permutation can be broken into cycles. Superfluid behavior can occur at low temperature when the probability of exchange cycles on the order of the system size is non-negligible. The *superfluid fraction* can be computed in a path integral Monte Carlo calculation as described in Ref. Pollock and Ceperley [1987]. The same method could be used to calculate the *superconducting fraction* in Jellium at low temperature. However, the straightforward application of those techniques to Fermi systems means that odd permutations subtract from the integrand. This is the “fermions sign problem” Ceperley [1991] which will be discussed in the next section.

Thermodynamic properties are averages over the thermal N -fermion density matrix which is defined as a thermal occupation of the exact eigenstates $\phi_i(R)$

$$\rho_F(R, R'; \beta) = \sum_i \phi_i^*(R) e^{-\beta E_i} \phi_i(R'). \quad (7.3.5)$$

The partition function is the trace of the density matrix

$$Z(\beta) = e^{-\beta F} = \int dR \rho_F(R, R; \beta) = \sum_i e^{-\beta E_i}. \quad (7.3.6)$$

Other thermodynamic averages are obtained as

$$\langle \mathcal{O} \rangle = Z(\beta)^{-1} \int dR dR' \langle R | \mathcal{O} | R' \rangle \rho(R', R; \beta). \quad (7.3.7)$$

Note that for any density matrix the diagonal part is always positive

$$\rho(R, R; \beta) \geq 0, \quad (7.3.8)$$

so that $Z^{-1} \rho(R, R; \beta)$ is a proper probability distribution. It is the diagonal part which we need for many observables, so that probabilistic ways of calculating those observables are, in principle, possible.

Path integrals are constructed using the product property of density matrices

$$\rho(R_2, R_0; \beta_1 + \beta_2) = \int dR_1 \rho(R_2, R_1; \beta_2) \rho(R_1, R_0; \beta_1), \quad (7.3.9)$$

which holds for any sort of density matrix. If the product property is used M times we can relate the density matrix at a temperature β^{-1} to the density matrix at a temperature $M\beta^{-1}$. The sequence of intermediate points $\{R_1, R_2, \dots, R_{M-1}\}$ is the path, and the time step is $\tau = \beta/M$. As the time step gets sufficiently small the Trotter theorem tells us that we can assume that the kinetic \mathcal{T} and potential \mathcal{V} operator commute so that: $e^{-\tau\mathcal{H}} = e^{-\tau\mathcal{T}}e^{-\tau\mathcal{V}}$ and the primitive approximation for the Boltzmann density matrix is found Ceperley [1995]. The Feynman-Kac formula for the Boltzmann density matrix results from taking the limit $M \rightarrow \infty$. The price we have to pay for having an explicit expression for the density matrix is additional integrations; all together $3N(M-1)$. Without techniques for multidimensional integration, nothing would have been gained by expanding the density matrix into a path. Fortunately, simulation methods can

accurately treat such integrands. It is feasible to make M rather large, say in the hundreds or thousands, and thereby systematically reduce the time-step error.

In addition to the internal energy and the static structure of the Jellium one could also measure its dynamic structure, the “superconducting fraction”, the specific heat, and the pressure Ceperley [1995].

The direct path integral method

In the *direct fermion method* one sums over permutations just as bosonic systems. Odd permutations then contribute with a negative weight. The direct method has a major problem because of the cancellation of positive and negative permutations. This was first noted by Feynman and Hibbs Feynman and Hibbs [1965] who after describing the path integral theory for boson superfluid ^4He , noted: “The [path integral] expression for Fermi particles, such as ^3He , is also easily written down. However in the case of liquid ^3He , the effect of the potential is very hard to evaluate quantitatively in an accurate manner. The reason for this is that the contribution of a cycle to the sum over permutations is either positive or negative depending whether the cycle has an odd or an even number of atoms in its length L . At very low temperature, the contributions of cycles such as $L = 51$ and $L = 52$ are very nearly equal but opposite in sign, and therefore they very nearly cancel. It is necessary to compute the difference between such terms, and this requires very careful calculation of each term separately. It is very difficult to sum an alternating series of large terms which are decreasing slowly in magnitude when a precise analytic formula for each term is not available.”

Progress could be made in this problem if it were possible to arrange the mathematics describing a Fermi system in a way that corresponds to a sum of positive terms. Some such schemes have been tried, but the resulting terms appear to be much too hard to evaluate even qualitatively.

[...]

The [explanation] of the superconducting state was first answered in a convincing way by Bardeen, Cooper, and Schrieffer. The path integral approach played no part in their analysis and *in fact has never proved useful for degenerate Fermi systems. [D. M. Ceperley *italics*]“*

When we measure a property \mathcal{O} in a Monte Carlo calculation Ceperley [1991, 1996]

$$\langle \mathcal{O} \rangle = \frac{\int \Pi \mathcal{O}}{\int \Pi}, \quad (7.3.10)$$

where π is a function with both positive and negative pieces and the integrals are not only over coordinates but a sum over permutations is also tacitly assumed.

One introduces the distribution function for the importance sampling P

$$\langle \mathcal{O} \rangle = \frac{\int P[\Pi \mathcal{O}/P]}{\int P[\Pi/P]}, \quad (7.3.11)$$

and calculates

$$\langle \mathcal{O} \rangle = \frac{\sum_i \omega_i \mathcal{O}_i}{\sum_i \omega_i}, \quad (7.3.12)$$

where $\omega_i = \Pi_i/P_i$ and the sums are over M points distributed according to P . Then the variance

of the measure is

$$\begin{aligned}
\sigma_{\mathcal{O}}^2 &= \left\langle \left(\frac{\sum_i \omega_i \mathcal{O}_i}{\sum_i \omega_i} - \langle \mathcal{O} \rangle \right)^2 \right\rangle_P \\
&= \frac{1}{(\sum_i \omega_i)^2} \left\langle \left[\sum_i \omega_i (\mathcal{O}_i - \langle \mathcal{O} \rangle) \right]^2 \right\rangle_P \\
&\approx \frac{1}{(\sum_i \omega_i)^2} \left\langle \sum_i \omega_i^2 (\mathcal{O}_i - \langle \mathcal{O} \rangle)^2 \right\rangle_P \\
&= \frac{1}{M (\int \Pi)^2} \langle \omega^2 (\mathcal{O} - \langle \mathcal{O} \rangle)^2 \rangle_P \\
&= \frac{1}{M (\int \Pi)^2} \int \frac{\Pi^2 (\mathcal{O} - \langle \mathcal{O} \rangle)^2}{P} ,
\end{aligned} \tag{7.3.13}$$

where we assumed that the sampled points were uncorrelated. Choosing $P = q^2 / \int q^2$ and solving $\delta \sigma_{\mathcal{O}}^2 / \delta q = 0$ we find as the optimal distribution

$$P^* \propto |\Pi(\mathcal{O} - \langle \mathcal{O} \rangle)| . \tag{7.3.14}$$

The usually one chooses $P = |\Pi| / \int |\Pi|$. For bosons there are no problems since Π is everywhere positive, but for fermions one finds

$$\sigma_F^2 = \sigma_B^2 / \xi , \tag{7.3.15}$$

where the efficiency is

$$\xi = \left[\frac{\int \Pi}{\int |\Pi|} \right]^2 = \left[\frac{M_+ - M_-}{M} \right]^2 = \left[\frac{\Theta_F}{\Theta_B} \right]^2 = e^{-2\beta(\Omega_F - \Omega_B)} . \tag{7.3.16}$$

The average time that the simulation spend in the positive region of P is M_+/M and M_-/M is the average time spent in the negative region. The efficiency for the fermionic case is proportional to the square of the average sign: the positive sampled points in excess over the negative ones. From the expressions for the grand-thermodynamic potentials for the ideal Bose, Ω_B , and Fermi, Ω_F , gas we find for example

$$\xi = \begin{cases} e^{-N\rho^3\Lambda^3/(\sqrt{2}g)} & z \rightarrow 0 \\ e^{-N\rho 2g(b_{5/2}(1) - f_{5/2}(1))/\Lambda^3} & z \rightarrow 1 \end{cases} , \tag{7.3.17}$$

where $b_{5/2}(1) - f_{5/2}(1) \approx 0.4743$. We then see that for any z the efficiency becomes exponentially small in the number of particles. Moreover for a fixed N we find $\xi = e^{-2\beta(F_F - F_B)}$, with F_B the Helmholtz free energy of the Bose gas and F_F the one of the Fermi gas, and in the high temperature limit we find [Landau and Lifshitz \[1951\]](#)

$$\xi \approx e^{-2\rho N (2\pi\lambda\beta)^{3/2}/g} . \tag{7.3.18}$$

Whereas in the low temperature limit

$$F_F = F_F^0 - \frac{1}{4\lambda} \frac{N}{\beta^2} \left(\frac{\pi}{3\rho} \right)^{2/3} , \tag{7.3.19}$$

$$F_B = -\frac{N}{\beta} \frac{b_{5/2}(1)}{b_{3/2}(1)} \left(\frac{T}{T_c} \right)^{3/2} , \tag{7.3.20}$$

where $T_c \simeq T_D 2\pi/(2.612g)^{2/3}$ is the Bose-Einstein condensation temperature, $F_F^0 = N\epsilon_F + \Omega_F^0$ with $\epsilon_F = \mu$ the Fermi energy and $\Omega_F^0 = -gV\epsilon_F^{5/2}/(15\pi^2\lambda^{3/2})$, and $N = gV(2m\epsilon_F)^{3/2}/6\pi^2\hbar^3$. So that in the limit $\beta \rightarrow \infty$ we find

$$\xi = e^{-2\beta F_F^0}, \quad (7.3.21)$$

with $F_F^0 = g(1/6 - 1/15)V\epsilon_F^{5/2}/(\pi^2\lambda^{3/2}) > 0$, which shows how the efficiency of a direct Monte Carlo calculation on fermions becomes exponentially small as β and N increases. Exactly where the physics becomes more interesting.

Restricted Path Integral Monte Carlo

The Fermion density matrix is defined [Ceperley \[1991, 1996\]](#) by the Bloch equation which describes its evolution in imaginary time

$$\frac{\partial}{\partial \beta} \rho_F(R, R_0; \beta) = -\mathcal{H}\rho_F(R, R_0; \beta), \quad (7.3.22)$$

$$\rho_F(R, R_0; 0) = \mathcal{A}\delta(R - R_0), \quad (7.3.23)$$

where $\beta = 1/k_B T$ with T the absolute temperature and \mathcal{A} is the operator of antisymmetrization. The *reach* of R_0 , $\gamma(R_0, t)$, is the set of points $\{R_t\}$ for which

$$\rho_F(R_{t'}, R_0; t') > 0 \quad 0 \leq t' \leq t, \quad (7.3.24)$$

where t is the imaginary thermal time. Note that

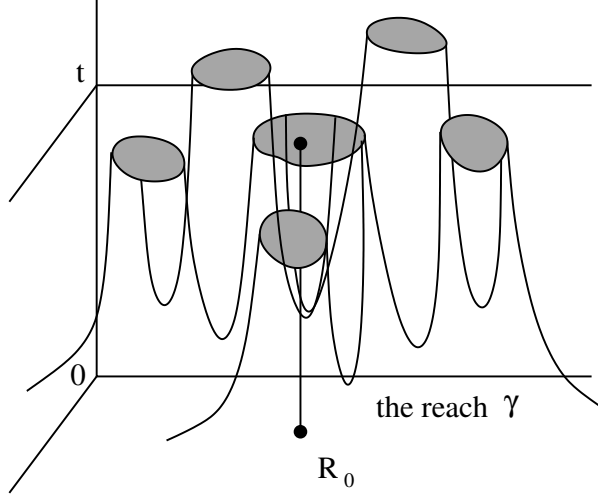


Figure 7.3.1: Illustration of the reach $\gamma(R_0, t)$ of the fermion density matrix.

$$\rho_F(R_0, R_0; t) > 0, \quad (7.3.25)$$

and clearly

$$\rho_F(R, R_0; t)|_{R \in \partial\gamma(R_0, t)} = 0. \quad (7.3.26)$$

We want to show that (7.3.26) uniquely determines the solution. Suppose $\delta(R, t)$ satisfies the Bloch equation

$$\left(\mathcal{H} + \frac{\partial}{\partial t} \right) \delta(R, t) = 0, \quad (7.3.27)$$

in a space-time domain $\alpha = \{t_1 \leq t \leq t_1, R \in \Omega_t\}$. And the two conditions

$$\delta(R, t_1) = 0, \quad (7.3.28)$$

$$\delta(R, t)|_{R \in \partial \Omega_t} = 0 \quad t_1 \leq t \leq t_2, \quad (7.3.29)$$

are also satisfied. Consider

$$\int_{t_1}^{t_2} dt \int_{\Omega_t} dR e^{2V_0 t} \delta(R, t) \left(\mathcal{H} + \frac{\partial}{\partial t} \right) \delta(R, t) = 0, \quad (7.3.30)$$

where V_0 is a lower bound for $V(R)$.

We have

$$\frac{\partial}{\partial t} [e^{2V_0 t} \delta^2(R, t)] = 2V_0 e^{2V_0 t} \delta^2(R, t) + 2e^{2V_0 t} \delta(R, t) \frac{\partial}{\partial t} \delta(R, t). \quad (7.3.31)$$

Since

$$\begin{aligned} \int_{t_1}^{t_2} dt \int_{\Omega_t} dR \frac{\partial}{\partial t} \left(\frac{e^{2V_0 t}}{2} \delta^2(R, t) \right) &= \int_{t_1}^{t_2} dt \frac{\partial}{\partial t} \left(\frac{e^{2V_0 t}}{2} \int_{\Omega_t} dR \delta^2(R, t) \right) \\ &= \frac{e^{2V_0 t_2}}{2} \int_{\Omega_{t_2}} dR \delta^2(R, t_2), \end{aligned} \quad (7.3.32)$$

where in the last equality we used Eq. (7.3.28). Then from Eq. (7.3.30) follows

$$\frac{e^{2V_0 t}}{2} \int_{\Omega_{t_2}} dR \delta^2(R, t_2) - e^{2V_0 t} \int_{t_1}^{t_2} dt \int_{\Omega_t} dR [V_0 \delta^2(R, t) - \delta(R, t) \mathcal{H} \delta(R, t)] = 0. \quad (7.3.33)$$

Then using Eq. (7.3.29) we find

$$\begin{aligned} \frac{e^{2V_0 t}}{2} \int_{\Omega_{t_2}} dR \delta^2(R, t_2) + \\ e^{2V_0 t} \int_{t_1}^{t_2} dt \int_{\Omega_t} dR [(V(R) - V_0) \delta^2(R, t) + \lambda (\nabla \delta(R, t))^2] = 0. \end{aligned} \quad (7.3.34)$$

Each term in Eq. (7.3.34) is non-negative so it must be

$$\delta(R, t) = 0 \quad \text{in } \alpha. \quad (7.3.35)$$

Let ρ_1 and ρ_2 be two solutions of the restricted path problem and let $\delta = \rho_1 - \rho_2$. Then $\delta(R, t)|_{R \in \partial \gamma(R_0, t)} = 0$ for $t_1 \leq t \leq t_2$. By taking t_2 to infinity and t_1 to zero we conclude that the fermion density matrix is the unique solution.

Eq (7.3.34) also shows that the reach γ has the *tiling* property Ceperley [1991]. Suppose it did not. Then there would exist a space-time domain with the density matrix non-zero inside and from which it is only possible to reach R_0 or any of its images $\mathcal{P}R_0$, with \mathcal{P} any permutation of the particles, crossing the nodes of the density matrix. But such a domain cannot extend to

$t = 0$ because in the classical limit there are no nodes. Then this density matrix satisfies for some $t_1 > 0$ the boundary conditions (7.3.28) and (7.3.29) and as a consequence it must vanish completely inside the domain contradicting the initial hypothesis.

We now derive the restricted path identity. Suppose ρ_F is the density matrix corresponding to some set of quantum numbers which is obtained by using the projection operator \mathcal{A} on the distinguishable particle density matrix. Then it is a solution to the Bloch equation (7.3.22) with boundary condition (7.3.23). Thus we have proved the *Restricted Path Integral* identity

$$\rho_F(R_\beta, R_0; \beta) = \int_{R' \rightarrow R_\beta \in \gamma(R_0)} dR' \rho_F(R', R_0; 0) \oint dR_t e^{-S[R_t]}, \quad (7.3.36)$$

where the subscript means that we restrict the path integration to paths starting at R' , ending at R_β and node-avoiding. The weight of the walk is $\rho_F(R', R_0; 0)$. It is clear that the contribution of all the paths for a single element of the density matrix will be of the same sign; positive if $\rho_F(R', R_0; 0) > 0$, negative otherwise.

Important in this argument is that the random-walk is a continuous process so we can say definitely that if sign of the density matrix changed, it had to have crossed the nodes at some point.

The restricted path identity is one solution to Feynman's task of rearranging terms to keep only positive contributing paths for diagonal expectation values.

The problem we now face is that the unknown density matrix appears both on the left-hand side and on the right-hand side of Eq. (7.3.36) since it is used to define the criterion of node-avoiding paths. To apply the formula directly, we would somehow have to self-consistently determine the density matrix. In practice what we need to do is make an *ansatz*, which we call ρ_T , for the nodes of the density matrix needed for the restriction. The *trial density matrix*, ρ_T , is used to define trial nodal cells: $\gamma_T(R_0)$.

Then if we know the reach of the fermion density matrix we can use the Monte Carlo method to solve the fermion problem restricting the path integral (RPIMC) to the space-time domain where the density matrix has a definite sign (this can be done, for example, using a trial density matrix whose nodes approximate well the ones of the true density matrix) and then using the antisymmetrization operator to extend it to the whole configuration space. This will require the complicated task of sampling the permutation space of the N -particles Ceperley [1995]. Recently it has been devised an intelligent method to perform this sampling through a new algorithm called the *worm* algorithm Boninsegni et al. [2006]. In order to sample the path in coordinate space one generally uses various generalizations of the Metropolis rejection algorithm Metropolis et al. [1953] and the *bisection method* Ceperley [1995] in order to accomplish multislice moves which becomes necessary as τ decreases.

The *pair-product approximation* was used Brown et al. [2013] (see appendix 7.G) to write the many-body density matrix as a product of high-temperature two-body density matrices Ceperley [1995]. The pair Coulomb density matrix was determined using the results of Pollock Pollock [1988] even if these could be improved using the results of Vieillefosse Vieillefosse [1994, 1995]. This procedure comes with an error that scales as $\sim \tau^3/r_s^2$ where $\tau = \beta/M$ is the time step, with M the number of imaginary time discretizations. A more dominate form of time step error originates from paths which cross the nodal constraint in a time less than τ . To help alleviate this effect, Brown et al. Brown et al. [2013] use an image action to discourage paths from getting too close to nodes. Additional sources of error are the finite size one and the sampling error of the Monte Carlo algorithm itself. For the highest density points, statistical errors are an order of magnitude higher than time step errors.

The results at a given temperature T were obtained starting from the density matrix in the

classical limit, at small thermal times, and using repetitively the *squaring* method

$$\rho_F(R_1, R_2; \beta) = \int dR' \rho_F(R_1, R'; \beta/2) \rho_F(R', R_2; \beta/2). \quad (7.3.37)$$

Time doubling is an improvement also because if we have accurate nodes down to a temperature T , we can do accurate simulations down to $T/2$. Eq. (7.3.37) is clearly symmetric in R_1 and R_2 . The time doubling cannot be repeated without reintroducing the sign problem.

Brown *et al.* Brown et al. [2013] use $N = 33$ electrons for the fully spin polarized system and $N = 66$ electrons for the unpolarized system.

7.3.2 Results for the radial distribution function and structure factor

In the classical Debye-Hückel limit one has Hansen and McDonald [1986]; Hansen [1973]

$$g_{DH}(r) = \exp \left[-\frac{\Gamma}{r} \exp(-k_D r_s a_0 r) \right], \quad (7.3.38)$$

were $k_D = \sqrt{4\pi\beta n e^2}$. And for the structure factor, after linearizing Eq. (7.3.38) for $r \gg 1/k_D r_s a_0$,

$$S_{DH}(k) = \frac{k^2}{k^2 + 3\Gamma}. \quad (7.3.39)$$

A serious weakness of the linearized approximation is the fact that it allows $g(r)$ to become negative at small r . This failing is rectified in the non-linear version (7.3.38).

In the ground state the radial distribution function and structure factor have been calculated by Ortiz and Ballone Ortiz and Ballone [1994].

In Fig. 7.3.2 we present the RPIMC results of Brown *et al.* Brown et al. [2013].

7.3.3 Results for the internal energy

Given the total internal energy per particle of the fluid e_{tot} , the exchange and correlation energy per particle is

$$e_{xc}(T) = e_{tot}(T) - e_0(T). \quad (7.3.40)$$

where $e_0(T)$ is the kinetic energy of a free Fermi gas at temperature T . And

$$e_{xc}(T) = e_x(T) + e_c(T). \quad (7.3.41)$$

where $e_x(T)$ is the Hartree-Fock exchange energy for a Fermi gas at temperature T (see Eq. (7) of Ref. Perdew and Zunger [1981]).

For fixed polarizations $\xi = 0$, the unpolarized case, and for $\xi = 1$, the fully polarized case, one has

$$e_0 = (2 - \xi) \frac{r_s^3}{3\pi\beta^{5/2}} \frac{1}{Ry^{5/2}} I(3/2, \kappa), \quad (7.3.42)$$

$$e_x = -(2 - \xi) \frac{r_s^3}{6\pi^2\beta^2} \frac{1}{Ry^2} \int_0^\infty \frac{dx}{1 + e^{x-\kappa}} \int_0^\infty \frac{dy}{1 + e^{y-\kappa}} \int_{-1}^1 \frac{dz}{\sqrt{x/y} + \sqrt{y/x} - 2z}, \quad (7.3.43)$$

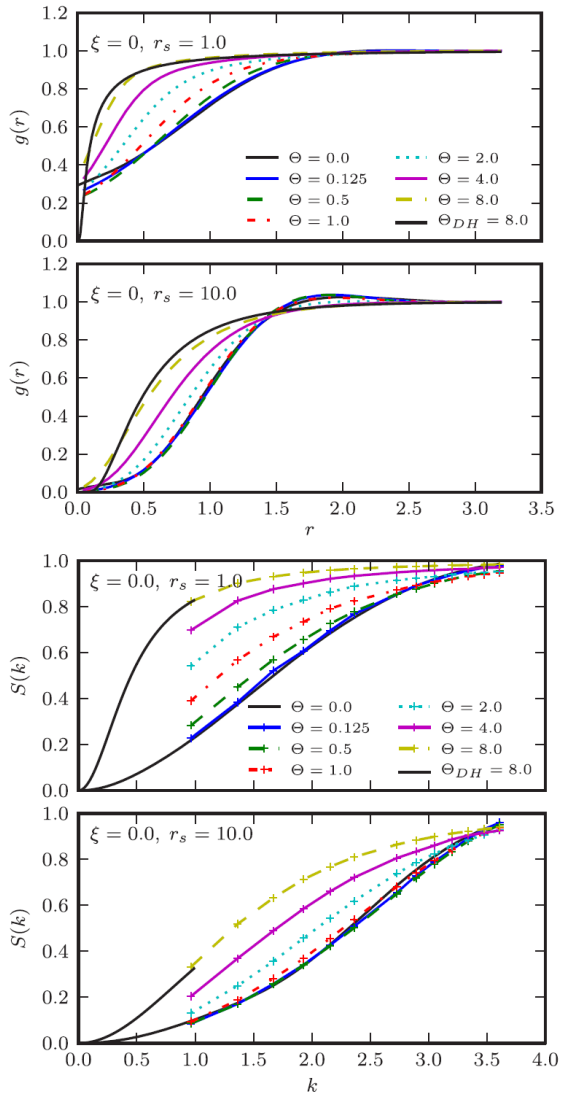


Figure 7.3.2: Pair correlation functions (on the left) for $r_s = 1.0$ and $r_s = 10.0$ in the unpolarized state. Also shown is the small r part of the classical Debye-Hückel limit at $\Theta = 8.0$; see Eq. (7.3.38). The Debye-Hückel limit is not yet reached at $\Theta = 8.0$ for the lower density $r_s = 10.0$. Static structure factors (on the right) for $r_s = 1.0$ and $r_s = 10.0$ in the unpolarized state. Also shown is the small k part of the classical Debye-Hückel limit at $\Theta = 8.0$; see Eq. (7.3.39). (Figure reproduced here by courtesy of the authors of Ref. Brown et al. [2013])

where

$$I(\nu, \kappa) = \int_0^\infty \frac{x^\nu}{1 + e^{x-\kappa}} dx, \quad (7.3.44)$$

and κ is determined from

$$I(1/2, \kappa) = \frac{2}{3} \Theta^{-3/2}. \quad (7.3.45)$$

For the expressions at an intermediate polarization $0 < \xi < 1$ see the appendix 7.A. It is still missing an analysis of the finite temperature Jellium at intermediate polarizations. This would be important for a clearer determination of the Jellium phase diagram.

In Fig. 7.3.3 we present the RPIMC results of Brown *et al.* [Brown et al. \[2013\]](#).

In Ref. [Brown et al. \[2014\]](#) a comparison is given between these calculations to previous estimations of the Jellium correlation energy. Such parameterizations generally fall into two categories: those which extend down from the classical regime and those which assume some interpolation between the $T = 0$ and high- T regimes. From the former group, in Fig. 7.3.4, Brown *et al.* plot e_c coming from Debye-Hückel (DH) theory which solves for the Poisson-Boltzmann equations for the classical one component plasma and the quantum corrections of Hansen *et al.* [Hansen \[1973\]](#); [Hansen and Vieillefosse \[1975\]](#) of the Coulomb system both with Wigner-Kirkwood corrections (H+WK) and without (H). Clearly these methods do not perform well in the quantum regime below the Fermi temperature since they lack quantum exchange.

The Random-Phase-Approximation (RPA) [Gupta and Rajagopal \[1980\]](#); [Perrot and Dharma-wardana \[1984\]](#) is a reasonable approximation in the low-density, high-temperature limit (where it reduces to DH) and the low-temperature, high-density limit, since these are both weakly interacting regimes. Its failure, however, is most apparent in its estimation of the equilibrium, radial distribution function $g(r)$ which becomes negative for stronger coupling. Extensions of the RPA into intermediate densities and temperatures have largely focused on constructing local-field corrections (LFC) through interpolation since diagrammatic resummation techniques often become intractable in strongly-coupled regimes. Singwi *et al.* [Singwi et al. \[1968\]](#) introduced one such strategy. Tanaka and Ichimaru [Tanaka and Ichimaru \[1986\]](#) (TI) extended this method to finite temperatures and provided the shown parameterization of the Jellium correlation energy. This method appears to perform marginally better than the RPA at all temperatures, though it still fails to produce a positive-definite $g(r)$ at values of $r_s > 2$. A third, more recent approach introduced by Perrot and Dharma-wardana (PDW) [Perrot and Dharma-wardana \[2000\]](#) relies on a classical mapping where the distribution functions of a classical system at temperature T_{cf} , solved for through the hypernetted-chain equation, reproduce those for the quantum system at temperature T . In a previous work, PDW showed such a temperature T_q existed for the classical system to reproduce the correlation energy of the quantum system at $T = 0$ [Dharma-wardana and Perrot \[2000\]](#). To extend this work to finite temperature quantum systems, they use the simple interpolation formula $T_{cf} = \sqrt{T^2 + T_q^2}$. This interpolation is clearly valid in the low- T limit where Fermi liquid theory gives the quadratic dependence of the energy on T . Further in the high- T regime, T dominates over T_q as the system becomes increasingly classical. The PDW line in Fig. 7.3.4 clearly matches well with the RPIMC results in these two limits. It is not surprising, however, that in the intermediate temperature regime, where correlation effects are greatest, the quadratic interpolation fails. A contemporary, but similar approach by Dutta and Dufty [Dutta and Dufty \[2013\]](#) uses the same classical mapping as PDW which relies on matching the $T = 0$ pair correlation function instead of the correlation energy. While we expect this to give more accurate results near $T = 0$, we would still expect a breakdown of the assumed Fermi liquid behavior near the Fermi temperature. Future Jellium work will include creating a

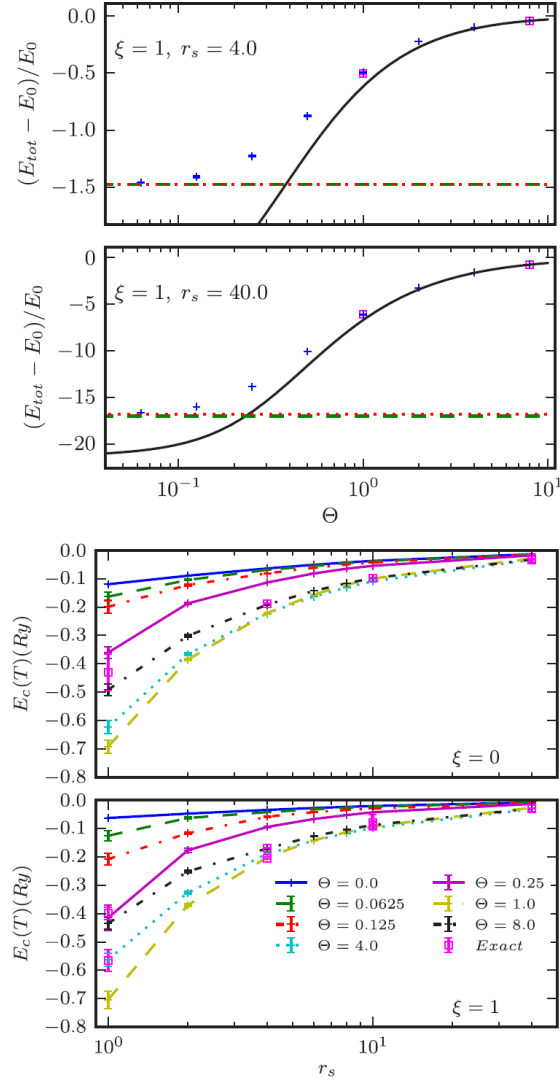


Figure 7.3.3: Excess energies $E_{xc} = e_{xc}$ (on the left) for $r_s = 4.0$ and $r_s = 40.0$ for the polarized state ($E_0 = e_0$). For both densities the high temperature results fall smoothly on top of previous Monte Carlo energies for the classical electron gas Pollock and Hansen [1973] (solid line). Differences from the classical Coulomb gas occur for $\Theta < 2.0$ for $r_s = 4.0$ and $\Theta < 4.0$ for $r_s = 40.0$. Simulations with the Fermion sign (squares) confirm the fixed-node results at $\Theta = 1.0$ and 8.0. The zero-temperature limit (dotted line) smoothly extrapolates to the ground state QMC results of Ceperley-Alder Ceperley and Alder [1980] (dashed line). Correlation energy $E_c(T) = e_c(T)$ (on the right) of the 3D Jellium at several temperatures and densities for the unpolarized (top) and fully spin-polarized (bottom) states. Exact (signful) calculations (squares) confirm the fixed-node results where possible ($\Theta = 8.0$ for $\xi = 0$ and $\Theta = 4.0, 8.0$ for $\xi = 1$). (Figure reproduced here by courtesy of the authors of Ref. Brown et al. [2013])

new parameterization of the correlation energy which uses the RPIMC data directly. In doing so, simulations at higher densities and both lower and higher temperatures may be necessary in order to complete the interpolation between the ground state and classical limits.

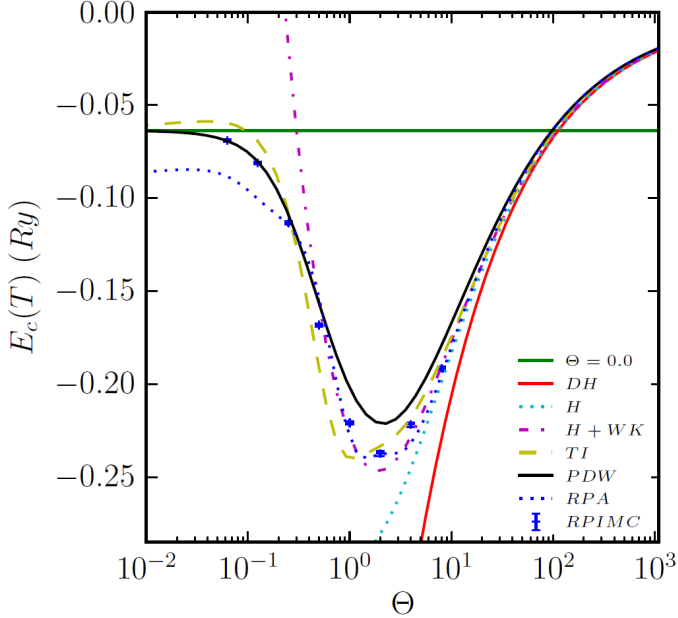


Figure 7.3.4: Correlation energy $E_c(T) = e_c(T)$ of the Jellium at $r_s = 4.0$ for the unpolarized $\xi = 0$ state from the RPIMC calculations (RPIMC) and several previous parameterizations as a function of Θ . The latter include Debye-Hückel (DH), Hansen (H), Hansen+Wigner-Kirkwood (H+WK), Random-Phase-Approximation (RPA), Tanaka and Ichimaru (TI), and Perrot and Dharma-wardana (PDW). Also included is the ground state $\Theta = 0.0$ result for comparison. (Figure reproduced here by courtesy of the authors of Ref. Brown et al. [2014])

7.3.4 Phase diagram

The *worm-dense* regime for both the fully spin-polarized $\xi = 1$ and unpolarized $\xi = 0$ systems has been studied through RPIMC by Brown et al. Brown et al. [2013]. This study complements the previous Monte Carlo studies on the classical one component plasma Pollock and Hansen [1973] and the inclusion of first order quantum mechanical effects by Jancovici Jancovici [1978] and Hansen and Vieillefosse Hansen and Vieillefosse [1975]. However, the accuracy of these results quickly deteriorates as the temperature is lowered and quantum correlations play a greater role Jones and Ceperley [1996]. This breakdown is most apparent in the *warm-dense regime* where both Γ and Θ are close to unity as shown in Fig. 7.3.5.

In the RPIMC of Brown et al. Brown et al. [2013] the trial density matrix was taken as the free electron density matrix

$$\rho_T(R, R'; \tau) = (4\pi\tau/r_s^2)^{-3N/2} \mathcal{A} \exp \left[-\frac{(R - R')^2}{4\tau/r_s^2} \right], \quad (7.3.46)$$

where $\tau = \beta/M$ with M the number of imaginary time discretizations. This approximation should be best at high temperature and low density when correlation effects are weak. The free-particle nodal approximation performs well for the densities studied by Brown et al. [Brown et al. \[2013\]](#). Further investigation is needed at even smaller values of r_s and lower temperatures in order to determine precisely where this approximation begins to fail. Such studies will necessarily require algorithmic improvements, however, because of difficulty in sampling paths at low density and low temperature.

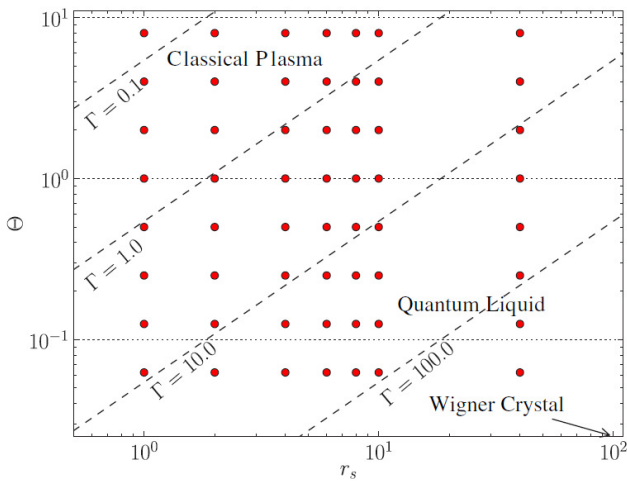


Figure 7.3.5: Temperature-density phase diagram showing the points considered in Ref. [Brown et al. \[2013\]](#). Several values of the Coulomb coupling parameter Γ (dashed lines) and the electron degeneracy parameter Θ (dotted lines) are also shown. (Figure reproduced here by courtesy of the authors of Ref. [Brown et al. \[2013\]](#))

7.4 Some physical realizations and phenomenology

The Jellium model is a system of pointwise electrons of charge e and number density n in the three dimensional Euclidean space filled with an uniform neutralizing background of charge density $-en$. The zero temperature, ground-state, properties of the statistical mechanical system thus depends just on the electronic density n , or the Wigner-Seitz radius $r_s = (3/4\pi n)^{1/3}/a_0$ where a_0 is Bohr radius, or the Coulomb coupling parameter Γ .

The model can be used for example as a first approximation to describe free electrons in metallic elements [Ashcroft and Mermin \[1976\]](#) ($2 \lesssim r_s \lesssim 4$) or the interior of a white dwarf [Shapiro and Teukolsky \[1983\]](#) ($r_s \simeq 0.01$). More generally it is an essential ingredient for the study of ionic liquids (see Ref. [Hansen and McDonald \[1986\]](#) Chapter 10 and 11): *molten-salts*, *liquid-metals*, and *ionic-solutions*. In molten alkali halides the masses of the cation and the anion are comparable whereas in liquid metals the anions are replaced by electrons from the valence or conduction bands. The very small mass of the electron leads to a pronounced dissymmetry between the two species present in the metal. In particular, whereas the behavior of

the cations can be discussed in the framework of classical statistical mechanics, the electrons form a degenerate Fermi gas for which a quantum-mechanical treatment is required. Restricting to the class of simple metals in which the electronic valence states are well separated in energy from the tightly-bound core states; their properties are reasonably well described by the nearly-free-electron model. Metals that are classified in this sense include the alkali metals, magnesium, zinc, mercury, gallium, and aluminium. Other liquid metals (noble and transition metals, alkaline earths, lanthanides, and actinides) have more complicated electronic structures, and the theory of such systems is correspondingly less well advanced. Molten-salt solutions are mixtures of liquid metals and molten salts. Ionic-solutions are liquids consisting of a solvent formed by neutral, polar molecules, and a solute that dissociates into positive and negative ions. They vary widely in complexity: in the classic electrolyte solutions, the cations and anions are comparable in size and absolute charge, whereas macromolecular ionic solutions contain both macroions (charged polymers chains or coils, micelles, charged colloidal particles, etc.) and microscopic counterions.

Experimentally, Wigner crystallization was first unambiguously observed to occur in a quasi-classical, quasi-two-dimensional fluid of electrons floating on top of liquid ^4He substrate [Grimes and Adams \[1979\]](#). Such quasi-two-dimensional electron systems are currently realized in the laboratory in various semiconductors structures, but it has proven difficult to reach the very low temperatures needed for Wigner crystallization of electrons in the quantal regime without losing their collective behavior through the unavoidable presence of impurities. Furthermore, the application of a strong magnetic field to a quasi-two-dimensional electron fluid in semiconductor structures provides a very effective way to squeeze out the translational kinetic energy without going to very low densities. The Wigner crystallization in the exactly-two-dimensional Jellium has been found by DMC calculations to be past $r_s = 37 \pm 5$ [Tanatar and Ceperley \[1989\]](#).

Whereas the finite temperature properties of Jellium depends additionally on the electron degeneracy parameter Θ . Apart from its purely speculative interest, the temperature dependence of the Jellium properties are certainly of great astrophysical relevance. Examples are dense plasmas in the interior of giant planets [M. D. Knudson et al. \[2012\]](#) and brown dwarfs atmospheres. Other uses could be in highly compressed laboratory plasmas, such as laser plasmas [R. Ernstorfer et al. \[2009\]](#), inertial confinement fusion plasmas [L. B. Fletcher et al. \[2014\]](#), and pressure-induced modifications of solids, such as insulator-metal transitions [Mazzola et al. \[2014\]](#). These examples justify the growing interest recently emerged in matter under extreme conditions in the warm-dense regime [Dornheim et al. \[2016\]](#).

It would be desirable to perform a full quantum Monte Carlo simulation for the Restricted Primitive Model (RPM), an electrically neutral fluid of particles of opposite charge made thermodynamically stable by preventing the particles collapse through the inclusion of a hard core of a certain radius centered on each particle. Some attempts have been made for large mass asymmetries between the positive and negative charges requiring a mixed MC (classical) - DMC (quantum) treatment [Dewing and Ceperley \[2002\]](#); [Ceperley et al. \[2002\]](#) where one treats the slow ions through the Born-Oppenheimer approximation and the fast ones at zero temperature. Other alternatives could be a mixed MC - PIMC or more generally a full PIMC one.

Follows an excerpt from the last March and Tosi book [March and Tosi \[2002\]](#).

7.4.1 Molten halides and some alloys of metallic elements

Unlike monatomic fluid like liquid argon already for liquid sodium it is necessary to view it as formed of positive ions and conduction electrons. More obviously, one has to start from an ionic picture in describing a sodium chloride melt or liquid lithium iodide.

The crystal structures of halide compounds arise from electronic charge transfer and local compensation of positive and negative ionic charges through chemical order. Nature achieves

charge compensation in two qualitatively distinct ways. The first involves halogen sharing and high coordination for the metal ions, as for example in alkali, alkaline-earth and lanthanide metal halides. In the second type charge compensation takes place within well defined molecular units, either monomeric ones as for example in HgCl_2 and SbCl_3 or dimeric ones as in AlBr_3 .

Neutron diffraction studies of metal halide melts have shown that melting usually preserves the type of chemical order found in the crystal. For example, the melting of MgCl_2 or YC_3 can be viewed as a transition from an ionic crystal to an ionic liquid (ionic-to-ionic, in short) and that of SbCl_3 or AlBr_3 as a molecular-to-molecular transition. However, AlBr_3 and FeCl_3 are known instances of ionic-to-molecular melting. Intermediate-range order (IRO), extending over distances of 5 to 10 Å say, has been revealed in both network-type and molecular-type melts. This type of order is well known in glassy materials.

Alkali halide vapours

Even for alkali halides, the vapour at coexistence with the hot melt is made of molecular monomers and dimers. The same basic ionic model can account for cohesion in these molecules as in the solid and dense liquid states, provided that distortions of the electron shells of the ions from electrical and overlap effects are accounted for.

Coulomb ordering in monohalides and dihalides

Alkali halides

The nature of Coulomb ordering in a molten salt like NaCl is such that the distribution of the screening charge density around any given ion oscillates in space, rather than being a monotonic function of distance as in the Debye-Hückel theory. Nevertheless, a meaningful definition of screening length in a dense ionic fluid can be based on the Debye-Hückel concept of the potential drop across the dipole layer formed by an ion and by the screening charge distribution.

Noble-metal halides

The monovalent Cu^+ and Ag^+ ions, with an outer shell of ten *d*-electrons, have small ionic radius and large electronic polarisability in comparison with the corresponding alkali ions. These properties lead to some hybridisation and covalent binding in copper and silver halides, tending to favor low coordination of first neighbors and promoting remarkable transport behaviors.

The ionic conductivity of solid CuBr and CuI increases rapidly with temperature, already reaching values of $\approx 0.1 \Omega^{-1}\text{cm}^{-1}$ before attaining, through two structural phase transitions, fast-ion (superionic) behavior of the Cu^+ ions before melting. A phase transition is also exhibited by AgI at 147°C and is accompanied by a jump in ionic conductivity to a values of $\approx 1 \Omega^{-1}\text{cm}^{-1}$, typical of ionic melts. The Ag^+ ions in the α phase are disordered over many interstitial sites. Solid CuCl , AgCl and AgBr also show premelting phenomena, with the ionic conductivity rising to values of $0.1 - 0.5 \Omega^{-1}\text{cm}^{-1}$.

These materials melt at relatively low temperature with a relatively low entropy change, while the ionic conductivity of the melt is comparable to that of molten alkali halides. Excess entropy has been released in the crystal before melting through the massive disordering of the metal ions. Diffraction data are available for all melts of this family: overall, their liquid structure can be described in term of a random close-packing of halogens, accommodating the metal ions in tetrahedral-like coordinations.

Fluorite-type superionic conductors

Fluorite-type materials such as SrCl₂ undergo a diffuse transition to a high-conductivity state before melting. The ionic conductivity and the entropy increase rapidly but continuously with temperature across the transition, whereas the heat capacity shows a peak. A high dynamic concentration of anionic Frenkel defects (interstitial-vacancy pairs) is gradually created across the transition, as revealed by neutron diffraction and diffuse quasi-elastic scattering studies on a variety of materials including SrCl₂, CaF₂, PbF₂ and UO₂. In other materials, such as BaCl₂ and SrBr₂, a superionic state is attained through a structural phase transition to the fluorite structure.

The liquid structure of BaCl₂ and SrCl₂ has been determined by neutron diffraction using isotopic substitution. In both melts, within the frame of the divalent cations, the halogen ion component is more weakly ordered. The liquid structure thus shows a remnant of the fast-ion conducting state that the solid attains through an extensive disordering of the anions.

The observed short-range ordering in molten SrCl₂ and BaCl₂ suggests that freezing may be viewed as a process in which the cationic component is independently crystallising and at the same time modulating the anions into the lattice periodicity. The anionic component in the hot crystal near melting may thus be described as a modulated “lattice liquid”. In turn, the diffuse transition from the superionic to the “normal” state on cooling the SrCl₂ crystal may be viewed as a continuous process of anionic freezing inside the periodic force field of the metal-ion lattice.

Tetrahedral-network structure in ZnCl₂

The pair structure is also experimentally known for a number of other dihalide melts. The evolution of the liquid structure with increasing covalency versus ionicity of the bonding brings it from a cation-dominated structure to one in which the anions provide a “deformable frame” accommodating the doubly-charged cations. The Cl⁻-Cl⁻ structural correlations are not especially affected: the Cl-Cl bond length stays in the range 3.6 to 3.8 Å.

The state of pronounced IRO in molten ZnCl₂ arises from strongly stable local tetrahedral structures through the formation of a network of chlorines. The partial distribution functions can be interpreted as describing a disordered close-packed arrangement of chlorine ions which provides tetrahedral sites for the Zinc ions. Such a structural arrangement is very similar to that of the glassy state of ZnCl₂: the Zn-Cl bond length is practically the same in the two states and the average coordination number of Zn is reported as 3.8 in the glass and ≈ 4 in the melt.

7.4.2 Structure of trivalent-metal halides

Two main trends emerge from liquid structure studies on trichlorides: (i) the trend from cation-dominated Coulomb ordering to loose octahedral-network structures across the series of lanthanide compounds including YCl₃, and (ii) the stabilization of molecular structures with strong intermolecular correlations leading to IRO. The overall structural evolution is governed by the increasing weight of covalency versus ionicity.

Octahedral-network formation in lanthanide chlorides

X-ray diffraction data on the series of molten rare-earth trichlorides show similar structural characters. The d_{MCl} bond length lies in the range 2.7-2.9 Å while the second-neighbor bond lengths are $d_{MM} \approx 5$ Å and $d_{ClCl} \approx 4$ Å, indicating a Coulomb ordering primarily ruled by the repulsion between the cations as discussed earlier for SrCl₂. Ionic conductivity and Raman

scattering data suggest that the coordination of the metal ions is becoming more stable through the series, leading to a liquid structure which resembles a loose network of Cl-sharing octahedra.

Ionic-to-molecular melting in AlCl_3 and FeCl_3

YCl_3 is structurally isomorphous to AlCl_3 in the crystal phase. The octahedral coordination of the Y, Al and Fe ions in the crystal is apparent, which is basically preserved in YCl_3 on melting. The upper cluster illustrates the cooperative mechanism of metal-ion displacements by which the Al_2Cl_6 and Fe_2Cl_6 molecules can form on melting, each dimer being in the shape of two tetrahedra sharing an edge. In AlBr_3 such an arrangement of Al ions in tetrahedral sites already exists in the crystal. The melting of AlCl_3 and FeCl_3 also involves expansion of the chlorine packing.

Liquid haloaluminates

In AlCl_3 and AlBr_3 , while the pure melt is a molecular liquid, molten-salt behavior emerges on mixing with alkali halides. Complex anions are formed with the alkalis playing the role of counterions. Thus, starting from neutral Al_2Cl_6 dimers in the AlCl_3 liquid, the $(\text{Al}_2\text{Cl}_7)^-$ anion in the shape of two tetrahedra sharing a corner has been identified in mixtures with alkali chlorides. This anion is ultimately replaced by $(\text{AlCl}_4)^-$ anions at 1 : 1 stoichiometry.

The fluoroaluminates behave quite differently. The Na_3AlF_4 compound, known as cryolite, presents special interest because of its role in the industrial Haïl-Héroult process for the electrodeposition of Al metal from alumina. The Raman spectra of molten $(\text{AlF}_3)_c \cdot (\text{NaF})_{l-c}$ and other Al-alkali fluoride mixtures give evidence for a gradual conversion of $(\text{AlF}_4)^-$ into $(\text{AlFs})^{2-}$ and $(\text{AlF}_6)^-$ as the solution becomes more basic with c decreasing below 0.5.

Molecular-to-molecular melting in GaCl_3 and SbCl_3

For other trihalides, such as GaCl_3 and SbCl_3 molecular units can be recognized as constituents in the crystal structure. Crystalline GaCl_3 can be viewed as composed of Ga_2Cl_6 dimers. The crystal structure of SbCl_3 is instead built by packing chains of monomers in the shape of trigonal pyramids with metal ions at the apices. The stable molecular units in the vapour phase are the Ga_2Cl_6 dimer and the SbCl_3 monomer.

The liquid structure of SbCl_3 at 80 °C has been studied by a combination of X-ray and neutron diffraction. It can be described as arising from separate monomeric units with strong intermolecular correlations. Each metal ion has three additional chlorine neighbors from other molecules: such a strongly distorted octahedral arrangement could result from stacking the monomers in chains like umbrellas, the dipole axes of molecules within a chain being strongly correlated over at least one or two molecular diameters.

The neutron diffraction patterns measured for molten AlBr_3 , GaBr_3 and GaI_3 show three peaks at approximately 1.0, 1.9 and 3.4 \AA^{-1} . The corresponding pair distribution functions exhibit a very well defined coordination shell of first neighbors, with coordination number 4.0 ± 0.2 for AlBr_3 and GaBr_3 and 3.75 ± 0.2 for GaI_3 . The intermolecular correlations between halogens are quite significant, the corresponding coordination number being in the range typical of a random close-packing in the liquid state.

7.4.3 Chemical short-range order in liquid alloys

Fully ionized salts with a large band gap, like the alkali halides, remain ionic across melting. At the opposite extreme, melting of covalent semiconductors such as Ge and InSb involves a

collapse of the covalent structure, which is directly revealed by an increase of coordination from 4 to values in the range 6-8 and by a sharp increase in electrical conductivity to an essentially metallic type. Between these extremes a number of systems have been identified which show a variety of intermediate electronic behavior in the liquid phase.

The CsAu compound

The stoichiometric CsAu compound crystallizes in the CsCl-type structure and is a strongly polar semiconductor with an optical band gap of 2.6 eV at room temperature. Its electrical conductivity drops on melting to a value which is comparable to molten salts. Electromigration experiments give evidence that Cs migrates to the cathode and Au to the anode, one Cs^+ and one Au^- being transported per elementary charge to the electrodes.

A neutron diffraction study of the liquid structure of the Cs-Au alloy shows a structure in the neutron structure factor at $k = 1.2 \text{ \AA}^{-1}$, which is interpreted as the “Coulomb prepeak” characteristic of chemical order. After Fourier transform of these data, the Cs-Au first neighbor distance at 3.6 Å can be followed up to 80% Cs, while the Cs-Cs distance at 5.3 Å characteristic of the pure Cs metal start emerging at 70% Cs.

Other alkali-based alloys with chemical short-range order

Interspecies ordering as shown by the Cs-Au system has been reported for a number of other alkali-based alloys, the alloying partners being elements of group III, IV or V. The formation of chemical short-range order at certain compositions is signalled by anomalies in electronic properties such as the electrical resistivity and the magnetic susceptibility, which reflect a minimum in the electron density of states at the Fermi level if not the opening of a gap due to full charge transfer. Three different kinds of compound formation can be identified: (i) compound formation near the electronic octet composition A_4B as in Li-Pb or Li-Sn; (ii) compound formation near the equimolar composition AB, as in K-Pb or Rb-Pb; and (iii) compound formation near both these compositions, as in Li-Si, Li-Ge or Na-Sn. The data show increasing stability of the octet composition through the sequence Si, Ge, Sn and Pb, and decreasing stability through the sequence from Li to Cs.

A neutron diffraction measurement of the Bhatia-Thornton⁸ concentration-structure factor in Li_4Pb has shown chemical order extending over a range of about 20 Å in the corresponding $g_{cc}(r)$ distribution function. With regard to alkali-group IV alloys in the second and third classes mentioned above, such as K-Pb or Na-Sn, it has proposed a model for order at equimolar composition which invokes formation of essentially tetrahedral Pb_4 or Sn_4 polyanions. Such tetrahedral “Zintl ions” are seen in the crystal structure of the equiatomic compound. In such a tetrahedral cluster the p-type electron states of Pb, say, would be split into bonding and antibonding states and the former could be filled by electron transfer from the alkali atoms.

The presence of polyanions in Zintl alloys also has dynamical consequences. A striking case is NaSn, in which the Sn_4 polyanions are observed to undergo jump reorientations and thereby to enhance the diffusivity of the Na cations by a paddle-wheel mechanism. These two types of disorder appear simultaneously as the melting point is approached.

7.4.4 Liquid metals

Some properties of simple liquid metals having conduction electrons in *s* and *p* states, that specifically reflect their nature as two component liquids of ions and electrons are: (i) the effective

⁸A. B. Bhatia and D. E. Thornton, *Phys. Rev. B* **2**, 3004 (1970)

interaction between pairs of ions as determined by screening of their bare Coulomb repulsions by the conduction electrons; (ii) the structural correlation functions involving the conduction electrons and supplementing the nuclear structure factor $S(k)$ in a full description of the liquid-metal structure; and (iii) the theory of electrical resistivity and viscosity of liquid metals. For a general account of liquid metals the book of March [1990] may be consulted. in the limit when the effects of the ionic cores become negligible, we shall call the plasma particles “Jellium”.

References

- M. P. Allen and D. J. Tildesley. *Computer Simulation of Liquids*. Oxford University Press Inc, New York, 1987.
- J. B. Anderson. Quantum chemistry by random walk. $H\ ^2P$, $H_3^+ \ D_{3h} \ ^1A'_1$, $H_2 \ ^3\Sigma_u^+$, $H^4 \ ^1\Sigma_g^+$, $Be\ ^1S$. *J. Chem. Phys.*, 65:4121, 1976. doi: [10.1063/1.432868](https://doi.org/10.1063/1.432868).
- N. W. Ashcroft and N. D. Mermin. *Solid State Physics*. Thomson Learning Inc, Australia, 1976.
- R. Assaraf and M. Caffarel. Zero-variance zero-bias principle for observables in quantum Monte Carlo: Application to forces. *J. Chem. Phys.*, 119:10536, 2003. doi: [10.1063/1.1621615](https://doi.org/10.1063/1.1621615).
- R. N. Barnett, P. J. Reynolds, and J. W. A. Lester. Monte Carlo algorithms for expectation values of coordinate operators. *J. Comp. Phys.*, 96:258, 1991. doi: [10.1016/0021-9991\(91\)90236-E](https://doi.org/10.1016/0021-9991(91)90236-E).
- S. Baroni and S. Moroni. Reptation Quantum Monte Carlo: A Method for Unbiased Ground-State Averages and Imaginary-Time Correlations. *Phys. Rev. Lett.*, 82:4745, 1999. doi: [10.1103/PhysRevLett.82.4745](https://doi.org/10.1103/PhysRevLett.82.4745).
- A. Bijl. The lowest wave function of the symmetrical many particles system. *Physica*, 7:869, 1940. doi: [10.1016/0031-8914\(40\)90166-5](https://doi.org/10.1016/0031-8914(40)90166-5).
- M. Boninsegni, N. Prokof'ev, and B. Svistunov. Worm Algorithm for Continuous-Space Path Integral Monte Carlo Simulations. *Phys. Rev. Lett.*, 96:070601, 2006. doi: [10.1103/PhysRevLett.96.070601](https://doi.org/10.1103/PhysRevLett.96.070601).
- E. Brown, M. A. Morales, C. Pierleoni, and D. M. Ceperley. Quantum monte carlo techniques and applications for warm dense matter. In F. G. et al., editor, *Frontiers and Challenges in Warm Dense Matter*, pages 123–149. Springer, 2014.
- E. W. Brown, B. K. Clark, J. L. DuBois, and D. M. Ceperley. Path-Integral Monte Carlo Simulation of the Warm Dense Homogeneous Electron Gas. *Phys. Rev. Lett.*, 110:146405, 2013. doi: [10.1103/PhysRevLett.110.146405](https://doi.org/10.1103/PhysRevLett.110.146405).
- J. M. Caillol. Exact results for a two-dimensional one-component plasma on a sphere. *J. Phys. (France) - Lett.*, 42:L–245, 1981. doi: [10.1051/jphyslet:019810042012024500](https://doi.org/10.1051/jphyslet:019810042012024500).
- D. M. Ceperley. Ground state of the fermion one-component plasma: A Monte Carlo study in two and three dimensions. *Phys. Rev. B*, 18:3126, 1978. doi: [10.1103/PhysRevB.18.3126](https://doi.org/10.1103/PhysRevB.18.3126).
- D. M. Ceperley. Fermion nodes. *J. Stat. Phys.*, 63:1237, 1991. doi: [10.1007/BF01030009](https://doi.org/10.1007/BF01030009).
- D. M. Ceperley. Path integrals in the theory of condensed helium. *Rev. Mod. Phys.*, 67:279, 1995. doi: [10.1103/RevModPhys.67.279](https://doi.org/10.1103/RevModPhys.67.279).

- D. M. Ceperley. Path integral monte carlo methods for fermions. In K. Binder and G. Ciccotti, editors, *Monte Carlo and Molecular Dynamics of Condensed Matter Systems*, Bologna, Italy, 1996. Editrice Compositori.
- D. M. Ceperley. Introduction to quantum monte carlo methods applied to the electron gas. In G. F. Giuliani and G. Vignale, editors, *Proceedings of the International School of Physics Enrico Fermi*, pages 3–42, Amsterdam, 2004. IOS Press. Course CLVII.
- D. M. Ceperley and B. J. Alder. Ground State of the Electron Gas by a Stochastic Method. *Phys. Rev. Lett.*, 45:566, 1980. doi: [10.1103/PhysRevLett.45.566](https://doi.org/10.1103/PhysRevLett.45.566).
- D. M. Ceperley and M. H. Kalos. Quantum many-body problems. In K. Binder, editor, *Monte Carlo Methods in Statistical Physics*, page 145. Springer-Verlag, Heidelberg, 1979.
- D. M. Ceperley, M. Dewing, and C. Pierleoni. The coupled electronic-ionic monte carlo simulation method. In *Bridging Time Scales: Molecular Simulations for the Next Decade*, pages 473–500. Springer-Verlag, 2002.
- S. Chiesa, D. M. Ceperley, R. M. Martin, and M. Holzmann. Finite-Size Error in Many-Body Simulations with Long-Range Interactions. *Phys. Rev. Lett.*, 97:076404, 2006. doi: [10.1103/PhysRevLett.97.076404](https://doi.org/10.1103/PhysRevLett.97.076404).
- P. Choquard. The two-dimensional one-component plasma on a periodic strip. *Helv. Phys. Acta*, 54:332, 1981.
- M. Dewing and D. M. Ceperley. Methods for Coupled Electronic-Ionic Monte Carlo. In W. A. Lester, S. M. Rothstein, and S. Tanaka, editors, *Recent Advances in Quantum Monte Carlo Methods, II*. World Scientific, Singapore, 2002.
- M. W. C. Dharma-wardana and F. Perrot. Simple Classical Mapping of the Spin-Polarized Quantum Electron Gas: Distribution Functions and Local-Field Corrections. *Phys. Rev. Lett.*, 84:959, 2000. doi: [10.1103/PhysRevLett.84.959](https://doi.org/10.1103/PhysRevLett.84.959).
- R. B. Dingle. LI. The zero-point energy of a system of particles. *Philos. Mag.*, 40:573, 1949. doi: [10.1080/14786444908521743](https://doi.org/10.1080/14786444908521743).
- T. Dornheim, S. Groth, T. Sjostrom, F. D. Malone, W. M. C. Foulkes, and M. Bonitz. *Ab Initio* Quantum Monte Carlo Simulation of the Warm Dense Electron Gas in the Thermodynamic Limit. *Phys. Rev. Lett.*, 117:156403, 2016. doi: [10.1103/PhysRevLett.117.156403](https://doi.org/10.1103/PhysRevLett.117.156403).
- S. Dutta and J. Dufty. Classical representation of a quantum system at equilibrium: Applications. *Phys. Rev. E*, 87:032102, 2013. doi: [10.1103/PhysRevE.87.032102](https://doi.org/10.1103/PhysRevE.87.032102).
- R. Fantoni. Two component plasma in a Flamm's paraboloid. *J. Stat. Mech.*, page P04015, 2012. doi: [10.1088/1742-5468/2012/04/P04015](https://doi.org/10.1088/1742-5468/2012/04/P04015).
- R. Fantoni. Radial distribution function in a diffusion Monte Carlo simulation of a Fermion fluid between the ideal gas and the Jellium model. *Solid State Communications*, 159:106, 2013. doi: [10.1140/epjb/e2013-40204-3](https://doi.org/10.1140/epjb/e2013-40204-3).
- R. Fantoni. Exact results for one dimensional fluids through functional integration. *J. Stat. Phys.*, 163:1247, 2016. doi: [10.1007/s10955-016-1510-3](https://doi.org/10.1007/s10955-016-1510-3).
- R. Fantoni. One-component fermion plasma on a sphere at finite temperature. *Int. J. Mod. Phys. C*, 29:1850064, 2018. doi: [10.1142/S012918311850064X](https://doi.org/10.1142/S012918311850064X).

- R. Fantoni. How Should We Choose the Boundary Conditions in a Simulation Which Could Detect Anyons in One and Two Dimensions? *J. Low Temp. Phys.*, 202:247, 2021. doi: [10.1007/s10909-020-02532-0](https://doi.org/10.1007/s10909-020-02532-0).
- R. Fantoni. One-component fermion plasma on a sphere at finite temperature. The anisotropy in the paths conformations. *J. Stat. Mech.*, page 083103, 2023. doi: [10.1088/1742-5468/aceb54](https://doi.org/10.1088/1742-5468/aceb54).
- R. Fantoni and G. Téllez. Two dimensional one-component plasma on a Flamm's paraboloid. *J. Stat. Phys.*, 133:449, 2008. doi: [10.1007/s10955-008-9616-x](https://doi.org/10.1007/s10955-008-9616-x).
- R. Fantoni, B. Jancovici, and G. Téllez. Pressures for a One-Component Plasma on a Pseudo-sphere. *J. Stat. Phys.*, 112:27, 2003. doi: [10.1023/A:1023671419021](https://doi.org/10.1023/A:1023671419021).
- E. Feenberg. *Theory of Quantum Fluids*. Academic Press Inc, New York, 1969.
- R. P. Feynman. The λ -Transition in Liquid Helium. *Phys. Rev.*, 90:1116, 1953a. doi: [10.1103/PhysRev.90.1116.2](https://doi.org/10.1103/PhysRev.90.1116.2).
- R. P. Feynman. Atomic Theory of the λ Transition in Helium. *Phys. Rev.*, 91:1291, 1953b. doi: [10.1103/PhysRev.91.1291](https://doi.org/10.1103/PhysRev.91.1291).
- R. P. Feynman. Atomic Theory of Liquid Helium Near Absolute Zero. *Phys. Rev.*, 91:1301, 1953c. doi: [10.1103/PhysRev.91.1301](https://doi.org/10.1103/PhysRev.91.1301).
- R. P. Feynman. *Statistical Mechanics: A Set of Lectures*. Addison-Wesley Publishing Company Inc, Reading, 1972. Section 9.6; Chapter 8.
- R. P. Feynman and M. Cohen. Energy Spectrum of the Excitations in Liquid Helium. *Phys. Rev.*, 102:1189, 1956. doi: [10.1103/PhysRev.102.1189](https://doi.org/10.1103/PhysRev.102.1189).
- R. P. Feynman and A. R. Hibbs. *Quantum Mechanics and Path Integrals*. McGraw-Hill Inc, New York, 1965. pp. 292-293.
- W. M. C. Foulkes, L. Mitas, R. J. Needs, and G. Rajagopal. Quantum Monte Carlo simulations of solids. *Rev. Mod. Phys.*, 73:33, 2001. doi: [10.1103/RevModPhys.73.33](https://doi.org/10.1103/RevModPhys.73.33).
- T. Gaskell. The Collective Treatment of a Fermi Gas: II. *Proc. Phys. Soc.*, 77:1182, 1961. doi: [10.1088/0370-1328/77/6/312](https://doi.org/10.1088/0370-1328/77/6/312).
- T. Gaskell. The Collective Treatment of Many-body Systems: III. *Proc. Phys. Soc.*, 80:1091, 1962. doi: [10.1088/0370-1328/80/5/307](https://doi.org/10.1088/0370-1328/80/5/307).
- R. Gaudoin and J. M. Pitarke. Hellman-Feynman Operator Sampling in Diffusion Monte Carlo Calculations. *Phys. Rev. Lett.*, 99:126406, 2007. doi: [10.1103/PhysRevLett.99.126406](https://doi.org/10.1103/PhysRevLett.99.126406).
- G. F. Giuliani and G. Vignale. *Quantum Theory of the Electron Liquid*. Cambridge University Press, Cambridge, 2005.
- C. C. Grimes and G. Adams. Evidence for a Liquid-to-Crystal Phase Transition in a Classical, Two-Dimensional Sheet of Electrons. *Phys. Rev. Lett.*, 42:795, 1979. doi: [10.1103/PhysRevLett.42.795](https://doi.org/10.1103/PhysRevLett.42.795).
- U. Gupta and A. K. Rajagopal. Exchange-correlation potential for inhomogeneous electron systems at finite temperatures. *Phys. Rev. A*, 22:2792, 1980. doi: [10.1103/PhysRevA.22.2792](https://doi.org/10.1103/PhysRevA.22.2792).

- J. M. Hammersley and D. C. Handscomb. *Monte Carlo Methods*. Fletcher & Son Ltd, Norwich, 1964. pp. 57-59.
- J. P. Hansen. Statistical Mechanics of Dense Ionized Matter. I. Equilibrium Properties of the Classical One-Component Plasma. *Phys. Rev. A*, 8:3096, 1973. doi: [10.1103/PhysRevA.8.3096](https://doi.org/10.1103/PhysRevA.8.3096).
- J. P. Hansen and I. R. McDonald. *Theory of Simple Liquids*. Academic Press, Amsterdam, 1986.
- J. P. Hansen and P. Vieillefosse. Quantum corrections in dense ionized matter. *Phys. Lett. A*, 53:187, 1975. doi: [10.1016/0375-9601\(75\)90523-X](https://doi.org/10.1016/0375-9601(75)90523-X).
- T. L. Hill. *Statistical Mechanics. Principles and Selected Applications*. McGraw-Hill Book Company Inc, Toronto, 1956.
- S. Ichimaru. Strongly coupled plasmas: high-density classical plasmas and degenerate electron liquids. *Rev. Mod. Phys.*, 54:1017, 1982. doi: [10.1103/RevModPhys.54.1017](https://doi.org/10.1103/RevModPhys.54.1017).
- B. Jancovici. *Physica (Amsterdam)*, 91A:152, 1978.
- B. Jancovici. Exact Results for the Two-Dimensional One-Component Plasma. *Phys. Rev. Lett.*, 46:386, 1981. doi: [10.1103/PhysRevLett.46.386](https://doi.org/10.1103/PhysRevLett.46.386).
- R. Jastrow. Many-Body Problem with Strong Forces. *Phys. Rev.*, 98:1479, 1955. doi: [10.1103/PhysRev.98.1479](https://doi.org/10.1103/PhysRev.98.1479).
- M. D. Jones and D. M. Ceperley. Crystallization of the One-Component Plasma at Finite Temperature. *Phys. Rev. Lett.*, 76:4572, 1996. doi: [10.1103/PhysRevLett.76.4572](https://doi.org/10.1103/PhysRevLett.76.4572).
- M. H. Kalos and P. A. Whitlock. *Monte Carlo Methods*. John Wiley & Sons Inc, New York, 1986.
- M. H. Kalos, D. Levesque, and L. Verlet. Helium at zero temperature with hard-sphere and other forces. *Phys. Rev. A*, 9:2178, 1974. doi: [10.1103/PhysRevA.9.2178](https://doi.org/10.1103/PhysRevA.9.2178).
- J. Kolorenc and L. Mitas. Applications of quantum Monte Carlo methods in condensed systems. *Rep. Prog. Phys.*, 74:026502, 2011. doi: [10.1088/0034-4885/74/2/026502](https://doi.org/10.1088/0034-4885/74/2/026502).
- Y. Kwon, D. M. Ceperley, and R. M. Martin. Effects of three-body and backflow correlations in the two-dimensional electron gas. *Phys. Rev. B*, 48:12037, 1993. doi: [10.1103/PhysRevB.48.12037](https://doi.org/10.1103/PhysRevB.48.12037).
- Y. Kwon, D. M. Ceperley, and R. M. Martin. Effects of backflow correlation in the three-dimensional electron gas: Quantum Monte Carlo study. *Phys. Rev. B*, 58:6800, 1998. doi: [10.1103/PhysRevB.58.6800](https://doi.org/10.1103/PhysRevB.58.6800).
- L. B. Fletcher *et al.* Observations of Continuum Depression in Warm Dense Matter with X-Ray Thomson Scattering. *Phys. Rev. Lett.*, 112:145004, 2014. doi: [10.1103/PhysRevLett.112.145004](https://doi.org/10.1103/PhysRevLett.112.145004).
- L. Šamaj. Is the Two-Dimensional One-Component Plasma Exactly Solvable? *J. Stat. Phys.*, 117:131, 2004. doi: [10.1023/B:JOSS.0000044056.19438.2c](https://doi.org/10.1023/B:JOSS.0000044056.19438.2c).
- L. D. Landau and E. M. Lifshitz. *Statistical Physics*, volume 5 of *Course of Theoretical Physics*. Butterworth-Heinemann, Oxford, 1951.

- L. D. Landau and E. M. Lifshitz. *Quantum Mechanics. Non-relativistic Theory*, volume 3. Pergamon Press Ltd, Oxford, 1977. Course of Theoretical Physics.
- A. J. Leggett. A theoretical description of the new phases of liquid ^3He . *Rev. Mod. Phys.*, 47: 331, 1975. doi: [10.1103/RevModPhys.47.331](https://doi.org/10.1103/RevModPhys.47.331).
- A. Lerda. *Anyons. Quantum Mechanics of Particles with Fractional Statistics*. Springer-Verlag, Berlin, 1992.
- C. Lin, F. H. Zong, and D. M. Ceperley. Twist-averaged boundary conditions in continuum quantum Monte Carlo algorithms. *Phys. Rev. E*, 64:016702, 2001. doi: [10.1103/PhysRevE.64.016702](https://doi.org/10.1103/PhysRevE.64.016702).
- K. S. Liu, M. H. Kalos, and G. V. Chester. Quantum hard spheres in a channel. *Phys. Rev. A*, 10:303, 1974. doi: [10.1103/PhysRevA.10.303](https://doi.org/10.1103/PhysRevA.10.303).
- M. D. Knudson et al. Probing the Interiors of the Ice Giants: Shock Compression of Water to 700GPa and $3.8\text{g}/\text{cm}^3$. *Phys. Rev. Lett.*, 108:091102, 2012. doi: [10.1103/PhysRevLett.108.091102](https://doi.org/10.1103/PhysRevLett.108.091102).
- N. H. March. *Liquid Metals. Concepts and theory*. Cambridge University Press, Cambridge, 1990.
- N. H. March and M. P. Tosi. *Coulomb Liquids*. Academic Press Inc Ltd, London, 1984.
- N. H. March and M. P. Tosi. *Introduction to Liquid State Physics*. World Scientific Publishing Co Pte Ltd, Singapore, 2002.
- P. A. Martin. Sum rules in charged fluids. *Rev. Mod. Phys.*, 60:1075, 1988. doi: [10.1103/RevModPhys.60.1075](https://doi.org/10.1103/RevModPhys.60.1075).
- G. Mazzola, S. Yunoki, and S. Sorella. Unexpectedly high pressure for molecular dissociation in liquid hydrogen by electronic simulation. *Nat. Commun.*, 5:3487, 2014. doi: [10.1038/ncomms4487](https://doi.org/10.1038/ncomms4487).
- N. Metropolis, A. W. Rosenbluth, M. N. Rosenbluth, A. M. Teller, and E. Teller. Equations of State Calculations by Fast Computing Machines. *J. Chem. Phys.*, 1087:21, 1953. doi: [10.1063/1.1699114](https://doi.org/10.1063/1.1699114).
- V. Natoli and D. M. Ceperley. An Optimized Method for Treating Long-Range Potentials. *Comput. Phys.*, 117:171, 1995. doi: [10.1006/jcph.1995.1054](https://doi.org/10.1006/jcph.1995.1054).
- G. Ortiz and P. Ballone. Correlation energy, structure factor, radial distribution function, and momentum distribution of the spin-polarized uniform electron gas. *Phys. Rev. B*, 50:1391, 1994. doi: [10.1103/PhysRevB.50.1391](https://doi.org/10.1103/PhysRevB.50.1391).
- R. M. Panoff and J. Carlson. Fermion Monte Carlo algorithms and liquid ^3He . *Phys. Rev. Lett.*, 62:1130, 1989. doi: [10.1103/PhysRevLett.62.1130](https://doi.org/10.1103/PhysRevLett.62.1130).
- S. Paziani, S. Moroni, P. Gori-Giorgi, and G. B. Bachelet. Local-spin-density functional for multideterminant density functional theory. *Phys. Rev. B*, 73:155111, 2006. doi: [10.1103/PhysRevB.73.155111](https://doi.org/10.1103/PhysRevB.73.155111).
- J. P. Perdew and A. Zunger. Self-interaction correction to density-functional approximations for many-electron systems. *Phys. Rev. B*, 23:5048, 1981. doi: [10.1103/PhysRevB.23.5048](https://doi.org/10.1103/PhysRevB.23.5048).

- F. Perrot and M. W. C. Dharma-wardana. Exchange and correlation potentials for electron-ion systems at finite temperatures. *Phys. Rev. A*, 30:2619, 1984. doi: [10.1103/PhysRevA.30.2619](https://doi.org/10.1103/PhysRevA.30.2619).
- F. Perrot and M. W. C. Dharma-wardana. Spin-polarized electron liquid at arbitrary temperatures: Exchange-correlation energies, electron-distribution functions, and the static response functions. *Phys. Rev. B*, 62:16536, 2000. doi: [10.1103/PhysRevB.62.16536](https://doi.org/10.1103/PhysRevB.62.16536).
- D. Pines and P. Nozières. *Theory of Quantum Liquids*. W. A. Benjamin Inc, New York, 1966.
- E. L. Pollock. Properties and computation of the Coulomb pair density matrix. *Computer Physics Communications*, 52:49, 1988. doi: [10.1016/0010-4655\(88\)90171-3](https://doi.org/10.1016/0010-4655(88)90171-3).
- E. L. Pollock and D. M. Ceperley. Path-integral computation of superfluid densities. *Phys. Rev. B*, 36:8343, 1987. doi: [10.1103/PhysRevB.36.8343](https://doi.org/10.1103/PhysRevB.36.8343).
- E. L. Pollock and J. P. Hansen. Statistical Mechanics of Dense Ionized Matter. II. Equilibrium Properties and Melting Transition of the Crystallized One-Component Plasma. *Phys. Rev. A*, 8:3110, 1973. doi: [10.1103/PhysRevA.8.3110](https://doi.org/10.1103/PhysRevA.8.3110).
- R. Ernststorfer *et al.* The formation of warm dense matter: experimental evidence for electronic bond hardening in gold. *Science*, 323:5917, 2009. doi: [10.1126/science.1162697](https://doi.org/10.1126/science.1162697).
- S. L. Shapiro and S. A. Teukolsky. *Black Holes, White Dwarfs, and Neutron Stars. The Physics of Compact Objects*. John Wiley & Sons Inc, New York, 1983.
- K. S. Singwi and M. P. Tosi. *Sol. State Phys.*, 36:177, 1981. ed. H. Ehrenreich, F. Seitz and D. Turnbull (Academic, New York, 1981) Vol. 36, p. 177.
- K. S. Singwi, M. P. Tosi, R. H. Land, and A. Sjölander. Electron Correlations at Metallic Densities. *Phys. Rev.*, 176:589, 1968. doi: [10.1103/PhysRev.176.589](https://doi.org/10.1103/PhysRev.176.589).
- S. Tanaka and S. Ichimaru. Thermodynamics and Correlational Properties of Finite-Temperature Electron Liquids in the Singwi-Tosi-Land-Sjölander Approximation. *Journal of the Physical Society of Japan*, 55:2278, 1986. doi: [10.1143/JPSJ.55.2278](https://doi.org/10.1143/JPSJ.55.2278).
- B. Tanatar and D. M. Ceperley. Ground state of the two-dimensional electron gas. *Phys. Rev. B*, 39:5005, 1989. doi: [10.1103/PhysRevB.39.5005](https://doi.org/10.1103/PhysRevB.39.5005).
- J. Toulouse, R. Assaraf, and C. J. Umrigar. Zero-variance zero-bias quantum Monte Carlo estimators of the spherically and system-averaged pair density. *J. Chem. Phys.*, 126:244112, 2007. doi: [10.1063/1.2746029](https://doi.org/10.1063/1.2746029).
- C. J. Umrigar, M. P. Nightingale, and K. J. Runge. A diffusion Monte Carlo algorithm with very small time-step errors. *J. Chem. Phys.*, 99:2865, 1993. doi: [10.1063/1.465195](https://doi.org/10.1063/1.465195).
- P. Vieillefosse. Coulomb pair density matrix I. *J. Stat. Phys.*, 74:1195, 1994. doi: [10.1007/BF02188223](https://doi.org/10.1007/BF02188223).
- P. Vieillefosse. Coulomb pair density matrix. II. *J. Stat. Phys.*, 80:461, 1995. doi: [10.1007/BF02178368](https://doi.org/10.1007/BF02178368).
- E. P. Wigner. On the Interaction of Electrons in Metals. *Phys. Rev.*, 46:1002, 1934. doi: [10.1103/PhysRev.46.1002](https://doi.org/10.1103/PhysRev.46.1002).

Appendices

7.A Ideal gas energy and exchange energy as a function of polarization

For the general case of N_+ spin-up particles the Fermi wave-vector for the spin-up (spin-down) particles will be

$$k_F^\pm = (1 \pm \xi)^{1/3} k_F, \quad (7.A.1)$$

with

$$k_F = (3\pi^2 n)^{1/3} = (9\pi/4)^{1/3}/a_0 r_s, \quad (7.A.2)$$

the Fermi wave-vector of the unpolarized fluid.

The Fermi energy will be

$$k_B T_F = \sum_{\sigma} \frac{(\hbar k_F^{\sigma})^2}{2m} \quad (7.A.3)$$

$$= \frac{\hbar^2 [(1 + \xi)^{2/3} + (1 - \xi)^{2/3}] k_F^2}{2m}. \quad (7.A.4)$$

The degeneracy parameter will then be

$$\Theta = \frac{2m}{\hbar^2} \left(\frac{1}{3\pi^2 n} \right)^{2/3} \left(\frac{k_B T}{[(1 + \xi)^{2/3} + (1 - \xi)^{2/3}]} \right). \quad (7.A.5)$$

Then finding κ^+ and κ^- from the following equations

$$I(1/2, \kappa^+) = \frac{2}{3} \Theta^{-3/2} \frac{(1 + \xi)}{[(1 + \xi)^{2/3} + (1 - \xi)^{2/3}]^{3/2}}, \quad (7.A.6)$$

$$I(1/2, \kappa^-) = \frac{2}{3} \Theta^{-3/2} \frac{(1 - \xi)}{[(1 + \xi)^{2/3} + (1 - \xi)^{2/3}]^{3/2}}, \quad (7.A.7)$$

we can determine the kinetic energy per particle of the partially polarized, $0 < \xi < 1$, ideal Fermi gas

$$e_0 = \frac{2r_s^3}{3\pi\beta^{5/2}} \frac{1}{Ry^{5/2}} \left[\frac{I(3/2, \kappa^+)}{(1 + \xi)} + \frac{I(3/2, \kappa^-)}{(1 - \xi)} \right]. \quad (7.A.8)$$

The exchange energy on the other hand will be

$$\begin{aligned} e_x &= -\frac{r_s^3}{3\pi^2\beta^2} \frac{1}{\text{Ry}^2} \times \\ &\left[\frac{1}{(1+\xi)} \int_0^\infty \frac{dx}{1+e^{x-\kappa^+}} \int_0^\infty \frac{dy}{1+e^{y-\kappa^+}} \int_{-1}^1 \frac{dz}{\sqrt{x/y} + \sqrt{y/x} - 2z} \right. \\ &\left. + \frac{1}{(1-\xi)} \int_0^\infty \frac{dx}{1+e^{x-\kappa^-}} \int_0^\infty \frac{dy}{1+e^{y-\kappa^-}} \int_{-1}^1 \frac{dz}{\sqrt{x/y} + \sqrt{y/x} - 2z} \right], \end{aligned} \quad (7.A.9)$$

7.B Jastrow, backflow, and three-body

In terms of the stochastic process governed by $f(R, t)$ one can write, using Kac theorem [Kac 1959, 1951]

$$\int dR f(R, \tau) = \left\langle \exp \left[- \int_0^\tau dt E_L(R^t) \right] \right\rangle_{\text{DRW}}, \quad (7.B.1)$$

where $\langle \dots \rangle_{\text{DRW}}$ means averaging with respect to the diffusing and drifting random-walk. Choosing a complete set of orthonormal wave-functions Ψ_i we can write for the true time dependent many-body wave-function

$$\begin{aligned} \phi(R, \tau) &= \sum_i \Psi_i(R) \int dR' \Psi_i(R') \phi(R', \tau) \approx \Psi(R) \int dR f(R, \tau) \\ &= \Psi(R) \left\langle \exp \left[- \int_0^\tau dt E_L(R^t) \right] \right\rangle_{\text{DRW}}, \end{aligned} \quad (7.B.2)$$

where Ψ is the wave-function, of the set, of maximum overlap with the true ground-state, the trial wave-function. Assuming that at time zero we are already close to the stationary solution, for sufficiently small τ we can approximate

$$\left\langle \exp \left[- \int_0^\tau dt E_L(R^t) \right] \right\rangle_{\text{DRW}} \approx e^{-\tau E_L(R^\tau)}. \quad (7.B.3)$$

By antisymmetrising we get the Fermion wave-function

$$\phi_F(R, \tau) \approx \mathcal{A} \left[e^{-\tau E_L(R)} \Psi(R) \right], \quad (7.B.4)$$

where given a function $f(R)$ we define the operator (a symmetry of the Hamiltonian)

$$\mathcal{A}[f(R)] = \frac{1}{N_{\mathcal{P}}} \sum_{\mathcal{P}} (-1)^{\mathcal{P}} f(\mathcal{P}R), \quad (7.B.5)$$

here $N_{\mathcal{P}} = N_+!N_-!$ is the total number of allowed permutations \mathcal{P} .

This is called the local energy method to improve a trial wave-function. Suppose we start from a simple unsymmetrical product of single particle plane waves of N_+ spin-up particles with $k < k_F^+$ occupied and N_- spin-up particles with $k < k_F^-$ occupied, for the zeroth order trial wave-function. Equation (7.B.4) will give us a first order wave-function of the Slater-Jastrow type (see

equation (7.2.16)). If we start from an unsymmetrical Hartree-Jastrow trial wave-function the local energy with the Jastrow factor has the form

$$E_L = V - \lambda \sum_i \left[-k_i^2 - 2ik_i \cdot \nabla_i \sum_{j < k} u(r_{jk}) - \nabla_i^2 \sum_{j < k} u(r_{jk}) + \left| \nabla_i \sum_{j < k} u(r_{jk}) \right|^2 \right], \quad (7.B.6)$$

where $V = V(R)$ is the total potential energy and $r_{ij} = |\mathbf{r}_{ij}| = |\mathbf{r}_i - \mathbf{r}_j|$. Then the antisymmetrized second order wave-function has the form in Eq. (7.2.31), which includes backflow (see the third term), which is the correction inside the determinant and which affects the nodes, and three-body boson-like correlations (see last term) which do not affect the nodes.

7.C The Random-Phase-Approximation

In this Appendix we will work on an unpolarized system.

Within the linear density response theory Hansen and McDonald [1986]⁹ one introduces the space-time Fourier transform, $\chi(\mathbf{k}, \omega)$, of the linear density response function. Which is related through the fluctuation dissipation theorem, $S(\mathbf{k}, \omega) = -(2\hbar/n)\Theta(\omega)\text{Im}\chi(\mathbf{k}, \omega)$, to the space-time Fourier transform, $S(\mathbf{k}, \omega)$ (dynamic structure factor), of the van Hove correlation function van Hove [1954], $\langle \rho(\mathbf{r}, t)\rho(\mathbf{0}, 0) \rangle / n$, where $\rho(\mathbf{r}, t) = \exp(iHt/\hbar)\rho(\mathbf{r})\exp(-iHt/\hbar)$.

In the Random-Phase-Approximation (RPA) we have Pines and Nozières [1966]

$$\frac{1}{\chi_{RPA}(\mathbf{k}, \omega)} = \frac{1}{\chi_0(\mathbf{k}, \omega)} - e^2 \tilde{v}_\mu(\mathbf{k}), \quad (7.C.1)$$

where χ_0 is the response function of the non-interacting Fermions (ideal Fermi gas), known as the Lindhard susceptibility Lindhard [1954]. This corresponds to taking the “proper polarizability” (the response to the Hartree potential) equal to the response of the ideal Fermi gas Tosi [1999]. With the help of the fluctuation dissipation theorem, $S_0(\mathbf{k}, \omega) = -(2\hbar/n)\Theta(\omega)\text{Im}\chi_0(\mathbf{k}, \omega)$ gives the differential cross-section for inelastic scattering from the ideal Fermi gas (at energy transfer $\omega \geq 0$). Scattering is due to the excitation of single particle-hole pairs

$$S_0(\mathbf{k}, \omega) = 2\pi \sum_{\mathbf{q}, \sigma} n_{\mathbf{q}}^0 [1 - n_{\mathbf{q}+\mathbf{k}}^0] \delta \left[\omega - \frac{1}{\hbar} (e_{\mathbf{q}+\mathbf{k}} - e_{\mathbf{q}}) \right], \quad (7.C.2)$$

where $e_{\mathbf{k}} = \hbar^2 k^2 / (2m)$ and $n_{\mathbf{k}}^0 = \Theta(|\mathbf{k}| - k_F)$ is the momentum distribution of the ideal Fermi gas. We thus find

$$S_0(\mathbf{k}, \omega) = \begin{cases} \hbar \pi \nu_F \frac{\omega}{k v_F} & 0 \leq \omega \leq -\omega_2(k) \\ \hbar \pi \nu_F \frac{k_F}{2k} \left[1 - \left(\frac{\omega}{k v_F} - \frac{k}{2k_F} \right)^2 \right] & |\omega_2(k)| \leq \omega \leq \omega_1(k) \\ 0 & \omega \geq \omega_1(k) \end{cases} \quad (7.C.3)$$

with $\nu_F = m k_F / (n \pi^2 \hbar^2)$ the density of states for particles at the Fermi level, $v_F = \hbar k_F / m$ the velocity of a free particle on the Fermi surface, $\omega_1(k) = \hbar(kk_F + k^2/2)/m$, and $\omega_2(k) = \hbar(-kk_F + k^2/2)/m$. Naturally we also have $S^x(k) = \int S_0(\mathbf{k}, \omega) d\omega / (2\pi)$.

The RPA static structure factor is then recovered through

$$S_{RPA}(k) = -\frac{\hbar}{n} \int_0^\infty \frac{d\omega}{\pi} \text{Im}\chi(k, \omega). \quad (7.C.4)$$

⁹Note that, unlike in the classical case, in quantum statistical physics even the linear response to a static perturbation requires the use of imaginary time correlation functions Martin [1988].

where

$$\text{Im}\chi = \frac{\text{Im}\chi_0}{(1 - e^2\tilde{v}_\mu \text{Re}\chi_0)^2 + (e^2\tilde{v}_\mu \text{Im}\chi_0)^2} , \quad (7.C.5)$$

and

$$\text{Im}\chi_0 = -\frac{n}{2\hbar}S_0 , \quad \omega > 0 , \quad (7.C.6)$$

$$\text{Re}\chi_0 = -n\nu_F \left\{ \frac{1}{2} + \frac{1-(x-y)^2}{8y} \ln \left| \frac{x-1-y}{x+1-y} \right| + \frac{1-(x+y)^2}{8y} \ln \left| \frac{x+1+y}{x-1+y} \right| \right\} \quad (7.C.7)$$

where $x = \omega/kv_F$ and $y = k/2k_F$. In deriving Eq. (7.C.7) we used the fact that $\text{Im}\chi_0(k, \omega)$ is an odd function of ω and the Kramers-Kronig relations.

7.D Analytic expressions for the non-interacting fermions ground state

Usually $g_{\sigma,\sigma'}$ is conventionally divided into the (known) exchange and the (unknown) correlation terms

$$g_{\sigma,\sigma'} = g_{\sigma,\sigma'}^x + g_{\sigma,\sigma'}^c , \quad (7.D.1)$$

where the exchange term corresponds to the uniform system of non-interacting fermions.

7.D.1 Radial distribution function

We thus have (from the definition of the RDF (7.2.37) and using Slater determinants for the wave-function)

$$g_{+-}^x(r) = 1 , \quad (7.D.2)$$

$$g_{\sigma,\sigma}^x(r) = 1 - \left[\frac{3j_1(k_F^\sigma r)}{k_F^\sigma r} \right]^2 , \quad (7.D.3)$$

where $j_1(x) = [\sin(x) - x \cos(x)]/x^2$ is the spherical Bessel function of the first kind and $(k_F^\sigma)^3 = 6\pi^2 n_\sigma$ is the Fermi wave-number for particles of spin σ .

7.D.2 Static structure factor

Again we will have the splitting $S_{\sigma,\sigma'} = S_{\sigma,\sigma'}^x + S_{\sigma,\sigma'}^c$ into the exchange and the correlation parts. So that for the non-interacting fermions we get

$$S_{+-}^x(k) = 0 , \quad (7.D.4)$$

$$\begin{aligned} S_{\sigma,\sigma}^x(k) &= \frac{n_\sigma}{n} - \frac{n_\sigma^2}{n} \Theta(2k_F^\sigma - k) \frac{3\pi^2}{(k_F^\sigma)^3} \left(1 - \frac{k}{2k_F^\sigma} \right)^2 \left(2 + \frac{k}{2k_F^\sigma} \right) \\ &= \frac{n_\sigma}{n} \begin{cases} 1 & k > 2k_F^\sigma \\ \frac{3}{4} \frac{k}{k_F^\sigma} - \frac{1}{16} \left(\frac{k}{k_F^\sigma} \right)^3 & k < 2k_F^\sigma \end{cases} , \end{aligned} \quad (7.D.5)$$

where $\Theta(x)$ is the Heaviside step function.

7.D.3 Internal energy

The Hartree-Fock approximation [Hartree \[1928\]](#); [Fock \[1930\]](#); [Slater \[1930\]](#) for the ground state of a system of interacting fermions assumes that the many-body wave function is a Slater determinant built from single-particle states, which are to be determined self-consistently by minimization of the expectation value of the Hamiltonian. Whereas for an inhomogeneous many-electron system (e.g. an atom or a molecule) the solution of the Hartree-Fock self-consistent problem can usually be obtained only in a numerical form involving further approximations, the exact Hartree-Fock solution is immediate in the case of a homogeneous fluid: in this case the self-consistent single-particle states are necessarily plane waves, from translational invariance. Hence, the Hartree-Fock wave function for the ground-state of a homogeneous fluid is the same as the ground-state wave function of the ideal Fermi gas.

Including explicitly the spin indices we get

$$E_g^{\text{HF}} = \sum_{\mathbf{k},\sigma} n_{\mathbf{k},\sigma}^0 \left[\epsilon_{\mathbf{k}} + \frac{1}{2} \Sigma_{\text{HF}}(\mathbf{k}) \right], \quad (7.\text{D}.6)$$

where $n_{\mathbf{k},\sigma}^0$ is the ideal Fermi distribution, $\epsilon_{\mathbf{k}} = \hbar^2 k^2 / 2m$ and for an unpolarized system

$$\Sigma_{\text{HF}}(\mathbf{k}) = v_0 + \frac{1}{N} \sum_q v_q n_{\mathbf{k}+\mathbf{q},\sigma}^0 \quad (7.\text{D}.7)$$

$$= -\frac{e^2 k_F}{\pi} \left[1 + \frac{k_F^2 - k^2}{2k k_F} \ln \left| \frac{k + k_F}{k - k_F} \right| \right], \quad (7.\text{D}.8)$$

here $v_0 = v_{\mathbf{q}=0}$ and $v_q = 4\pi e^2/q^2$. So that

$$e_g^{\text{HF}} = E_g^{\text{HF}}/N = \left(\frac{3}{5\alpha^2 r_s^2} - \frac{3}{2\pi\alpha r_s} \right) \text{Ry} = \left(\frac{2.21}{r_s^2} - \frac{0.916}{r_s} \right) \text{Ry}, \quad (7.\text{D}.9)$$

with $\alpha = (9\pi/4)^{-1/3}$. As already remarked, the gain in potential energy found in Hartree-Fock derives from the fact that the exclusion principle is built into the many-body wave function and keeps apart pairs of electrons with parallel spins, thus lowering their Coulomb repulsive interaction energy on average. Notice that the ratio between potential and kinetic energy is proportional to r_s : this dimensionless length gives a measure of the coupling strength, which increases with decreasing density. The main problem with the Hartree-Fock approximation is that, by including exchange between electrons with parallel spins but neglecting correlations due to the Coulomb repulsions (which are most effective for electrons with antiparallel spins), it includes neither dielectric screening nor the collective plasma excitation. As shown in section [7.2.4](#) the Hartree-Fock ground-state can be determined from the exchange part of the radial distribution function (see Eqs. [\(7.D.2\)-\(7.D.3\)](#)).

When one proceeds to evaluate the ground-state energy of Jellium by perturbation theory beyond first order (i.e. beyond Hartree-Fock), one meets divergences arising from the long-range character of the Coulomb interactions. On summing to infinite order the most strongly divergent terms of the perturbative expansion (corresponding to the RPA theory), screening introduces a cut-off as the lower end of integrals over wave vector space and cures the divergences [Gell-Mann and Bruckner \[1957\]](#). Such a calculation, supplemented by the inclusion of a contribution from second-order exchange processes, yields the low r_s expansion

$$e_g(r_s) = \left[\frac{2.21}{r_s^2} - \frac{0.916}{r_s} + 0.0622 \ln r_s - 0.096 + \dots \right] \text{Ry}, \quad (7.\text{D}.10)$$

plus terms going like r_s , $r_s \ln r_s$, etc. The results of such a truncated expansion is reasonably accurate only up to $r_s = 1$, whereas the values of r_s that are relevant in the physics of normal metals extend up to $r_s = 6$.

In the thirties Wigner [1934, 1938] had already noticed that an optimal value $e_{\text{pot}} = -(1.8/r_s)\text{Ry}$ is obtained for the potential energy if the electrons are placed on the sites of a crystalline lattice having body-centered-cubic (bcc) structure. The gain by a factor ≈ 2 over the potential energy in Hartree-Fock is clearly related to the fact that in the crystal all pairs of electrons keep apart irrespectively of their relative spin orientation. Using the crystalline result at large r_s in combination with an estimate of the correlation energy at low r_s , Wigner proposed the interpolation formula

$$e_g^W = \left[\frac{2.21}{r_s^2} - \frac{0.916}{r_s} - \frac{0.88}{7.8 + r_s} \right] \text{Ry}, \quad (7.D.11)$$

as approximately valid at metallic densities.

7.E Radial distribution functions sum rules for the electron gas ground state

Both the behavior of the RDF at small r and at large r has to satisfy to general exact relations or sum rules.

7.E.1 Cusp conditions

When two electrons ($\mu = \infty$) get closer and closer together, the behavior of $g_{\sigma,\sigma'}(r)$ is governed by the exact cusp conditions Kimball [1973]; Rajagopal et al. [1978]; Hoffmann-Ostenhof et al. [1992]

$$\left. \frac{d}{dr} g_{\sigma,\sigma}(r) \right|_{r \rightarrow 0} = 0, \quad (7.E.1)$$

$$\left. \frac{d^3}{dr^3} g_{\sigma,\sigma}(r) \right|_{r \rightarrow 0} = \frac{3}{2a_0} \left. \frac{d^2}{dr^2} g_{\sigma,\sigma}(r) \right|_{r \rightarrow 0}, \quad (7.E.2)$$

$$\left. \frac{d}{dr} g_{+,-}(r) \right|_{r \rightarrow 0} = \frac{1}{a_0} g_{+,-}(0), \quad (7.E.3)$$

where in the adimensional units $a_0 \rightarrow 1/r_s$. For finite μ we only have the condition $g_{\sigma,\sigma}(0) = 0$ due to Pauli exclusion principle.

7.E.2 The Random-Phase-Approximation (RPA) and the long range behavior of the RDF

The small k behavior of the RPA, summarized in Appendix 7.C, is exact Pines and Nozières [1966]. One finds

$$S_{RPA}(k) = \frac{\hbar k^2}{2m\omega_p}, \quad k \ll k_F, \quad (7.E.4)$$

where $\omega_p = \sqrt{4\pi ne^2/m}$ is the plasmon frequency Giuliani and Vignale [2005]. This is also known as the second-moment sum rule for the exact RDF and can be rewritten as $n \int dr r^2[g(r) -$

$1] = -6(\hbar/2m\omega_p)$. We can then say that $g(r) - 1$ has to decay faster than r^{-5} at large r . The fourth-moment (or compressibility) sum rule links the thermodynamic compressibility, $\chi = [nd(n^2 de_0/dn)/dn]^{-1}$, Tosi [1999] to the fourth-moment of the RDF. For the equivalent classical system it is well known that the correlation functions have to decay faster than any inverse power of the distance Alastuey and Martin [1985]; Martin [1988]; Lighthill [1959] (in accord with the Debye-Hückel theory). To the best of our knowledge we do not know, yet, the exact decay for the zero temperature quantum case.

7.F The primitive action

Suppose the Hamiltonian is split into two pieces $\mathcal{H} = \mathcal{T} + \mathcal{V}$, where $\mathcal{C}\text{al}$ and \mathcal{V} are the kinetic and potential operators. Recall the exact Baker-Campbell-Hausdorff formula to expand $\exp(-\tau\mathcal{H})$ into the product $\exp(-\tau\mathcal{T})\exp(-\tau\mathcal{V})$. As $\tau \rightarrow 0$ the commutator terms which are of order higher than τ^2 become smaller than the other terms and thus can be neglected. This is known as the *primitive approximation*

$$e^{-\tau(\mathcal{T}+\mathcal{V})} \approx e^{-\tau\mathcal{T}} e^{-\tau\mathcal{V}}. \quad (7.F.1)$$

hence we can approximate the exact density matrix by product of the density matrices for \mathcal{T} and \mathcal{V} alone. One might worry that this would lead to an error as $M \rightarrow \infty$, with small errors building up to a finite error. According to the Trotter Trotter [1959] formula, one does not have to worry

$$e^{-\beta(\mathcal{T}+\mathcal{V})} = \lim_{M \rightarrow \infty} [e^{-\tau\mathcal{T}} e^{-\tau\mathcal{V}}]^M. \quad (7.F.2)$$

The Trotter formula holds if the three operators \mathcal{T} , \mathcal{V} , and $\mathcal{T} + \mathcal{V}$ are self-adjoint and make sense separately, for example, if their spectrum is bounded below Simon [1979]. This is the case for the Hamiltonian describing Jellium.

Let us now write the primitive approximation in position space

$$\rho(R_0, R_2; \tau) \approx \int dR_1 \langle R_0 | e^{-\tau\mathcal{T}} | R_1 \rangle \langle R_1 | e^{-\tau\mathcal{V}} | R_2 \rangle, \quad (7.F.3)$$

and evaluate the kinetic and potential density matrices. Since the potential operator is diagonal in the position representation, its matrix elements are trivial

$$\langle R_1 | e^{-\tau\mathcal{V}} | R_2 \rangle = e^{-\tau V(R_1)} \delta(R_2 - R_1). \quad (7.F.4)$$

The kinetic matrix can be evaluated using the eigenfunction expansion of \mathcal{T} . Consider, for example, the case of distinguishable particles in a cube of side L with periodic boundary conditions. Then the exact eigenfunctions and eigenvalues of \mathcal{T} are $L^{-3N/2} e^{iK_n R}$ and λK_n^2 , with $K_n = 2\pi n/L$ and n a $3N$ -dimensional integer vector. We are using here dimensional units. Then

$$\langle R_0 | e^{-\tau\mathcal{T}} | R_1 \rangle = \sum_n L^{-3N} e^{-\tau\lambda K_n^2} e^{-iK_n(R_0 - R_1)} \quad (7.F.5)$$

$$= (4\pi\lambda\tau)^{-3N/2} \exp\left[-\frac{(R_0 - R_1)^2}{4\lambda\tau}\right], \quad (7.F.6)$$

where $\lambda = \hbar^2/2m$. Eq. (7.F.6) is obtained by approximating the sum by an integral. This is appropriate only if the thermal wavelength of one step is much less than the size of the box,

$\lambda\tau \ll L^2$. In some special situations this condition could be violated, in which case one should use Eq. (7.F.5) or add periodic “images” to Eq. (7.F.6). The exact kinetic density matrix in periodic boundary conditions is a theta function, $\prod_{i=1}^{3N} \theta_3(z_i, q)$, where $z = \pi(R_0^i - R_1^i)/L$, R^i is the i th component of the $3N$ dimensional vector R , and $q = e^{-\lambda\tau(2\pi/L)^2}$ (see chapter 16 of Ref. Abramowitz and Stegun [1970]). Errors from ignoring the boundary conditions are $O(q)$, exponentially small at large M .

A *link* m is a pair of time slices (R_{m-1}, R_m) separated by a *time step* $\tau = \beta/M$. The *action* S^m of a link is defined as minus the logarithm of the exact density matrix. Then the exact path integral expression becomes

$$\rho(R_0, R_M; \beta) = \int dR_1 \dots dR_{M-1} \exp \left[- \sum_{m=1}^M S^m \right], \quad (7.F.7)$$

It is convenient to separate out the *kinetic action* from the rest of the action. The exact kinetic action for link m will be denoted K^m

$$K^m = \frac{3N}{2} \ln(4\pi\lambda\tau) + \frac{(R_{m-1} - R_m)^2}{4\lambda\tau}, \quad (7.F.8)$$

The *inter-action* is then defined as what is left

$$U^m = U(R_{m-1}, R_m; \tau) = S^m - K^m. \quad (7.F.9)$$

In the primitive approximation the inter-action is

$$U_1^m = \frac{\tau}{2} [V(R_{m-1}) + V(R_m)], \quad (7.F.10)$$

where we have symmetrized U_1^m with respect to R_{m-1} and R_m , since one knows that the exact density matrix is symmetric and thus the symmetrized form is more accurate.

A capital letter U refers to the total link inter-action. One should not think of the exact U as being strictly the potential action. That is true for the primitive action but, in general, is only correct in the small- τ limit. The exact U also contains kinetic contributions of higher order in τ . If a subscript is present on the inter-action, it indicates the order of approximation; the primitive approximation is only correct to order τ . No subscript implies the exact inter-action.

The *residual energy* of an approximate density matrix is defined as

$$E_A(R, R'; t) = \frac{1}{\rho_A(R, R'; t)} \left[\mathcal{H} + \frac{\partial}{\partial t} \right] \rho_A(R, R'; t). \quad (7.F.11)$$

The residual energy for an exact density matrix vanishes; it is a local measure of the error of an approximate density matrix. The Hamiltonian \mathcal{H} is a function of R ; thus the residual energy is not symmetric in R and R' .

It is useful to write the residual energy as a function of the inter-action. We find

$$E_A(R, R'; t) = V(R) - \frac{\partial U_A}{\partial t} - \frac{(R - R') \cdot \nabla U_A}{t} + \lambda \nabla^2 U_A - \lambda (\nabla U_A)^2. \quad (7.F.12)$$

The terms on the right hand side are ordered in powers of τ , keeping in mind that $U(R)$ is of order τ , and $|R - R'|$ is of order $\tau^{1/2}$. One obtains the primitive action by setting the residual energy to zero and dropping the last three terms on the right hand side.

The residual energy of the primitive approximation is

$$E_1(R, R'; t) = \frac{1}{2} [V(R) - V(R')] - \frac{1}{2} (R - R') \cdot \nabla V + \frac{\lambda t}{2} \nabla^2 V - \frac{\lambda t^2}{4} (\nabla V)^2. \quad (7.F.13)$$

With a leading error of $\sim \lambda\tau^2$.

7.G The pair-product action

An often useful method to determine the many-body action is to use the exact action for two electrons Barker [1979]. To justify this approach, first assume that the potential energy can be broken into a pairwise sum of terms

$$V(R) = \sum_{i < j} v(|\mathbf{r}_i - \mathbf{r}_j|), \quad (7.G.1)$$

with $|\mathbf{r}_i - \mathbf{r}_j| = r_{ij}$. Next, apply the Feynman-Kac formula for the inter-action

$$e^{-U(R_0, R_F; \tau)} = \left\langle \exp \left[- \int_0^\tau dt V(R(t)) \right] \right\rangle_{\text{RW}}, \quad (7.G.2)$$

where the notation $\langle \dots \rangle_{\text{RW}}$ means the average over all Gaussian random-walks from R_0 to R_F in a “time” τ . So that

$$e^{-U(R_0, R_F; \tau)} = \left\langle \exp \left[- \int_0^\tau dt \sum_{i < j} v(r_{ij}(t)) \right] \right\rangle_{\text{RW}} \quad (7.G.3)$$

$$= \left\langle \prod_{i < j} \exp \left[- \int_0^\tau dt v(r_{ij}(t)) \right] \right\rangle_{\text{RW}} \quad (7.G.4)$$

$$\approx \prod_{i < j} \left\langle \exp \left[- \int_0^\tau dt v(r_{ij}(t)) \right] \right\rangle_{\text{RW}} \quad (7.G.5)$$

$$= \prod_{i < j} \exp [-u_2(r_{ij}, r'_{ij}; \tau)] \quad (7.G.6)$$

$$= \exp \left[- \sum_{i < j} u_2(r_{ij}, r'_{ij}; \tau) \right] = e^{-U_2(R_0, R_F; \tau)}, \quad (7.G.7)$$

where U_2 is the *pair-product* action and u_2 is the exact action for a pair of electrons. At low temperatures the pair action approaches the solution of the two particle wave equation. The result is the pair-product or Jastrow ground-state wave function, which is the ubiquitous choice for a correlated wave function because it does such a good job of describing most ground-state correlations.

The residual energy (see Eq. (7.F.11)) for the pair-product action is less singular than for other forms. We have that

$$u_2(r_{ij}, r'_{ij}; \tau) = -\ln \left\langle \exp \left(- \int_0^\tau dt v(r_{ij}(t)) \right) \right\rangle_{\text{RW}}, \quad (7.G.8)$$

is of order τ^2 since the two body problem can be factorized into a center-of-mass term and a term that is a function of the relative coordinates. Moreover we must have

$$\frac{\partial u_2}{\partial \tau} = v(r_{ij}(\tau)), \quad (7.G.9)$$

so that

$$\frac{\partial U_2}{\partial \tau} = V(R(\tau)), \quad (7.G.10)$$

which tells that only the last three terms on the right hand side of Eq. (7.F.12) contribute to the residual energy. We also have

$$\nabla U_2 = \sum_i \sum_{i \neq j} \nabla_i u_2(r_{ij}, r'_{ij}; \tau), \quad (7.G.11)$$

where the indices run over the particles. So the leading error of the pair-product action is $\sim \lambda \tau^3$.

7.H Linear-Response-Theory

Linear response theory e Ph. Nozières [1966]; March and Tosi [1984]; Hansen and McDonald [1986] is a well known framework to describe the approach to thermal equilibrium in response to an external perturbation acting on a many-body quantum fluid.

Let us introduce the density linear response function $K(\mathbf{r} - \mathbf{r}', t - t')$ for a homogeneous fluid. Let us indicate with V_b the “bare” potential in vacuum.

The coupling of the fluid to the perturbing potential is described by the Hamiltonian

$$H'(t) = \int d\mathbf{r} \rho(\mathbf{r}) V_b(\mathbf{r}, t), \quad (7.H.1)$$

where $\rho(\mathbf{r})$ is the density operator (here we implicitly assume that the mean value of the density has been subtracted from $\rho(\mathbf{r})$). We will just consider the linear effect of this perturbation. The change in density is given by

$$\delta n(\mathbf{r}, t) = \langle \rho(\mathbf{r}) \rangle - \langle \rho(\mathbf{r}) \rangle_0 = \text{tr}\{[w(t) - w_0]\rho(\mathbf{r})\}, \quad (7.H.2)$$

where tr denotes the trace, $w(t) = \int \psi^*(\mathbf{R}, t)\psi(\mathbf{R}, t) d^{3N}R$ is the perturbed density matrix whose unperturbed counterpart is $w_0 = \exp(-\beta H_0)/\text{tr}\{\exp(-\beta H_0)\}$, and $\beta = 1/k_B T$ with k_B the Boltzmann constant and T the absolute temperature. We are indicating with $\psi(\mathbf{R}, t)$ the many-body wave function of the fluid with particles at positions $\mathbf{R} = (\mathbf{r}_1, \mathbf{r}_2, \dots, \mathbf{r}_N)$ at time t . This satisfies to the Schrödinger equation

$$i\hbar \frac{\partial \psi(\mathbf{R}, t)}{\partial t} = [H_0 + H'(t)]\psi(\mathbf{R}, t), \quad (7.H.3)$$

where H is the Hamiltonian of the unperturbed fluid. Then the perturbed density matrix satisfies to

$$\begin{aligned} i\hbar \frac{\partial w(t)}{\partial t} &= [H_0 + H'(t), w(t)] \\ &\approx [H_0, w(t) - w_0] + [H'(t), w_0], \end{aligned} \quad (7.H.4)$$

where $[A, B]$ denotes the commutator $AB - BA$ and in the last step we have linearized the effect of the perturbation and used $[H_0, w_0] = 0$. This equation is subject to the initial condition

$$\lim_{t \rightarrow -\infty} w(t) = w_0, \quad (7.H.5)$$

representing a state of thermal equilibrium.

The linearized equation (7.H.4) has the following solution

$$w(t) - w_0 = (i\hbar)^{-1} \int_{-\infty}^t dt' \exp\{-iH_0(t-t')/\hbar\} [H'(t'), w_0] \exp\{iH_0(t-t')/\hbar\}. \quad (7.H.6)$$

Inserting this result into Eq. (7.H.2) and using the cyclic invariance of the trace, $\text{tr}\{AB\} = \text{tr}\{BA\}$, we can write the desired result as follows

$$\delta n(\mathbf{r}, t) = (-i/\hbar) \int d\mathbf{r}' \int_{-\infty}^t dt' \langle [\rho(\mathbf{r}, t), \rho(\mathbf{r}', t')] \rangle_0 V_b(\mathbf{r}', t). \quad (7.H.7)$$

Again the angle parenthesis $\langle A \rangle_0 = \text{tr}\{w_0 A\}$ denotes the mean value on the equilibrium state and $\rho(\mathbf{r}, t)$ is the Heisenberg operator

$$\rho(\mathbf{r}, t) = \exp(iH_0 t/\hbar) \rho(\mathbf{r}) \exp(-iH_0 t/\hbar). \quad (7.H.8)$$

So

$$K(\mathbf{r} - \mathbf{r}', t - t') = (-i/\hbar) \theta(t - t') \langle [\rho(\mathbf{r}, t), \rho(\mathbf{r}', t')] \rangle_0. \quad (7.H.9)$$

This result clearly embodies the causality property through the Heaviside step function θ .

Introducing the notation

$$\chi''(k, t - t') = (1/2\hbar) \int d(\mathbf{r} - \mathbf{r}') \exp[-i\mathbf{k} \cdot (\mathbf{r} - \mathbf{r}')] \langle [\rho(\mathbf{r}, t), \rho(\mathbf{r}', t')] \rangle_0, \quad (7.H.10)$$

we see, from Eq. (7.H.9) that the Fourier transform of K is the convolution integral of the Fourier transform of $\chi''(k, t)$, that we will indicate with $\chi''(k, \omega)$, and of the Heaviside step function, that is equal to $i/(\omega + i\eta)$ with η a small positive quantity. We can then write the space-time Fourier transform of K like so

$$\chi(k, \omega) = - \int_{-\infty}^{\infty} \frac{d\omega'}{\pi} \chi''(k, \omega') / (\omega - \omega' + i\eta). \quad (7.H.11)$$

Using the rule $(\omega + i\eta)^{-1} = P(1/\omega) - i\pi\delta(\omega)$, where P denotes the Cauchy principal part, this can be written like so

$$\chi(k, \omega) = -P \int_{-\infty}^{\infty} \frac{d\omega'}{\pi} \chi''(k, \omega') / (\omega - \omega') + i\chi''(k, \omega). \quad (7.H.12)$$

Since $\chi''(k, t)$ is written in terms of the commutator of Hermitian operators it can be readily shown that $\chi''(k, \omega)$ must be real. So we can write

$$\text{Im}\chi(k, \omega) = \chi''(k, \omega). \quad (7.H.13)$$

7.H.1 Fluctuation-dissipation theorem

We now worry about the relationship between the density response function and the van Hove dynamic response $S(\mathbf{k}, \omega)$. Let us define the autocorrelation density function as

$$G(\mathbf{r} - \mathbf{r}', t - t') = \frac{1}{n} \langle \rho(\mathbf{r}, t) \rho(\mathbf{r}', t') \rangle_0, \quad (7.H.14)$$

whose space-time Fourier transform is $S(\mathbf{k}, \omega)$. The connection between G e K that gush from Eq. (7.H.9) can be rewritten in Fourier transform like so

$$\chi(\mathbf{k}, \omega) = (n/\hbar) \int_{-\infty}^{\infty} \frac{d\omega'}{2\pi} [S(\mathbf{k}, \omega) - S(-\mathbf{k}, -\omega)] / (\omega - \omega' + i\eta). \quad (7.H.15)$$

This has the same form of Eq. (7.H.11) so that

$$\text{Im}\chi(\mathbf{k}, \omega) = (-n/2\hbar)[S(\mathbf{k}, \omega) - S(-\mathbf{k}, -\omega)]. \quad (7.\text{H}.16)$$

For a fluid in thermodynamic equilibrium we must have

$$S(-\mathbf{k}, -\omega) = \exp(-\hbar\beta\omega)S(\mathbf{k}, \omega). \quad (7.\text{H}.17)$$

In order to prove this property we observe that its inverse space-time Fourier transform reads

$$G(-\mathbf{r}, -t) = \exp\left(-i\hbar\beta\frac{\partial}{\partial t}\right)G(\mathbf{r}, t), \quad (7.\text{H}.18)$$

since under time Fourier transform $\partial/\partial t \rightarrow -i\omega$. But Eq. (7.H.18) can readily be proven through the following steps (where, once again we use the cyclic invariance of the trace and the definition of the Heisenberg operator, Eq. (7.H.8))

$$\begin{aligned} \text{tr}\{\exp(-\beta H_0)\rho(\mathbf{0}, 0)\rho(\mathbf{r}, t)\} &= \text{tr}\{\rho(\mathbf{r}, t)\exp(-\beta H_0)\rho(\mathbf{0}, 0)\} \\ &= \text{tr}\{\exp(-\beta H_0)\rho(\mathbf{r}, t - i\hbar\beta)\rho(\mathbf{0}, 0)\} \\ &= \exp(-i\hbar\beta\partial/\partial t)\text{tr}\{\exp(-\beta H_0)\rho(\mathbf{r}, t)\rho(\mathbf{0}, 0)\}. \end{aligned} \quad (7.\text{H}.19)$$

In the classical limit, for β small, Eq. (7.H.16) becomes

$$\text{Im}\chi(\mathbf{k}, \omega) = (-n\beta\omega/2)S(\mathbf{k}, \omega). \quad (7.\text{H}.20)$$

7.H.2 Kramers-Kronig relations

Causality imposes that the response function $K(\mathbf{r}, t)$ vanish for $t < 0$. In other words the fluid is influenced only by the action of the external perturbation in the past. Introducing the “intermediate” response function $\chi(\mathbf{k}, t)$ as the space Fourier transform of $K(\mathbf{r}, t)$, we have

$$\chi(\mathbf{k}, t) = 0 \quad \text{for } t < 0. \quad (7.\text{H}.21)$$

On the other hand

$$\chi(\mathbf{k}, t) = \int_{-\infty}^{\infty} \frac{d\omega}{2\pi} \exp(-i\omega t)\chi(\mathbf{k}, \omega). \quad (7.\text{H}.22)$$

Extending the definition of $\chi(\mathbf{k}, \omega)$ from real to complex frequencies, we can calculate this integral through contour methods and for $t < 0$ we can close the contour with the semicircle at infinity above the real axis. The contribution from the integration on the semicircle vanishes since $\chi(\mathbf{k}, \omega) \propto \omega^{-2}$ at high frequency. So the causality property (7.H.21) is guaranteed if $\chi(\mathbf{k}, \omega)$ is analytic in the upper part of the complex frequency plane.

Let us now consider the integral

$$\oint \frac{\chi(\mathbf{k}, \omega')}{\omega - \omega'} d\omega' = 0, \quad (7.\text{H}.23)$$

on the contour Γ shown in Fig. 7.H.1. This contour integral vanishes due to the analyticity of $\chi(\mathbf{k}, \omega)$. The contribution from the semicircle at infinity is again zero, so that

$$P \int_{-\infty}^{\infty} d\omega' \frac{\chi(\mathbf{k}, \omega')}{\omega' - \omega} - i\pi\chi(\mathbf{k}, \omega) = 0, \quad (7.\text{H}.24)$$

where again P denotes the Cauchy principal part of the integral on the real frequency axis and the second term comes from the integration over the small semicircle around the point ω . If we now separate $\chi(\mathbf{k}, \omega)$ into its real and imaginary parts we find

$$P \int_{-\infty}^{\infty} d\omega' \frac{\text{Re}\chi(\mathbf{k}, \omega')}{\omega' - \omega} + \pi \text{Im}\chi(\mathbf{k}, \omega) = 0, \quad (7.\text{H}.25)$$

and

$$P \int_{-\infty}^{\infty} d\omega' \frac{\text{Im}\chi(\mathbf{k}, \omega')}{\omega' - \omega} - \pi \text{Re}\chi(\mathbf{k}, \omega) = 0. \quad (7.\text{H}.26)$$

These are the Kramers-Kronig relations.

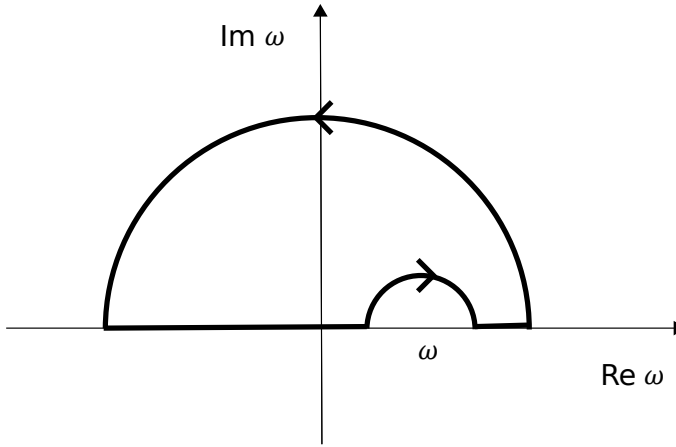


Figure 7.H.1: Integration contour on the complex ω plane.

7.H.3 The dielectric function

In a Coulomb liquid, the connection with the longitudinal dielectric function $\epsilon(\mathbf{k}, \omega)$, becomes apparent from the Poisson equations

$$\nabla \cdot \mathbf{D}(\mathbf{r}, t) = -4\pi e n_e(\mathbf{r}, t), \quad (7.\text{H}.27)$$

$$\nabla \cdot \mathbf{E}(\mathbf{r}, t) = -4\pi e [n_e(\mathbf{r}, t) + \delta n(\mathbf{r}, t)], \quad (7.\text{H}.28)$$

which yield

$$\frac{1}{\epsilon(\mathbf{k}, \omega)} = \frac{\mathbf{k} \cdot \mathbf{E}(\mathbf{k}, \omega)}{\mathbf{k} \cdot \mathbf{D}(\mathbf{k}, \omega)} = 1 + \frac{\delta n(\mathbf{k}, \omega)}{n_e(\mathbf{k}, \omega)} = 1 + \frac{4\pi e^2}{k^2} \chi(\mathbf{k}, \omega), \quad (7.\text{H}.29)$$

since from Eqs. (7.H.7) and (7.H.9) follows $\delta n(\mathbf{k}, \omega) = \chi(\mathbf{k}, \omega) V_b(\mathbf{k}, \omega)$ where $\chi(\mathbf{k}, \omega)$ is the Fourier transform of $K(|\mathbf{r} - \mathbf{r}'|, t - t')$ and

$$V_b(\mathbf{k}, \omega) = \frac{4\pi e^2}{k^2} n_e(\mathbf{k}, \omega). \quad (7.\text{H}.30)$$

Of course the field \mathbf{E} and the associated screened or “Hartree” potential $V_H(\mathbf{k}, \omega) = V_b(\mathbf{k}, \omega)/\epsilon(\mathbf{k}, \omega)$ would be experienced by a second test charge introduced into the plasma, rather than by the particles of the plasma. The latter also experience effects which involve the precise “hole” a particle of the plasma digs around itself. This latter effect brings about the so called local field corrections.

In addition to $\chi(\mathbf{k}, \omega)$ which relates the displaced charge density to the potential *in vacuo*, it is useful to introduce yet another longitudinal response function, $\tilde{\chi}(\mathbf{k}, \omega)$ say, by exploiting further the analogy with elementary electrostatics. This relates $n(\mathbf{k}, \omega)$ directly to the Hartree potential through

$$n(\mathbf{k}, \omega) = \tilde{\chi}(\mathbf{k}, \omega)V_H(\mathbf{k}, \omega). \quad (7.H.31)$$

We then have

$$\epsilon(\mathbf{k}, \omega) = 1 - \frac{4\pi e^2}{k^2} \tilde{\chi}(\mathbf{k}, \omega). \quad (7.H.32)$$

The expression $\chi(\mathbf{k}, \omega) = \tilde{\chi}(\mathbf{k}, \omega)/\epsilon(\mathbf{k}, \omega)$ accounts at one stroke for the *long range* effects of the Coulomb interactions (the resonance at the plasma frequency, determined by $\epsilon(\mathbf{k}, \omega) = 0$, is brought about explicitly in the denominator).

The simplest useful approximation to the dielectric function of the plasma is obtained by approximating $\tilde{\chi}$ by the density response function of an ideal gas. This corresponds to the Vlasov theory for the classical plasma and to the Lindhard theory for the degenerate electron fluid. Refinements of these theories aims at incorporating the effects of “exchange and correlation” in $\tilde{\chi}$. This expression being an abbreviation for the short range effects arising from the statistics (“exchange”) and long range effect arising from the Coulomb interaction (“correlation”). Of course the exchange effects are absent in the classical limit.

7.I Long-range potentials with the Ewalds image technique

Suppose the bare potential in infinite d dimensional space is $v(r)$. Let us define the Fourier transform by

$$\tilde{v}_{\mathbf{k}} = \int_{-\infty}^{\infty} d^d r e^{-i\mathbf{k}\cdot\mathbf{r}} v(r) . \quad (7.I.1)$$

Then its inverse is

$$v(r) = \int_{-\infty}^{\infty} \frac{d^d \mathbf{k}}{(2\pi)^d} e^{i\mathbf{k}\cdot\mathbf{r}} \tilde{v}_{\mathbf{k}} . \quad (7.I.2)$$

Now let us find the energy of a single particle interacting with an infinite rectangular lattice of another particle a distance r away. To make it converge we also add a uniform background of the same density (Ω =volume) of opposite charge. Thus the “image pair-potential” is equal to

$$v_I(r) = \sum_{\mathbf{L}} v(\mathbf{r} + \mathbf{L}) - \tilde{v}_0/\Omega . \quad (7.I.3)$$

The \mathbf{L} sum is over the Bravais lattice of the simulation cell $\mathbf{L} = (m_x L_x, m_y L_y, \dots)$ where m_x, m_y, \dots range over all positive and negative integers. Converting this to k -space and using the Poisson sum formula we get

$$v_I(r) = \frac{1}{\Omega} \sum'_{\mathbf{k}} \tilde{v}_{\mathbf{k}} e^{i\mathbf{k}\cdot\mathbf{r}} , \quad (7.I.4)$$

where the prime indicates that we omit the $\mathbf{k} = 0$ term; it cancels out with the background. The \mathbf{k} -sum is over reciprocal lattice vectors of the simulation box $\mathbf{k} = (2\pi n_x/L_x, 2\pi n_y/L_y, \dots)$.

Because both sums are so poorly convergent, we make the division into \mathbf{k} -space and \mathbf{r} -space; taking the long-range part into \mathbf{k} -space. We write

$$v(\mathbf{r}) = v_s(\mathbf{r}) + v_l(\mathbf{r}), \quad (7.I.5)$$

and equivalently (since Fourier transform is linear)

$$\tilde{v}_{\mathbf{k}} = \tilde{v}_{s\mathbf{k}} + \tilde{v}_{l\mathbf{k}}. \quad (7.I.6)$$

Then the image pair-potential is written as

$$v_I(\mathbf{r}) = \sum_{\mathbf{L}} v_s(|\mathbf{r} + \mathbf{L}|) + \frac{1}{\Omega} \sum'_{\mathbf{k}} \tilde{v}_{l\mathbf{k}} e^{i\mathbf{k}\cdot\mathbf{r}} - \frac{1}{\Omega} \tilde{v}_0. \quad (7.I.7)$$

Now let us work with N particles of charge q_i in a periodic box and let us compute the total potential energy of the unit cell. Particles i and j are assumed to interact with a pair-potential $q_i q_j v(r_{ij})$. The image potential energy for the N -particle system is

$$V_I = \sum_{i < j} q_i q_j v_I(r_{ij}) + \sum_i q_i^2 v_M, \quad (7.I.8)$$

where v_M is the interaction of a particle with its own images; it is a Madelung constant for particle i interacting with the perfect lattice of the simulation cell. If this term were not present, particle i would only see $N - 1$ particles in the surrounding cells instead of N . We can find its value by considering the limit as two particles get close together with the image pair-potential. Hence

$$v_M = \frac{1}{2} \lim_{r \rightarrow 0} [v_I(r) - v(r)]. \quad (7.I.9)$$

Now we substitute the split up image pair-potential and collect all the terms together

$$\begin{aligned} V_I &= \sum_{i < j} \sum_{\mathbf{L}} q_i q_j v_s(|\mathbf{r}_{ij} + \mathbf{L}|) + \frac{1}{\Omega} \sum'_{\mathbf{k}} \tilde{v}_{l\mathbf{k}} \sum_{i < j} q_i q_j e^{i\mathbf{k}\cdot\mathbf{r}_{ij}} - \frac{1}{\Omega} \sum_{i < j} \tilde{v}_{s0} q_i q_j + \\ &\quad \sum_i q_i^2 v_M, \end{aligned} \quad (7.I.10)$$

$$v_M = \frac{1}{2} \left[\sum_{\mathbf{L}} v_s(|\mathbf{L}|) + \frac{1}{\Omega} \sum'_{\mathbf{k}} \tilde{v}_{l\mathbf{k}} - \frac{1}{\Omega} \tilde{v}_{s0} - v(0) \right], \quad (7.I.11)$$

or,

$$V_I = \sum_{i < j} \sum_{\mathbf{L}} q_i q_j v_s(|\mathbf{r}_{ij} + \mathbf{L}|) + \frac{1}{2\Omega} \sum'_{\mathbf{k}} \tilde{v}_{l\mathbf{k}} |\rho_{\mathbf{k}}|^2 + \frac{1}{2} \sum_i q_i^2 v_c - \frac{1}{2\Omega} \tilde{v}_{s0} \left[\sum_i q_i \right]^2, \quad (7.I.12)$$

where

$$\rho_{\mathbf{k}} = \sum_i q_i e^{i\mathbf{k}\cdot\mathbf{r}_i}, \quad (7.I.13)$$

$$|\rho_{\mathbf{k}}|^2 = \sum_i q_i^2 + 2 \sum_{i < j} q_i q_j \cos(\mathbf{k} \cdot \mathbf{r}_{ij}), \quad (7.I.14)$$

$$v_c = \lim_{r \rightarrow 0} \left[\sum_{\mathbf{L}} v_s(|\mathbf{r} + \mathbf{L}|) - v(r) \right]. \quad (7.I.15)$$

REFERENCES

Now we give the standard forms for the breakup which is done with a Gaussian charge distribution. α is a free parameter related to the width of the distribution. It gives nice analytic results but is not necessarily optimal. See the paper by Natoli and Ceperley Ref. [Natoli and Ceperley \[1995\]](#).

For an interaction that goes as $v(r) = r^{-n}$ the needed functions are

$$v_s(r) = \frac{\Gamma(\nu, (\alpha r)^2)}{\Gamma(\nu)r^n}, \quad (7.I.16)$$

$$\tilde{v}_{lk} = \frac{\pi^{d/2}(2/k)^{2\mu}\Gamma(\mu, (k/2\alpha)^2)}{\Gamma(\nu)}, \quad (7.I.17)$$

$$\tilde{v}_{s0} = \frac{\pi^{d/2}}{\Gamma(\nu)\mu\alpha^{2\mu}}, \quad (7.I.18)$$

$$v_c = -\frac{\alpha^n}{\nu\Gamma(\nu)}, \quad (7.I.19)$$

where $\Gamma(a, z)$ is the incomplete gamma function (see Abramowitz and Stegun [Abramowitz and Stegun \[1970\]](#)) and $\nu = n/2$ and $\mu = (d - n)/2$.

Specializing for the usual case of the Coulomb interaction ($n = 1$) in three dimensions $d = 3$, we get

$$v_s(r) = \text{erfc}(\alpha r)/r, \quad (7.I.20)$$

$$\tilde{v}_{lk} = \frac{4\pi e^{-(k/2\alpha)^2}}{k^2} \quad (7.I.21)$$

$$\tilde{v}_{s0} = \frac{\pi}{\alpha^2}, \quad (7.I.22)$$

$$v_c = -\frac{2\alpha}{\sqrt{\pi}}. \quad (7.I.23)$$

One usually chooses α so that the short-ranged potential is nearly zero at the edge of the box ($\pm L/2, \pm L/2, \pm L/2$) and then increases the number of k points until convergence is achieved.

References

- M. Abramowitz and I. A. Stegun. *Handbook of mathematical functions*. Dover, New York, 1970.
- A. Alastuey and P. A. Martin. Decay of correlations in classical fluids with long-range forces. *J. Stat. Phys.*, 39:405, 1985. doi: [10.1007/BF01018670](https://doi.org/10.1007/BF01018670).
- J. A. Barker. A quantum statistical Monte Carlo method; path integrals with boundary conditions. *J. Chem. Phys.*, 70:2914, 1979. doi: [10.1063/1.437829](https://doi.org/10.1063/1.437829).
- D. P. e Ph. Nozières. *The Theory of Quantum Liquids*. W. A. Benjamin, Inc., New York, 1966. Chapter 2.
- V. Fock. Naherungsmethode zur Lösung des quantenmechanischen Mehrkörperproblems. *Zs. Phys.*, 61:126, 1930. doi: [10.1007/BF01340294](https://doi.org/10.1007/BF01340294).
- M. Gell-Mann and K. A. Bruckner. Correlation Energy of an Electron Gas at High Density. *Phys. Rev.*, 106:364, 1957. doi: [10.1103/PhysRev.106.364](https://doi.org/10.1103/PhysRev.106.364).

- G. F. Giuliani and G. Vignale. *Quantum Theory of the Electron Liquid*. Cambridge University Press, Cambridge, 2005.
- J. P. Hansen and I. R. McDonald. *Theory of Simple Liquids*. Academic Press, Amsterdam, 1986.
- D. R. Hartree. The Wave Mechanics of an Atom with a Non-Coulomb Central Field. Part I. Theory and Methods. *Proc. Cambridge Phil. Soc.*, 24:89 and 111, 1928. doi: [10.1017/S0305004100011919](https://doi.org/10.1017/S0305004100011919).
- M. Hoffmann-Ostenhof, T. Hofmann-Ostenhof, and H. Stremnitzer. Electronic wave functions near coalescence points. *Phys. Rev. Lett.*, 68:3857, 1992. doi: [10.1103/PhysRevLett.68.3857](https://doi.org/10.1103/PhysRevLett.68.3857).
- M. Kac. Proceedings of the second berkeley symposium on probability and statistics. Berkeley, 1951. University of California Press. Sec. 3.
- M. Kac. *Probability and Related Topics in Physical Sciences*. Interscience Publisher Inc, New York, 1959.
- J. C. Kimball. Short-Range Correlations and Electron-Gas Response Functions. *Phys. Rev. A*, 7:1648, 1973. doi: [10.1103/PhysRevA.7.1648](https://doi.org/10.1103/PhysRevA.7.1648).
- M. J. Lighthill. *Introduction to Fourier analysis and generalized functions*. Cambridge University Press, 1959.
- J. Lindhard. *Mat.-Fys. Medd.*, 28(8), 1954.
- N. H. March and M. P. Tosi. *Coulomb Liquids*. Academic Press Inc Ltd, London, 1984.
- P. A. Martin. Sum rules in charged fluids. *Rev. Mod. Phys.*, 60:1075, 1988. doi: [10.1103/RevModPhys.60.1075](https://doi.org/10.1103/RevModPhys.60.1075).
- V. Natoli and D. M. Ceperley. An Optimized Method for Treating Long-Range Potentials. *Comput. Phys.*, 117:171, 1995. doi: [10.1006/jcph.1995.1054](https://doi.org/10.1006/jcph.1995.1054).
- D. Pines and P. Nozières. *Theory of Quantum Liquids*. W. A. Benjamin Inc, New York, 1966.
- A. K. Rajagopal, J. C. Kimball, and M. Banerjee. Short-ranged correlations and the ferromagnetic electron gas. *Phys. Rev. B*, 18:2339, 1978. doi: [10.1103/PhysRevB.18.2339](https://doi.org/10.1103/PhysRevB.18.2339).
- B. Simon. *Functional integration and quantum physics*. Academic, New York, 1979.
- J. C. Slater. Note on Hartree's Method. *Phys. Rev.*, 35:210, 1930. doi: [10.1103/PhysRev.35.210.2](https://doi.org/10.1103/PhysRev.35.210.2).
- M. P. Tosi. Many-body effects in jellium. In N. H. March, editor, *Electron Correlation in the Solid State*, chapter 1, pages 1–42. Imperial College Press, London, 1999.
- H. F. Trotter. On the Product of Semi-Groups of Operators. *Proc. Am. Math. Soc.*, 10:545, 1959. doi: [10.1090/S0002-9939-1959-0108732-6](https://doi.org/10.1090/S0002-9939-1959-0108732-6).
- L. van Hove. Correlations in Space and Time and Born Approximation Scattering in Systems of Interacting Particles. *Phys. Rev.*, 95:249, 1954. doi: [10.1103/PhysRev.95.249](https://doi.org/10.1103/PhysRev.95.249).
- E. P. Wigner. On the Interaction of Electrons in Metals. *Phys. Rev.*, 46:1002, 1934. doi: [10.1103/PhysRev.46.1002](https://doi.org/10.1103/PhysRev.46.1002).
- E. P. Wigner. Effects of the Electron Interaction on the Energy Levels of Electrons in Metals. *Trans. Faraday Soc.*, 34:678, 1938. doi: [10.1039/tf9383400678](https://doi.org/10.1039/tf9383400678).

Chapter 8

The White Dwarf

In this chapter we study the effect of having a finite temperature on the equation of state and structure of a white dwarf. In order to keep the treatment as general as possible we carry on our discussion for ideal quantum gases obeying to both the Fermi-Dirac and the Bose-Einstein statistics even if we will only use the results for the free electron gas inside a white dwarf. We discuss the effect of temperature on the stability of the star and on the Fermi hole.

8.1 Introduction

A white dwarf below the regime of neutron drip, at mass densities less than $4 \times 10^{11} \text{ g cm}^{-3}$, are stars which emit light of a white color due to their relatively high surface temperature of about 10^4 K . Because of their small radii R , luminous white dwarfs, radiating away their residual thermal energy, are characterized by much higher effective temperatures, T , than normal stars even though they have lower luminosities (which varies as $R^2 T^4$). In other words, white dwarfs are much “whiter” than normal stars, hence their name [Balian and Blaizot \[1999\]](#); [Silbar and Reddy \[2004\]](#); [Jackson et al. \[2005\]](#).

White dwarfs life begins when a star dies, they are therefore *compact objects* [Shapiro and Teukolsky \[1983\]](#). Star death begins when most of the nuclear fuel has been consumed. White dwarfs has about one solar mass M_\odot with characteristic radii of about 5000km and mean densities of around 10^6 g cm^{-3} . They are no longer burning nuclear fuel and are slowly cooling down as they radiate away their residual thermal energy.

They support themselves against gravity by the pressure of cold electrons, near their degenerate, zero temperature, state. In 1932 L. D. Landau [Landau \[1932\]](#) presented an elementary explanation of the equilibrium of a white dwarf which had been previously discovered by Chandrasekhar in 1931 [Chandrasekhar and Milne \[1931\]](#); [Chandrasekhar \[1931a,b\]](#) building on the formulation of the Fermi-Dirac statistics in August 1926 [Dirac \[1926\]](#) and the work of R. H. Fowler in December 1926 [Fowler \[1926\]](#), on the role of the *electron degeneracy pressure* to keep the white dwarf from gravitational collapse. Landau explanation can be found in §3.4 of the book of Shapiro and Teukolsky [Shapiro and Teukolsky \[1983\]](#), and fixes the equilibrium maximum mass of the white dwarf to $M_{\max} \sim 1.5 M_\odot$. Whereas Chandrasekhar result was $M_{\text{Ch}} = 1.456 M_\odot$ for completely ionized matter made of elements with a ratio between mass number and atomic number equal to 2. Strictly speaking one would have a matter made of a fluid of electrons and a fluids of nuclei. In the work of Chandrasekhar the fluid of electrons is treated as an ideal gas where the electrons are not interacting among themselves and the nuclei thousands times heavier are neglected.

Despite the high surface temperature these stars are still considered cold, however, because on a first approximation temperature does not affect the equation of state of its matter. White dwarfs are described as faint stars below the main sequence in the Hertzsprung-Russell diagram. In other words, white dwarfs are less luminous than main-sequence stars of corresponding colors. While slowly cooling, the white dwarfs are changing in color from white to red and finally to black. White dwarfs can be considered as one possibility of a final stage of stellar evolution since they are considered static over the lifetime of the Universe.

White dwarfs were established in the early 20th century and have been studied and observed ever since. They comprise an estimated 3% of all the stars of our galaxy. Because of their low luminosity, white dwarfs (except the very nearest ones) have been very difficult to detect at any reasonable distance and that is why there was very little observational data supporting the theory in the time of them being discovered. The companion of Sirius, discovered in 1915 by W. S. Adams [1915, 1925], was among the earliest to become known. The cooling of white dwarfs is not only a fascinating phenomenon but in addition offers information of many body physics in a new setting since the circumstances of an original star can not be built up in a laboratory. More over, the evolution and the equation of state for white dwarfs can be useful on Earth providing us more understanding of matter and physics describing the Universe.

In this chapter, we discuss how the Chandrasekhar analysis at zero temperature should be changed in order to take into account the effect of having a quantum ideal gas at finite (non-zero) temperature. For the sake of generality we will treat in parallel the case of the Fermi and the Bose ideal gases. Even if only the Fermi case is appropriate for the description of the white dwarf interior made of ionized matter characterized by a sea of free cold electrons (as Chandrasekhar did, we will neglect the Coulomb interaction between the electrons and disregards the nuclei in order to keep the treatment analytically solvable. We will also use Newtonian gravity to study the star stability disregarding general relativistic effects). At the typical surface temperature and density of a white dwarf the momentum thermal average fraction of particles having momentum $\hbar k$ and a full relativistic dispersion relation (C_k/C_0 where C_k is given by Eq. (8.2.25) below) varies appreciably over a k range which is a fraction of 0.933 ¹ of the k range where it is different from zero. So we generally expect the effect of temperature to play a role on the behavior of the ideal quantum gas. We will pursue our analysis for both the thermodynamic properties, as the validity of the various polytropic adiabatic equation of state as a function of density, and for the structural properties, as the Fermi hole.

The chapter is organized as follows: In section 8.2 we review the thermodynamic properties of the ideal quantum gases at finite temperatures. This section contains three subsections, in the first one 8.2.1 we discuss the importance of a full relativistic treatment at high densities, in the second one 8.2.2 we discuss the onset of quantum statistics as the star collapses, and in the third one 8.2.3 we present the revised Chandrasekhar analysis. In the second section 8.3 we present our study of the structure of the ideal quantum gases at finite temperature and in the full relativistic regime.

8.2 The thermodynamics of the ideal quantum gas

We want to find the thermodynamic grand potential of a system of many free fermions or bosons with a rest mass m in thermodynamic equilibrium at an inverse temperature $\beta = 1/k_B T$.

¹This value will get smaller as the star cools down in view of Eq. (8.2.20) and eventually become close to zero as the momentum thermal average fraction approaches a step function

The Hamiltonian of the system is

$$\mathcal{H} = \sum_i (-\hbar^2 c^2 \Delta_i + m^2 c^4)^{1/2}, \quad (8.2.1)$$

with Δ the Laplacian and c the speed of light.

Assuming the many particles are distinguishable (Boltzmannons) the density matrix operator, $\hat{\rho}_D$, satisfies to the Bloch equation

$$\frac{\partial \hat{\rho}_D(\beta)}{\partial \beta} = -\mathcal{H}\hat{\rho}_D(\beta), \quad (8.2.2)$$

$$\hat{\rho}_D(0) = \mathcal{I}, \quad (8.2.3)$$

where \mathcal{I} is the identity operator. The solution of Eq. (8.2.2) in coordinate representation $\mathbf{R} = (\mathbf{r}_1, \dots, \mathbf{r}_N)$, where \mathbf{r}_i is the position of i th spinless particle in the three dimensional space, has the following solution

$$\rho_D(R_0, R_1; \beta) = \langle R_0 | e^{-\beta \mathcal{H}} | R_1 \rangle = \int \frac{dK}{(2\pi)^{3N}} e^{-i\mathbf{K} \cdot (\mathbf{R}_0 - \mathbf{R}_1)} e^{-\beta \sum_i (\hbar^2 c^2 k_i^2 + m^2 c^4)^{1/2}}, \quad (8.2.4)$$

where $\mathbf{K} = (k_1, \dots, k_N)$ and $\mathbf{R}_n = (r_1^n, \dots, r_N^n)$. A very simple calculation yields the propagator ρ_D in closed form. The result can be cast in the following form

$$\rho_D = \prod_i \mathcal{R}(r_i^1, r_i^0), \quad (8.2.5)$$

where \mathcal{R} in one dimension is

$$\mathcal{R}_{1d}(r^1, r^0) = \frac{mc^2 \beta}{\pi \Psi^{1/2}} K_1\left(\frac{mc}{\hbar} \Psi^{1/2}\right), \quad (8.2.6)$$

where $\Psi = (r^1 - r^0)^2 + (\hbar c \beta)^2$ and K_ν is the familiar modified Bessel functions of order ν . In three dimensions we thus find

$$\begin{aligned} \mathcal{R}(r^1, r^0) &= -\frac{1}{2\pi|r^1 - r^0|} \frac{d\mathcal{R}_{1d}(r^1, r^0)}{d|r^1 - r^0|} \\ &= \frac{mc^2 \beta}{4\pi^2 \Psi^{3/2}} \left[\frac{mc}{\hbar} \Psi^{1/2} K_0\left(\frac{mc}{\hbar} \Psi^{1/2}\right) + 2K_1\left(\frac{mc}{\hbar} \Psi^{1/2}\right) + \frac{mc}{\hbar} \Psi^{1/2} K_2\left(\frac{mc}{\hbar} \Psi^{1/2}\right) \right], \end{aligned} \quad (8.2.7)$$

Note that for the non relativistic gas, when $\mathcal{H} = -\lambda \sum_i \Delta_i$, ρ_D would have been the usual Gaussian $\Lambda^{-3N} e^{-(\mathbf{R}_1 - \mathbf{R}_0)^2/4\lambda\beta}$, with $\lambda = \hbar^2/2m$ and $\Lambda = \sqrt{4\pi\beta\lambda}$ the de Broglie thermal wavelength.

Taking care of the indistinguishability of the particles we can describe a system of bosons and fermions with spin $s = (g - 1)/2$ through density matrices, $\hat{\rho}_{B,F}$, that are obtained from the distinguishable one opportunely symmetrized or antisymmetrized, respectively. The corresponding grand canonical partition functions can then be found through a standard procedure Feynman [1972] from $\Theta_{B,F} = e^{-\beta\Omega_{B,F}} = \sum_{N=0}^{\infty} Z_{B,F}^N e^{N\mu\beta}$ where $Z_{B,F}^N = e^{-\beta F_{B,F}^N}$ is the trace of $\hat{\rho}_{B,F}$. Here $\mu = (\ln z)/\beta$ is the chemical potential, F is the Helmholtz free energy, and Ω is the grand thermodynamic potential.

If V is the volume occupied by the system of particles, the pressure is given by $P = -\Omega/V$, and the average number of particles, $N = nV = -z\partial\beta\Omega/\partial z$, where n is the number density. We find for bosons

$$\beta P = \frac{gm^2 c}{2\pi^2 \beta \hbar^3} \sum_{\nu=1}^{\infty} \frac{z^\nu}{\nu^2} K_2(\beta mc^2 \nu), \quad (8.2.8)$$

$$n = \frac{gm^2 c}{2\pi^2 \beta \hbar^3} \sum_{\nu=1}^{\infty} \frac{z^\nu}{\nu} K_2(\beta mc^2 \nu), \quad (8.2.9)$$

and for fermions

$$\beta P = \frac{gm^2c}{2\pi^2\beta\hbar^3} \sum_{\nu=1}^{\infty} \frac{(-1)^{\nu-1}z^\nu}{\nu^2} K_2(\beta mc^2\nu) , \quad (8.2.10)$$

$$n = \frac{gm^2c}{2\pi^2\beta\hbar^3} \sum_{\nu=1}^{\infty} \frac{(-1)^{\nu-1}z^\nu}{\nu} K_2(\beta mc^2\nu) . \quad (8.2.11)$$

Clearly in the zero temperature limit ($\beta \rightarrow \infty$) these reduce to (see §2.3 of Ref. [Shapiro and Teukolsky \[1983\]](#) and our appendix [8.A](#))

$$P = \frac{g}{2} \frac{mc^2}{\lambda^3} \phi(x) , \quad (8.2.12)$$

$$n = \frac{g}{2} \frac{x^3}{3\pi^2\lambda^3} , \quad (8.2.13)$$

$$\phi(x) = \frac{1}{8\pi^2} \left[x\sqrt{1+x^2} \left(\frac{2}{3}x^2 - 1 \right) + \ln \left(x + \sqrt{1+x^2} \right) \right] , \quad (8.2.14)$$

where $\lambda = \hbar/mc$, with m the electron mass, is the electron Compton wavelength.

We can then introduce the polylogarithm, b_μ , of order μ and the companion f_μ function,

$$b_\mu(z) = \sum_{\nu=1}^{\infty} \frac{z^\nu}{\nu^\mu} , \quad (8.2.15)$$

$$f_\mu(z) = \sum_{\nu=1}^{\infty} \frac{(-1)^{\nu-1}z^\nu}{\nu^\mu} = -b_\mu(-z) = (1 - 2^{1-x}) b_\mu(z) . \quad (8.2.16)$$

At finite temperatures, in the extreme relativistic case, we find for bosons

$$\beta P = \frac{g}{\pi^2(\beta\hbar c)^3} b_4(z) , \quad (8.2.17)$$

$$n = \frac{g}{\pi^2(\beta\hbar c)^3} b_3(z) , \quad (8.2.18)$$

where we used the property $zdb_\mu(z)/dz = b_{\mu-1}(z)$, and for fermions

$$\beta P = \frac{g}{\pi^2(\beta\hbar c)^3} f_4(z) , \quad (8.2.19)$$

$$n = \frac{g}{\pi^2(\beta\hbar c)^3} f_3(z) , \quad (8.2.20)$$

In agreement with §61 of Landau [Landau and Lifshitz \[1951\]](#). And in the non relativistic case, we find for bosons

$$\beta P = \frac{g}{\Lambda^3} b_{5/2}(z) , \quad (8.2.21)$$

$$n = \frac{g}{\Lambda^3} b_{3/2}(z) , \quad (8.2.22)$$

and for fermions

$$\beta P = \frac{g}{\Lambda^3} f_{5/2}(z) , \quad (8.2.23)$$

$$n = \frac{g}{\Lambda^3} f_{3/2}(z) , \quad (8.2.24)$$

In agreement with §56 of Landau [Landau and Lifshitz \[1951\]](#). Recalling that the internal energy of the system is given by $E = -\partial \ln \Theta / \partial \beta$ we find in the extreme relativistic case $E = 3PV$ and in the non relativistic case $E = 3PV/2$. At very low density n , and high temperature T , when $n/T^{3/2}$ is very small, $b_{3/2}(z) \approx f_{3/2}(z)$ is very small and z is also very small. In this case $b_{3/2}(z) \approx b_{5/2}(z) \approx f_{3/2}(z) \approx f_{5/2}(z) \approx z$ and we find for the quantum gas $E/V \approx (3/2)K_B T n$. That is the non relativistic classical limit. For the bosons, as the temperature gets small at fixed density $b_{3/2}(z)$ increases (see Eq. (8.2.22)) and z gets close to 1. $b_\mu(z)$ is a monotonically increasing function of z which is only defined in $0 \leq z \leq 1$, so the bosons ideal gas must have a chemical potential less than zero. $b_{3/2}(1) = \zeta(3/2) \approx 2.612$ and $b_{5/2}(1) = \zeta(5/2) \approx 1.341$ where ζ is the Riemann zeta function. The temperature $T_c = \frac{2\pi\hbar^2}{mk_B} \left(\frac{n/g}{\zeta(3/2)} \right)^{2/3}$ at which $z = 1$ is called the *critical temperature* for the Bose-Einstein condensation in the non relativistic case. For $T < T_c$ the number of bosons with energy greater than zero will then be $N_> = N(T/T_c)^{3/2}$. The rest $N_0 = N[1 - (T/T_c)^{3/2}]$ bosons are in the lowest energy state, i.e. have zero energy. For the fermions the activity is allowed to vary in $0 \leq z < \infty$ and the functions $f_\mu(z)$ can be extended at $z > 1$ by using the following integral representation $f_x(z) = [\int_0^\infty dy y^{x-1} / (e^y/z + 1)]/\Gamma(x)$, where Γ is the usual gamma function.

Given the entropy $S = -\partial \Omega / \partial T$ we immediately see that, in both the extreme relativistic and the non relativistic cases, S/N must be a homogeneous function of order zero in z and that along an adiabatic process (S/N constant) we must have z constant. Then on an adiabatic, in the extreme relativistic case, $P \propto n^{1+1/3}$, a polytrope of index 3, and in the non relativistic case, $P \propto n^{1+2/3}$, a polytrope of index 3/2. This conclusions clearly continue to hold at zero temperature when $z \rightarrow \infty$ and the entropy is zero.

8.2.1 Relativistic effects at high density in a gas of fermions

The thermal average fraction of particles having momentum $p = \hbar k$ is given by

$$\mathcal{C}_k = \frac{g}{N} \frac{1}{e^{\beta[\epsilon(k)-\mu]} - \xi} = \frac{g}{N\xi} b_0(\xi z e^{-\beta\epsilon_k}), \quad V \int \frac{dk}{(2\pi)^3} \mathcal{C}_k = 1, \quad (8.2.25)$$

where $\xi = +1, -1, 0$ refer to the Bose, Fermi, and Boltzmann gas respectively.

In a degenerate ($T = 0$) Fermi gas we can define a Fermi energy as $\epsilon_F = \mu = \sqrt{p_F^2 c^2 + m^2 c^4}$, in terms of the Fermi momentum p_F . From Eq. (8.2.25) follows that the thermal average fraction of particles having momentum $p = \hbar k$ is $\mathcal{C}_k = (g/N)\Theta[\mu - \epsilon(k)]$, where Θ is the Heaviside unit step function and $\epsilon(k) = \sqrt{\hbar^2 k^2 c^2 + m^2 c^4}$ is the full relativistic dispersion relation. We will then have for the density

$$n = \frac{g}{h^3} \int_0^{p_F} 4\pi p^2 dp = \frac{4\pi g}{3h^3} p_F^3. \quad (8.2.26)$$

We then see immediately that at high density the Fermi momentum is also large and as a consequence the Fermi gas becomes relativistic. On the contrary the degenerate Bose gas will undergo the Bose Einstein condensation and have all the particles in the zero energy state.

At finite temperature from the results of the previous section we find that since $f_\mu(z)$ is a monotonously increasing function of z then at large density n also z is large and at fixed temperature this implies that the chemical potential μ is also large. In view of Eq. (8.2.25) this means that in the gas there are fermions of ever increasing momentum so that a relativistic treatment becomes necessary.

From Eqs. (8.2.10) and (8.2.11) it is possible (see appendix 8.A) to extract the full relativistic adiabatic equation of state as a function of temperature and observe the transition from the low

density regime to the high density extreme relativistic one. In Fig. 8.2.1 we show the exponent $\Gamma = d \ln P / d \ln n$ for the adiabatic full relativistic equation of state as a function of density. For the sake of the calculation it may be convenient to use natural units $\hbar = c = k_B = 1$. From the figure we see how at high density (which implies high activity) $\Gamma \rightarrow 4/3$. This figure should be compared with Fig. 2.3 of Ref. [Shapiro and Teukolsky \[1983\]](#) for the degenerate Fermi gas. In particular we see how at a temperature of $T = 20000\text{K}$ the Fermi gas can be considered extremely relativistic already at an electron number density $n \gtrsim 10^{25}\text{cm}^{-3}$. While we know (see Ref. [Shapiro and Teukolsky \[1983\]](#) and Eqs. (8.2.12)-(8.2.14)) that the completely degenerate gas becomes extremely relativistic for $n \gtrsim 10^{31}\text{cm}^{-3}$.

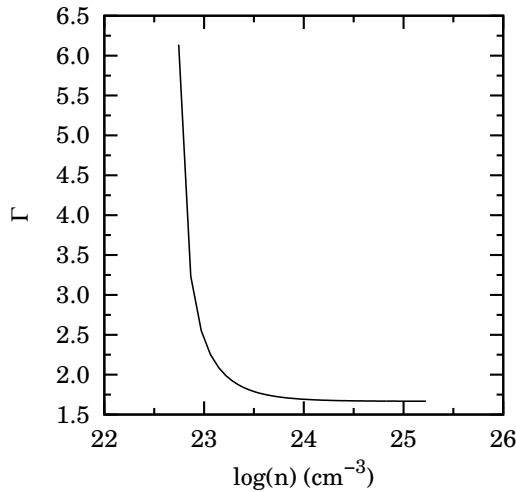


Figure 8.2.1: The exponent $\Gamma = d \ln P / d \ln n$ for the adiabatic full relativistic equation of state as a function of density. We chose a temperature $T = 20000\text{K}$ and zero entropy, $g = 2$, and m is the mass of an electron. n is in cm^{-3} .

8.2.2 The onset of quantum statistics

For a spherically symmetric distribution of matter, the mass interior to a radius r is given by

$$m(r) = \int_0^r \rho 4\pi r'^2 dr' , \quad \text{or} \quad \frac{dm(r)}{dr} = 4\pi r^2 \rho . \quad (8.2.27)$$

Here, since as we are considering non relativistic matter made of completely ionized elements of atomic number Z and mass number A , $\rho = \rho_0 = \mu_e m_u n$ is the rest mass density with $\mu_e = A/Z$ the mean molecular weight per electron and $m_u = 1.66 \times 10^{-24}\text{g}$ the atomic mass unit. If the star is in a steady state, the gravitational force balances the pressure force at every point. To derive the *hydrostatic equilibrium* equation, consider an infinitesimal fluid element lying between r and $r + dr$ and having an area dA perpendicular to the radial direction. The gravitational attraction between $m(r)$ and the mass $dm = \rho dA dr$ is the same as if $m(r)$ were concentrated in a point at the center, while the mass outside exerts no force on dm . The net outward pressure force on dm

is $-[P(r + dr) - P(r)]dA$, where P is the pressure. So in equilibrium

$$\frac{dP}{dr} = -\frac{Gm(r)\rho}{r^2}, \quad (8.2.28)$$

where G is the universal gravitational constant.²

A consequence of the hydrostatic equilibrium is the *virial theorem*. The gravitational potential energy of the star of radius R is

$$\begin{aligned} W &= - \int_0^R \frac{Gm(r)}{r} \rho 4\pi r^2 dr \\ &= \int_0^R \frac{dP}{dr} 4\pi r^3 dr \\ &= -3 \int_0^R P 4\pi r^2 dr, \end{aligned} \quad (8.2.29)$$

where we have integrated by parts.

Now we assume that the gas of fermions is characterized by an adiabatic equation of state

$$P = K\rho_0^\Gamma, \quad K, \Gamma = 1 + \frac{1}{n} \text{ constants}, \quad (8.2.30)$$

which is also called a *polytrope* of polytropic index n . For example for fermions in the extreme relativistic limit we find

$$K = \frac{P}{\rho^{4/3}} = \frac{\pi^{2/3}\hbar c}{g^{1/3}(\mu_e m_u)^{4/3}} \frac{f_4(z)}{f_3^{4/3}(z)}, \quad (8.2.31)$$

where z depends on the temperature and density and goes to infinity in the degenerate limit ($\lim_{z \rightarrow \infty} f_4(z)/f_3^{4/3}(z) = 3^{1/3}/2^{5/3}$). At the temperature and density typical of a white dwarf z is very large so the equation of state is practically indistinguishable from the one in the degenerate limit.

Calling u' the energy density of the gas, excluding the rest mass energy, we must have from the first law of thermodynamics, assuming adiabatic changes,

$$d(u'/\rho_0) = -Pd(1/\rho_0), \quad (8.2.32)$$

and integration leads to

$$u' = \rho_0 c^2 + \frac{P}{\Gamma - 1}, \quad (8.2.33)$$

which gives $u' = P/(\Gamma - 1)$. Now Eq. (8.2.29) can be rewritten as

$$W = -3(\Gamma - 1)U, \quad (8.2.34)$$

where $U = \int_0^R u' 4\pi r^2 dr$ is the total internal energy of the star. The total energy of the star, $E = W + U$, is then

$$E = -\frac{3\Gamma - 4}{3(\Gamma - 1)} |W|. \quad (8.2.35)$$

²Here we are assuming Newtonian theory of gravity. For the general relativistic stability analysis see for example §6.9 of Ref. [Shapiro and Teukolsky \[1983\]](#).

If Eq. (8.2.30) holds everywhere inside the star of total mass M and constant density, then the gravitational potential energy is given by

$$W = -3 \int_0^M \frac{P}{\rho} dm(r) = -\frac{3(\Gamma - 1)}{5\Gamma} \frac{GM^2}{R}, \quad (8.2.36)$$

where we used $d(P/\rho) = [(\Gamma - 1)/\Gamma]Gm(r)d(1/r)$ and integrated by parts using $\Gamma > 1$.

Without nuclear fuel, E decreases due to radiation. According to Eqs. (8.2.35) and (8.2.36), $\Delta E < 0$ implies $\Delta R < 0$ whenever $\Gamma > 4/3$. That is the star contracts and the gas will soon become quantum (see Ref. [Shapiro and Teukolsky \[1983\]](#) §3.2). Can the star contract forever, extracting energy from the infinite supply of gravitational potential energy until R goes to zero or until the star undergoes total collapse? The answer is no for stars with $M \sim M_\odot$, as is demonstrated by Chandrasekhar [Chandrasekhar \[1938\]](#) or in the book of Shapiro and Teukolsky [Shapiro and Teukolsky \[1983\]](#). We will reproduce their treatments in the next section.

8.2.3 The Chandrasekhar limit

The hydrostatic equilibrium Eqs. (8.2.27) and (8.2.28) can be combined to give

$$\frac{1}{r^2} \frac{d}{dr} \left(\frac{r^2}{\rho} \frac{dP}{dr} \right) = -4\pi G\rho. \quad (8.2.37)$$

Substituting the equation of state (8.2.30) and reducing the result to dimensionless form with

$$\rho = \rho_c \theta^n, \quad (8.2.38)$$

$$r = a\eta, \quad (8.2.39)$$

$$a = \sqrt{\frac{(n+1)K\rho_c^{1/n-1}}{4\pi G}}, \quad (8.2.40)$$

where $\rho_c = \rho(r=0)$ is the central density, we find

$$\frac{1}{\eta^2} \frac{d}{d\eta} \eta^2 \frac{d\theta}{d\eta} = -\theta^n. \quad (8.2.41)$$

This is the *Lane-Emden equation* for the structure of a polytrope of index n . The boundary conditions at the center of a polytropic star are

$$\theta(0) = 1, \quad (8.2.42)$$

$$\theta'(0) = 0. \quad (8.2.43)$$

The condition (8.2.42) follows directly from Eq. (8.2.38). Eq. (8.2.43) follows from the fact that near the center $m(r) \approx 4\pi\rho_cr^3/3$, so that by Eq. (8.2.27) $d\rho/dr = 0$.

Eq. (8.2.41) can be easily integrated numerically, starting at $\eta = 0$ with the boundary conditions (8.2.42) and (8.2.43). One finds that for $n < 5$ ($\Gamma > 6/5$), the solutions decreases monotonically and have a zero at a finite value $\eta = \eta_n$: $\theta(\eta_n) = 0$. This point corresponds to the surface of the star, where $P = \rho = 0$. Thus the radius of the star is

$$R = a\eta_n, \quad (8.2.44)$$

while the mass is

$$\begin{aligned} M &= \int_0^R 4\pi r^2 \rho dr \\ &= 4\pi a^3 \rho_c \int_0^{\eta_n} \eta^2 \theta^n d\eta \\ &= -4\pi a^3 \rho_c \int_0^{\eta_n} \frac{d}{d\eta} \left(\eta^2 \frac{d\theta}{d\eta} \right) d\eta \\ &= 4\pi a^3 \rho_c \eta_n |\theta'(\eta_n)| . \end{aligned} \quad (8.2.45)$$

Eliminating ρ_c between Eqs. (8.2.44) and (8.2.45) gives the mass-radius relation for polytropes

$$M = 4\pi R^{(3-n)/(1-n)} \left[\frac{(n+1)K}{4\pi G} \right]^{n/(n-1)} \eta_n^{(3-n)/(1-n)} \eta_n^2 |\theta'(\eta_n)| . \quad (8.2.46)$$

The solutions we are particularly interested in are

$$\Gamma = \frac{5}{3}, \quad n = \frac{3}{2}, \quad \eta_{3/2} = 3.65375, \quad \eta_{3/2}^2 |\theta'(\eta_{3/2})| = \omega_{3/2} = 2.71406, \quad (8.2.47)$$

$$\Gamma = \frac{4}{3}, \quad n = 3, \quad \eta_3 = 6.89685, \quad \eta_3^2 |\theta'(\eta_3)| = \omega_3 = 2.01824, \quad (8.2.48)$$

which as explained in section 8.2.1 corresponds to the low density non relativistic case and to the high density relativistic case respectively. Note that for $\Gamma = 4/3$, M is independent of ρ_c and hence R . We conclude that as $\rho_c \rightarrow \infty$, the electrons become more and more relativistic throughout the star, and the mass asymptotically approaches the value

$$M_{\text{Ch}} = 4\pi \omega_3 \left(\frac{K}{\pi G} \right)^{3/2}, \quad (8.2.49)$$

as $R \rightarrow 0$. The mass limit (8.2.49) is called *Chandrasekhar limit* (see Eq. (36) in Ref. Chandrasekhar and Milne [1931], Eq. (58) in Chandrasekhar [1935], or Eq. (43) in Chandrasekhar [1983]) and represents the maximum possible mass of a white dwarf.

In Fig. 8.2.2 we show the temperature dependence of the Chandrasekhar limit at $\mu_e = 2$.

For the dependence of the star mass on the central density as it develops through the various polytropes, as shown in Fig. (8.2.1), see for example Fig. 3.2 of Ref. Shapiro and Teukolsky [1983]. Clearly in the high $\rho_c \rightarrow \infty$ limit we will have in the degenerate limit $z \rightarrow \infty$, from Eq. (8.2.31),

$$M \rightarrow M_{\text{Ch}} = 1.45639 \left(\frac{2}{\mu_e} \right)^2 M_\odot, \quad (8.2.50)$$

where μ_e can be taken approximately equal to 2 or to 56/26 assuming that all the elements have been subject to nuclear fusion into the stable iron ^{56}Fe .

The star will not become a black hole if $R > r_s$ (see Fig. 1.1 of Ref. Shapiro and Teukolsky [1983]), with $r_s = 2GM_{\text{Ch}}/c^2$ the Schwarzschild radius in the Chandrasekhar limit, i.e.

$$K < \frac{\eta_3 c^2}{2^3 \omega_3 \rho_c^{1/3}}, \quad (8.2.51)$$

where K is given by (8.2.31). This suggests that at high enough central densities the star fate is to become a black hole. The critical central density is given in the degenerate $z \rightarrow \infty$ limit by $\bar{\rho}_c = g(\mu_e/2)^4 (2.3542 \times 10^{17} \text{ g cm}^{-3})$ which is well above the one required for the neutron drip.

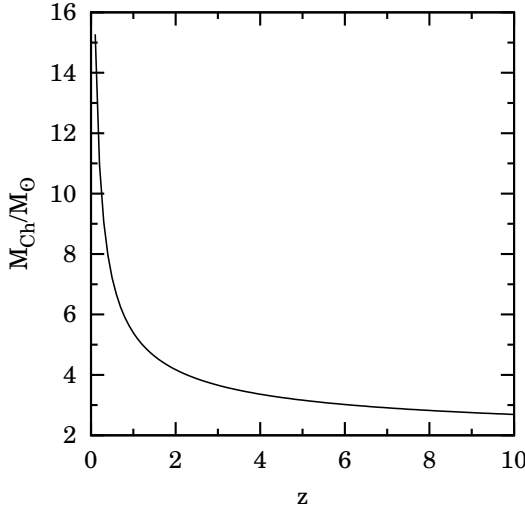


Figure 8.2.2: Temperature dependence of the Chandrasekhar limit at $\mu_e = 2$. We recall that $z = e^{\beta\mu}$.

If the star has a mass lower than M_{Ch} it will not reach the Chandrasekhar limit but will remain on a polytrope with $n < 3$. If the star has a mass higher than M_{Ch} it will eventually evolve through a supernovae explosion into a more compact object as a neutron star (when electrons are captured by protons to form neutrons by β^+ decay), a quark star, or a black hole.

8.3 The structure of the ideal quantum gas

The radial distribution function $g(r)$ is related to the structure factor $S(k)$ by the following Fourier transform

$$n[g(r) - 1] = \frac{1}{V} \sum_k e^{ik \cdot r} [S(k) - 1]. \quad (8.3.1)$$

Taking into account that the operator of the particle number N_0 is a constant of motion, the fluctuation-dissipation theorem (see appendix 5 of Ref. [March and Tosi \[1984\]](#)) $\chi''(k, \omega) = (n\pi/\hbar)(1 - e^{-\beta\hbar\omega})S(k, \omega)$, can be solved for the van Hove function

$$S(k, \omega) = \frac{\hbar}{n\pi} [1 - \delta_k] \frac{\chi''(k, \omega)}{1 - e^{-\beta\hbar\omega}} + \left\langle \frac{(\delta N)^2}{N} \right\rangle \delta_k \delta(\omega), \quad (8.3.2)$$

where $\langle \dots \rangle$ represents averaging in the grand canonical ensemble. The static structure factor $S(k) = \int_{-\infty}^{\infty} d\omega S(k, \omega)$ then is

$$S(k) = \frac{\hbar}{n\pi} [1 - \delta_k] \int_0^{\infty} d\omega \chi''(k, \omega) \coth\left(\frac{\beta\hbar\omega}{2}\right) + \left\langle \frac{(\delta N)^2}{N} \right\rangle \delta_k \delta(\omega), \quad (8.3.3)$$

where the last term does not contribute in the thermodynamic limit [Bosse et al. \[2011\]](#). We substitute (see appendix 8 of Ref. [March and Tosi \[1984\]](#))

$$\chi''(k, \omega) = N\pi \int \frac{dk'}{(2\pi)^3} C_{k'} \{ \delta[\hbar\omega - \Delta_{k'}(\mathbf{k})] - \delta[\hbar\omega + \Delta_{k'}(\mathbf{k})] \}, \quad (8.3.4)$$

with $\Delta_{k'}(\mathbf{k}) = \epsilon(|\mathbf{k}' + \mathbf{k}|) - \epsilon(\mathbf{k}')$, and obtain for $\mathbf{k} \neq \mathbf{0}$

$$S(k) = V \int \frac{dk'}{(2\pi)^3} \mathcal{C}_{k'} \coth \left\{ \frac{1}{2} \beta [\epsilon(|\mathbf{k}' + \mathbf{k}|) - \epsilon(\mathbf{k}')] \right\}, \quad k > 0, \quad (8.3.5)$$

where \mathcal{C}_k denotes the thermal average fraction of particles having momentum $\hbar\mathbf{k}$ defined in Eq. (8.2.25).

For further analytical manipulation we rewrite

$$\frac{\beta}{2} [\epsilon(k) - \mu] = \ln \sqrt{\frac{g}{N\mathcal{C}_k} + \xi}, \quad (8.3.6)$$

One rewrites Eq. (8.3.5) changing variables first $\mathbf{k} + \mathbf{k}' \rightarrow \mathbf{k}$ and subsequently $\mathbf{k} \rightarrow -\mathbf{k}$ to find

$$S(k) = V \int \frac{dk'}{(2\pi)^3} \mathcal{C}_{|\mathbf{k}+\mathbf{k}'|} \coth \left\{ \frac{1}{2} \beta [\epsilon(k) - \epsilon(|\mathbf{k} + \mathbf{k}'|)] \right\}. \quad (8.3.7)$$

Adding Eqs. (8.3.5) and (8.3.7) and making use of the fact that the hyperbolic cotangent is an odd function, one finds

$$2S(k) = V \int \frac{dk'}{(2\pi)^3} (\mathcal{C}_{k'} - \mathcal{C}_{|\mathbf{k}+\mathbf{k}'|}) \coth \left\{ \frac{1}{2} \beta [\epsilon(|\mathbf{k}' + \mathbf{k}|) - \epsilon(k')] \right\}. \quad (8.3.8)$$

Now using Eq. (8.3.6) we find

$$\begin{aligned} S(k) &= \frac{V}{2} \int \frac{dk'}{(2\pi)^3} (\mathcal{C}_{k'} - \mathcal{C}_{|\mathbf{k}+\mathbf{k}'|}) \coth \left[\ln \sqrt{\frac{g}{N\mathcal{C}_{|\mathbf{k}+\mathbf{k}'|}}} + \xi - \ln \sqrt{\frac{g}{N\mathcal{C}_{k'}}} + \xi \right] \\ &= \frac{V}{2} \int \frac{dk'}{(2\pi)^3} \left(\mathcal{C}_{k'} + \mathcal{C}_{|\mathbf{k}+\mathbf{k}'|} + \frac{2N\xi}{g} \mathcal{C}_{k'} \mathcal{C}_{|\mathbf{k}+\mathbf{k}'|} \right) \\ &= 1 + \frac{VN\xi}{g} \int \frac{dk'}{(2\pi)^3} \mathcal{C}_{k'} \mathcal{C}_{|\mathbf{k}+\mathbf{k}'|}, \quad k > 0, \end{aligned} \quad (8.3.9)$$

where $\coth[\ln \sqrt{x}] = (x+1)/(x-1)$ was used in the middle step. From this follows

$$\frac{1}{V} \sum_{\mathbf{k} \neq \mathbf{0}} e^{i\mathbf{k} \cdot \mathbf{r}} [S(k) - 1] = \frac{n\xi}{g} \left\{ 2\mathcal{C}_0 \sum_{\mathbf{k} \neq \mathbf{0}} \mathcal{C}_k e^{i\mathbf{k} \cdot \mathbf{r}} + \left| \sum_{\mathbf{k} \neq \mathbf{0}} \mathcal{C}_k e^{i\mathbf{k} \cdot \mathbf{r}} \right|^2 \right\}, \quad (8.3.10)$$

where $\mathcal{C}_0 = \delta_{\xi,1} \Theta(T_c - T) N_0 / N$, with Θ the Heaviside step function, denotes the fraction of particles which occupy the zero momentum state. We then introduce the function $F(r) = \sum_{\mathbf{k}} \mathcal{C}_k e^{i\mathbf{k} \cdot \mathbf{r}}$. This assume the following forms

$$F_r(r) = \mathcal{C}_0(T) + \frac{g}{2\pi^2 n (\beta \hbar c)^2 \xi} \int_0^\infty \kappa d\kappa b_0 \left(\xi z e^{-\sqrt{\kappa^2 + \beta^2 m^2 c^4}} \right) \sin \left(\frac{1}{\beta \hbar c} \kappa r \right) / r \quad (8.3.11)$$

$$F_{er}(r) = \mathcal{C}_0(T) + \frac{g}{2\pi^2 n (\beta \hbar c)^2 \xi} \int_0^\infty \kappa d\kappa b_0 \left(\xi z e^{-\kappa} \right) \sin \left(\frac{1}{\beta \hbar c} \kappa r \right) / r, \quad (8.3.12)$$

$$F_{nr}(r) = \mathcal{C}_0(T) + \frac{2g}{\pi n \Lambda^2 \xi} \int_0^\infty \kappa d\kappa b_0 \left(\xi z e^{-\kappa^2} \right) \sin \left(\frac{2\sqrt{\pi}}{\Lambda} \kappa r \right) / r. \quad (8.3.13)$$

in the relativistic $\epsilon(k) = \sqrt{\hbar^2 k^2 c^2 + m^2 c^4}$, extreme relativistic $\epsilon(k) = c\hbar k$, and non relativistic $\epsilon(k) = \lambda k^2$ cases respectively. Inserting Eq. (8.3.9) into Eq. (8.3.1) we find

$$g(r) = 1 + \frac{\xi}{g} [F^2(r) - \mathcal{C}_0^2(T)]. \quad (8.3.14)$$

which generalizes Eq. (117.8) of Landau [Landau and Lifshitz \[1951\]](#). In Fig. 8.3.1 we show the radial distribution function for fermions in the relativistic and the non relativistic cases. From the figure we see how the Fermi hole becomes larger in the non relativistic case at smaller number densities. Increasing the temperature by one order of magnitude (see Fig. 3.3 of Ref. [Shapiro and Teukolsky \[1983\]](#)) keeping the density fixed produces a change in the radial distribution function of the order of 10^{-2} , with the Fermi hole getting smaller.

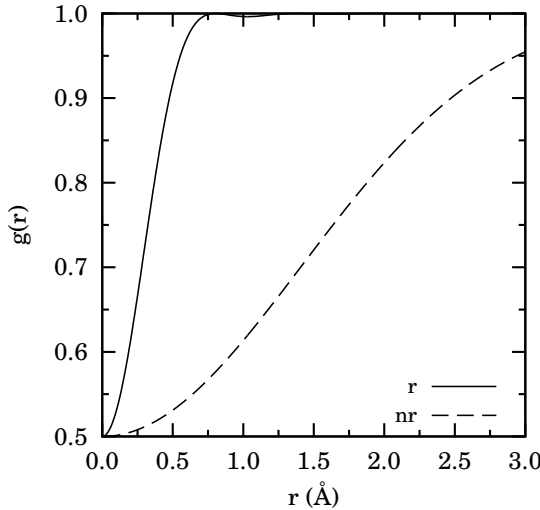


Figure 8.3.1: The radial distribution function for ideal electrons ($\xi = -1, g = 2$) in the relativistic and the non relativistic cases. Here we chose $T = 20000\text{K}$ and $n = 1.04 \times 10^{22}\text{cm}^{-3}$ in the non relativistic case and $n = 5.93 \times 10^{24}\text{cm}^{-3}$ in the relativistic case. r is in Angstroms.

For the electron gas we should include the Coulomb interaction between the particles: the *jellium*. The radial distribution function of jellium cannot of course be calculated exactly analytically, for a Monte Carlo simulation of the degenerate ($T = 0$) jellium see for example Ref. [Fantoni \[2013\]](#) and for jellium at finite temperature see for example Ref. [Militzer et al. \[2003\]](#).

Actually a more accurate result could be found by treating the white dwarf matter as a binary mixture of electrons and nuclei which can today be done exactly with Monte Carlo simulations techniques like the one devised in Ref. [Dewitt and Ceperley \[2002\]](#).

From these numerical studies one could extract a more accurate value for the constant K in the adiabatic equation of state and thus the critical central density $\bar{\rho}_c = (\eta_3 c^2 / 2^3 \omega_3 K)^3$.

8.4 Conclusions

In this chapter we studied the importance of temperature dependence on ideal Quantum gases relevant for white dwarfs interior. Even if the temperature of the star is six orders of magnitudes smaller than the Fermi energy of the electron gas inside the star, we find that the temperature effects are quite relevant at the white dwarf densities and temperatures. In particular we show that the adiabatic equation of state becomes extremely relativistic, with $\Gamma = 4/3$, at densities six orders of magnitude lower than the ones required for the completely degenerate, $T = 0$, case. Even if the polytropic form of the adiabatic equation of state remains the same as that at zero

temperature, the proportionality constant K changing by just a 10^{-10} relative factor between the finite temperature case and the zero temperature case, we think that an accurate analysis of the star evolution, at least at the level of the ideal electron gas approximation in absence of the nuclei, should properly take into account the temperature effects. This gives us a complete exactly solvable analytic approximation for the compact star interior at a finite temperature. We could comment that the temperature effects are smaller than the corrections necessary to take into account of the Coulomb interactions between the electrons and of the presence of the nuclei, but from a calculation point of view it is still desirable to keep under control the magnitude of the temperature corrections alone. Since this can be done analytically we think that their analysis is relevant by itself.

We gave the generalization to finite temperature of all the zero temperature results used by Chandrasekhar and in order to keep the treatment as general as possible we studied in parallel the Fermi and the Bose gas. Clearly only the Fermi gas results were used for the description of the ideal electron gas in the star interior.

We then studied the structure of the ideal quantum gas as a function of temperature. We found the Fermi hole for the cold electron gas in a white dwarf which turned out to be of the order of 1\AA in the full relativistic regime at a number density of the order of $n \sim 10^{26}\text{cm}^{-3}$ and bigger in the non relativistic regime at smaller densities and fixed temperature. The radial distribution function is also affected by the temperature and the Fermi hole gets smaller as the temperature increases at fixed density.

We also point out that in order to correct our result for the Coulomb interaction among the electrons and for the presence of the nuclei, it is necessary to abandon the analytic treatment in favor of the numerical simulation. We gave some relevant references of Monte Carlo methods which are important to adopt to solve this fascinating subject. These corrections to the Chandrasekhar result or to our temperature dependent treatment are important more from a philosophical point of view rather than an experimental or observational point of view. They would lead us to the exact knowledge of the properties of a mixture of electrons and nuclei at astrophysical conditions such as the ones found in white dwarfs.

More over let us observe that only a general relativistic statistical physics theory would give us fully correct results for the stability of a white dwarf. But since this theory has not yet been formulated [Rovelli \[2013\]](#) we will have to wait till the theory becomes available.

References

- W. S. Adams. *Pub. Astron. Soc. Pac.*, 27:236, 1915.
- W. S. Adams. The Relativity Displacement of the Spectral Lines in the Companion of Sirius. *Proc. Natl. Acad. Sci. USA*, 11:382, 1925. doi: [10.1073/pnas.11.7.382](https://doi.org/10.1073/pnas.11.7.382). Erratum: *Observatory* **49**, 88.
- R. Balian and J. P. Blaizot. Stars and statistical physics: A Teaching experience. *Am. J. Phys.*, 67:1189, 1999. doi: [10.1119/1.19105](https://doi.org/10.1119/1.19105).
- J. Bosse, K. N. Pathak, and G. S. Singh. Analytical pair correlations in ideal quantum gases: Temperature-dependent bunching and antibunching. *Phys. Rev. E*, 84:042101, 2011. doi: [10.1103/PhysRevE.84.042101](https://doi.org/10.1103/PhysRevE.84.042101).
- S. Chandrasekhar. XLVIII. The density of white dwarf stars. *The London, Edinburgh, and Dublin Philosophical Magazine and Journal of Science*, 11:592, 1931a. doi: [10.1080/14786443109461710](https://doi.org/10.1080/14786443109461710).

- S. Chandrasekhar. The maximum mass of ideal white dwarfs. *Astrophys. J.*, 74:81, 1931b. doi: [10.1086/143324](https://doi.org/10.1086/143324).
- S. Chandrasekhar. The Highly Collapsed Configurations of a Stellar Mass. (Second Paper.). *Monthly Notices of the Royal Astronomical Society*, 95:207, 1935. doi: [10.1093/mnras/95.3.207](https://doi.org/10.1093/mnras/95.3.207).
- S. Chandrasekhar. *An introduction to the study of stellar structure*. The University of Chicago Press, Chicago, Illinois, 1938.
- S. Chandrasekhar. On Stars, Their Evolution and Their Stability. *Nobel Prize lecture*, December 1983.
- S. Chandrasekhar and E. A. Milne. The Highly Collapsed Configurations of a Stellar Mass. *Monthly Notices of the Royal Astronomical Society*, 91:456, 1931. doi: [10.1093/mnras/91.5.456](https://doi.org/10.1093/mnras/91.5.456).
- M. Dewing and D. M. Ceperley. Methods for Coupled Electronic-Ionic Monte Carlo. In W. A. Lester, S. M. Rothstein, and S. Tanaka, editors, *Recent Advances in Quantum Monte Carlo Methods, II*. World Scientific, Singapore, 2002.
- P. A. M. Dirac. On the Theory of Quantum Mechanics. *Proc. Roy. Soc. Lond. A*, 112:661, 1926. doi: [10.1098/rspa.1926.0133](https://doi.org/10.1098/rspa.1926.0133).
- R. Fantoni. Radial distribution function in a diffusion Monte Carlo simulation of a Fermion fluid between the ideal gas and the Jellium model. *Eur. Phys. J. B*, 86:286, 2013. doi: [10.1140/epjb/e2013-40204-3](https://doi.org/10.1140/epjb/e2013-40204-3).
- R. P. Feynman. *Statistical Mechanics: A Set of Lectures*. Addison-Wesley Publishing Company Inc, Reading, 1972. Section 9.6; Chapter 8.
- R. H. Fowler. On dense matter. *Mon. Not. Roy. Astron. Soc.*, 87:114, 1926.
- C. B. Jackson, J. Taruna, S. L. Pouliot, B. W. Ellison, D. D. Lee, and J. Piekarewicz. Compact objects for everyone: I. White dwarf stars. *European J. Phys.*, 26:695, 2005. doi: [10.1088/0143-0807/26/5/003](https://doi.org/10.1088/0143-0807/26/5/003).
- L. D. Landau. On the theory of stars. *Phys. Z. Sowjetunion*, 1:285, 1932. doi: [10.1016/B978-0-08-010586-4.4.50013-4](https://doi.org/10.1016/B978-0-08-010586-4.4.50013-4).
- L. D. Landau and E. M. Lifshitz. *Statistical Physics*, volume 5 of *Course of Theoretical Physics*. Butterworth-Heinemann, Oxford, 1951.
- N. H. March and M. P. Tosi. *Coulomb Liquids*. Academic Press Inc Ltd, London, 1984.
- B. Militzer, E. L. Pollock, and D. M. Ceperley. Path integral Monte Carlo calculation of the momentum distribution of the homogeneous electron gas at finite temperature. *High Energy Density Physics*, 30:13, 2003. doi: [10.1016/j.hedp.2018.12.004](https://doi.org/10.1016/j.hedp.2018.12.004).
- C. Rovelli. General relativistic statistical mechanics. *Phys. Rev. D*, 87:084055, 2013. doi: [10.1103/PhysRevD.87.084055](https://doi.org/10.1103/PhysRevD.87.084055).
- S. L. Shapiro and S. A. Teukolsky. *Black Holes, White Dwarfs, and Neutron Stars. The Physics of Compact Objects*. John Wiley & Sons Inc, New York, 1983.
- R. Silbar and S. Reddy. Neutron stars for undergraduates. *Am. J. Phys.*, 72:892, 2004. doi: [10.1119/1.1703544](https://doi.org/10.1119/1.1703544).

Appendices

8.A The adiabatic equation of state for a relativistic ideal electron gas at finite temperature

Using the dispersion relation $\epsilon(k) = \sqrt{\hbar^2 k^2 c^2 + m^2 c^4}$, with m the rest mass of an electron, we find the pressure and the density from,

$$\beta P = g \int \frac{dk}{(2\pi)^3} \ln \left(1 + ze^{-\beta\epsilon(k)} \right), \quad (8.A.1)$$

$$n = g \int \frac{dk}{(2\pi)^3} \frac{1}{e^{\beta\epsilon(k)}/z + 1}. \quad (8.A.2)$$

Integrating by parts the pressure equation and changing variable $\kappa = \beta\hbar ck$ we find

$$\beta P = \frac{g}{(\beta\hbar c)^3} \frac{1}{2\pi^2} \frac{1}{3} \int d\kappa \frac{\kappa^3 / \sqrt{\kappa^2 + (\beta mc^2)^2}}{e^{\sqrt{\kappa^2 + (\beta mc^2)^2}/z} + 1}, \quad (8.A.3)$$

$$n = \frac{g}{(\beta\hbar c)^3} \frac{1}{2\pi^2} \int d\kappa \frac{\kappa^2}{e^{\sqrt{\kappa^2 + (\beta mc^2)^2}/z} + 1}. \quad (8.A.4)$$

These equations are equivalent to Eqs. (8.2.10) and (8.2.11) in the main text. Then the entropy is given by

$$S/Vk_B = g \int \frac{dk}{(2\pi)^3} \ln \left(1 + ze^{-\beta\epsilon(k)} \right) - g \int \frac{dk}{(2\pi)^3} \frac{\ln z - \beta\epsilon(k)}{e^{\beta\epsilon(k)}/z + 1}. \quad (8.A.5)$$

On an adiabatic the entropy per particle $s = S/Nk_B$ is constant, and from Eq. (8.A.1) follows

$$\beta P = g \int \frac{dk}{(2\pi)^3} \frac{\ln z - \beta\epsilon(k)}{e^{\beta\epsilon(k)}/z + 1} + sn. \quad (8.A.6)$$

Chapter 9

The Renormalization Group

We review some of the ideas of the renormalization group in the statistical physics of classical and quantum fluids theory. The origin, the nature, the basis, the formulation, the critical exponents and scaling, relevance, irrelevance, and marginality, universality, and Wilson's concept of flows and fixed point in a space of Hamiltonians.

In a recent Review of Modern Physics, M. E. Fisher [Fisher \[1998\]](#) presented, to a wide audience, the ideas of the Renormalization Group (RG) theory behind statistical mechanics of matter physics and Quantum Field Theory (QFT).

We will also follow the lectures given by N. Goldenfeld [Goldenfeld \[1992\]](#) at the University of Illinois at Urbana-Champaign in 1992.

Despite its name the theory is not really about a group but about a *semigroup* since the set of transformations involved is not necessarily invertible. The theory is thought as one of the underlying ideas in the theoretical structure of QFT even if the roots of RG theory has to be looked upon the theory of critical phenomena of the statistical mechanics of matter physics.

9.1 Notation

In specifying critical behavior (and asymptotic variation more generally) a little more precision than normally used is really called for. Following well established custom, we use \simeq for “approximately equals” in a rough and ready sense, as in $\pi^2 \simeq 10$. But to express “ $f(x)$ varies like x^λ when x is small and positive” i.e., just to specify a critical exponent, we write:

$$f(x) \sim x^\lambda \quad (x \rightarrow 0^+). \quad (9.1.1)$$

Then the precise implication is

$$\lim_{x \rightarrow 0^+} \ln |f(x)| / \ln x = \lambda. \quad (9.1.2)$$

We define \approx as “asymptotically equals” so that

$$f(x) \approx g(x) \quad (x \rightarrow 0^+), \quad (9.1.3)$$

implies

$$\lim_{x \rightarrow 0^+} f(x)/g(x) = 1. \quad (9.1.4)$$

We define the $o(\cdot)$ symbol as follows:

$$f = o(g) \quad (x \rightarrow 0), \quad (9.1.5)$$

means that $|f| < c|g|$ for some constant c and $|x|$ small enough.

9.2 The origin of RG

The history of the RG has to be reckoned on the work of Lev D. Landau who can be regarded as the founder of systematic effective field theories and of the concept of the *order parameter* (Landau and Lifshitz [1958] sec. 135). That is one recognizes that there is a microscopic level of description and believes it should have certain general, overall properties especially as regards locality and symmetry. Those then serve to govern the most characteristic behavior on scales greater than atomic. Known the nature of the order parameter, suppose, for example, it is a complex number and like a wave function, then one knows much about the macroscopic nature of a physical system.

Traditionally, one characterizes statistical mechanics as directly linking the *microscopic* world of nuclei and atoms (on length scales of 10^{-13} to 10^{-8} cm) to the *macroscopic* world of say, millimeters to meters. But the order parameter, as a dynamic, fluctuating object in many cases intervenes on an intermediate or *mesoscopic* level characterized by scales of tens or hundreds of angstroms up to microns. A major collaborator of Landau and developer of the concept was V. L. Ginzburg Ginzburg and Landau [1959]; Ginzburg [1997] in particular for the theory of superconductivity.

Landau's concept of the order parameter brought light, clarity, and form to the general theory of phase transitions, leading eventually, to the characterization of multicritical points and the understanding of many characteristic features of ordered states. But in 1944 Lars Onsager, by a mathematical tour de force, computed exactly the partition function and thermodynamic properties of the simplest model of a ferromagnet or a fluid Onsager [1944, 1949]; Kaufman and Onsager [1949]. This model, the Ising model, exhibited a sharp critical point: But the explicit properties, in particular, the nature of the critical singularities disagreed profoundly with essentially all the detailed predictions of the Landau theory (and of all foregoing, more specific theories). From this challenge, and from experimental evidence pointing in the same direction Fisher [1965], grew the ideas of universal but nontrivial critical exponents Domb [1960, 1996], special relations between different exponents Essam and Fisher [1963], and then, scaling descriptions of the region of a critical point Widom [1965a,b]; Domb and Hunter [1965]; Kadanoff [1966]; Patashinskii and Pokrovskii [1966]. These insights served as stimulus and inspiration to Kenneth Wilson in his pursuit of an understanding of QFTs Wilson [1983]. Indeed, once one understood the close mathematical analogy between doing statistical mechanics with effective Hamiltonians and doing quantum field theory (especially with the aid of Feynman's path integral) the connections seemed almost obvious. Needless to say, however, the realization of the analogy did not come overnight: In fact, Wilson himself was the individual who first understood clearly the analogies at the deepest levels.

In 1971, Wilson, having struggled with the problem of the systematic integrating out of appropriate degrees of freedom and the resulting RG flows for four or five years, was able to cast his RG ideas into a conceptually effective framework Wilson [1971a,b, 1983]. Effective in the sense that one could do certain calculations with it. And Franz Wegner, very soon afterwards Wegner [1972a,b], further clarified the foundations and exposed their depth and breadth. An early paper by Kadanoff and Wegner Kadanoff and Wegner [1971] showing when and how universality could fail was particularly significant in demonstrating the richness of Wilson's conception. Their

focus on relevant, irrelevant, and marginal operators (or perturbations) has played a central role Kadanoff [1976]; Wegner [1976]. The advent of Wilson's concept of the RG gave more precise meaning to the effective ("coarse-grained") Hamiltonians that stemmed from the work of Landau and Ginzburg. One now pictures the Landau-Ginzburg-Wilson (LGW) Hamiltonians as true but significantly renormalized Hamiltonians in which finer microscopic degrees of freedom have been integrated out.

So our understanding of "anomalous" i.e., non-Landau-type but, in reality, standard critical behaviour was greatly enhanced. The epsilon expansion (see chapter 12 of the Goldenfeld book Goldenfeld [1992]), which used as a small, perturbation parameter the deviation of the spatial dimensionality, d , from four dimensions, namely, $\epsilon = 4 - d$, provided a powerful and timely tool Wilson and Fisher [1972]. It had the added advantage, if one wanted to move ahead, that the method looked something like a cookbook so that "any fool" could do or check the calculations, whether they really understood, at a deeper level, what they were doing or not. But in practice that also has a real benefit in that a lot of calculations do get done, and some of them turn up new and interesting things or answer old or new questions in instructive ways. A few calculations reveal apparent paradoxes and problems which serve to teach one and advance understanding.

The foundations of RG theory are in the *critical exponent relations* and the crucial *scaling concepts* developed in 1963-66 Essam and Fisher [1963]; Widom [1965a,b]; Kadanoff [1966]; Fisher [1967a].

Some antedating reviews on RG theory are to be found in the following Refs. Domb [1960]; Fisher [1965, 1967b]; Kadanoff et al. [1967]; Stanley [1971]. Retrospective reviews can be found in the following books Baker Jr. [1990]; Creswick et al. [1992]; Domb [1996]. Introductory accounts in an informal lecture style are presented by M. E. Fisher in Refs. Fisher [1965, 1983].

9.3 The decay of correlation functions

Consider a locally defined microscopic variable which we will denote $\psi(\mathbf{r})$. In a ferromagnet this might well be the local magnetization, $M(\mathbf{r})$, or spin vector, $S(\mathbf{r})$, at point \mathbf{r} in ordinary d -dimensional (Euclidean) space; in a fluid it might be the deviation $\delta\rho(\mathbf{r})$, of the fluctuating density at \mathbf{r} from the mean density. In QFT the local variables $\psi(\mathbf{r})$ are the basic quantum fields which are "operator valued". For a magnetic system, in which quantum mechanics was important, $M(\mathbf{r})$ and $S(\mathbf{r})$ would, likewise, be operators. However, the distinction is of relatively minor importance so that we may, for ease, suppose $\psi(\mathbf{r})$ is a simple classical variable. It will be most interesting when ψ is closely related to the order parameter for the phase transition and critical behavior of concern.

By means of a scattering experiment (using light, x rays, neutrons, electrons, etc.) one can often observe the corresponding pair correlation function (or basic "two-point function")

$$G(\mathbf{r}) = \langle \psi(\mathbf{0})\psi(\mathbf{r}) \rangle, \quad (9.3.1)$$

where the angular brackets $\langle \cdot \rangle$ denote a statistical average over the thermal fluctuations that characterize all equilibrium systems at nonzero temperature. (Also understood, when $\psi(\mathbf{r})$ is an operator, are the corresponding quantum-mechanical expectation values).

Physically, $G(\mathbf{r})$ is important since it provides a direct measure of the influence of the leading microscopic fluctuations at the origin $\mathbf{0}$ on the behavior at a point distance $r = |\mathbf{r}|$ away. But, almost by definition, in the vicinity of an appropriate critical point, for example the Curie point of a ferromagnet when $\psi = M$ or the gas-liquid critical point when $\psi = \delta\rho$, a strong "ordering" influence or correlation spreads out over, essentially, macroscopic distances. As a consequence,

precisely at criticality one rather generally finds a power-law decay, namely,

$$G_c(r) \approx D/r^{d-2+\eta} \quad \text{as } r \rightarrow \infty, \quad (9.3.2)$$

which is characterized by the critical exponent (or critical index) $d - 2 + \eta$.

Now all the theories one first encounters, the so-called “classical” or Landau-Ginzburg or van der Waals theories, etc., predict, quite unequivocally, that η vanishes. In QFT this corresponds to the behavior of a free massless particle. Mathematically, the reason underlying this prediction is that the basic functions entering the theory have (or are assumed to have) a smooth, analytic, nonsingular character so that, following Newton, they may be freely differentiated and, thereby expanded in Taylor series with positive integral powers even at the critical point. In QFT the classical exponent value $d - 2$ (implying $\eta = 0$) can often be determined by naive dimensional analysis or “power counting”: Then $d - 2$ is said to represent the “canonical dimension” while η , if nonvanishing, represents the “dimensional anomaly”. Physically, the prediction $\eta = 0$ typically results from a neglect of fluctuations or, more precisely as Wilson emphasized, from the assumption that only fluctuations on much smaller scales can play a significant role: In such circumstances the fluctuations can be safely incorporated into effective (or renormalized) parameters (masses, coupling constants, etc.) with no change in the basic character of the theory.

But a power-law dependence on distance implies a *lack* of a definite length scale and, hence, a *scale invariance*. To illustrate this, let us rescale distances by a factor b so that $r \rightarrow r' = br$, and, at the same time, rescale the order parameter ψ by some “covariant” factor b^ω where ω will be a critical exponent characterizing ψ . Then we have that if one has $\omega = \frac{1}{2}(d - 2 + \eta)$, the factors of b drop out and the form in Eq. (9.3.2) is recaptured. In other words $G_c(r)$ is *scale invariant* (or covariant): Its variation reveals no characteristic lengths, large, small, or intermediate.

Since power laws imply scale invariance and the absence of well separated scales, the classical theories should be suspect at (and near) criticality. Indeed, one finds that the “anomaly” η does *not* normally vanish (at least for dimensions d less than 4, which is the only concern in a physics of matter laboratory). In particular, from the work of Kaufman and Onsager [Kaufman and Onsager \[1949\]](#) one can show analytically that $\eta = \frac{1}{4}$ for the $d = 2$ Ising model. Consequently, the analyticity and Taylor expansions presupposed in the classical theories are *not* valid. Therein lies the challenge to theory. Indeed, it proved hard even to envisage the nature of a theory that would lead to $\eta \neq 0$. The power of the renormalization group is that it provides a conceptual and, in many cases, a computational framework within which anomalous values for η (and for other exponents like ω and its analogs for all local quantities such as the energy density \mathcal{E}) arise naturally.

In applications to matter physics, it is clear that the power law in Eq. (9.3.2) can hold only for distances relatively large compared to atomic lengths or lattice spacings which we will denote a . In this sense the scale invariance of correlation functions is only *asymptotic* hence the symbol \approx , for “asymptotically equals”, and the proviso $r \rightarrow \infty$ in Eq. (9.3.2). A more detailed description would account for the effects of nonvanishing a , at least in leading order. By contrast, in QFT the microscopic distance a represents an “ultraviolet” cutoff which, since it is in general unknown, one normally wishes to remove from the theory. If this removal is not done with surgical care, which is what the renormalization program in QFT is all about, the theory remains plagued with infinite divergencies arising when $a \rightarrow 0$, i.e., when the “cutoff is removed”. But in statistical physics one always anticipates a short-distance cutoff that sets certain physical parameters such as the value of T_c ; infinite terms *per se* do not arise and certainly do not drive the theory as in QFT.

One may, however, provide a more concrete illustration of scale dependence by referring again to the power law Eq. (9.3.2). If the exponent η vanishes, or equivalently, if ψ has its canonical dimension, so that $\omega = \omega_{\text{can}} = \frac{1}{2}(d - 2)$, one may regard the amplitude D as a fixed, measurable

parameter which will typically embody some real physical significance. Suppose, however, η does not vanish but is nonetheless relatively small: Indeed, for many ($d = 3$)-dimensional systems, one has $\eta \simeq 0.035$ Fisher and Burford [1967]; Fisher [1983]; Baker Jr. [1990]; Domb [1996]. Then we can introduce a “renormalized” or “scale-dependent” parameter

$$\tilde{D}(r) \approx D/r^\eta \quad \text{as } r \rightarrow \infty, \quad (9.3.3)$$

and rewrite the original result simply as

$$G_c(r) = \tilde{D}(r)/r^{d-2}. \quad (9.3.4)$$

Since η is small we see that $\tilde{D}(r)$ varies slowly with the scale r on which it is measured. In many cases in QFT the dimensions of the field ψ (alias the order parameter) are subject only to marginal perturbations (see below) which translate into a $\ln r$ dependence of the renormalized parameter $\tilde{D}(r)$; the variation with scale is then still weaker than when $\eta \neq 0$.

9.4 The challenges posed by critical phenomena

Physics is an experimental science. So let us briefly review a few experimental findings that serves to focus attention on the principal theoretical challenges faced by, and rather fully met by RG theory.

In 1869 Andrews reported to the Royal Society his observations of carbon dioxide sealed in a (strong) glass tube at a mean overall density, ρ , close to 0.5 gm cm^{-3} . At room temperatures the fluid breaks into two phases: A liquid of density $\rho_{\text{liq}}(T)$ that coexists with a lighter vapor or gas phase of density $\rho_{\text{gas}}(T)$ from which it is separated by a visible meniscus or interface; but when the temperature, T , is raised and reaches a sharp critical temperature, $T_c \simeq 31.04^\circ\text{C}$, the liquid and gaseous phases become identical, assuming a common density $\rho_{\text{liq}} = \rho_{\text{gas}} = \rho_c$ while the meniscus disappears in a “mist” of “critical opalescence”. For all T above T_c there is a complete “continuity of state”, i.e., no distinction whatsoever remains between liquid and gas (and there is no meniscus). A plot of $\rho_{\text{liq}}(T)$ and $\rho_{\text{gas}}(T)$, as illustrated somewhat schematically in Fig. 9.4.1(d), represents the so-called gas-liquid coexistence curve or *binodal*: The two halves, $\rho_{\text{liq}} > \rho_c$ and $\rho_{\text{gas}} < \rho_c$, meet smoothly at the critical point (T_c, ρ_c) , shown as a small circle in Fig. 9.4.1: The dashed line below T_c represents the diameter defined by $\rho(T) = \frac{1}{2}[\rho_{\text{liq}}(T) + \rho_{\text{gas}}(T)]$.

The same phenomena occur in all elemental and simple molecular fluids and in fluid mixtures. The values of T_c , however, vary widely: e.g., for helium-four one finds 5.20 K while for mercury $T_c \simeq 1764$ K. The same is true for the critical densities and concentrations: These are thus “nonuniversal parameters” directly reflecting the atomic and molecular properties, i.e., the physics on the scale of the cutoff a . Hence, in Fig. 9.4.1, ρ_{max} (which may be taken as the density of the corresponding crystal at low T) is of order $1/a^3$, while the scale of $k_B T_c$ is set by the basic microscopic potential energy of attraction denoted ε . While of considerable chemical, physical, and engineering interest, such parameters will be of marginal concern to us here. The point, rather, is that the shapes of the coexistence curves, $\rho_{\text{liq}}(T)$ and $\rho_{\text{gas}}(T)$ versus T , become asymptotically universal in character as the critical point is approached.

To be more explicit, note first an issue of symmetry. In QFT, symmetries of many sorts play an important role: They may (or must) be built into the theory but can be “broken” in the physically realized vacuum state(s) of the quantum field. In the physics of fluids the opposite situation pertains. There is no real physical symmetry between coexisting liquid and gas: They are just different states, one a relatively dense collection of atoms or molecules, the other a relatively dilute collection, see Fig. 9.4.1(d). However, if one compares the two sides of the

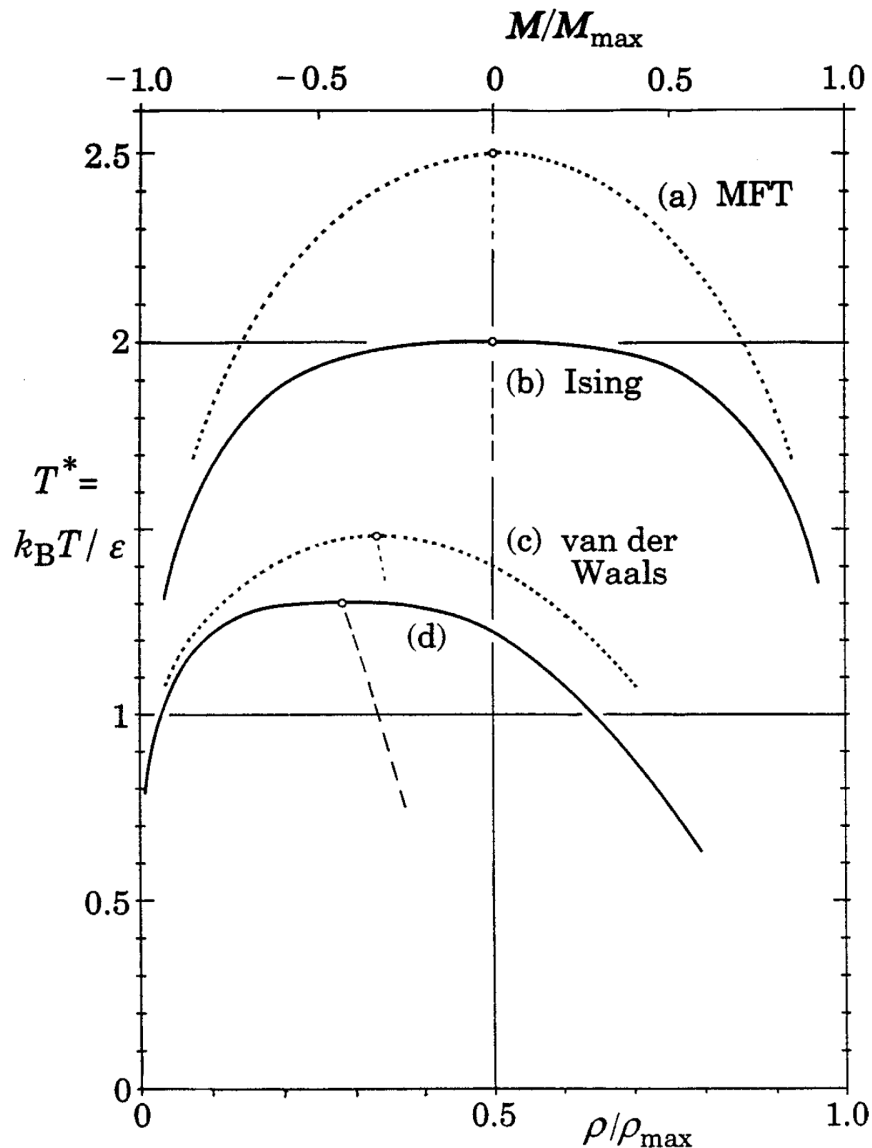


Figure 9.4.1: Temperature variation of gas-liquid coexistence curves (temperature, T , versus density, ρ) and corresponding spontaneous magnetization plots (magnetization, M , versus T). The solid curves, (b) and (d), represent (semiquantitatively) observation and modern theory, while the dotted curves (a) and (c) illustrate the corresponding “classical” predictions (mean-field theory and van der Waals approximation). These latter plots are parabolic through the critical points (small open circles) instead of obeying a power law with the universal exponent $\beta \simeq 0.325$: See Eqs. (9.4.3) and (11). The energy scale ϵ , and the maximal density and magnetization, ρ_{\max} and M_{\max} , are nonuniversal parameters particular to each physical system; they vary widely in magnitude.

coexistence curve, gas and liquid, by forming the ratio

$$R(T) = [\rho_c - \rho_{\text{gas}}(T)]/[\rho_c - \rho_{\text{liq}}(T)], \quad (9.4.1)$$

one discovers an extraordinarily precise asymptotic symmetry. Explicitly, when T approaches T_c from below or, introducing a convenient notation,

$$t \equiv (T - T_c)/T_c \rightarrow 0^-, \quad (9.4.2)$$

one finds $R(T) \rightarrow 1$. This simply means that the physical fluid builds for itself an exact mirror symmetry in density (and other properties) as the critical point is approached. And this is a universal feature for all fluids near criticality. (This symmetry is reflected in Fig. 9.4.1(d) by the high, although not absolutely perfect, degree of asymptotic linearity of the coexistence-curve diameter, $\bar{\rho}(T)$, the dashed line described above).

More striking than the (asymptotic) symmetry of the coexistence curve is the universality of its shape close to T_c , visible in Fig. 9.4.1(d) as a flattening of the graph relative to the parabolic shape of the corresponding classical prediction, see plot (c) in Fig. 9.4.1, which is derived from the famous van der Waals equation of state. Rather generally one can describe the shape of a fluid coexistence curve in the critical region via the power law

$$\Delta\rho \equiv \frac{1}{2}[\rho_{\text{liq}}(T) - \rho_{\text{gas}}(T)] \approx B|t|^\beta \quad \text{as } t \rightarrow 0^-, \quad (9.4.3)$$

where B is a nonuniversal amplitude while the critical exponent β takes a universal value

$$\beta \simeq 0.325, \quad (9.4.4)$$

(in which the last figure is uncertain). To stress the point: β is a nontrivial number, not known exactly, but it is the same for all fluid critical points! This contrasts starkly with the classical prediction $\beta = \frac{1}{2}$ [corresponding to a parabola: See Fig. 9.4.1(c)]. The value in Eq. (9.4.4) applies to ($d = 3$)-dimensional systems. Classical theories make the same predictions for all d . On the other hand, for $d = 2$, Onsager's work [Onsager \[1949\]](#) on the square-lattice Ising model leads to $\beta = \frac{1}{8}$. This value has since been confirmed experimentally by Kim and Chan [Kim and Chan \[1984\]](#) for a “two-dimensional fluid” of methane (CH_4) adsorbed on the flat, hexagonal-lattice surface of graphite crystals.

Not only does the value in Eq. (9.4.4) for β describe many types of fluid system, it also applies to anisotropic magnetic materials, in particular to those of Ising-type with one “easy axis”. For that case, in vanishing magnetic fields, H , below the Curie or critical temperature, T_c , a ferromagnet exhibits a spontaneous magnetization and one has $M = \pm M_0(T)$. The sign, + or −, depends on whether one lets H approach zero from positive or negative values. Since, in equilibrium, there is a full, natural physical symmetry under $H \rightarrow -H$ and $M \rightarrow -M$ (in contrast to fluid systems) one clearly has $M_c = 0$: Likewise, the asymptotic symmetry corresponding to Eq. (9.4.1) is, in this case exact for all T : See Fig. 9.4.1, plots (a) and (b). Thus, as is evident in Fig. 9.4.1, the global shape of a spontaneous magnetization curve does not closely resemble a normal fluid coexistence curve. Nevertheless, in the asymptotic law

$$M_0(T) \approx B|t|^\beta \quad \text{as } t \rightarrow 0^-, \quad (9.4.5)$$

the exponent value in Eq. (9.4.4) still applies for $d = 3$: See Fig. 9.4.1(b); the corresponding classical “mean-field theory” in plot (a), again predicts $\beta = \frac{1}{2}$. For $d = 2$ the value $\beta = \frac{1}{8}$ is once more valid.

And, beyond fluids and anisotropic ferromagnets many other systems belong, more correctly their critical behavior belongs, to the “Ising universality class”. Included are other magnetic materials (antiferromagnets and ferrimagnets), binary metallic alloys (exhibiting order-disorder transitions), certain types of ferroelectrics, and so on.

For each of these systems there is an appropriate order parameter and, via Eq. (9.3.2), one can then define (and usually measure) the correlation decay exponent η which is likewise universal. Indeed, essentially any measurable property of a physical system displays a universal critical singularity. Of particular importance is the exponent $\alpha \approx 0.11$ (Ising, $d = 3$) which describes the divergence to infinity of the specific heat via

$$c(T) \approx A^\pm / |t|^\alpha \quad \text{as} \quad t \rightarrow 0^\pm, \quad (9.4.6)$$

(at constant volume for fluids or in zero field, $H = 0$, for ferromagnets, etc.). The amplitudes A^+ and A^- are again nonuniversal; but their dimensionless ratio, A^+/A^- , is universal, taking a value close to 0.52. When $d = 2$, as Onsager [\[1944\]](#) found, $A^+/A^- = 1$ and $|t|^{-\alpha}$ is replaced by $\ln |t|$. But classical theory merely predicts a jump in specific heat, $\Delta c = c_c^- - c_c^+ > 0$ for all d .

Two other central quantities are a divergent isothermal compressibility $\chi(T)$ (for a fluid) or isothermal susceptibility, $\chi(T) \propto (\partial M / \partial H)_T$ (for a ferromagnet) and, for all systems, a *divergent correlation length*, $\xi(T)$, which measures the growth of the “range of influence” or of correlation observed say, via the decay of the correlation function $G(\mathbf{r}; T)$, see Eq. (9.3.1) above, to its long-distance limit. For these functions we write

$$\chi(T) \approx C^\pm / |t|^\gamma \quad \text{and} \quad \xi(t) \approx \xi_0^\pm / |t|^\nu, \quad (9.4.7)$$

as $t \rightarrow 0^\pm$, and find, for $d = 3$ Ising-type systems,

$$\gamma \approx 1.24 \quad \text{and} \quad \nu \approx 0.63, \quad (9.4.8)$$

(while $\gamma = 1\frac{3}{4}$ and $\nu = 1$ for $d = 2$).

As hinted, there are other universality classes known theoretically although relatively few are found experimentally [Fisher \[1974b\]](#); [Aharony \[1976\]](#). Indeed, one of the early successes of RG theory was delineating and sharpening our grasp of the various important universality classes. To a significant degree one found that only the vectorial or tensorial character of the relevant order parameter (e.g., scalar, complex number alias two-component vector, three-component vector, etc.) plays a role in determining the universality class. But the whys and the wherefores of this self-same issue represent, as does the universality itself, a prime challenge to any theory of critical phenomena.

9.5 The critical exponents

It has been believed for a long time that the critical exponents were the same above and below the critical temperature. It has now been shown that this is not necessarily true: When a continuous symmetry is explicitly broken down to a discrete symmetry by irrelevant (in the renormalization group sense) anisotropies, then the exponents γ and γ' are not identical [Leonard and Delamotte \[2015\]](#). Here we indicate with a prime the critical exponents for $t < 0$ (ordered phase) and without the prime the critical exponent for $t > 0$ (disordered phase).

9.5.1 The classical exponent values

The classical Landau theory (aka mean-field theory) values of the critical exponents for a scalar field are given by (see chapter 5 of Goldenfeld book [Goldenfeld \[1992\]](#))

$$\alpha = 0, \quad (9.5.1)$$

$$\beta = \frac{1}{2}, \quad (9.5.2)$$

$$\gamma = 1, \quad (9.5.3)$$

$$\delta = 3, \quad (9.5.4)$$

adding derivative terms turning it into a mean-field Ginzburg-Landau theory, we get

$$\eta = 0, \quad (9.5.5)$$

$$\nu = \frac{1}{2}. \quad (9.5.6)$$

They are valid for $d > d_{uc} = 4$, the upper critical dimension [Wilson and Fisher \[1972\]](#); [Wilson and Kogut \[1974\]](#); [Fisher \[1974a,b, 1983\]](#).

The problem with mean-field theory is that the critical exponents do not depend on the space dimension. This leads to a quantitative discrepancy in space dimensions 2 and 3, where the true critical exponents differ from the mean-field values. It leads to a qualitative discrepancy in space dimension 1, where a critical point in fact no longer exists, even though mean-field theory still predicts there is one. The space dimension where mean-field theory becomes qualitatively incorrect is called the lower critical dimension.

9.5.2 The Ising exponent values

We list in Table 9.5.1 the critical exponents of the ferromagnetic transition in the Ising model (see also Goldenfeld book [Goldenfeld \[1992\]](#) p. 111).

Table 9.5.1: This table lists the critical exponents of the ferromagnetic transition in the Ising model. In statistical physics, the Ising model describes a continuous phase transition with scalar order parameter. The critical exponents of the transition are universal values and characterize the singular properties of physical quantities. The ferromagnetic transition of the Ising model establishes an important universality class, which contains a variety of phase transitions as different as ferromagnetism close to the Curie point and critical opalescence of liquid near its critical point.

	$d = 2$	$d = 3$	$d = 4$
α	0	0.11008(1)	0
β	1/8	0.326419(3)	1/2
γ	7/4	1.237075(10)	1
δ	15	4.78984(1)	3
η	1/4	0.036298(2)	0
ν	1	0.629971(4)	1/2
ω	2	0.82966(9)	0

9.5.3 Exponent relations

Critical exponents obey the following *exponent relations* independently of the universality class

$$\nu d = 2 - \alpha = 2\beta + \gamma = \beta(\delta + 1) = \gamma \frac{\delta + 1}{\delta - 1}, \quad (9.5.7)$$

$$2 - \eta = \frac{\gamma}{\nu} = d \frac{\delta - 1}{\delta + 1}. \quad (9.5.8)$$

These equations imply that there are only two independent exponents, e.g., ν and η . All this follows from the theory of the RG.

The relations Fisher [1959, 1962, 1964, 1967b]; Essam and Fisher [1963]

$$\gamma = (2 - \eta)\nu, \quad (9.5.9)$$

$$\alpha + 2\beta + \gamma = 2, \quad (9.5.10)$$

hold exactly for the $d = 2$ Ising models and are valid when $d = 3$ to within the experimental accuracy or the numerical precision (of the theoretical estimates Fisher [1967b]; Baker Jr. [1990]; Domb [1996]). They are even obeyed exactly by the classical exponent values (which, today, we understand as valid for $d > 4$).

The first relation (9.5.9) pertains just to the basic correlation function $G(r; T)$ as defined previously in Eq. (9.3.1). It follows from the assumption Fisher [1959, 1962], supported in turn by an examination of the structure of Onsager's matrix solution to the Ising model Onsager [1944]; Kaufman and Onsager [1949] that in the critical region all lengths (much larger than the lattice spacing a) scale like the correlation length $\xi(T)$, introduced in Eq. (9.4.7). Formally one expresses this principle by writing, for $t \rightarrow 0$ and $r \rightarrow \infty$,

$$G(r; T) \approx \frac{D}{r^{d-2+\eta}} \mathcal{G}\left(\frac{r}{\xi(T)}\right), \quad (9.5.11)$$

where, for consistency with (9.3.2), the scaling function, $\mathcal{G}(x)$, satisfies the normalization condition $\mathcal{G}(0) = 1$. Integrating r over all space yields the compressibility/susceptibility $\chi(T)$ and, thence, the relation $\gamma = (2 - \eta)\nu$. This scaling law highlights the importance of the correlation length ξ in the critical region, a feature later stressed and developed further, especially by Widom Widom [1965a,b], Kadanoff Kadanoff [1966, 1976], and Wilson Wilson [1983]; Wilson and Kogut [1974]. It is worth remarking that in QFT the inverse correlation length ξ^{-1} , is basically equivalent to the renormalized mass of the field ψ : Masslessness then equates with criticality since $\xi^{-1} \rightarrow 0$.

The second relation (9.5.10) is proven in section 9.8.

9.6 The Gaussian model and the upper critical dimension

See chapters 6 and 7 of the book of Goldenfeld Goldenfeld [1992].

9.7 The task of RG

One would wish the RG theory to:

- (i) explain the ubiquity of power laws at and near critical points (as opposed to the exponential laws which governs, for example, the decay of correlation in Coulomb liquids Martin [1988]; Das et al. [2011]);

- (ii) explain the values of the leading *thermodynamic and correlation exponents*, $\alpha, \beta, \gamma, \delta, \nu, \eta$, and ω ;
- (iii) clarify why and how the classical values are in error, including the existence of *borderline dimensionalities*, like $d_{uc} = 4$, above which classical theories become valid;
- (iv) find the *correction-to-scaling exponent* θ (and, ideally, the higher-order correction exponents);
- (v) give a method to compute *crossover exponents*, ϕ , to check for the *relevance* or *irrelevance* of a multitude of possible perturbations;
- (vi) give understanding of *universality* with nontrivial exponents;
- (vii) give a derivation of *scaling*;
- (viii) allow to understand the *breakdown* of universality and scaling in certain circumstances;
- (ix) handle effectively *logarithmic* and more exotic dependences on temperature.

We may start by supposing that one has a set of microscopic, fluctuating, mechanical variables: In QFT these would be the various quantum fields, $\psi(r)$, defined at all points in a Euclidean (or Minkowski) space. In statistical physics the phase space variables $PS = \{R^N, P^N\}$ of N particles of coordinates $R^N = \{r_1, \dots, r_N\}$ and momenta $P^N = \{p_1, \dots, p_N\}$ in a volume V .

In terms of the basic variables PS one can form various “local operators” (or “physical quantities” or “observables”) like, for a real fluid, the pressure P , the energy density \mathcal{E} , the specific heat c , the isothermal compressibility χ , etc. or, for the Ising model, the pressure P , the spontaneous magnetization M , the energy density \mathcal{E} , the specific heat c , the isothermal magnetic susceptibility χ , etc. For a mapping between the Ising model and a real fluid see Goldenfeld book [Goldenfeld \[1992\]](#) section 2.12.

A physical system of interest is then specified by its *Hamiltonian* $\mathcal{H}[PS; L]$ which is usually just a spatially uniform sum of local operators made up from the phase space operators and the coupling constant $L = \{L\}$. The crucial function is the “reduced Hamiltonian”

$$\bar{\mathcal{H}}[PS; K] = -\mathcal{H}[PS; L]/k_B T, \quad (9.7.1)$$

where k_B is Boltzmann constant, T the absolute temperature, and $K = \{T, L\}$, are the various “thermodynamic fields” (or coupling constants in QFT). We may suppose that one or more of the thermodynamic fields, in particular the temperature, can be controlled directly by the experimenter; but others may be “given” since they will, for example, embody details of the physical system that are “fixed by nature”.

An important feature of Wilson’s approach, however, is to regard any “physical Hamiltonian” as merely specifying a subspace in a very large space of possible (reduced) Hamiltonians, \mathcal{H} . This change in perspective proves crucial to the proper formulation of a renormalization group: In principle, it enters also in QFT although in practice, it is usually given little attention.

The partition function will be

$$Z_N[\bar{\mathcal{H}}] = \text{Tr}_N \left\{ e^{\bar{\mathcal{H}}[PS]} \right\}, \quad (9.7.2)$$

where the trace operator $\text{Tr}_N \{\cdot\}$, denotes a summation or integration over the possible values of all the $2dN$ variables PS . Then the thermodynamics follow from the total free energy density,

which is given by

$$f[\bar{\mathcal{H}}] \equiv f(K) = \lim_{N,V \rightarrow \infty} \frac{\ln Z_N[\bar{\mathcal{H}}]}{V}, \quad (9.7.3)$$

where N and V becomes infinite maintaining the ratio $V/N = a^d$ fixed: In QFT this corresponds to an infinite system with an ultraviolet lattice cutoff.

To the degree that one can actually perform the trace operation in Eq. (9.7.2) for a particular model system and take the “thermodynamic limit” in Eq. (9.7.3) one will obtain the precise critical exponents, scaling functions, and so on. This was Onsager’s (1944) [Onsager \[1944\]](#) route in solving the $d = 2$, spin 1/2 Ising models in zero magnetic field. At first sight one then has no need of RG theory. While one knows for sure that $\alpha = 0$ (\ln), $\beta = \frac{1}{8}$, $\gamma = 1\frac{3}{4}$, $\nu = 1$, $\eta = \frac{1}{4}$, … for the planar Ising models one does not know why the exponents have these values. Indeed, the seemingly inevitable mathematical complexities of solving even such physically oversimplified models exactly [Baxter \[1982\]](#) serve to conceal almost all traces of general, underlying mechanisms and principles that might “explain” the results. Also, should one ever achieve truly high precision in simulating critical systems on a computer (a prospect which still seems some decades away [Ceperley \[1995\]](#)) the same problem would remain. Thus it comes to pass that even a rather crude and approximate solution of a two-dimensional Ising model by a RG method can be truly instructive.

9.8 The basis and formulation

At the heart of (real space ¹) RG theory there is the renormalization of the spatial scale via $r \rightarrow r' = br$ which produces on the reduced Hamiltonian the following *renormalization transformation*

$$\bar{\mathcal{H}}'[PS'; K'] = \mathcal{R}_b \bar{\mathcal{H}}[PS, K], \quad (9.8.1)$$

where we have elected to keep track of the spatial rescaling factor, b , as a subscript of the RG operator \mathcal{R} . Thus successive renormalizations with scaling factors b_1 and b_2 yield the quite general relation $\mathcal{R}_{b_2} \mathcal{R}_{b_1} = \mathcal{R}_{b_2 b_1}$, which essentially defines a unitary *semigroup* of transformations. the formal algebraic definition [MacLane and Birkhoff \[1967\]](#) of a unitary semigroup (or “monoid”) is a set M of elements, u, v, w, x, \dots with a binary operation, $xy = w \in M$, which is associative, so $v(wx) = (vw)x$, and has a unit u , obeying $ux = xu = x$ (for all $x \in M$). In RG theory, the unit transformation corresponds simply to $b = 1$.

It is more fruitful to iterate the transformation so obtaining a sequence, $\bar{\mathcal{H}}^{(l)}$, of renormalized Hamiltonians, namely,

$$\bar{\mathcal{H}}^{(l)} = \mathcal{R}_b \bar{\mathcal{H}}^{(l-1)} = \mathcal{R}_{b^l} \bar{\mathcal{H}}. \quad (9.8.2)$$

Hille [Hille \[1948\]](#) and Riesz and Sz.-Nagy [Riesz and Sz.-Nagy \[1955\]](#) describe semigroups within a continuum, functional analysis context and discuss the existence of an infinitesimal generator when the flow parameter l is defined for continuous values $l \geq 0$. One may regard

$$l = \log_b(|r'|/|r|), \quad (9.8.3)$$

as measuring, logarithmically, the scale on which the system is being described; but note that, in general, the form of the Hamiltonian is also changing as the “scale” is changed or l increases.

¹As opposed to the *momentum-shell* RG [Wilson and Fisher \[1972\]](#).

Thus a partially renormalized Hamiltonian can be expected to take on a more-or-less generic, mesoscopic form: Hence it represents an appropriate candidate to give meaning to a Landau-Ginzburg or, now, LGW effective Hamiltonian.

It is also worth mentioning that by letting $b \rightarrow 1^+$, one can derive a *differential* or continuous RG flow and rewrite the recursion relation (9.8.2) as

$$\frac{d}{dl} \bar{\mathcal{H}} = \mathbf{B} \bar{\mathcal{H}}. \quad (9.8.4)$$

In this form the RG semigroup can typically be extended to an Abelian group MacLane and Birkhoff [1967]. But as already stressed this fact plays a negligible role. Such continuous flows are illustrated in Fig. 9.8.1.²

The recursive application of an RG transformation \mathcal{R}_b induces a *flow* in the space of Hamiltonians, \mathcal{H} . Then one observes that “sensible”, “reasonable”, or, better, “well-designed” RG transformations are *smooth*, so that points in the original physical manifold, $\mathcal{H}^{(0)}$, that are close, say in temperature, remain so in $\mathcal{H}^{(1)}$, i.e., under renormalization, and likewise as the flow parameter l increases, in $\mathcal{H}^{(l)}$.

Thanks to the smoothness of the RG transformation, if one knows the free energy $f_l \equiv f[\mathcal{H}^{(l)}]$ at the l -th stage of renormalization, then one knows the original free energy $f[\mathcal{H}]$ and its critical behavior: Explicitly one has

$$f(K) \equiv f[\bar{\mathcal{H}}] = b^{-dl} f[\bar{\mathcal{H}}^{(l)}] \equiv b^{-dl} f_l(K^{(l)}). \quad (9.8.5)$$

Furthermore, the smoothness implies that all the universal critical properties are preserved under renormalization. Similarly one finds Wilson [1971a]; Wilson and Kogut [1974]; Fisher [1983] that the critical point of $\bar{\mathcal{H}}^{(0)} \equiv \bar{\mathcal{H}}$ maps on to that of $\bar{\mathcal{H}}^{(1)} \equiv \bar{\mathcal{H}}'$, and so on, as illustrated by the flow lines in Fig. 9.8.1. Thus it is instructive to follow the *critical trajectories* in \mathcal{H} , i.e., those RG flow lines that emanate from a physical critical point. In principle, the topology of these trajectories could be enormously complicated and even chaotic: In practice, however, for a well-designed or “apt” RG transformation, one most frequently finds that the critical flows terminate, or, more accurately, come to an asymptotic halt, at a *fixed point* \mathcal{H}^* , of the RG: See Fig. 9.8.1. Such a fixed point is defined simply by

$$\mathcal{R}_b \bar{\mathcal{H}}^* = \bar{\mathcal{H}}^* \quad \text{or} \quad \mathbf{B} \bar{\mathcal{H}}^* = 0. \quad (9.8.6)$$

One then searches for fixed point solutions.

Why are the fixed points so important? Some, in fact, are *not*, being merely *trivial*, corresponding to *no interactions* or to all spins frozen, etc. But the *nontrivial* fixed points represent critical states; furthermore, the nature of their criticality, and of the free energy in their neighborhood, must, as explained, be *identical* to that of all those distinct Hamiltonians whose critical trajectories converge to the same fixed point. In other words, a particular fixed point defines a *universality class*³ of critical behavior which “governs” or “attracts” all those systems whose critical points eventually map onto it: See Fig. 9.8.1.

²If it happens that $\bar{\mathcal{H}}$ can be represented, in general only approximately, by a single coupling constant, say, g , then \mathbf{B} reduces to the so-called beta-function $\beta(g)$ of QFT.

³This retrospective statement may, perhaps, warrant further comment. First, the terms “universal” and “universality class” came into common usage only after 1974 when the concept of various types of RG fixed point had been well recognized (see Fisher Ref. Fisher [1974b]). Kadanoff Kadanoff [1976] deserves credit not only for introducing and popularizing the terms but especially for emphasizing, refining, and extending the concepts. On the other hand, Domb’s Domb [1960] review made clear that all (short-range) Ising models should have the same critical exponents irrespective of lattice structure but depending strongly on dimensionality. The excluded-volume problem for polymers was known to have closely related but distinct critical exponents from the Ising

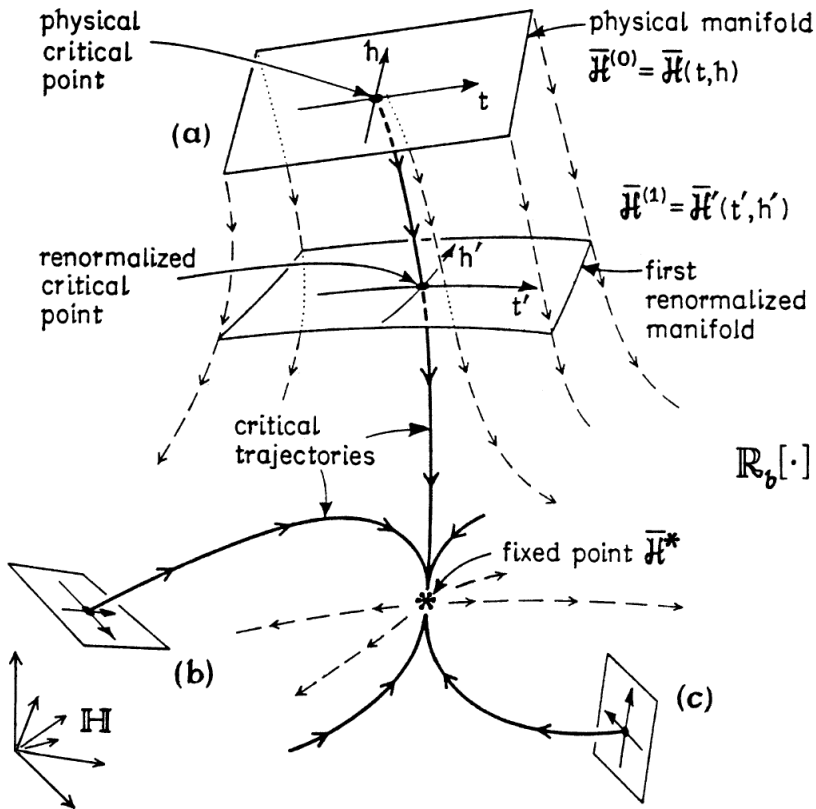


Figure 9.8.1: A depiction of the space of Hamiltonians \mathcal{H} showing initial or physical manifolds, $K = \{t, h\}$ with $t = (T - T_c)/T_c$ and T_c the critical temperature, [labelled (a), (b), ...] and the flows induced by repeated application of a discrete RG transformation \mathcal{R}_b with a spatial rescaling factor b (or induced by a corresponding continuous or differential RG). Critical trajectories are shown bold: They all terminate, in the region of \mathcal{H} shown here, at a fixed point $\bar{\mathcal{H}}^*$. The full space contains, in general, other nontrivial, critical fixed points, describing multicritical points and distinct critical-point universality classes; in addition, trivial fixed points, including high-temperature ‘‘sinks’’ with no outflowing or relevant trajectories, typically appear. Lines of fixed points and other more complex structures may arise and, indeed, play a crucial role in certain problems. (After Ref. Fisher [1983])

Here, then we at last have the natural explanation of universality: Systems of quite different physical character may, nevertheless, belong to the domain of attraction of the same fixed point $\bar{\mathcal{H}}^*$ in \mathcal{H} . The distinct sets of inflowing trajectories reflect their varying physical content of associated irrelevant variables and the corresponding nonuniversal rates of approach to the asymptotic power laws dictated by \mathcal{H}^* .

From each critical fixed point, there flow at least two “unstable” or outgoing trajectories. These correspond to one or more relevant variables, specifically, for the case illustrated in Fig. 9.8.1, to the temperature or thermal field, $t = (T - T_c)/T_c$, with T_c the critical temperature, and the magnetic or ordering field, h . If there are further relevant trajectories then one can expect crossover to different critical behavior. In the space \mathcal{H} , such trajectories will then typically lead to distinct fixed points describing (in general) completely new universality classes. A skeptical reader may ask: “But what if no fixed points are found?” This can well mean, as it has frequently meant in the past, simply that the chosen RG transformation was poorly designed or “not apt”. On the other hand, a fixed point represents only the simplest kind of asymptotic flow behavior: Other types of asymptotic flow may well be identified and translated into physical terms.

But what about power laws and scaling?

The smoothness of a well-designed RG transformation means that it can always be expanded locally, to at least some degree, in a Taylor series Wilson [1971a]; Wilson and Kogut [1974]; Fisher [1974b]; Wegner [1972a,b, 1976]; Kadanoff [1976]. It is worth stressing that it is this very property that fails for free energies in a critical region: To regain this ability, the large space of Hamiltonians is crucial. Near a fixed point satisfying Eq. (9.8.5) we can, therefore, rather generally expect to be able to linearize by writing

$$\mathcal{R}_b[\bar{\mathcal{H}}^* + g\mathcal{Q}] = \bar{\mathcal{H}}^* + g\mathcal{L}_b\mathcal{Q} + o(g), \quad (9.8.7)$$

as $g \rightarrow 0$, or in differential form,

$$\frac{d}{dl}(\bar{\mathcal{H}}^* + g\mathcal{Q}) = g\mathcal{B}\mathcal{Q} + o(g). \quad (9.8.8)$$

Now \mathcal{L}_b and \mathcal{B} are *linear operators* (albeit acting in a large space \mathcal{H}). As such we can seek eigenvalues and corresponding “eigenoperators”, say \mathcal{Q}_k (which will be “partial Hamiltonians”). Thus, we may write

$$\mathcal{L}_b\mathcal{Q}_k = \Lambda_k(b)\mathcal{Q}_k \quad \text{or} \quad \mathcal{B}\mathcal{Q}_k = \lambda_k\mathcal{Q}_k, \quad (9.8.9)$$

where, in fact, (by the semigroup property) the eigenvalues must be related by $\Lambda_k(b) = b^{\lambda_k}$. As in any such linear problem, knowing the spectrum of eigenvalues and eigenoperators or, at least,

model, depending similarly on dimensionality but not lattice structure Fisher and Sykes [1959]. And, as regards the Heisenberg model, which possesses what we would now say is an ($n = 3$)-component vector or $O(3)$ order parameter, there were strong hints that the exponents were again different Rushbrooke and Wood [1958]; Domb and Sykes [1962]. On the experimental front matters might, possibly be viewed as less clear-cut: Indeed, for ferromagnets, nonclassical exponents were unambiguously revealed only in 1964 by Kouvel and Fisher Kouvel and Fisher [1964]. However, a striking experiment by Heller and Benedek Heller and Benedek [1962] had already shown that the order parameter of the antiferromagnet MnF₂, namely, the sublattice magnetization $M_0^\dagger(T)$, vanishes as $|t|^\beta$ with $\beta = 0.335$. Furthermore, for fluids, the work of the Dutch school under Michels and the famous analysis of coexistence curves by Guggenheim Guggenheim [1949] allowed little doubt, see Rowlinson book Rowlinson [1959], Chap. 3, especially, pp. 91–95 that all reasonably simple atomic and molecular fluids displayed the same but nonclassical critical exponents with $\beta \simeq \frac{1}{3}$: And, also well before 1960, Widom and Rice Widom and Rice [1955] had analyzed the critical isotherms of a number of simple fluids and concluded that the corresponding critical exponent δ (see, e.g., Ref. Fisher [1967b]) took a value around 4.2 in place of the van der Waals value $\delta = 3$. In addition, evidence was in hand showing that the consolute point in binary fluid mixtures was similar (see Rowlinson book Rowlinson [1959], pp. 165–166).

its dominant parts, tells one much of what one needs to know. Reasonably, the \mathcal{Q}_k should form a basis for a general expansion

$$\overline{\mathcal{H}} \cong \overline{\mathcal{H}}^* + \sum_{k \geq 1} g_k \mathcal{Q}_k. \quad (9.8.10)$$

Physically, the expansion coefficient g_k ($\equiv g_k^{(0)}$) then represents the thermodynamic field (reduced, as always, by the factor $1/k_B T$) conjugate to the “critical operator” \mathcal{Q}_k which, in turn, will often be close to some combination of *local* operators. Indeed, in a characteristic critical-point problem one finds two *relevant operators*, say \mathcal{Q}_1 and \mathcal{Q}_2 with $\lambda_1, \lambda_2 > 0$. Invariably, one of these operators can, say by its symmetry, be identified with the local energy density, $\mathcal{Q}_1 \cong \mathcal{E}$, so that $g_1 \cong t$ is the thermal field; the second then characterizes the order parameter, $\mathcal{Q}_2 \cong \Psi$ with field $g_2 \cong h$. Under renormalization each g_k varies simply as $g_k^{(l)} \approx b^{\lambda_k l} g_k^{(0)}$.

Finally, one examines the flow equation (9.8.5) for the free energy. The essential point is that the degree of renormalization, b^l , can be chosen as large as one wishes. When $t \rightarrow 0$, i.e., in the critical region which it is our aim to understand, a good choice proves to be $b^l = 1/|t|^{1/\lambda_1}$, which clearly diverges at ∞ . One then finds that Eq. (9.8.5) leads to the following *basic scaling relation*

$$f_s(t, h, \dots, g_j, \dots) \approx |t|^{2-\alpha} \mathcal{F}\left(\frac{h}{|t|^\Delta}, \dots, \frac{g_j}{|t|^{\phi_j}}, \dots\right), \quad (9.8.11)$$

where f_s is the “singular part” of the free energy found by subtracting from the free energy all the analytic terms. α is the specific heat exponent introduced while the exponent, Δ , which determines how h scales with t , is given by

$$\Delta = \beta + \gamma, \quad (9.8.12)$$

Widom observed, incidentally, that the classical theories themselves obey scaling: One then has $\alpha = 0, \Delta = 1\frac{1}{2}, \phi = -\frac{1}{2}$. The exponent, ϕ , did not appear in the original critical-point scaling formulations Widom [1965a,b]; Domb and Hunter [1965]; Kadanoff [1966]; Patashinskii and Pokrovskii [1966]; Fisher [1967b]; Stanley [1971]; neither did the argument $g/|t|^\phi$ appear in the *scaling function* \mathcal{F} . It is really only with the appreciation of RG theory that we know that such a dependence should in general be present and, indeed, that a full spectrum $\{\phi_j\}$ of such higher-order exponents with $\phi \equiv \phi_1 > \phi_2 > \phi_3 > \dots$ must normally appear Wilson [1971a]; Fisher [1974a].

Eq. (9.8.11) is the essential result. Recall, for example, that: (i) it very generally *implies* the thermodynamic exponent relation Eq. (9.5.10) connecting α, β , and γ (since the derivative of the free energy with respect to h is proportional to minus the magnetization); and (ii) since all leading exponents are determined entirely by the two exponents α and Δ ($= \beta + \gamma$), it predicts similar exponent relations for any other exponents one might define, such as δ specified on the critical isotherm by $H \sim M^\delta$. Beyond that, (iii) if one fixes P (or g) and similar parameters and observes the free energy or, in practice, the *equation of state*, the data one collects amount to describing a function, say $M(T, H)$, of two variables. Typically this would be displayed as sets of *isotherms*: i.e., many plots of M vs. H at various closely spaced, fixed values of T near T_c . But according to the scaling law Eq. (9.8.11) if one plots the *scaled variables* $f_s/|t|^{2-\alpha}$ or $M/|t|^\beta$ vs. the scaled field $h/|t|^\Delta$, for appropriately chosen exponents and critical temperature T_c , one should find that all these data “collapse” (in Stanley’s Stanley [1971] picturesque terminology) onto a single curve, which then just represents the scaling function $x = \mathcal{F}(y)$ itself. This collapse is sometimes also called *law of corresponding states* (see for instance section 4.1 in Ref. Hansen and McDonald [1986]).

Now, however, the critical exponents can be expressed directly in terms of the RG eigenexponents λ_k (for the fixed point in question). Specifically one finds

$$2 - \alpha = \frac{d}{\lambda_1}, \quad \Delta = \frac{\lambda_2}{\lambda_1}, \quad \phi_j = \frac{\lambda_j}{\lambda_1}, \quad \nu = \frac{1}{\lambda_1}. \quad (9.8.13)$$

Then, the sign of a given ϕ_j and, hence, of the corresponding λ_j determines the relevance (for $\lambda_j > 0$), *marginality* (for $\lambda_j = 0$), or *irrelevance* (for $\lambda_j < 0$) of the corresponding critical operator Q_j (or “perturbation”) and of its conjugate field g_j : This field might, but for most values of j will not, be under direct experimental control. The first and last of the equations (9.8.13) yield the *hyperscaling relation*: $d\nu = 2 - \alpha$ which explicitly involve the spatial dimensionality Fisher [1974a]. This relation holds exactly for the $d = 2$ Ising model and also for all other exactly soluble models when $d < 4$ Fisher [1983]; Baxter [1982].⁴

When a coupling constant g is irrelevant then $z = g/|t|^\phi \rightarrow 0$ on approaching the critical point. Consequently, $\mathcal{F}(y, z)$ can be replaced simply by $\mathcal{F}(y, 0)$ which is a function of just a *single variable*. Furthermore, asymptotically when $T \rightarrow T_c$ we get the same function whatever the actual value of g . Clearly this is an example of *universality*.⁵ Then one can, fairly generally, hope to expand the scaling function $\mathcal{F}(y, z)$ in powers of z and thereby obtain the so called “*correction-to-scaling*” exponent θ , which is also universal (for $d = 3$ Ising-type systems one finds $\theta \simeq 0.54$ Zinn and Fisher [1996]).

When a coupling constant g is relevant then when $t \rightarrow 0$ the scaled variable $g/|t|^\phi$ grows larger and larger. Two possibilities then arise: *Either* the critical point may be destroyed altogether. This is, in fact, the effect of the magnetic field, which must itself be regarded as a relevant perturbation since $\phi \equiv \Delta = \beta + \gamma > 0$. *Alternatively*, when z grows, the true, asymptotic critical behavior may *crossover* Fisher [1974b]; Aharony [1976] to a new, quite *distinct* universality class with different exponents and a new asymptotic scaling function, say, $\mathcal{F}_\infty(y)$.⁶

When a coupling constant g is marginal then when $t \rightarrow 0$ this may lead to *logarithmic* modifications of the classical critical power laws (by factors diverging as $\ln |t|$ to various powers). The predicted logarithmic behavior has, in fact, been verified experimentally by Ahlers et al. Ahlers et al. [1975]. In other cases, especially for $d = 2$, marginal variables lead to continuously variable exponents such as $\alpha(g)$, and to quite different thermal variation, like $\exp(A/|t|^\nu)$; such results have been checked both in exactly solved statistical mechanical models and in physical systems such as superfluid helium films Nelson [1983]; Kadanoff and Wegner [1971].

Because of the multifaceted character of matter physics these are rather different and more diverse than those aspects of RG theory of significance for QFT. When there are no marginal variables and the least negative ϕ_j is larger than unity in magnitude, a simple scaling description

⁴Unlike the previous exponent relations (all being independent of d) hyperscaling fails for the classical theories unless $d = 4$. And since one knows (rigorously for certain models) that the classical exponent values are valid for $d > 4$, it follows that hyperscaling cannot be generally valid. Thus something is certainly missing from Kadanoff’s picture. Now, thanks to RG insights, we know that the breakdown of hyperscaling is to be understood via the second argument in the “fuller” scaling form Eq. (9.8.11): when d exceeds the appropriate borderline dimension, d_{uc} , a “dangerous irrelevant variable” appears and must be allowed for (see Fisher in Ref. Gunton and Green [1973] p. 66 where a “dangerous irrelevant variable” is characterized as a “hidden relevant variable” and Ref. Fisher [1983], appendix D). In essence one finds that the scaling function limit $\mathcal{F}(y, z \rightarrow 0, \dots)$, previously accepted without question, is no longer well defined but, rather, diverges as a power of z : asymptotic scaling survives but $d^* \equiv (2 - \alpha)/\nu$ sticks at the value 4 for $d > d_{uc} = 4$.

⁵Note that T_c for example, will usually be a function of any irrelevant parameter such as g_j . This comes about because, in a full scaling formulation, the variables t , h , and $\{g_j\}$ appearing in Eq. (9.8.11) must be replaced by nonlinear scaling fields $t(t, h, \{g_j\})$, $h(t, h, \{g_j\})$, and $g_j(t, h, \{g_j\})$ which are smooth functions of t , h , and g_j Wegner [1972a,b, 1976]; Fisher [1983]. By the same token it is usually advantageous to introduce a prefactor A_0 in Eq. (9.8.11) and “metrical factors” E_j in the arguments of \mathcal{F} (see, e.g., Ref. Fisher [1983]).

⁶Formally, one might write $\mathcal{F}_\infty(y) = \mathcal{F}(y, z \rightarrow z_\infty)$ where z_∞ is a critical value which could be ∞ ; but a more subtle relationship is generally required since the exponent α in the prefactor in Eq. (9.8.11) changes

will usually work well and the Kadanoff picture almost applies. When there are no relevant variables and only one or a few marginal variables, field-theoretic perturbative techniques of the Gell-Mann-Low Gell-Mann and Low [1954], Callan-Symanzik Wilson [1975]; Brézin et al. [1976]; Amit [1978]; Itzykson and Drouffe [1989] or so-called “parquet diagram” varieties Larkin and Khmel’nitskii [1969] may well suffice (assuming the dominating fixed point is sufficiently simple to be well understood). There may then be little incentive for specifically invoking general RG theory. This seems, more or less, to be the current situation in QFT and it applies also in certain physics of matter problems.

Within RG theory the general mechanism of universality is as follows: In a very large (generally infinitely large) space of Hamiltonians \mathcal{H} , parametrized by t, h , and all the g_j , there is a controlling critical point (a fixed point) about which each variable enters with a characteristic exponent. All systems with Hamiltonians differing only through the values of the g_j (within suitable bounds) will exhibit the same critical behavior determined by the same free-energy scaling function \mathcal{F} , dropping the irrelevant arguments. Different universality classes will be associated with different controlling critical points in the space of Hamiltonians with, once one recognizes the concept of RG flows, different “domains of attraction” under the flow. Indeed, the expectation of a general form of scaling is frequently the most important consequence of RG theory for the practicing experimentalist or theorist.

References

- A. Aharony. Dependence of Universal Critical Behavior on Symmetry and Range of Interaction. In C. Domb and M. S. Green, editors, *Phase Transitions and Critical Phenomena*, page 357. Academic, London, 1976.
- G. A. Ahlers, A. Kornblit, and H. J. Guggenheim. Logarithmic Corrections to the Landau Specific Heat near the Curie Temperature of the Dipolar Ising Ferromagnet LiTbF₄. *Phys. Rev. Lett.*, 34:1227, 1975. doi: [10.1103/PhysRevLett.34.1227](https://doi.org/10.1103/PhysRevLett.34.1227).
- D. J. Amit. *Field Theory, the Renormalization Group and Critical Phenomena*. McGraw-Hill Inc., London, 1978. see also 1993, the expanded Revised 2nd Edition (World Scientific, Singapore).
- G. A. Baker Jr. *Quantitative Theory of Critical Phenomena*. Academic, San Diego, 1990.
- R. J. Baxter. *Exactly Solved Models in Statistical Mechanics*. Academic, London, 1982.
- E. Brézin, J. C. L. Guillou, and J. Zinn-Justin. Field Theoretical Approach to Critical Phenomena. In C. Domb and M. S. Green, editors, *Phase Transitions and Critical Phenomena*, page 125. Academic, London, 1976.
- D. M. Ceperley. Path integrals in the theory of condensed helium. *Rev. Mod. Phys.*, 67:279, 1995. doi: [10.1103/RevModPhys.67.279](https://doi.org/10.1103/RevModPhys.67.279).
- R. J. Creswick, H. A. Farach, and C. P. Poole Jr. *Introduction to Renormalization Group Methods in Physics*. John Wiley & Sons, Inc., New York, 1992.
- S. K. Das, Y. C. Kim, and M. E. Fisher. When Is a Conductor Not Perfect? Sum Rules Fail Under Critical Fluctuations. *Phys. Rev. Lett.*, 107:215701, 2011. doi: [10.1103/PhysRevLett.107.215701](https://doi.org/10.1103/PhysRevLett.107.215701).

- C. Domb. On the Theory of Cooperative Phenomena in Crystals. *Adv. Phys. (Philos. Mag. Suppl.)*, 9:149, 1960. doi: [10.1080/00018736000101189](https://doi.org/10.1080/00018736000101189).
- C. Domb. *The Critical Point: A Historical Introduction to the Modern Theory of Critical Phenomena*. Taylor and Francis, London, 1996.
- C. Domb and D. L. Hunter. On the Critical Behavior of Ferromagnets. *Proc. Phys. Soc. (London)*, 86:1147, 1965. doi: [10.1088/0370-1328/86/5/127](https://doi.org/10.1088/0370-1328/86/5/127).
- C. Domb and M. F. Sykes. Effect of Change of Spin on the Critical Properties of the Ising and Heisenberg Models. *Phys. Rev.*, 128:168, 1962. doi: [10.1103/PhysRev.128.168](https://doi.org/10.1103/PhysRev.128.168).
- J. W. Essam and M. E. Fisher. Padé Approximant Studies of the Lattice Gas and Ising Ferromagnet below the Critical Point. *J. Chem. Phys.*, 38:802, 1963. doi: [10.1063/1.1733766](https://doi.org/10.1063/1.1733766).
- M. E. Fisher. The Susceptibility of the Plane Ising Model. *Physica (Amsterdam)*, 25:521, 1959. doi: [10.1016/S0031-8914\(59\)95411-4](https://doi.org/10.1016/S0031-8914(59)95411-4).
- M. E. Fisher. On the Theory of Critical Point Density Fluctuations. *Physica (Amsterdam)*, 28: 172, 1962. doi: [10.1016/0031-8914\(62\)90102-7](https://doi.org/10.1016/0031-8914(62)90102-7).
- M. E. Fisher. Correlation Functions and the Critical Region of Simple Fluids. *J. Math. Phys.*, 5:944, 1964. doi: [10.1063/1.1704197](https://doi.org/10.1063/1.1704197).
- M. E. Fisher. The Nature of Critical Points. In *Lectures in Theoretical Physics*, page 1. University of Colorado Press, Boulder, 1965.
- M. E. Fisher. The Theory of Condensation and the Critical Point. *Physics*, 3:255, 1967a. doi: [10.1103/PHYSICSPHYSIQUEFIZIKA.3.255](https://doi.org/10.1103/PHYSICSPHYSIQUEFIZIKA.3.255). (Long Island City, NY).
- M. E. Fisher. The Theory of Equilibrium Critical Phenomena. *Rep. Prog. Phys.*, 30:615, 1967b. doi: [10.1088/0034-4885/30/2/306](https://doi.org/10.1088/0034-4885/30/2/306).
- M. E. Fisher. General Scaling Theory for Critical Points. In B. Lundqvist and S. Lundqvist, editors, *Proceedings of the Nobel Symp. XXIV, Aspensgården, Lerum, Sweden, June 1973, in Collective Properties of Physical Systems*, page 16. Academic, New York, 1974a.
- M. E. Fisher. The Renormalization Group in the Theory of Critical Phenomena. *Rev. Mod. Phys.*, 46:597, 1974b. doi: [10.1103/Revmodphys.46.597](https://doi.org/10.1103/Revmodphys.46.597).
- M. E. Fisher. Scaling, Universality and Renormalization Group Theory. In F. J. Hahne, editor, *Critical Phenomena*, volume 186, page 1. Springer, Berlin, 1983.
- M. E. Fisher. Renormalization group theory: Its basis and formulation in statistical physics. *Rev. Mod. Phys.*, 70:653, 1998. doi: [10.1103/Revmodphys.70.653](https://doi.org/10.1103/Revmodphys.70.653).
- M. E. Fisher and R. J. Burford. Theory of Critical Point Scattering and Correlations. I. The Ising Model. *Phys. Rev.*, 156:583, 1967. doi: [10.1103/Physrev.156.583](https://doi.org/10.1103/Physrev.156.583).
- M. E. Fisher and M. F. Sykes. Excluded Volume Problem and the Ising Model of Ferromagnetism. *Phys. Rev.*, 114:45, 1959. doi: [10.1103/Physrev.114.45](https://doi.org/10.1103/Physrev.114.45).
- M. Gell-Mann and F. E. Low. Quantum Electrodynamics at Small Distances. *Phys. Rev.*, 95: 1300, 1954. doi: [10.1103/PhysRev.95.1300](https://doi.org/10.1103/PhysRev.95.1300).

REFERENCES

- V. L. Ginzburg. Superconductivity and Superfluidity (What was done and what was not). *Phys. Usp.*, 40:407, 1997. doi: [10.1070/PU1997v04n04ABEH000230](https://doi.org/10.1070/PU1997v04n04ABEH000230).
- V. L. Ginzburg and L. D. Landau. On the Theory of Superconductivity. *Zh. Eksp. Teor. Fiz.*, 20:1064, 1959.
- N. Goldenfeld. *Lectures on Phase Transitions and the Renormalization Group*. Frontiers in Physics. Westview Press, University of Illinois at Urbana-Champaign, 1992.
- E. A. Guggenheim. *Thermodynamics*. North Holland, Amsterdam, 1949. Fig. 4.9.
- J. D. Gunton and M. S. Green, editors. *Renormalization Group in Critical Phenomena and Quantum Field Theory: Proceedings of a Conference*, Chestnut Hill, Pennsylvania, 29-31 May 1973. Temple University, Philadelphia.
- J. P. Hansen and I. R. McDonald. *Theory of Simple Liquids*. Academic Press, Amsterdam, 1986.
- P. Heller and G. B. Benedek. Nuclear Magnetic Resonance in MnF_2 near the Critical Point. *Phys. Rev. Lett.*, 8:428, 1962. doi: [10.1103/PhysRevLett.8.428](https://doi.org/10.1103/PhysRevLett.8.428).
- E. Hille. *Functional Analysis and Semi-Groups*. American Mathematical Society, New York, 1948.
- D. Itzykson and J.-M. Drouffe. *Statistical Field Theory*. Cambridge University Press, Cambridge, 1989.
- L. Kadanoff. Scaling Laws for Ising Models near T_c . *Physics*, 2:263, 1966. doi: [10.1103/PhysiqueFizika.2.263](https://doi.org/10.1103/PhysiqueFizika.2.263). (Long Island City, NY).
- L. P. Kadanoff. Scaling, Universality and Operator Algebras. In C. Domb and M. S. Green, editors, *Phase Transitions and Critical Phenomena*, volume 5a, page 1. Academic, London, 1976.
- L. P. Kadanoff and F. J. Wegner. Some Critical Properties of the Eight-Vertex Model. *Phys. Rev. B*, 4:3989, 1971. doi: [10.1103/PhysRevB.4.3989](https://doi.org/10.1103/PhysRevB.4.3989).
- L. P. Kadanoff et al. Static Phenomena near Critical Points: Theory and Experiment. *Rev. Mod. Phys.*, 39:395, 1967. doi: [10.1103/RevModPhys.39.395](https://doi.org/10.1103/RevModPhys.39.395).
- B. Kaufman and L. Onsager. Crystal Statistics II. Short-Range Order in a Binary Lattice. *Phys. Rev.*, 76:1244, 1949. doi: [10.1103/PhysRev.76.1244](https://doi.org/10.1103/PhysRev.76.1244).
- H. K. Kim and M. H. W. Chan. Experimental Determination of a Two-Dimensional Liquid-Vapor Critical-Point Exponent. *Phys. Rev. Lett.*, 53:170, 1984. doi: [10.1103/PhysRevLett.53.170](https://doi.org/10.1103/PhysRevLett.53.170).
- J. S. Kouvel and M. E. Fisher. Detailed Magnetic Behavior of Nickel near its Curie Point. *Phys. Rev. A*, 136:1626, 1964. doi: [10.1103/Physrev.136.A1626](https://doi.org/10.1103/Physrev.136.A1626).
- L. D. Landau and E. M. Lifshitz. *Statistical Physics*, volume 5 of *Course of Theoretical Physics*. Pergamon, London, 1958.
- A. I. Larkin and D. E. Khmel'nitskii. Phase Transition in Uniaxial Ferroelectrics. *Zh. Eksp. Teor. Fiz.*, 56:2087, 1969.
- F. Leonard and B. Delamotte. Critical exponents can be different on the two sides of a transition. *Phys. Rev. Lett.*, 115:200601, 2015. doi: [10.1103/PhysRevLett.115.200601](https://doi.org/10.1103/PhysRevLett.115.200601).

- S. MacLane and G. Birkhoff. *Algebra*. MacMillan, New York, 1967. Chap. II, Sec. 9 and Chap. III, Sec. 1.2.
- P. A. Martin. Sum rules in charged fluids. *Rev. Mod. Phys.*, 60:1075, 1988. doi: [10.1103/RevModPhys.60.1075](https://doi.org/10.1103/RevModPhys.60.1075).
- D. R. Nelson. Defect-mediated Phase Transitions. In C. Domb and M. S. Green, editors, *Phase Transitions and Critical Phenomena*, page 1. Academic, London, 1983.
- L. Onsager. Crystal Statistics I. A Two-dimensional Model with an Order-Disorder Transition. *Phys. Rev.*, 62:117, 1944. doi: [10.1103/PhysRev.65.117](https://doi.org/10.1103/PhysRev.65.117).
- L. Onsager. Discussion remark following a paper by G. S. Rushbrooke at the International Conference on Statistical Mechanics in Florence. *Nuovo Cimento Suppl.*, 9:261, 1949.
- A. Z. Patashinskii and V. L. Pokrovskii. Behavior of ordering systems near the transition point. *Zh. Eksp. Teor. Fiz.*, 50:439, 1966.
- F. Riesz and B. Sz.-Nagy. *Functional Analysis*. F. Ungar, New York, 1955. Chap. X, Secs. 141 and 142.
- J. S. Rowlinson. *Liquids and Liquid Mixtures*. Butter-Worth Scientific, London, 1959.
- G. S. Rushbrooke and P. J. Wood. On the Curie Points and High-Temperature Susceptibilities of Heisenberg Model Ferromagnetics. *Mol. Phys.*, 1:257, 1958. doi: [10.1080/00268975800100321](https://doi.org/10.1080/00268975800100321).
- H. E. Stanley. *Introduction to Phase Transitions and Critical Phenomena*. Oxford University, New York, 1971.
- F. J. Wegner. Corrections to Scaling Laws. *Phys. Rev. B*, 5:4529, 1972a. doi: [10.1103/PhysRevB.5.4529](https://doi.org/10.1103/PhysRevB.5.4529).
- F. J. Wegner. Critical Exponents in Isotropic Spin Systems. *Phys. Rev. B*, 6:1891, 1972b. doi: [10.1103/PhysRevB.6.1891](https://doi.org/10.1103/PhysRevB.6.1891).
- F. J. Wegner. The Critical State, General Aspects. In C. Domb and M. S. Green, editors, *Phase Transitions and Critical Phenomena*, volume 6, page 6. Academic, London, 1976.
- B. Widom. Surface Tension and Molecular Correlations near the Critical Point. *J. Chem. Phys.*, 43:3892, 1965a. doi: [10.1063/1.1696617](https://doi.org/10.1063/1.1696617).
- B. Widom. Equation of State in the Neighborhood of the Critical Point. *J. Chem. Phys.*, 43: 3898, 1965b. doi: [10.1063/1.1696618](https://doi.org/10.1063/1.1696618).
- B. Widom and O. K. Rice. Critical Isotherm and the Equation of State of Liquid-Vapor Systems. *J. Chem. Phys.*, 23:1250, 1955. doi: [10.1063/1.1742251](https://doi.org/10.1063/1.1742251).
- K. G. Wilson. Renormalization Group and Critical Phenomena I. Renormalization Group and Kadanoff Scaling Picture. *Phys. Rev. B*, 4:3174, 1971a. doi: [10.1103/PhysRevB.4.3174](https://doi.org/10.1103/PhysRevB.4.3174).
- K. G. Wilson. Renormalization Group and Critical Phenomena II. Phase-Space Cell Analysis of Critical Behavior. *Phys. Rev. B*, 4:3184, 1971b. doi: [10.1103/PhysRevB.4.3184](https://doi.org/10.1103/PhysRevB.4.3184).
- K. G. Wilson. The Renormalization Group: Critical Phenomena and the Kondo Problem. *Rev. Mod. Phys.*, 47:773, 1975. doi: [10.1103/RevModPhys.47.773](https://doi.org/10.1103/RevModPhys.47.773).

REFERENCES

- K. G. Wilson. The Renormalization Group and Critical Phenomena. *Rev. Mod. Phys.*, 55:583, 1983. doi: [10.1103/RevModPhys.55.583](https://doi.org/10.1103/RevModPhys.55.583). (1982, Nobel Prize Lecture).
- K. G. Wilson and M. E. Fisher. Critical Exponents in 3.99 Dimensions. *Phys. Rev. Lett.*, 28: 240, 1972. doi: [10.1103/Physrevlett.28.240](https://doi.org/10.1103/Physrevlett.28.240).
- K. G. Wilson and J. Kogut. The Renormalization Group and the ϵ Expansion. *Phys. Rep.*, 12: 75, 1974. doi: [10.1016/0370-1573\(74\)90023-4](https://doi.org/10.1016/0370-1573(74)90023-4).
- S.-Y. Zinn and M. E. Fisher. Universal Surface-Tension and Critical-Isotherm Amplitude Ratios in Three Dimensions. *Physica A*, 226:168, 1996. doi: [10.1016/0378-4371\(95\)00382-7](https://doi.org/10.1016/0378-4371(95)00382-7).

List of Figures

1.1 Radiation zone of a current system. The shaded area is where are the currents. The origin of the coordinate system O is chosen inside this region. Q is any point of the currents. P is where we measure the electromagnetic field radiated out. d is the linear extension of the current system.	10
3.7.1 Shows the deviations (3.7.1) for a simulation with $S = 60$ and $S = 52.5$, $\tau = 0.025$, $l = 9$. The free particle standard deviations (3.7.2) are plotted for comparison. For $S = 60$ the path is localized while for $S = 52.5$ is unlocalized i.e. closer to the free particle path.	97
3.8.1 Shows the time step, τ , extrapolation for the potential energy, $P = \langle \mathcal{P} \rangle$. We run at $\beta = 15$, $\gamma = 0.02$, and $S = 60$. The extrapolated value to the continuum limit is in this case $P = -16.1(5)$ which is in good agreement with the result of Ref. X. Wang [1998].	98
3.8.2 At $S = 60$ the results for the potential energy \mathcal{P} at each MC block (5×10^3 MCS) starting from an initial unlocalized path obtained by a previous simulation at $S = 52.5$. We can see that after about 30 blocks there is a transition from the ES state to the ST state. In the inset is shown the autocorrelation function, defined in Eq. (3.A.8), for the potential energy, for the two states. The correlation time, in MC blocks, is shorter in the unlocalized phase than in the localized one. The computer time necessary to carry on a given number of Monte Carlo steps is longer for the unlocalized phase.	99
3.8.3 The top panel shows the polaron (closed) path $x(t)$ as a function of Euclidean time t in units of τ at equilibrium during the simulation. The middle panel shows the projection on the $x - y$ plane of the path. The bottom panel shows the three-dimensional path. We see clearly how both path has moved from the initial path located on the origin but the path at $S = 52.5$ is much less localized than the one at $S = 60$	100
3.8.4 Shows the behavior of the potential energy P as a function of the coupling constant S . The points are the MC results (see Tab. 3.8.1), the dashed line is the second order perturbation theory result (perturbation) valid in the weak coupling regime and the dot-dashed line is the variational approach from Ref. Sumi and Toyozawa [1973] (variational) in the weak and strong coupling regimes.	101
4.2.1 Ionization potentials of elements that are known from spectroscopic data.	115
6.2.1 The Riemannian surface \mathcal{S} of Eq. (6.2.124).	145

LIST OF FIGURES

6.2.2 The one body density $n^{\text{hs}}(r)/n$ of Eq. (6.2.178), for the 2D OCP on just one universe of the surface \mathcal{S} , obtained with $N = 300$. On the left at fixed $M = 1$ and on the right at fixed $n = 1$	152
6.2.3 The one body density $n^{(1)}(s)/n$, where $s = 2Mx$, for the 2D OCP on the whole manifold, obtained using Eq. (6.2.192) with $N = 300$. On the left at fixed $M = 1$ and on the right at fixed $n = 1$	155
6.2.4 The one body density $n^{(1)}(r)/n$, for the 2D OCP on just one universe of the surface \mathcal{S} , obtained using both the pair potential $-\ln z - z' $ and $-\ln(z - z' /\sqrt{ zz' })$ at fixed $M = n = 1$	156
6.2.5 The one body density $n^{\text{gh}}(r)/n$ obtained truncating the sum of Eq. (6.2.223) after the first 300 terms and choosing $(\sqrt{R} + \sqrt{R - 2M})^2/2M = 10$. On top on the left at fixed $M = \zeta = 1$ and on the right at fixed $n = \zeta = 1$. On the bottom at fixed $M = n = 1$	160
7.2.1 Radial distribution function $g(r)$ computed by DMC method (mixed estimator) for the unpolarized $\xi = 0$ case and the fully polarized $\xi = 1$ case. $r_s = 1$ (dotted line), $r_s = 3$ (dash-dotted line), $r_s = 5$ (dashed line), and $r_s = 10$ (full line). r is in units of a Bohr radius. (Figure reproduced here by courtesy of the authors of Ref. Ortiz and Ballone [1994])	198
7.2.2 Structure factor $S(k)$ computed by the DMC method (mixed estimator). The r_s considered and the symbols are the same as those of Fig. 7.2.1. (Figure reproduced here by courtesy of the authors of Ref. Ortiz and Ballone [1994])	199
7.2.3 The energy of the four phases studied relative to that of the lowest boson state times r_s^2 in Rydbergs as a function of r_s in Bohr radii. The boson system undergoes Wigner crystallization at $r_s = 160 \pm 10$. The fermion system has two phase transitions, crystallization at $r_s = 100 \pm 20$ and depolarization at $r_s = 75 \pm 5$. (Figure reproduced here by courtesy of the authors of Ref. Ceperley and Alder [1980])	200
7.3.1 Illustration of the reach $\gamma(R_0, t)$ of the fermion density matrix.	204
7.3.2 Pair correlation functions (on the left) for $r_s = 1.0$ and $r_s = 10.0$ in the unpolarized state. Also shown is the small r part of the classical Debye-Hückel limit at $\Theta = 8.0$; see Eq. (7.3.38). The Debye-Hückel limit is not yet reached at $\Theta = 8.0$ for the lower density $r_s = 10.0$. Static structure factors (on the right) for $r_s = 1.0$ and $r_s = 10.0$ in the unpolarized state. Also shown is the small k part of the classical Debye-Hückel limit at $\Theta = 8.0$; see Eq. (7.3.39). (Figure reproduced here by courtesy of the authors of Ref. Brown et al. [2013])	208
7.3.3 Excess energies $E_{xc} = e_{xc}$ (on the left) for $r_s = 4.0$ and $r_s = 40.0$ for the polarized state ($E_0 = e_0$). For both densities the high temperature results fall smoothly on top of previous Monte Carlo energies for the classical electron gas Pollock and Hansen [1973] (solid line). Differences from the classical Coulomb gas occur for $\Theta < 2.0$ for $r_s = 4.0$ and $\Theta < 4.0$ for $r_s = 40.0$. Simulations with the Fermion sign (squares) confirm the fixed-node results at $\Theta = 1.0$ and 8.0 . The zero-temperature limit (dotted line) smoothly extrapolates to the ground state QMC results of Ceperley-Alder Ceperley and Alder [1980] (dashed line). Correlation energy $E_c(T) = e_c(T)$ (on the right) of the 3D Jellium at several temperatures and densities for the unpolarized (top) and fully spin-polarized (bottom) states. Exact (signful) calculations (squares) confirm the fixed-node results where possible ($\Theta = 8.0$ for $\xi = 0$ and $\Theta = 4.0, 8.0$ for $\xi = 1$). (Figure reproduced here by courtesy of the authors of Ref. Brown et al. [2013])	210

7.3.4 Correlation energy $E_c(T) = e_c(T)$ of the Jellium at $r_s = 4.0$ for the unpolarized $\xi = 0$ state from the RPIMC calculations (RPIMC) and several previous parameterizations as a function of Θ . The latter include Debye-Hückel (DH), Hansen (H), Hansen+Wigner-Kirkwood (H+WK), Random-Phase-Approximation (RPA), Tanaka and Ichimaru (TI), and Perrot and Dharma-wardana (PDW). Also included is the ground state $\Theta = 0.0$ result for comparison. (Figure reproduced here by courtesy of the authors of Ref. Brown et al. [2014])	211
7.3.5 Temperature-density phase diagram showing the points considered in Ref. Brown et al. [2013]. Several values of the Coulomb coupling parameter Γ (dashed lines) and the electron degeneracy parameter Θ (dotted lines) are also shown. (Figure reproduced here by courtesy of the authors of Ref. Brown et al. [2013])	212
7.H.1 Integration contour on the complex ω plane.	237
8.2.1 The exponent $\Gamma = d \ln P / d \ln n$ for the adiabatic full relativistic equation of state as a function of density. We chose a temperature $T = 20000\text{K}$ and zero entropy, $g = 2$, and m is the mass of an electron. n is in cm^{-3}	248
8.2.2 Temperature dependence of the Chandrasekar limit at $\mu_e = 2$. We recall that $z = e^{\beta\mu}$	252
8.3.1 The radial distribution function for ideal electrons ($\xi = -1, g = 2$) in the relativistic and the non relativistic cases. Here we chose $T = 20000\text{K}$ and $n = 1.04 \times 10^{22}\text{cm}^{-3}$ in the non relativistic case and $n = 5.93 \times 10^{24}\text{cm}^{-3}$ in the relativistic case. r is in Angstroms.	254
9.4.1 Temperature variation of gas-liquid coexistence curves (temperature, T , versus density, ρ) and corresponding spontaneous magnetization plots (magnetization, M , versus T). The solid curves, (b) and (d), represent (semiquantitatively) observation and modern theory, while the dotted curves (a) and (c) illustrate the corresponding “classical” predictions (mean-field theory and van der Waals approximation). These latter plots are parabolic through the critical points (small open circles) instead of obeying a power law with the universal exponent $\beta \simeq 0.325$: See Eqs. (9.4.3) and (11). The energy scale ε , and the maximal density and magnetization, ρ_{\max} and M_{\max} , are nonuniversal parameters particular to each physical system; they vary widely in magnitude.	264
9.8.1 A depiction of the space of Hamiltonians \mathcal{H} showing initial or physical manifolds, $K = \{t, h\}$ with $t = (T - T_c)/T_c$ and T_c the critical temperature, [labelled (a), (b), ...] and the flows induced by repeated application of a discrete RG transformation \mathcal{R}_b with a spatial rescaling factor b (or induced by a corresponding continuous or differential RG). Critical trajectories are shown bold: They all terminate, in the region of \mathcal{H} shown here, at a fixed point $\bar{\mathcal{H}}^*$. The full space contains, in general, other nontrivial, critical fixed points, describing multicritical points and distinct critical-point universality classes; in addition, trivial fixed points, including high-temperature “sinks” with no outflowing or relevant trajectories, typically appear. Lines of fixed points and other more complex structures may arise and, indeed, play a crucial role in certain problems. (After Ref. Fisher [1983])	272

LIST OF FIGURES

List of Tables

3.8.1 MC results for P as a function of S at $\beta = 15$ and $\gamma = 0.02$ displayed in Fig. 3.8.4. The runs where made of 5×10^5 MCS (with 5×10^4 MCS for the equilibration) for the ES states and 5×10^6 MCS (with 5×10^5 MCS for the equilibration) for the ST states.	102
9.5.1 This table lists the critical exponents of the ferromagnetic transition in the Ising model. In statistical physics, the Ising model describes a continuous phase transi- tion with scalar order parameter. The critical exponents of the transition are uni- versal values and characterize the singular properties of physical quantities. The ferromagnetic transition of the Ising model establishes an important universality class, which contains a variety of phase transitions as different as ferromagnetism close to the Curie point and critical opalescence of liquid near its critical point. .	267

LIST OF TABLES

Index

Follows the analytic index of some of the most significant terms.

A

- antiparticle 2, 27, 77, 80
- anyons 184
- atom 4, 5, 12, 111–114, 117, 118, 229

B

- Bijl-Dingle-Jastrow 191
- black hole 251

C

- Chandrasekhar limit 250, 251
- chemical element 114, 117, 118
- chemical reaction 117
- correlation exponent 269
- correlation function 261, 262, 266, 268
- correlation length 266, 268
- critical exponent 259, 262, 266, 273
- critical point 260–265, 267, 271, 275, 276

D

- density matrix 197, 201, 204–206, 211, 231, 232, 234
- differential forms 8
- diffusion Monte Carlo 12, 188, 189

E

- Einstein Relativity 38
- electromagnetic wave 9
- electron 1–3, 5–7, 9, 11–13, 17, 89–92, 112–114, 117, 118, 183–185, 211–214, 217, 238, 243, 246, 248, 255, 257

- electron fluid 213
- electron gas 4, 7, 12, 13, 183, 185, 192, 210, 230, 254, 255, 257
- electron plasma 2
- electronegativity 117, 118
- elementary particle 1, 2, 27
- exterior derivative 8

F

- fermions nodes 205, 206, 227
- fermions sign problem 201, 207
- fine-structure constant 7
- fixed point 259, 271–273, 275, 276
- flow 259, 260, 270–274, 276
- fractional statistics 184

G

- Galilean relativity 31
- Galileo group 33, 42
- graphene 7

H

- Hartree potential 227, 238
- Hartree-Fock 207, 229, 230
- Hartree-Jastrow 227
- Hodge star 8
- Hyper-Netted-Chain 183

I

- internal energy 12, 197, 202, 207, 229, 247, 249
- invariance 27, 28, 31
- irrelevance 259, 269, 275

INDEX

J

Jastrow factor 192, 194, 226, 233
jellium 12, 13, 183, 185, 188, 192,
197, 201, 202, 209–213, 229, 231

K

Kosterlitz-Thouless phenomenon 8, 125

L

Landau problem 7, 173
Lie group 82, 85
Linear-Response-Theory 227, 234
locality 2, 27, 57, 76, 77, 79
localization 102
Lorentz group 38–40, 42, 53, 57, 58, 61
luminosity 244

M

marginality 259, 261, 263, 275
Maxwell equations 8
Mean-Spherical-Approximation 183
Metropolis algorithm 90, 94, 102, 206
molecule 4, 118, 183, 229

N

neutron drip 243, 251

O

one component plasma 127, 183, 209, 211

P

path integral 12, 184, 197, 201, 202, 232
Percus-Yevick 183
periodic table 5, 113
phase diagram 211
phase transition 7, 12, 89, 90, 98, 100,
102, 103, 118, 119,
214, 215, 260, 261, 267
phonons 89, 90, 102, 103
Poincaré group 41, 42, 54, 55, 57, 60,
64, 65, 67, 68, 73, 75, 76, 80
polaron 89–91, 93, 98, 100–102, 110
positron 2
Poynting vector 11

pressure 12, 13, 119, 120, 196, 202, 243,
245, 248, 257

primitive approximation 201, 231, 232

primitive model 183, 213

Q

quantum field theory 259, 261, 263, 269
Quantum Hall Effect 5, 7

R

radial distribution function 195,
197, 198, 207, 209, 228–230,
252, 254, 255
Random-Phase-Approximation 186,
192, 194, 209, 211, 227, 230
random-walk 188, 206, 226, 233
RedOx 117
renormalization group 259, 262, 266, 269
restricted path integral 204–206

S

scaling 259, 260, 268–270, 273–276
Slater determinant 191, 192, 228, 229
Slater-Jastrow 188, 226
spin-statistics theorem 2, 27, 76, 77, 79
structure factor 192, 193, 196, 197, 199,
207, 208, 217, 218, 227, 228, 252
superconductivity 12, 13, 185, 201, 202
superfluidity 201, 202
superionic 214, 215
supernovae 252

T

two component plasma 119, 161, 183

U

universality 259, 263–269, 271, 273, 275, 276

V

variational Monte Carlo 12, 189

W

white dwarf 243, 244, 251, 254, 255

